Millennial-scale rates of erosion and change in relief in north Queensland using cosmogenic nuclide ^{10}Be

Thesis submitted by

Ashish Kumar Mishra

B.Tech, M.Sc

March 2019

for the degree of

Doctor of Philosophy

College of Science and Engineering,

James Cook University

Declaration of Authorship

I, Ashish Kumar Mishra, declare that this thesis, submitted in fulfilment of the requirements for the award of Doctor of Philosophy, in the College of Science and Engineering, James Cook University, is my own work unless otherwise referenced or acknowledged.

This thesis has been prepared in journal article compilation style format.

This work was done while in candidature for a research degree at James Cook University, and this thesis has not been submitted for qualification at any other academic institution.

Ashish Kumar Mishra

4 March 2019

Statement of Contribution of Others

The financial support for this thesis was provided by James Cook University Postgraduate Research Scholarship (JCUPRS), James Cook University Graduate Research School HDR Enhancement Scheme, and my supervisor at James Cook University Dr. Christa Placzek. My stipend was funded through James Cook University Postgraduate Research Scholarship (JCUPRS). The cost of analysis of my samples at Australia's Nuclear Science and Technology Organization (ANSTO) was funded by ANSTO Facility Access Grant.

My advisors gave advice throughout the project on study design, research methodology, data collection techniques and analysis as well as manuscript preparation.

Two chapters of this thesis, namely Chapter 2 and 4, has been published in two international peer reviewed journals (below):

1. Mishra, A. K., Placzek, C., & Jones, R. (2019). Coupled influence of precipitation and vegetation on millennial-scale erosion rates derived from 10Be. *PLOS ONE, 14*(1), e0211325. doi:10.1371/journal.pone.0211325

2. Mishra, A. K., Placzek, C., Wurster, C., & Whitehead, P. W. (2018). New radiocarbon age constraints for the 120 km-long Toomba flow, north Queensland, Australia. *Australian Journal of Earth Sciences*, 1-9. doi:10.1080/08120099.2019.1523227

Both papers have multiple co-authors, which include Rhondda Jones, Peter Whitehead, and Chris Wurster. Toshiyuki Fujioka, Charles Mifsud, and David Fink from ANSTO also had contribution towards the work presented in this thesis. Specific contribution of all these members are indicated below:
Rhondda Jones provided training in statsitical analyses for paper (1). Chris Wurster performed hydrogen pyrolysis pre-treatment on radiocarbon samples for paper (2). Chris Wurster also helped in preparation of manuscript for paper (2). Peter Whitehead helped in preparation of manuscript and added more constraints on geological description for paper (2). David Fink, Toshiyuki Fujioka, and Chrales Mifsud operated the accelerator mass spectrometers at ANSTO.

Acknowledgements

First and foremost I would like to thank my supervisors Dr Christa Placzek, Professor Michael Bird, and Dr Carl Spandler. Their constant support and guidance made this thesis possible. I would also like to thank Dr Christa Placzek for providing me the support I needed to get started, the freedom to explore new ideas, and suggestions for new techniques. She was always available to share ideas and knowledge, discuss new methods, and developments in the field. She also provided me with field support and training on samples collection, processing and preparation.

I would also like to thank David Fink, Toshi Fujioka, and Charles Mifsud from Australia's Nuclear Science and Technology Organisation (ANSTO) for sharing their ideas, knowledge, and time, and for their support in sample analyses.

I would also like to thank my colleagues at James Cook University for sharing their ideas and knowledge during my candidature. Special mention to Dr James Daniels and Dr Stephanie Duce for their help with GIS. I would also like to thank Dr Eric Roberts, Dr Carl Splander, Dr Cassian Pirard, Dr Bob Henderson, Yi Hu (Advance Analytical Centre), Dr Chris Wurster, Dr Han She Lim, and Mr Peter Whitehead for generously sharing their knowledge with me. I would also like to thank members of Centre for Tropical Environmental and Sustainability Science (TESS) and Economic Geology Research Centre (EGRU).

I would also like to specially thank Rebecca Steele, Judy Botting, Melissa Norton, Alaina Jones, and team for always making things easier for us. I could not have made it without their support. I would also like to thank Andrew Norton for magically solving all the IT problems during my candidature.

I would like to specially thank my friends Veer, Laura, Connor, Tiffany, Marcus, Claudia, Jaime, Joao, Alexia, Avishek, Arup, Padma, Tegan, Jonathan, Justin, Abhinav, Ricky, Manish, Priya, Bew, Benham, Beatrice, Michelle and many more, for their constant support and more making this a memorable experience. I would also like to thank my family - my Mom, my Dad, and my Sister for their support, guidance, and love.

And finally I would like to thank Sybille, for her continuous love and support, and for making this entire experience memorable and awesome. Without her support, I could not have finished this.

I would also like to thank Miss Sushi @JCU for morning coffees.

Contents

List of Tables:

List of Figures:

Thesis Abstract

Although water is one of the main agents of erosion in many environmental settings, many erosion rates derived from beryllium-10 (^{10}Be) suggests that a relationship between precipitation and erosion rate is statistically non-significant on a global scale. This might be because of the strong influence of other variables on erosion rate. The first chapter of this thesis contains global ^{10}Be compilation, in which I examine if mean annual precipitation has a statistically significant secondary control on erosion rate. My secondary variable assessment suggests a significant secondary influence of precipitation on erosion rate. This is the first time that the influence of precipitation on ^{10}Be-derived erosion rate is recognized on global scale. In fact, in areas where slope is <200m/km (~11°), precipitation influences erosion rate as much as mean basin slope, which has been recognized as the most important variable in previous ^{10}Be compilations. In areas where elevation is <1000m and slope is <11°, the correlation between precipitation and erosion rate improves considerably. These results also suggest that erosion rate responds to change in mean annual precipitation nonlinearly and in three regimes: 1) it increases with an increase in precipitation until ~1000 mm/yr; 2) erosion rate stabilizes at ~1000 mm/yr and decreases slightly with increased precipitation until ~2200 mm/yr; and 3) it increases again with further increases in precipitation. This complex relationship between erosion rate and mean annual precipitation is best explained by the interrelationship between mean annual precipitation and vegetation. Increased vegetation, particularly the presence of trees, is widely recognized to lower erosion rate. Our results suggest that tree cover of 40% or more reduces erosion rate enough to outweigh the direct erosive effects of increased rainfall. Thus, precipitation emerges as a stronger secondary control on erosion rate in hyper-arid areas, as well as in hyper-wet areas. In contrast, the regime between ~1000 and ~2200 mm/yr is dominated by opposing relationships where higher rainfall acts to increase erosion rate, but more water also increases vegetation/tree

cover, which slows erosion. These results suggest that when interpreting the sedimentological record, high sediment fluxes are expected to occur when forests transition to grasslands/savannahs; however, aridification of grasslands or savannahs into deserts will result in lower sediment fluxes. This study also implies that anthropogenic deforestation, particularly in regions with high rainfall, can greatly increase erosion.

Quantification of long-term erosion rates is important in north Queensland, which is proximal to the Great Barrier Reef. One of the main threats to the Great Barrier Reef is sediment generated by erosion. Recent applications of ^{10}Be in north Queensland has contributed significantly towards understanding erosion rates in the region. However, the existing information has a limited spatial distribution and information on bedrock erosion rates in north Queensland are very limited. Here, I focus on quantifying erosion rates across north Queensland and investigating how erosion rate varies across different slopes, rock types, and precipitation values. I also determined paleoerosion rates for the Burdekin River, and quantified erosion rates from bedrock samples and compared these to adjacent basins to explore the implications for rates of relief generation and landscape evolution.

The erosion rates of basins in north Queensland range from 2.2 to 53.6m/My and bedrock rates range from 3.6 to 70.2m/My. These rates are slow, compared to basins in other parts of the world that experience similar precipitation. Basins in northern part of north Queensland are eroding faster than the southern part, because the northern part experiences higher rainfall. Precipitation has strong influence on basin erosion rate (R^2=0.71), whereas the influence of mean basin slope is negligible (R^2=0.09). The strong influence of precipitation and weak influence of slope on erosion rates in north Queensland is consistent with the fact that most sampling sites are from areas where slope was low (~<13°). The bedrock erosion rates in north Queensland are mainly governed by lithology; sedimentary rocks are eroding faster than granites, and precipitation has no influence on bedrock erosion rate.

Unlike most places in the world, bedrock in north Queensland erodes faster than basins. This implies that relief is being lost over time. My results also suggests minimal temporal variation for erosion rates in north Queensland, and that these erosion rates were consistently slow for ~120,000 years, implying that landscapes in north Queensland have most likely attained steady state.

In order to obtain the paleoerosion rate of Burdekin River, sediments buried under the Toomba flow were collected. The Toomba flow is the youngest flow of the Nulla volcanic province, located in north Queensland. This 120 km long flow has a published $^{40}Ar/^{39}Ar$ age of 21,000 ± 3000 years. In contrast, seven conventional radiocarbon (^{14}C) analyses of carbon-bearing material beneath the flow yielded radiocarbon ages of 16,000 to <2500 BP. Published radiocarbon ages are younger than the $^{40}Ar/^{39}Ar$ age, potentially due to contamination of the charcoal by younger carbon that was not removed by acid-base pre-treatment methodology used. I have, therefore, re-examined the radiocarbon age of the Toomba flow using newly sampled charcoal buried beneath the Toomba flow in combination with hydrogen pyrolysis pre-treatment and accelerated mass spectrometer (AMS) measurements. I determined a calibrated radiocarbon age of 20,815–19,726 calBP (2σ) for the material beneath the Toomba flow. Our radiocarbon age, therefore: (1) is older than previous radiocarbon ages for the Toomba flow, (2) provides the most precise age yet available for the Toomba flow, (3) is in agreement with the $^{40}Ar/^{39}Ar$ age, and (4) validates that hydrogen pyrolysis is a robust and effective pre-treatment method for subtropical conditions where samples are susceptible to contamination by younger carbon. The Toomba flow erupted during the Last Glacial Maximum, but the preserved surface suggests that the rate of weathering and soil formation has been almost negligible on this flow, despite being situated in a subtropical climate that experiences highly variable, often intense rainfall. The age of Toomba flow also allowed determination of paleoerosion rates for the Burdekin River, and the present erosion rate

derived from modern Burdekin samples is not very different from the erosion rate derived from sediment deposited ~20,000 years ago.

Chapter 1: Rationale

1.1. Introduction

Erosion is the transfer or removal of bedrock and Earth materials (Olvmo, 2010). It is closely associated with sediment yield, and plays an important indirect role in sediment transport (Pimentel et al., 1995). Sediment yield, the quantity of sediment reaching the catchment outlet per unit time and per unit area (García-Ruiz et al., 2015), affects many environmental processes, including formation of river deltas, sedimentation in reservoirs and channels, and sediment storages (Quinton, 2004). The role of erosion and sediment transport has been modelled extensively and its impact on water quality is significant (e.g. Reusser et al., 2015; Whiting, 2006; Merritt et al., 2003; Pimentel et al., 1995). Though rapid erosion is natural, and depends on topography, geology, and Pleistocene history, land-use can accelerate erosion by several folds (e.g. García-Ruiz et al., 2015; Reusser et al., 2015; Whiting, 2006; Pimentel & Kounang, 1998; Stallard, 1998).

Understanding rates of erosion and weathering can also provide deeper insights into pedogenesis, soil morphology, and soil classification (e.g. Riebe et al., 2001b). Comprehending rates of erosion and weathering is also important to understand the process of supplying material to the earth's surface (von Blanckenburg, 2005). Furthermore, quantifying erosion is important to understand climatic evolution (e.g. Rea et al., 1998; Raymo & Ruddiman, 1992; Ruddiman & Kutzbach, 1989; Ruddiman et al., 1989; Raymo et al., 1988; Berner et al., 1983).

Increased erosion and weathering have been linked to the uplift of major mountain belts because it influences silicate weathering, which reduces atmospheric CO_2, thereby regulating global temperature (e.g. Rea et al., 1998; Raymo & Ruddiman, 1992; Ruddiman & Kutzbach, 1989; Ruddiman et al., 1989; Raymo et al., 1988; Berner et al., 1983). Most notably, many

have argued that increased weathering due to uplift of the Himalayas, may be responsible for low atmospheric CO_2 concentration and resultant global cooling over the Cenozoic (Raymo & Ruddiman, 1992; Raymo et al., 1988). Further quantitative understanding of variables controlling rates of erosion and weathering rate is required to understand uplift-erosion model and global carbon-cycle climate models (Raymo & Ruddiman, 1992).

1.2. Difficulty in quantifying rate of erosion

Early geomorphic studies used sediment yield to quantify erosion rate (e.g. Summerfield & Hulton, 1994; Meade, 1988; Walling & Webb, 1983; Schumm, 1973; Schumm, 1963; Langbein & Schumm, 1958). However, quantifying erosion rate using sediment yield is difficult because it requires constant monitoring of sediment fluxes (Meade, 1988) and the timeperiod of monitoring is relatively long. Ideally, 20-25 years of data is required for estimating a reliable sediment yield through sediment fluxes (García-Ruiz et al., 2015). Additionally, the present day flux can be affected by sediment storage or remobilization. Erosion rates derived using modern sediment yield also represents a combination of both natural and anthropogenic-induced erosion (Hewawasam et al., 2003; Summerfield & Hulton, 1994) and is subjected to a degree of uncertainty, primarily because of the episodic nature of sediment delivery (Trimble & Crosson, 2000; Summerfield & Hulton, 1994).

Quantifying erosion rate using sediment yield can also be determined from unique sedimentary deposits. These deposits must have captured all sediment generated in the catchment (Meade, 1988), and require unique conditions where the chronology of depositional units is determined precisely (e.g. Summerfield & Hulton, 1994; Meade, 1988; Walling & Webb, 1983; Schumm, 1973; Schumm, 1963; Langbein & Schumm, 1958).

Over the last several decades, the use of terrestrial cosmogenic nuclides, particularly ^{10}Be and ^{26}Al, has provided unprecedented insight into quantification of erosion rate over millennial

timescales (10^2 to 10^5 years), giving critical insight into factors influencing erosion rate (Willenbring et al., 2013; Portenga & Bierman, 2011; von Blanckenburg, 2005; Brown et al., 1998; Bierman & Steig, 1996; Granger et al., 1996; Brown et al., 1995; Lal, 1991; Brown et al., 1988). Concentration of ^{10}Be have also been widely used to estimate soil production, and erosional histories across many climatic regions (Codilean et al., 2018; Portenga et al., 2013; Heimsath et al., 2010; Bierman & Steig, 1996; Granger et al., 1996; Brown et al., 1995; Lal, 1991). These millennial scale erosion rates can also provide a baseline against, which anthropogenically influence erosion rates can be assessed (Hewawasam et al., 2003; Summerfield & Hulton, 1994)

1.3. An overview of cosmogenic nuclide methods

Cosmogenic nuclides are produced by the interaction of cosmic rays and the particles on Earth's surface, and can be used to estimate amount of time that a rock or sediment has been exposed near the Earth's surface (Bierman & Steig, 1996; Granger et al., 1996; Brown et al., 1995; Lal, 1991; Lal & Peters, 1967). The concentration of CNs is the key parameter from which rate of erosion and/or exposure ages are determined (e.g. Bierman & Steig, 1996; Granger et al., 1996; Brown et al., 1995; Lal, 1991). Higher concentrations of CNs indicates that the sample has been exposed to the cosmic rays for longer time (Bierman & Steig, 1996; Granger et al., 1996; Brown et al., 1995; Lal, 1991). This exposure age inversely correlates with rate of erosion (von Blanckenburg, 2005; Bierman & Steig, 1996; Granger et al., 1996; Brown et al., 1995; Lal, 1991) and long exposure ages are only possible where rates of erosion are slow (von Blanckenburg & Willenbring, 2014; von Blanckenburg, 2005; Bierman & Nichols, 2004; Lal, 1991).

1.3.1. Types of cosmogenic nuclides:

There are two types of cosmogenic nuclides:

- *Meteoric* cosmogenic nuclides
- *In-situ* cosmogenic nuclides

1.3.2. Meteoric cosmogenic nuclides:

Cosmic rays interact with Earth's atmosphere producing *meteoric* cosmogenic nuclide (also known as atmospheric cosmogenic nuclide) and secondary particles. Some of the common *meteoric* cosmogenic nuclides are ^{7}Be, ^{9}Be, ^{10}Be, ^{14}C, and ^{36}Cl. The production rate of *meteoric* cosmogenic nuclides in Earth's atmosphere is generally greater than *in-situ* cosmogenic nuclides, because of the effect of atmospheric shielding (Lal, 1991; Lal, 1988).

1.3.3. In-situ cosmogenic nuclides:

Some cosmic rays and secondary particles produced along with *meteoric* cosmogenic nuclides have enough energy to reach the surface of Earth and undergo nuclear reactions with surface materials, producing *in-situ* cosmogenic nuclides or Terrestrial Cosmogenic Nuclides (TCN) (Lal, 1991; Nishiizumi et al., 1986; Lal & Peters, 1967). There are two kinds of *in-situ* cosmogenic nuclides: stable and unstable. As the names suggest, stable nuclides (^{21}Ne, ^{4}He) are the *in-situ* cosmogenic nuclides that do not decay, and unstable nuclides (^{26}Al, ^{10}Be, ^{36}Cl) are radioactive. The unstable *in-situ* cosmogenic nuclides are more commonly used in quantifying rate of erosion and exposure age. This is in part because stable *in-situ* cosmogenic nuclides are mostly gases, and can leak through the surface of rocks. Additionally, stable *in-situ* cosmogenic nuclides inherit nuclides from past exposure events. However, many studies have used stable *in-situ* cosmogenic nuclides such as ^{21}Ne, to derive erosion rates (e.g. Codilean et al., 2008; Summerfield et al., 1999).

The two most frequently measured unstable *in-situ* cosmogenic nuclides are ^{26}Al and ^{10}Be (Gosse & Phillips, 2001). The radioactive isotope of beryllium, ^{10}Be, with a half-life of 1.39

Ma (1.39 x 10^6 years), is formed by cosmic ray spallation of oxygen (Nishiizumi et al., 1989). In contrast, ^{26}Al forms through spallation of silicon (Si) (Nishiizumi et al., 1989).

1.3.4. Rate of erosion using cosmogenic ^{10}Be and ^{26}Al:

For ^{10}Be and ^{26}Al, quartz is generally analysed (von Blanckenburg, 2005). Oxygen and silicon are the constituent atoms of quartz (SiO_2), which is one of the most common and widely distributed minerals in Earth's crust (Bierman & Steig, 1996; Granger et al., 1996; Brown et al., 1995; Lal, 1991). Other reasons that make quartz preferable are:

- Quartz is available in abundance in silicate rocks and sediments.
- Quartz is resistant to the loss of *in-situ* cosmogenic nuclides.
- Quartz is resist to chemical weathering.
- Quartz has a simple chemistry and is easy to separate from other minerals.

To measure the concentration of ^{10}Be and ^{26}Al, sensitive techniques are required. Developments in the field of Accelerated Mass Spectrometer (AMS) allows measurement of cosmogenic nuclides (Tuniz et al., 1998). However, the concentration of the *in-situ* cosmogenic nuclides is very small (up to few thousand atoms per gram of sample), so tens to hundreds of grams of quartz generally needs to be processed (von Blanckenburg, 2005).

1.4. Outline of the thesis

In this thesis, I aim to determine millennial scale erosion rate in basins and bedrock of north Queensland. In this thesis, I aim to incorporate cosmogenic nuclide data from basins and bedrock from tropical and subtropical areas to determine erosion rate. Terrestrial cosmogenic nuclides, especially ^{10}Be, have been widely applied, but their application in tropical and subtropical landscapes is small compared to arid, semi-arid, and temperate climatic regimes

(Harel et al., 2016; Sosa Gonzalez et al., 2016; Portenga & Bierman, 2011). Erosion rates from north Queensland are limited.

North Queensland is home to the Great Barrier Reef (GBR), which is a World Heritage Area and the largest reef ecosystem in the world. Various studies have found that sediments from adjacent catchments are impacting the health of coral reef in GBR (Bainbridge et al., 2018; Hess et al., 2017; Fabricius et al., 2016; Bartley et al., 2015; Brodie et al., 2012; Fabricius, 2005; Furnas, 2003; Brodie, 2002). However, identification of source of sediments for the large catchments of GBR has been challenging. In particular, sediment yield estimates are often considered high and potentially subjected to a degree of uncertainty because of the episodic nature of sediment delivery (Trimble & Crosson, 2000; Summerfield & Hulton, 1994).

Quantification of erosion rate over millennial timescales (10^2 to 10^5 years) allows determination of which environmental parameters affects erosion rate. This is crucial in order to quantify anthropogenic induced erosion rate (e.g. García-Ruiz et al., 2015; Reusser et al., 2015; Whiting, 2006; Pimentel & Kounang, 1998). Additionally, the influence of environmental parameters, especially precipitation, on erosion rates is not well established.

In this thesis, I first assessed precipitation's influence on ^{10}Be-derived erosion rate on a global scale. I assessed primary as well as secondary influences of environmental parameters on ^{10}Be-derived erosion rate by compiling erosion rates from 93 studies from around the world, and assessed the interrelationship between variables. After the role of precipitation on ^{10}Be-derived erosion rate was established on a global scale, I quantified erosion rate in north Queensland and assessed the relationship between slope, lithology, and precipitation on erosion in north Queensland. To add additional constraints on temporal variation in erosion rate, I also determined past erosion rates from sediments buried beneath the Toomba lava

flow. Since the precise age of the Toomba flow was debatable, I determined a new age for Toomba flow using radiocarbon dating. The outline of the thesis is discussed in detail in the chapters below:

1.4.1. Chapter 2: Coupled influence of precipitation and vegetation on millennial-scale erosion rates derived from ^{10}Be

Chapter 2 of this thesis aims to determine which environmental parameters exert control on rates of erosion on a global scale. The focus of this chapter is on the role of precipitation on ^{10}Be-derived erosion rate on global scale, which has been a matter of debate within the cosmogenic community for decades. This is primarily because, although many studies acknowledge precipitation's influence on erosion rate on global scale (Yanites & Kesler, 2015; Pimentel, 2006; Lal, 2001; Pimentel & Kounang, 1998; Pimentel et al., 1995), other ^{10}Be studies suggest that precipitation's influence on erosion rate is either small or negligible (Nichols et al., 2014; Scherler et al., 2014; Bermúdez et al., 2013; Willenbring et al., 2013; Portenga & Bierman, 2011; Binnie et al., 2007; Wittmann et al., 2007; von Blanckenburg, 2005; Riebe et al., 2001b, 2001a). In this chapter, I compiled data from 93 published studies (n=1790) and investigates not only primary correlation, but also secondary correlation between variables and ^{10}Be-derived erosion rate. In this chapter, I also examined the interrelationship between variables, specially precipitation and vegetation, to find out if the interrelationship between variables obscures their primary influence on erosion rate.

This Chapter is published in a peer-reviewed international journal (Plos One; Mishra et al., 2019).

1.4.2. Chapter 3: Millennial-scale erosion rates in north Queensland determined using ^{10}Be

Chapter 3 of this thesis aims to quantify erosion rates across north Queensland using ^{10}Be. The focus of this chapter is to add constraints on rates of sediment generation and delivery in

north Queensland. This chapter discusses methods of sample collection, processing, and analysis and presents data for 40 samples processed for ^{10}Be and ^{26}Al. The samples for this study were analysed at ANSTO, with the help of ANSTO facility request grant. We have also processed ^{26}Al samples for this chapter and are waiting for the results. In this chapter, I also aim at understanding the spatial and temporal variability of long-term erosion rates in north Queensland and aims to identify how ^{10}Be-derived erosion rates correlate with variability in slope, lithology, and precipitation across north Queensland. In this chapter, I also incorporates erosion rate from bedrock in north Queensland, to understand how rock type affects erosion rate and rates of landscape transformation in north Queensland. This is the first time bedrock erosion rate are published for this region, and I compare these erosion rate from bedrock to basin erosion rate in north Queensland. In this chapter, I also quantified paleoerosion rate for Burdekin River, using sediments buried beneath Toomba flow. Since that required precise age of burial, in this case precise age of Toomba flow, we determined age of Toomba flow using radiocarbon dating (discussed in next chapter).

This chapter is ready to be submitted to a peer-reviewed international journal (Geomorphology) once ^{26}Al data is received.

1.4.3. Chapter 4: New radiocarbon age constraints for the 120 km long Toomba flow, north Queensland, Australia

Chapter 4 of this thesis aims to determine a precise age for the Toomba flow through accelerator mass spectrometer radiocarbon dating. This was done using recently collected charcoal from sediments buried under the Toomba flow that were pre-treated with hydrogen pyrolysis, which preserves only the stable polycyclic aromatic carbon and is an excellent method to avoid radiocarbon contamination. This chapter also compares new radiocarbon ages of the Toomba flow with ^{40}Ar/^{39}Ar ages to understand precision of ^{40}Ar/^{39}Ar method.

With the precise age of Toomba flow determined in this chapter, paleoerosion rate for Burdekin River was determined using sediments buried beneath Toomba flow.

This chapter is published in a peer-reviewed journal (Australian Journal of Earth Science; Mishra et al., 2018)

1.4.4. Chapter 5: Thesis conclusion

The ‘Thesis conclusion’ chapter at the end of this thesis combines all findings and implications from the chapters of this thesis.

Chapter 2: Coupled influence of precipitation and vegetation on millennial-scale erosion rates derived from ^{10}Be

[This chapter is published as **Mishra, A. K., Placzek, C., & Jones, R. (2019). Coupled influence of precipitation and vegetation on millennial-scale erosion rates derived from 10Be. *PLOS ONE, 14*(1), e0211325. doi:10.1371/journal.pone.0211325**]

2.1. Abstract

Water is one of the main agent of erosion in many environmental settings, but erosion rates derived from beryllium-10 (^{10}Be) suggests that a relationship between precipitation and erosion rate is statistically non-significant on a global scale. This might be because of the strong influence of other variables on erosion rate. In this global ^{10}Be compilation, we examine if mean annual precipitation has a statistically significant secondary control on erosion rate. Our secondary variable assessment suggests a significant secondary influence of precipitation on erosion rate. This is the first time that the influence of precipitation on ^{10}Be-derived erosion rate is recognized on global scale. In fact, in areas where slope is <200m/km (~11°), precipitation influences erosion rate as much as mean basin slope, which has been recognized as the most important variable in previous ^{10}Be compilations. In areas where elevation is <1000m and slope is <11°, the correlation between precipitation and erosion rate improves considerably. These results also suggest that erosion rate responds to change in mean annual precipitation nonlinearly and in three regimes: 1) it increases with an increase in precipitation until ~1000 mm/yr; 2) erosion rate stabilizes at ~1000 mm/yr and decreases slightly with increased precipitation until ~2200 mm/yr; and 3) it increases again with further increases in precipitation. This complex relationship between erosion rate and mean annual precipitation is best explained by the interrelationship between mean annual precipitation and vegetation. Increased vegetation, particularly the presence of trees, is widely recognized to lower erosion rate. Our results suggest that tree cover of 40% or more reduces erosion rate

enough to outweigh the direct erosive effects of increased rainfall. Thus, precipitation emerges as a stronger secondary control on erosion rate in hyper-arid areas, as well as in hyper-wet areas. In contrast, the regime between ~1000 and ~2200 mm/yr is dominated by opposing relationships where higher rainfall acts to increase erosion rate, but more water also increases vegetation/tree cover, which slows erosion. These results suggest that when interpreting the sedimentological record, high sediment fluxes are expected to occur when forests transition to grasslands/savannahs; however, aridification of grasslands or savannahs into deserts will result in lower sediment fluxes. This study also implies that anthropogenic deforestation, particularly in regions with high rainfall, can greatly increase erosion.

2.2. Introduction

The interrelated processes of erosion and weathering are critical components of Earth's biogeochemical cycles because they regulate the supply of sediments and nutrients to soils, streams, and ultimately the ocean (e.g. von Blanckenburg, 2005; Pimentel et al., 1995). Over geologic timescales, the chemical components of erosion and weathering are crucial in understanding climatic evolution (e.g. Rea et al., 1998; Raymo & Ruddiman, 1992; Ruddiman & Kutzbach, 1989; Ruddiman et al., 1989; Raymo et al., 1988; Berner et al., 1983). Erosion also leads to long-term transformation and development of landscapes (e.g. Acosta et al., 2015; Portenga et al., 2013; DiBiase et al., 2010; Dixon et al., 2009a; Quigley et al., 2007; Vanacker et al., 2007; Riebe et al., 2004; Bonnet & Crave, 2003; Tucker & Bras, 1998) and is closely associated with sediment yield, which controls the volume and characteristics of material preserved in the rock record. Sediment yield can also have important environmental management implications because the quantity of sediment moving out of a catchment is important for water quality (Reusser et al., 2015; Whiting, 2006; Merritt et al., 2003; Pimentel et al., 1995). Therefore, it is important to understand the factors that

impact erosion, in order to understand biogeochemical cycles (e.g. von Blanckenburg, 2005; Pimentel et al., 1995), interpret the sediment record (e.g. Walling & Webb, 1987; Langbein & Schumm, 1958), implement effective land-use strategies, (e.g. Lal, 2001; Pimentel et al., 1995; Lal, 1990) and quantify human influences (e.g. García-Ruiz et al., 2015; Reusser et al., 2015; Whiting, 2006; Pimentel & Kounang, 1998).

Early geomorphic studies suggest that rapid uplift (Schumm, 1963), higher relief (Summerfield & Hulton, 1994), and/or shifts in climate (Langbein & Schumm, 1958) can result in high sediment yield. However, quantifying erosion rate using sediment yield is difficult because it either requires constant monitoring of sediment fluxes or sediment deposits that have captured all sediment generated in a specific area (Meade, 1988). Over the last several decades, the use of terrestrial cosmogenic nuclides, particularly ^{10}Be, has provided unprecedented insight into quantification of erosion rate over millennial timescales (10^2 to 10^5 years), giving critical insight into factors influencing erosion rate (Willenbring et al., 2013; Portenga & Bierman, 2011; von Blanckenburg, 2005; Brown et al., 1998; Bierman & Steig, 1996; Granger et al., 1996; Brown et al., 1995; Lal, 1991; Brown et al., 1988).

Efforts to quantify erosion rate using ^{10}Be broadly fall into two categories: local to regional scale studies that generally aim to determine the effects of key variables in a specific region, and global compilations of data from various parts of the globe that seek to understand which variables are most important across different regions. These ^{10}Be-based studies suggest that a multitude of variables influence erosion rate, including: channel steepness (e.g. Harel et al., 2016), mean basin slope (e.g. Nichols et al., 2014; Placzek et al., 2014; Carretier et al., 2013; Willenbring et al., 2013; Portenga & Bierman, 2011), vegetation (e.g. Acosta et al., 2015; Carretier et al., 2013; Hewawasam et al., 2003), elevation (e.g. Portenga & Bierman, 2011), relief (e.g. Portenga & Bierman, 2011), temperature and mean annual precipitation (e.g. Moon et al., 2011; Heimsath et al., 2010; Dixon et al., 2009a; Dixon et al., 2009b; Grujic et

al., 2006; Bonnet & Crave, 2003; Montgomery et al., 2001), variability in precipitation (e.g. Carretier et al., 2013), and tectonic uplift (e.g. Henck et al., 2011; Cyr et al., 2010; von Blanckenburg, 2005; Riebe et al., 2001b, 2001a).

Many ^{10}Be studies, both local and global, have recognized mean basin slope to be significantly correlated with erosion rate (e.g. Nichols et al., 2014; Placzek et al., 2014; Carretier et al., 2013; Willenbring et al., 2013; Portenga & Bierman, 2011; von Blanckenburg, 2005). This relationship between slope and erosion rate is unsurprising as steeper slopes have more gravitational energy, which facilitates the movement of sediments. Some studies suggest that erosion rate increases with steepness in slope only up to a threshold value (Montgomery & Brandon, 2002; Roering et al., 1999), whereas others suggest in areas with high uplift rate, relief correlates best with erosion rate (Henck et al., 2011; Burbank et al., 2003). However, overall slope is observed as the dominant variable influencing erosion rate in previous global ^{10}Be compilations (Willenbring et al., 2013; Portenga & Bierman, 2011).

2.3. Precipitation's influence on erosion rate

Intuitively, precipitation should have a strong influence on erosion rate, as water facilitates the weathering process that precedes erosion in most environmental settings and is also one of the main agents for transport of sediments (Lal, 2001; Pimentel & Kounang, 1998; Langbein & Schumm, 1958). Indeed, many studies assert that rainfall is the primary cause of erosion in many environmental settings (Yanites & Kesler, 2015; Pimentel, 2006; Lal, 2001; Pimentel & Kounang, 1998; Pimentel et al., 1995). In contrast, many ^{10}Be-based studies on the correlation between various environmental variables and erosion rate suggest a small to nonexistent relationship between precipitation and erosion rate (Nichols et al., 2014; Scherler et al., 2014; Bermúdez et al., 2013; Willenbring et al., 2013; Portenga & Bierman, 2011;

Binnie et al., 2007; Wittmann et al., 2007; von Blanckenburg, 2005; Riebe et al., 2001b, 2001a).

Local to regional-scale ^{10}Be studies suggest that higher precipitation results in faster erosion in some regions, but not in others. For example, Matmon et al. (2009) suggest that the oldest surfaces on Earth are found in hyper-arid areas, such as the Negev and Atacama Deserts; and Heimsath et al. (2010) also observed an increase in erosion rate with an increase in precipitation across all of Australia. In contrast, this relationship between increased aridity and slow erosion is not observed in the semi-arid Namib Desert (Bierman & Caffee, 2001) or across semi-arid Australia (Bierman & Caffee, 2002). In the case of the Namibian margin, it is suggested that the entire region had attained steady state and has been eroding at similar rates over the past 36 Million years, making climatic influences less significant (Bierman & Caffee, 2001). In similarly contrasting findings, Dixon et al. (2009b) found that the combined influence of temperature and precipitation do influence erosion rate in the western Sierra Nevada Mountains, California, USA; however, Riebe et al. (2001a) notes only a weak climatic control on the erosion rates across the Sierra Nevada. In another example, Reiners et al. (2003) notes strong coupling between precipitation and long-term erosion rate in a mountainous setting (Washington Cascades); but, Burbank et al. (2003) finds no influence of precipitation on erosion rate in the Himalayas.

This contrast between the role of climatic (e.g. precipitation and temperature) verses tectonically linked variables (e.g. slope, channel steepness, and uplift rate) observed in various ^{10}Be studies could be partly related to the landscape obtaining steady state (DiBiase & Whipple, 2011; DiBiase et al., 2010). For instance, a landscape that has reached a steady state with respect to external factors will have its erosion rate controlled by the uplift rate that provides material for erosion (DiBiase & Whipple, 2011; von Blanckenburg, 2005). Conversely, if the landscape has not yet reached steady state and is in transition phase, then

factors such as precipitation, vegetation, and temperature will control erosion rate (DiBiase & Whipple, 2011).

The complex interrelationship between these different factors is also evident in sediment yield studies. Some sediment yield studies suggest precipitation is extremely important to erosion and that there is a strong correlation between erosion and precipitation and/or vegetation (e.g. Schaller et al., 2018; Jansson, 1988; Walling & Webb, 1987; Walling & Webb, 1983; Knox, 1972; Douglas, 1967; Fournier, 1960; Langbein & Schumm, 1958). For instance, Langbein and Schumm (1958) found that sediment yield increases with an increase in precipitation, reaching a maximum at approximately 254-355 mm/yr; beyond this sediment yield decreases when precipitation increases further. This decrease in sediment yield beyond 355 mm/yr of precipitation is attributed to an increase in vegetation density (Langbein & Schumm, 1958). Knox (1972) observed that sediment yield reaches a maximum when climate transitions from an arid environment into a semi-arid or humid environment. However, some studies emphasize the role of relief in controlling variability in sediment yield on a global scale (Walling & Webb, 1996; Summerfield & Hulton, 1994; Milliman & Meade, 1983). For instance, Summerfield and Hulton (1994) analysed sediment yield data from 33 major rivers and found that basin relief provides the best statistical explanation for variation in sediment yield. Similarly, Dedkov and Mozzherin (1984) found that sediment yields from "mountain" rivers were three times higher than "plains" rivers, but within the two groups, sediment yield varied with climate.

Despite the seemingly obvious link between erosion and precipitation, ^{10}Be-based global compilations (e.g. Harel et al., 2016; Willenbring et al., 2013; Portenga & Bierman, 2011) do not show any statistically significant numerical relationship between long-term erosion and precipitation. Instead, Portenga and Bierman (2011), in their global compilation concluded that mean annual precipitation might be important on the local scale, but is non-significant at

global scale. Similarly, the percentage of vegetation cover is non-significant at influencing ^{10}Be-derived erosion rates (Portenga & Bierman, 2011).

One reason for the lack of a statistically meaningful correlation between precipitation and erosion rate in global compilations could be that other variables, such as slope, lithology, relief, or rock uplift rate, have greater significance (e.g. Willenbring et al., 2013; Henck et al., 2011; Portenga & Bierman, 2011) and obscure the correlation with precipitation. For example, Henck et al. (2011) found that tectonic setting and the rate of rock uplift determines if precipitation or relief will have the strongest influence on erosion rate. Another possibility is that intrinsic characteristics of the precipitation regime, such as precipitation variability (Carretier et al., 2013; DiBiase & Whipple, 2011; Tucker & Bras, 2000), magnitude of maximum precipitation events (Dadson et al., 2003) and the relationship between precipitation and vegetation (Schaller et al., 2018; Acosta et al., 2015; Jiongxin, 2005) might be more important than mean annual precipitation itself. In particular, the evidence from sediment yield studies clearly suggest that vegetation may obscure any potential impact that precipitation has on erosion rate because high rainfall increases erosive power but results in dense vegetation that holds back sediments (Acosta et al., 2015; Jiongxin, 2005; Pimentel & Kounang, 1998; Walling & Webb, 1987; Walling & Webb, 1983; Knox, 1972; Douglas, 1967; Fournier, 1960; Langbein & Schumm, 1958).

2.4. Aim of this compilation

There exists a contrast between the intuitive link between precipitation and erosion and comparisons of ^{10}Be results and precipitation. In this compilation, we examine precipitation and ^{10}Be-derived erosion rate in a global context that acknowledges the important influence of other variables, particularly slope, which emerges as the dominant variable in previous

^{10}Be compilations, and vegetation, which may complicate the correlation between precipitation and erosion by interacting with both erosion and precipitation.

2.5. Methods

2.5.1. Erosion rates compilation and standardization:

Terrestrial or in-situ ^{10}Be is a radioactive isotope of beryllium with a half-life of 1.39 My (1.39 x 10^6 years) (Chmeleff et al., 2010; Korschinek et al., 2010) and is formed by cosmic-ray spallation of an oxygen atom (Balco & Shuster, 2009). The concentration of ^{10}Be in quartz-bearing rocks is inversely proportional to the erosion rate of these rocks (Bierman & Steig, 1996; Granger et al., 1996; Brown et al., 1995; Lal, 1991; Nishiizumi et al., 1986) because more ^{10}Be is produced during longer exposure to secondary cosmic rays as a result of slower erosion. Similarly, where erosion is fast, exposure to secondary cosmic rays is shorter, resulting in a lower concentration of ^{10}Be nuclides (Bierman & Steig, 1996; Granger et al., 1996; Brown et al., 1995; Lal, 1991; Nishiizumi et al., 1986). Erosion rates derived from ^{10}Be are generally averaged over the past several thousand years and are calculated based on the assumption that the rock is eroding at a constant rate, and that the concentration of ^{10}Be is at steady state (Bierman & Steig, 1996; Granger et al., 1996; Brown et al., 1995; Lal, 1991; Nishiizumi et al., 1986). When sediment is collected for ^{10}Be-derived erosion rates, the result is generally considered to be the basin-averaged erosion rate. The primary assumptions for calculating basin-averaged erosion rates are: (1) all lithologies in the catchment are eroding at the same rate; (2) all rock types contributing to erosion have similar grain sizes; (3) there is minimal time spent in sediment storage; and (4) the timescale of erosion is smaller than the timescale of radioactive decay of ^{10}Be (Bierman & Steig, 1996; Granger et al., 1996; Brown et al., 1995; Lal, 1991; Nishiizumi et al., 1986).

The timescale of ^{10}Be-derived erosion rates is calculated by dividing the erosion rate by the absorption depth of secondary cosmic rays (von Blanckenburg, 2005). An erosion rate of 1000 m/My is averaged over a timescale of 600 years; in contrast, an erosion rate of 10 m/My is averaged over 60 ky. For this reason, ^{10}Be-derived erosion rates are often considered millennial-scale erosion rates (Bierman & Steig, 1996; Granger et al., 1996; Brown et al., 1995; Lal, 1991; Nishiizumi et al., 1986). Some studies quantifies erosion rate over short-term, which is usually calculated from contemporary sediment yields (Summerfield & Hulton, 1994), and is averaged over few years or decades. Short-term erosion rates represent a combination of both natural and anthropogenic-induced erosion (Hewawasam et al., 2003; Summerfield & Hulton, 1994) and are potentially subject to a degree of uncertainty, primarily because of the episodic nature of sediment delivery (Trimble & Crosson, 2000; Summerfield & Hulton, 1994). For example, Kirchner et al. (2001) found in central Idaho that long-term erosion rates were on average seven times higher than the short-term erosion rate and suggested that this is because the sediment delivery is episodic in the mountainous terrain (Kirchner et al., 2001). Similarly, in central Europe, Schaller et al. (2001) found that long-term erosion rates are 1.5-10 times higher than short-term erosion rates because short-term erosion rate underestimate the amount of sediment generated. Long-term erosion rate on contrary integrates erosion rate over millennial timescale, therefore includes the entire range of episodic discharges, and loads (e.g. Schaller et al., 2001).

We recognize that the timescale over which ^{10}Be-derived erosion rates are determined is dependent on the rate of erosion itself, and is generally longer than the timescale over which variables, such as precipitation and vegetation cover are determined. However, although not constant, paleo-precipitation and paleo-temperature over the past several thousand years exhibit broadly similar gradients (Mutz et al., 2018). Furthermore, global climate zones over the timescale of ^{10}Be-derived erosion rates are not dramatically different from today (Mutz et

al., 2018). Thus, we compared ^{10}Be-derived erosion rates with modern precipitation and vegetation cover following a similar approach to previous global compilations, such as Portenga and Bierman (2011) and Harel et al. (2016). Comparing modern vegetation cover with long-term erosion rate is imperfect, but it does broadly allow exploration of the influence of vegetation cover, if any, on long-term erosion rate on global scale.

Here, we have compiled data (n=1790) from 93 published studies that use the concentration of ^{10}Be in sediment samples to determine millennial-scale erosion rates (**Error! Reference source not found.**). The scope of our compilation is similar to that of Portenga and Bierman (2011), Willenbring et al. (2013), and Harel et al. (2016). The data was collected from various studies and compilations published prior to 2016, so erosion rates were recalculated based on the new update of CRONUS (Version 2.3) (Balco et al., 2008)(hess.ess.washington.edu). We used Lal (1991) and Stone (2000) scaling scheme for our entire dataset. Erosion rates from Antarctica are excluded in this compilation.

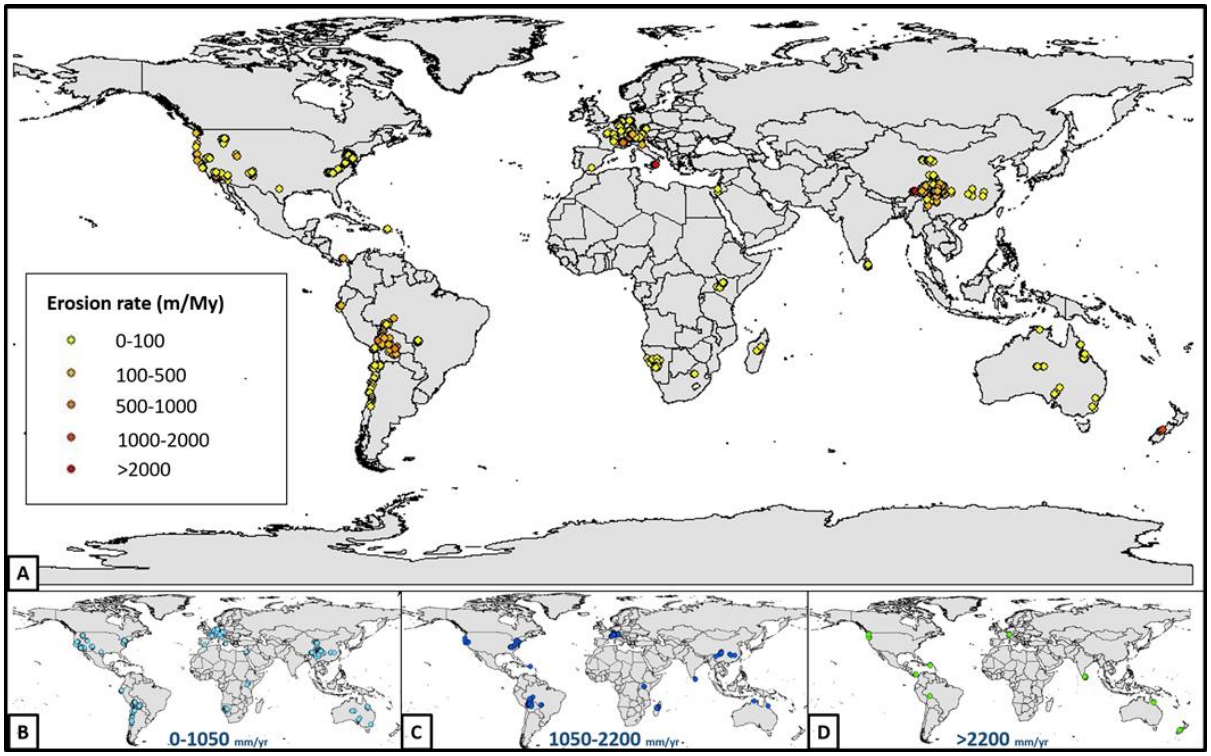

Figure 1: (A.) Geographic distribution of basin averaged 10Be-derived erosions rate samples (refer to appendix 1 for data and the list of source publications). (B.) Samples with mean annual precipitation between 0-1050 mm/yr. (C.) Samples with mean annual precipitation between 1050-2200 mm/yr. (D.) Samples with mean annual precipitation >2200 mm/yr**.**

2.5.2. Mean basin slope, mean annual precipitation, and tree cover:

'Mean basin slope' for this compilation was retrieved using DEM with ArcGIS, using ~3 arc-seconds (90m) SRTM data (http://srtm.csi.cgiar.org), ensuring that all mean basin slope values in our compilation were calculated using similar DEM and SRTM resolution. Mean annual precipitation values for the entire dataset were retrieved using available data set from Hijmans et al. (2005). Tree cover data was retrieved from an existing dataset using 1-km resolution by Defries et al. (2000). Following similar approaches of Portenga and Bierman (2011) and Harel et al. (2016), 0-10% values in the data set were replaced with 5% and non-vegetated areas were replaced with 0%. To standardize our data, all parameters were retrieved using similar method, and erosion rates were re-calculated based on the latest updated version of CRONUS.

2.5.3. Statistics:

All statistical analyses used R (R Core Team, 2016). Univariate and multiple regressions and R^2 estimates used the base statistics package. Mixed-effects models used the nlme and lme4 packages, with pseudo-R^2 values provided by the MuMIn package. We performed all statistical analyses assessing significance at the 95% confidence level; therefore, p-values > 0.05 are not statistically significant (Neyman, 1937).

To check for secondary influences of mean annual precipitation and tree cover on erosion rate, we used multiple regression models and mixed effect models. The main objective is to examine if the model between response variable (in this case erosion rate) and the predicting variable improves by adding another variable to the model. Thus, if adding a particular parameter improves the explanation of the variances (R^2 value), then that parameter is of secondary statistical significance.

We undertook three sets of analyses. The first used unadjusted univariate linear and polynomial regressions to evaluate the overall relationship of each of three individual explanatory variables (mean basin slope, precipitation and tree-cover percentage) with the log-transformed erosion rate. The second set of analyses included all three of these explanatory variables in the same model. These two sets of analyses treat every available data point as independent and do not consider correlation between erosion rates observed within different studies. The mixed-effects analyses described below, which allowed for intra-study correlation, indicated that greater complexity was not justified, so we restricted the polynomial fits to linear, quadratic or cubic regressions. Inflection points for the tree-cover and precipitation curves were also identified.

Within individual studies, estimates of erosion rate tended to be very similar, indicating that individual measurements within a study could not be regarded as completely independent,

presumably because they shared a range of other attributes (e.g. rock type, tectonic setting) with local influences. The third set of analyses, therefore, used an additive, mixed-effects random intercept model with citation (the study providing the data) as a random effect, and with the fixed effects listed below:

- Mean basin slope
- Tree cover percentage (as a quadratic polynomial)
- Precipitation (as a cubic polynomial)

Aikake Information Criterion (AIC) and Analysis of variance (ANOVA) comparisons identified the level of polynomial used for each explanatory variable. All analyses are attached as appendix 1.

2.6. Results

Erosion rates determined using CRONUS 2.3 range from 0.07 m/My to 4119.53 m/My. The slowest erosion rates are observed in the driest regions of the Atacama Desert, Chile (Slope= 2.4°; Precipitation= 3 mm/yr) (Placzek et al., 2014; Placzek et al., 2010), whereas the fastest is observed in Namche Barwa-Gyala Peri Massif, Tibet (Slope= 21.6°; Precipitation= 559 mm/yr)(Finnegan et al., 2008).

2.6.1. Primary influence:

Results of the correlation of variables with ^{10}Be-derived erosion rate is expressed according to their R^2 values in Table 1. On a global scale, a significant positive, but moderate correlation is observed between rate of erosion and mean basin slope, with an R^2 value of 0.28 and p-value <2.2e-16 (Figure 2). There is no evidence of curvature in this relationship. For all areas where slope is <11°, correlation of mean basin slope with erosion rate weakens to R^2=0.08, p-value = 2.4e-13.

Table 1: Variables with their R^2 value using erosion rate as response variable.

Predictors/Variables	R^2 Value of this compilation	P-value	R^2 value from Portenga and Bierman (2011)	R^2 values from Willenbring et al., 2013)	R^2 values from Harel et al., (2016) (used channel steepness index)
Slope	0.284	<2.2e-16	0.346	0.48	_
Precipitation	0.017	0.0000001	0.008	_	-0.003
Precipitation (polynomial)	0.049	<2.2e-16	_	_	_
Vegetation	0.006	0.0006457	0.028	_	-0.034
Vegetation (polynomial)	0.124	<2.2e-16	_	_	_

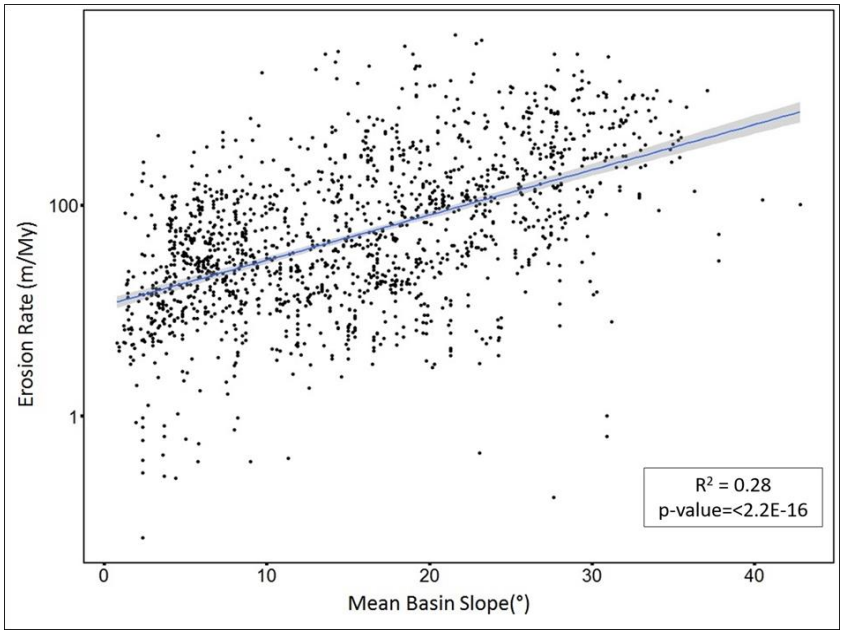

Figure 2: Mean basin slope (x-axis) versus log erosion rate (y-axis). The blue line indicates the linear relationship best-fit line between erosion rate and mean basin slope. The grey area around the blue line represents confidence interval.

Mean annual precipitation shows a very weakly significant primary linear correlation with erosion rate (R^2 = 0.017 and p-value = 0.000001; Figure 3). However, the data and its distribution indicates a non-linear relationship. The polynomial correlation between erosion rate and mean annual precipitation has R^2 value of 0.05, and p-value <2.2e-16 (Figure 4). The

relationship is best described by a 3rd order polynomial model according to the AIC values (See appendix 1). The AIC values for each model was very close, which might be due to the variability within a study and the variability between studies with similar values of the explanatory variables. Therefore, we analyzed the AIC values for models using single data points per study (i.e. by calculating average values for each study for both the explanatory variables and log erosion rates). The analysis of AIC values for order 3 and above in the mixed effects model are very close, and the higher-order polynomials do not retain their advantage when each study is allowed to contribute only a single data point. Therefore, we decided to take the most conservative option and use the 3rd-order polynomial. Inflection points denoting the maxima and minima of the best fit curve are points where the fitted relationship between erosion rate and precipitation changes its trend. In this case, erosion rate continues to increase with precipitation until the precipitation value reaches ~1050 mm/yr (first inflection point). From there, the relationship between erosion rate and precipitation is inverse until the precipitation value of ~2200 mm/yr (second inflection point), after which erosion rate again increases with further increase in precipitation.

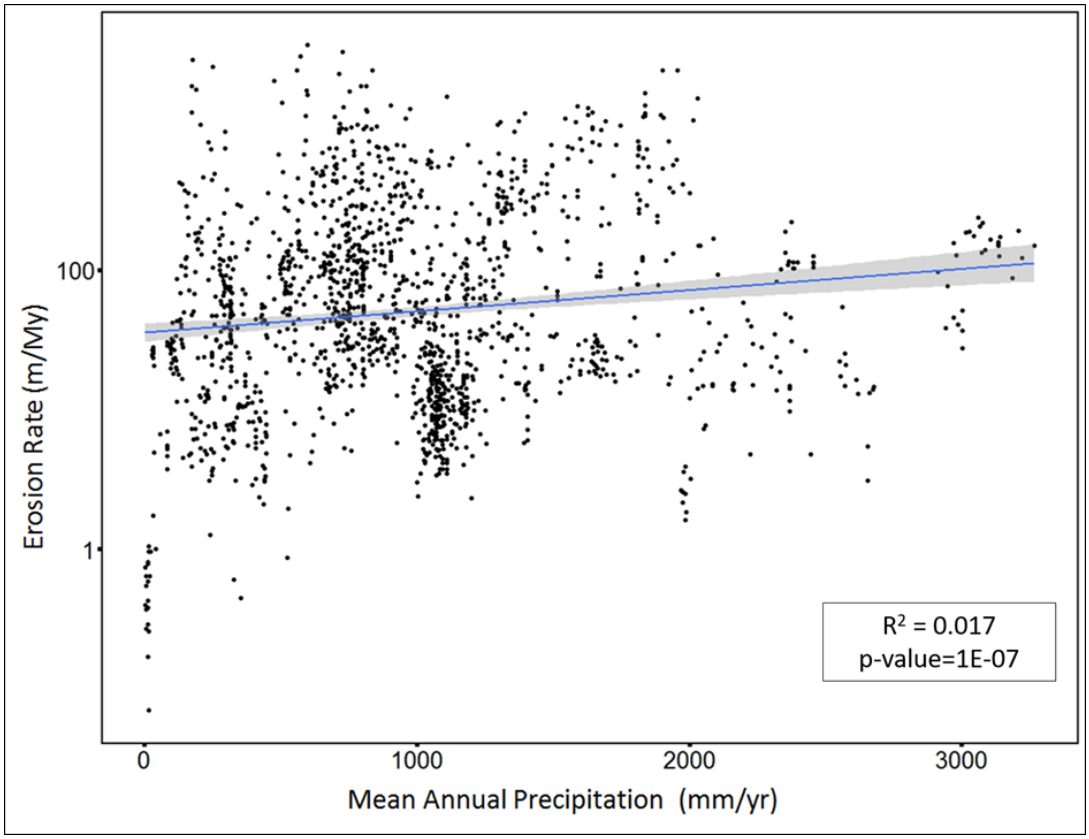

Figure 3: Linear regression: mean annual precipitation (x-axis) versus log erosion rate (y-axis). Blue line indicates linear relationship best fit line between erosion rate and mean annual precipitation. The grey area around the blue line represents confidence interval.

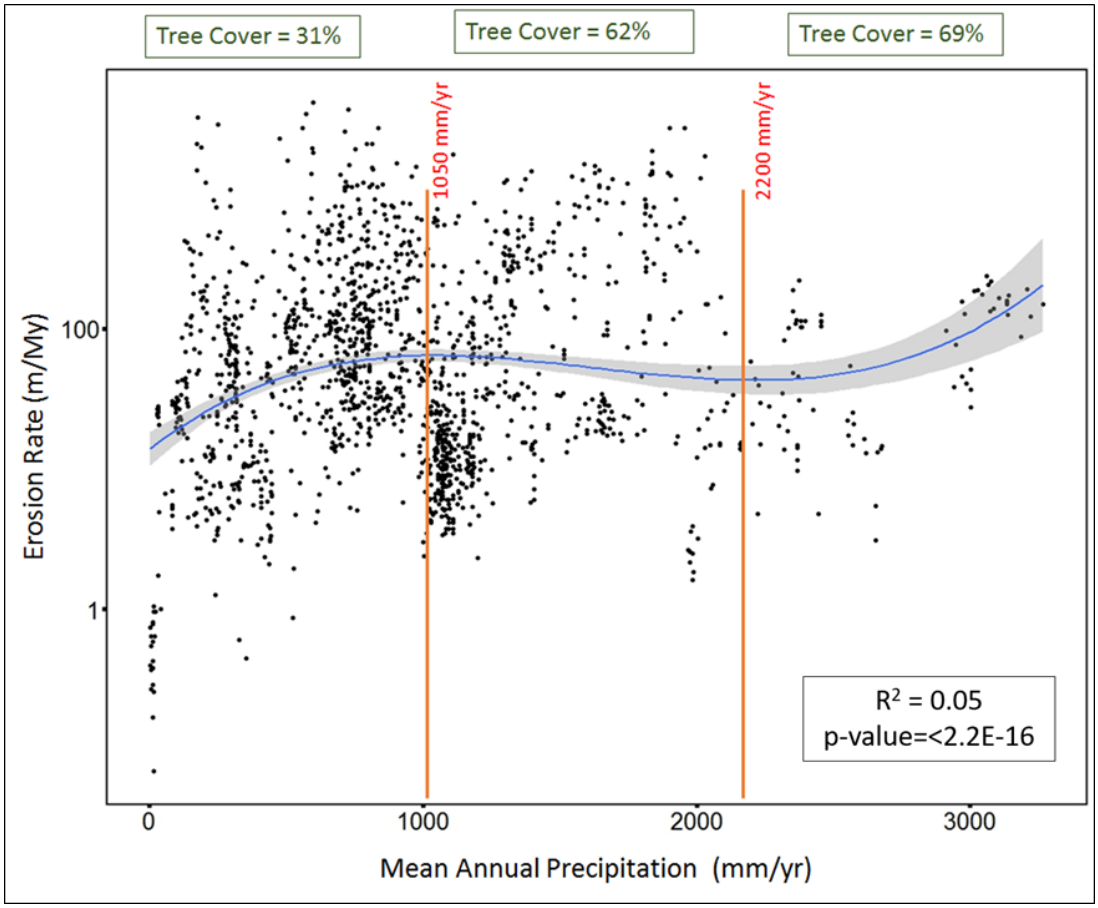

Figure 4: Non-linear regression: mean annual precipitation (x-axis) versus log erosion rate (y-axis). Blue line indicates the non-linear relationship curve between erosion rate and mean annual precipitation. The grey area around the blue line represents confidence interval. Orange vertical line represents inflection points, where the relationship curve trend changes. Green box on top represents average tree cover percentage in each regime.

The percentage of tree cover also shows a weak linear correlation with erosion rate, with R^2 value of 0.006 and p-value = 0.0006457. Allowing for curvature via a quadratic fit increases the R^2 value to 0.12, p-value <2.2e-16 (Figure 5). The inflection point of the relationship implies that the maxima is at 40% tree cover. The percentage of tree cover is linearly correlated with precipitation, with R^2 value of 0.30 and p-value < 2.2e-16 (Figure 6).

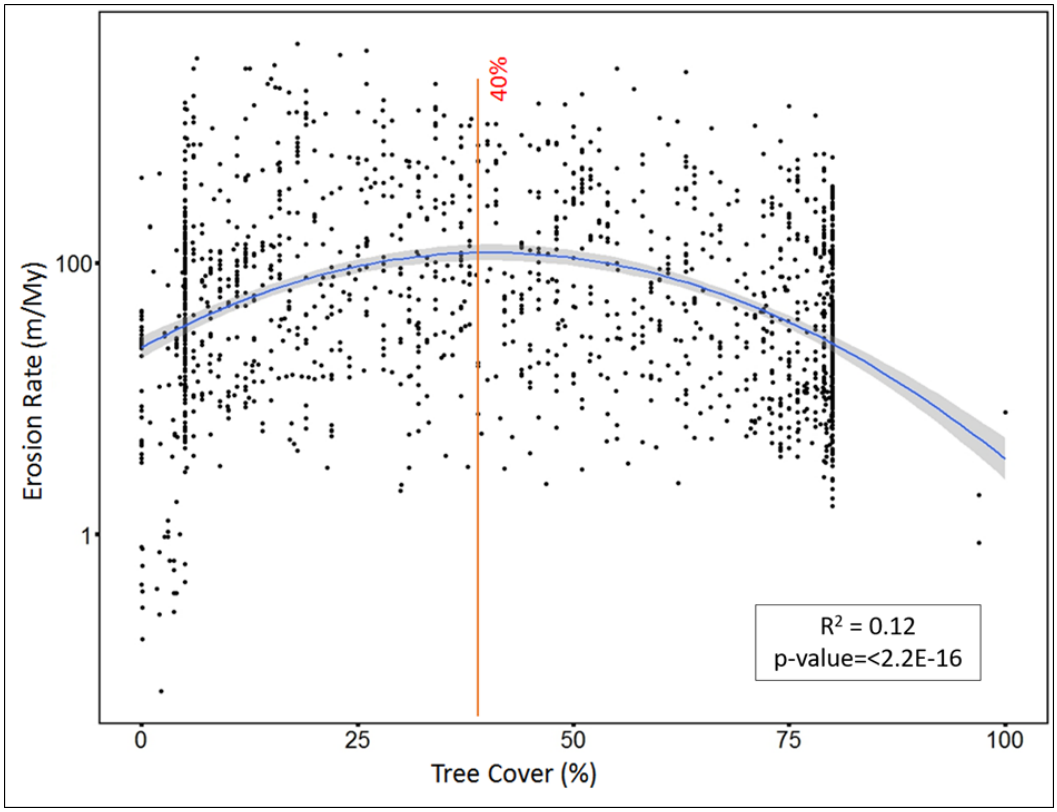

Figure 5: Non-linear regression: percentage of tree cover (x-axis) versus log erosion rate (y-axis). Blue curve line indicates non-linear relationship curve between erosion rate and tree cover percentage. Orange vertical line indicates the maxima or threshold value of tree cover percentage.

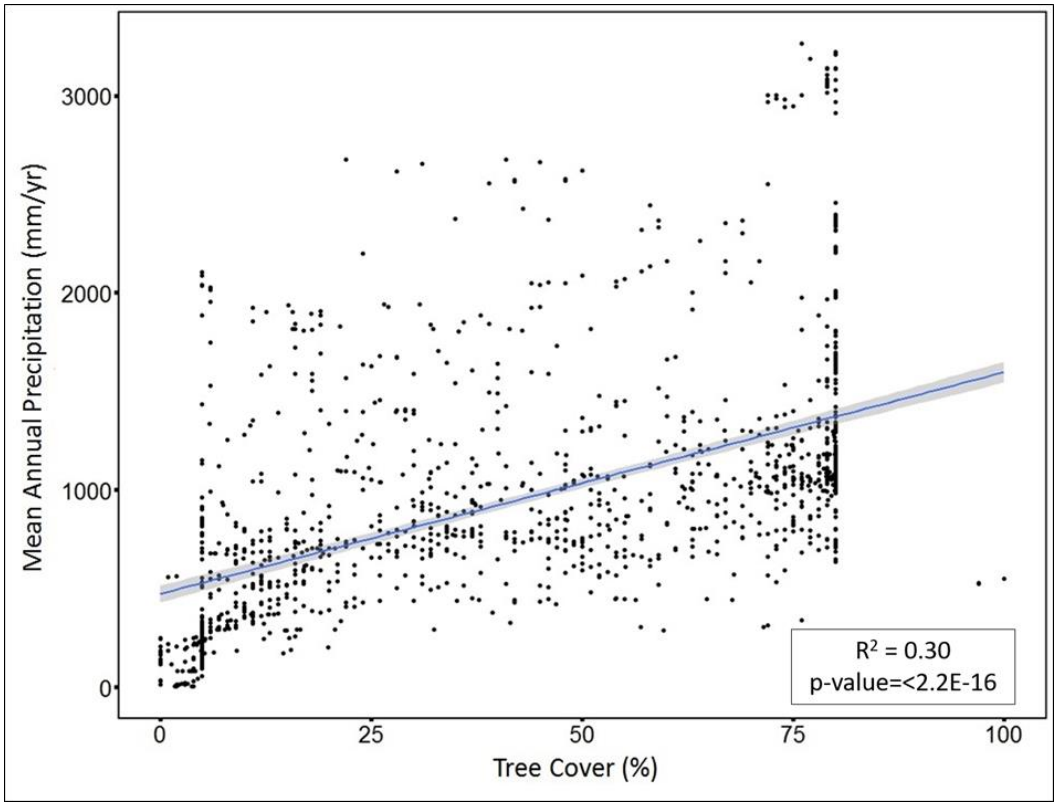

Figure 6: Linear regression: percentage of tree cover (x-axis) versus mean annual precipitation (y-axis).

The R^2 values here indicates the variation in response variable (in this case erosion rate) explained by the model. The R^2 values reported are extremely low because data was compiled from different environmental settings that are widely scattered. However, with such a large dataset that consists of wide range of variables, having low R^2 value to express correlation is not unusual.

2.6.2. Secondary influence of precipitation and percentage of tree cover:

The relationship between precipitation and percentage of tree cover has a slightly better correlation with erosion rate when curvature is allowed (R^2 value increasing from 0.01 to 0.05 for precipitation, and from 0.006 to 0.13 for vegetation). However, when the percentage of tree cover and precipitation both were added to the model, the combined correlation between them and erosion rate increased the R^2 value to 0.18 (p-value <2.2e-16), suggesting

that precipitation and tree cover together better explains the variation in erosion rate data (See appendix 1). However, in the combined model, precipitation and vegetation have opposite effects on rate of erosion (see estimated regression coefficients in S2 file), suggesting both mechanistically and statistically, precipitation and tree cover act in different directions in terms of their influence on erosion.

Of the compared variables, mean basin slope has the most dominant correlation with erosion rate (R^2 value of 0.28 and p-value <2.2e-16). Adding precipitation and tree cover to the model between erosion rate and mean basin slope increases the R^2 value to 0.40 and the p-value is <2.2e-16. This indicates that the explanation of the variances in the erosion rate data is improved when mean basin slope, precipitation and tree cover are all considered.

We included study identifier (i.e. citation) as a random effect in the mixed effect model. This improved the explanatory power of the model substantially (R^2 = 0.81 and p-value 0.0015). In order to check how much of this explanatory power is improved by mean annual precipitation alone, we considered another mixed effect model, without precipitation, and compared the R^2 values. Our comparisons suggests that precipitation improves the explanation of variance in the model by ~40% (fixed effect R^2 value improves from 0.138 to 0.194) (Table 2).

Table 2: Statistical models and their R^2 value and p value

Model	R^2 value	p-value
Erosion rate ~ Precipitation(poly)	0.05	<2.2E-16
Erosion rate ~ Tree Cover (poly)	0.12	<2.2E-16
Erosion rate ~ Precipitation(poly) + Tree cover(poly)	0.18	<2.2E-16
Erosion rate ~ Slope	0.28	<2.2E-16
Erosion rate ~ Slope + Precipitation(poly) + Tree Cover(poly)	0.4	<2.2E-16
Erosion rate ~ Slope + Precipitation(poly) + Tree Cover(poly) (Random effect = Citation)	0.81	0.0015

Erosion rate ~ Slope (for all areas with <11° slope)	0.08	2.48E-15
Erosion rate ~ Precipitation(poly) (for all areas with <11° slope)	0.08	2.98E-13

We also examined the correlation of both slope and precipitation with erosion rate for areas with slope <11° and found that mean annual precipitation has a similar correlation (R^2 =0.08, p-value =2.98e-13) as mean basin slope (R^2=0.08, p-value = 2.48e-15) (Figure 7). Correspondingly, we also found that the correlation between mean annual precipitation and erosion rate is better (R^2=0.1717, p-value = <2.2e-16) in areas where elevation is <1000m and slope is <11° (Table 3). In addition to that, the response of erosion rate to change in mean annual precipitation was also examined for different lithologies (Figure 8). The correlation between mean annual precipitation and erosion rate was found to be highest for 'mixed' lithologies (R^2=0.1063, p-value= 2.89e-15). However, in areas with elevation <1000m, the correlation between mean annual precipitation and erosion rate was highest when the lithology was 'igneous' (R^2=0.6681, p-value= <2.2e-16; Table 3).

Table 3: R^2 value and p-value of erosion rate vs. mean annual precipitation when other variables are constant

Condition	**All Data**		**Elevation>1000m**		**Elevation<1000m**	
Erosion vs. Precipitation in areas where:	**R^2 value**	**p-value**	**R^2 value**	**p-value**	**R^2 value**	**p-value**
Igneous lithology	0.0019	0.299	-0.00952	0.9084	0.6681	<2.2E-16
Metamorphic lithology	-0.0000903	0.3985	0.036	0.003906	0.077	0.0034
Mixed lithology	0.1063	2.89E-15	0.315	<2.2E-16	0.009	0.1408
Sedimentary lithology	0.0052	0.1873	0.1515	0.00021	0.005	0.2363
Slope <11°	0.05	<2.2E-16	0.0143	0.06079	0.1717	<2.2E-16
Slope>11°	-0.0017	0.7784	0.0089	0.0255	0.024	0.007541

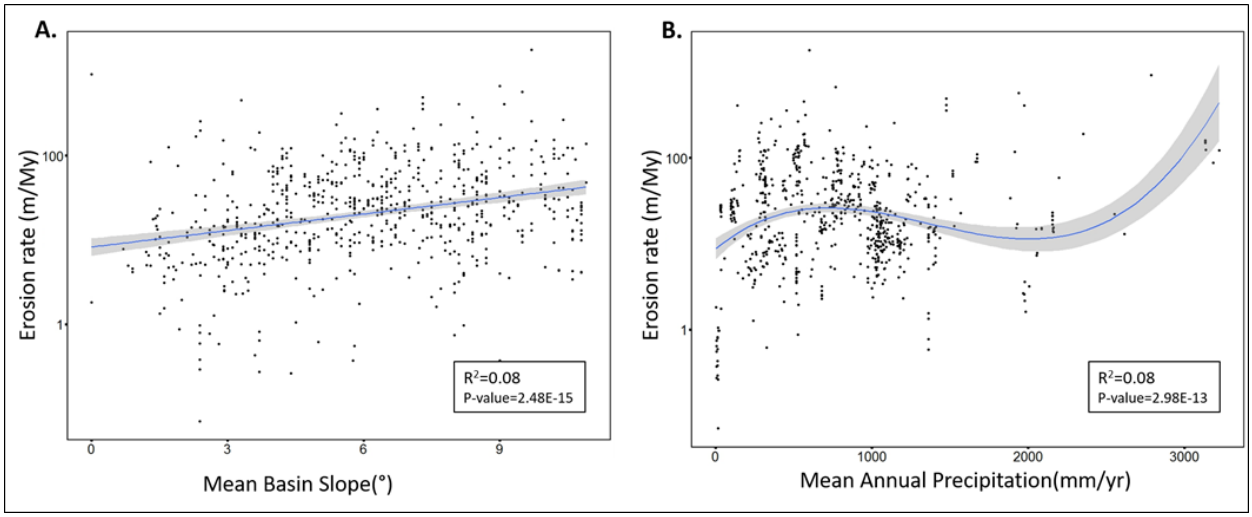

Figure 7: Plots of mean basin slope and precipitation with erosion rate in areas with <11° slope. A. Mean basin slope (x-axis) versus log erosion rate (y-axis). B. mean annual precipitation (x-axis) versus log erosion rate (y-axis).

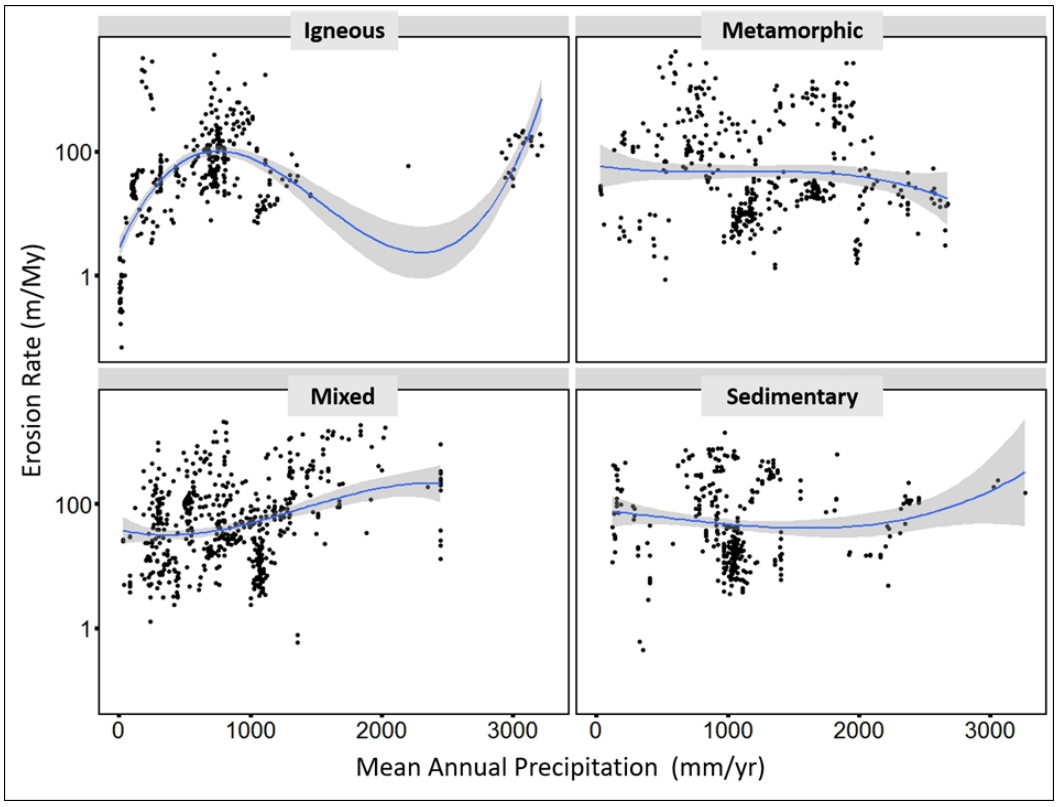

Figure 8: Plots of mean annual Precipitation (x-axis) vs Erosion rate (y-axis) in for each lithology. Clockwise from top-left is Igneous, Metamorphic, Sedimentary and Mixed.

2.7. Discussion

Our results suggest a relationship between mean basin slope and erosion rate that is similar to that observed in previous studies and compilations (Nichols et al., 2014; Placzek et al., 2014; Carretier et al., 2013; Willenbring et al., 2013; Portenga & Bierman, 2011). Observationally, sites (e.g. Atacama, Namibian Desert and Escarpment, Sechura Desert) in hyper-arid areas have average basin slopes (11°, 6.1°, and 0.8°, respectively) that are lower than the average slopes for the entire dataset (15.1°) (refer to appendix 1) and sites with higher mean annual precipitation tend to have higher mean basin slope (e.g. Southern Alps in New Zealand - 31°, Tibetan Plateau - 16.08°, and Sri Lankan escarpment - 28.6°) (refer to appendix 1). However, mean basin slope and mean annual precipitation do not show any direct significant statistical correlation (R^2=0.08, p-value = 2.48e-13) (Figure 9).

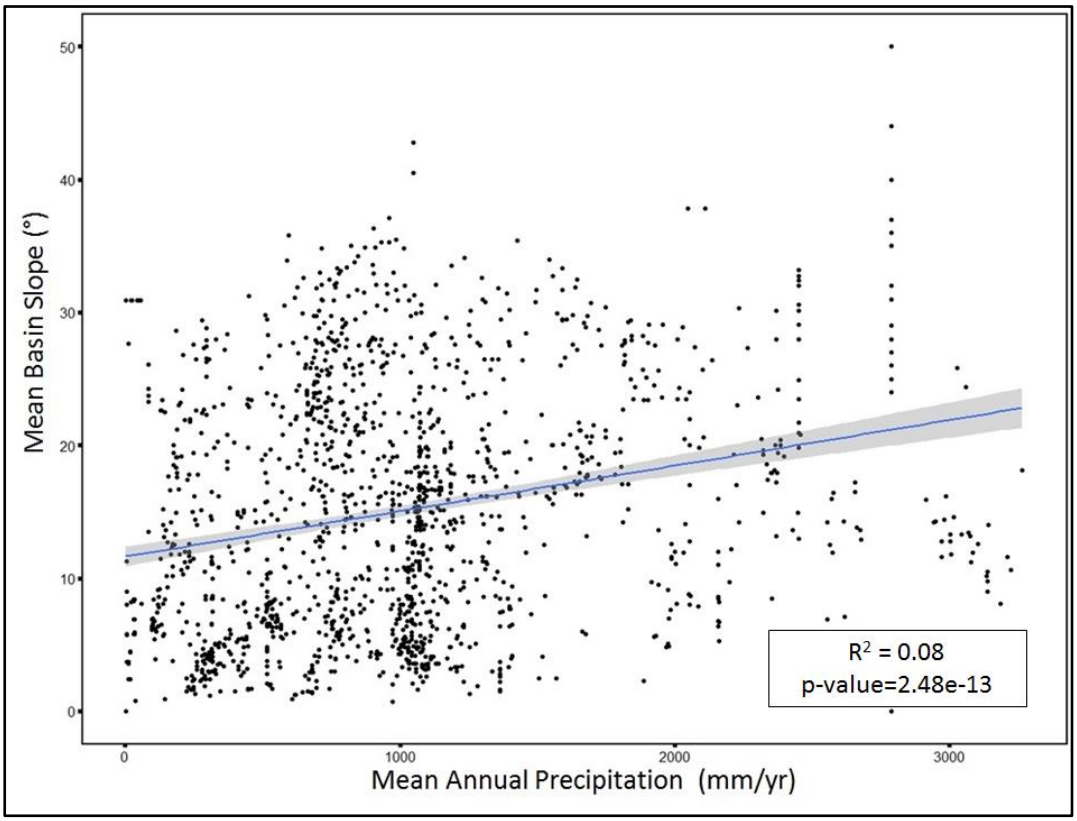

Figure 9: Mean annual precipitation (x-axis) versus mean basin slope (y-axis). The blue line indicates the linear relationship best-fit line between mean annual precipitation and mean basin slope. The grey area around the blue line represents confidence interval.

2.7.1. Precipitation's influence:

Across the entire data set, mean annual precipitation has a very weak correlation with erosion rate when compared linearly and directly (Figure 3). However, the relationship between erosion rate and precipitation is somewhat better (R^2 value 0.05) when polynomial fit is allowed (Figure 4). The correlation remains weak, indicating that noise created by other variables significantly influences erosion rate. However, including precipitation in a statistical model of erosion rate with mean basin slope gives a significantly improved model. Absence of precipitation from the model decreases the explanatory power of fixed effects by ~40%, which again indicates that the optimum model for factors influencing erosion rate must include precipitation. The large variation attributable to individual studies suggests that other locally specific environmental attributes, such as lithology, uplift rate, or relief, also have a major influence on erosion rate. This response of erosion rate to precipitation is valid only for silicate terrains, and carbonate terrains might have different response, as rate and characteristics of weathering of carbonate terrains is different and are beyond the scope of this study (Ryb et al., 2014; Gabrovšek, 2009).

In areas with slope less than 11°, which includes more than 92% of Earth's surface (Willenbring et al., 2013), mean annual precipitation correlates with erosion rate (R^2 value 0.08) as much as mean basin slope (R^2 value 0.08). This correlation between mean annual precipitation and erosion rate further improves in areas where slope <11° and elevation is <1000m (R^2 value 0.1717) (Table 3). This implies that when topographic influence is low (i.e. when elevation and slope are low), the correlation between mean annual precipitation and erosion rate improves. Lithology also plays an important role in this correlation. Mixed lithology favors a stronger influence of mean annual precipitation on erosion rate in areas where elevation is >1000m (R^2 value 0.315). However, in areas where elevation is <1000m, igneous lithology strengthens precipitation's influence on erosion rate (R^2 value 0.6681).

The non-linear relationship between erosion rate and mean annual precipitation suggests that erosion rate responds to change in mean annual precipitation in three different regimes. First, it tends to increase with an increase in mean annual precipitation until ~1000 mm/yr, after which it starts decreasing with an increase in mean annual precipitation until ~2200 mm/yr. At greater than ~2200 mm/yr erosion rate again starts increasing with further increase in mean annual precipitation (Figure 4). This complex trend also potentially lowers the overall statistical correlation of precipitation with erosion rate.

The percentage of tree cover correlates with erosion rate non-linearly, and the threshold (maxima) value of this correlation is 40%. In other words, once tree cover reaches more than 40%, it starts to counteract precipitation's influence on erosion rate, thereby slowing down erosion rate. This is consistent with several simulation studies (e.g. Durán Zuazo & Rodríguez Pleguezuelo, 2008; Bochet et al., 2006; Rogers & Schumm, 1991) that found that vegetation fails to slow down erosion rate significantly until vegetation cover reaches a threshold value. This complex interaction between tree cover and erosion rate, and a threshold value for tree cover acting against precipitation's influence on erosion rate, explains the three regimes of mean annual precipitation's influences on erosion rate:

- **First regimes:** In the first regime, erosion rate increases with increased mean annual precipitation (from 0-1050 mm/yr). Over this regime, the mean value of tree cover is 31%. Although tree cover increases with increasing precipitation, the influence of tree cover is not enough to counteract the erosive ability of higher rainfall, and therefore erosion rate increases with increased mean annual precipitation. This observation is consistent with observations made in previous studies that indicated slow erosion in arid and hyper arid environments (Placzek et al., 2014; Placzek et al., 2010; Matmon et al., 2009). However, it is also noteworthy that vegetation does not always acts against the erosive ability of precipitation. In some

settings, such as in transition from arid to semi-arid environment, vegetation facilitates erosion by promoting weathering in the root zone due to high pCO_2 (Matmon et al., 2018).

- **Second regime:** The second regime (1050-2200 mm/yr) is characterized by erosion rates that do not increase with an increase in mean annual precipitation. The mean value of tree cover in this regime is ~62%. In this regime, the combined effect of mean annual precipitation and tree cover results in decreasing erosion rate with further increase in precipitation. Although an increase in precipitation tends to increase erosion rate, the response of vegetation to higher rainfall neutralizes precipitation's influence and ultimately stabilizes and lowers the erosion rate. A similar response has been noted in sediment yield studies (Walling & Webb, 1983; Knox, 1972; Langbein & Schumm, 1958), where the response of vegetation lowers sediment yield despite increasing precipitation.
- **Third regime:** The third regime (>2200 mm/yr) is characterized by erosion rates increasing with increased mean annual precipitation, and is quite complex. In this regime the mean value of tree cover is ~69%. In spite of the tree cover percentage being greater than the threshold value, erosion rate in this regime tends to increase with an increase in precipitation. This is likely due to the mechanism of how trees lower soil erosion against high intensity of rainfall. Trees primarily control soil erosion in two ways: first, roots hold the soil together; and second, leaf litter accumulates on the topsoil and protects it from eroding (Zimmermann et al., 2012; Kaspari & Yanoviak, 2009; Kaspari & Yanoviak, 2008). Areas where the percentage of tree cover and precipitation are both high are often rich in nutrients (Zimmermann et al., 2012; Kaspari & Yanoviak, 2008). This abundance of nutrients means that the roots don't spread laterally and leaf litter decomposes faster (Zimmermann et al.,

2012; Kaspari & Yanoviak, 2008) resulting in a lower protection of soil against erosion. High tree cover percentage often also means a thick canopy, which ultimately restricts under-story growth, resulting in less protection against erosion (Rey, 2003). Furthermore, areas with high mean annual precipitation experience a higher frequency of landslides, resulting in a high erosion rate (e.g. Dadson et al., 2003). The influence of relief is also apparent in this high rainfall regime. For instance, sites from Sri Lanka (Hewawasam et al., 2003) with average slope of ~13.3° and average precipitation of ~2610 mm/yr yielded an average erosion rate of ~18m/My. Conversely, sites from Swiss Alps (Buechi et al., 2014) with average slope ~26.6° and average precipitation of ~2450mm/yr recorded an average erosion rate of ~217m/My. Thus, the erosion rates from Swiss Alps are ~10 times higher than average erosion rate observed from Sri Lankan sites, although both sites experience almost same average precipitation. This further implies that areas with lower relief, but very high precipitation will have lower erosion rate, despite the fact that high precipitation acts toward increasing erosion rate.

This three-regime relationship accounts for the response of erosion rate to both change in precipitation and the co-related change in tree cover percentage. This non-linear relationship between erosion rate and mean annual precipitation also suggests similarity to the curve observed by previous sediment yield studies (Walling & Webb, 1983; Knox, 1972; Langbein & Schumm, 1958)(Figure 10). Although, not entirely comparable, the sediment yield curves attest the non-linearity of the relationship between precipitation and erosion rate. This observation is also consistent with the findings of Schaller et al. (2018) in Chilean Coastal Cordillera, where denudation rates increased with increase in mean annual precipitation until ~1000 +/- 500 mm/yr; after this value, denudation rates did not increase with further increase in mean annual precipitation (Schaller et al., 2018). This stability in denudation rate at ~1000

mm/yr is attributed to vegetation cover, suggesting a vegetation-induced non-linear relationship between precipitation and erosion rate (Schaller et al., 2018). Our results suggests that this interrelationship operates on a global scale.

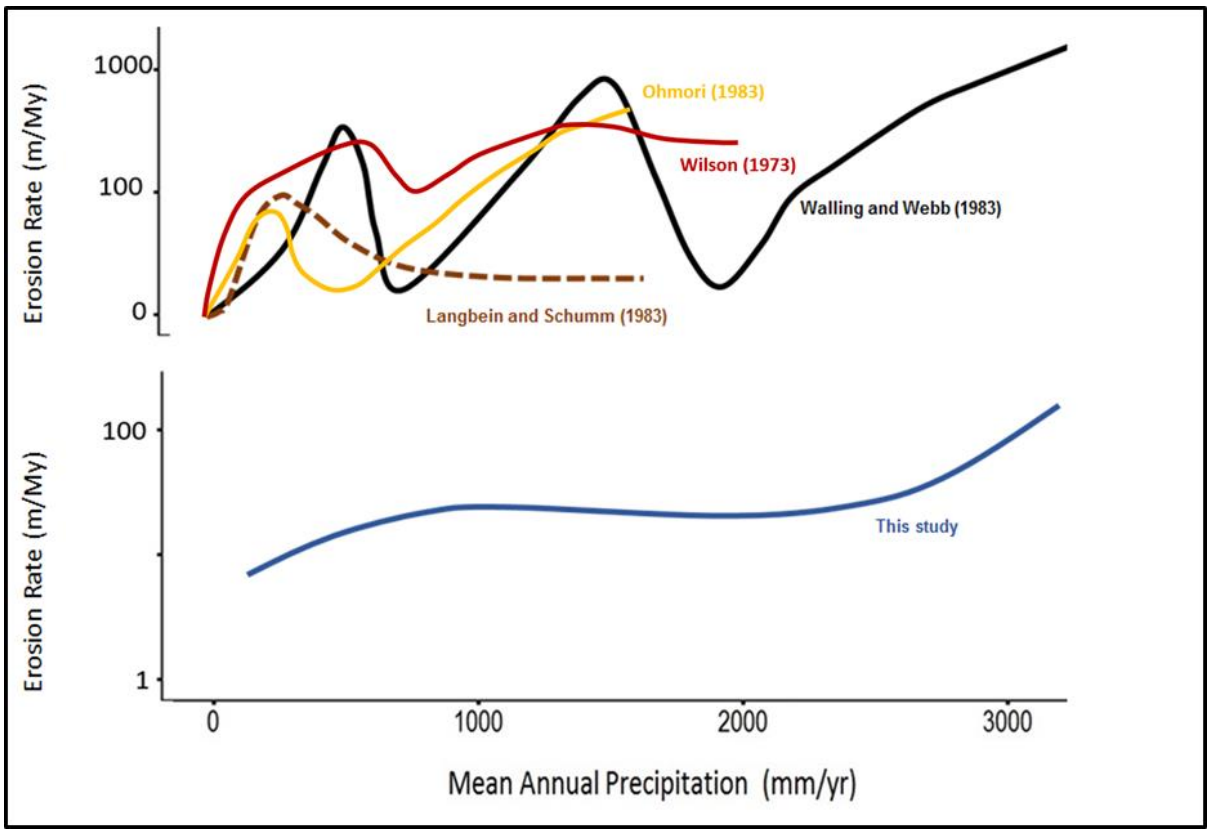

Figure 10: Comparison of the relationship between erosion rate and mean annual precipitation from different studies. Black solid curve represents the relationship between precipitation and erosion rate from Wailing and Webb (1983), Brown dashed curve represents the relationship from Langbein and Schumm (1958), yellow solid curve represents relationship from Ohmori (1983), Red solid curve represents the relationship from Wilson (1973), and the blue solid curve represents the curve from this study. Wailing and Webb (1983) and Langbein and Schumm (1958) originally depicted the relationship between sediment yield and precipitation; sediment yield (t km-2yr-1) is converted to m/My using 1 m/My = 2.7 t km-2yr-1

Results of our compilation highlight the critical role of vegetation and tree cover, and illustrates how tree cover is inseparable from precipitation's influence on erosion rate. From an erosion management perspective high tree cover is widely recognized and associated with lower erosion rate (Acosta et al., 2015; Jiongxin, 2005; Pimentel & Kounang, 1998; Pimentel et al., 1995). Additionally, soil production rates decline exponentially with soil depth

(Heimsath et al., 1997) and forested landscapes are characterized by thick soils, so production of material available to erode should be less in environments where tree cover is high. However, our results suggests that at very high precipitation, erosion rate increases in-spite of high tree cover percentage.

This response of erosion rate to high mean annual precipitation and high tree cover percentage in third regime is based on limited data available from these areas. Indeed, there is an overall lack of erosion rate studies from areas with very high precipitation (>2000mm/yr). Addition of sites with very high precipitation and high tree cover percentage could potentially affect the reported trend of the third regime. For example, sites from Shillong plateau (Rosenkranz et al., 2018), where precipitation ranges between 4000 to 6000mm/yr and vegetation cover is >90%, reported average erosion rate of <100m/My. The erosion rate was higher for areas that were recently deforested (Rosenkranz et al., 2018). Therefore, more detailed constraints are required to understand this relationship in areas where tree cover percentage and precipitation both are high. Such areas currently constitute only ~10% of our dataset and further data in such regions may further inform on this regime.

2.8. Conclusions and implications

Although it is consistently suggested that precipitation is an important factor impacting erosion rate, global ^{10}Be compilations have failed to find its significance. This may be because previous global ^{10}Be compilations focused on precipitation's primary and linear correlation with erosion rate. The relationship between mean annual precipitation and erosion rate is best explained non-linearly. From this compilation of ^{10}Be-derived erosion rates, several important conclusions can be made: 1) the relationship between mean annual precipitation and erosion rate is non-linear and significant; 2) mean annual precipitation influences erosion rate in three regimes i.e. erosion rate first increases, then decreases, and

then again increases with an increase in mean annual precipitation; 3) increased precipitation results in increased vegetation, causing a complex and competing influence on erosion rate that is responsible for the three regimes. These competing trends intersect at precipitation values between ~1000 and 2200 mm/yr; 4) tree cover lowers the influence of increased precipitation on erosion rate when the percentage of tree cover is 40% or more; 5) the influence of mean annual precipitation on erosion rate is often non-apparent because it is obscured by its closed coupled interaction with vegetation; and 6) in areas where slope is low (~90% of the Earth's surface (Willenbring et al., 2013)), slope's influence on erosion rate is not clear, and mean annual precipitation correlates with erosion rate as much as mean basin slope.

In the geologic record, high sediment yields are often interpreted as a result of climate change and our results suggest that high sediment fluxes occur when forests transition to grasslands/savannahs; however, over millennial timescales, aridification of grasslands or savannahs into deserts will result in lower sediment fluxes. These results also have relevance to anthropogenic influences on sediment yield, as it is widely asserted that changes in land use have increased short-term (e.g. Pimentel, 2006; Hewawasam et al., 2003; Pimentel & Kounang, 1998; Pimentel et al., 1995) or mid-term (Portenga et al., 2016) erosion. Our results suggest that vegetation loss will result in significantly higher sediment yield. In particular, deforestation in areas with high precipitation should result in very high rates of erosion.

Chapter 3: Millennial-scale erosion rates in north Queensland determined using ^{10}Be

3.1. Abstract

Quantification of long-term erosion rates is important for reliable estimates of sediment generation rates and accurate identification of its sources. It is also important to determine effective land-use strategies. Quantifying long-term erosion rates is particularly important in north Queensland, which is proximal to the Great Barrier Reef. One of the main threats to the Great Barrier Reef is sediment generated by erosion.

Recent applications of ^{10}Be in north Queensland has contributed significantly towards understanding erosion rates in the region. However, the existing information has a limited spatial distribution and information on bedrock erosion rates in north Queensland are very limited. Here, we focus on quantifying erosion rates across north Queensland and investigating how erosion rate varies across different slopes, rock types, and precipitation values. We also determined paleoerosion rates for the Burdekin River, and quantified erosion rates from bedrock samples and compared these to adjacent basins to explore the implications for rates of relief generation and landscape evolution.

The erosion rates of basins in north Queensland range from 2.2 to 53.6m/My and bedrock rates range from 3.6 to 70.2m/My. These rates are slow, compared to basins in other parts of the world that experience similar precipitation. Basins in the northern part of north Queensland are eroding faster than the southern part, because the northern part experiences higher rainfall. Precipitation has a strong influence on basin erosion rate (R^2=0.71), whereas the influence of mean basin slope is negligible (R^2=0.09). The strong influence of precipitation and weak influence of slope on erosion rates in north Queensland is consistent with the fact that most sampling sites are from areas where slope was low (~<13°). The bedrock erosion rates in north Queensland are mainly governed by lithology: sedimentary

rocks are eroding faster than granites, and precipitation has no influence on bedrock erosion rate.

Unlike most places in the world, bedrock in north Queensland erodes faster than basins. This implies that relief is being lost over time. Our results also suggest minimal temporal variation for erosion rates in north Queensland, and that these erosion rates were consistently slow for ~120,000 years, implying that landscapes in north Queensland have most likely attained steady state.

3.2. Introduction

Erosion regulates the supply of sediments and nutrients to soils, streams, and ultimately the ocean, and is a significant component of Earth's biogeochemical cycle (e.g. von Blanckenburg, 2005; Pimentel et al., 1995). Erosion is also important in understanding the long-term transformation and development of landscapes (e.g. Acosta et al., 2015; Portenga et al., 2013; DiBiase et al., 2010; Dixon et al., 2009; Quigley et al., 2007b; Vanacker et al., 2007; Riebe et al., 2004; Bonnet & Crave, 2003; Tucker & Bras, 1998). Although erosion is a natural process, anthropogenic influences have intensified rates by several folds in many locations (Bainbridge et al., 2018; Coates-Marnane et al., 2016; Bartley et al., 2015; Hewawasam et al., 2003; Pimentel et al., 1995). Therefore, it is important to quantify background erosion rates and to understand the factors that impact erosion, in order to understand biogeochemical cycles (e.g. von Blanckenburg, 2005; Pimentel et al., 1995), interpret the sediment record (e.g. Walling & Webb, 1987; Langbein & Schumm, 1958), quantify human influences (e.g. García-Ruiz et al., 2015; Reusser et al., 2015; Whiting, 2006; Pimentel & Kounang, 1998), and implement effective land-use strategies, (e.g. Lal, 2001; Pimentel et al., 1995; Lal, 1990).

Erosion is closely associated with sediment yield, which is the quantity of sediment moving out of a catchment (Reusser et al., 2015; Whiting, 2006; Merritt et al., 2003; Pimentel et al., 1995). Sediment yield is important for water quality as increased sediment and nutrients degrade water quality and affect terrestrial and marine ecosystems (Brodie et al., 2012; Furnas, 2003; O'Reagain et al., 2005). This is particularly important for north Queensland, which is adjacent to the Great Barrier Reef (GBR). The GBR is a World Heritage area and the largest reef ecosystem in the world. Degradation of marine ecosystems due to sediment deposition is a global issue, but damage to coral reefs of the GBR is a widely noted impact (e.g. Brodie et al., 2012; Burke et al., 2011; Doney, 2010). Sediment and nutrient delivery to the GBR is mainly generated from erosion (Bainbridge et al., 2018; Hess et al., 2017; Fabricius et al., 2016; Bartley et al., 2015; Brodie et al., 2012; Fabricius, 2005; Furnas, 2003; Brodie, 2002), and it is suggested that this has significantly increased due to land use changes since 1850. The Burdekin catchment is the largest contributor of sediment to the GBR (Bartley et al., 2015; Croke et al., 2015; Furnas, 2003), but there is a lack of information on key sources of sediment generation and transport to the GBR (Bainbridge et al., 2018; Oleson et al., 2017; Kroon et al., 2014). Furthermore, estimates of contemporary sediment yield (e.g. Herr & Kuhnert, 2007; Prosser et al., 2001) are often considered high and unreliable because of the episodic nature of sediment delivery (Trimble & Crosson, 2000; Summerfield & Hulton, 1994). Nichols et al. (2014) quantified long-term erosion rates in the northern GBR over millennial time-scales using terrestrial cosmogenic nuclides and compared these with contemporary sediment yields. Nichols et al. (2014) found that the contemporary sediment yield estimates were almost similar to long-term erosion rates, implying that changes in land-use post European settlements had not changed sediment generation in Barron catchment. This is unusual because various studies in the region have confirmed an increase in sediment

generation due to changes in land-use (e.g. Brodie et al., 2012; Hughes et al., 2009; Furnas, 2003; Brodie, 2002).

The development and application of ^{10}Be allows quantification of erosion rates over the timescale of thousands of years. In particular, the use of fluvial sediments to quantify erosion rate averaged over an entire catchment has increased (Bierman & Steig, 1996; Granger et al., 1996; Brown et al., 1995b), and it is now widely applied to small (e.g. Croke et al., 2015; Nichols et al., 2014) and large river catchments (e.g. Lupker et al., 2012; Wittmann et al., 2011). Recent applications of ^{10}Be has also contributed significantly towards an understanding of Australia's erosional history (e.g. Croke et al., 2015; Nichols et al., 2014; Heimsath et al., 2010; Bierman et al., 2009; Heimsath et al., 2009; Heimsath et al., 2006; Heimsath et al., 2001; Heimsath et al., 2000; Heimsath et al., 1997). TCN based studies in Australia suggest that landscapes evolve very slowly (Portenga et al., 2013; Quigley et al., 2007a; Heimsath et al., 2006; Bierman & Caffee, 2002) and are characterised by erosion rates as low as ~1m/My (Pillans & Fifield, 2013; Belton et al., 2004; Bierman & Caffee, 2002), falling within the lower range of global ^{10}Be-derived erosion rates (Mishra et al., 2019; Portenga & Bierman, 2011). This slow erosion is often broadly attributed to tectonic stability and the low-gradient of Australia (e.g. Pillans & Fifield, 2013; Belton et al., 2004; Bierman & Caffee, 2002), but the influence of variables such as mean basin slope, uplift rate, relief, vegetation, and precipitation on erosion rate remains unclear, both globally and within Australia. Information on ^{10}Be-derived erosion rates from bedrock is also very limited in Australia and is required to understand landscape transformation and rates of change in relief. This is particularly significant for landscapes of north Queensland, which despite being mostly low-gradient and low-relief, also consists of steep gorges (such as Porcupine Gorge and Tully Gorge) and relief features such as the Great Dividing Range and the Great Escarpment. Most studies suggest that the formation of the Great Divide and major river

formation, followed by widespread basalt flow and uplift subsequently lead to formation and retreat of the Great Escarpment (Matmon et al., 2002; Ollier, 1979; Oilier, 1982).

Globally, ^{10}Be studies suggest variability in the influence of climatic (e.g. precipitation and temperature) and tectonically linked factors (e.g. slope, channel steepness, and uplift rate) on ^{10}Be-derived erosion rates. Even within catchments of the GBR, the influence of a multitude of variables on ^{10}Be-derived erosion rates is not yet clearly established. For example, Nichols et al. (2014) observed a strong correlation between mean basin slope and ^{10}Be-derived erosion rates in far north Queensland; however, further south, Croke et al. (2015) did not observe this correlation when the smaller basin of the Upper Burdekin were examined. However, when the larger sub-basin samples were considered, Croke et al. (2015) observed significant correlation between slope and erosion rate. Similarly, Heimsath et al. (2010) suggests a strong climatic influence on erosion rates across Australia, but Nichols et al. (2014) does not observe significant correlation between precipitation and erosion. Within the Upper Burdekin, Croke et al. (2015) also did not observe any correlation between precipitation and erosion, but found a moderate correlation when the larger sub-basins were considered. The impacts of lithology on long-term erosion rates in north Queensland is also not very clear. Croke et al. (2015) found that erosion rates were higher when the percentage of granitic lithology in a catchment was high. However, this observation is in contrast to what is observed in global data sets (e.g. Portenga & Bierman, 2011) and requires further investigation.

3.2.1. Aim of this study:

This study aims to add constraints on rates of sediment generation and landscape evolution in north Queensland by quantifying erosion rates across north Queensland using ^{10}Be. Much of this study aims to understanding the spatial variability of long-term erosion rates in north Queensland, and how this variability relates to lithology, slope, and precipitation. We also try

understanding temporal variability, enabling comparison between long-term and recent erosion rates. A comparison of bedrock erosion rates to the basin averaged erosion rates will further enhance understanding of the rate of landscape transformation in north Queensland.

3.3. Study Site

3.3.1. Sampling Strategy:

Samples for this study were collected from north Queensland, between 16.4°S and 21.5°S. Sample locations were primarily divided into two study areas – a northern study area and a southern study area. The 'northern study area' consisted primarily of the Mitchell drainage basin; and the 'southern study area' focused on the Burdekin, Copper Creek, and Flinders drainage basins. This strategy was devised to explore the differences in slope, lithology, and precipitation across north Queensland. Sampling locations were selected to complement previous studies (Figure 11 and Table 4).

3.3.2. Geologic and Climatic Setting:

The geology of Queensland is dominated by three structural units – the Precambrian Shield, the Palaeozoic Tasman Orogenic Belt and the Great Artesian Basin (McNeil et al., 2005; Day, 1983; Day et al., 1978; Hill & Denmead, 1960). The Precambrian Shield is located primarily in central and northwest of Queensland and forms the drainage divide between coastal and inland drainage systems (McNeil et al., 2005). It consists mainly of granitic and metamorphic rocks (Plumb et al., 1980), but also includes dolomites, quartzose sandstone and meta basalts (Plumb et al., 1980). The Tasman Orogenic Belt, located primarily along the eastern coastline of Queensland, forms the Great Dividing Range (McNeil et al., 2005). It consists of mostly volcanic rocks with granitic intrusions, with some areas containing limestone (McNeil et al., 2005). The Great Artesian Basin is the largest of the three structural units and is dominated by Mesozoic sediments (McNeil et al., 2005). Samples from northern

study area were located in the Tasman Orogenic Belt, and were primarily granitic rocks. In contrast, samples from southern study area are located partly in the Tasman Orogenic Belt and partly in the Great Artesian Basin. Most samples in southern study area were quartz-rich sedimentary rocks.

The major topographic features of north Queensland are the Great Dividing Range and the Great Escarpment. The Great Dividing Range is one the most important mountain ranges in Australia and the Great Escarpment runs eastward of the Great Dividing Range, spanning much of the eastern coast of Australia. The Great Dividing Range is believed to have formed over 300 million years ago, and uncertainties exist around the age of the Great Escarpment (Nott et al., 1991; Young, 1983). Some studies indicate that the Great Escarpment formed and took its modern shape in Oligocene (e.g. Nott et al., 1991; Young, 1983), while others (e.g. Matmon et al., 2002; Oilier, 1982) suggest that it might have largely formed during intial rifting. Nevertheless, both the Great Dividing Range and the Great Escarpment have experienced substantial erosion since they have formed.

The climate of north Queensland is characterised as semi-arid to wet-tropical. Mean annual precipitation ranges from <500mm/yr to >3000mm/yr ("BoM," 2018), whereas mean annual temperature ranges from 18°C to 25°C ("BoM," 2018). Precipitation in the northern sampling area is higher than the southern sampling area. The northern sampling area is associated with the wet-tropical vegetation and high tree-cover. In contrast, southern sampling area mainly experiences sub-tropical climate and has a savannah landscape, with an average annual rainfall of ~600mm/yr and average annual temperature ranging from 23°C to 25°C (Alexander et al., 2001; Pillans, 1997; Fielding & Alexander, 1996). The location of samples from this study and previous studies (Croke et al., 2015; Nichols et al., 2014), along with the climatic and geological data is presented in Figure 11 and Figure 12.

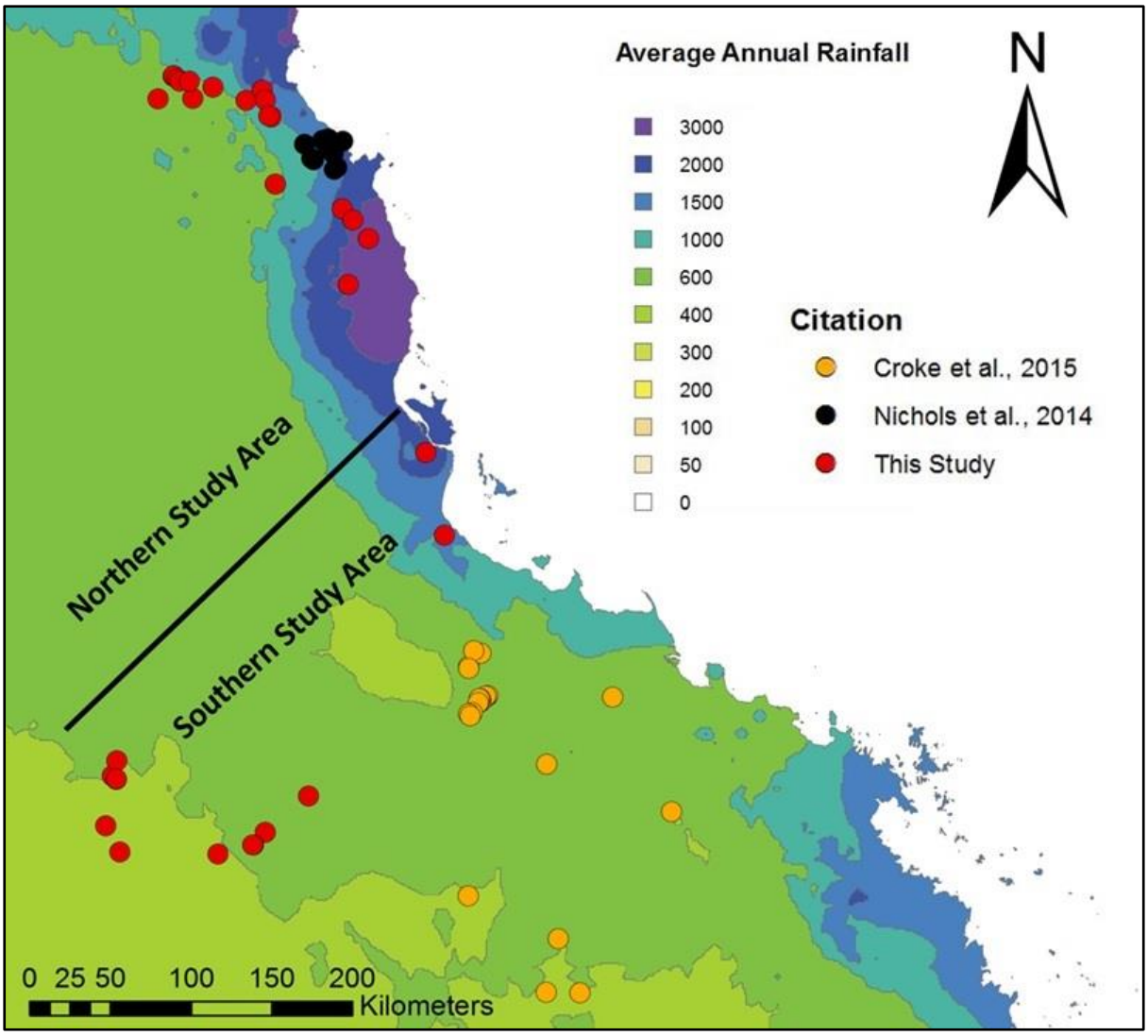

Figure 11: Location of samples from north Queensland along with precipitation. Red dots represents samples from this study, black dots represents samples from Nichols et al., 2014 , and orange dots represents samples from Croke et al., 2015. Black diagonal line shows the divide between northern study area and southern study area of this study.

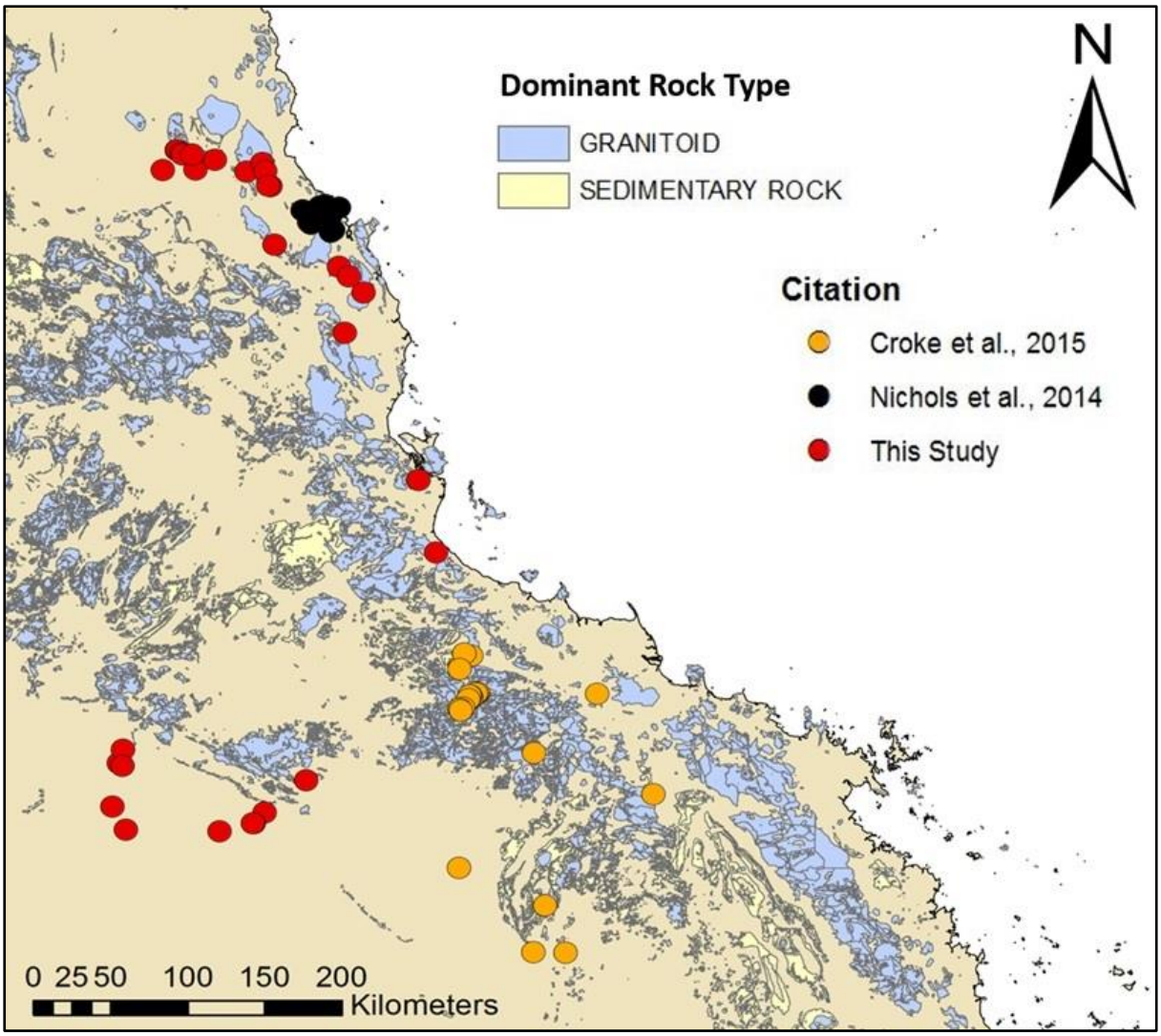

Figure 12: Location of samples from north Queensland along with dominant rock type. Red dots represents samples from this study, black dots represents samples from Nichols et al., 2014 , and orange dots represents samples from Croke et al., 2015.

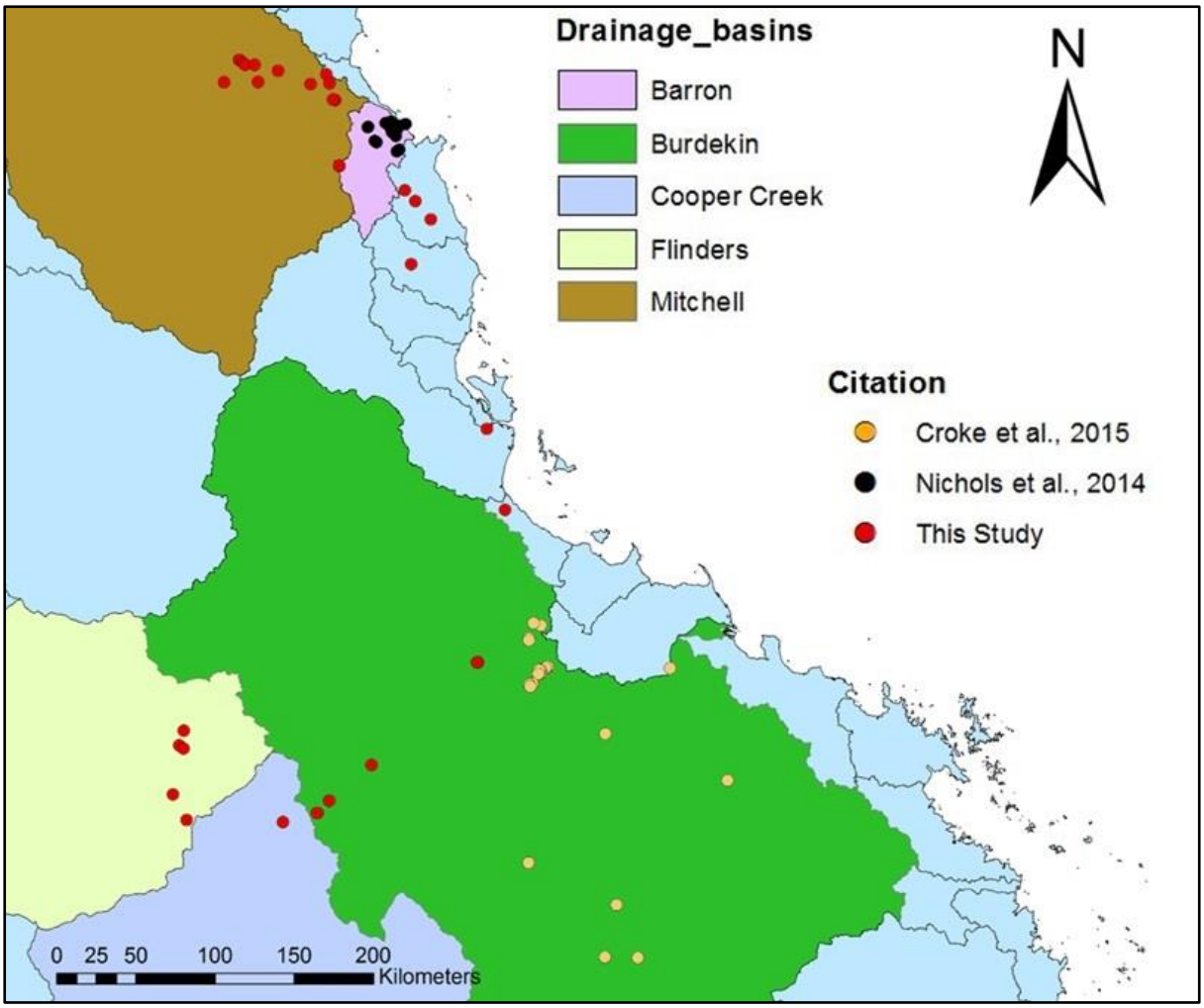

Figure 13: Location of samples from north Queensland along with catchment boundaries. Red dots represents samples from this study, black dots represents samples from Nichols et al., 2014 , and orange dots represents samples from Croke et al., 2015. Black line represents direction of flow (i.e. inland or seaward)

Table 4: Sample locations and types. The coordinates (WGS 84) were noted using Garmin eTrex 10 brand GPS device, with horizontal precision of ±10m.

SAMPLE ID	Location	Type	Latitude (decimal degrees)	Longitude (decimal degrees)
BR1	Toomba basalt(Burdekin river),Qld, Australia	Sediments	-20.331433	144.440417
CN2	Toomba basalt, Qld, Australia	Buried sediments	-19.8601	146.137767
CN3	Toomba basalt, Qld, Australia	Buried sediments	-19.8592	146.132617
PG1	flinders creek, Qld, Australia	sediments	-20.755967	144.4822
PG2	Porcupine gorge creek, Qld, Australia	sediments	-20.24795	144.465983
PG3	Porcupine creek, Qld, Australia	sediments	-20.61015	144.404183
PG4	Torrens creek, Qld, Australia	sediments	-20.767167	145.028983
PG5	Warrigal Creek, Qld, Australia	sediments	-20.6456	145.292167
PG6	Campaspe river, Qld, Australia	sediments	-20.442217	145.53335
PGBR2	Porcupine gorge, Qld, Australia	Bedrock	-20.3495	144.462867
PGBR3	Porcupine gorge, Qld, Australia	Bedrock	-20.349167	144.46285
PGBR6	white Mountains, Qld, Australia	Bedrock	-20.715617	145.225333
PGBR7	white Mountains, Qld, Australia	Bedrock	-20.715283	145.22475
PGBR8	white Mountains, Qld, Australia	Bedrock	-20.71585	145.22335
NQ1	Henrietta Creek, Qld,Australia	sediments	-17.59745	145.75739
NQ2	Kelly St. George Creek, Qld, Australia	sediments	-16.43639	144.78011
NQ3	Boulder creek, Qld, Australia	sediments	-16.56328	144.69536
NQ4	Mitchell river, Qld, Australia	sediments	-16.56049	144.88808
NQ5	McLeod river Qld, Australia	sediments	-16.49823	145.00208
NQ6	Granite gorge, Qld, Australia	sediments	-17.038116	145.34903
NQ7	Mary Creek, Qld, Australia	sediments	-16.57277	145.18692
NQ8	Rifle Creek, Qld, Australia	sediments	-16.66477	145.3269
NQ9	Creek 1(from top), Mt. Lewis National Park	sediments	-16.51646	145.27654
NQ10	creek 2 (from top), Mt. Lewis, Qld	sediments	-16.56949	145.2942
NQ11	Babinda boulders, Qld, Australia	sediments	-17.3416	145.86955
NQ13	Mulgrave river, Qld, Australia	sediments	-17.17688	145.72331
NQBR1	Mt carbine, Qld, Australia	Bedrock	-16.435	144.78174
NQBR2	Mt carbine, Qld, Australia	Bedrock	-16.45232	144.80215
NQBR3	Mt carbine, Qld, Australia	Bedrock	-16.46419	144.81448
NQBR4	Mt carbine, Qld, Australia	Bedrock	-16.46419	144.86877
NQBR5	Granite Gorge, Qld, Australia	Bedrock	-17.03805	145.3501
NQBR7	Mt carbine, Qld, Australia	Bedrock	-16.65986	145.31317
NQBR8	The track Crest, Gordonvale, Qld, Australia	Bedrock	-17.23764	145.78204
NQBR9	Hinchinbrook Lookout, Qld, Australia	Bedrock	-18.53297	146.18896
NQBR10	Paluma Range, Qld, Australia	Bedrock	-18.99236	146.29106

3.4. Methods

3.4.1. Sample Collection:

Twenty-one fluvial-sediments and 14 bedrock samples were collected from north Queensland. For the fluvial-sediments, 9 were collected from the southern study area and 12 were from the northern study area. Five bedrock samples were collected from southern study area and nine bedrock samples were collected from the northern study area.

Buried samples were also collected to assess temporal variation in erosion rate, allowing assesment of isotopic and geomorphic steady state. Temporal variation in long-term erosion rate can be determined by comparing ^{10}Be inventory from buried samples to the ^{10}Be inventory of non-buried samples (Schaller et al., 2002). Sediments samples were collected for ^{10}Be from recently exposed gullies beneath the Toomba flow, and the precise age of Toomba flow was recently determined using radiocarbon (Mishra et al., 2018)(Chapter-4 of this thesis).

3.4.2. Cosmogenic ^{10}Be:

Berryllium-10 (^{10}Be) is the most commonly used cosmogenic nuclide for determining erosion rates and has been successfully applied to obtain basin-averaged erosion rates in a variety of settings (Bierman & Steig, 1996; Granger et al., 1996; Brown et al., 1995b; Lal, 1991). The primary assumption of this approach is that the cosmogenic nuclide concentration of a fluvial sediment sample is a good approximation for the nuclide concentration on the hillslopes, and the erosion rate derived using fluvial sediment is known as the basin-average erosion rate. This approach assumes that there are negligible changes to the nuclide inventory as sediment is transported. Concentrations of ^{10}Be have also been widely used to estimate soil production, and erosional histories across many climatic regions (Codilean et al., 2018; Portenga et al.,

2013; Heimsath et al., 2010; Bierman & Steig, 1996; Granger et al., 1996; Brown et al., 1995b; Lal, 1991).

The application of cosmogenic ^{10}Be approaches to determining basin averaged erosion rates has several assumptions (von Blanckenburg, 2005; Bierman & Steig, 1996; Granger et al., 1996), which include - (1) the rate of erosion is uniform throughout the basin and all lithologies are eroding at same rate; (2) the production of nuclides within the basin is in steady-state; (3) all rock types contributing to erosion have similar grain sizes; (4) the loss of mass in the basin occurs primarily by surface lowering; (5) the timescale of erosion is smaller than the decay timescale of ^{10}Be; and (6) there is minimal time spent in sediment storage and it does affects the concentrations of isotopes.

This also should probably explain why many studies use the concentration of ^{26}Al, along with ^{10}Be to assess for long-term sediment storage and/or to determine if significant quantities of material are produced in the subsurface (e.g. Clapp et al., 2002; Granger et al., 2001a; Granger & Smith, 2000; Kubik et al., 1998; Brown et al., 1995a; Nishiizumi et al., 1989).

Radioactive *in-situ* cosmogenic nuclides, such as ^{10}Be, decay at a rate given by their decay constant. The production of cosmogenic nuclides varies with rock depth, rock density, latitude, and elevation. Production of *in-situ* cosmogenic nuclides varies inversely with increasing rock depth and occurs dominantly within the first 1.5-2 meters (Ivy-Ochs & Kober, 2008; Gosse & Phillips, 2001; Masarik & Reedy, 1995). The production rate of *in-situ* cosmogenic nuclides varies proportionally with latitudes and with altitude because of the higher intensity of cosmic rays at higher altitude and at polar regions (Ivy-Ochs & Kober, 2008; Gosse & Phillips, 2001; Stone, 2000; Lal, 1991). Tools like the CRONUS online calculator (Balco et al., 2008) normalise production rate to sea level high latitude (SLHL) and

allow determination of erosion rate from the concentration of cosmogenic nuclides (Balco et al., 2008).

3.4.3. Sample processing:

Quartz was separated from samples and ^{10}Be was isolated from the quartz in the clean lab at James Cook University using standard methods (Clifton et al., 2005; Kohl & Nishiizumi, 1992). Sediment samples were sieved to a grain size of 0.25-0.50 mm. This was to ensure that any windblown detritus is not included in the sample. The samples then underwent treatment with concentrated HNO_3 for dissolution of carbonate. Samples were next soaked overnight in an aqua-regia solution in order to remove metals. Thereafter, magnetic minerals were removed in a magnetic separator, after which they underwent heavy-liquid separation using lithium heteropolytungstate (LST heavy liquid) to remove heavy minerals. The remaining samples were primarily quartz and feldspar.

Samples were split into ~60-65 gram fractions and subjected to at least three 24-hour cycles in a continuously agitated 5% HF/HNO_3 solution to obtain clean quartz (Child et al., 2000). The samples were then rinsed with milli-Q, dried, and tested for aluminium content. Sufficiently clean quartz samples (generally <400ppm Al) were then treated with a 2% HF/HNO_3 solution overnight in an ultrasonic bath to assure removal of meteoric ^{10}Be (Child et al., 2000). The clean quartz was spiked with ~300µg of ^{9}Be in a weak HNO_3 carrier solution and dissolved in a 5:1 solution of concentrated HF and HNO_3. After the quartz was completely dissolved, the resulting sample solution was evaporated and dried in Teflon beakers (Child et al., 2000).

Fluorides were removed by treating the sample with concentrated $HClO_3$. The resulting cake was dissolved in concentrated HCl, transferred to a Teflon beaker, and dried. This sample cake was next dissolved in oxalic acid and beryllium was retrieved through standard ion

chromatography methods (Clifton et al., 2005). Beryllium hydroxide was precipitated at pH ~9-10 using NH_4OH and EDTA. The samples were centrifuged and rinsed three times. The samples were sent to Australian Nuclear Science and Technology Organization (ANSTO) for analysis by accelerator mass spectrometry (AMS) on the ANTARES accelerator (Fink and Smith, 2007). Five blanks were also added to the analyses to assess the sample preparation method. The blanks were prepared with the same Be spike and gave a mean $^{10}Be/^{9}Be$ value of $1.116 \pm 0.6 \times 10^{-15}$, which represents < 1% of the lowest $^{10}Be/^{9}Be$ ratio from the collected samples. The concentration of ^{10}Be in atoms/gram was derived from the AMS measurements of $^{10}Be/^{9}Be$ and the concentration of the added ^{9}Be. The AMS standard for ^{10}Be was 07KNSTD (Nishiizumi et al., 2007).

3.4.4. Erosion rate calculations:

The rates of production and decay can be combined to give the total concentration of cosmogenic radionuclides in a sample, which is a function of age (Lal, 1987):

$$N_i(t) = \left(\frac{P_i}{\rho E \Lambda^{-1} + \lambda_i}\right)\left(1 - e^{-(\rho E \Lambda^{-1} + \lambda_i)t}\right) \qquad \textbf{(Equation 1)}$$

Where, the concentration (N) of a cosmogenic nuclide (i) in a rock depends on the erosion rate (E) and the exposure time (t), where P_i is the production rate, ρ *is* the rock density, Λ is the effective cosmic-ray nucleon attenuation length, and is λ_i the decay constant ($\lambda_{Be\text{-}10} = 5.00 \times 10\text{-}7\ yr^{-1}$) (Chmeleff et al., 2010; Korschinek et al., 2010).

In order to examine temporal variation in erosion rate, the erosion rate of the buried samples was calculated and compared to the non-buried samples. The concentration of ^{10}Be retrieved from the buried samples (CN-2 and CN-3) were used to calculate the initial concentration of ^{10}Be in these samples before burial (~20, 000 years ago). The equation used was:

$$N = N°e^{-\lambda t}$$ **(Equation 2)**

Where, (N) is the final concentration of ^{10}Be from the buried samples, (N°) is the initial ^{10}Be concentration before burial time (t), and is (λ) the decay constant of ^{10}Be. The burial time (t) is the age of Toomba flow, which is 19,726-20,815 cal BP (2σ) (Mishra et al., 2018). The average age was 20,260 years; however, for ease of calculation, the burial time (t) was assumed 20,000 years, and the decay constant (λ) was assumed to be 5.00 x 10-7 yr^{-1}) (Chmeleff et al., 2010; Korschinek et al., 2010).

The CRONUS online calculator version 2.3 was used to compute the erosion rate from concentrations of ^{10}Be. In this study, we used the CRONUS online calculator (https://hess.ess.washington.edu/). The scaling model of Lal (1991) /Stone (2000) was used. CRONUS topographic shielding calculator (http://stoneage.ice-d.org/math/skyline/skyline_in.html) was used for shielding corrections for the samples that were geographically shielded (see appendix-3). The sample thickness for sediment samples was assumed 1 cm and the rock density was assumed to be 2.7g/cm^3, following the widely used approach of other studies (e.g. Portenga and Bierman, 2011; Harel et al., 2016). For bedrock samples, the measured average sample thickness was used (see appendix-3). We also recalculated the erosion rate of the previously published studies (Croke et al., 2015; Nichols et al., 2014) using the ^{10}Be concentration, shielding correction, and AMS standard published by these studies.

3.4.5. Mean basin slope and precipitation calculations:

The mean basin slope was calculated using DEM with ArcGIS using ~3 arc-seconds (90m) SRTM data (http://srtm.csi.cgiar.org). Mean annual precipitation values for the sample locations were retrieved using weather station directory of Bureau of Meteorology's climate data (http://www.bom.gov.au/climate/data/). Precipitation data was retrieved from the nearest

weather station using coordinates of the samples. We recalculated precipitation for previous studies using weather station data to standardize precipitation data between studies. For statistical analyses, statistical package R was used.

3.4.6. Relief generation and landscape transformation:

The rate of landscape change over millennial time scales can be determined using cosmogenic methods, by comparing bedrock and basin erosion rates (e.g. Meyer et al., 2010; Quigley et al., 2007a; Bierman & Caffee, 2002; Brown et al., 1995b; Lal, 1991). Comparisons of the erosion rate of a ridge-top or ridgeline with the adjacent basin erosion rates allows determination of the contrast in the rate of lowering of the topographic highs and the drainage basin in general (Portenga et al., 2013). Such comparison allows determination of the rate of change in relief, which is one of the main drivers of landscape transformation (Portenga et al., 2013; Quigley et al., 2007a). In order to generate relief, rates of erosion in drainage basins must be higher than the adjacent summit surface so that incision occurs in the landscape (Quigley et al., 2007a). If the erosion rate of adjacent summit surface exceeds erosion rates of drainage basin, the landscape experiences reduction in relief (Meyer et al., 2010; Quigley et al., 2007a).

Such comparisons of erosion rates is widely used (e.g. Portenga et al., 2013; Quigley et al., 2007a; Bierman & Caffee, 2002), but has limitations (Portenga et al., 2013). For example, when determining the exposure history of bedrock samples, it is assumed that they are constantly eroding (Portenga et al., 2013; Bierman & Caffee, 2002; Small et al., 1997). In some case, bedrock loses a large portion of mass by landslides (e.g. Niemi et al., 2005) or by loss of blocks (e.g. Bierman & Caffee, 2002; Small et al., 1997). In these cases, if the outcrop sample is collected after block removal, the erosion rate measured through ^{10}Be concentrations will be overestimating the actual erosion rates (Portenga et al., 2013; Niemi et al., 2005; Small et al., 1997). Therefore, to ensure proper examination of the response of

landscape through bedrock erosion and to avoid overestimation or underestimation of erosion rates of bedrock, it is extremely important to quantify bedrock erosion rate at various levels of a landscape, such as at summit, hillslopes, and floors of the landscape (Quigley et al., 2007a). In addition to that, ^{26}Al concentration along with ^{10}Be are helpful in avoiding samples with complex exposure history (e.g. Clapp et al., 2002; Kubik et al., 1998).

To understand the rate of change in relief, erosion rates from bedrock samples were compared to erosion rates from adjacent basins. Locations of these samples are shown in Figure 14. In northern study area, bedrock outcrops from Mt. Carbine (NQBR-7) were compared to the adjacent Rifle Creek (NQ-8). Similarly, a bedrock sample from Gordonvale (NQBR-8) was compared to the adjacent Mulgrave River (NQ-13). We sampled exposed bedrock at the crest (PGBR-8) and ridgelines (PGBR-6 and PGBR-7) of the White Mountains (Great Dividing Range) and compared these to the erosion rate of Warrigal Creek on the eastern side (PG-5) and Torrens Creek on the western side (PG-4) of the Great Dividing Range.

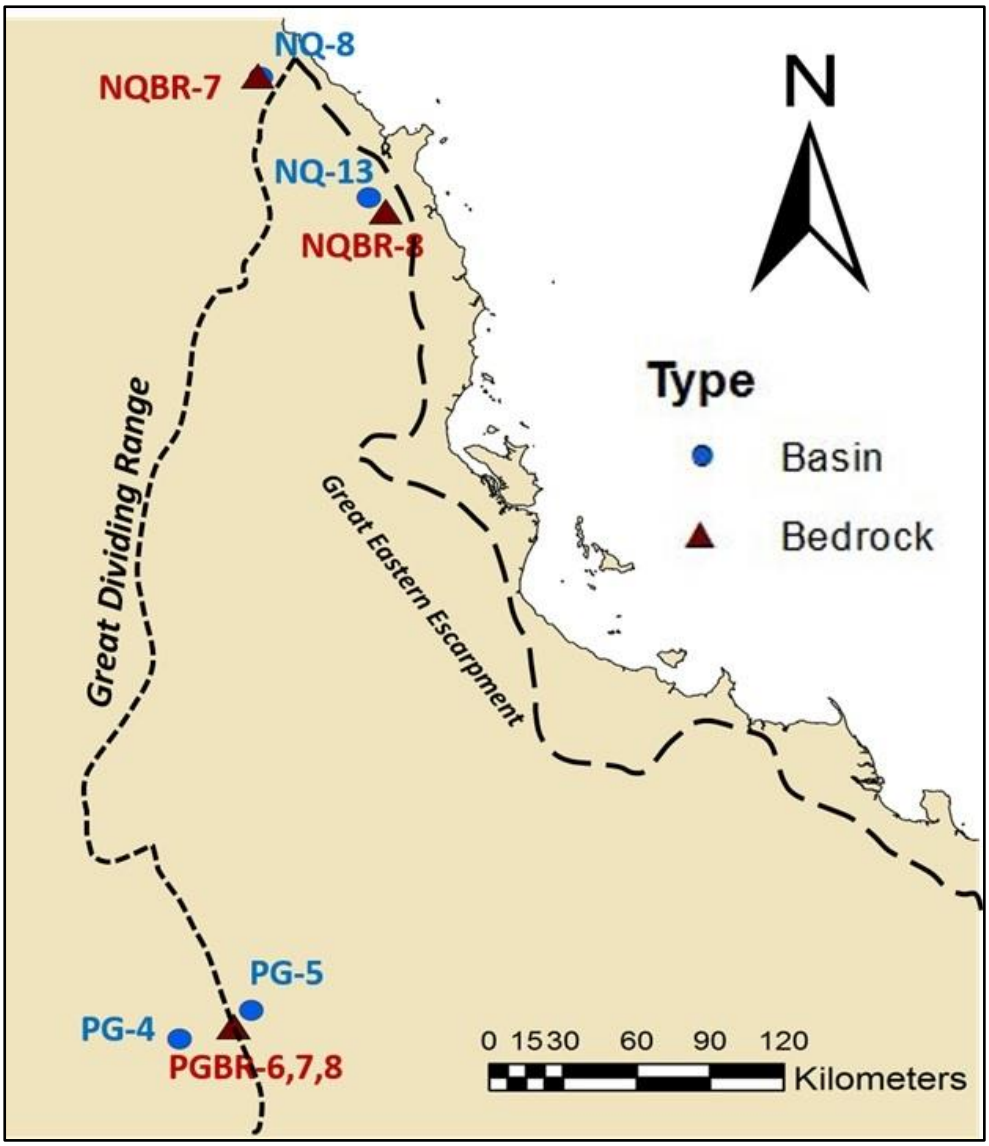

Figure 14: Location of bedrock samples and adjacent basin samples used for determination of rates of relief change.

3.5. Results

3.5.1. Basin-averaged erosion rate in north Queensland:

Erosion rates determined in this study ranged from 2.2m/My to 53.6m/My (Figure 15). The median erosion rate of basins in northern study area was 16.9m/My, whereas median erosion rate of basins from southern study area was 14.65m/My (Figure 16). When all north Queensland studies are considered, the median erosion rate of basins of northern study area is 16.2m/My, whereas that of southern study area is 12.6m/My (Figure 17).

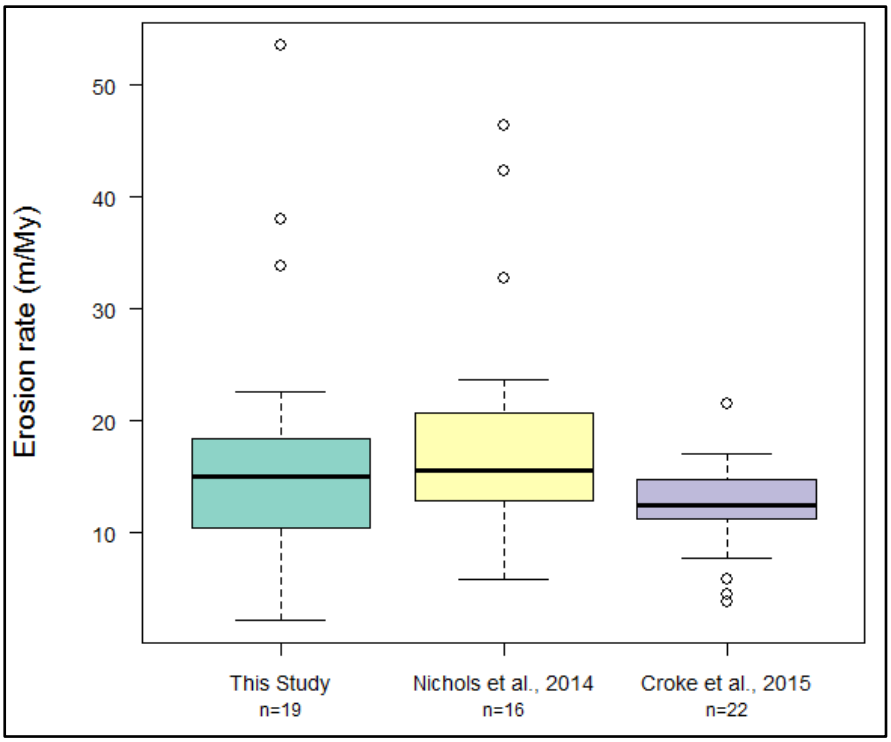

Figure 15: Box and whisker plots of erosion rates. The central thick line represents the median value, the edge of the box represents 25th percentile and 75th percentile, and the whiskers represents 1.5 times of the inter-quartile range. Blue box represents erosion rates from this study; yellow box represents erosion rates from Nichols et al., 2014; and purple box represents erosion rates from Croke et al., 2015.

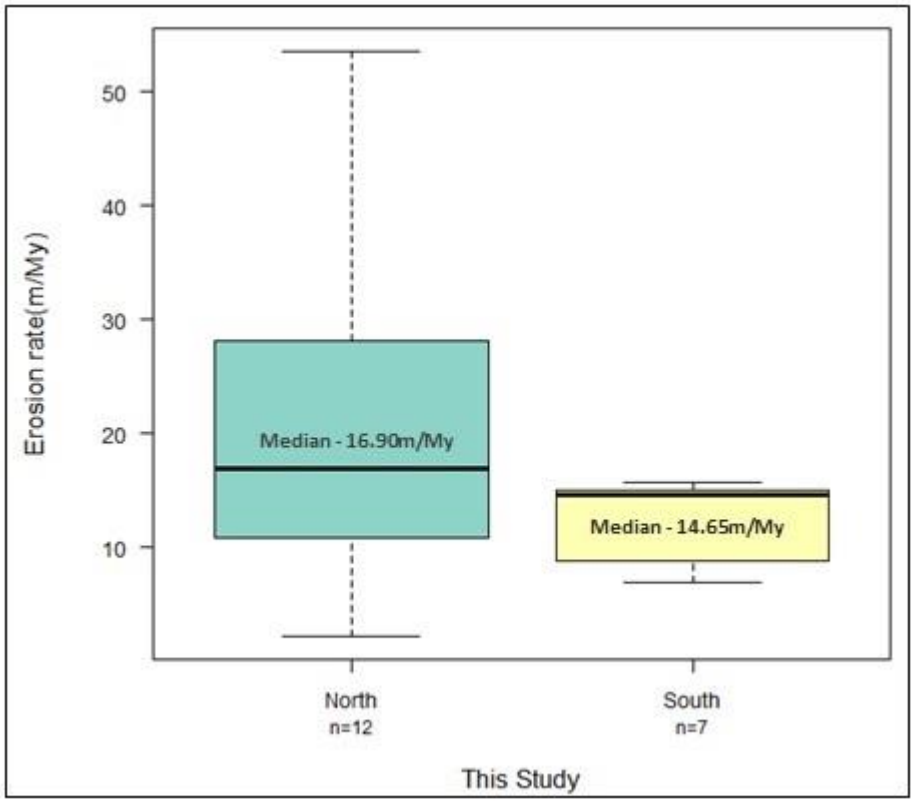

Figure 16: Box and whisker plot of erosion rate of northern and southern study area of this study. The central thick line represents the median value, the edge of the box represents 25th percentile and 75th percentile, and the whiskers represents 1.5 times of the inter-quartile range. Blue box represents erosion rates of northern study area and yellow box represents erosion rates of southern study area. Median erosion rate of northern study area is 16.9m/My and southern study area is 14.65m/My.

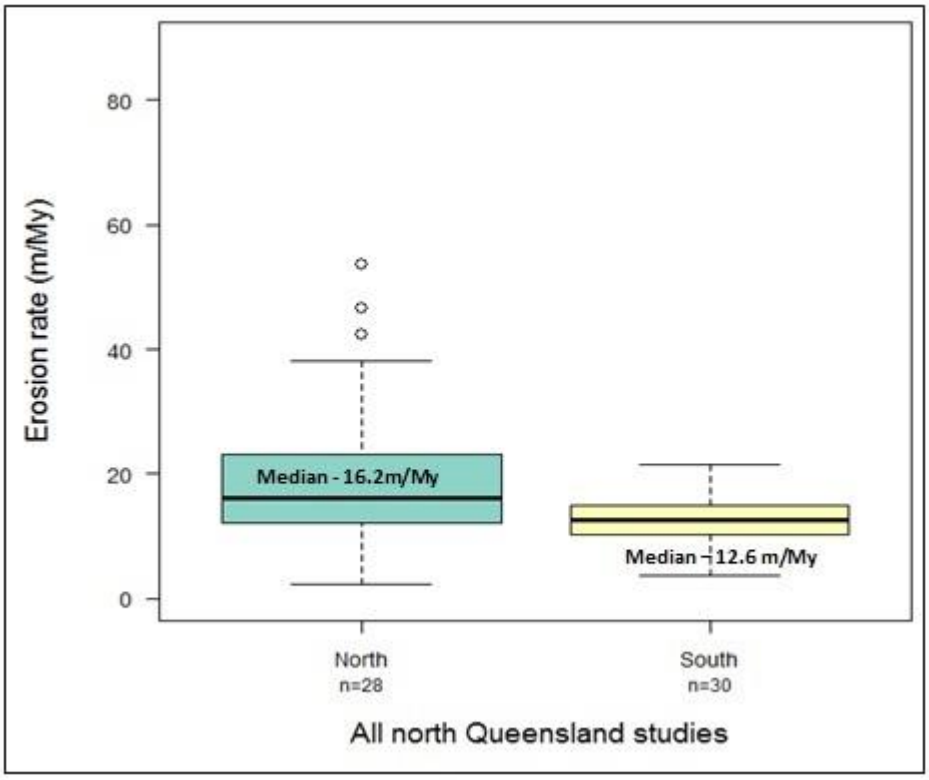

Figure 17: Box and whisker plot of erosion rates of northern and southern study areas from all studies of north Queensland combined (this study, Croke et al., 2015, and Nichols et al., 2014). The central thick line represents the median value, the edge of the box represents 25th percentile and 75th percentile, and the whiskers represents 1.5 times of the inter-quartile range. Blue box represents erosion rates from northern study area and yellow box represents erosion rates from southern study area. Median erosion rate of northern study area is 16.2m/My and southern study area is 12.6m/My.

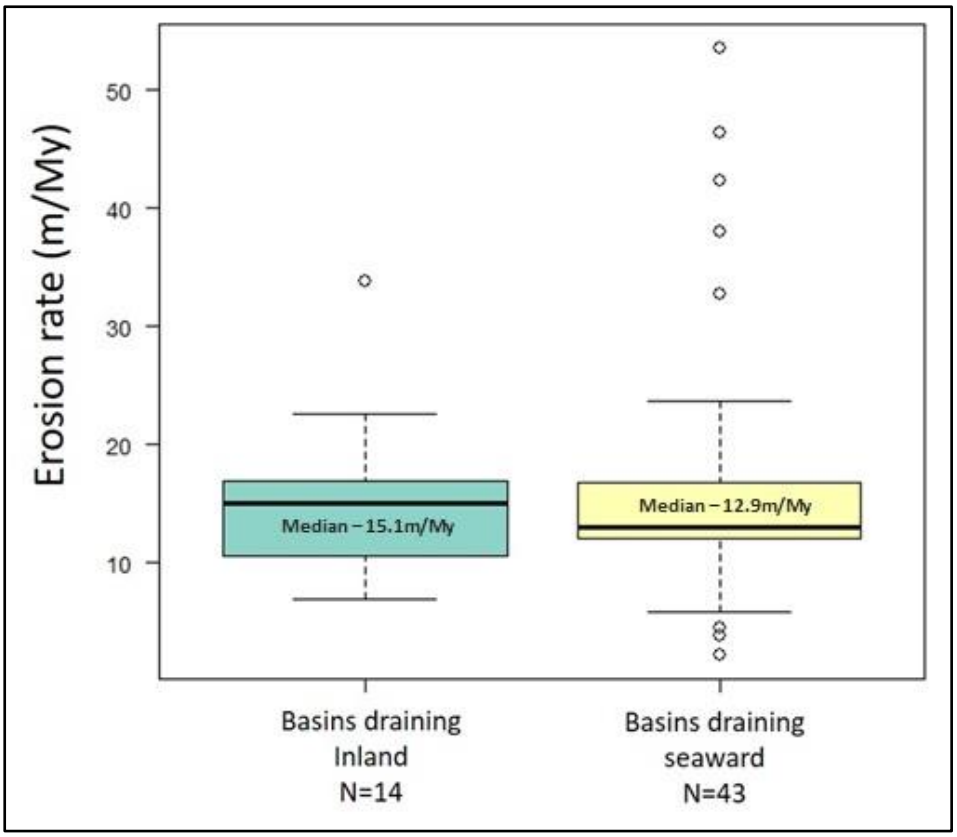

Figure 18: Box and whisker plot of erosion rates of all studies of north Queensland combined (this study, Croke et al., 2015, and Nichols et al., 2014). The central thick line represents the median value, the edge of the box represents 25th percentile and 75th percentile, and the whiskers represents 1.5 times of the inter-quartile range. Blue box represents erosion rates from basins draining inland and yellow box represents erosion rates from basins draining seaward.

3.5.2. Variables influencing erosion rate:

The erosion rate derived from the concentration of ^{10}Be for the basins from this study shows no statistically meaningful correlation with mean basin slope, when compared linearly (R^2 = 0.09 and p-value = 0.2 (Figure 19)). Erosion rates of the basins from this study exhibits a very strong and statistically significant correlation with mean annual precipitation (R^2 =0.71 and p-value = 6.5E-06) (Figure 19).

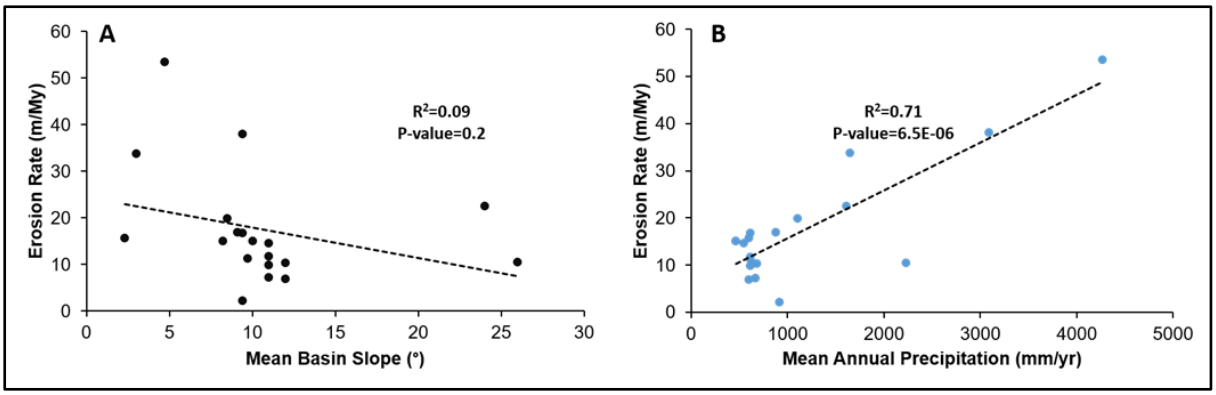

Figure 19: A. Erosion rate versus mean basin slope for samples from this study only. Black dotted line represents the trend-line between erosion rate and mean basin slope. B. Erosion rate versus mean annual precipitation for samples of this study only. Black dotted line represents trend-line between mean annual precipitation and erosion rate.

The correlation between mean annual precipitation and erosion rate of the basins from all ^{10}Be studies in north Queensland is represented in Figure 20 and the correlation between mean basin slope is represented in Figure 21. The correlation between mean annual precipitation and erosion rate of the upper Burdekin basins from Croke et al. (2015) yielded R^2 = 0.01; Nichols et al. (2014) yielded an R^2 = 0.06 (Figure 20). The correlation between mean basin slope and erosion rate of the basins from Croke et al. (2015) yielded R^2 = 0.06, and from Nichols et al. (2014) yielded R^2 = 0.35 (Figure 21). However, the correlation of mean basin slope and mean annual precipitation with erosion rate observed by Croke et al. (2015) improved when all sub-basin samples were included.

Erosion rates in north Queensland (this study, Croke et al., 2015; Nichols et al., 2014) exhibits moderately strong correlation (R^2=0.40; Figure 22) when compared to mean annual precipitation; whereas erosion rates from all other ^{10}Be studies in Australia (Godard et al., 2019; Croke et al., 2015; Nichols et al., 2014; Heimsath et al., 2010; Bierman et al., 2009; Heimsath et al., 2009; Heimsath et al., 2006; Heimsath et al., 2001; Heimsath et al., 2000) exhibit no correlation, (R^2=0.03; Figure 22) when compared with mean annual precipitation.

When mean basin slope is <11°, the correlation between erosion rates and precipitation in north Queensland yielded $R^2 = 0.48$; this contrast with an $R^2 = 0.18$ when mean basin slope was >11° (Figure 23).

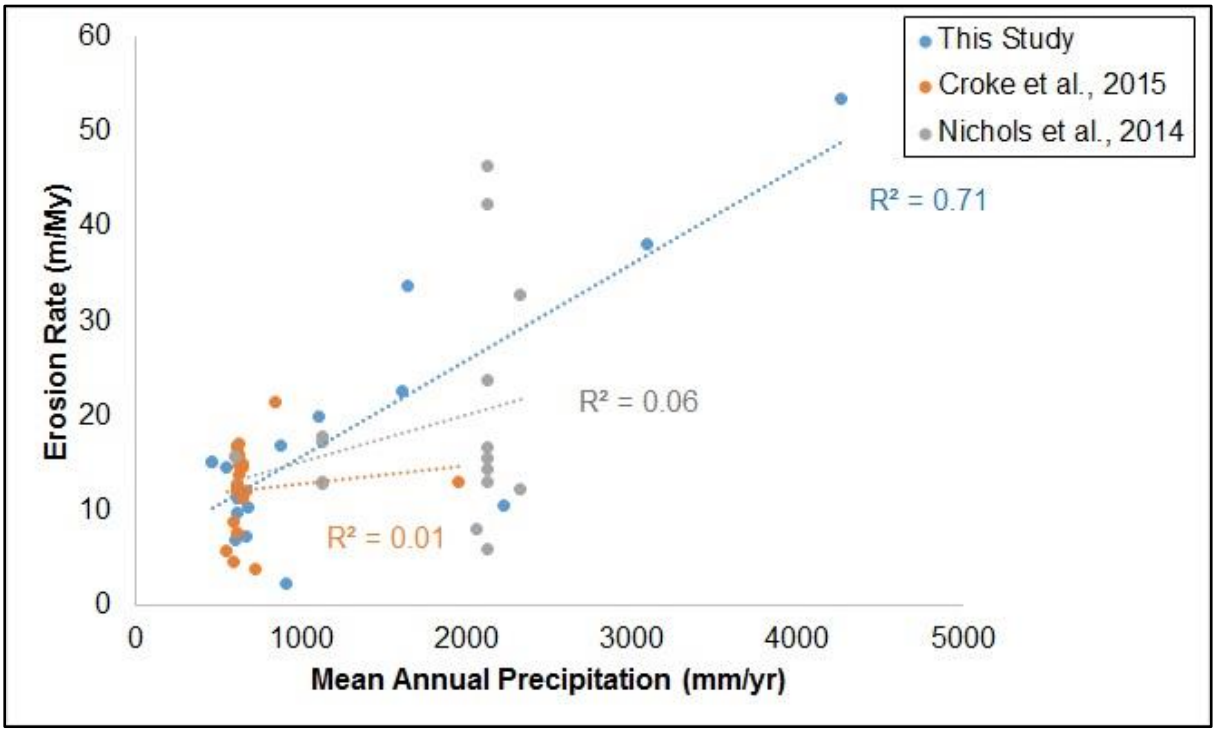

Figure 20: Erosion rate versus mean annual precipitation. Blue dots represents samples from this study, orange points represents samples from Croke et al., 2015, and grey points represents samples from Nichols et al., 2014.

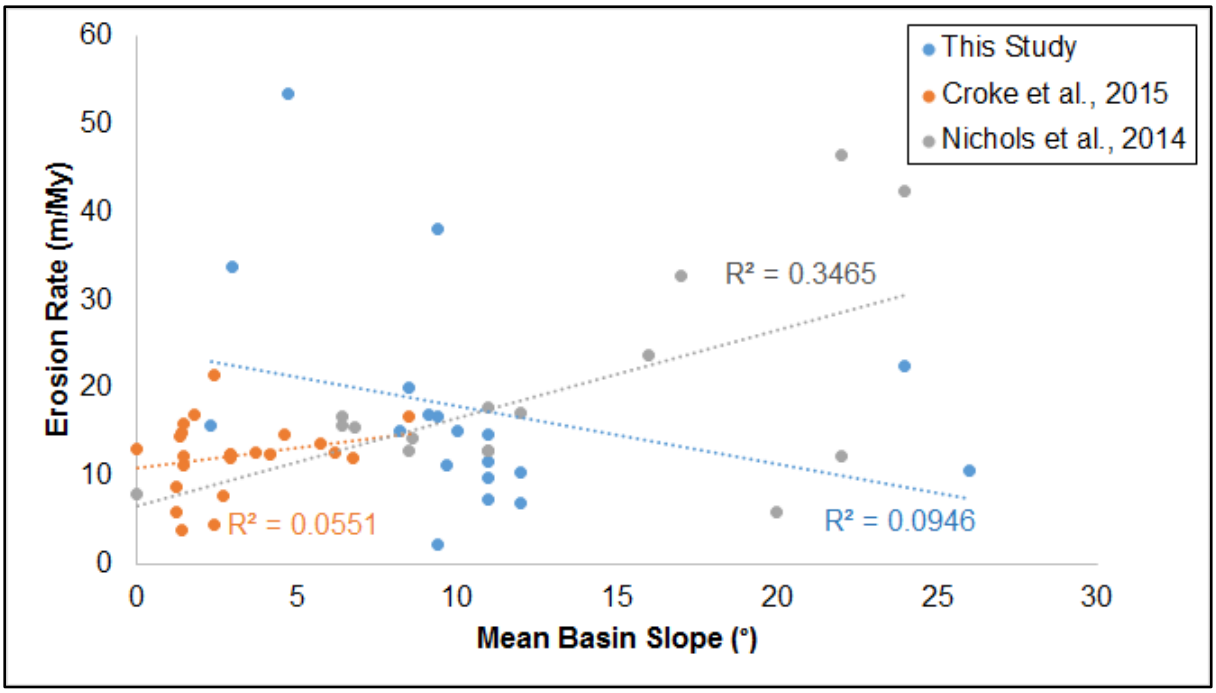

Figure 21: Erosion rate versus mean basin slope. Blue points represent samples from this study, orange points represents samples from Croke et al., 2015, and grey points represents samples from Nichols et al., 2014.

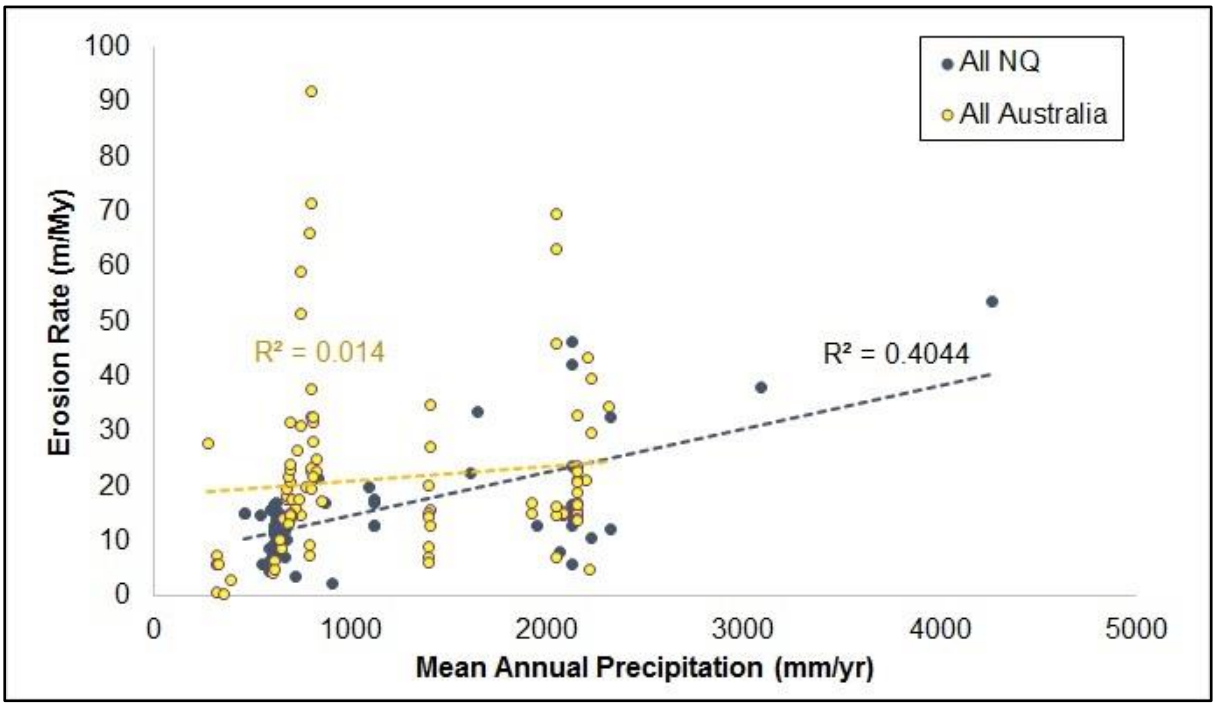

Figure 22: Erosion rate versus mean annual precipitation. Blue dots represent samples from this study, Croke et al., 2015, and Nichols et al., 2014. Orange dots represents samples from all other Australian ^{10}Be studies (Godard et al., 2019; Croke et al., 2015; Nichols et al., 2014; Heimsath et al., 2010; Bierman et al., 2009; Heimsath et al., 2009; Heimsath et al., 2006; Heimsath et al., 2001; Heimsath et al., 2000)

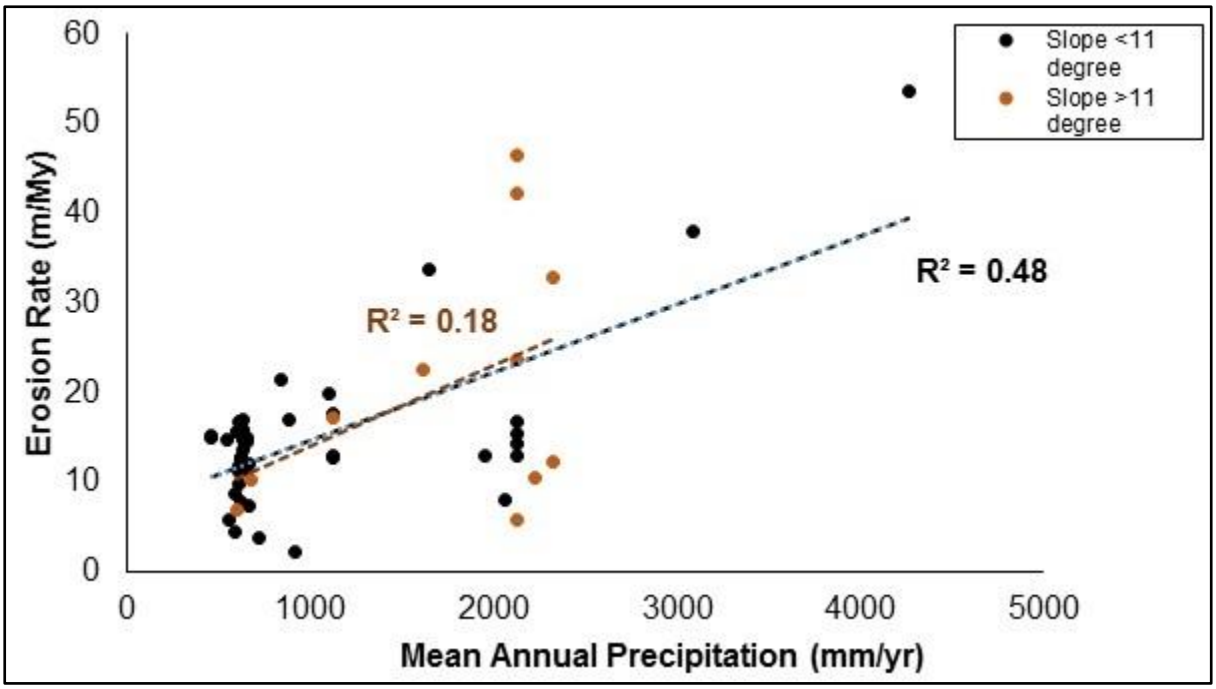

Figure 23: Erosion rate versus mean annual precipitation for all studies in north Queensland. Black points represent samples with mean basin slope < 11 degrees, orange points represent samples with mean basin slope >11 degrees.

Table 5: R^2 value of erosion rate and other parameters for this study, prior studies, and all of these combined.

Relation	R^2 value			
	This Study	Croke et al., 2015	Nichols et al., 2014	All north Queensland
Erosion vs Slope	0.09	0.06	0.35	0.09
Erosion vs Precipitation	0.71	0.01*	0.06	0.40
Erosion vs Precipitation (when slope<11°)	-	-	-	0.48
Erosion vs Precipitation (when slope>11°)	-	-	-	0.18

*This R^2 observed by Croke et al., 2015 improved significantly when only major sub-basin samples were included.

3.5.3. Bedrock erosion rate and comparison with basins:

The erosion rate of bedrock derived from concentrations of ^{10}Be ranged from 3.6 to 79.2m/My. The fastest erosion rate was observed at an outcrop sample from Porcupine Gorge National Park, whereas the slowest erosion rate was observed from an outcrop sample from Mount Carbine. The erosion rate of bedrock collected from northern study area (median-15.8m/My) was slower than the erosion rate of bedrock collected from southern study area (median- 37.6m/My)(Figure 24).

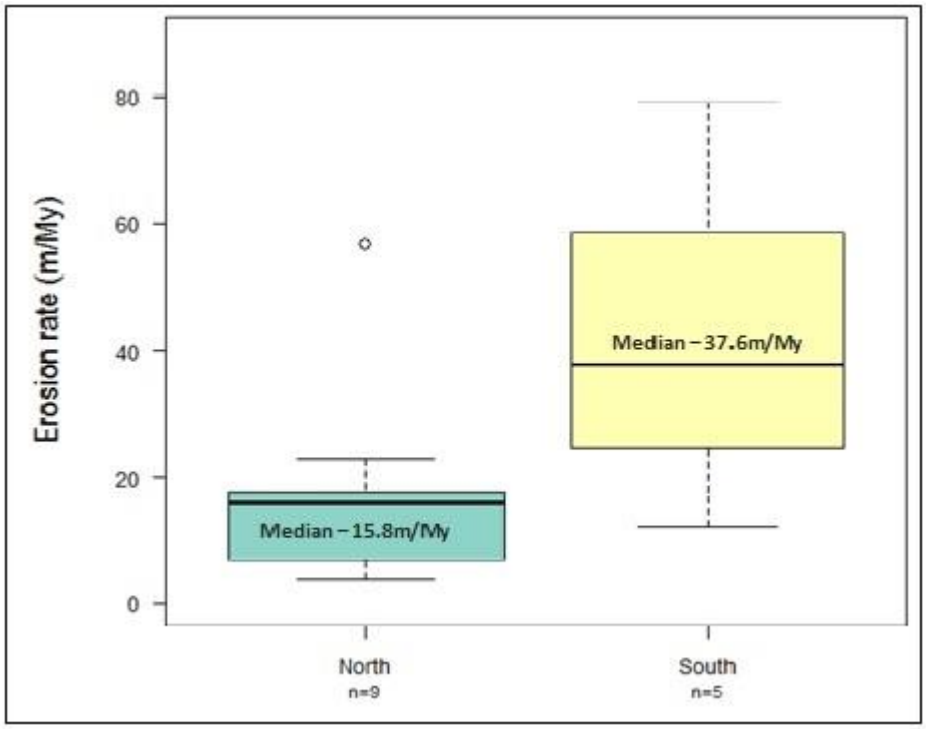

Figure 24: Box and whisker plot of erosion rates of bedrock from the northern and southern study areas from this study. The central thick line represents the median value, the edge of the box represents 25th percentile and 75th percentile, and the whiskers represents 1.5 times of the inter-quartile range. Blue box represents erosion rates from northern study area and yellow box represents erosion rates from the southern study area. Median erosion rate of bedrock collected from the northern study area is 15.8m/My, whereas median erosion rate of samples from the southern study area is 37.6m/My.

The erosion rate of all bedrock samples (median-17.3m/My) was higher than the erosion rate of basin samples from this study (median-15.1m/My) (Figure 25), as well as the erosion rate

of all basins in north Queensland (this study, Croke et al., 2015; Nichols et al., 2014)(median-14m/My) (Figure 26).

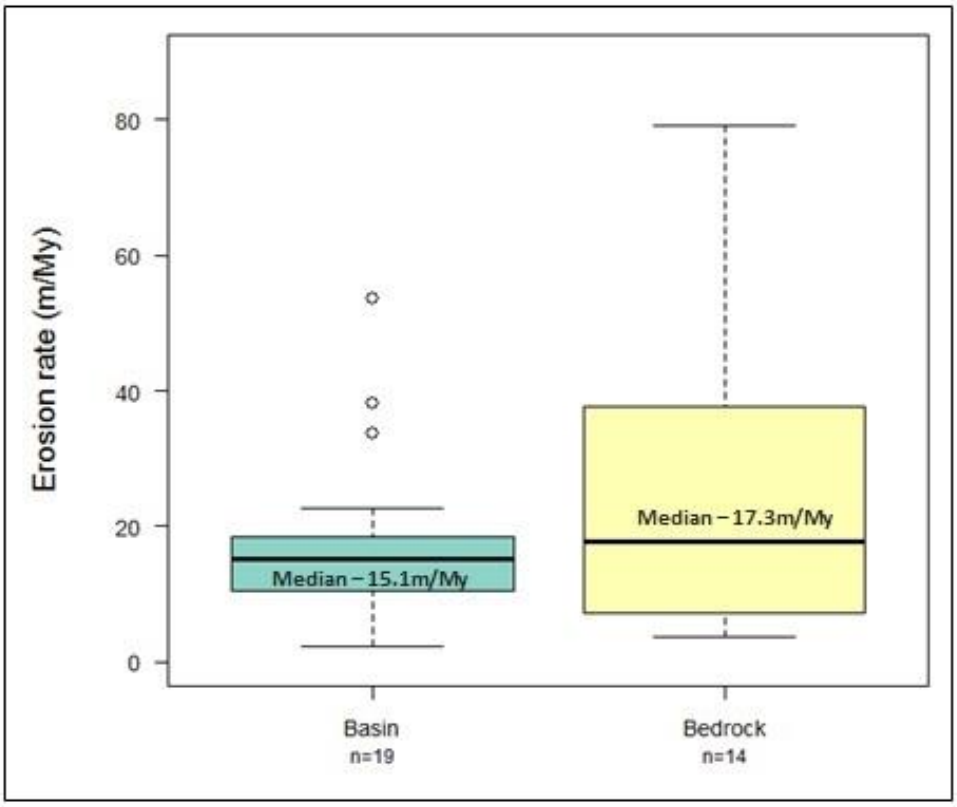

Figure 25: Box and whisker plot of erosion rates of basin and bedrock samples from this study. The central thick line represents the median value, the edge of the box represents 25th percentile and 75th percentile, and the whiskers represents 1.5 times of the inter-quartile range. Blue box represents erosion rate of basins and yellow box represents erosion rates of bedrock. Median erosion rate of all bedrock in this study is 17.3m/My, whereas median erosion rate of basin samples of this study is 15.1m/My.

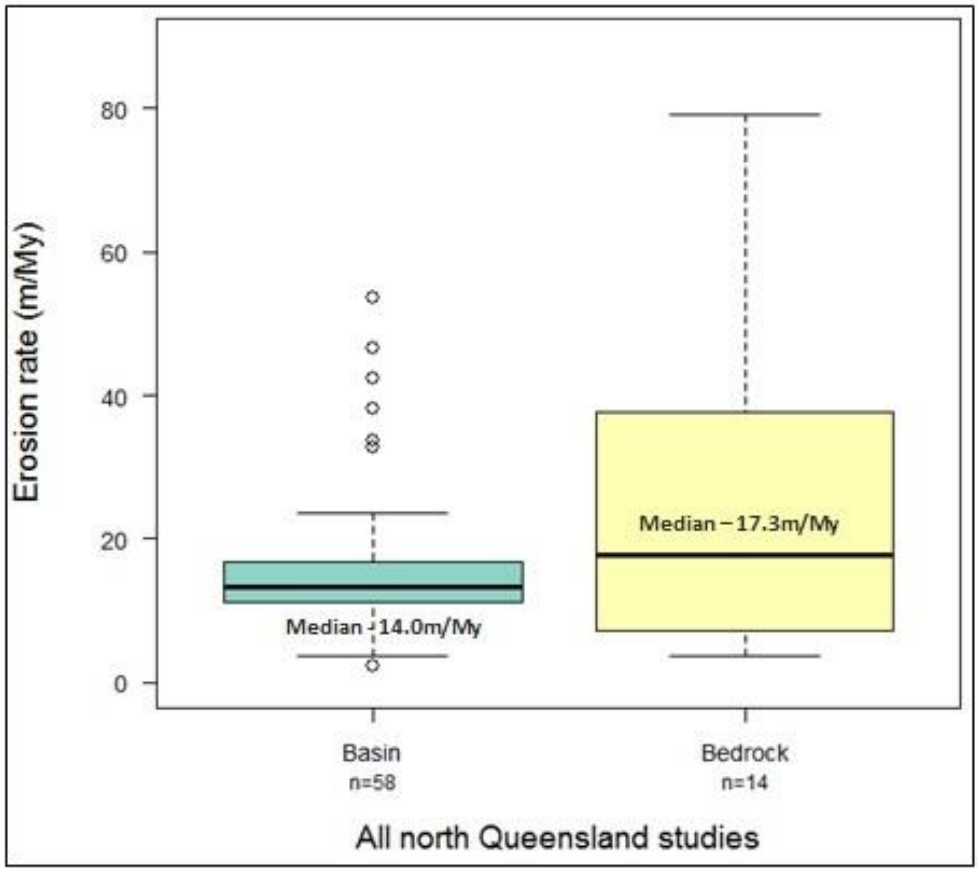

Figure 26: Box and whisker plot of erosion rate of basins and bedrock samples from all north Queensland studies (this study, Croke et al., 2015, and Nichols et al., 2014). The central thick line represents the median value, the edge of the box represents 25th percentile and 75th percentile, and the whiskers represents 1.5 times of the inter-quartile range. Blue box represents erosion rate of basins and yellow box represents erosion rates of bedrock. Median erosion rate from all bedrock in this study is 17.3m/My, whereas median erosion rate of all basin samples in north Queensland is 14m/My.

The influence of lithology on the erosion rate of bedrock was also examined. The erosion rate observed in sedimentary bedrock samples (median-30.9m/My) was higher than the erosion rate of granitic bedrock samples (median-11.4m/My) (Figure 27). The correlation between the erosion rate of bedrock and precipitation was also assessed, and no significant correlation was observed (R^2=0.08)(Figure 28).

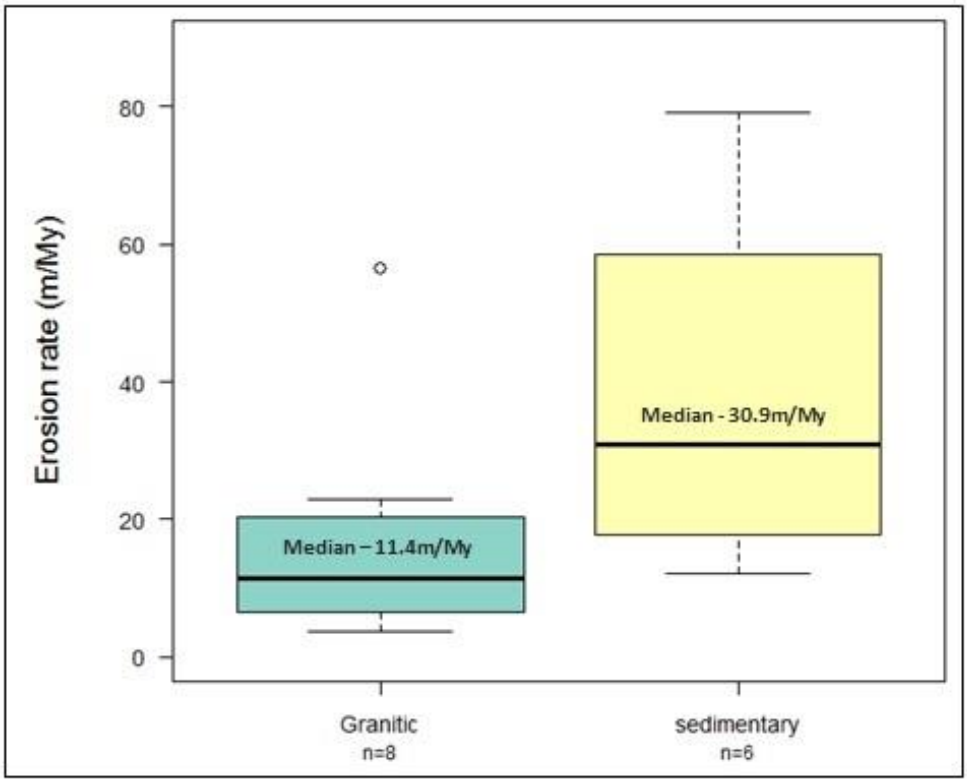

Figure 27: Box and whisker plot of the erosion rate of bedrock from granitic and sedimentary lithology from this study. The central thick line represents the median value, the edge of the box represents 25th percentile and 75th percentile, and the whiskers represents 1.5 times of the inter-quartile range. Blue box represents erosion rate of granitic rocks and yellow box represents erosion rate of sedimentary rocks. Median erosion rate of sedimentary bedrock is 30.9m/My, whereas median erosion rate of granitic bedrock is 11.4m/My.

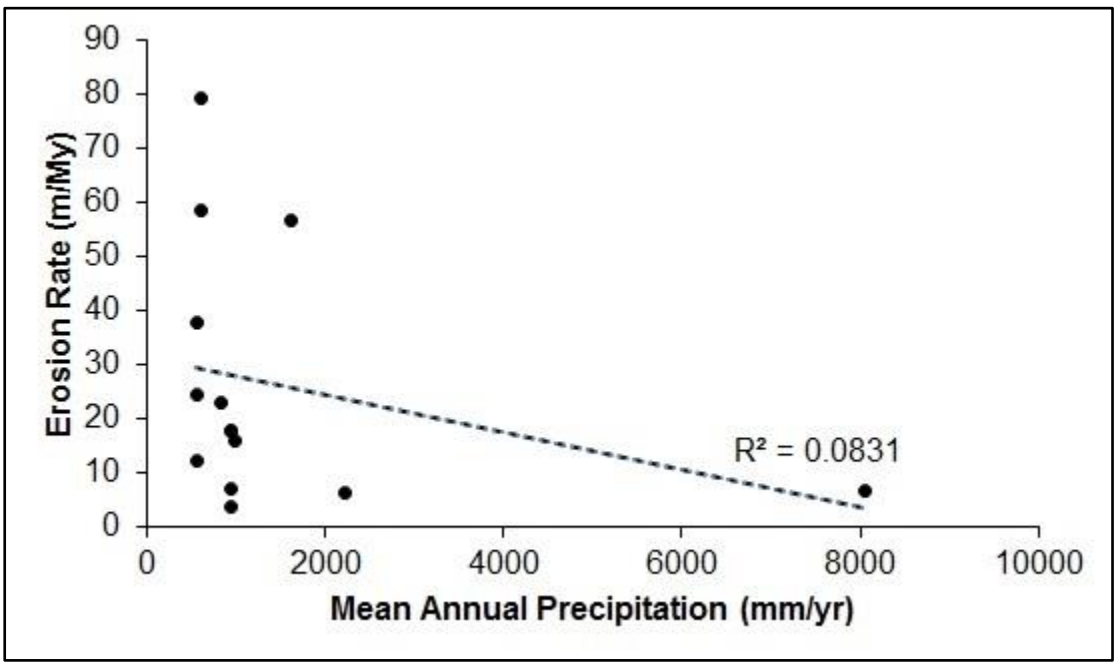

Figure 28: Erosion rate versus mean annual precipitation for bedrock samples. Black dotted line represents the trend-line between erosion rate and mean annual precipitation.

3.5.4. Relief generation and landscape transformation:

The erosion rate of adjacent bedrock and basin samples from both northern and southern study areas of north Queensland were compared (Figure 29). In the northern study area, a bedrock outcrop at Mt. Carbine (NQBR-7) erodes at the rate of 22.9m/My, higher than the adjacent Rifle Creek (NQ-8), which is eroding at a rate of 19.9m/My. Similarly, bedrock at Gordonvale (NQBR-8) erodes at the rate of 56.5m/My, which is faster than the adjacent Mulgrave River (NQ-13) which erodes at the rate of 33.8m/My. Ridgeline samples (PGBR-6 and PGBR-7) of the White Mountains erodes at rates of 12.1m/My and 37.6m/My, whereas a crest sample (PGBR-8) erodes at the rate of 24.2m/My. On the other hand, Warrigal Creek (PG-5) on the eastern side erodes at a rate of 7.27m/My and Torrens Creek (PG-4) on the western side erodes at a rate of 14.65m/My (Figure 29).

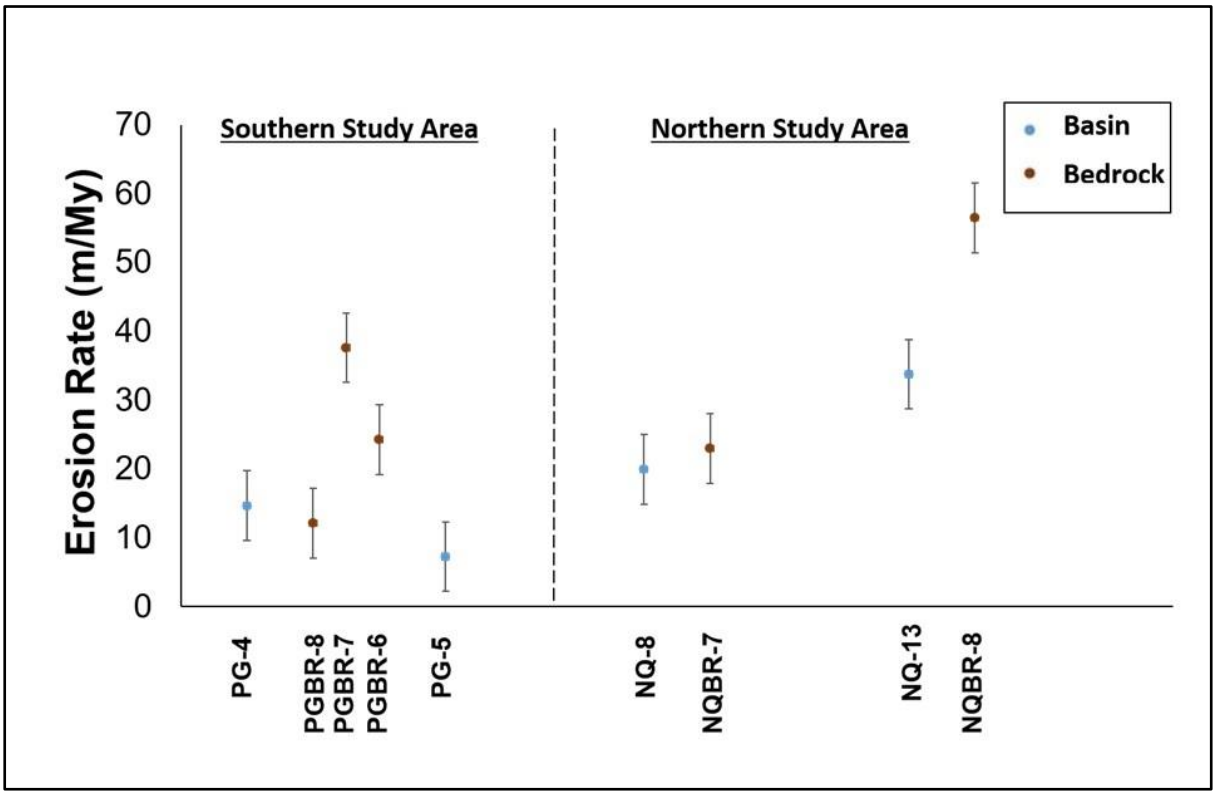

Figure 29: Erosion rate of various bedrock samples with their adjacent basin samples. Blue points represent basin samples and the dark-brown points represent bedrock samples. The vertical bar with the data label represents error. From right, the NQ-8, NQ-13, NQBR-7, and NQBR-8 samples are from northern study area, and the samples PG-4, PG-5, PGBR6, PGBR-7, and PGBR-8 are from southern study area.

3.5.5. Temporal variation in erosion rate:

The ^{10}Be concentration of the buried samples CN-2 and CN-3 were 1,220,519 atoms/gram and 254,644 atoms/gram, respectively. Using these concentrations, the decay constant, and burial time from equation-2, we calculated the initial concentration of ^{10}Be in these samples, and used these concentrations to derive erosion rate of the buried samples (Table 6). The paleoerosion rate of the buried sediment samples CN-2 and CN-3 is 1.45 ± 0.15m/My and 9.05 ± 0.73m/My, respectively (Table 6). The erosion rate of closest non-buried sample (BR-1) is 15.72 ± 1.34m/My. The erosion rate of another nearby non-buried sample (PG-2) is 6.93 ± 0.63m/My. Thus, the erosion rate of the buried and non-buried samples are not significantly different from each other.

Table 6: Erosion rate determined using ^{10}Be concentration obtained using radioactive decay formula

Sample	Present concentration(N)	Burial time (t)	Decay constant(λ)	λ t	$e^{-\lambda t}$	(N_o)	Erosion rate (m/My)
CN-2	1220519.276	20,000	0.0000005	-0.01	0.990049834	1232786	1.45±0.15
CN-3	254644.6019	20,000	0.0000005	-0.01	0.990049834	257203.8	9.05±0.73

Table 7: Erosion rate (m/My) and timescale for all samples of this study

Sample ID	Erosion rate(m/My)	Timescale (years)
BR1	15.72	37696.72981
CN2	1.82	325600.3256
CN3	10.72	55279.15976
PG1	15.06	39348.77773
PG2	6.93	85511.19662
PG3	15.09	39270.54954
PG4	14.65	40450.00632
PG5	7.27	81512.0485
PG6	10.31	57477.45806
PGBR2	58.54	10122.86629
PGBR3	79.22	7480.34073
PGBR6	12.1	48974.59443
PGBR7	37.6	15760.44129
PGBR8	24.21	24477.18268
NQ1	38.08	15561.78027
NQ2	16.83	35210.49273
NQ3	11.73	50519.40261
NQ4	11.22	52815.73909
NQ5	9.82	60345.47786
NQ6	2.23	265736.5886
NQ7	16.94	34981.85316
NQ8	19.96	29689.00764
NQ9	10.52	56330.09435
NQ10	22.57	26255.76396
NQ11	53.56	11064.08873
NQ13	33.76	17553.09812
NQBR1	17.82	33254.35424
NQBR2	7.07	83817.9056
NQBR3	3.57	165992.3229
NQBR4	17.75	33385.49817
NQBR5	15.75	37624.92651
NQBR7	22.94	25832.2839
NQBR8	56.49	10490.22115
NQBR9	6.68	88711.46596
NQBR10	6.28	94361.8778
Croke-Hillslope	13.02	45514.02401
Croke-1	11.28	52534.80431
Croke-2	14.51	40840.28895
Croke-3	14.94	39664.83217
Croke-4	12.23	48454.01411
Croke-5	7.73	76661.3962
Croke-6	15.9	37269.97438

Croke-7	16.73	35420.95592
Croke-8	17.04	34776.5606
Croke-9	12.66	46808.26166
Croke-10	13.71	43223.38385
Croke-11	14.72	40257.64895
Croke-12	12.39	47828.29642
Croke-13	12.75	46477.8504
Croke-14	12.12	48893.77827
Croke-15	12.39	47828.29642
Croke-16	12.54	47256.18761
Croke-17	12	49382.71605
Croke-18	21.47	27600.95913
Croke-19	3.76	157604.4129
Croke-20	8.81	67263.6314
Croke-21	5.81	101995.2827
Croke-22	4.53	130815.1419
QLD1	15.64	37889.55196
QLD2	16.76	35357.55326
QLD3	32.76	18088.90698
QLD4	12.35	47983.20588
QLD5	14.36	41266.89363
QLD6	5.83	101645.3847
QLD7	17.75	33385.49817
QLD8	17.16	34533.36787
QLD9	12.8	46296.2963
QLD9xb	12.96	45724.73708
QLD10	12.96	45724.73708
QLD11	15.5	38231.78017
QLD12	23.68	25025.02503
QLD13	46.47	12752.15392
QLD14	42.31	14005.97004
QLD15	7.97	74352.89744

3.6. Discussion

3.6.1. Slow erosion rates in north Queensland

The results of this study suggest that, compared to other parts of the world with similar precipitation, erosion rates in north Queensland are slow. The median erosion rate of other parts of the world within a similar precipitation bracket (400-4000mm/yr) is at least 5 times higher than the median erosion rate of north Queensland's basin (Figure 30). This is in agreement with studies conducted in other parts of Australia, which also concluded that erosion rates in Australia are uniquely slow (Heimsath et al., 2010; Heimsath et al., 2006). The uniformly slow erosion rates of erosion across Australia is likely due to the tectonic stability of the continent (Pillans & Fifield, 2013; Belton et al., 2004; Bierman & Caffee, 2002) and is observed across Australia despite different types of rock and across variable slopes (Heimsath et al., 2010; Heimsath et al., 2006; Pillans & Fifield, 2013; Belton et al., 2004).

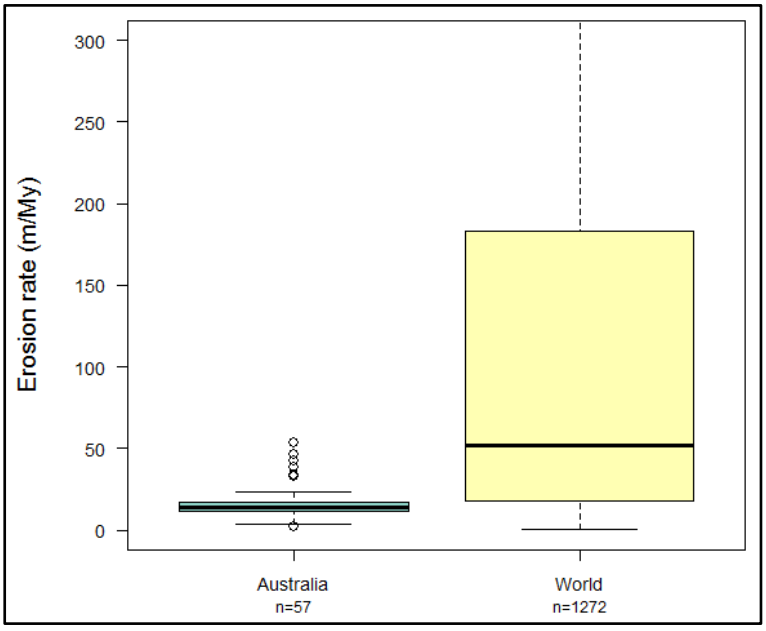

Figure 30: Boxplot of erosion rate of basins from north Queensland and basins from other parts of the world within a similar bracket of precipitation. The blue box represents north Queensland basins, including site from this study, Croke et al., 2015 and Nichols et al., 2014. Yellow box represents sites from all over the world with mean annual precipitation between 400-4000mm/yr.

3.6.2. Influence of storage and sediment remobilization:

One of the primary assumptions in determining erosion rate from ^{10}Be concentration is that the erosion rates are uniform throughout the basin and that the basin is in isotopic steady state. Most samples from this study were collected from landscapes that are tectonically stable, especially in southern study area. Additionally, most of the sampling sites lacks evidence of episodic sediment discharge events such as landslides. However, most sites are located in low-gradient areas and sediment storage may affect the basin-average erosion rate by leading to excess accumulation of ^{10}Be concentration, which can result in an underestimation of the basin-average erosion rate (Croke et al., 2015; Bierman & Steig, 1996; Granger et al., 1996; Brown et al., 1995b). Most samples in this study were collected from small drainage areas. In small drainage areas, sediments are delivered directly to the drainage network, thereby restricting any potential effects of sediment storage or remobilization on ^{10}Be inventory. Furthermore, Croke et al. (2015) found nested drainage networks of the Burdekin River catchment have consistant ^{10}Be concentrations, thereby suggesting uniform erosion rate.

In northern study area, Nichols et al. (2014) concluded that approximately 40% of sediment generated in the Barron River catchment is stored in the catchments, indicating that the likelihood of storage is higher in northern study area. More information about the residence time of the sediments and storage history can be obtained by using more than one cosmogenic nuclide, and often ^{26}Al is used along with ^{10}Be (Clapp et al., 2002; Clapp et al., 2000; Granger et al., 1996; Lal, 1991). In this study, we have processed ^{26}Al for all samples, and are awaiting results.

3.6.3. Sediment yield:

The mean basin erosion rate reported here is approximately 15.9 m/My, which is equivalent to approximately 49.3 $t.km^{-2}.yr^{-1}$ of sediment, assuming a rock density of 2.7 $g.cm^{-3}$ (Kirchner et al., 2001; Schaller et al., 2001). The corresponding sediment yield from northern study area is 43.74 $t.km^{-2}.yr^{-1}$, whereas from southern study area is 34.02 $t.km^{-2}.yr^{-1}$. This sediment yield is lower than contemporary sediment yield for the catchments of GBR, which are approximately 66 $t.km^{-2}.yr^{-1}$ (Nichols et al., 2014; Prosser et al., 2001; Neil, 1995). This is not surprising as it is suggested that sediment generation has likely increased after European settlement (Brodie et al., 2012; Hughes et al., 2009; Furnas, 2003; Brodie, 2002). However, the difference between ^{10}Be-derived sediment yield and contemporary sediment yield is not large and is similar to the finding of Nichols et al. (2014). Nichols et al. (2014) suggest that the reason for similar sediment yields across timescales is that much of the anthropogenic increase in sediment is stored. Such sediment might remobilise during the next extreme event (Tomkins et al., 2007). More widespread estimates of background erosion rate and sediment storage from other catchments draining to the GBR is required to understand how extreme events and storage impact sediment delivery to the GBR.

3.6.4. Influence of mean basin slope:

The results of this study suggest that the correlation between erosion rate derived from ^{10}Be concentration and mean basin slope is weak (R^2= 0.09) for the basins of this study (Figure 19). This is surprising because many studies recognize mean basin slope as significantly correlated with ^{10}Be-derived erosion rate (e.g. Nichols et al., 2014; Placzek et al., 2014; Carretier et al., 2013; Willenbring et al., 2013; Portenga & Bierman, 2011; von Blanckenburg, 2005). In a global compilation of ^{10}Be-studies in Chapter-2 of this thesis (Mishra et al., 2019) and several other studies, mean basin slope emerged as the single variable with strongest influence on erosion rate at global scale. Similarly, Nichols et al.

(2014) in their study of the Barron River catchments of north Queensland found a strong correlation (R^2=0.35) between erosion rate and mean basin slope. This correlation observed in Nichols et al. (2014) is likely because the sampling area of that study focused on the eastern escarpment and incorporated higher slopes areas (up to ~25°). In contrast, the mean basin slope of samples locations from this study ranged from ~2° to 26°, but only 2 samples (i.e. NQ-9 and NQ-10) have mean basin slopes >20°. All remaining samples from this study were collected from areas with mean basin slopes <13°. Our results are similar to results from the low-gradient Burdekin River catchment of north Queensland (Croke et al. 2015), where a weak correlation between mean basin slope and erosion rate was observed.

The absence of a strong influence of mean basin slope on ^{10}Be-derived erosion rates in north Queensland is in agreement with findings of Chapter-2 of this thesis (Mishra et al., 2019) and Willenbring et al. (2013), which found that when slope is less than 200m/km or ~11°, the influence of mean basin slope on erosion rate is not clear and other variables have more influence on erosion rate. Furthermore, the lack of slope's influence on erosion rate may be because high slope and fast uplift are often linked, and relatively speaking, Australia is tectonically stable and the influence of mean basin slope on erosion rate may be limited to tectonically active landscapes (Montgomery & Brandon, 2002; Montgomery, 2001).

3.6.5. Influence of lithology:

Lithology influences the erosion rate of both basin and bedrock samples. Basins from the northern study area (dominated by granitic rocks) eroded faster when compared to basins from the southern study area (dominated by sedimentary rocks). In contrast, bedrock samples from northern study area (granitic rocks) eroded more slower compared to bedrock from the southern study area (sedimentary rocks).

In general, granites are more resistant to erosion than sedimentary rocks (e.g. Jessup et al., 2011; Granger et al., 2001b; Small et al., 1999). However, Croke et al. (2015) found that the erosion rate of drainage basins were higher when the percentage of granitic rocks was high. A situation where granitic rocks erode faster than sedimentary rocks might be due to higher rates of chemical weathering in tropics as temperature and runoff strongly influence the rate of chemical weathering in granitic rock (Oliva et al., 2003; Sverdrup & Warfvinge, 1995; White, 1994) because of the presence of easily weatherable minerals (such as feldspar, mica, apatite etc.). As such the suggestion by Croke et al. (2015) that in north Queensland granitic rocks erode more quickly than sedimentary rocks requires further investigation. However, we take a different approach and examine the effects of lithology on erosion rates in north Queensland only from bedrock samples. This is because, given the strong correlation between faster erosion rate from northern study area (which is dominated by granitic rocks) and higher precipitation, it is possible that the relationships between lithology and erosion rate in basin samples in the region are compounded by other variables.

Granitic bedrock samples from the northern study area eroded more slowly than sedimentary bedrock samples from the southern study area. This suggests that this situation in north Queensland is consistent with previous studies that have observed that sedimentary rocks generally erode faster than granitic rocks (e.g. Portenga & Bierman, 2011). Portenga and Bierman (2011) found that sedimentary outcrops erode approximately 2.5 times faster than igneous outcrop; and within Australia, granitic rocks erode approximately 2.7 times more slowly. In this study, granitic rock eroded 2.7 times more slowly than sedimentary rocks.

3.6.6. Influence of mean annual precipitation:

Influence of precipitation on erosion rates in north Queensland is strong and clear. This study suggests that mean annual precipitation correlates strongly with ^{10}Be-derived erosion rate (R^2=0.71) (Figure 19). This strong correlation is observed in spite of samples that were

collected from various lithologies and across different slopes. We speculate that if homogenous rock types were sampled, precipitation's influence will be stronger.

The strong correlation between mean annual precipitation and ^{10}Be-derived erosion rate observed in this study is consistent with Heimsath et al. (2010), who suggested a strong climatic influence on erosion rates within Australia. Locally, these results contrast with Croke et al. (2015), who did not find a strong correlation between mean annual precipitation and ^{10}Be-derived erosion rates for the Upper Burdekin, and observe only a moderate correlation when sub-basin samples were included. This might be due to the fact that range of precipitation explored by Croke et al. (2015) is smaller than the range of precipitation explored in this study. However, Nichols et al. (2014) also did not observe a strong correlation between precipitation and erosion, despite being in northern study area, where precipitation is high. This might again be due to a narrow range of precipitation, coupled with high mean basin slope in that study. Indeed, ~55% of samples from Nichols et al. (2014) were collected from the escarpment, mean basin slope was usually >11° or 200m/km. When the mean basin slope is approximately >11° or 200m/km, precipitation's influence on ^{10}Be-derived erosion rate is clear and strong (e.g. Mishra et al., 2019; Willenbring et al., 2013). When all basins of north Queensland are considered, a moderately strong correlation is observed between basin erosion rate and mean annual precipitation (R^2=0.4). This is likely due to the wide range of precipitation gradients that these basins experiences.

This strong influence of precipitation on erosion rate is consistent with the observation of Chapter-2 (Mishra et al., 2019), who found that when mean basin slope's influence on erosion rate is weak, mean annual precipitation will have a stronger influence. In this case, where a weak correlation is observed between mean basin slope and erosion rate (R^2=0.09 for this study; R^2=0.08 for all of north Queensland), a strong correlation between mean annual precipitation and erosion rate is observed (R^2=0.71 for this study; R^2=0.40 for all of North

Queensland) (Table 5). This further suggests that even though basins in north Queensland erode slowly compared to rest of the world, this is not because of the weak influence of precipitation on erosion rates in north Queensland. The reason north Queensland erodes slowly despite higher precipitation is its tectonic stability and/or low-gradient/low-relief landscapes.

Although mean annual precipitation influences erosion rate of basins in north Queensland, its influence on bedrock erosion rate is almost negligible (R^2=0.08). Elsewhere in Australia, some influence is observed. For example, Bierman and Caffee (2002) concluded that an increase in mean annual precipitation increased the lowest calculated granite erosion rate of inselbergs on the Eyre Peninsula (Bierman & Caffee, 2002), and Quigley et al. (2007a) inferred that the rate of chemical and physical weathering of bedrock increases with an increase in precipitation. The absence of precipitation's influence on bedrock erosion rate in this study might be due to the strong influence of lithology.

Steady state in north Queensland:

The role of precipitation and slope observed in various ^{10}Be studies is often related to whether landscape has obtained steady state (DiBiase & Whipple, 2011; DiBiase et al., 2010). A landscape that is in steady state will be more influenced by factors like slope, whereas if the landscape is in transition, its erosion rate will be influenced by factors such as precipitation (DiBiase & Whipple, 2011; von Blanckenburg, 2005). A question naturally arises as to if sites from north Queensland are strongly influenced by mean annual precipitation because these sites are not in steady state. However, the overall tectonic stability of Australia supports that the landscape is in steady state. Furthermore, Heimsath et al. (2009) found that ^{10}Be concentrations have attained stead-state in Arnhem Land, Australia. Another approach to verify if erosion rates are consistent or not is through a comparison of present erosion rate with paleoerosion rates.

The similarity of erosion rates from buried and non-buried samples suggests that erosion rates in the study area have been consistently slow. The average timescale of erosion rate of basins in north Queensland is ~54,000 years (Table 7). The consistency of erosion rates between modern and 20,000 year old samples also suggests that there are negligible changes in sediment supply and transport in the region over a timescale of approximately 7,000 to 325,000 years.

3.6.7. Implications for landscape evolution and relief generation:

Usually, basins erode either at the same rate or faster than the bedrock outcrops (Portenga et al., 2013; Portenga & Bierman, 2011). This is because bedrock is usually more resilient in comparison to material found under soil and/or because the most resistant rocks are inherently the ones to crop out in a steady-state landscape. However, in north Queensland bedrock samples erode faster than the drainage basins (Figure 25 and Figure 26). In order to generate relief in catchments, rates of erosion in basins must be higher than the adjacent bedrock surface (Quigley et al., 2007a), and if the bedrock in the region continues eroding faster than adjacent basins, relief will not be generated but will be lost over the long term.

In spite of this, the north Queensland landscape has a large escarpment, mountain ranges, and ridgelines that are incised by steep and narrow gorges. Relief features in other parts of Australia, such as Flinders Range might have developed in response to the uplift rate and the intraplate tectonism during and after the terminal Miocene (Célérier et al., 2005; Sandiford, 2003). However, unlike north Queensland, these parts of Australia are actively generating relief (Quigley et al., 2007a). The presence of several steep gorges in north Queensland (e.g. Porcupine Gorge, Barron Gorge, Tully Gorge etc.) suggests another possible mechanism of formation of relief features in north Queensland, fluvial incision. This type of incision (Quigley et al., 2007a; Quigley et al., 2006) is more likely when large amount of coarse material is transported during large stream discharges, usually associated with large-scale

flood events. Thus, it is probable that the steep gorges of north Queensland were formed through large flood events, as opposed to hillslope evolution.

3.7. Conclusion and Implication

This study uses the terrestrial cosmogenic nuclide ^{10}Be to determine erosion rates for drainage basins and bedrock of north Queensland. The results of this study found that rates of erosion are very slow in north Queensland, like rest of the Australia. The rate of erosion of basins from this study are consistent with those reported by previous studies in north Queensland (Croke et al., 2015; Nichols et al., 2014) and suggest that basins in north Queensland erodes more slowly than other part of the world, despite similar precipitation. This slow erosion is not because the influence of precipitation on erosion rate is weak. Instead, the influence of precipitation on erosion rates in north Queensland is strong and clear (R^2=0.71). This strong influence of precipitation in north Queensland is significant, because very few regional to local scale studies observe such a strong correlation between precipitation and erosion rate. This furthers the assertion that even though precipitation might not be the primary influence on ^{10}Be-derived erosion rate on global scale (Mishra et al., 2019), its influence can be dominant on regional/local scale. The strong influence of precipitation on erosion rates in north Queensland also adds more constraints on the relationship between erosion and precipitation in tropical and subtropical areas.

This study also concludes that rock type has a significant influence on erosion rate in north Queensland, especially on bedrock erosion rate. Sedimentary rocks in north Queensland erode ~2.7 times faster than granitic rock types, which is consistent with the findings of Portenga and Bierman (2011).

This one of the first studies in north Queensland to determine bedrock erosion rates, and compare these rates to the basin erosion rates. Bedrock erosion rates are faster than basin

erosion rate in north Queensland, implying that relief is lost over the long-term in north Queensland. Erosion rates in north Queensland have been slow and consistent for approximately 10^3 to 10^5 years, indicating that Australian landscape have also attained steady state. Thus, the strong influence of precipitation on erosion rates in north Queensland is not because the landscape is in transition and suggest that precipitation may influence erosion rates across a variety of landscape types.

Chapter 4: New radiocarbon age constraints for the 120 km long Toomba flow, north Queensland, Australia

[This chapter is published as **Mishra, A. K., Placzek, C., Wurster, C., & Whitehead, P. W. (2018). New radiocarbon age constraints for the 120 km-long Toomba flow, north Queensland, Australia.** ***Australian Journal of Earth Sciences*****, 1-9. doi:10.1080/08120099.2019.1523227]**

4.1. Abstract

The Toomba flow is the youngest flow of the Nulla volcanic province, located in north Queensland. This 120 km long flow has a published $^{40}Ar/^{39}Ar$ age of 21 000 ± 3000 years. In contrast, seven conventional radiocarbon (^{14}C) analyses of carbon-bearing material beneath the flow yielded radiocarbon ages of 16 000 to <2500 BP. Published radiocarbon ages are younger than the $^{40}Ar/^{39}Ar$ age, potentially due to contamination of the charcoal by younger carbon that was not removed by acid-base pre-treatment methodology used. We have, therefore, re-examined the radiocarbon age of Toomba flow using newly sampled charcoal buried beneath the Toomba flow in combination with hydrogen pyrolysis pre-treatment and accelerated mass spectrometer (AMS) measurements. We determined a calibrated radiocarbon age of 20 815–19 726 calBP (2σ) for the material beneath the Toomba flow. Our radiocarbon age, therefore: (1) is older than previous radiocarbon ages for the Toomba flow, (2) provides the most precise age yet available for the Toomba flow, (3) is in agreement with the $^{40}Ar/^{39}Ar$ age, and (4) validates that hydrogen pyrolysis is a robust and effective pre-treatment method, for subtropical conditions where samples are susceptible to contamination by younger carbon. The Toomba flow erupted during the Last Glacial Maximum, but the preserved surface suggests that the rate of weathering and soil formation has been almost negligible in this region on this flow, despite being situated in a subtropical climate that experiences highly variable often intense rainfall.

4.2. Introduction

Quaternary volcanism is important to understanding tectonic and/or geomorphic histories of a region (e.g. Blondes, Reiners, Edwards, & Biscontini, 2007; Wagner, 1998; Zreda, Phillips, Kubik, Sharma, & Elmore, 1993). It also provides crucial information about crustal and mantle geochemistry (e.g. Blondes et al., 2007; Wheller, Varne, Foden, & Abbott, 1987). Additionally, weathering and erosion of basalt impacts nutrient cycling and the chemical composition of seawater (e.g. Chadwick, Derry, Vitousek, Huebert, & Hedin, 1999; Gordon, 2005; Jenny, 1941). Young basalts with well-constrained ages allow for determination of soil chronosequences, which leads to understanding of changes in soil over time (e.g. Jenny, 1941; Pillans, 1997). Moreover, young basalts not only have geomorphological significance, but can also have association with cultural heritage (Chivas, Barnes, Evans, Lupton, & Stone, 1987; Cohen, Mark, Fallon, & Stephenson, 2017; Dixon & Irvine, 1991; Murray-Wallace, 2011; Sutherland, 1995).

Cenozoic volcanism in the Eastern Australian Volcanic Zone (EAVZ), runs broadly parallel to the eastern coast of Australia and extends up to 4000 km, stretching from Torres Strait in the north to Tasmania in the south (Johnson, Knutson, & Taylor, 1989; Stephenson, Burch-Johnston, Stanton, & Whitehead, 1998; Wellman & McDougall, 1974). In north Queensland, Cenozoic volcanism covers an area of about 28 000 km^2, and is part of this long volcanic belt (Figure 31) (Stephenson et al., 1998; Wyatt & Webb, 1970). Mafic volcanic flows in north Queensland are globally significant long lava flows, being the longest flows recorded on the planet, outside of large igneous provinces (Self, Keszthelyi, & Thordarson, 1998). The volcanoes in north Queensland range from *ca* 50 Ma to the Holocene, although most are younger than 9 Ma (Cohen et al., 2017; Stephenson et al., 1998). The Kinrara and Toomba eruptions are the youngest known flows within the volcanic provinces of north Queensland,

although there are also late Pleistocene and Holocene maar eruptions in the region (Cohen et al., 2017; Stephenson et al., 1998; Whitehead et al., 2007).

The Toomba flow is located on the southern side of the Nulla volcanic province, a Neogene to Quaternary volcanic outpouring that lies approximately 160 km southwest of Townville and approximately 90 km west of Charters Towers (Figure 31). The flows of the Nulla province overlie Paleozoic basement rocks and early Cenozoic sediments (Burch, 1991; Wyatt & Webb, 1970). The Nulla province covers an area of approximately 7500 km^2 (Johnson et al., 1989), and is located to the east of the Great Divide that separates drainage towards the Gulf of Carpentaria from drainage towards the eastern coast of Australia.

The Toomba flow was dated using conventional (beta-counting) radiocarbon dating in 1978 by Stephenson, Polach, and Wyatt (1978). Stephenson et al. (1978) measured nine samples, which were clayey sandstone, sands, or loams containing small carbonised stems, and finer disseminated carbonaceous material (Appendix B, Cohen et al., 2017). The uncalibrated ages for the nine carbonaceous samples dated by Stephenson et al. (1978) ranged from 13 100 to 2390 BP. The six oldest samples (all >10 000 yr) were considered robust, and the oldest age (13 100 BP) was interpreted as most closely related to burial time (Stephenson et al., 1978). The uncalibrated radiocarbon ages of Stephenson et al. (1978) were calibrated by Cohen et al. (2017) using the SHCal13 calibration dataset (Hogg et al., 2013). Relative to the SHCal13 calibration of Hogg et al. (2013), these radiocarbon analyses yield calibrated ages of *ca* 16 cal ka to <2.5 ka BP (Cohen et al. 2017).

Recent improvements in $^{40}Ar/^{39}Ar$ geochronology, particularly the development of multi-collector noble gas mass spectrometers, has allowed for determination of ages for mafic volcanoes well into the Holocene (e.g. Cohen et al., 2017; Wijbrans et al., 2011). Recently, Cohen et al. (2017) used the laser step-heating $^{40}Ar/^{39}Ar$ method to determine the age of

Toomba flow and determined an age of 21 000 ± 3000 years ago (2σ), which is significantly older than either the uncalibrated or calibrated existing radiocarbon ages (Cohen et al., 2017; Stephenson et al., 1978).

The possibility of contamination in radiocarbon samples was discussed by both Stephenson et al. (1978) and Cohen et al. (2017), and is widely recognised as a challenge in radiocarbon geochronology (Bird et al., 2014; Cheng & Lehmann, 2009; Czimczik, Preston, Schmidt, & Schulze, 2003; Mellars, 2006). Radiocarbon samples can be contaminated in the form of either inorganic $CaCO_3$ or labile organic compounds, such as humic or fulvic acids (Bird et al., 2014; Cheng & Lehmann, 2009; Czimczik et al., 2003; Mellars, 2006). In most situations, this secondary organic carbon is younger than the original samples and results in ages that are too young. This situation is magnified by the fact that the older the sample is, the more sensitive it is to modern contamination. For instance, a 40 000 year old sample with just 1% contamination by young carbon will yield an age of *ca* 33 000 years (Mellars, 2006). In comparison a 20 000 year old sample with 1% contamination by young carbon, will yield an age of *ca* 19 100 years (Polach & Gulson, 1966).

In this study, we aim to determine a precise age for the Toomba flow through accelerator mass spectrometer radiocarbon dating. We use recently collected charcoal from sediments buried under the Toomba flow, pre-treated with hydrogen pyrolysis that preserves only the stable polycyclic aromatic carbon (Bird et al., 2014) and is thus an excellent method to avoid contamination. We also aim to compare the radiocarbon ages of the Toomba flow with $^{40}Ar/^{39}Ar$ ages to understand precision of $^{40}Ar/^{39}Ar$ method.

4.3. Geological background

The Toomba flow extends from its volcano at 20.022°S 145.132°E to its terminus at 19.884°S 146.220°E, following the regional gradient to the east (Figure 31). It is located near

the southern edge of the Nulla province and is approximately 120 km long, spreading across 670 km^2 (Burch, 1991; Cohen et al., 2017; Whitehead & Stephenson, 1998). The most distal flows occupied a previous channel of the Burdekin River, which is the single largest river draining into the Great Barrier Reef (Bainbridge et al., 2012; Kroon et al., 2012). After emplacement of the Toomba flow, the Burdekin River was subsequently diverted to the east. The Toomba flow is the most recent flow to have diverted the Burdekin River in this fashion, with the Birdbush and Kangerong flows occupying earlier channels (Whitehead & Stephenson, 1998). The Toomba flow is locally known as the 'Great Basalt Wall', and comprises of a distinctive group of basalt flows known for their rough terrain (Whitehead & Stephenson, 1998).

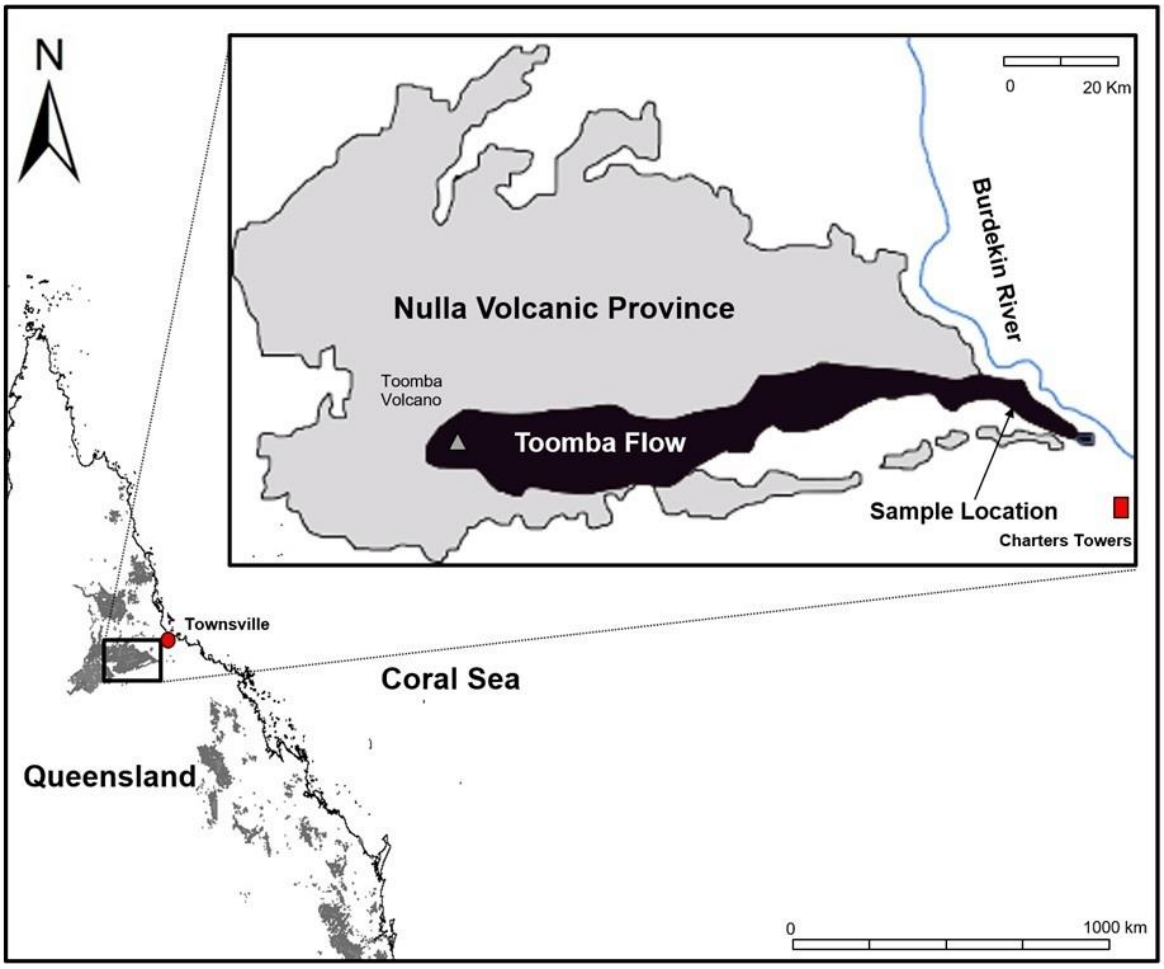

Figure 31: Location of Toomba flow showing the extent of the flow (modified from Whitehead & Stephenson, 1998). The Toomba flow is 120 km long and spreads across an area of 670 km^2.

Various lava rise features, such as lava rise ridges and lava inflation pits, are well developed and are abundant throughout Toomba flow. These lava features at some places rise up to 20 m above adjacent lava surfaces (Stephenson et al., 1998; Whitehead & Stephenson, 1998). Close to Toomba volcano there are well-preserved lava tunnels and lava tubes (Burch, 1991; Wyatt & Webb, 1970). Lava inflation pits are common in the central section of the flow, 20 to 40 km down-flow from the vent, where depressions over 100 m long and up to 20 m deep are formed in an otherwise relatively flat plateau (Stephenson et al., 1998; Whitehead & Stephenson, 1998). Lava clefts are present at the edges and slopes of these depressions. In the more distal portions, lava inflation ridges occur where flows were confined to drainage channels, including that of the Burdekin River (Whitehead & Stephenson, 1998). The small-scale surface characteristics of the Toomba flow include prevalent pahoehoe textures, with lesser a'a and localised chilled surfaces (Stephenson et al., 1998; Whitehead & Stephenson, 1998; Wyatt & Webb, 1970).

The composition of Toomba flow is largely hawaiite and ne-hawaitte, with some basanite (Burch, 1991; Johnson et al., 1989; Whitehead & Stephenson, 1998). Chilled surfaces of the distal flows are comprised of a glassy groundmass with up to 12 vol% olivine phenocrysts and microphenocrysts and about 10 vol% of plagioclase microphenocrysts (Whitehead & Stephenson, 1998).

Located in the subtropics, the present climate of the region is semi-arid, with a mean annual rainfall ranging from 400–650 mm/yr and mean annual temperature ranging from 23 to 25 °C (Pillans, 1997). The Burdekin River catchment is prone to extreme rainfall events, which influences the local geomorphology significantly, particularly sediment and soil redistribution (Alexander, Fielding, Wakefield, George, & Cottnam, 2001; Fielding & Alexander, 1996). There is little development of an internal drainage system within the flow, so the margins are

largely undissected (Burch, 1991; Wyatt & Webb, 1970). The Toomba flow has negligible soil cover, which may be due to its young age, slow rates of soil formation, or soil removal during extreme rainfall events. Its black and unweathered outcrop makes the whole flow very distinctive. This rock outcrop is also associated with distinctive vegetation (e.g. vine scrub) that grows through cracks in the flow (Willmott, 2009).

4.4. Methodology

4.4.1. Radiocarbon dating (^{14}C) sampling location and methods

Charcoal samples were collected from beneath the eastern edge of the Toomba flow, in the 'basalt corner' of the Toomba flow near a recreational area known as 'Big Bend'. Our radiocarbon sampling site is close to the localities from which the K–Ar and $^{40}Ar/^{39}Ar$ samples were collected (Cohen et al., 2017; Wyatt & Webb, 1970), and is 2.5–3 km from the radiocarbon sampling site of Stephenson et al. (1978) (Figure 32). As part of our collection effort we revisited the sampling area of Stephenson et al. (1978); however no radiocarbon samples were found at that location.

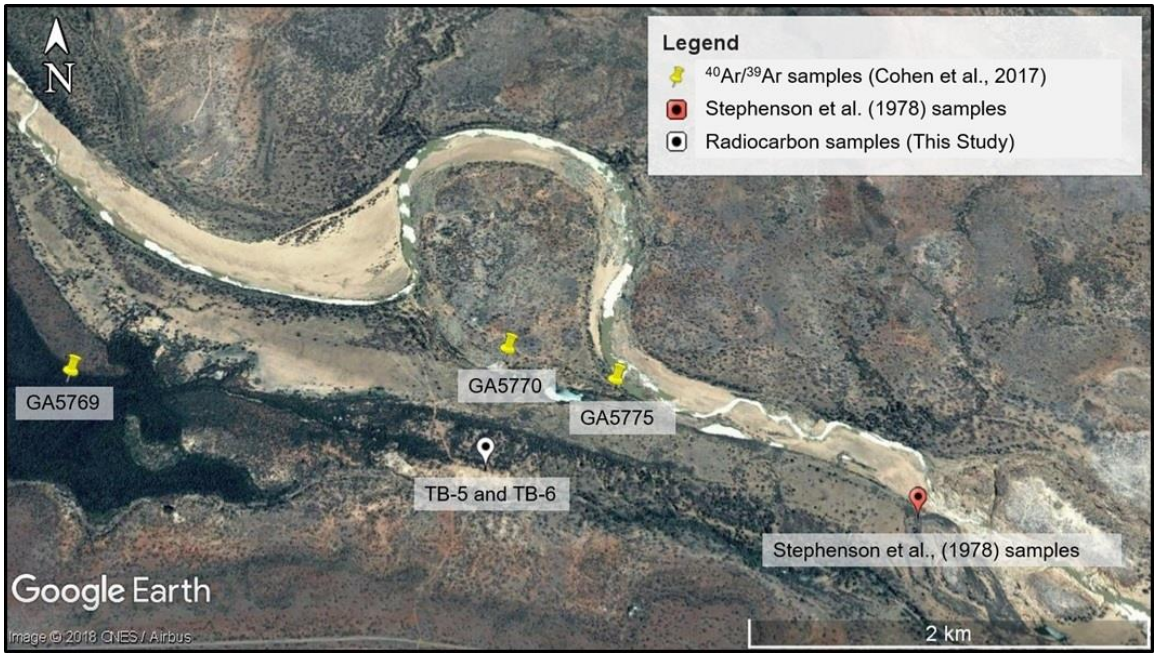

Figure 32: Satellite image of Toomba flow with sample locations in the Big Bend area of the Burdekin River. Yellow pins represent $^{40}Ar/^{39}Ar$ sampling sites (Cohen et al., 2017); the red squares represents the conventional radiocarbon sample location (Stephenson et al., 1978); and the white pins represents radiocarbon sampling sites in this study

Our sampling area is incised by a nearby creek and has sparse modern vegetation, with some trees, mainly eucalyptus, and tussock grasses (Figure 33). Sediment under the lava flow is primarily sand and loam and is highly oxidised, with an orange-red colour. Both samples (TB-5 and TB-6) were collected from a zone of oxidised sediment directly below the basalt flow. Both samples (TB-5 and TB-6) were approximately 5 cm below the basalt, which is between 0.5–1 m thick at this point (Figure 34). A shovel was used to dig out the sediment until charcoal was visible. Underlying charcoal was retrieved from sediment using a knife and collected directly onto aluminium foil, minimising exposure to the adjacent sediments. The charcoal consisted of multiple elongated centimetre-scale fragments, and each fragment had visible wood-like texture. The fragments were black and extremely brittle, powdering easily (Figure 34).

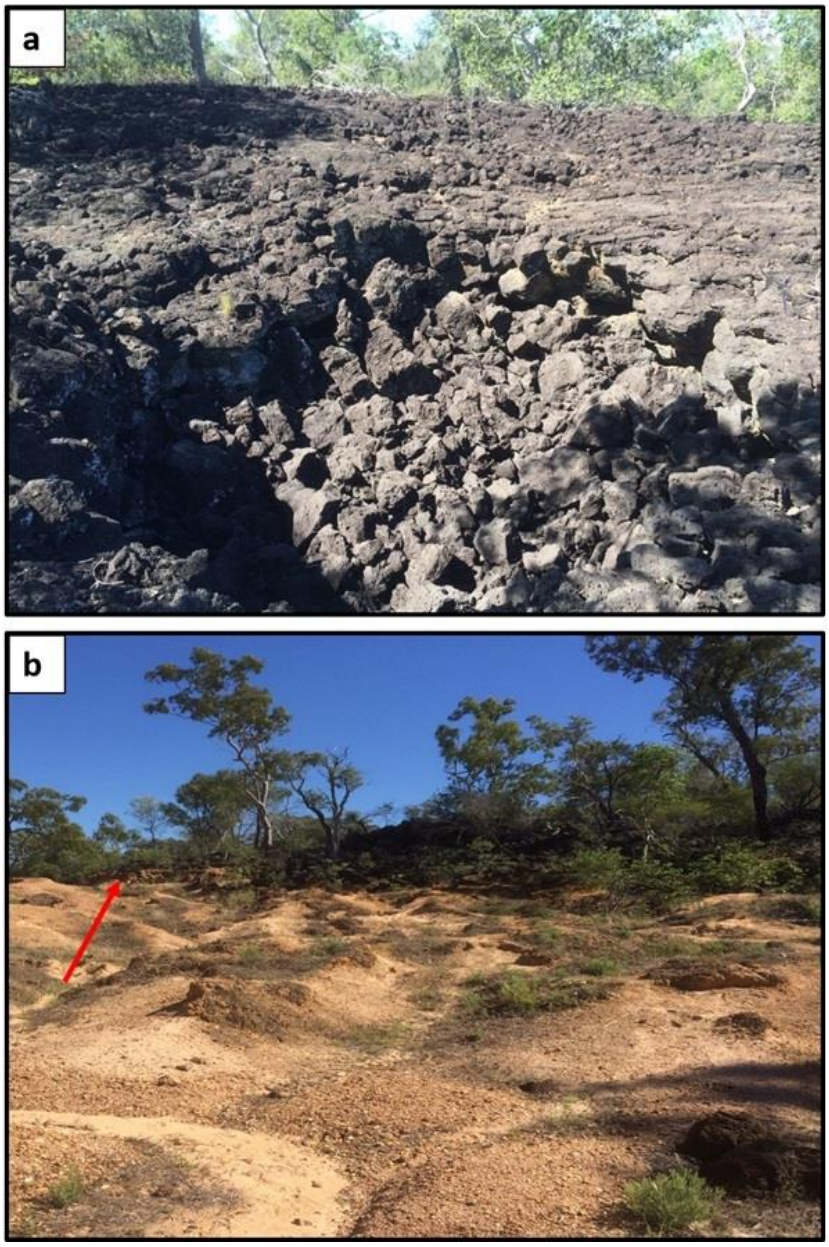

Figure 33: (a) Toomba flow with the original lava-flow structures such as depressions and pahoehoe structures approximately 50 m away from the sample location. (b) The sampling area with moderate vegetation in the ‘basalt corner’ of the Burdekin section of the Toomba flow. The Toomba flow occupies the uppermost portions of this outcrop, in the portions with increased vegetation and dark-coloured rocks. The lighter orange-brown coloured hummocky terrain in the foreground is comprised of weathered sediments beneath the flow. The red arrow points to the exact sampling site.

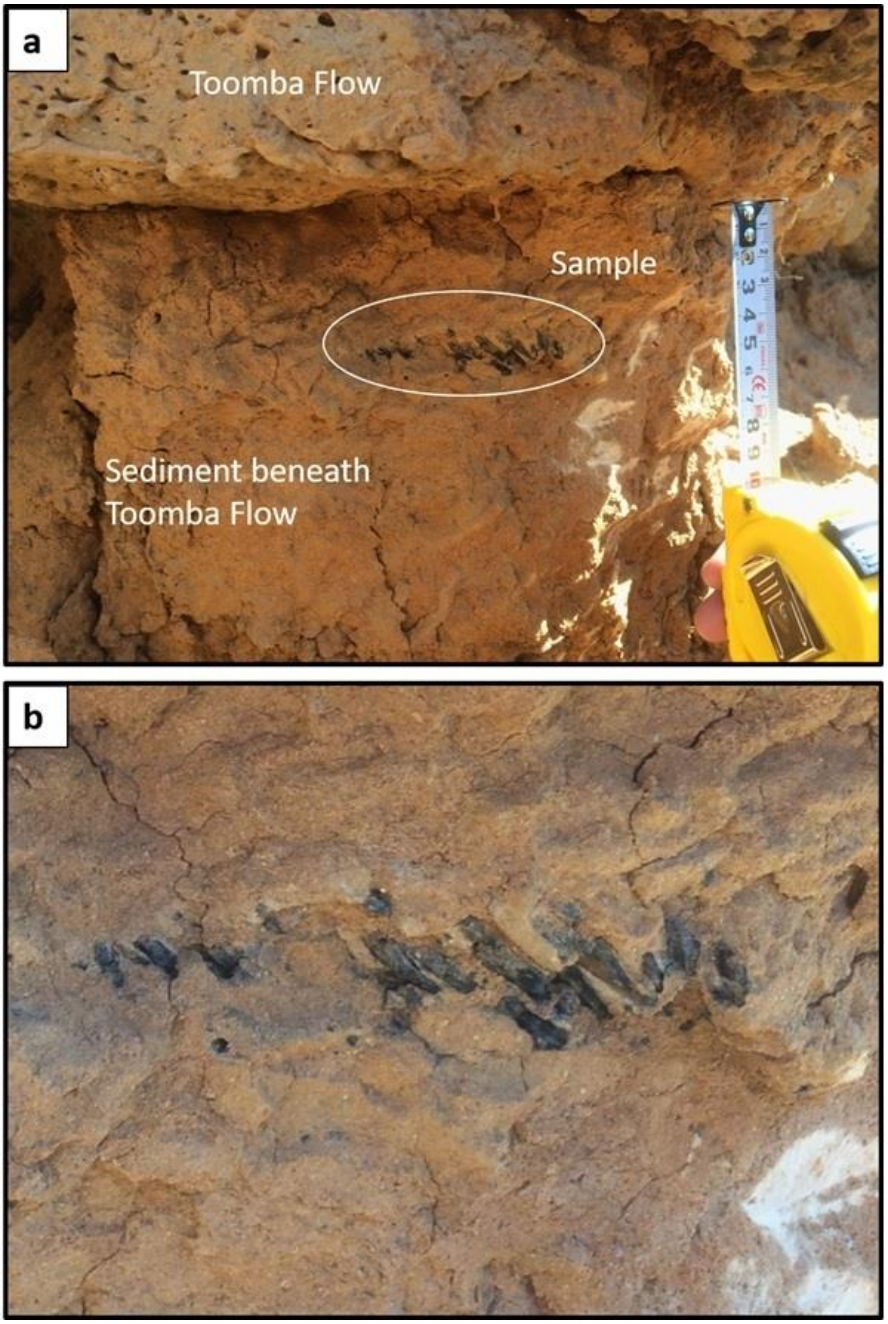

Figure 34: (a) Sample location for TB-5 and TB-6 (19.860100° S, 146.137767° E, and elevation 257 m). Sediments in the area are mainly sandy and loamy, and are highly oxidised (orange-red colour). (b) Close-up image of the material being sampled, showing clear charcoal fragments that had visible wood-like texture. The measuring tape pictured has a scale in centimetres.

4.4.2. Hydrogen pyrolysis pre-treatment

The range of radiocarbon ages determined by Stephenson et al. (1978) indicates that their pre-treatment method, which was Acid-Base-Acid method (using HCl and NaOH leaching) was insufficient to remove contamination from their samples. In this study,

therefore, we used a different pre-treatment method – hydrogen pyrolysis (hypy) – a technique that is specifically designed to remove labile carbon (Ascough et al., 2009; Bird et al., 2014) and yield more reliable radiocarbon measurements.

The hypy sample pre-treatment was undertaken at James Cook University, Cairns, Australia. Samples were immersed in 30% hydrogen peroxide overnight. This is not a standard part of the hypy methodology, but we included it as an extra step to enhance the removal of labile carbon. Radiocarbon measurements using hypy alone have not always resulted in the elimination of exogenous carbon (Bird et al., 2014; Wurster, Lloyd, Goodrick, Saiz, & Bird, 2012), however, ongoing work has indicated that an initial step for removing labile carbon, such as hydrogen peroxide has been more effective than hydrogen pyrolysis alone (unpublished data). The samples were then loaded with a Mo catalyst using an aqueous/methanol (1:1) solution of ammonium dioxydithiomolybdate [$(NH_4)_2MoO_2S_2$]. Catalyst weight was 10% sample weight for all samples to give a nominal loading of 1% Mo. Catalyst loaded samples were then lyophilised and placed in the hypy reactor, pressurised with hydrogen to 15 GPa with a sweep gas flow of 5 $Lmin^{-1}$, then heated using a pre-programmed temperature profile. We used the recommended temperature program previously optimised for pyrogenic carbon quantification where samples are initially heated at rate of 300 °C min^{-1} to 250 °C, then heated at a rate of 8 °C min^{-1} until the final hold temperature of 550 °C for 2 min (Ascough et al., 2009). The hypy residue was the material used for radiocarbon analysis. The samples underwent ^{14}C AMS analysis at Beta Analytics commercial laboratory located in Miami, USA. and were calibrated to southern hemisphere terrestrial calibration curve (SHCal13; Hogg et al., 2013).

4.5. Result and discussion

The sample TB-5 yielded a calibrated radiocarbon age of 20 815–20 429 calBP, while TB-6 yielded a calibrated age of 20 148–19 726 calBP (2σ, Table 8).

Table 8: Radiocarbon analysis of samples TB-5 and TB-6. Calibration output from Beta Analytics calibration program BetaCal v3.21 based on OxCal *(Bronk Ramsey, 2009)* and using SHCal13 curve (Hogg et al., 2013). Calibrated age range is the 95.4% probability for these samples. The age uncertainties reported are 2σ.

Sample ID	Sample Location (Decimal Degrees[a])	Measured Radiocarbon Age (^{14}C yr BP[b])	Lab Code	δ^{13}C (‰ VPDB[c])	Percent Modern Carbon (pMC)	Calibrated age (cal yr BP[b])	Probality (%)
TB-5	–19.860100, 146.137767	17130 ± 50	Beta-467008	–29.1	11.85 ± 0.07	20 815–20 429	95.4%
TB-6	–19.860100, 146.137767	16580 ±50	Beta-469112	–35.7	12.69 ±0.08	20 148–19 726	95.4%

[a]The sampling locality (WGS 84) was determined using Garmin eTrex 10 brand GPS device, with horizontal precision of ±10 m; [b]BP, Before Present; [c]VPDB, Vienna Pee Dee Belemnite

Our two calibrated radiocarbon ages from beneath the Toomba flow are within 300 years of each other. Overall, this agreement between two distinct samples indicates robust ages that are largely free from contamination by secondary carbon. To determine the age of burial by the Toomba flow, one argument might be to follow Stephenson et al. (1978) and adopt the oldest age as most accurate. However, when lava overruns vegetation, the flows can bury dead trees and other organic debris that can have ages several hundred years older than the flow. For example, consider a tree that had died 50 years before being buried by a basalt flow. The tree itself may have been 150 years old at the time of death. In this case, the wood in the centre of the tree will be 200 years old at the time of burial. In this scenario, the youngest radiocarbon age – representing vegetation that was alive during the eruption – would represent the time of burial. In the Toomba situation, with only two analyses, we choose a conservative approach that incorporates the age from the full range of analytical and

calibration uncertainty of both samples, and determines that the age of sediments buried beneath the Toomba flow is between 20 815 to 19 726 calBP (2σ).

Our new age for the Toomba flow is older than the previous radiocarbon ages from charcoal (Stephenson et al., 1978), but is in agreement with laser step-heating $^{40}Ar/^{39}Ar$ age of 21 000 ± 3000 years (Cohen et al., 2017). The wide range of radiocarbon ages reported by Stephenson et al. (1978) is entirely consistent with contamination by modern carbon and carbonate that was not fully removed by the pre-treatment methods used previously. The presence of such contamination in radiocarbon samples is unsurprising. Although charcoal is used widely for radiocarbon dating because of its chemical and biological stability, charcoal commonly reacts with exogenous carbon, and can undergo modification and environmental degradation (Ascough et al., 2011; Bird et al., 2014; Cheng & Lehmann, 2009; Czimczik et al., 2003; Mellars, 2006).

In tropical and subtropical conditions, radiocarbon samples are more susceptible to contamination (Bird et al., 2017; Harkness, Roobol, Smith, Stipp, & Baker, 1994). This contamination can have critical implications on archeological and environmental studies, and pre-treating the samples with an effective pre-treatment method is extremely important. Acid-base-acid (ABA) pre-treatment is the most commonly used method, but is not always effective in removing contamination (Ascough et al., 2016; Bird et al., 2014; Chappell, Head, & Magee, 2015; Gillespie et al., 2016; Goh & Molloy, 1979; Higham, McGovern-Wilson, & Hogg, 1998). On the other hand, acid–base-oxidation (ABOX) technique is effective, but requires large amounts of material, and increases the cost and time of analyses (Bird et al., 2014). Alternately, hypy is extremely effective in removing labile organic matter, and is not very expensive. Here, hypy pre-treatment was used to eliminate contamination and yielded radiocarbon ages older than those previously reported.

The efficient modern hypy pre-treatment technique was not available for 1978 radiocarbon dating by Stephenson et al. (1978). Indeed, the weak 2% NaOH treatment applied to these samples was likely insufficient in removing contamination. Many studies across other localities have also found that such treatment is insufficient to remove all the labile humic and fulvic acids (Ascough et al., 2016; Bird et al., 2014; Chappell et al., 2015; Gillespie et al., 2016; Goh & Molloy, 1979; Higham et al., 1998). Moreover, sampling conditions of Stephenson et al. (1978) were susceptible to contamination by modern carbon as their sampling site was submerged by the Burdekin River for approximately three months per year and shielding by the overlying lava kept the sediments moist for the remaining months of the year (Cohen et al., 2017). Additionally, the larger sample size of conventional radiocarbon dating would have made it much more difficult to separate modern rootlets from older charcoal. In spite of that, the four older samples (>10 000 calBP) of Stephenson et al. (1978) closely approached our sediment burial age and the $^{40}Ar/^{39}Ar$ age for the Toomba flow.

As stated earlier, at the Toomba flow, the fact that the $^{40}Ar/^{39}Ar$ and hypy radiocarbon ages agree within analytical uncertainty enhances confidence that both methods are accurately recording the timing of the Toomba eruption. The reliability of the $^{40}Ar/^{39}Ar$ analysis at Toomba is important, because the same technique was also used to determine an age of 7000 ± 2000 years for the Kinrara flow (Cohen et al., 2017), located approximately 200 km further north, in the McBride province. Aboriginal verbal traditions in the Kinrara region describe features that are consistent with a volcanic eruption, which would necessitate that the traditions were successfully passed on through 230 ± 70 generations (Cohen et al., 2017). Therefore, the Kinrara eruption has cultural significance in north Queensland.

The well-preserved surface of Toomba flow such as pahoehoe textures have been preserved for *ca* 20 000 years, in-spite of mean annual temperature ranging from 23 to 25 °C and mean annual rainfall ranging from 400–650 mm/yr, implying that the rate of soil formation and

weathering in the area has been relatively slow. However, the region also experience high-intensity rainfall events. This has considerable influence on rates of weathering, soil formation and soil loss. For example, the rate of soil formation might also appear slow due to the influence of high intensity rainfall, which will wash away soil that forms or settles on the flow. Furthermore, the new age of sediments buried beneath the Toomba flow adds new age constraints to the soil chronosequence used as a guide to understand earlier stages of soil development (Pillans, 1997), as the Toomba flow was previously assumed to be only 13,100 ± 200 year old.

4.6. Conclusion and implications

From our study, we conclude that the calibrated radiocarbon burial age of sediments beneath the Toomba flow is between 20 815 and 19 726 calBP (2σ). Our calibrated radiocarbon age, which used hypy pre-treatment, is older than the conventional radiocarbon analyses of Stephenson et al. (1978), who used acid–base pre-treatment. These results indicate that hypy was an effective pre-treatment method at this location.

Our calibrated radiocarbon age is in excellent agreement with the laser step-heating $^{40}Ar/^{39}Ar$ result of 21 000 ± 3000 years (Cohen et al., 2017). This concordance of ages by two techniques support the conclusion that both the radiocarbon and $^{40}Ar/^{39}Ar$ results are accurately dating the eruption of the Toomba flow, and burial of carbon-bearing sediments beneath the flow. Importantly, the calibrated radiocarbon age provides the most precise age available for the timing of this eruption, which produced lavas that extend an exceptional distance of 120 km from the vent. This new radiocarbon age, coupled with the well-preserved nature such as pahoehoe textures of the Toomba flow, implies that soil formation has been slow in this subtropical region.

Chapter 5: Thesis conclusions

In this thesis, I aim to add constraints on rates of sediment generation and landscape evolution in north Queensland by quantifying erosion rates across north Queensland using ^{10}Be. The main conclusions that can be drawn from the results of this thesis is that the rate of erosion in north Queensland is slow. In fact, results of this thesis indicates that erosion rates for basins and bedrock in north Queensland are slower than most other parts of the world. This thesis also determined the first published bedrock erosion rates from north Queensland, and compared these rates to the basin erosion rates. The bedrock data suggested that there is a strong influence of rock type on bedrock erosion rates, and sedimentary rocks in north Queensland erode ~2.7 times faster than granitic rocks. This study also found that bedrock erosion rates are faster than basin erosion rate in north Queensland, implying that relief is lost over the long-term.

In this thesis, I also examined precipitation' influence on ^{10}Be-derived erosion rate in a global context, which acknowledges the important influence of other variables, particularly slope and vegetation (Chapter 2). The results suggested that precipitation's influence on ^{10}Be-derived erosion rate on global scale is not absent or negligible, as suggested by various studies (Nichols et al., 2014; Scherler et al., 2014; Bermúdez et al., 2013; Willenbring et al., 2013; Portenga & Bierman, 2011; Binnie et al., 2007; Wittmann et al., 2007; von Blanckenburg, 2005; Riebe et al., 2001b, 2001a). Instead, precipitation's influence on ^{10}Be-derived erosion rate is secondary on global scale, after mean basin slope. The primary reason that the direct influence of precipitation on erosion rate is obscured is the interrelationship between vegetation and precipitation. This is in agreement with previous sediment yield studies that suggested that precipitation and vegetation are interrelated (e.g. Walling & Webb, 1983; Langbein & Schumm, 1958), and is consistent with findings of Schaller et al. (2018)

from Chilean Coastal Cordillera, where denudation rates increase with an increase in mean annual precipitation until ~1000 +/- 500 mm/yr; after this value, denudation rates did not increase with further increase in mean annual precipitation (Schaller et al., 2018). This plateauing of denudation rate at ~1000 mm/yr in our global compilation suggests that a vegetation-induced non-linear relationship between precipitation and erosion rate (Schaller et al., 2018) operates across a range of environments.

The results of this study is also consistent with findings of Willenbring et al. (2013), which states that this strong correlation of the mean basin slope with ^{10}Be-derived erosion rate is valid only for landscapes where slope is >11°. For areas where slope is <11°, which comprises approximately 90% of the Earth's surface (Willenbring et al., 2013), influence of mean basin slope is not very strong, and is almost equal to the influence of mean annual precipitation. The influence of precipitation on erosion rate in north Queensland is strong and clear (R^2=0.71), and is consistent with the findings of this study (Chapter 2), which showed that when slope is <11°, precipitation will have a stronger influence on erosion rate. In this case, most of north Queensland is characterised by a low-gradient landscape (slope is <11°). This furthers confirms the assertion that even though precipitation does not have a primary influence on ^{10}Be-derived erosion rate on global scale (Mishra et al., 2019), its influence can be dominant on a regional/local scale.

In this thesis, I also aimed to address the lack of paleoerosion information for Burdekin River, which is the largest draining river to the Great Barrier Reef. In order to obtain paleoerosion rates, buried samples were collected beneath Toomba flow and compared to non-buried samples. To establish the timescale of paleoerosion rates, a precise age of burial was required. Thus, precise age of Toomba flow was determined using the radiocarbon dating method and hydrogen pyrolysis. The results of this thesis concluded that the calibrated radiocarbon burial age of sediments beneath the Toomba flow is between 20,815 and 19,726

calBP (2σ). The results also concluded that both the radiocarbon results and $^{40}Ar/^{39}Ar$ results by Cohen et al. (2017) accurately date the eruption of the Toomba flow. The calibrated radiocarbon age provides the most precise age available for the timing of this eruption. The results of this thesis suggest that the long-term erosion rate of Burdekin River from modern samples is not very different than that from sediment deposited ~20,000 years ago. Using chronologic data (from chapter 4 of this thesis), it is also shown that erosion rates in north Queensland have been consistently slow for approximately 10^3 to 10^5 years, indicating that Australian landscape have attained steady state.

Chapter 6: Bibliography

Acosta, V. T., Schildgen, T. F., Clarke, B. A., Scherler, D., Bookhagen, B., Wittmann, H., von Blanckenburg, F., & Strecker, M. R. (2015). Effect of vegetation cover on millennial-scale landscape denudation rates in East Africa. *Lithosphere*, L402. 401.

Alexander, J., Fielding, C. R., Wakefield, S. J., George, M. T., & Cottnam, C. F. (2001). Fluvial Geochemistry through a Short-Duration, Tropical-Cyclone Induced Discharge event in the Burdekin River and Hann Creek, North Queensland, Australia. *Aquatic Geochemistry, 7*(4), 275-293. doi:10.1023/a:1015203127320

Ascough, P. L., Bird, M. I., Brock, F., Higham, T. F. G., Meredith, W., Snape, C. E., & Vane, C. H. (2009). Hydropyrolysis as a new tool for radiocarbon pre-treatment and the quantification of black carbon. *Quaternary Geochronology, 4*(2), 140-147. doi:10.1016/j.quageo.2008.11.001

Ascough, P. L., Bird, M. I., Francis, S. M., Thornton, B., Midwood, A. J., Scott, A. C., & Apperley, D. (2011). Variability in oxidative degradation of charcoal: Influence of production conditions and environmental exposure. *Geochimica et Cosmochimica Acta, 75*(9), 2361-2378. doi:10.1016/j.gca.2011.02.002

Ascough, P. L., Bird, M. I., Meredith, W., Wood, R. E., Snape, C. E., Brock, F., Higham, T. F. G., Large, D. J., & Apperley, D. C. (2016). Hydropyrolysis: Implications for Radiocarbon Pretreatment and Characterization of Black Carbon. *Radiocarbon, 52*(3), 1336-1350. doi:10.1017/S0033822200046427

Bainbridge, Z., Lewis, S., Bartley, R., Fabricius, K., Collier, C., Waterhouse, J., Garzon-Garcia, A., Robson, B., Burton, J., Wenger, A., & Brodie, J. (2018). Fine sediment and particulate organic matter: A review and case study on ridge-to-reef transport, transformations, fates, and impacts on marine ecosystems. *Marine Pollution Bulletin, 135*, 1205-1220. doi:https://doi.org/10.1016/j.marpolbul.2018.08.002

Balco, G., & Shuster, D. L. (2009). 26Al–10Be–21Ne burial dating. *Earth and Planetary Science Letters, 286*(3–4), 570-575. doi:http://dx.doi.org/10.1016/j.epsl.2009.07.025

Balco, G., Stone, J. O., Lifton, N. A., & Dunai, T. J. (2008). A complete and easily accessible means of calculating surface exposure ages or erosion rates from 10 Be and 26 Al measurements. *Quaternary Geochronology, 3*(3), 174-195.

Bartley, R., Croke, J., Bainbridge, Z. T., Austin, J. M., & Kuhnert, P. M. (2015). Combining contemporary and long-term erosion rates to target erosion hot-spots in the Great Barrier Reef, Australia. *Anthropocene, 10*, 1-12. doi:https://doi.org/10.1016/j.ancene.2015.08.002

Belton, D., Brown, R., Kohn, B., Fink, D., & Farley, K. (2004). Quantitative resolution of the debate over antiquity of the central Australian landscape: implications for the tectonic and geomorphic stability of cratonic interiors. *Earth and Planetary Science Letters, 219*(1), 21-34.

Bermúdez, M. A., van der Beek, P. A., & Bernet, M. (2013). Strong tectonic and weak climatic control on exhumation rates in the Venezuelan Andes. *Lithosphere, 5*(1), 3-16.

Berner, R. A., Lasaga, A. C., & Garrels, R. M. (1983). The carbonate-silicate geochemical cycle and its effect on atmospheric carbon dioxide over the past 100 million years. *Am. J. Sci, 283*(7), 641-683.

Bierman, P. R., & Caffee, M. (2001). Slow rates of rock surface erosion and sediment production across the Namib Desert and escarpment, southern Africa. *American Journal of Science, 301*(4-5), 326-358.

Bierman, P. R., & Caffee, M. (2002). Cosmogenic exposure and erosion history of Australian bedrock landforms. *Geological Society of America Bulletin, 114*(7), 787-803.

Bierman, P., & Steig, E. J. (1996). Estimating rates of denudation using cosmogenic isotope abundances in sediment. *Earth surface processes and landforms, 21*(2), 125-139.

Bierman, P., Reusser, L., Nichols, K., Matmon, A., & Rood, D. (2009). *Where is the sediment coming from and where is it going-A 10Be examination of the northern Queensland escarpment, Australia.* Paper presented at the 2009 Portland GSA Annual Meeting: Portland, Or.

Binnie, S. A., Phillips, W. M., Summerfield, M. A., & Fifield, L. K. (2007). Tectonic uplift, threshold hillslopes, and denudation rates in a developing mountain range. *Geology, 35*(8), 743-746.

Bird, M. I., Levchenko, V., Ascough, P. L., Meredith, W., Wurster, C. M., Williams, A., Tilston, E. L., Snape, C. E., & Apperley, D. C. (2014). The efficiency of charcoal decontamination for radiocarbon dating by three pre-treatments – ABOX, ABA and hypy. *Quaternary Geochronology, 22*, 25-32. doi:10.1016/j.quageo.2014.02.003

Bird, M. I., McBeath, A. V., Ascough, P. L., Levchenko, V. A., Wurster, C. M., Munksgaard, N. C., Smernik, R. J., & Williams, A. (2017). Loss and gain of carbon during char degradation. *Soil Biology and Biochemistry, 106*, 80-89. doi:10.1016/j.soilbio.2016.12.012

Blondes, M. S., Reiners, P. W., Edwards, B. R., & Biscontini, A. (2007). Dating young basalt eruptions by (U-Th)/He on xenolithic zircons. *Geology, 35*(1), 17-20. doi:10.1130/G22956A.1

Bochet, E., Poesen, J., & Rubio, J. L. (2006). Runoff and soil loss under individual plants of a semi-arid Mediterranean shrubland: influence of plant morphology and rainfall intensity. *Earth surface processes and landforms, 31*(5), 536-549. doi:10.1002/esp.1351

BoM. (2018). *Bureau of Meteorology.* Retrieved from http://www.bom.gov.au/climate/data/stations/

Bonnet, S., & Crave, A. (2003). Landscape response to climate change: Insights from experimental modeling and implications for tectonic versus climatic uplift of topography. *Geology, 31*(2), 123-126.

Brodie, J. E., Kroon, F. J., Schaffelke, B., Wolanski, E. C., Lewis, S. E., Devlin, M. J., Bohnet, I. C., Bainbridge, Z. T., Waterhouse, J., & Davis, A. M. (2012). Terrestrial pollutant runoff to the Great Barrier Reef: An update of issues, priorities and management responses. *Marine Pollution Bulletin, 65*(4–9), 81-100. doi:http://dx.doi.org/10.1016/j.marpolbul.2011.12.012

Brodie, J. (2002). *Keeping the wolf from the door: managing land-based threats to the Great Barrier Reef.* Paper presented at the Proceedings of the Ninth International Coral Reef Symposium, Bali, 23-27 October 2000.

Bronk Ramsey, C. (2009). Bayesian Analysis of Radiocarbon Dates. *Radiocarbon, 51*(1), 337-360. doi:10.1017/S0033822200033865

Brown, E. T., Bourlès, D. L., Colin, F., Raisbeck, G. M., Yiou, F., & Desgarceaux, S. (1995a). Evidence for muon-induced production of 10Be in near-surface rocks from the Congo. *Geophysical Research Letters, 22*(6), 703-706.

Brown, E. T., Stallard, R. F., Larsen, M. C., Bourlès, D. L., Raisbeck, G. M., & Yiou, F. (1998). Determination of predevelopment denudation rates of an agricultural watershed (Cayaguas River, Puerto Rico) using in-situ-produced 10Be in river-borne quartz. *Earth and Planetary Science Letters, 160*(3-4), 723-728. doi:10.1016/S0012-821X(98)00123-X

Brown, E. T., Stallard, R. F., Larsen, M. C., Raisbeck, G. M., & Yiou, F. (1995). Denudation rates determined from the accumulation of in situ-produced 10Be in the luquillo experimental forest, Puerto Rico. *Earth and Planetary Science Letters, 129*(1-4), 193-202. doi:10.1016/0012-821X(94)00249-X

Brown, L., Pavich, M. J., Hickman, R. E., Klein, J., & Middleton, R. (1988). Erosion of the eastern United States observed with 10Be. *Earth surface processes and landforms, 13*(5), 441-457. doi:10.1002/esp.3290130509

Buechi, M. W., Kober, F., Ivy-Ochs, S., Salcher, B., Kubik, P. W., & Christl, M. (2014). Denudation rates of small transient catchments controlled by former glaciation: The Hörnli nunatak in the northeastern Swiss Alpine Foreland. *Quaternary Geochronology, 19*(0), 135-147. doi:http://dx.doi.org/10.1016/j.quageo.2013.06.005

Burbank, D. W., Blythe, A. E., Putkonen, J., Pratt-Sitaula, B., Gabet, E., Oskin, M., Barros, A., & Ojha, T. P. (2003). Decoupling of erosion and precipitation in the Himalayas. *Nature, 2003 v.426 no.6967*(no. 6967), pp. 652-655. doi:10.1038/nature02187

Burch, A. (1991). Flow discrimination in the Toomba Basalt. *BSc (Hons) thesis. James Cook University, Townsville (unpubl.).*

Burke, L., Reytar, K., Spalding, M., & Perry, A. (2011). *Reefs at risk revisited*.

Carretier, S., Regard, V., Vassallo, R., Aguilar, G., Martinod, J., Riquelme, R., Pepin, E., Charrier, R., Hérail, G., & Farías, M. (2013). Slope and climate variability control of erosion in the Andes of central Chile. *Geology, 41*(2), 195-198.

Célérier, J., Sandiford, M., Hansen, D. L., & Quigley, M. (2005). Modes of active intraplate deformation, Flinders Ranges, Australia. *Tectonics, 24*(6). doi:doi:10.1029/2004TC001679

Chadwick, O. A., Derry, L. A., Vitousek, P. M., Huebert, B. J., & Hedin, L. O. (1999). Changing sources of nutrients during four million years of ecosystem development. *Nature, 397*, 491. doi:10.1038/17276

Chappell, J., Head, J., & Magee, J. (2015). Beyond the radiocarbon limit in Australian archaeology and Quaternary research. *Antiquity, 70*(269), 543-552. doi:10.1017/S0003598X00083708

Cheng, C. H., & Lehmann, J. (2009). Ageing of black carbon along a temperature gradient. *Chemosphere, 75*(8), 1021-1027. doi:10.1016/j.chemosphere.2009.01.045

Child, D., Elliott, G., Mifsud, C., Smith, A. M., & Fink, D. (2000). Sample processing for earth science studies at ANTARES. *Nuclear Instruments and Methods in Physics Research Section B: Beam Interactions with Materials and Atoms, 172*(1), 856-860. doi:https://doi.org/10.1016/S0168-583X(00)00198-1

Chivas, A. R., Barnes, I., Evans, W. C., Lupton, J. E., & Stone, J. O. (1987). Liquid carbon dioxide of magmatic origin and its role in volcanic eruptions. *Nature, 326*, 587. doi:10.1038/326587a0

Chmeleff, J., von Blanckenburg, F., Kossert, K., & Jakob, D. (2010). Determination of the 10Be half-life by multicollector ICP-MS and liquid scintillation counting. *Nuclear Instruments and Methods in Physics Research Section B: Beam Interactions with Materials and Atoms, 268*(2), 192-199. doi:https://doi.org/10.1016/j.nimb.2009.09.012

Clapp, E. M., Bierman, P. R., & Caffee, M. (2002). Using 10Be and 26Al to determine sediment generation rates and identify sediment source areas in an arid region drainage basin. *Geomorphology, 45*(1), 89-104. doi:https://doi.org/10.1016/S0169-555X(01)00191-X

Clapp, E. M., Bierman, P. R., Schick, A. P., Lekach, J., Enzel, Y., & Caffee, M. (2000). Sediment yield exceeds sediment production in arid region drainage basins. *Geology, 28*(11), 995-998. doi:10.1130/0091-7613(2000)28<995:SYESPI>2.0.CO;2

Clifton, T., Granger, D. E., Gilbert, Z., & Caffee, M. (2005). *Quartz sample preparation for AMS.* Paper presented at the The 10th International Conference on Accelerator Mass Spectrometry.

Coates-Marnane, J., Olley, J., Burton, J., & Sharma, A. (2016). Catchment clearing accelerates the infilling of a shallow subtropical bay in east coast Australia. *Estuarine, Coastal and Shelf Science, 174*, 27-40. doi:https://doi.org/10.1016/j.ecss.2016.03.006

Codilean, A. T., Struck, M., Fülöp, R.-H., Egholm, D. L., Jansen, J. D., Fink, D., Wilcken, K. M., Kotevski, S., & Fujioka, T. (2018). Soil production and transport on postorogenic desert hillslopes quantified with 10Be and 26Al. *GSA Bulletin, 130*(5-6), 1017-1040. doi:10.1130/b31767.1

Cohen, B. E., Mark, D. F., Fallon, S. J., & Stephenson, P. J. (2017). Holocene-Neogene volcanism in northeastern Australia: Chronology and eruption history. *Quaternary Geochronology, 39*, 79-91. doi:10.1016/j.quageo.2017.01.003

Croke, J., Bartley, R., Chappell, J., Austin, J. M., Fifield, K., Tims, S. G., Thompson, C. J., & Furuichi, T. (2015). 10 Be-derived denudation rates from the Burdekin catchment: The largest contributor of sediment to the Great Barrier Reef. *Geomorphology, 241*, 122-134. doi:https://doi.org/10.1016/j.geomorph.2015.04.003

Cyr, A. J., Granger, D. E., Olivetti, V., & Molin, P. (2010). Quantifying rock uplift rates using channel steepness and cosmogenic nuclide–determined erosion rates: Examples from northern and southern Italy. *Lithosphere, 2*(3), 188-198.

Czimczik, C. I., Preston, C. M., Schmidt, M. W. I., & Schulze, E. D. (2003). How surface fire in Siberian Scots pine forests affects soil organic carbon in the forest floor: Stocks, molecular structure, and conversion to black carbon (charcoal). *Global Biogeochemical Cycles, 17*(1). doi:10.1029/2002GB001956

Dadson, S. J., Hovius, N., Chen, H., Dade, W. B., Hsieh, M.-L., Willett, S. D., Hu, J.-C., Horng, M.-J., Chen, M.-C., Stark, C. P., Lague, D., & Lin, J.-C. (2003). Links between erosion, runoff variability and seismicity in the Taiwan orogen. *Nature, 426*, 648. doi:10.1038/nature02150

Day, R. (1983). *Queensland Geology: A companion volume to the 1: 2,500,000 scale geological map (1975)*: Geological Survey of Queensland.

Day, R. W., Murray, C. G., & Whitaker, W. G. (1978). The eastern part of the Tasman Orogenic Zone. *Tectonophysics, 48*(3), 327-364. doi:https://doi.org/10.1016/0040-1951(78)90123-3

Dedkov, A., & Mozzherin, V. (1984). Erosion and Sediment Runoff on the Earth: Kazan: Izd-vo Kazansk. un-ta.

Defries, R. S., Hansen, M. C., Townshend, J. R. G., Janetos, A. C., & Loveland, T. R. (2000). A new global 1-km dataset of percentage tree cover derived from remote sensing. *Global Change Biology, 6*(2), 247-254. doi:10.1046/j.1365-2486.2000.00296.x

DiBiase, R. A., & Whipple, K. X. (2011). The influence of erosion thresholds and runoff variability on the relationships among topography, climate, and erosion rate. *Journal of Geophysical Research: Earth Surface, 116*(F4).

DiBiase, R. A., Whipple, K. X., Heimsath, A. M., & Ouimet, W. B. (2010). Landscape form and millennial erosion rates in the San Gabriel Mountains, CA. *Earth and Planetary Science Letters, 289*(1), 134-144.

Dixon, J. L., Heimsath, A. M., & Amundson, R. (2009). The critical role of climate and saprolite weathering in landscape evolution. *Earth surface processes and landforms, 34*(11), 1507-1521. doi:10.1002/esp.1836

Dixon, J. L., Heimsath, A. M., Kaste, J., & Amundson, R. (2009b). Climate-driven processes of hillslope weathering. *Geology, 37*(11), 975-978.

Dixon, R. M. W., & Irvine, T. (1991). Words of our country : stories, place names, and vocabulary in Yidiny, the Aboriginal language of the Cairns-Yarrabah region. *University of Queensland Press ; Portland, Or. : Distributed in the USA and Canada by International Specialized Book Services, St. Lucia, Qld., Australia*.

Doney, S. C. (2010). The Growing Human Footprint on Coastal and Open-Ocean Biogeochemistry. *Science, 328*(5985), 1512-1516. doi:10.1126/science.1185198

Douglas, I. (1967). MAN VEGETATION AND SEDIMENT YIELDS OF RIVERS. *Nature, 215*(5104), 925-&. doi:10.1038/215925a0

Durán Zuazo, V. H., & Rodríguez Pleguezuelo, C. R. (2008). Soil-erosion and runoff prevention by plant covers. A review. *Agronomy for Sustainable Development, 28*(1), 65-86. doi:10.1051/agro:2007062

Fabricius, K. E. (2005). Effects of terrestrial runoff on the ecology of corals and coral reefs: review and synthesis. *Marine Pollution Bulletin, 50*(2), 125-146. doi:https://doi.org/10.1016/j.marpolbul.2004.11.028

Fabricius, K. E., Logan, M., Weeks, S. J., Lewis, S. E., & Brodie, J. (2016). Changes in water clarity in response to river discharges on the Great Barrier Reef continental shelf: 2002–2013. *Estuarine, Coastal and Shelf Science, 173*, A1-A15. doi:https://doi.org/10.1016/j.ecss.2016.03.001

Fielding, C. R., & Alexander, J. (1996). Sedimentology of the Upper Burdekin River of North Queensland, Australia—an example of a tropical, variable discharge river. *Terra Nova, 8*(5), 447-457. doi:10.1111/j.1365-3121.1996.tb00770.x

Finnegan, N. J., Hallet, B., Montgomery, D. R., Zeitler, P. K., Stone, J. O., Anders, A. M., & Yuping, L. (2008). Coupling of rock uplift and river incision in the Namche Barwa–Gyala Peri massif, Tibet. *Geological Society of America Bulletin, 120*(1-2), 142-155. doi:http://dx.doi.org/10.1130/B26224.1

Fournier, F. (1960). *Climat et érosion: la relation entre l'érosion du sol par l'eau et les précipitations atmosphériques*. Retrieved from

Furnas, M. M. (2003). *Catchments and corals: terrestrial runoff to the Great Barrier Reef*: Australian Institute of Marine Science & CRC Reef Research Centre.

Gabrovšek, F. (2009). On concepts and methods for the estimation of dissolutional denudation rates in karst areas. *Geomorphology, 106*(1-2), 9-14. doi:10.1016/j.geomorph.2008.09.008

García-Ruiz, J. M., Beguería, S., Nadal-Romero, E., González-Hidalgo, J. C., Lana-Renault, N., & Sanjuán, Y. (2015). A meta-analysis of soil erosion rates across the world. *Geomorphology, 239*, 160-173.

Gillespie, R., Hammond, A. P., Goh, K. M., Tonkin, P. J., Lowe, D. C., Sparks, R. J., & Wallace, G. (2016). AMS Dating of a Late Quaternary Tephra at Graham's Terrace, New Zealand. *Radiocarbon, 34*(1), 21-27. doi:10.1017/S0033822200013382

Godard, V., Dosseto, A., Fleury, J., Bellier, O., Siame, L., & ASTER Team. (2019). Transient landscape dynamics across the Southeastern Australian Escarpment. *Earth and Planetary Science Letters, 506*, 397-406

Goh, K. M., & Molloy, B. P. (1979). Contaminants in charcoals used for radiocarbon dating. *New Zealand journal of science*.

Gordon, S. J. (2005). Effect of environmental factors on the chemical weathering of plagioclase in Hawaiian basalt. *Physical Geography, 26*(1), 69-84. doi:10.2747/0272-3646.26.1.69

Gosse, J. C., & Phillips, F. M. (2001). Terrestrial in situ cosmogenic nuclides: theory and application. *Quaternary Science Reviews, 20*(14), 1475-1560. doi:http://dx.doi.org/10.1016/S0277-3791(00)00171-2

Granger, D. E., Fabel, D., & Palmer, A. N. (2001a). Pliocene–Pleistocene incision of the Green River, Kentucky, determined from radioactive decay of cosmogenic 26Al and 10Be in Mammoth Cave sediments. *GSA Bulletin, 113*(7), 825-836. doi:10.1130/0016-7606(2001)113<0825:ppiotg>2.0.co;2

Granger, D. E., Riebe, C. S., Kirchner, J. W., & Finkel, R. C. (2001b). Modulation of erosion on steep granitic slopes by boulder armoring, as revealed by cosmogenic 26Al and 10Be. *Earth and Planetary Science Letters, 186*(2), 269-281. doi:https://doi.org/10.1016/S0012-821X(01)00236-9

Granger, D. E., Kirchner, J. W., & Finkel, R. (1996). Spatially Averaged Long-Term Erosion Rates Measured from in Situ-Produced Cosmogenic Nuclides in Alluvial Sediment. *The Journal of Geology, 104*(3), 249-257. doi:10.1086/629823

Granger, D., & Smith, A. (2000). Dating buried sediments using radioactive decay and muogenic production of 26Al and 10Be. *Nuclear Instruments and Methods in Physics Research Section B: Beam Interactions with Materials and Atoms, 172*(1), 822-826. doi:https://doi.org/10.1016/S0168-583X(00)00087-2

Grujic, D., Coutand, I., Bookhagen, B., Bonnet, S., Blythe, A., & Duncan, C. (2006). Climatic forcing of erosion, landscape, and tectonics in the Bhutan Himalayas. *Geology, 34*(10), 801-804.

Harel, M. A., Mudd, S. M., & Attal, M. (2016). Global analysis of the stream power law parameters based on worldwide 10Be denudation rates. *Geomorphology, 268*, 184-196. doi:https://doi.org/10.1016/j.geomorph.2016.05.035

Harkness, D. D., Roobol, M. J., Smith, A. L., Stipp, J. J., & Baker, P. E. (1994). Radiocarbon redating of contaminated samples from a tropical volcano: the Mansion 'Series' of St Kitts, West Indies. *Bulletin of Volcanology, 56*(5), 326-334. doi:10.1007/bf00326459

Heimsath, A. M., Chappell, J., & Fifield, K. (2010). Eroding Australia: rates and processes from Bega Valley to Arnhem land. *Geological Society, London, Special Publications, 346*(1), 225-241.

Heimsath, A. M., Chappell, J., Dietrich, W. E., Nishiizumi, K., & Finkel, R. C. (2000). Soil production on a retreating escarpment in southeastern Australia. *Geology, 28*(9), 787-790.

Heimsath, A. M., Chappell, J., Finkel, R. C., Fifield, K., & Alimanovic, A. (2006). Escarpment erosion and landscape evolution in southeastern Australia. *Geological Society of America Special Papers, 398*, 173-190.

Heimsath, A. M., Dietrich, W. E., Nishiizumi, K., & Finkel, R. C. (1997). The soil production function and landscape equilibrium. *Nature, 388*(6640), 358-361.

Heimsath, A. M., Dietrich, W. E., Nishiizumi, K., & Finkel, R. C. (2001). Stochastic processes of soil production and transport: Erosion rates, topographic variation and cosmogenic nuclides in the Oregon Coast Range. *Earth surface processes and landforms, 26*(5), 531-552.

Heimsath, A. M., Fink, D., & Hancock, G. R. (2009). The 'humped'soil production function: eroding Arnhem Land, Australia. *Earth surface processes and landforms, 34*(12), 1674-1684.

Henck, A. C., Huntington, K. W., Stone, J. O., Montgomery, D. R., & Hallet, B. (2011). Spatial controls on erosion in the Three Rivers Region, southeastern Tibet and southwestern China. *Earth and Planetary Science Letters, 303*(1), 71-83. doi:https://doi.org/10.1016/j.epsl.2010.12.038

Herr, A., & Kuhnert, P. (2007). Assessment of uncertainty in Great Barrier Reef catchment models. *Water Science and Technology, 56*(1), 181-188.

Hess, S., Prescott, L. J., Hoey, A. S., McMahon, S. A., Wenger, A. S., & Rummer, J. L. (2017). Species-specific impacts of suspended sediments on gill structure and function in coral reef fishes. *Proceedings of the Royal Society B: Biological Sciences, 284*(1866), 20171279. doi:doi:10.1098/rspb.2017.1279

Hewawasam, T., von Blanckenburg, F., Schaller, M., & Kubik, P. (2003). Increase of human over natural erosion rates in tropical highlands constrained by cosmogenic nuclides. *Geology, 31*(7), 597-600.

Hewawasam, T., von Blanckenburg, F., Schaller, M., & Kubik, P. (2003). Increase of human over natural erosion rates in tropical highlands constrained by cosmogenic nuclides. *Geology, 31*(7), 597-600.

Higham, T. F. G., McGovern-Wilson, R. J., & Hogg, A. G. (1998). Chemical pretreatment and radiocarbon dating of samples from the prehistoric site of Killermont Nr. 2, Mackenzie Basin, New Zealand. *New Zealand Journal of Archaeology*, 75-90.

Hijmans, R. J., Cameron, S. E., Parra, J. L., Jones, P. G., & Jarvis, A. (2005). Very high resolution interpolated climate surfaces for global land areas. *International Journal of Climatology, 25*(15), 1965-1978. doi:10.1002/joc.1276

Hill, D., & Denmead, A. K. (1960). The geology of Queensland.

Hogg, A. G., Hua, Q., Blackwell, P. G., Niu, M., Buck, C. E., Guilderson, T. P., Heaton, T. J., Palmer, J. G., Reimer, P. J., Reimer, R. W., Turney, C. S. M., & Zimmerman, S. R. H. (2013). SHCal13 Southern Hemisphere Calibration, 0–50,000 Years cal BP. *Radiocarbon, 55*(4), 1889-1903. doi:10.2458/azu_js_rc.55.16783

Hughes, A. O., Olley, J. M., Croke, J. C., & McKergow, L. A. (2009). Sediment source changes over the last 250 years in a dry-tropical catchment, central Queensland, Australia. *Geomorphology, 104*(3), 262-275. doi:https://doi.org/10.1016/j.geomorph.2008.09.003

Ivy-Ochs, S., & Kober, F. (2008). Surface exposure dating with cosmogenic nuclides. *Quaternary Science Journal, 57*(1-2), 179-209.

Jansson, M. B. (1988). A Global Survey of Sediment Yield. *Geografiska Annaler. Series A, Physical Geography, 70*(1/2), 81-98. doi:10.2307/521127

Jenny, H. (1941). Factors of soil formation: A system of quantitative pedology, 281 pp: McGraw-Hill, New York.

Jessup, B. S., Jesse Hahm, W., Miller, S. N., Kirchner, J. W., & Riebe, C. S. (2011). Landscape response to tipping points in granite weathering: The case of stepped topography in the Southern Sierra Critical Zone Observatory. *Applied Geochemistry, 26*, S48-S50. doi:https://doi.org/10.1016/j.apgeochem.2011.03.026

Jiongxin, X. (2005). Precipitation–vegetation coupling and its influence on erosion on the Loess Plateau, China. *CATENA, 64*(1), 103-116. doi:http://dx.doi.org/10.1016/j.catena.2005.07.004

Johnson, R. W., Knutson, J., & Taylor, S. R. (1989). *Intraplate volcanism: in eastern Australia and New Zealand*: Cambridge University Press.

Kaspari, M., & Yanoviak, S. P. (2008). Biogeography of litter depth in tropical forests: evaluating the phosphorus growth rate hypothesis. *Functional Ecology, 22*(5), 919-923. doi:10.1111/j.1365-2435.2008.01447.x

Kaspari, M., & Yanoviak, S. P. (2009). Biogeochemistry and the structure of tropical brown food webs. *Ecology, 90*(12), 3342-3351. doi:10.1890/08-1795.1

Kirchner, J. W., Finkel, R. C., Riebe, C. S., Granger, D. E., Clayton, J. L., King, J. G., & Megahan, W. F. (2001). Mountain erosion over 10 yr, 10 ky, and 10 my time scales.

Geology, 29(7), 591-594. doi:10.1130/0091-7613(2001)029<0591:MEOYKY>2.0.CO;2

Knox, J. C. (1972). Valley Alluiviation in Southwestern Wisconsin *Annals of the Association of American Geographers, 62*(3), 401-410. doi:10.1111/j.1467-8306.1972.tb00872.x

Kohl, C. P., & Nishiizumi, K. (1992). Chemical isolation of quartz for measurement of in-situ -produced cosmogenic nuclides. *Geochimica et Cosmochimica Acta, 56*(9), 3583-3587. doi:https://doi.org/10.1016/0016-7037(92)90401-4

Korschinek, G., Bergmaier, A., Faestermann, T., Gerstmann, U. C., Knie, K., Rugel, G., Wallner, A., Dillmann, I., Dollinger, G., von Gostomski, C. L., Kossert, K., Maiti, M., Poutivtsev, M., & Remmert, A. (2010). A new value for the half-life of 10Be by Heavy-Ion Elastic Recoil Detection and liquid scintillation counting. *Nuclear Instruments and Methods in Physics Research Section B: Beam Interactions with Materials and Atoms, 268*(2), 187-191. doi:https://doi.org/10.1016/j.nimb.2009.09.020

Kroon, F. J., Schaffelke, B., & Bartley, R. (2014). Informing policy to protect coastal coral reefs: Insight from a global review of reducing agricultural pollution to coastal ecosystems. *Marine Pollution Bulletin, 85*(1), 33-41. doi:https://doi.org/10.1016/j.marpolbul.2014.06.003

Kubik, P., Ivy-Ochs, S., Schlüchter, C., Masarik, J., & Frank, M. (1998). 1998: 10Be and 26Al production rates deduced from an instantaneous event within the dendro-calibration curve, the landslide of the Köfels Otz Valley Austria. Earth and Planetary Science Letters 161, 231-241.

Lal, D. (1987). Production of 3He in terrestrial rocks. *Chemical Geology: Isotope Geoscience Section, 66*(1-2), 89-98. doi:10.1016/0168-9622(87)90031-5

Lal, D. (1991). Cosmic ray labeling of erosion surfaces: in situ nuclide production rates and erosion models. *Earth and Planetary Science Letters, 104*(2-4), 424-439. doi:10.1016/0012-821X(91)90220-C

Lal, R. (1990). Soil erosion and land degradation: the global risks *Advances in soil science* (pp. 129-172): Springer.

Lal, R. (2001). Soil degradation by erosion. *Land Degradation & Development, 12*(6), 519-539. doi:10.1002/ldr.472

Langbein, W. B., & Schumm, S. A. (1958). Yield of sediment in relation to mean annual precipitation. *Eos, Transactions American Geophysical Union, 39*(6), 1076-1084. doi:10.1029/TR039i006p01076

Lupker, M., Blard, P.-H., Lavé, J., France-Lanord, C., Leanni, L., Puchol, N., Charreau, J., & Bourlès, D. (2012). 10Be-derived Himalayan denudation rates and sediment budgets in the Ganga basin. *Earth and Planetary Science Letters, 333-334*, 146-156. doi:https://doi.org/10.1016/j.epsl.2012.04.020

Masarik, J., & Reedy, R. C. (1995). Terrestrial cosmogenic-nuclide production systematics calculated from numerical simulations. *Earth and Planetary Science Letters, 136*(3–4), 381-395. doi:http://dx.doi.org/10.1016/0012-821X(95)00169-D

Matmon, A., Enzel, Y., Vainer, S., Grodek, T., & Mushkin, A. (2018). The near steady state landscape of western Namibia. *Geomorphology, 313*, 72-87. doi:https://doi.org/10.1016/j.geomorph.2018.04.008

Matmon, A., Simhai, O., Amit, R., Haviv, I., Porat, N., McDonald, E., Benedetti, L., & Finkel, R. (2009). Desert pavement–coated surfaces in extreme deserts present the longest-lived landforms on Earth. *Geological Society of America Bulletin, 121*(5-6), 688-697.

Matmon, A., Bierman, P., & Enzel, Y. (2002). Pattern and tempo of great escarpment erosion. *Geology, 30*(12), 1135-1138. doi:10.1130/0091-7613(2002)030<1135:patoge>2.0.co;2

McNeil, V. H., Cox, M. E., & Preda, M. (2005). Assessment of chemical water types and their spatial variation using multi-stage cluster analysis, Queensland, Australia. *Journal of Hydrology, 310*(1), 181-200. doi:https://doi.org/10.1016/j.jhydrol.2004.12.014

Meade, R. H. (1988). Movement and storage of sediment in river systems *Physical and chemical weathering in geochemical cycles* (pp. 165-179): Springer.

Mellars, P. (2006). A new radiocarbon revolution and the dispersal of modern humans in Eurasia. *Nature, 439*, 931. doi:10.1038/nature04521

Merritt, W. S., Letcher, R. A., & Jakeman, A. J. (2003). A review of erosion and sediment transport models. *Environmental Modelling & Software, 18*(8–9), 761-799. doi:http://dx.doi.org/10.1016/S1364-8152(03)00078-1

Meyer, H., Hetzel, R., Fügenschuh, B., & Strauss, H. (2010). Determining the growth rate of topographic relief using in situ-produced 10Be: A case study in the Black Forest, Germany. *Earth and Planetary Science Letters, 290*(3), 391-402. doi:https://doi.org/10.1016/j.epsl.2009.12.034

Milliman, J. D., & Meade, R. H. (1983). World-wide delivery of river sediment to the oceans. *The Journal of Geology, 91*(1), 1-21.

Mishra, A. K., Placzek, C., & Jones, R. (2019). Coupled influence of precipitation and vegetation on millennial-scale erosion rates derived from 10Be. *PLOS ONE, 14*(1), e0211325. doi:10.1371/journal.pone.0211325

Mishra, A. K., Placzek, C., Wurster, C., & Whitehead, P. W. (2018). New radiocarbon age constraints for the 120 km-long Toomba flow, north Queensland, Australia. *Australian Journal of Earth Sciences*, 1-9. doi:10.1080/08120099.2019.1523227

Molnar, P. (2001). Climate change, flooding in arid environments, and erosion rates. *Geology, 29*(12), 1071-1074. doi:10.1130/0091-7613(2001)029<1071:CCFIAE>2.0.CO;2

Montgomery, D. R. (2001). Slope Distributions, Threshold Hillslopes, and Steady-state Topography. *American Journal of Science, 301*(4-5), 432-454. doi:10.2475/ajs.301.4-5.432

Montgomery, D. R., & Brandon, M. T. (2002). Topographic controls on erosion rates in tectonically active mountain ranges. *Earth and Planetary Science Letters, 201*(3), 481-489.

Montgomery, D. R., Balco, G., & Willett, S. D. (2001). Climate, tectonics, and the morphology of the Andes. *Geology, 29*(7), 579-582. doi:http://dx.doi.org/10.1130/0091-7613(2001)029<0579:CTATMO>2.0.CO;2

Moon, S., Chamberlain, C. P., Blisniuk, K., Levine, N., Rood, D. H., & Hilley, G. E. (2011). Climatic control of denudation in the deglaciated landscape of the Washington Cascades. *Nature Geoscience, 4*(7), 469-473.

Murray-Wallace, C. V. (2011). Comment on: "New $^{40}Ar/^{39}Ar$ ages for selected young (<1 Ma) basalt flows of the Newer Volcanic Province, southeastern Australia" by E. Matchan & D. Phillips. *Quaternary Geochronology, 6*(6), 598-599. doi:10.1016/j.quageo.2011.07.001

Mutz, S. G., Ehlers, T. A., Werner, M., Lohmann, G., Stepanek, C., & Li, J. (2018). Estimates of late Cenozoic climate change relevant to Earth surface processes in tectonically active orogens. *Earth Surface Dynamics, 6*(2), 271-301. doi:10.5194/esurf-6-271-2018

Neil, D. (1995). *Fluvial sediment yield to the Great Barrier Reef lagoon: spatial patterns and the effect of land use.* Paper presented at the Proceedings of the Conference on Downstream Effects of Land Use.

Neyman, J. (1937). Outline of a theory of statistical estimation based on the classical theory of probability. *Philosophical Transactions of the Royal Society of London. Series A, Mathematical and Physical Sciences, 236*(767), 333-380.

Nichols, K. K., Bierman, P. R., & Rood, D. H. (2014). 10Be constrains the sediment sources and sediment yields to the Great Barrier Reef from the tropical Barron River catchment, Queensland, Australia. *Geomorphology, 224*(0), 102-110. doi:http://dx.doi.org/10.1016/j.geomorph.2014.07.019

Niemi, N. A., Oskin, M., Burbank, D. W., Heimsath, A. M., & Gabet, E. J. (2005). Effects of bedrock landslides on cosmogenically determined erosion rates. *Earth and Planetary Science Letters, 237*(3), 480-498. doi:https://doi.org/10.1016/j.epsl.2005.07.009

Nishiizumi, K., Imamura, M., Caffee, M. W., Southon, J. R., Finkel, R. C., & McAninch, J. (2007). Absolute calibration of 10Be AMS standards. *Nuclear Instruments and Methods in Physics Research Section B: Beam Interactions with Materials and Atoms, 258*(2), 403-413.

Nishiizumi, K., Lal, D., Klein, J., Middleton, R., & Arnold, J. R. (1986). Production of 10Be and 26Al by cosmic rays in terrestrial quartz in situ and implications for erosion rates. *Nature, 319*, 134. doi:10.1038/319134a0

Nishiizumi, K., Winterer, E. L., Kohl, C. P., Klein, J., Middleton, R., Lal, D., & Arnold, J. R. (1989). Cosmic ray production rates of 10Be and 26Al in quartz from glacially polished rocks. *Journal of Geophysical Research: Solid Earth, 94*(B12), 17907-17915. doi:doi:10.1029/JB094iB12p17907

Nott, J. F., Young, R. W., & Idnurm, M. (1991). Sedimentology, weathering, age and geomorphological significance of Tertiary sediments on the far south coast of New South Wales. *Australian Journal of Earth Sciences, 38*(3), 357-373. doi:10.1080/08120099108727978

Oilier, C. D. (1982). The Great Escarpment of eastern Australia: Tectonic and geomorphic significance. *Journal of the Geological Society of Australia, 29*(1-2), 13-23. doi:10.1080/00167618208729190

Ollier, C. D. (1979). Evolutionary Geomorphology of Australia and Papua: New Guinea. *Transactions of the Institute of British Geographers, 4*(4), 516-539. doi:10.2307/622212

Oleson, K. L. L., Falinski, K. A., Lecky, J., Rowe, C., Kappel, C. V., Selkoe, K. A., & White, C. (2017). Upstream solutions to coral reef conservation: The payoffs of smart and cooperative decision-making. *Journal of Environmental Management, 191*, 8-18. doi:https://doi.org/10.1016/j.jenvman.2016.12.067

Oliva, P., Viers, J., & Dupré, B. (2003). Chemical weathering in granitic environments. *Chemical geology, 202*(3), 225-256. doi:https://doi.org/10.1016/j.chemgeo.2002.08.001

Pillans, B. (1997). Soil development at snail's pace: evidence from a 6 Ma soil chronosequence on basalt in north Queensland, Australia. *Geoderma, 80*(1), 117-128. doi:10.1016/S0016-7061(97)00068-2

Pillans, B., & Fifield, L. K. (2013). Erosion rates and weathering history of rock surfaces associated with Aboriginal rock art engravings (petroglyphs) on Burrup Peninsula, Western Australia, from cosmogenic nuclide measurements. *Quaternary Science Reviews, 69*, 98-106. doi:http://dx.doi.org/10.1016/j.quascirev.2013.03.001

Pimentel, D. (2006). Soil Erosion: A Food and Environmental Threat. *Environment, development and sustainability, 8*(1), 119-137. doi:10.1007/s10668-005-1262-8

Pimentel, D., & Kounang, N. (1998). Ecology of Soil Erosion in Ecosystems. *Ecosystems, 1*(5), 416-426. doi:10.1007/s100219900035

Pimentel, D., & Kounang, N. (1998). Ecology of Soil Erosion in Ecosystems. *Ecosystems, 1*(5), 416-426. doi:10.1007/s100219900035

Pimentel, D., Harvey, C., Resosudarmo, P., Sinclair, K., Kurz, D., McNair, M., Crist, S., Shpritz, L., Fitton, L., Saffouri, R., & Blair, R. (1995). Environmental and Economic costs of Soil Erosion and Conservation Benefits *Science, 267*(5201), 1117-1123. doi:10.1126/science.267.5201.1117

Placzek, C., Granger, D. E., Matmon, A., Quade, J., & Ryb, U. (2014). Geomorphic process rates in the central Atacama Desert, Chile: Insights from cosmogenic nuclides and implications for the onset of hyperaridity. *American Journal of Science, 314*(10), 1462-1512.

Placzek, C., Matmon, A., Granger, D., Quade, J., & Niedermann, S. (2010). Evidence for active landscape evolution in the hyperarid Atacama from multiple terrestrial cosmogenic nuclides. *Earth and Planetary Science Letters, 295*(1), 12-20.

Plumb, K., Derrick, G., & Wilson, I. (1980). Precambrian geology of the McArthur River—Mount Isa region, northern Australia. *The geology and geophysics of northeastern Australia*, 71-88.

Polach, H. A., & Gulson, J. (1966). Collection of specimens for radiocarbon dating and interpretation of results *Manual No. 2*: Australian Institute of Aboriginal Studies. Canberra. Australia.

Portenga, E. W., & Bierman, P. R. (2011). Understanding Earth's eroding surface with 10 Be. *GSA Today, 21*(8), 4-10.

Portenga, E. W., Bierman, P. R., Rizzo, D. M., & Rood, D. H. (2013). Low rates of bedrock outcrop erosion in the central Appalachian Mountains inferred from in situ 10Be. *Geological Society of America Bulletin, 125*(1-2), 201-215.

Portenga, E. W., Rood, D. H., Bishop, P., & Bierman, P. R. (2016). A late Holocene onset of Aboriginal burning in southeastern Australia. *Geology, 44*(2), 131-134. doi:https://doi.org/10.1130/G37257.1

Prosser, I., Rustomji, P., Young, B., Moran, C., & Hughes, A. (2001). Constructing river basin sediment budgets for the National Land and Water Resources Audit. *Land and Water Technical Report, CSIRO, Canberra*.

Quigley, M., Sandiford, M., & Cupper, M. (2006). Landscape expressions of late Quaternary climate change and large flood events, Flinders Ranges, South Australia. *ASEG Extended Abstracts, 2006*(1), 1-2. doi:https://doi.org/10.1071/ASEG2006AB144

Quigley, M., Sandiford, M., Fifield, K., & Alimanovic, A. (2007a). Bedrock erosion and relief production in the northern Flinders Ranges, Australia. *Earth surface processes and landforms, 32*(6), 929-944. doi:doi:10.1002/esp.1459

Quigley, M., Sandiford, M., Fifield, L. K., & Alimanovic, A. (2007b). Landscape responses to intraplate tectonism: Quantitative constraints from 10 Be nuclide abundances. *Earth and Planetary Science Letters, 261*(1), 120-133.

Raymo, M. E., Ruddiman, W. F., & Froelich, P. N. (1988). Influence of late Cenozoic mountain building on ocean geochemical cycles. *Geology, 16*(7), 649-653.

Raymo, M., & Ruddiman, W. F. (1992). Tectonic forcing of late Cenozoic climate. *Nature, 359*(6391), 117-122.

Rea, D. K., Snoeckx, H., & Joseph, L. H. (1998). Late Cenozoic eolian deposition in the North Pacific: Asian drying, Tibetan uplift, and cooling of the northern hemisphere. *Paleoceanography, 13*(3), 215-224.

Reiners, P. W., Ehlers, T. A., Mitchell, S. G., & Montgomery, D. R. (2003). Coupled spatial variations in precipitation and long-term erosion rates across the Washington Cascades. *Nature, 426*, 645. doi:10.1038/nature02111

Reusser, L., Bierman, P., & Rood, D. (2015). Quantifying human impacts on rates of erosion and sediment transport at a landscape scale. *Geology, 43*(2), 171-174. doi:http://dx.doi.org/10.1130/G36272.1

Rey, F. (2003). Influence of vegetation distribution on sediment yield in forested marly gullies. *CATENA, 50*(2), 549-562. doi:https://doi.org/10.1016/S0341-8162(02)00121-2

Riebe, C. S., Kirchner, J. W., & Finkel, R. C. (2004). Erosional and climatic effects on long-term chemical weathering rates in granitic landscapes spanning diverse climate regimes. *Earth and Planetary Science Letters, 224*(3), 547-562. doi:https://doi.org/10.1016/j.epsl.2004.05.019

Riebe, C. S., Kirchner, J. W., Granger, D. E., & Finkel, R. C. (2001a). Minimal climatic control on erosion rates in the Sierra Nevada, California. *Geology, 29*(5), 447-450.

Riebe, C. S., Kirchner, J. W., Granger, D. E., & Finkel, R. C. (2001b). Strong tectonic and weak climatic control of long-term chemical weathering rates. *Geology, 29*(6), 511-514.

Roering, J. J., Kirchner, J. W., & Dietrich, W. E. (1999). Evidence for nonlinear, diffusive sediment transport on hillslopes and implications for landscape morphology. *Water Resources Research, 35*(3), 853-870. doi:doi:10.1029/1998WR900090

Rogers, R. D., & Schumm, S. A. (1991). The effect of sparse vegetative cover on erosion and sediment yield. *Journal of Hydrology, 123*(1), 19-24. doi:https://doi.org/10.1016/0022-1694(91)90065-P

Rosenkranz, R., Schildgen, T., Wittmann, H., & Spiegel, C. (2018). Coupling erosion and topographic development in the rainiest place on Earth: Reconstructing the Shillong Plateau uplift history with in-situ cosmogenic 10Be. *Earth and Planetary Science Letters, 483*, 39-51. doi:https://doi.org/10.1016/j.epsl.2017.11.047

Ruddiman, W. F., Prell, W. L., & Raymo, M. E. (1989). Late Cenozoic uplift in southern Asia and the American West: Rationale for general circulation modeling experiments. *Journal of Geophysical Research: Atmospheres, 94*(D15), 18379-18391. doi:10.1029/JD094iD15p18379

Ryb, U., Matmon, A., Erel, Y., Haviv, I., Benedetti, L., & Hidy, A. J. (2014). Styles and rates of long-term denudation in carbonate terrains under a Mediterranean to hyper-arid climatic gradient. *Earth and Planetary Science Letters, 406*, 142-152. doi:https://doi.org/10.1016/j.epsl.2014.09.008

Sandiford, M. (2003). Neotectonics of southeastern Australia: linking the Quaternary faulting record with seismicity and in situ stress. *Special papers-geological society of america*, 107-120.

Schaller, M., Ehlers, T. A., Lang, K. A. H., Schmid, M., & Fuentes-Espoz, J. P. (2018). Addressing the contribution of climate and vegetation cover on hillslope denudation, Chilean Coastal Cordillera (26°–38°S). *Earth and Planetary Science Letters, 489*, 111-122. doi:https://doi.org/10.1016/j.epsl.2018.02.026

Schaller, M., von Blanckenburg, F., Hovius, N., & Kubik, P. W. (2001). Large-scale erosion rates from in situ-produced cosmogenic nuclides in European river sediments. *Earth and Planetary Science Letters, 188*(3), 441-458. doi:https://doi.org/10.1016/S0012-821X(01)00320-X

Schaller, M., von Blanckenburg, F., Veldkamp, A., Tebbens, L. A., Hovius, N., & Kubik, P. W. (2002). A 30 000 yr record of erosion rates from cosmogenic 10Be in Middle

European river terraces. *Earth and Planetary Science Letters, 204*(1), 307-320. doi:https://doi.org/10.1016/S0012-821X(02)00951-2

Scherler, D., Bookhagen, B., & Strecker, M. R. (2014). Tectonic control on 10Be-derived erosion rates in the Garhwal Himalaya, India. *Journal of Geophysical Research: Earth Surface, 119*(2), 83-105. doi:10.1002/2013JF002955

Schumm, S. A. (1963). *The disparity between present rates of denudation and orogeny*: US Government Printing Office.

Self, S., Keszthelyi, L., & Thordarson, T. (1998). THE IMPORTANCE OF PĀHOEHOE. *Annual Review of Earth and Planetary Sciences, 26*(1), 81-110. doi:10.1146/annurev.earth.26.1.81

Small, E. E., Anderson, R. S., & Hancock, G. S. (1999). Estimates of the rate of regolith production using 10Be and 26Al from an alpine hillslope. *Geomorphology, 27*(1), 131-150. doi:https://doi.org/10.1016/S0169-555X(98)00094-4

Small, E. E., Anderson, R. S., Repka, J. L., & Finkel, R. (1997). Erosion rates of alpine bedrock summit surfaces deduced from in situ 10Be and 26Al. *Earth and Planetary Science Letters, 150*(3), 413-425. doi:https://doi.org/10.1016/S0012-821X(97)00092-7

Stephenson, P., Burch-Johnston, A., Stanton, D., & Whitehead, P. (1998). Three long lava flows in north Queensland. *Journal of Geophysical Research: Solid Earth, 103*(B11), 27359-27370. doi:10.1029/98JB01670

Stephenson, P., Polach, H., & Wyatt, D. (1978). The age of the Toomba basalt, north Queensland. *Third Australian Geological Convention*(Stephenson P.J ed., Geological Society of Australia), 62-63

Stone, J. O. (2000). Air pressure and cosmogenic isotope production. *Journal of Geophysical Research: Solid Earth (1978–2012), 105*(B10), 23753-23759.

Summerfield, M. A., Stuart, F. M., Cockburn, H. A. P., Sugden, D. E., Denton, G. H., Dunai, T., & Marchant, D. R. (1999). Long-term rates of denudation in the Dry Valleys, Transantarctic Mountains, southern Victoria Land, Antarctica based on in-situ-produced cosmogenic 21Ne. Geomorphology, 27(1), 113-129. doi:https://doi.org/10.1016/S0169-555X(98)00093-2

Summerfield, M. A., & Hulton, N. J. (1994). Natural controls of fluvial denudation rates in major world drainage basins. *Journal of Geophysical Research: Solid Earth, 99*(B7), 13871-13883. doi:doi:10.1029/94JB00715

Sutherland, L. (1995). The Volcanic Earth: Sydney, University of New South Wales Press, 248 p. *University of New South Wales Press, Sydney*, 248 p.

Sverdrup, H., & Warfvinge, P. (1995). Chapter 11. ESTIMATING FIELD WEATHERING RATES USING LABORATORY KINETICS *Chemical Weathering Rates of Silicate Minerals* (Vol. 31).

Tomkins, K., Humphreys, G., Wilkinson, M., Fink, D., Hesse, P., Doerr, S., Shakesby, R., Wallbrink, P., & Blake, W. (2007). Contemporary versus long-term denudation along a passive plate margin: the role of extreme events. *Earth surface processes and landforms, 32*(7), 1013-1031.

Trimble, S. W., & Crosson, P. (2000). U.S. Soil Erosion Rates--Myth and Reality. *Science, 289*(5477), 248-250. doi:10.1126/science.289.5477.248

Tucker, G. E., & Bras, R. L. (1998). Hillslope processes, drainage density, and landscape morphology. *Water Resources Research, 34*(10), 2751-2764. doi:10.1029/98WR01474

Vanacker, V., Von Blanckenburg, F., Hewawasam, T., & Kubik, P. (2007). Constraining landscape development of the Sri Lankan escarpment with cosmogenic nuclides in river sediment. *Earth and Planetary Science Letters, 253*(3), 402-414.

von Blanckenburg, F. (2005). The control mechanisms of erosion and weathering at basin scale from cosmogenic nuclides in river sediment. *Earth and Planetary Science Letters, 237*(3), 462-479. doi:10.1016/j.epsl.2005.11.017

Wagner, G. A. (1998). *Age determination of young rocks and artifacts: physical and chemical clocks in quaternary geology and archaeology*: Springer Science & Business Media.

Walling, D. E., & Webb, B. (1983). Patterns of sediment yield. *BACKGROUND TO PALAEOHYDROLOGY. A PERSPECTIVE., 1983*, 69-100.

Walling, D. E., & Webb, B. (1996). *Erosion and Sediment Yield: Global and Regional Perspectives: Proceedings of an International Symposium Held at Exeter, UK, from 15 to 19 July 1996*: IAHS.

Walling, D., & Webb, B. (1987). Material transport by the world's rivers: evolving perspectives. *IN: Water for the Future: Hydrology in Perspective. IAHS Publication*(164).

Wellman, P., & McDougall, I. (1974). Cainozoic igneous activity in eastern australia. *Tectonophysics, 23*(1), 49-65. doi:https://doi.org/10.1016/0040-1951(74)90110-3

Wheller, G. E., Varne, R., Foden, J. D., & Abbott, M. J. (1987). Geochemistry of quaternary volcanism in the Sunda-Banda arc, Indonesia, and three-component genesis of island-arc basaltic magmas. *Journal of Volcanology and Geothermal Research, 32*(1), 137-160. doi:10.1016/0377-0273(87)90041-2

White, A. (1994). Effects of climate on chemical weathering in watersheds underlain by grantoid rocks. *Mineralogical Magazine, 58*, 967-968.

Whitehead, P., & Stephenson, P. (1998). Lava rise ridges of the Toomba basalt flow, north Queensland, Australia. *Journal of Geophysical Research: Solid Earth, 103*(B11), 27371-27382. doi:10.1029/98JB00029

Whitehead, P., Stephenson, P., McDougall, I., Hopkins, M. S., Graham, A. W., Collerson, K. D., & Johnson, D. P. (2007). Temporal development of the Atherton Basalt Province, north Queensland. *Australian Journal of Earth Sciences, 54*(5), 691-709. doi:10.1080/08120090701305236

Whiting, P. J. (2006). Estimating TMDL Background Suspended Sediment Loading To Great Lakes Tributaries from Existing Data. *JAWRA Journal of the American Water Resources Association, 42*(3), 769-776. doi:10.1111/j.1752-1688.2006.tb04491.x

Wijbrans, J., Schneider, B., Kuiper, K., Calvari, S., Branca, S., De Beni, E., Norini, G., Corsaro, R. A., & Miraglia, L. (2011). $^{40}Ar/^{39}Ar$ geochronology of Holocene basalts; examples from Stromboli, Italy. *Quaternary Geochronology, 6*(2), 223-232. doi:10.1016/j.quageo.2010.10.003

Willenbring, J. K., Codilean, A. T., & McElroy, B. (2013). Earth is (mostly) flat: Apportionment of the flux of continental sediment over millennial time scales. *Geology, 41*(3), 343-346. doi:https://doi.org/10.1130/G33918.1

Willmott, W. F. (2009). *Rocks and landscapes of the national parks of north Queensland*: Geological Society of Australia Queensland Division.

Wittmann, H., von Blanckenburg, F., Guyot, J. L., Laraque, A., Bernal, C., & Kubik, P. W. (2011). Sediment production and transport from in situ-produced cosmogenic 10Be and river loads in the Napo River basin, an upper Amazon tributary of Ecuador and Peru. *Journal of South American Earth Sciences, 31*(1), 45-53. doi:https://doi.org/10.1016/j.jsames.2010.09.004

Wittmann, H., von Blanckenburg, F., Kruesmann, T., Norton, K. P., & Kubik, P. W. (2007). Relation between rock uplift and denudation from cosmogenic nuclides in river sediment in the Central Alps of Switzerland. *Journal of Geophysical Research: Earth Surface (2003–2012), 112*(F4).

Wurster, C. M., Lloyd, J., Goodrick, I., Saiz, G., & Bird, M. I. (2012). Quantifying the abundance and stable isotope composition of pyrogenic carbon using hydrogen pyrolysis. *Rapid Communications in Mass Spectrometry, 26*(23), 2690-2696. doi:10.1002/rcm.6397

Wyatt, D. H., & Webb, A. W. (1970). Potassium-argon ages of some northern Queensland basalts and an interpretation of late Cainozoic history. *Journal of the Geological Society of Australia, 17*(1), 39-51. doi:10.1080/00167617008728722

Yanites, B. J., & Kesler, S. E. (2015). A climate signal in exhumation patterns revealed by porphyry copper deposits. *Nature Geosci, 8*(6), 462-465. doi:10.1038/ngeo2429.

Young, R. W. (1983). The Tempo of Geomorphological Change: Evidence from Southeastern Australia. *The Journal of Geology, 91*(2), 221-230. doi:10.1086/628758

Zimmermann, A., Francke, T., & Elsenbeer, H. (2012). Forests and erosion: Insights from a study of suspended-sediment dynamics in an overland flow-prone rainforest catchment. *Journal of Hydrology, 428*(Supplement C), 170-181. doi:https://doi.org/10.1016/j.jhydrol.2012.01.039

Zreda, M. G., Phillips, F. M., Kubik, P. W., Sharma, P., & Elmore, D. (1993). Cosmogenic 36Cl dating of a young basaltic eruption complex, Lathrop Wells, Nevada. *Geology, 21*(1), 57-60. doi:10.1130/0091-7613(1993)021<0057:CCDOAY>2.3.CO;2

Chapter 7: Appendices

7.1. Appendix 1 – Data and statistics for Chapter 2

7.2. Appendix 2 – Pictures of sample locations

7.3. Appendix 3 – Erosion rate data for Chapter 3

7.4. Appendix 4 – Permits to collect samples

7.5. Appendix 5 – Results for Chapter 4

Appendix 1

Supplementary material for: Coupled influence of precipitation and vegetation on millennial-scale erosion rates derived from ^{10}Be

Ashish Kumar Mishra[1*], Christa Placzek[1], and Rhondda Jones[2]

[1]Geosciences, College of Science and Engineering and Centre for Tropical Environmental and Sustainability Science (TESS), James Cook University, Townsville, Queensland, Australia, 4810

[2]Emeritus Professor, Coordinator, StatsHelp Service, Graduate Research School, James Cook University, Townsville, Queensland, Australia, 4810

DATA COMPILATION:

Cosmogenic ^{10}Be-derived basin average erosion rates were compiled from various published studies conducted all over the world. Most of the studies of this compilation were included in Portenga & Bierman (2011), and Willenbring (2013); however, we have added more studies conducted after these publications. We also recalculated erosion rate for all studies, based on the latest update of CRONUS (Version 2.3) (Balco, Stone, Lifton, & Dunai, 2008)(hess.ess.washington.edu). The information required for CRONUS erosion rate calculations was retrieved from published studies. Most studies did not have any information on sample thickness and crustal density. Therefore, sample thickness was assumed 1 cm and crustal density as 2.7g/cm^3. The geographic coordinates of the samples in the dataset are expressed in Decimal Degrees and the spatial reference system is WGS84.

REFERENCES FOR DATA:

1. Abbühl, L. M., Norton, K. P., Schlunegger, F., Kracht, O., Aldahan, A., and Possnert, G., 2010, El Niño forcing on ^{10}Be-based surface denudation rates in the north-western Peruvian Andes: Geomorphology, v. 123, p. 257-268.
2. Acosta, V. T., Schildgen, T. F., Clarke, B. A., Scherler, D., Bookhagen, B., Wittmann, H., Strecker, M. R. (2015). Effect of vegetation cover on millennial-scale landscape denudation rates in East Africa. Lithosphere, L402. 401.
3. Balco, G., Stone, J. O., Lifton, N. A., & Dunai, T. J. (2008). A complete and easily accessible means of calculating surface exposure ages or erosion rates from 10 Be and 26 Al measurements. Quaternary Geochronology, 3(3), 174-195.

4. Belmont, P., Pazzaglia, F. J., and Gosse, J. C., 2007, Cosmogenic ^{10}Be as a tracer for hillslope and channel sediment dynamics in the Clearwater River, western Washington State: Earth and Planetary Science Letters.
5. Bierman, P. R., Albrecht, A., Bothner, M., Brown, E., Bullen, T., Gray, L., and Turpin, L., 1998, Weathering, erosion and sedimentation, *in* Kendall, C., and McDonnell, J. J., eds., Isotope Tracers in Catchment Hydrology, Elsevier, p. 647-678.
6. Bierman, P. R., and Caffee, M. W., 2001, Slow rates of rock surface erosion and sediment production across the Namib Desert and escarpment, Southern Africa: American Journal of Science, v. 301, no. 4-5, p. 326-358.
7. Bierman, P. R., and Steig, E., 1996, Estimating rates of denudation and sediment transport using cosmogenic isotope abundances in sediment: Earth Surface Processes and Landforms, v. 21, p. 125-139.
8. Bierman, P. R., Clapp, E. M., Nichols, K. K., Gillespie, A. R., and Caffee, M., 2001, Using cosmogenic nuclide measurements in sediments to understand background rates of erosion and sediment transport,, *in* Harmon, R. S., and Doe, W. M., eds., Landscape Erosion and Evolution Modelling: New York, Kluwer, p. 89-116.
9. Bierman, P. R., Nichols, K. K., Matmon, A., Enzel, Y., Larsen, J., and Finkel, R., 2007, 10-Be shows that Namibian drainage basins are slowly, steadily and uniformly eroding: Quaternary International v. 167–168 no. 3, p. 33.
10. Bierman, P. R., Reusser, L. J., Nichols, K. K., Matmon, A., and Rood, D., 2009, Where is the sediment coming from and where is it going - A 10Be examination of the northern Queensland escarpment, Australia, 2009 Portland GSA Annual Meeting: Portland, Or.
11. Bierman, P. R., Reuter, J. M., Pavich, M., Gellis, A. C., Caffee, M. W., and Larsen, J., 2005, Using cosmogenic nuclides to contrast rates of erosion and sediment yield in a semi-arid, arroyo-dominated landscape, Rio Puerco Basin, New Mexico: Earth Surface Processes and Landforms, v. 30, no. 8, p. 935-953.
12. Binnie, S. A., Phillips, W. M., Summerfield, M. A., and Fifield, L. K., 2006, Sediment mixing and basin-wide cosmogenic nuclide analysis in rapidly eroding mountainous environments: Quaternary Geochronology v. 1, p. 4-14.
13. Binnie, S. A., Phillips, W. M., Summerfield, M. A., Fifield, L. K., and Spotila, J. A., 2008, Patterns of denudation through time in the San Bernardino Mountains, California: Implications for early-stage orogenesis Earth and Planetary Science Letters, v. In Press.
14. Brown, E. T., Stallard, R. F., Larsen, M. C., Bourles, D. L., Raisbeck, G. M., and Yiou, F., 1998, Determination of predevelopment denudation rates of an agricultural watershed (Cayaguas River, Puerto Rico) using in-situ-produced ^{10}Be in river-borne quartz: Earth and Planetary Science Letters, v. 160, no. 3-4, p. 723-728.
15. Buechi, M., Kober, F., Ivy-Ochs, S., Salcher, B., Kubik, P., & Christl, M. 2014. Denudation rates of small transient catchments controlled by former glaciation: The Hörnli nunatak in the northeastern Swiss Alpine Foreland. Quaternary Geochronology, 19, 135-147.

16. Carretier, S., Regard, V., Vassallo, R., Aguilar, G., Martinod, J., Riquelme, R., Farías, M. (2013). Slope and climate variability control of erosion in the Andes of central Chile. Geology, 41(2), 195-198.
17. Chappell, J., Zheng, H., and Fifield, K., 2006, Yangtse River sediments and erosion rates from source to sink traced with cosmogenic ^{10}Be: Sediments from major rivers: Palaeogeography, Palaeoclimatology, Palaeoecology, v. 241, no. 1, p. 79-94.
18. Clapp, E. M., Bierman, P. R., Nichols, K. K., Pavich, M., and Caffee, M., 2001, Rates of sediment supply to arroyos from upland erosion determined using in situ produced cosmogenic ^{10}Be and ^{26}Al: Quaternary Research (New York), v. 55, no. 2, p. 235-245.
19. Clapp, E. M., Bierman, P. R., Schick, A. P., Lekach, J., Enzel, Y., and Caffee, M., 2000, Sediment yield exceeds sediment production in arid region drainage basins: Geology, v. 28, no. 11, p. 995-998.
20. Clapp, E., Bierman, P. R., and Caffee, M., 2002, Using ^{10}Be and ^{26}Al to determine sediment generation rates and identify sediment source areas in an arid region drainage basin: Geomorphology, v. 45, no. 1,2, p. 89-104.
21. Codilean, A. T., Bishop, P., Stuart, F. M., Hoey, T. B., Fabel, D., & Freeman, S. P. 2008. Single-grain cosmogenic 21Ne concentrations in fluvial sediments reveal spatially variable erosion rates. Geology, 36(2), 159-162.
22. Codilean, A. T., Fenton, C. R., Fabel, D., Bishop, P., & Xu, S. (2014). Discordance between cosmogenic nuclide concentrations in amalgamated sands and individual fluvial pebbles in an arid zone catchment. Quaternary Geochronology, 19, 173-180.
23. Cox, R., Bierman, P. R., Jungers, M., Rakotondrazafy, A. F. M., and Finkel, R. C., 2006, Just how fast does Madagascar erode? Evidence from ^{10}Be analysis of lavaka, slope, and river sediment: Geological Society of America *Abstracts with Programs*, v. 38, no. 7, p. 278.
24. Croke, J., Bartley, R., Chappell, J., Austin, J. M., Fifield, K., Tims, S. G., Furuichi, T. (2015). 10Be-derived denudation rates from the Burdekin catchment: the largest contributor of sediment to the Great Barrier Reef. Geomorphology.
25. Cyr, A. J., and Granger, D. E., 2008, Dynamic equilibrium among erosion, river incision, and coastal uplift in the northern and central Apennines, Italy: Geology, v. 36, no. 2, p. 103- 106.
26. Cyr, A. J., Granger, D. E., Olivetti, V., and Molin, P., 2010, Quantifying rock uplift rates using channel steepness and cosmogenic nuclide-determined erosion rates: examples from northern and southern Italy: Lithosphere, v. 2, no. 3, p. 188-198.
27. Delunel, R., Beek, P. A. v. d., Carcaillet, J., Bourlès, D. L., and Valla, P. G., 2010, Frost- cracking control on catchment denudation rates: Insights from in situ produced ^{10}Be concentrations in stream sediments (Ecrins–Pelvoux massif, French Western Alps): Earth and Planetary Science Letters, v. 293, p. 72-83.
28. Delunel, R., van der Beek, P. A., Carcaillet, J., Bourlès, D. L., & Valla, P. G. (2010). Frost-cracking control on catchment denudation rates: Insights from in situ produced 10Be concentrations in stream sediments (Ecrins–Pelvoux massif, French Western

Alps). Earth and Planetary Science Letters, 293(1–2), 72-83. doi:http://dx.doi.org/10.1016/j.epsl.2010.02.020

29. Densmore, A. L., Hetzel, R., Ivy-Ochs, S., Krugh, W. C., Dawers, N., & Kubik, P. (2009). Spatial variations in catchment-averaged denudation rates from normal fault footwalls. Geology, 37(12), 1139-1142. doi:10.1130/g30164a.1
30. DiBiase, R. A., Whipple, K. X., Heimsath, A. M., and Ouimet, W. B., 2009, Landscape form and millennial erosion rates in the San Gabriel Mountains, CA: Earth and Planetary Science Letters, v. 289, p. 134-144.
31. Dirks, P. H. G. M., Placzek, C. J., Fink, D., Dosseto, A., & Roberts, E. (2016). Using 10Be cosmogenic isotopes to estimate erosion rates and landscape changes during the Plio-Pleistocene in the Cradle of Humankind, South Africa. *Journal of Human Evolution, 96*, 19-34. doi:http://dx.doi.org/10.1016/j.jhevol.2016.03.002
32. Duxbury, J., 2009, Erosion rates in and around Shenandoah National Park, VA, determined using analysis of cosmogenic 10Be: University of Vermont, 134 p.
33. Duxbury, J., Bierman, P. R., Portenga, E. W., Pavich, M. J., Southworth, S., & Freeman, S. P. (2015). Erosion rates in and around Shenandoah National Park, Virginia, determined using analysis of cosmogenic 10Be. American Journal of Science, 315(1), 46-76.
34. Ferrier, K. L., Kirchner, J. W., and Finkel, R. C., 2005, Erosion rates over millennial and decadal timescales at Caspar Creek and Redwood Creek, Northern California Coast Ranges: Earth Surface Processes and Landforms, v. 30, no. 8, p. 1025-1038.
35. Finnegan, N. J., Hallet, B., Montgomery, D. R., Zeitler, P., Stone, J., Anders, A. M., and Yuping, L., 2008, coupling of rock uplift and river incision in the Namche Barwa-Gyala peri massif, Tibet: 2007 GSA Denver Annual Meeting.
36. Glotzbach, C., Röttjer, M., Hampel, A., Hetzel, R., & Kubik, P. W. (2014). Quantifying the impact of former glaciation on catchment-wide denudation rates derived from cosmogenic 10Be. *Terra Nova*, *26*(3), 186-194. doi:10.1111/ter.12085
37. Godard, V., Lavé, J., Carcaillet, J., Cattin, R., Bourlès, D., and Zhu, J., 2010, Spatial distribution of denudation in Eastern Tibet and regressive erosion of plateau margins: Tectonophysics, v. 491, p.253-274.
38. Granger, D. E., Kirchner, J. W., and Finkel, R., 1996, Spatially averaged long-term erosion rates measured from in situ-produced cosmogenic nuclides in alluvial sediments: Journal of Geology, v. 104, no. 3, p. 249-257.
39. Guralnik, B., Matmon, A., Avni, Y., and Fink, D., 2010, ^{10}Be exposure ages of ancient desert pavements reveal Quaternary evolution of the Dead Sea drainage basin and rift margin tilting: Earth and Planetary Science Letters, v. 290, p. 132-141.
40. Harkins, N., Kirby, E., Heimsath, A., Robinson, R., and Reiser, U., 2007, Transient fluvial incision in the headwaters of the Yellow River, northeastern Tibet, China: Journal of Geophysical Research, v. 112., no. F03S04, p. 21.
41. Heimsath, A. M., Chappell, J., Fifield, K., 1999, Cosmogenic nuclides, topography, and the spatial variation of soil depth: Geomorphology, v. 27, no. 1-2, p. 151-172.

42. Heimsath, A. M., Chappell, J., Fifield, K., 2001a, Late Quaternary erosion in southeastern Australia: a field example using cosmogenic nuclides: Quaternary International, v. 83-85, p. 169-185.
43. Heimsath, A. M., Chappell, J., Fifield, K., 2001b, Stochastic processes of soil production and transport; erosion rates, topographic variation and cosmogenic nuclides in the Oregon Coast Range: Earth Surface Processes and Landforms, v. 26, no. 5, p. 531-552.
44. Heimsath, A. M., Chappell, J., Fifield, K., 2010, Eroding Australia: rates and processes from Bega Valley to Arnhem Land: Geological Society, London, Special Publications, v. 346, p. 225-241.
45. Heimsath, A. M., Fink, D., and Hancock, G. R., 2009, The 'humped' soil production function: eroding Arnhem Land, Australia: Earth Surface Processes and Landforms, vol. 34, p. 1674-1684.
46. Heimsath, A., Chappel, J., Finkel, R. C., Fifield, K., and Alimanovic, A., 2006, Escarpment Erosion and Landscape Evolution in Southeastern Australia: Special Papers-Geological Society of America, v. 398, p. 173.
47. Henck, A. C., Huntington, K. W., Stone, J. O., Montgomery, D. R., and Hallet, B., 2011, Spatial controls on erosion in the Three Rivers Region, southeastern Tibet and southwestern China: Earth and Planetary Science Letters, v. 303, p. 71-83.
48. Hewawasam, T., von Blackenburg, F., Schaller, M., and Kubik, P., 2003, Increase of human over natural erosion rates in tropical highlands constrained by cosmogenic nuclides: Geology, v. 31, no. 7, p. 597-600.
49. Hippe, K., Kober, F., Zeilinger, G., Ivy-Ochs, S., Maden, C., Wacker, L., Wieler, R. (2012). Quantifying denudation rates and sediment storage on the eastern Altiplano, Bolivia, using cosmogenic 10 Be, 26 Al, and in situ 14 C. Geomorphology, 179, 58-70.
50. Insel, N., Ehlers, T. A., Schaller, M., Barnes, J. B., Tawackoli, S., and Poulsen, C. J., 2010, Spatial and temporal variability in denudation across the Bolivian Andes from multiple geochronometers: 2010, v. 122, p. 65-77.
51. Kirchner, J. W., Finkel, R. C., Riebe, C. S., Granger, D. E., Clayton, J. L., King, J. G., and Megahan, W. F., 2001, Mountain erosion over 10 yr, 10 k.y., and 10 m.y. time scales: Geology, v. 29, no. 7, p. 591-594.
52. Kober, F., Ivy-Ochs, S., Zeilinger, G., Schlunegger, F., Kubik, P. W., Baur, H., and Wieler, R., 2009, Complex multiple cosmogenic nuclide concentration and histories in the arid Rio Lluta catchment, northern Chile: Earth Surface Processes and Landforms, v. 34, p. 398- 412.
53. Larsen, I. J., Almond, P. C., Eger, A., Stone, J. O., Montgomery, D. R., & Malcolm, B. (2014). Rapid soil production and weathering in the Southern Alps, New Zealand. Science, 343(6171), 637-640.
54. Matmon, A. S., Bierman, P., Larsen, J., Southworth, S., Pavich, M., Finkel, R., and Caffee, M., 2003, Erosion of an ancient mountain range, the Great Smoky Mountains, North Carolina and Tennessee: American Journal of Science, v. 303, p. 817-855.
55. Meyer, H., Hetzel, R., & Strauss, H. (2010). Erosion rates on different timescales derived from cosmogenic 10Be and river loads: implications for landscape evolution

in the Rhenish Massif, Germany. International Journal of Earth Sciences, 99(2), 395-412.
56. Miller, S. R., Sak, P. B., Kirby, E., & Bierman, P. R. (2013). Neogene rejuvenation of central Appalachian topography: Evidence for differential rock uplift from stream profiles and erosion rates. Earth and Planetary Science Letters, 369, 1-12.
57. Morel, P., von Blackenburg, F., Schaller, M., Kubik, P. W., and Hinderer, M., 2003, Lithology, landscape dissection and glaciation controls on catchment erosion as determined by cosmogenic nuclides in river sediment (the Wutach Gorge, Black Forest): Terra Nova, v. 15, no. 6, p. 398-404.
58. Nichols, K. K., Bierman, P. R., & Rood, D. H. (2014). 10Be constrains the sediment sources and sediment yields to the Great Barrier Reef from the tropical Barron River catchment, Queensland, Australia. Geomorphology, 224(0), 102-110. doi:http://dx.doi.org/10.1016/j.geomorph.2014.07.019
59. Nichols, K. K., Bierman, P. R., Eppes, M. C., Caffee, M., Finkel, R., and Larsen, J., 2005b, Late Quaternary history of the Chemehuevi Mountain piedmont, Mojave Desert, deciphered using ^{10}Be and ^{26}Al: American Journal of Science, v. 305, no. 5, p. 345-368.
60. Nichols, K. K., Bierman, P. R., Eppes, M. C., Caffee, M., Finkel, R., and Larsen, J., 2007, Timing of surficial process changes down a Mojave Desert piedmont: Quaternary Research, v. 68, no. 1, p. 151-161.
61. Nichols, K. K., Bierman, P. R., Hooke, R. L., Clapp, E., and Caffee, M., 2002, Quantifying sediment transport on desert piedmonts using ^{10}Be and ^{26}Al: Geomorphology, v. 45, no. 1,2, p. 89-104.
62. Nichols, K., Bierman, P., Finkel, R., and Larsen, J., 2005a, Long-Term (10 to 20 kyr) Sediment Generation Rates for the Upper Rio Chagres Basin Based on Cosmogenic ^{10}Be, *in* Harmon, R. S., ed., The Rio Chagres: A Multidisciplinary Profile of a Tropical Watershed, Kluwer Academic Publishers.
63. Norton, K. P., Blanckenburg, F. v., and Kubik, P. W., 2010, Cosmogenic nuclide-derived rates of diffusive and episodic erosion in the glacially sculpted upper Rhone Valley, Swiss Alps: Earth Surface Processes and Landforms, v. 35, p. 651-662.
64. Norton, K. P., Blanckenburg, F. v., Schlunegger, F., Schwab, M., and Kubik, P. W., 2008, Cosmogenic nuclide-based investigation of spatial erosion and hillslope channel coupling in the transient foreland of the Swiss Alps: Geomorphology, v. 95, p. 474-486.
65. Norton, K. P., von Blanckenburg, F., & Kubik, P. W. (2010). Cosmogenic nuclide-derived rates of diffusive and episodic erosion in the glacially sculpted upper Rhone Valley, Swiss Alps. Earth surface processes and landforms, 35(6), 651-662.
66. Norton, K. P., von Blanckenburg, F., DiBiase, R., Schlunegger, F., & Kubik, P. W. (2011). Cosmogenic 10Be-derived denudation rates of the Eastern and Southern European Alps. International Journal of Earth Sciences, 100(5), 1163-1179.

67. Ouimet, W. B., Whipple, K. X., and Granger, D. E., 2009, Beyond threshold hillslopes: Channel adjustment to base-level fall in tectonically active mountain ranges: Geology, v. 37, no. 7, p. 579-582.
68. Palumbo, L., Hetzel, R., Tao, M., & Li, X. (2011). Catchment-wide denudation rates at the margin of NE Tibet from in situ-produced cosmogenic 10Be. Terra Nova, 23(1), 42-48.
69. Palumbo, L., Hetzel, R., Tao, M., and Li, X., 2009, Topographic and lithologic control on catchment-wide denudation rates derived from cosmogenic ^{10}Be in two mountain ranges at the margin of NE Tibet: Geomorphology, v. 117, p. 130-142.
70. Perg, L., Anderson, R., and Finkel, R., 2003, Use of cosmogenic radionuclides as a sediment tracer in the Santa Cruz littoral cell, California, USA: Geology, v. 31, p. 299-302.
71. Placzek, C. J., Matmon, A., Granger, D. E., Quade, J., and Niedermann, S., 2010, Evidence for active landscape evolution in the hyperarid Atacama from multiple terrestrial cosmogenic nuclides: Earth and Planetary Science Letters, v. 295, p. 12-20.
72. Placzek, C., Granger, D. E., Matmon, A., Quade, J., & Ryb, U. (2014). Geomorphic process rates in the central Atacama Desert, Chile: Insights from cosmogenic nuclides and implications for the onset of hyperaridity. *American Journal of Science, 314*(10), 1462-1512.
73. Portenga, E. W., & Bierman, P. R. (2011). Understanding Earth's eroding surface with 10 Be. *GSA Today, 21*(8), 4-10.
74. Pupim, F. d. N., Bierman, P. R., Assine, M. L., Rood, D. H., Silva, A., & Merino, E. R. (2015). Erosion rates and landscape evolution of the lowlands of the Upper Paraguay river basin (Brazil) from cosmogenic 10Be. *Geomorphology, 234*(0), 151-160. doi:http://dx.doi.org/10.1016/j.geomorph.2015.01.016
75. Quigley, M., Sandiford, M., Fifield, K., and Alimanovic, A., 2007a, Bedrock erosion and relief production in the northern Flinders Ranges, Australia: Earth Surface Processes and Landforms, v. 32, no. 6, p. 929.
76. Quigley, M., Sandiford, M., Fifield, L. K., and Alimanovic, A., 2007b, Landscape responses to intraplate tectonism: Quantitative constraints from ^{10}Be nuclide abundances: Earth and Planetary Science Letters, v. 261, no. 1-2, p. 120-133.
77. Reinhardt, L. J., Bishop, P., Hoey, T. B., Dempster, T. J., and Sanderson, D. C. W., 2007, Quantification of the transient response to base-level fall in a small mountain catchment: Sierra Nevada, southern Spain Journal of Geophysical Research, v. 112, no. F03S05, p. 20.
78. Reuter, J. M., 2005, Erosion rates and patterns inferred from cosmogenic ^{10}Be in the Susquehanna River basin: University of Vermont, 172 p.
79. Riebe, C. S., Kirchner, J. W., and Finkel, R. C., 2003, Long-term rates of chemical weathering and physical erosion from cosmogenic nuclides and geochemical mass balance: Geochimica et Cosmochimica Acta, v. 67, no. 22, p. 4411-4427.

80. Riebe, C. S., Kirchner, J. W., Granger, D. E., and Finkel, R. C., 2000, Erosional equilibrium and disequilibrium in the Sierra Nevada, inferred from cosmogenic ^{26}Al and ^{10}Be in alluvial sediment: Geology, v. 28, no. 9, p. 803-806.
81. Riebe, C. S., Kirchner, J. W., Granger, D. E., and Finkel, R. C., 2001a, Minimal climatic control on erosion rates in the Sierra Nevada, California: Geology, v.29, no. 5, p. 447-450.
82. Riebe, C. S., Kirchner, J. W., Granger, D. E., and Finkel, R. C., 2001b, Strong tectonic and weak climatic control of long-term chemical weathering rates: Geology, v. 29, no. 6, p. 511–514.
83. Safran, E. B., Bierman, P. R., Aalto, R., Dunne, T., Whipple, K. X., and Caffee, M., 2005, Erosion rates driven by channel network incision in the Bolivian Andes: Earth Surface Processes and Landforms, v. 30, no. 8, p. 1007-1024.
84. Schaller, M., von Blanckenburg, F., Hovius, N., and Kubik, P. W., 2001, Large-scale erosion rates from In situ-produced cosmogenic nuclides in European river sediments: Earth and Planetary Science Letters, v. v. 188, p. 441-458.
85. Scharf, T. E. (2012). Denudation rates and geomorphic evolution of the Cape Mountains, determined by the analysis of the in situ-produced cosmogenic 10BE. University of Cape Town.
86. Stock, G. M., Frankel, K. L., Ehlers, T. A., Schaller, M., Briggs, S. M., and Finkel, R. C., 2009, Spatial and temporal variations in denudation of the Wasatch Mountains, Utah, USA: Lithosphere, v. 1, no. 1, p. 34-40.
87. Sullivan, C. L., 2007, ^{10}Be erosion rates and landscape evolution of the Blue Ridge Escarpment, southern Appalachian Mountains: University of Vermont, 76 p.
88. Tomkins, K. M., Humphreys, G. S., Wilkinson, M. T., Fink, D., Hesse, P. P., Doerr, S. H., Shakesby, R. A., Wallbrink, P. J., and Blake, W. H., 2007, Contemporary versus long- term denudation along a passive plate margin: the role of extreme events: Earth Surface Processes and Landforms, v. 32, no. 7, p. 1013.
89. Vanacker, V., von Blanckenburg, F., Hewawasam, T., and Kubik, P. W., 2007, Constraining landscape development of the Sri Lankan escarpment with cosmogenic nuclides in river sediment: Earth and Planetary Science Letters, v. 253, no. 3-4, p. 402-414.
90. Vance, D., Bickle, M., Ivy-Ochs, S., and Kubik, P. W., 2003, Erosion and exhumation in the Himalaya from cosmogenic isotope inventories of river sediments: Earth and Planetary Science Letters, v. 206, p. 273-288.
91. von Blanckenburg, F., Hewawasam, T., and Kubik, P. W., 2004, Cosmogenic nuclide evidence for low weathering and denudation in the wet, tropical highlands of Sri Lanka: Journal of Geophysical Research, v. 109, no. F3.
92. Willenbring, J. K., Codilean, A. T., & McElroy, B. (2013). Earth is (mostly) flat: Apportionment of the flux of continental sediment over millennial time scales. Geology, 41(3), 343-346.

93. Willenbring, J. K., Codilean, A. T., & McElroy, B. (2013). Earth is (mostly) flat: Apportionment of the flux of continental sediment over millennial time scales. *Geology, 41*(3), 343-346.
94. Wittmann, H., Blanckenburg, F. v., Guyot, J. L., Maurice, L., and Kubik, P. W., 2009, from source to sink: Preserving the cosmogenic ^{10}Be-derived denudation rate signal of the Bolivian Andes in sediment of the Beni and Mamoré foreland basins: Earth and Planetary Science Letters, v. 288, p. 463-474.
95. Wittmann, H., Blanckenburg, F. v., Kruesmann, T., Norton, K. P., and Kubik, P. W., 2007, Relation between rock uplift and denudation from cosmogenic nuclides in river sediment in the Central Alps of Switzerland: Journal of Geophysical Research, v. 112, no. F04010.
96. Wittmann, H., von Blanckenburg, F., Maurice, L., Guyot, J.-L., Filizola, N., & Kubik, P. W. (2010). Sediment production and delivery in the Amazon River basin quantified by in situ-produced cosmogenic nuclides and recent river loads. Geological Society of America Bulletin. doi:10.1130/b30317.1

Erosion Stats

```
library(ggplot2)
```

```
## Warning: package 'ggplot2' was built under R version 3.4.4
```

```
library(lmerTest)
```

```
## Loading required package: lme4
```

```
## Warning: package 'lme4' was built under R version 3.4.4
```

```
## Loading required package: Matrix
```

```
##
## Attaching package: 'lmerTest'
```

```
## The following object is masked from 'package:lme4':
##
##     lmer
```

```
## The following object is masked from 'package:stats':
##
##     step
```

```
library(lme4)
library(dplyr)
```

```
##
## Attaching package: 'dplyr'
```

```
## The following objects are masked from 'package:stats':
##
##     filter, lag
```

```
## The following objects are masked from 'package:base':
##
##     intersect, setdiff, setequal, union
```

```
b<-theme(

   panel.grid.major=element_blank(),
   panel.grid.minor=element_blank(),
   panel.background=element_rect(colour="black",size=1.2,fill=NA),
   axis.line=element_line(colour="black"),


   axis.title.y=element_text(vjust=1.5),
   axis.title.x=element_text(vjust=0.2),

   axis.text.x=element_text(size=20, colour="black"),
   axis.text.y=element_text(size=20, colour="black"),

   axis.ticks.x=element_line(size=2, colour="black"),
   axis.ticks.y=element_line(size=2, colour="black")

   )
```

```
nydata<-read.csv(file.choose())
summary(nydata)
```

```
##   Study.number                     Citation            Sample.ID
##  Min.   : 1.00   Schaller et al 2001   :  81   2            :   5
##  1st Qu.:26.00   Reuter 2005           :  79   4            :   5
##  Median :48.00   Duxbury 2008          :  70   3            :   4
##  Mean   :45.09   Duxbury et. al. (2014):  66   05-3R-11b-SAL:   3
##  3rd Qu.:69.00   Ouimet et al 2009     :  66   06-3R-26-MEK :   3
##  Max.   :82.00   Miller et al. (2013)  :  59   06-3R-27-MEK :   3
##                  (Other)               :1368   (Other)      :1766
##      Slope              RockType   Precipitation    Vegetation
##  Min.   : 0.00              : 68   Min.   :   3   Min.   :  0.00
##  1st Qu.: 7.00    Mixed     :  1   1st Qu.: 582   1st Qu.: 13.00
##  Median :14.40   Igneous    :354   Median : 949   Median : 45.00
##  Mean   :15.09   Metamorphic:416   Mean   :1009   Mean   : 43.84
##  3rd Qu.:21.70   Mixed      :606   3rd Qu.:1229   3rd Qu.: 76.00
##  Max.   :50.00   Sedimentary:344   Max.   :3265   Max.   :100.00
##                                                   NA's   :158
##     Erosion           X
##  Min.   :   0.07   Mode:logical
##  1st Qu.:  14.66   NA's:1789
##  Median :  40.55
##  Mean   : 167.87
##  3rd Qu.: 141.07
##  Max.   :4119.53
##
```

```
nydata = nydata[!is.na(nydata$Vegetation),]
```

Plotting erosion rate against Slope

```
ggplot(nydata, aes(x=Slope, y=Erosion)) + geom_point() +
  geom_smooth(method="lm") + b + scale_y_log10()
```

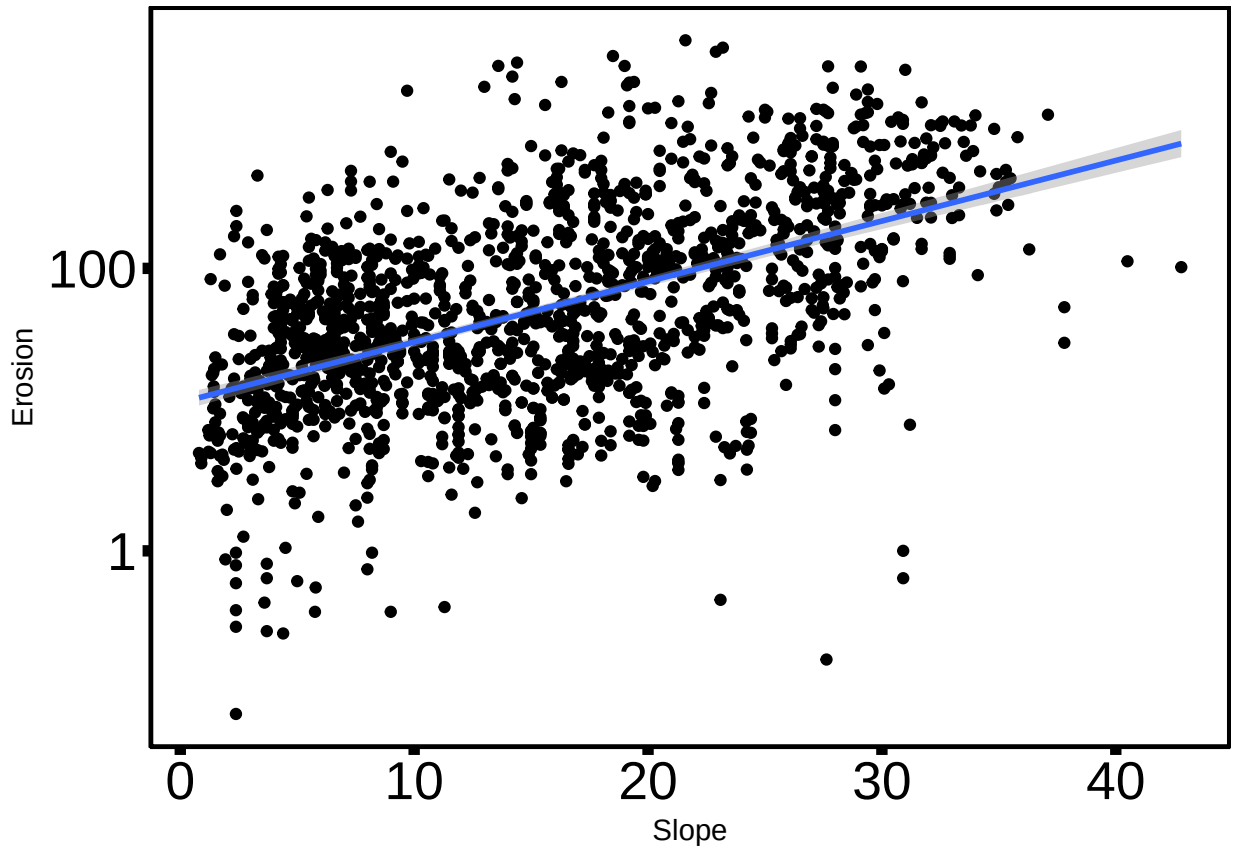

#correlation test for Slope:

```
regression.m1<-lm(log(Erosion) ~ Slope, data=nydata)
plot(regression.m1)
```

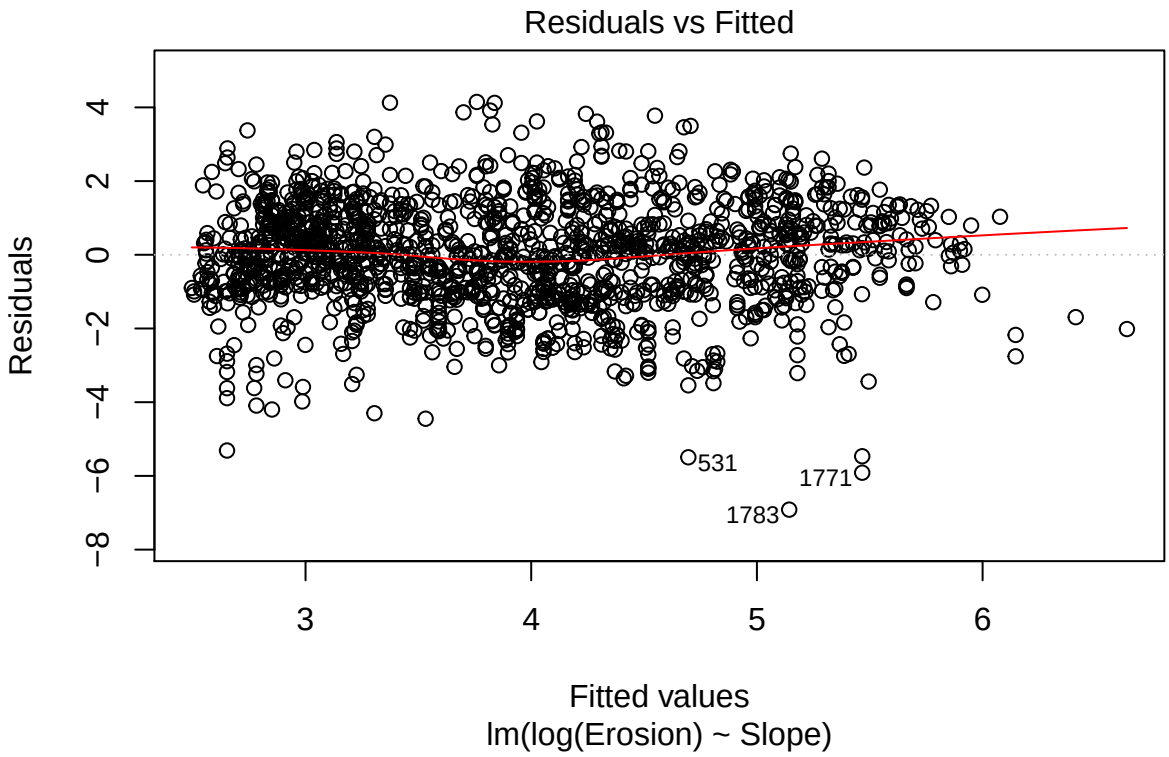
Residuals vs Fitted
Residuals
4
2
0
−2
−4
−6
−8
3
4
5
6
531
1771
1783
Fitted values
lm(log(Erosion) ~ Slope)

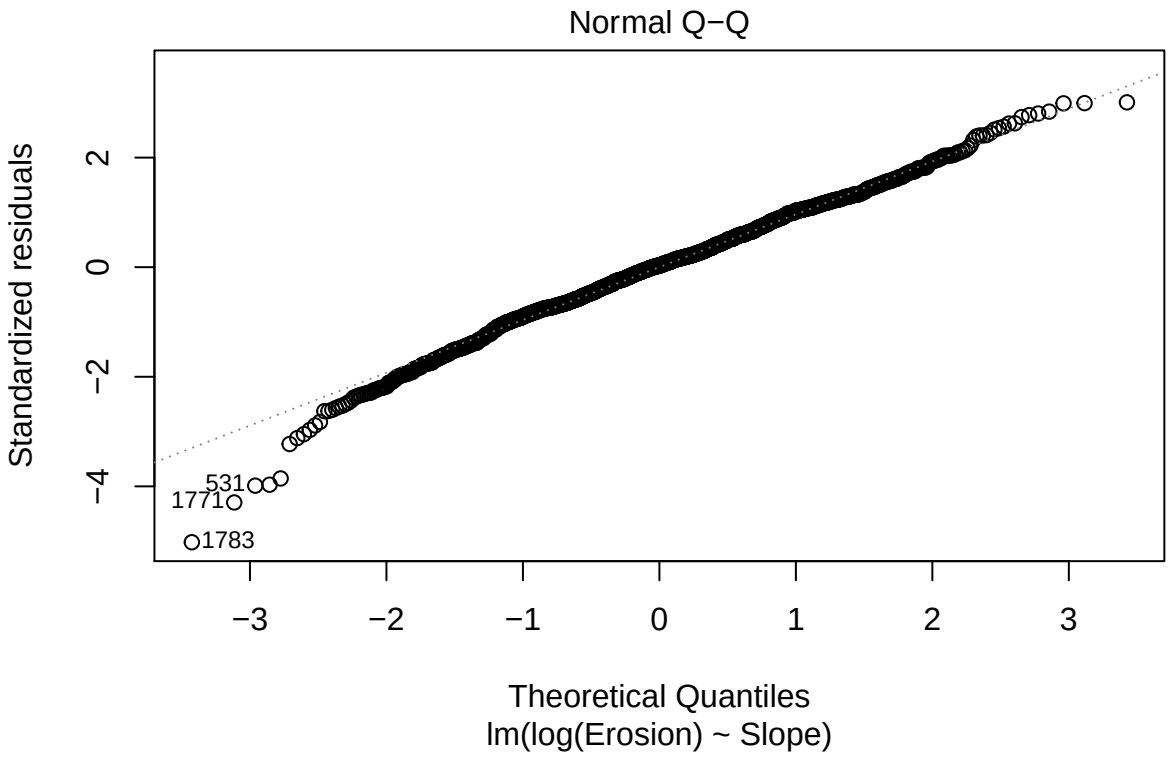
Normal Q−Q
Standardized residuals
2
0
−2
−4
531
1771
1783
−3
−2
−1
0
1
2
3
Theoretical Quantiles
lm(log(Erosion) ~ Slope)

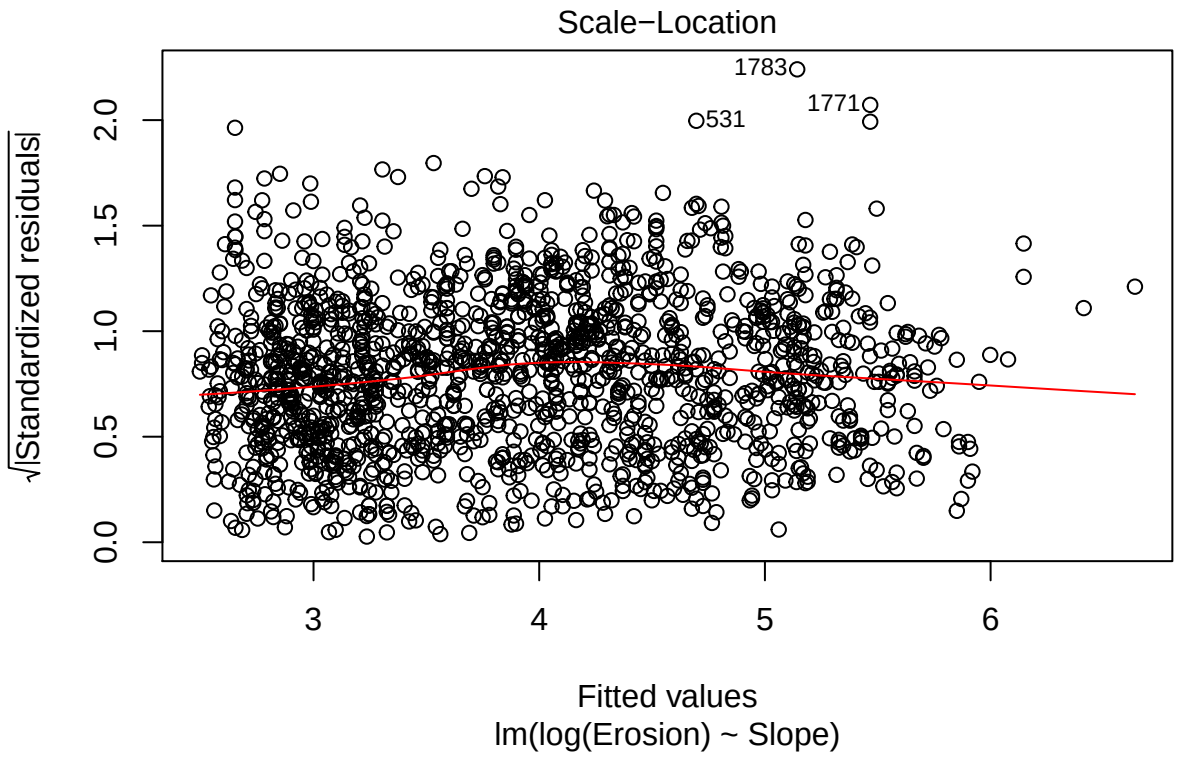
Scale−Location
1783
1771
531
√|Standardized residuals|
0.0
0.5
1.0
1.5
2.0
3
4
5
6
Fitted values
lm(log(Erosion) ~ Slope)

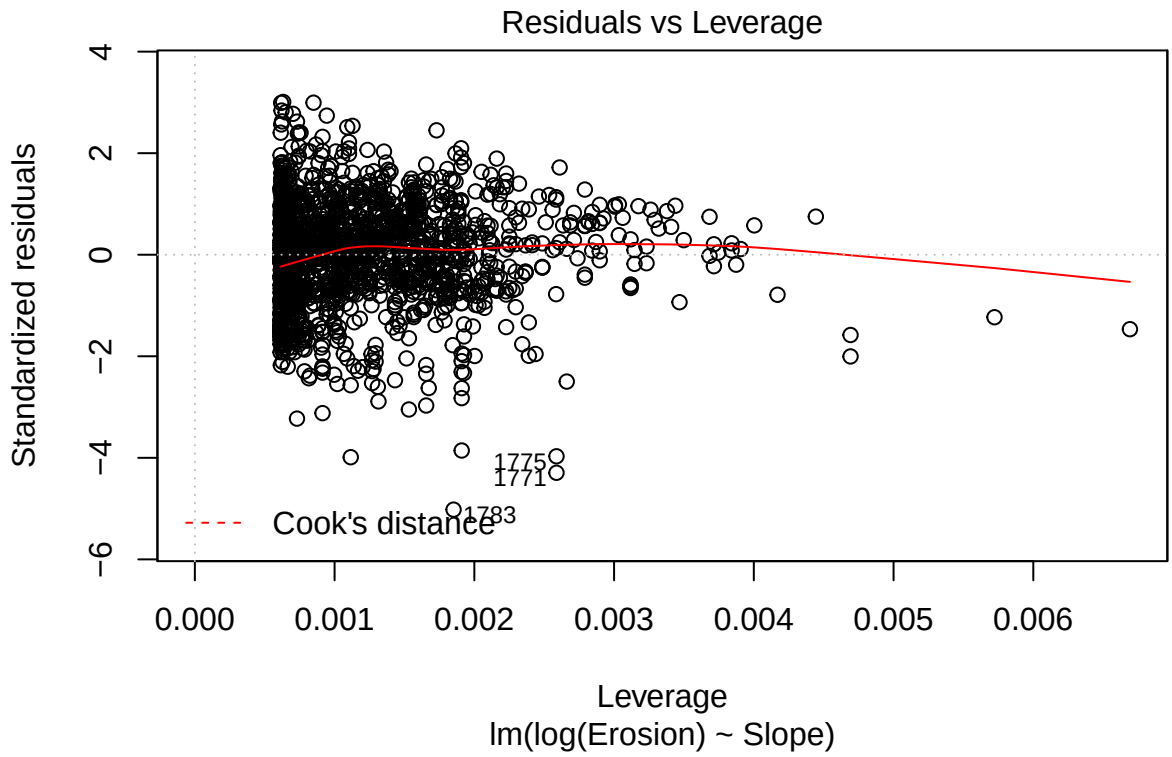


```
summary(regression.m1)
```

```
##
## Call:
## lm(formula = log(Erosion) ~ Slope, data = nydata)
##
## Residuals:
##     Min      1Q  Median      3Q     Max
## -6.9150 -0.8939  0.0420  0.8970  4.1471
##
## Coefficients:
##             Estimate Std. Error t value Pr(>|t|)
## (Intercept) 2.417298   0.068075   35.51   <2e-16 ***
## Slope       0.098653   0.003888   25.38   <2e-16 ***
## ---
## Signif. codes:  0 '***' 0.001 '**' 0.01 '*' 0.05 '.' 0.1 ' ' 1
##
## Residual standard error: 1.379 on 1629 degrees of freedom
## Multiple R-squared:  0.2833, Adjusted R-squared:  0.2829
## F-statistic:   644 on 1 and 1629 DF,  p-value: < 2.2e-16
```

Plotting erosion rate against precipitation:

```
ggplot(nydata, aes(x=Precipitation, y=Erosion)) + geom_point() +
  geom_smooth(method="lm") + b + scale_y_log10()
```

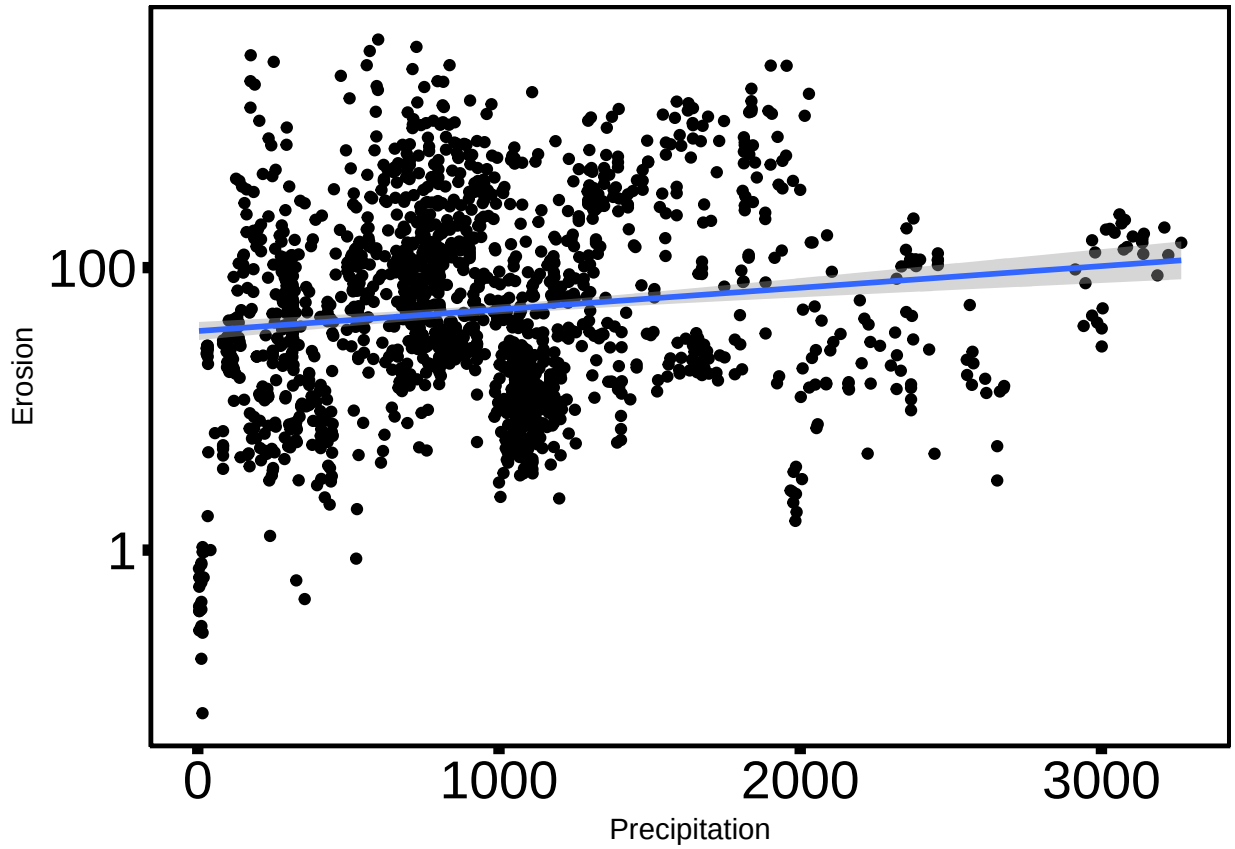

#correlation of precipitation with erosion rate:

```
regression.m2<-lm(log(Erosion) ~ Precipitation, data=nydata)
plot(regression.m2)
```

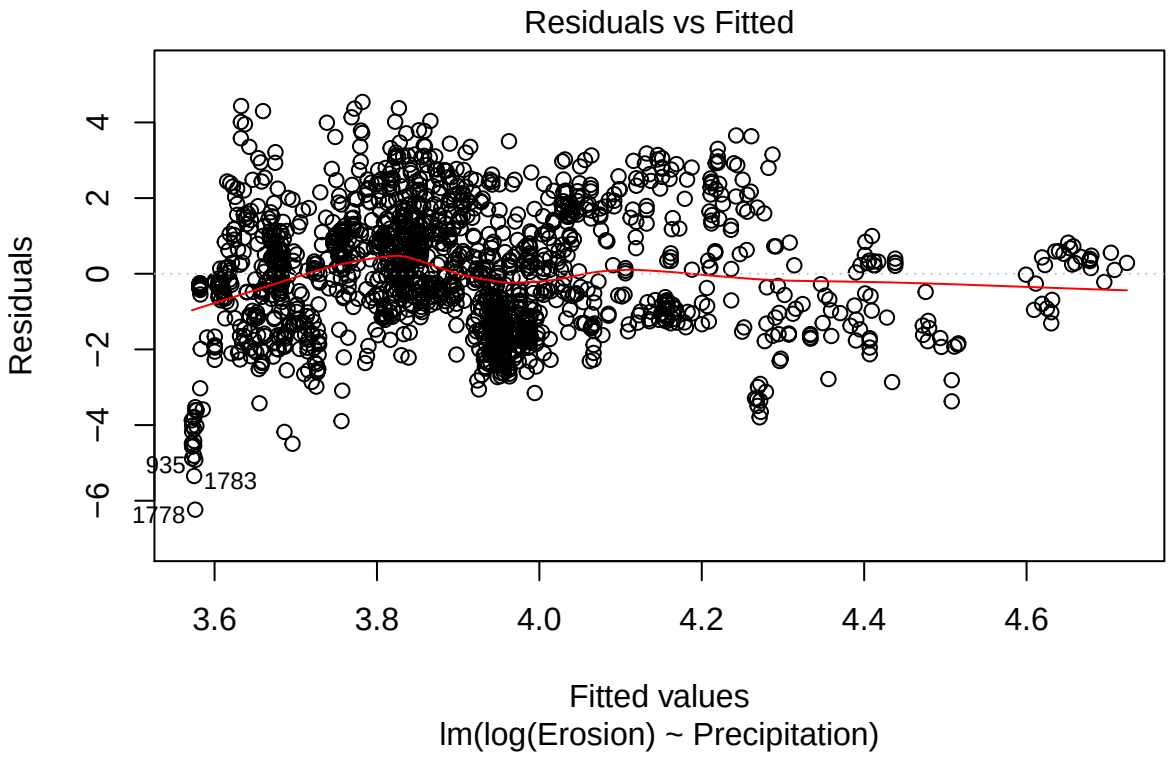
Residuals vs Fitted
Residuals
4
2
0
−2
−4
−6
935
1783
1778
3.6
3.8
4.0
4.2
4.4
4.6
Fitted values
lm(log(Erosion) ~ Precipitation)

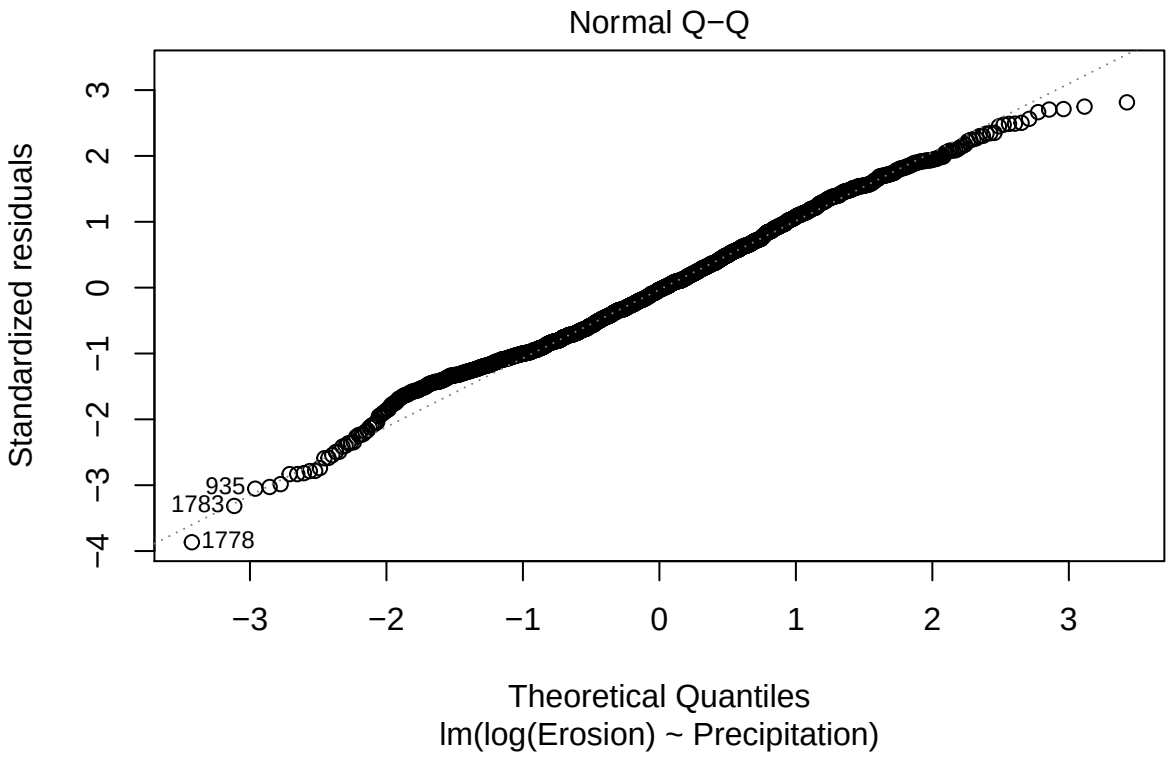
Normal Q−Q
Standardized residuals
Theoretical Quantiles
lm(log(Erosion) ~ Precipitation)
935
1783
1778

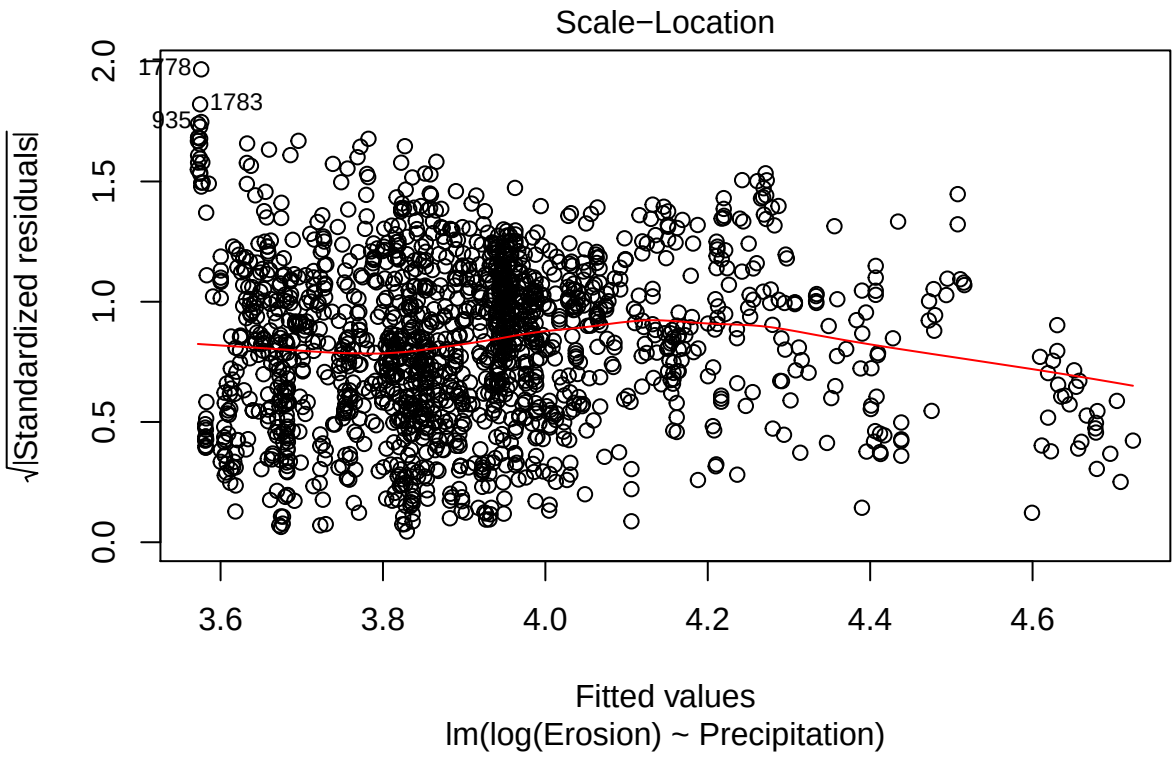
Scale−Location
√|Standardized residuals|
0.0
0.5
1.0
1.5
2.0
1778
1783
935
3.6
3.8
4.0
4.2
4.4
4.6
Fitted values
lm(log(Erosion) ~ Precipitation)

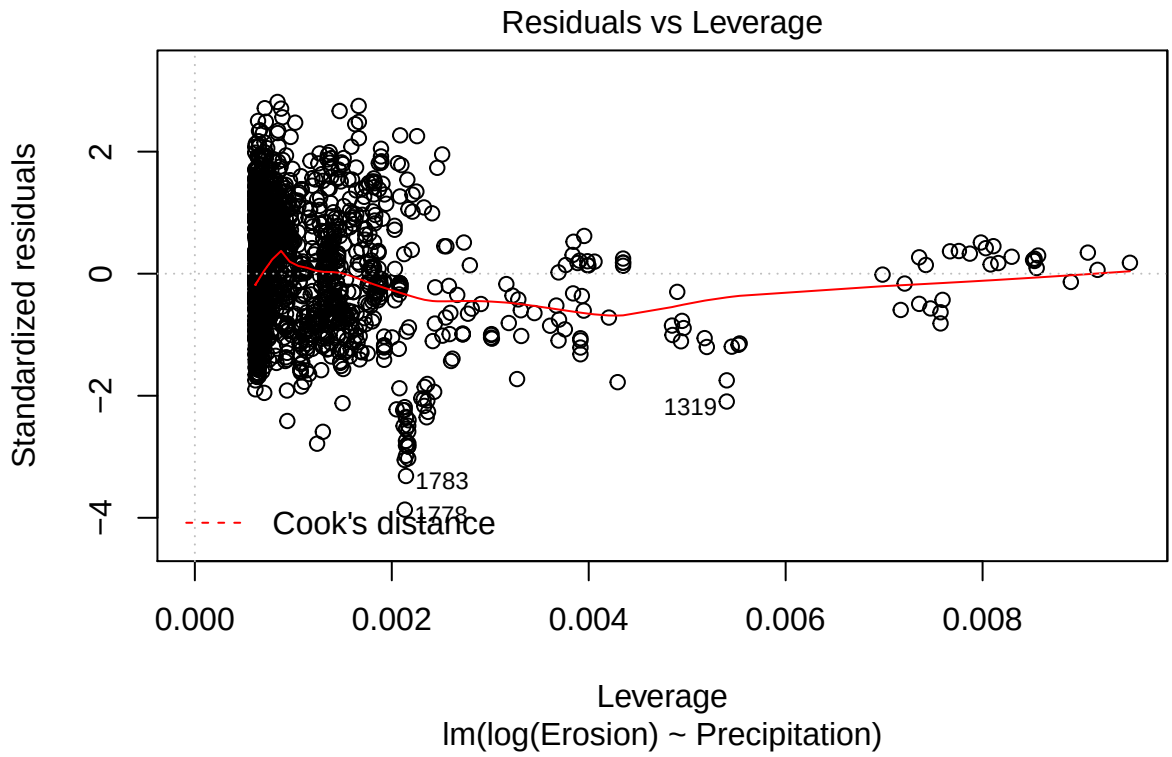


```
summary(regression.m2)
```

```
##
## Call:
## lm(formula = log(Erosion) ~ Precipitation, data = nydata)
##
## Residuals:
##     Min      1Q  Median      3Q     Max
## -6.2354 -1.1825 -0.0532  1.0871  4.5414
##
## Coefficients:
##                Estimate Std. Error t value Pr(>|t|)
## (Intercept)   3.5706068  0.0754383  47.332  < 2e-16 ***
## Precipitation 0.0003531  0.0000662   5.334 1.09e-07 ***
## ---
## Signif. codes:  0 '***' 0.001 '**' 0.01 '*' 0.05 '.' 0.1 ' ' 1
##
## Residual standard error: 1.615 on 1629 degrees of freedom
## Multiple R-squared:  0.01717,    Adjusted R-squared:  0.01656
## F-statistic: 28.46 on 1 and 1629 DF,  p-value: 1.093e-07
```

Selecting best suited model for Precipitation

```
nydata$Precipitation= as.numeric(nydata$Precipitation)
nydata = mutate(nydata,
              Precipitation2 = Precipitation * Precipitation,
              Precipitation3 = Precipitation * Precipitation* Precipitation,
              Precipitation4 = Precipitation * Precipitation * Precipitation * Precipitation,
              Precipitation5 = Precipitation * Precipitation * Precipitation* Precipitation * Precipita
              Precipitation6 = Precipitation * Precipitation * Precipitation* Precipitation * Precipita
              Precipitation7 = Precipitation * Precipitation * Precipitation* Precipitation * Precipita
              Precipitation8 = Precipitation * Precipitation * Precipitation* Precipitation * Precipita

model.1 = lm (log(Erosion) ~ Precipitation,                                  data=nydata)
model.2 = lm (log(Erosion) ~ Precipitation + Precipitation2,                 data=nydata)
model.3 = lm (log(Erosion) ~ Precipitation + Precipitation2 + Precipitation3, data=nydata)
model.4 = lm (log(Erosion) ~ Precipitation + Precipitation2 + Precipitation3 + Precipitation4, data=nyda
model.5 = lm (log(Erosion) ~ Precipitation + Precipitation2 + Precipitation3 + Precipitation4 + Precipi
model.6 = lm (log(Erosion) ~ Precipitation + Precipitation2 + Precipitation3 + Precipitation4 + Precipi
model.7 = lm (log(Erosion) ~ Precipitation + Precipitation2 + Precipitation3 + Precipitation4 + Precipi
model.8 = lm (log(Erosion) ~ Precipitation + Precipitation2 + Precipitation3 + Precipitation4 + Precipi
```

AIC Value of Models:

```
AIC(model.1)
```

```
## [1] 6195.295
```

```
AIC(model.2)
```

```
## [1] 6177.035
```

```
AIC(model.3)
```

```
## [1] 6141.354
```

```
AIC(model.4)
```

```
## [1] 6115.865
```

```
AIC(model.5)
```

```
## [1] 6026.973
```

```
AIC(model.6)
```

```
## [1] 6028.497
```

```
AIC(model.7)
```

```
## [1] 5998.598
```

```
AIC(model.8)
```

```
## [1] 5996.645
```

ANOVA of models:

```
anova(model.1, model.2, model.3, model.4, model.5, model.6, model.7, model.8)
```

```
## Analysis of Variance Table
##
## Model 1: log(Erosion) ~ Precipitation
## Model 2: log(Erosion) ~ Precipitation + Precipitation2
## Model 3: log(Erosion) ~ Precipitation + Precipitation2 + Precipitation3
## Model 4: log(Erosion) ~ Precipitation + Precipitation2 + Precipitation3 +
##     Precipitation4
## Model 5: log(Erosion) ~ Precipitation + Precipitation2 + Precipitation3 +
##     Precipitation4 + Precipitation5
## Model 6: log(Erosion) ~ Precipitation + Precipitation2 + Precipitation3 +
##     Precipitation4 + Precipitation5 + Precipitation6
## Model 7: log(Erosion) ~ Precipitation + Precipitation2 + Precipitation3 +
##     Precipitation4 + Precipitation5 + Precipitation6 + Precipitation7
## Model 8: log(Erosion) ~ Precipitation + Precipitation2 + Precipitation3 +
##     Precipitation4 + Precipitation5 + Precipitation6 + Precipitation7 +
##     Precipitation8
##   Res.Df    RSS Df Sum of Sq       F    Pr(>F)
## 1   1629 4246.5
## 2   1628 4194.1  1    52.424 22.8123 1.947e-06 ***
## 3   1627 4098.3  1    95.786 41.6815 1.415e-10 ***
## 4   1626 4029.8  1    68.493 29.8049 5.519e-08 ***
## 5   1625 3811.4  1   218.431 95.0507 < 2.2e-16 ***
## 6   1624 3810.3  1     1.110  0.4832   0.48707
## 7   1623 3736.5  1    73.798 32.1132 1.718e-08 ***
## 8   1622 3727.4  1     9.045  3.9358   0.04744 *
## ---
## Signif. codes:  0 '***' 0.001 '**' 0.01 '*' 0.05 '.' 0.1 ' ' 1
```

Plotting erosion rate against precipitation:

```
ggplot(nydata, aes(x=Precipitation, y=Erosion)) + geom_point() +
  stat_smooth(method="lm", formula=y ~ poly(x, 3, raw=TRUE)) + b +scale_y_log10()
```

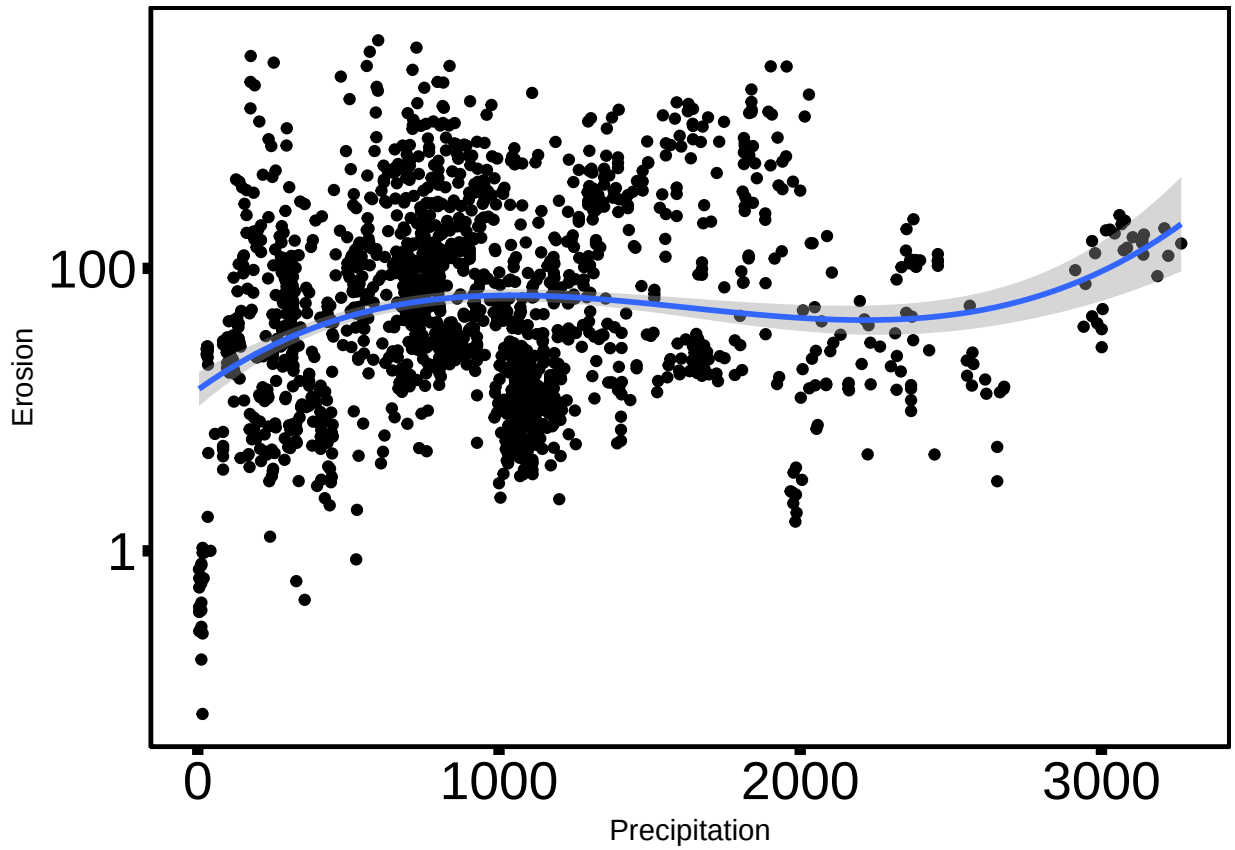

#Checking correlation of Precip in polynomial:

```
regression.m3<-lm(log(Erosion) ~ poly(Precipitation, 3), data=nydata)
plot(regression.m3)
```

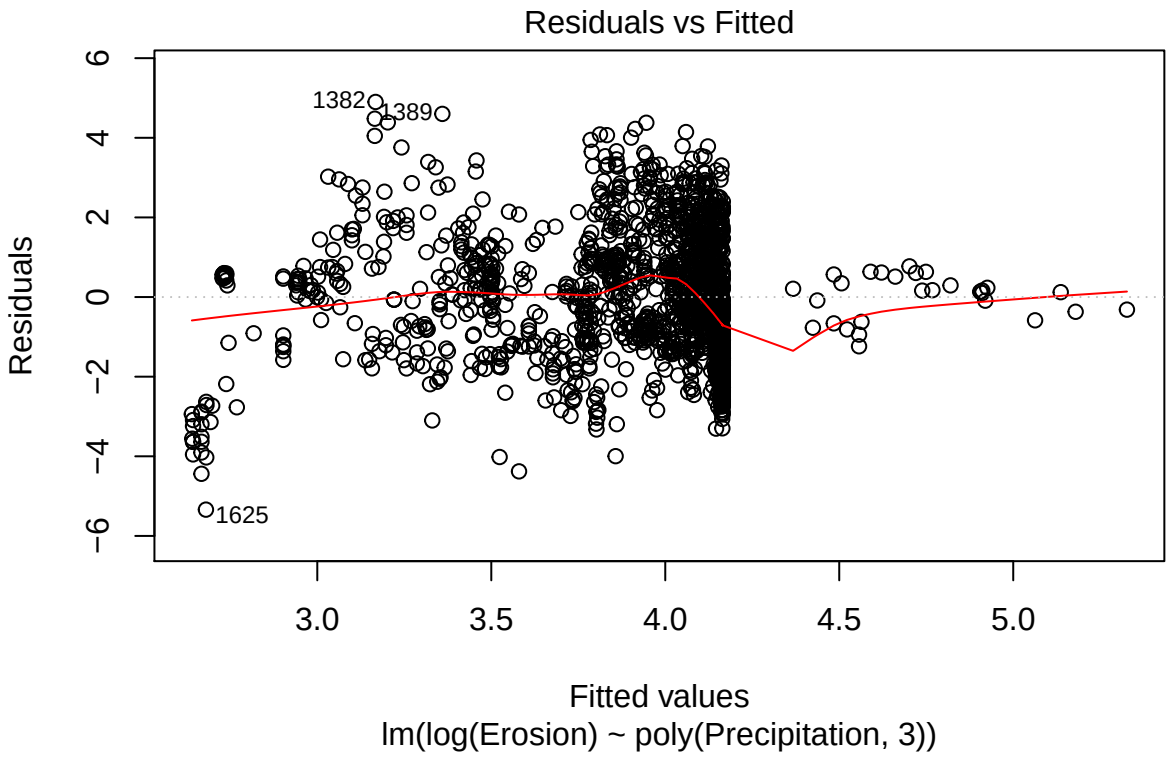
Residuals vs Fitted
Residuals
Fitted values
lm(log(Erosion) ~ poly(Precipitation, 3))
1382
1389
1625
6
4
2
0
−2
−4
−6
3.0
3.5
4.0
4.5
5.0

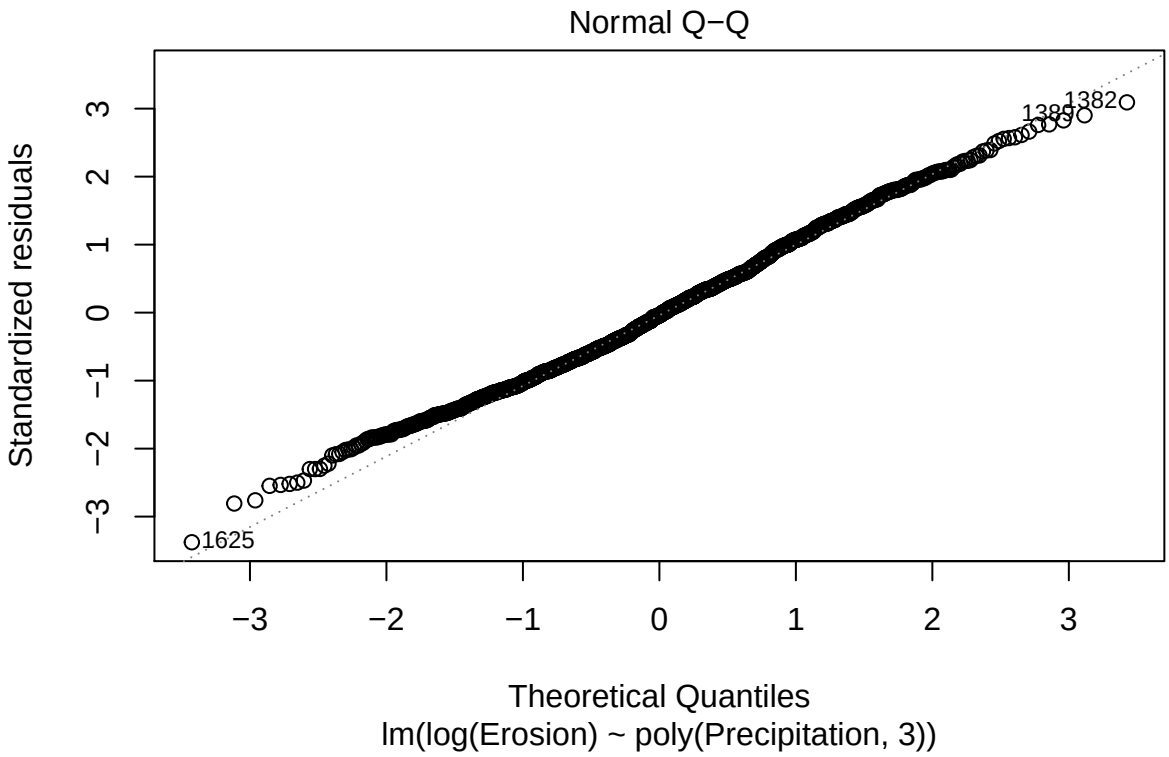
Normal Q−Q
Standardized residuals
Theoretical Quantiles
lm(log(Erosion) ~ poly(Precipitation, 3))
1625
1382
−3
−2
−1
0
1
2
3

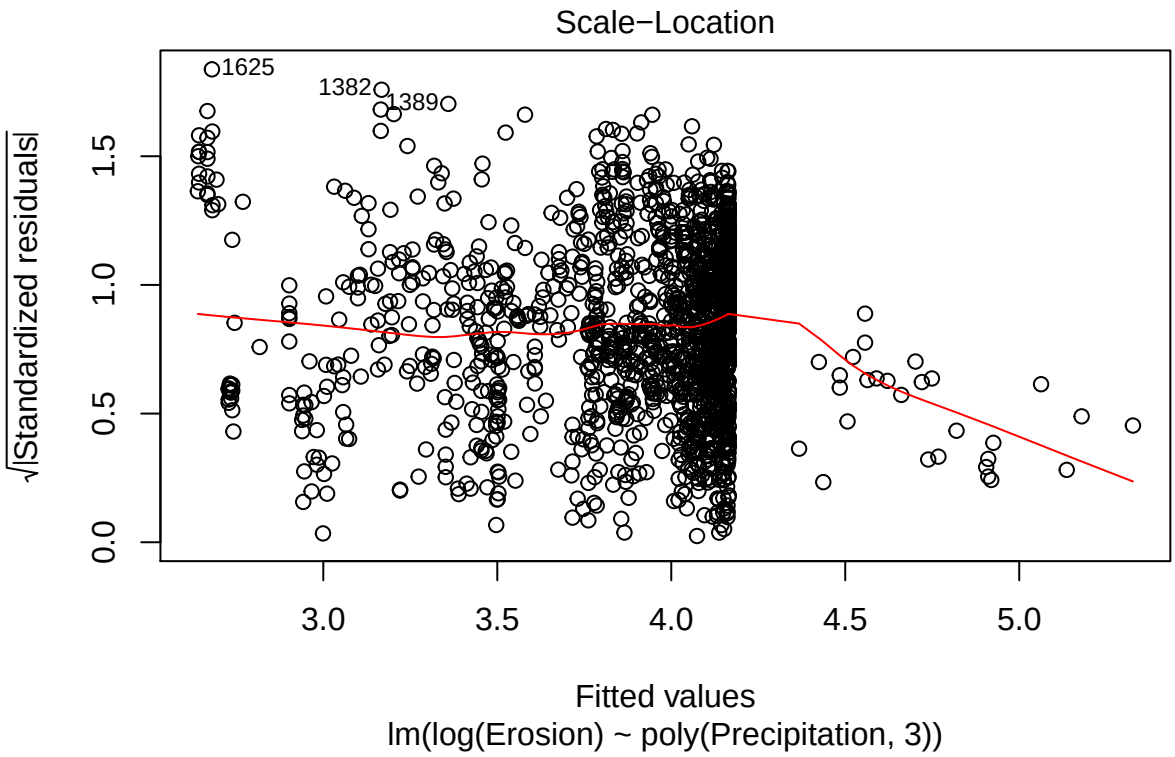
Scale−Location
1625
1382
1389
√|Standardized residuals|
0.0
0.5
1.0
1.5
3.0
3.5
4.0
4.5
5.0
Fitted values
lm(log(Erosion) ~ poly(Precipitation, 3))

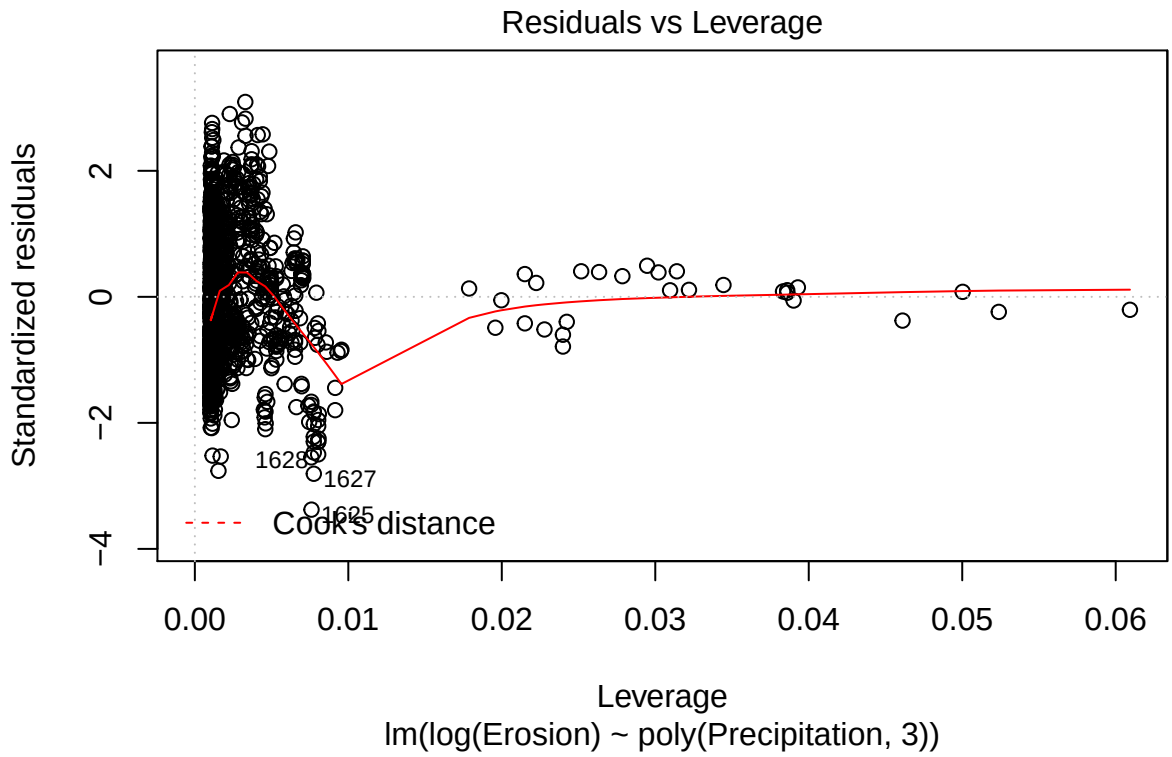


```
summary(regression.m3)
```

```
##
## Call:
## lm(formula = log(Erosion) ~ poly(Precipitation, 3), data = nydata)
##
## Residuals:
##     Min      1Q  Median      3Q     Max
## -5.3392 -1.1717 -0.0617  1.0488  4.8999
##
## Coefficients:
##                          Estimate Std. Error t value Pr(>|t|)
## (Intercept)                3.9119     0.0393  99.541  < 2e-16 ***
## poly(Precipitation, 3)1    8.6127     1.5871   5.427 6.61e-08 ***
## poly(Precipitation, 3)2   -7.2404     1.5871  -4.562 5.45e-06 ***
## poly(Precipitation, 3)3    9.7871     1.5871   6.167 8.79e-10 ***
## ---
## Signif. codes:  0 '***' 0.001 '**' 0.01 '*' 0.05 '.' 0.1 ' ' 1
##
## Residual standard error: 1.587 on 1627 degrees of freedom
## Multiple R-squared:  0.05147,    Adjusted R-squared:  0.04972
## F-statistic: 29.43 on 3 and 1627 DF,  p-value: < 2.2e-16
```

Plotting erosion rate against Vegtation:

```
ggplot(nydata, aes(x=Vegetation, y=Erosion)) + geom_point() +
  geom_smooth(method="lm") + b + scale_y_log10()
```

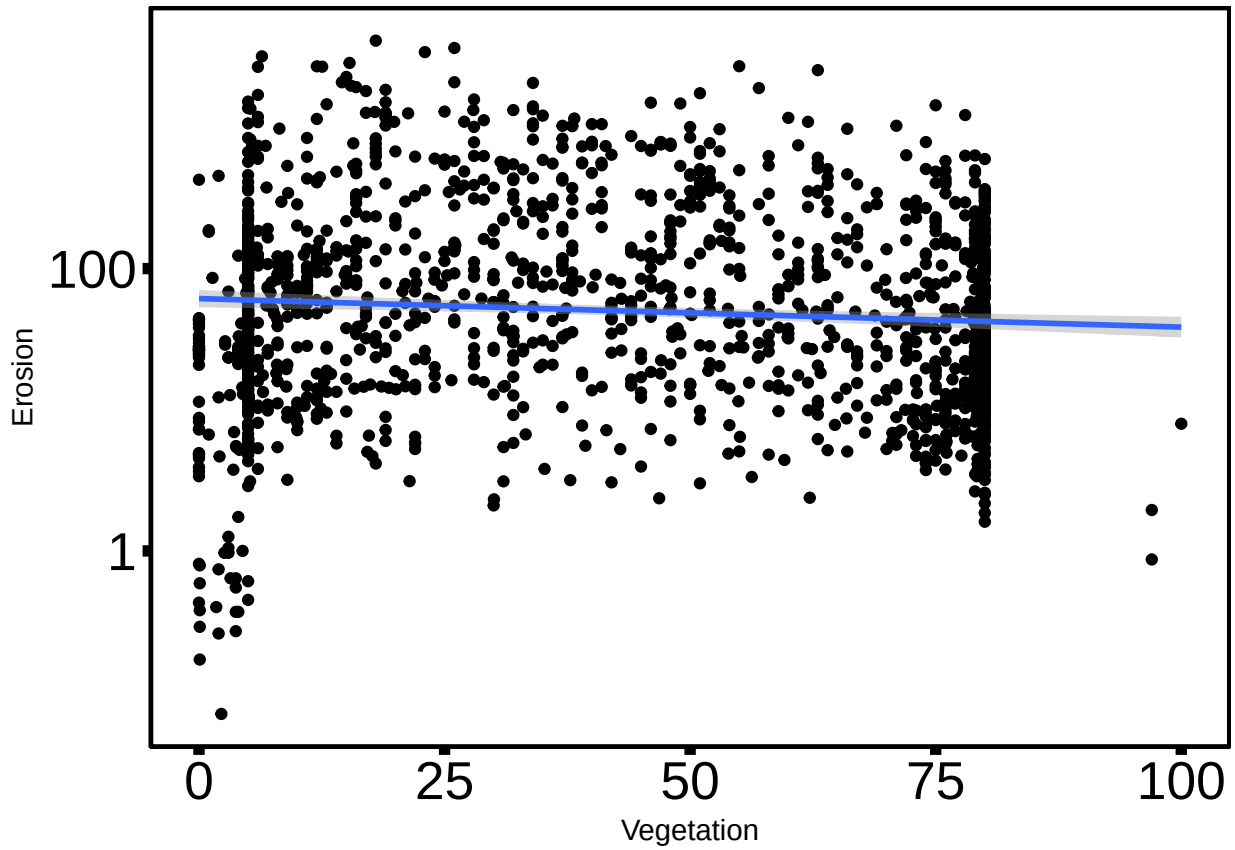

#correlation of vegetation with erosion:

```
regression.m4<-lm(log(Erosion) ~ Vegetation, data=nydata)
plot(regression.m4)
```

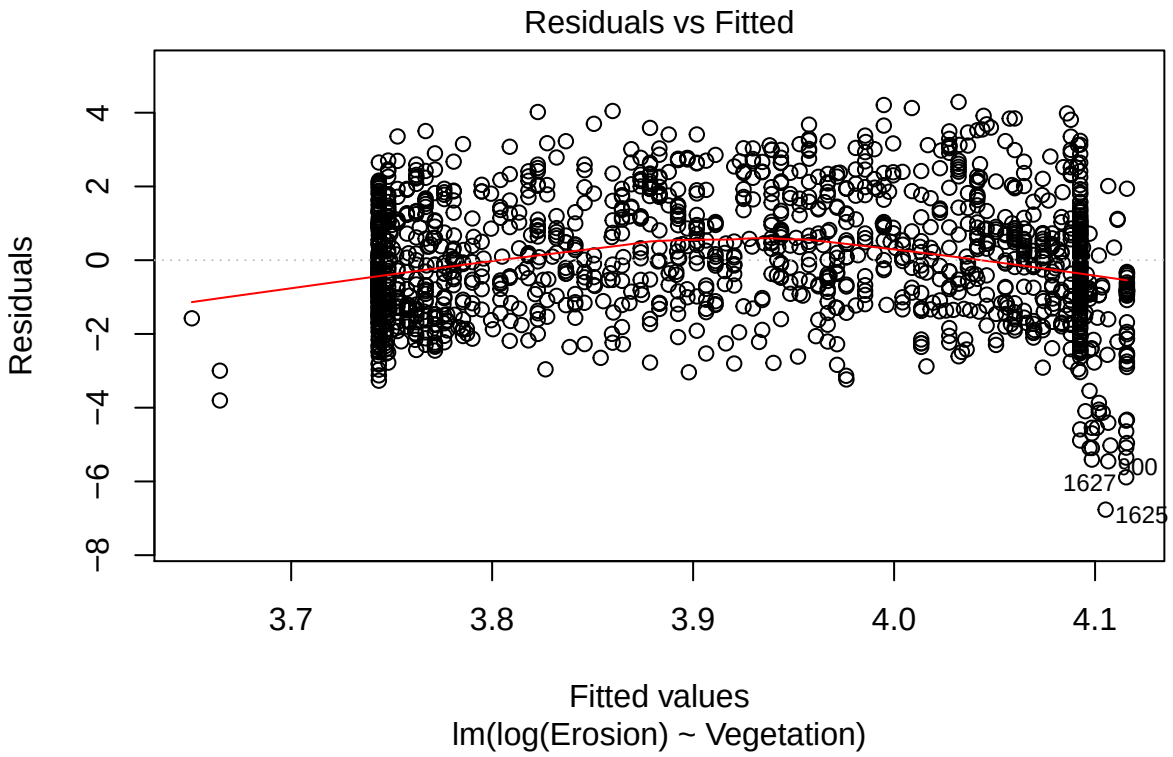
Residuals vs Fitted
Residuals
4
2
0
−2
−4
−6
−8
3.7
3.8
3.9
4.0
4.1
1627
900
1625
Fitted values
lm(log(Erosion) ~ Vegetation)

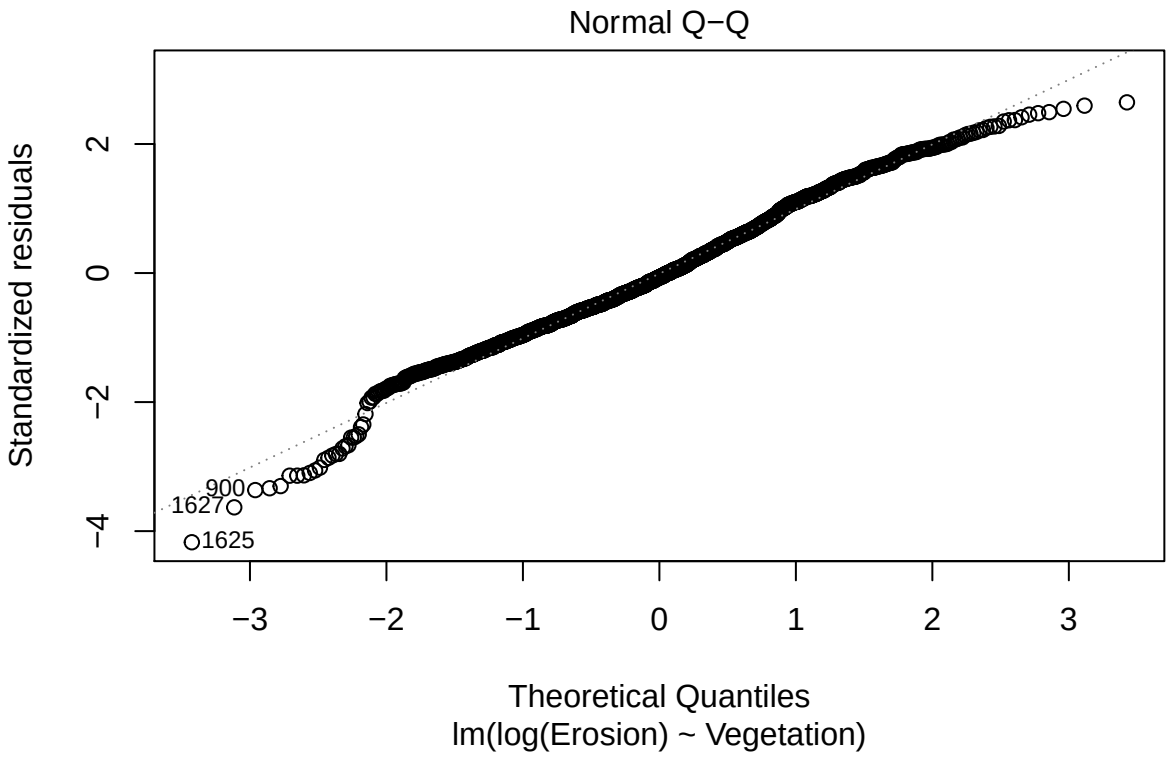
Normal Q−Q
Standardized residuals
Theoretical Quantiles
lm(log(Erosion) ~ Vegetation)
900
1627
1625
−4
−2
0
2
−3
−2
−1
0
1
2
3

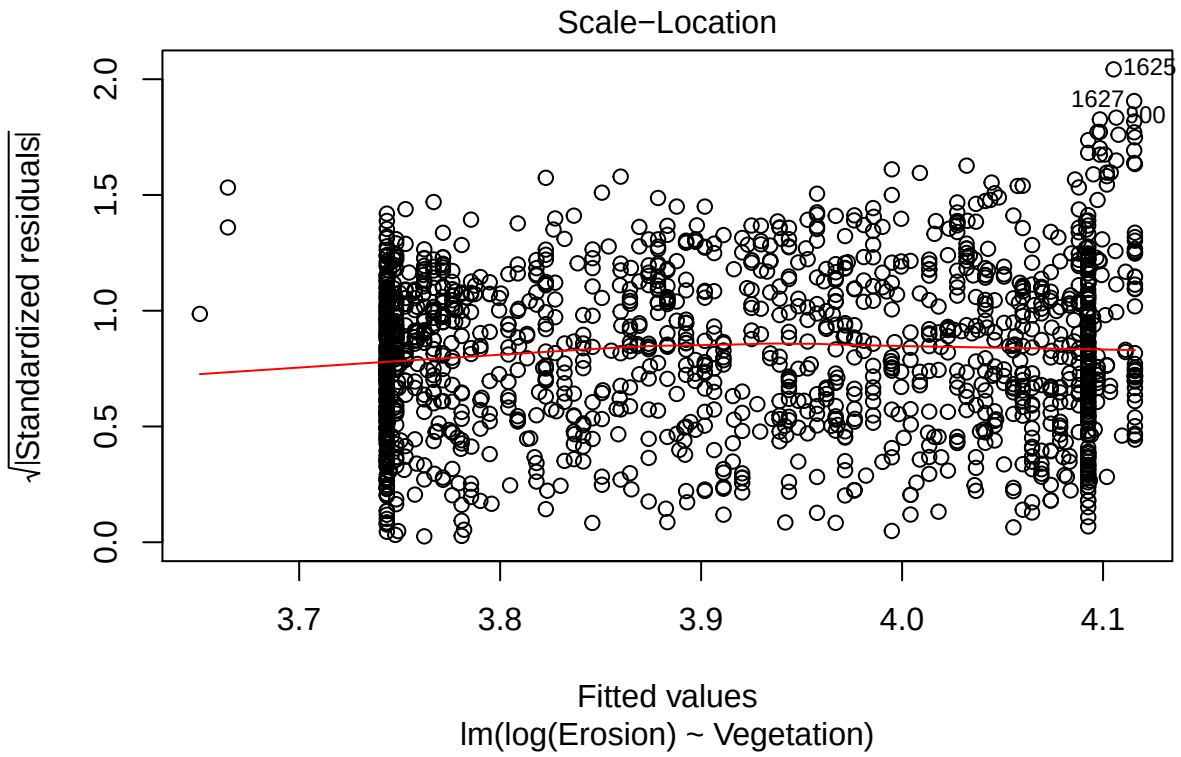
Scale−Location
√|Standardized residuals|
0.0
0.5
1.0
1.5
2.0
1625
1627
900
3.7
3.8
3.9
4.0
4.1
Fitted values
lm(log(Erosion) ~ Vegetation)

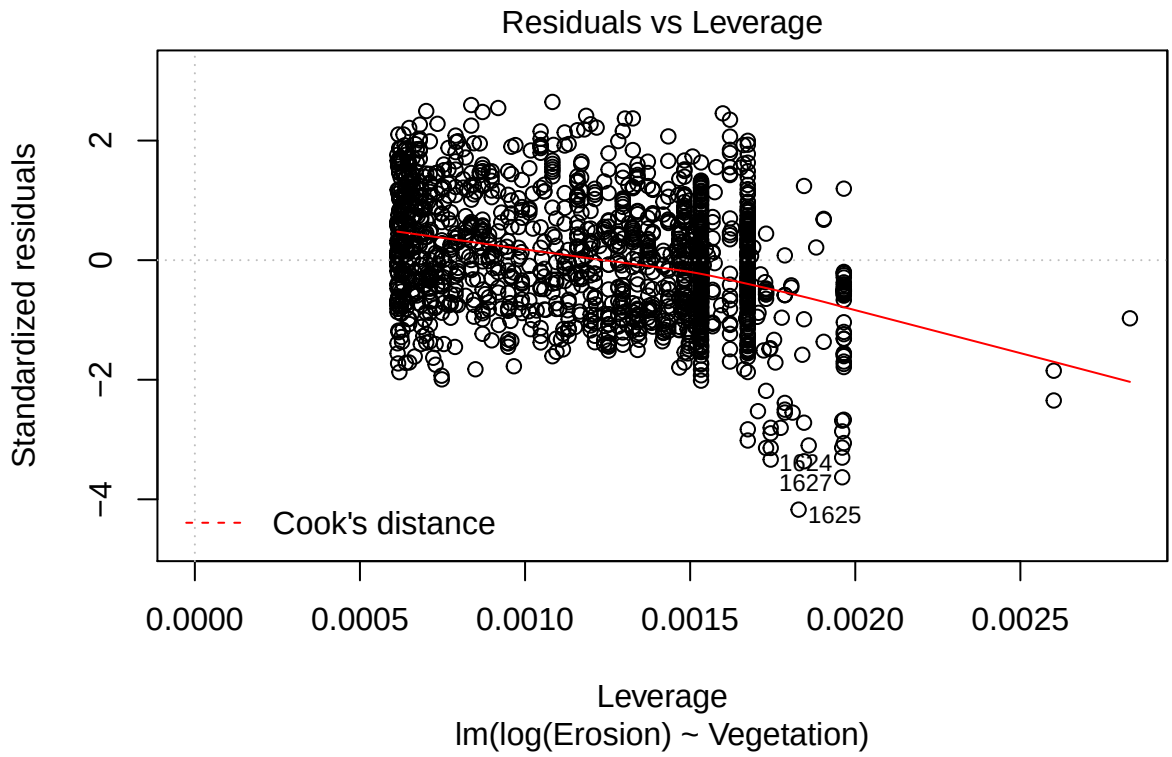


```
summary(regression.m4)
```

```
##
## Call:
## lm(formula = log(Erosion) ~ Vegetation, data = nydata)
##
## Residuals:
##     Min      1Q  Median      3Q     Max
## -6.7645 -1.1110 -0.1094  1.0805  4.2914
##
## Coefficients:
##             Estimate Std. Error t value Pr(>|t|)
## (Intercept)  4.115855   0.071943  57.210  < 2e-16 ***
## Vegetation  -0.004653   0.001361  -3.418 0.000646 ***
## ---
## Signif. codes:  0 '***' 0.001 '**' 0.01 '*' 0.05 '.' 0.1 ' ' 1
##
## Residual standard error: 1.623 on 1629 degrees of freedom
## Multiple R-squared:  0.007122,   Adjusted R-squared:  0.006512
## F-statistic: 11.68 on 1 and 1629 DF,  p-value: 0.0006457
```

plotting vegetation with erosion rate on polynomial:

```
ggplot(nydata, aes(x=Vegetation, y=Erosion)) + geom_point() +
  geom_smooth(method="lm", formula=y ~ poly(x, 2, raw=TRUE)) + b +scale_y_log10()
```

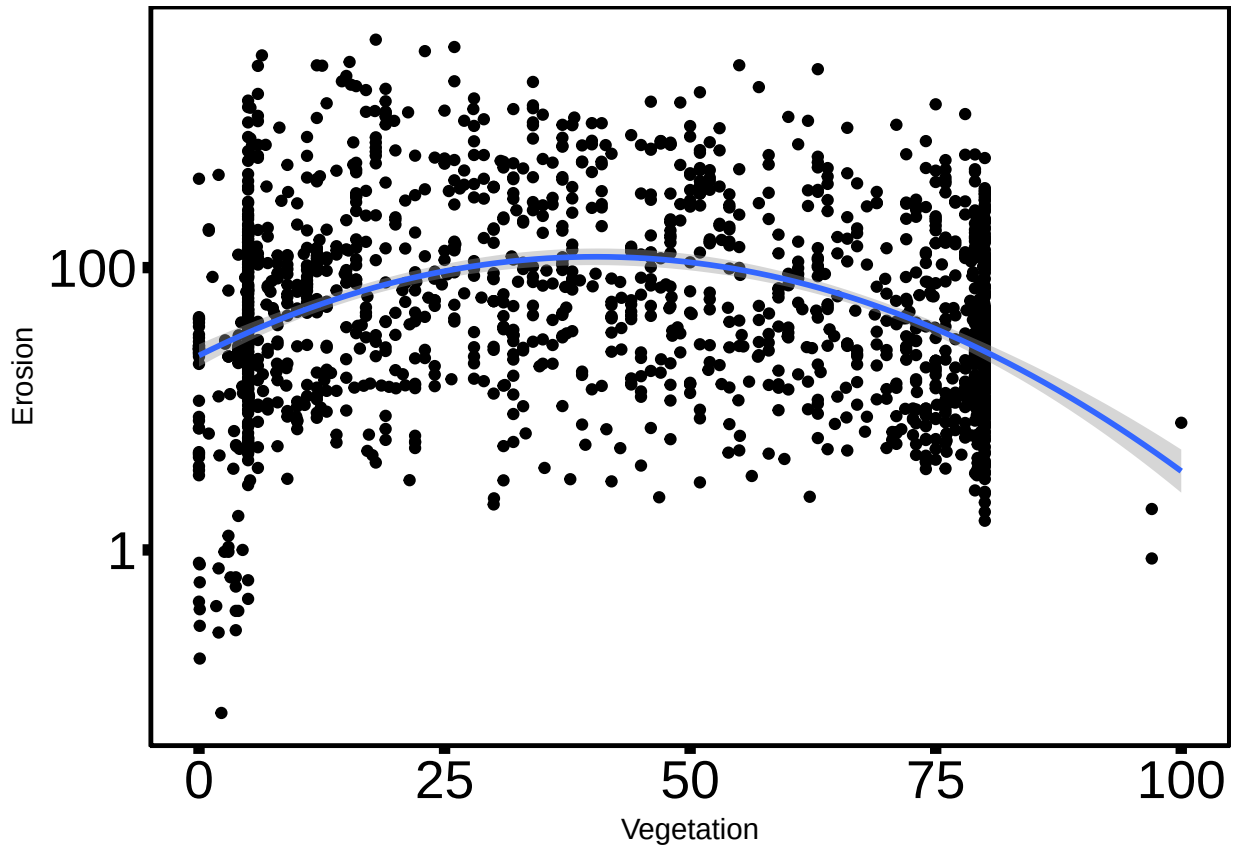

#correlation of erosion with poly vegetation:

```
regression.m5<-lm(log(Erosion) ~ poly(Vegetation, 2), data=nydata)
plot(regression.m5)
```

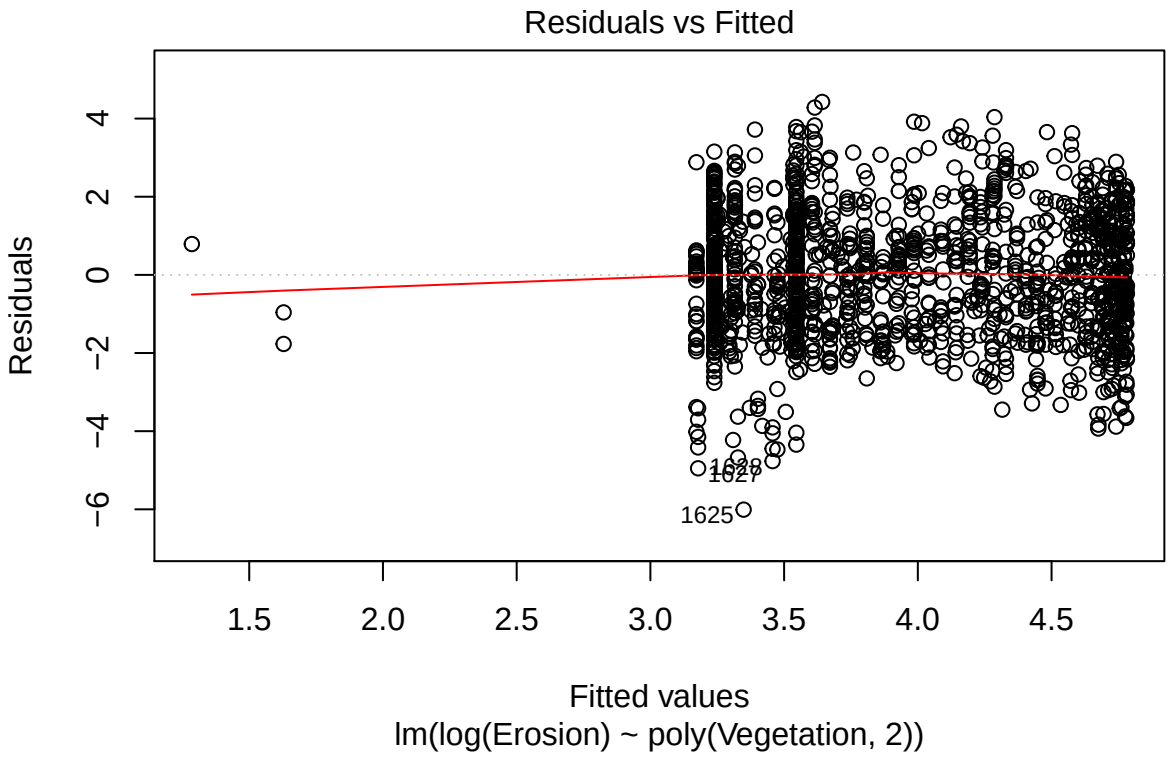
Residuals vs Fitted
Residuals
4
2
0
−2
−4
−6
1628
1627
1625
1.5
2.0
2.5
3.0
3.5
4.0
4.5
Fitted values
lm(log(Erosion) ~ poly(Vegetation, 2))

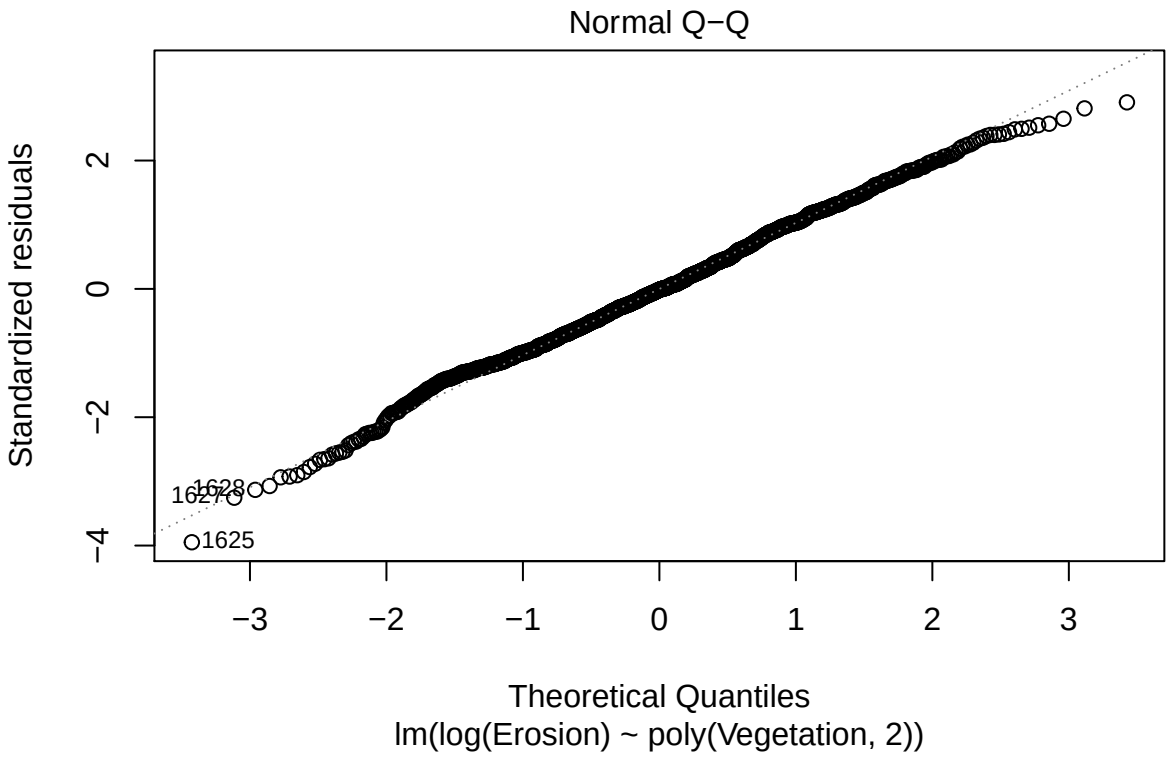
Normal Q−Q
Standardized residuals
2
0
−2
−4
1628
1627
1625
−3
−2
−1
0
1
2
3
Theoretical Quantiles
lm(log(Erosion) ~ poly(Vegetation, 2))

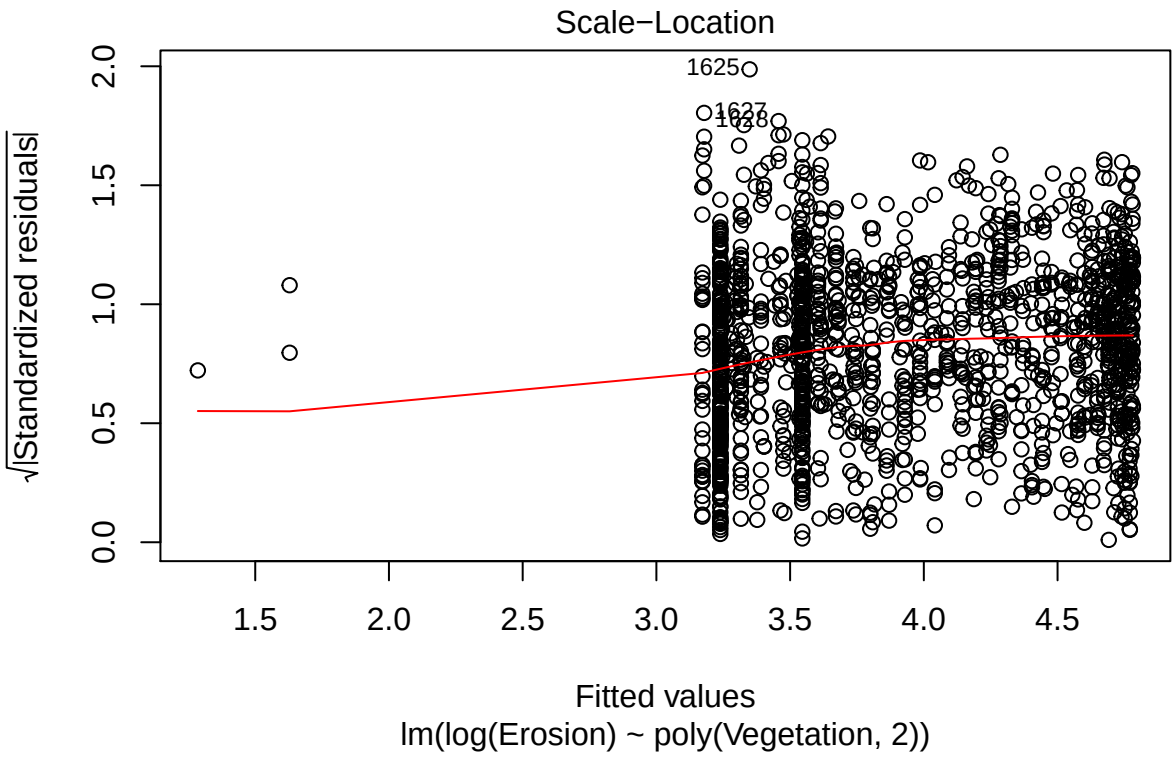
Scale−Location
√|Standardized residuals|
0.0
0.5
1.0
1.5
2.0
1625
1627
1628
1.5
2.0
2.5
3.0
3.5
4.0
4.5
Fitted values
lm(log(Erosion) ~ poly(Vegetation, 2))

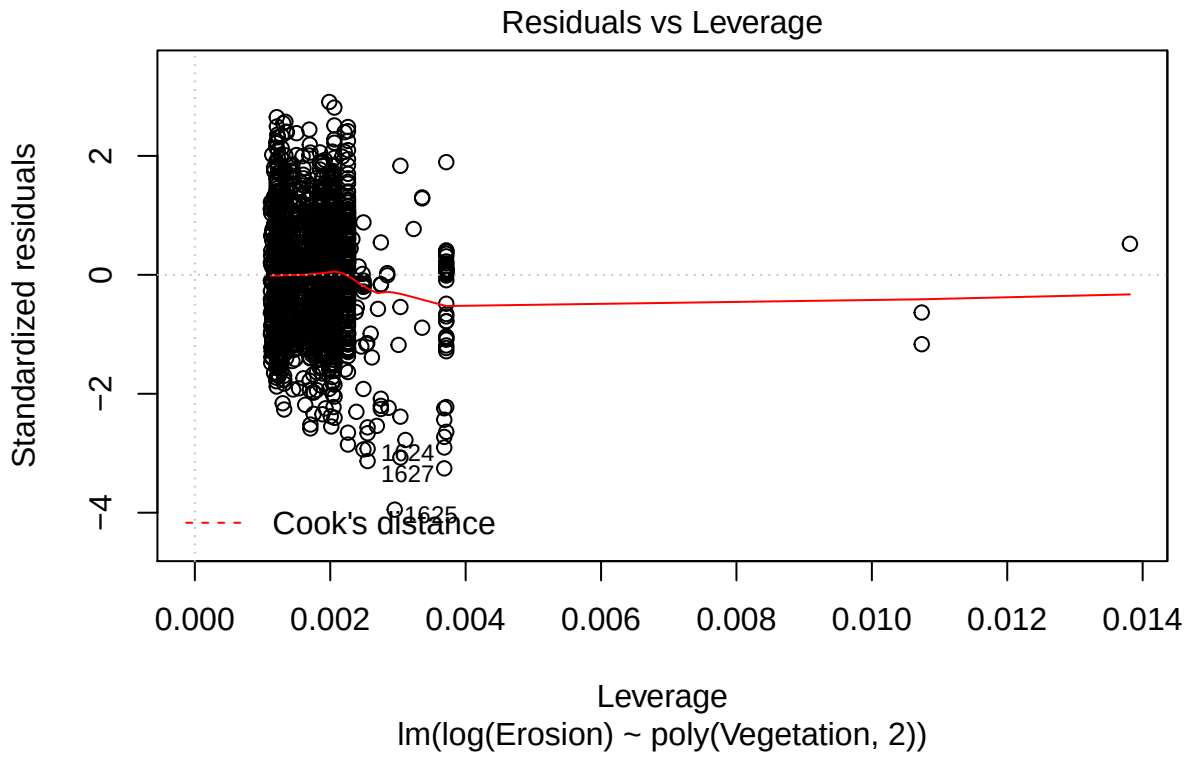


```
summary(regression.m5)
```

```
##
## Call:
## lm(formula = log(Erosion) ~ poly(Vegetation, 2), data = nydata)
##
## Residuals:
##     Min      1Q  Median      3Q     Max
## -6.0078 -1.0597 -0.0201  1.0565  4.4252
##
## Coefficients:
##                       Estimate Std. Error t value Pr(>|t|)
## (Intercept)            3.91187    0.03773  103.67  < 2e-16 ***
## poly(Vegetation, 2)1  -5.54718    1.52386   -3.64 0.000281 ***
## poly(Vegetation, 2)2 -22.57114    1.52386  -14.81  < 2e-16 ***
## ---
## Signif. codes:  0 '***' 0.001 '**' 0.01 '*' 0.05 '.' 0.1 ' ' 1
##
## Residual standard error: 1.524 on 1628 degrees of freedom
## Multiple R-squared:  0.125,  Adjusted R-squared:  0.124
## F-statistic: 116.3 on 2 and 1628 DF,  p-value: < 2.2e-16
```

plotting vegegtation vs precipitation

```
ggplot(nydata, aes(x=Vegetation, y=Precipitation)) + geom_point() +
  geom_smooth(method="lm") + b
```

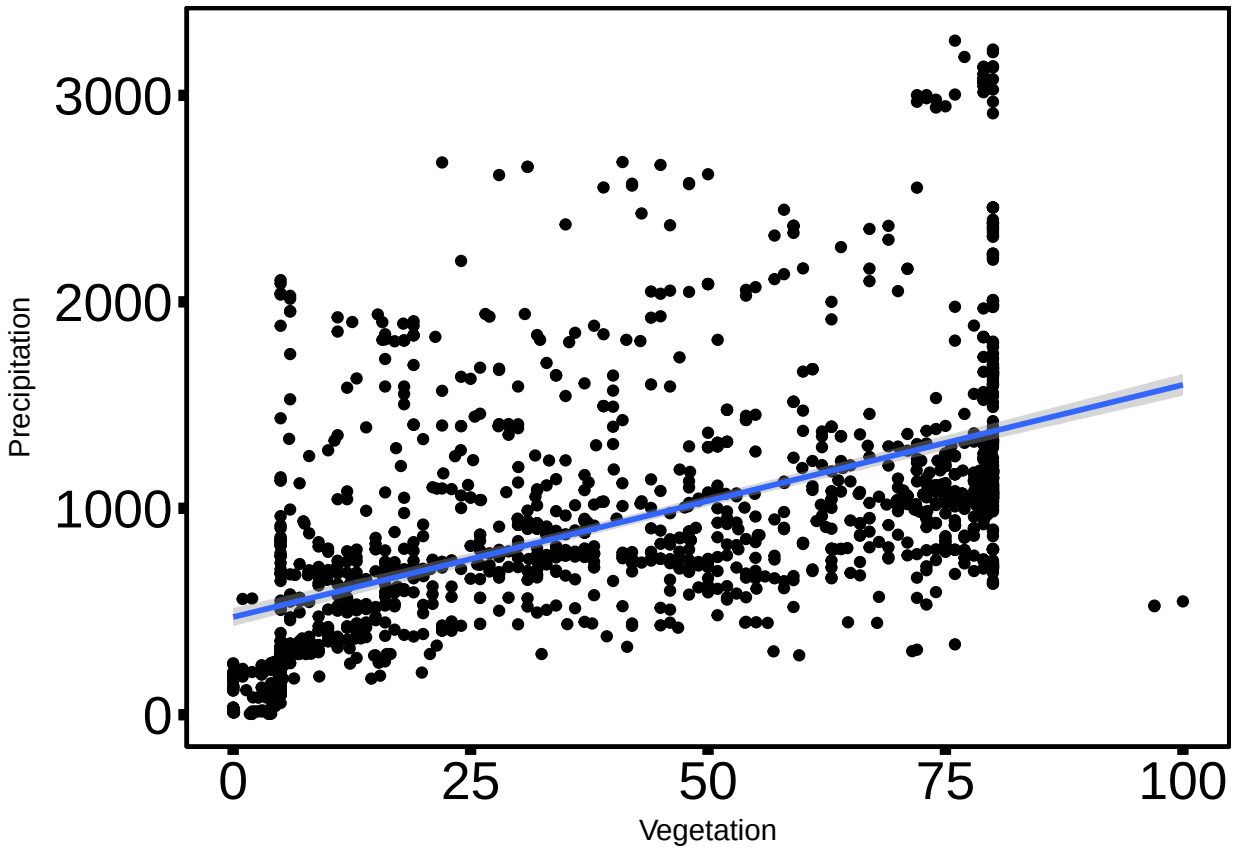

#Linear regression: do precip and vegcorrelate?

```
regression.m6<-lm(Precipitation ~ Vegetation, data=nydata)
plot(regression.m6)
```

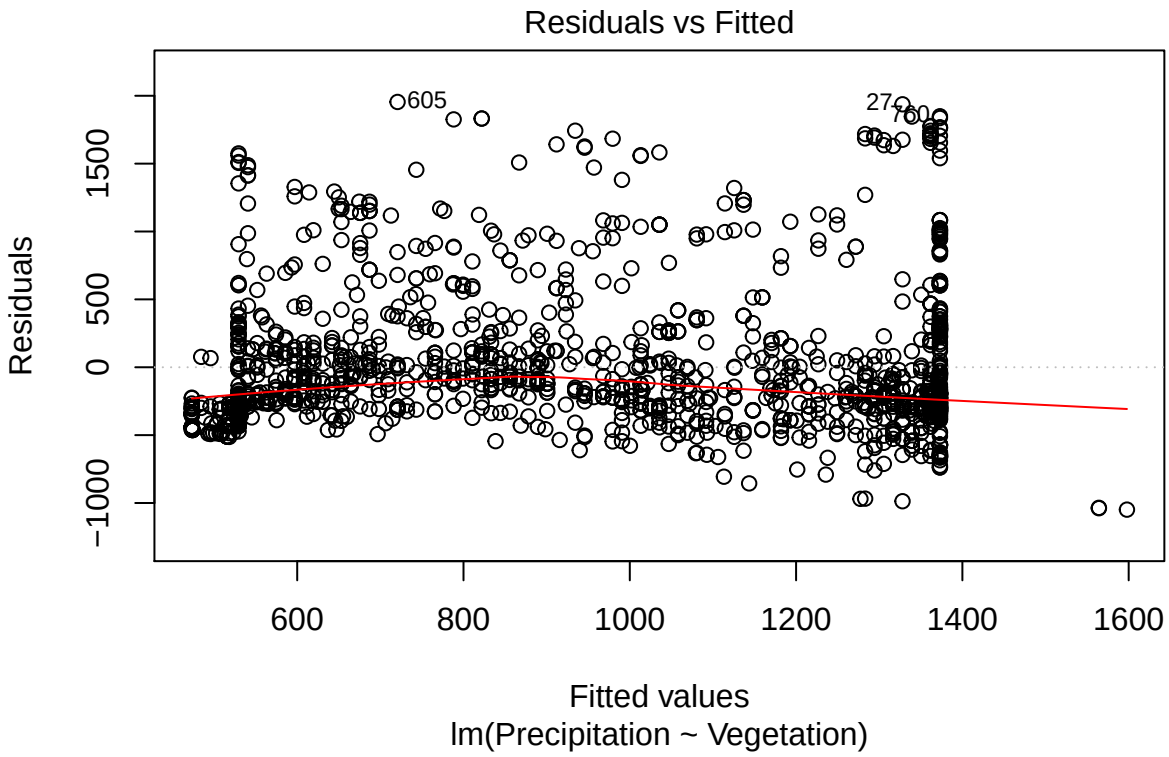
Residuals vs Fitted
605
27
760
Residuals
−1000
0
500
1500
600
800
1000
1200
1400
1600
Fitted values
lm(Precipitation ~ Vegetation)

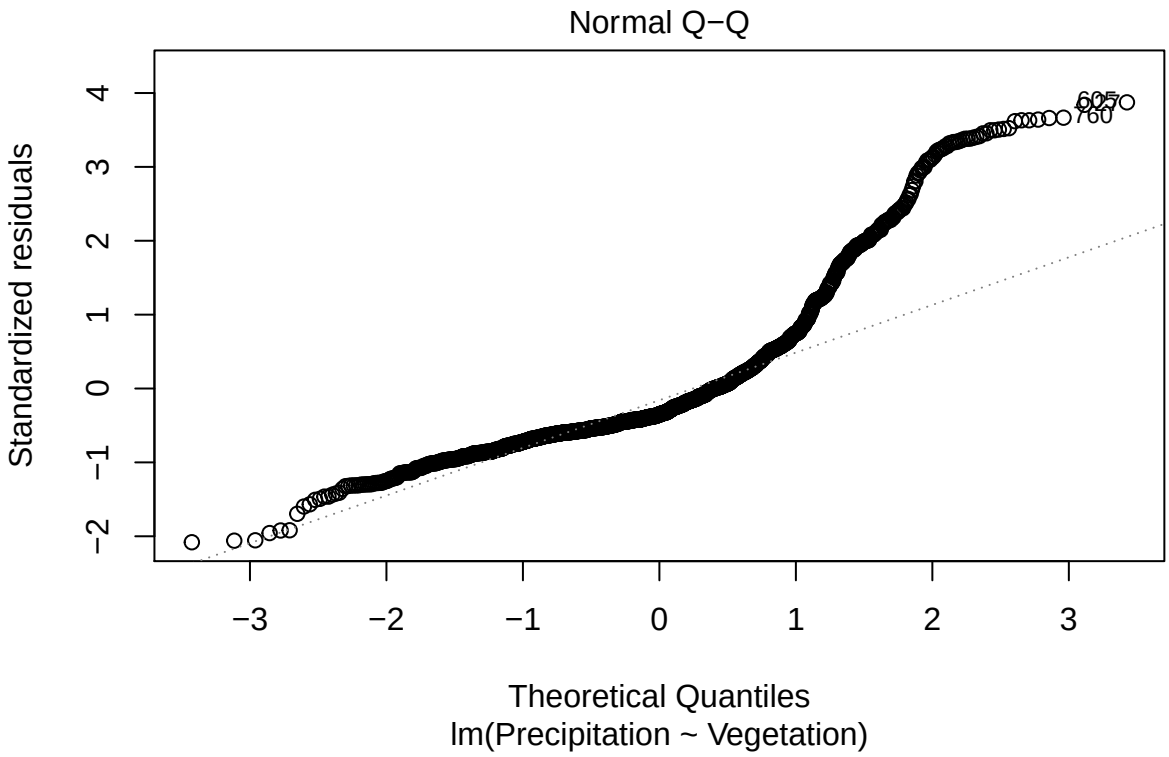
Normal Q−Q
Standardized residuals
Theoretical Quantiles
lm(Precipitation ~ Vegetation)
625
760

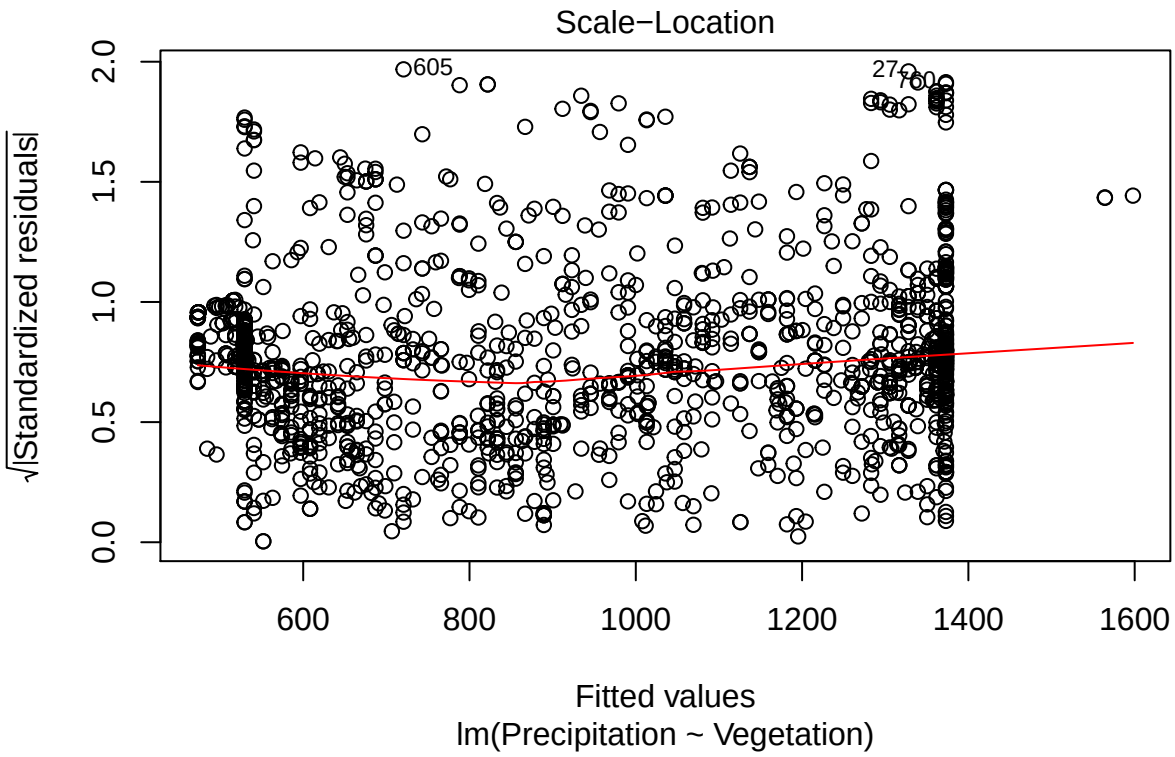
Scale−Location
√|Standardized residuals|
0.0
0.5
1.0
1.5
2.0
605
600
800
1000
1200
1400
1600
Fitted values
lm(Precipitation ~ Vegetation)

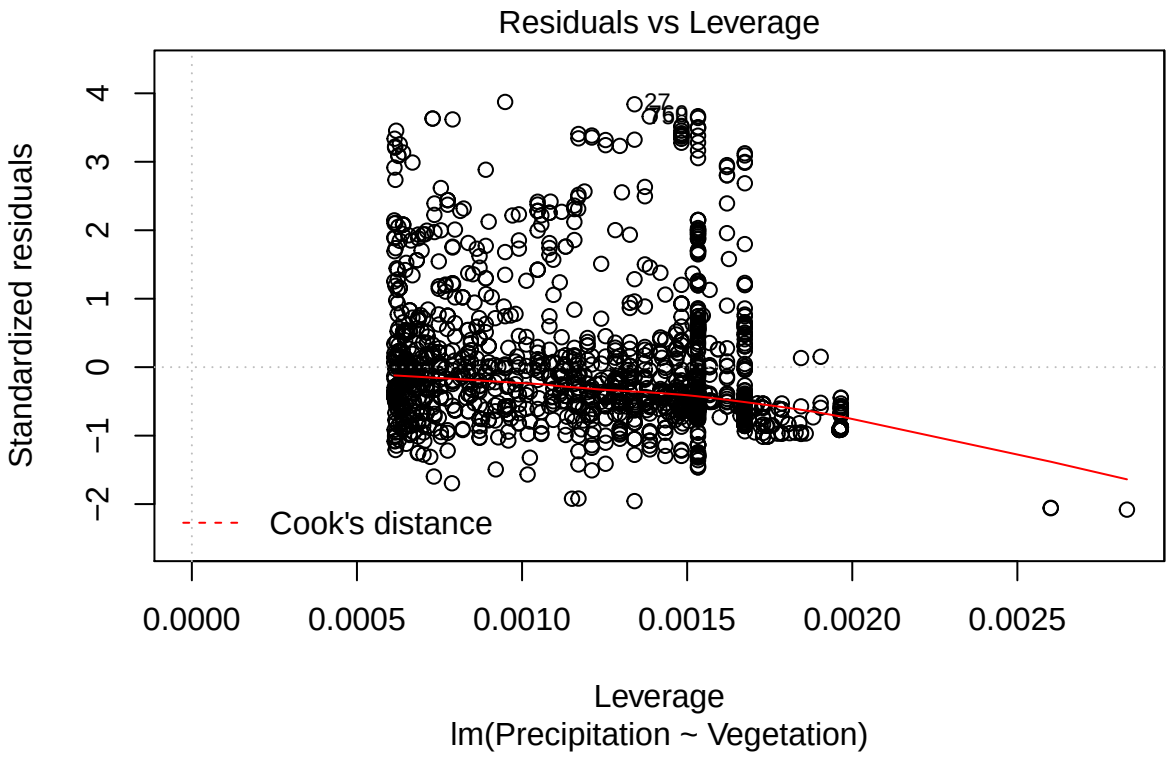


```
summary(regression.m6)
```

```
##
## Call:
## lm(formula = Precipitation ~ Vegetation, data = nydata)
##
## Residuals:
##     Min      1Q  Median      3Q     Max
## -1048.8  -299.2  -176.5   139.6  1954.3
##
## Coefficients:
##             Estimate Std. Error t value Pr(>|t|)
## (Intercept) 473.2666    22.3767   21.15   <2e-16 ***
## Vegetation   11.2466     0.4234   26.57   <2e-16 ***
## ---
## Signif. codes:  0 '***' 0.001 '**' 0.01 '*' 0.05 '.' 0.1 ' ' 1
##
## Residual standard error: 504.7 on 1629 degrees of freedom
## Multiple R-squared:  0.3023, Adjusted R-squared:  0.3018
## F-statistic: 705.7 on 1 and 1629 DF,  p-value: < 2.2e-16
```

Use citation as random effect

```
glob.all = read.csv(file.choose())
glob.all.complete = glob.all[!is.na(glob.all$Vegetation),]
```

```
str(glob.all)
```

```
## 'data.frame':    1789 obs. of  9 variables:
##  $ Study.number : int  1 1 1 1 1 1 1 1 1 1 ...
##  $ Citation     : Factor w/ 89 levels "Abbuhl et al. (2010)",..: 1 1 1 1 1 1 1 1 1 1 ...
##  $ Sample.ID    : Factor w/ 1633 levels " Piu11"," SH-32 ",..: 1132 195 1136 1134 1135 1137 1138 113
##  $ Slope        : num  10.8 12.4 14.9 19.3 18.6 19.2 20.8 21.4 21.1 20.1 ...
##  $ RockType     : Factor w/ 6 levels ""," Mixed","Igneous",..: 5 5 5 5 5 5 5 5 5 5 ...
##  $ Precipitation: num  338 378 429 510 626 639 716 743 763 815 ...
##  $ Vegetation   : num  8 8 9 10 9 9 9 13 13 9 ...
##  $ Erosion      : num  15.9 11.1 45.6 27.7 64.9 ...
##  $ X            : logi  NA NA NA NA NA NA ...
```

```
library(nlme)
```

```
##
## Attaching package: 'nlme'
```

```
## The following object is masked from 'package:dplyr':
##
##     collapse
```

```
## The following object is masked from 'package:lme4':
##
##     lmList
```

Improvemnent in model for precipitation + vegetation

```
lme3p = lm(log(Erosion) ~  poly(Precipitation, 3) + poly (Vegetation, 2),
              data =glob.all.complete)
```

R2 value of model

```
library(MuMIn)
r.squaredLR(lme3p)
```

```
## [1] 0.1831283
## attr(,"adj.r.squared")
## [1] 0.1872672
```

Improvement by addint Slope+precipitation+ vegetation

```
lme3pp = lm(log(Erosion) ~  Slope + poly(Precipitation, 3) + poly(Vegetation, 2),
              data =glob.all.complete)
library(MuMIn)
r.squaredLR(lme3pp)
```

```
## [1] 0.3939928
## attr(,"adj.r.squared")
## [1] 0.4028975
```

```r
summary(lme3pp)
```

```
##
## Call:
## lm(formula = log(Erosion) ~ Slope + poly(Precipitation, 3) +
##     poly(Vegetation, 2), data = glob.all.complete)
##
## Residuals:
##     Min      1Q  Median      3Q     Max
## -5.6522 -0.7913 -0.0053  0.8331  4.3113
##
## Coefficients:
##                            Estimate Std. Error t value Pr(>|t|)
## (Intercept)                2.553771   0.065211  39.161  < 2e-16 ***
## Slope                      0.089645   0.003771  23.771  < 2e-16 ***
## poly(Precipitation, 3)1   13.585700   1.723171   7.884 5.76e-15 ***
## poly(Precipitation, 3)2   -8.026773   1.591010  -5.045 5.04e-07 ***
## poly(Precipitation, 3)3   12.968986   1.393732   9.305  < 2e-16 ***
## poly(Vegetation, 2)1     -22.076652   1.887597 -11.696  < 2e-16 ***
## poly(Vegetation, 2)2      -7.330610   1.507246  -4.864 1.26e-06 ***
## ---
## Signif. codes:  0 '***' 0.001 '**' 0.01 '*' 0.05 '.' 0.1 ' ' 1
##
## Residual standard error: 1.27 on 1624 degrees of freedom
## Multiple R-squared:  0.394,  Adjusted R-squared:  0.3918
## F-statistic:   176 on 6 and 1624 DF,  p-value: < 2.2e-16
```

maximum likelihood fits for model comparison

```r
lme2a = lme(log(Erosion) ~  Slope + poly(Vegetation,2) + poly(Precipitation, 2),
            method="ML", random = ~1|Citation, data = glob.all.complete)
summary(lme2a)
```

```
## Linear mixed-effects model fit by maximum likelihood
##  Data: glob.all.complete
##        AIC     BIC    logLik
##   3514.235 3557.41 -1749.117
##
## Random effects:
##  Formula: ~1 | Citation
##         (Intercept)  Residual
## StdDev:    1.318831 0.6399108
##
## Fixed effects: log(Erosion) ~ Slope + poly(Vegetation, 2) + poly(Precipitation,      2)
##                              Value Std.Error   DF   t-value p-value
## (Intercept)               2.982093 0.1586054 1545 18.801969  0.0000
## Slope                     0.063651 0.0033328 1545 19.098523  0.0000
## poly(Vegetation, 2)1     -2.232718 1.3809897 1545 -1.616752  0.1061
## poly(Vegetation, 2)2     -3.797537 0.9845335 1545 -3.857195  0.0001
## poly(Precipitation, 2)1   6.238972 2.0052657 1545  3.111294  0.0019
## poly(Precipitation, 2)2 -5.794004 2.2379151 1545 -2.589019  0.0097
##  Correlation:
##                          (Intr) Slope  p(V,2)1 p(V,2)2 p(P,2)1
```

```
## Slope                    -0.312
## poly(Vegetation, 2)1     0.071 -0.187
## poly(Vegetation, 2)2    -0.032  0.100 -0.233
## poly(Precipitation, 2)1  0.041 -0.137 -0.189   0.034
## poly(Precipitation, 2)2 -0.118 -0.029  0.266  -0.185  -0.028
##
## Standardized Within-Group Residuals:
##         Min          Q1         Med          Q3         Max
## -5.13279248 -0.54032155  0.02167082  0.55967625  4.18226353
##
## Number of Observations: 1631
## Number of Groups: 81
```

```
lme3a = lme(log(Erosion) ~  Slope + poly(Vegetation,2) + poly(Precipitation, 3),
            method="ML", random = ~1|Citation, data = glob.all.complete)
summary(lme3a)
```

```
## Linear mixed-effects model fit by maximum likelihood
##  Data: glob.all.complete
##        AIC      BIC    logLik
##   3506.107 3554.679 -1744.053
##
## Random effects:
##  Formula: ~1 | Citation
##         (Intercept) Residual
## StdDev:    1.277552 0.638853
##
## Fixed effects: log(Erosion) ~ Slope + poly(Vegetation, 2) + poly(Precipitation,      3)
##                              Value Std.Error   DF   t-value p-value
## (Intercept)              2.973089 0.1543598 1544 19.260776  0.0000
## Slope                    0.064336 0.0033311 1544 19.313476  0.0000
## poly(Vegetation, 2)1    -3.288882 1.4159441 1544 -2.322748  0.0203
## poly(Vegetation, 2)2    -3.214717 0.9997377 1544 -3.215560  0.0013
## poly(Precipitation, 3)1  8.955289 2.1634181 1544  4.139417  0.0000
## poly(Precipitation, 3)2 -5.866888 2.2214915 1544 -2.640968  0.0084
## poly(Precipitation, 3)3  5.569072 1.7394381 1544  3.201650  0.0014
##  Correlation:
##                          (Intr) Slope  p(V,2)1 p(V,2)2 p(P,3)1 p(P,3)2
## Slope                    -0.321
## poly(Vegetation, 2)1     0.075 -0.194
## poly(Vegetation, 2)2    -0.036  0.109 -0.265
## poly(Precipitation, 3)1  0.032 -0.103 -0.262   0.104
## poly(Precipitation, 3)2 -0.120 -0.028  0.259  -0.183  -0.031
## poly(Precipitation, 3)3 -0.017  0.058 -0.230   0.184   0.388  -0.005
##
## Standardized Within-Group Residuals:
##          Min           Q1          Med           Q3          Max
## -5.206163840 -0.552850519  0.008293124  0.549472635  4.170585799
##
## Number of Observations: 1631
## Number of Groups: 81
```

```
lme4a = lme(log(Erosion) ~  Slope + poly(Vegetation,2) + poly(Precipitation, 4),
            method="ML", random = ~1|Citation, data = glob.all.complete)
summary(lme4a)
```

```
## Linear mixed-effects model fit by maximum likelihood
##  Data: glob.all.complete
##        AIC      BIC    logLik
##   3499.409 3553.379 -1739.705
##
## Random effects:
##  Formula: ~1 | Citation
##         (Intercept)  Residual
## StdDev:    1.278939 0.6370313
##
## Fixed effects: log(Erosion) ~ Slope + poly(Vegetation, 2) + poly(Precipitation,      4)
##                               Value Std.Error   DF   t-value p-value
## (Intercept)                3.000931 0.1547759 1543 19.388876  0.0000
## Slope                      0.063564 0.0033330 1543 19.070998  0.0000
## poly(Vegetation, 2)1      -2.990806 1.4159748 1543 -2.112189  0.0348
## poly(Vegetation, 2)2      -3.072036 0.9984301 1543 -3.076867  0.0021
## poly(Precipitation, 4)1    8.944013 2.1597292 1543  4.141266  0.0000
## poly(Precipitation, 4)2   -7.163302 2.2614720 1543 -3.167540  0.0016
## poly(Precipitation, 4)3    5.503288 1.7362207 1543  3.169694  0.0016
## poly(Precipitation, 4)4   -3.897136 1.3227742 1543 -2.946184  0.0033
##  Correlation:
##                           (Intr) Slope  p(V,2)1 p(V,2)2 p(P,4)1 p(P,4)2
## Slope                     -0.323
## poly(Vegetation, 2)1       0.079 -0.199
## poly(Vegetation, 2)2      -0.032  0.104 -0.260
## poly(Precipitation, 4)1    0.032 -0.103 -0.261   0.104
## poly(Precipitation, 4)2   -0.129 -0.013  0.240  -0.189  -0.030
## poly(Precipitation, 4)3   -0.018  0.058 -0.230   0.183   0.388  -0.002
## poly(Precipitation, 4)4   -0.061  0.077 -0.070  -0.049   0.001   0.196
##                           p(P,4)3
## Slope
## poly(Vegetation, 2)1
## poly(Vegetation, 2)2
## poly(Precipitation, 4)1
## poly(Precipitation, 4)2
## poly(Precipitation, 4)3
## poly(Precipitation, 4)4  0.011
##
## Standardized Within-Group Residuals:
##         Min          Q1         Med          Q3         Max
## -5.31628568 -0.54442487  0.01350764  0.55310783  4.18505556
##
## Number of Observations: 1631
## Number of Groups: 81
```

```
lme5a = lme(log(Erosion) ~  Slope + poly(Vegetation,2) + poly(Precipitation, 5),
            method="ML", random = ~1|Citation, data = glob.all.complete)
summary(lme5a)
```

```
## Linear mixed-effects model fit by maximum likelihood
##  Data: glob.all.complete
##        AIC      BIC    logLik
##   3499.023 3558.389 -1738.512
##
## Random effects:
```

```
##  Formula: ~1 | Citation
##         (Intercept)  Residual
## StdDev:    1.271842 0.6367208
##
## Fixed effects: log(Erosion) ~ Slope + poly(Vegetation, 2) + poly(Precipitation,      5)
##                               Value Std.Error   DF   t-value p-value
## (Intercept)              3.003097 0.1540844 1542 19.489944  0.0000
## Slope                    0.063659 0.0033324 1542 19.103030  0.0000
## poly(Vegetation, 2)1    -2.630610 1.4352916 1542 -1.832806  0.0670
## poly(Vegetation, 2)2    -3.034449 0.9984713 1542 -3.039095  0.0024
## poly(Precipitation, 5)1  8.915261 2.1571100 1542  4.132966  0.0000
## poly(Precipitation, 5)2 -7.322042 2.2606497 1542 -3.238911  0.0012
## poly(Precipitation, 5)3  5.500299 1.7345160 1542  3.171086  0.0015
## poly(Precipitation, 5)4 -4.403993 1.3625733 1542 -3.232114  0.0013
## poly(Precipitation, 5)5  1.681510 1.0902895 1542  1.542260  0.1232
##  Correlation:
##                         (Intr) Slope  p(V,2)1 p(V,2)2 p(P,5)1 p(P,5)2
## Slope                   -0.324
## poly(Vegetation, 2)1     0.080 -0.193
## poly(Vegetation, 2)2    -0.032  0.105 -0.253
## poly(Precipitation, 5)1  0.032 -0.103 -0.259   0.103
## poly(Precipitation, 5)2 -0.130 -0.013  0.229  -0.190  -0.030
## poly(Precipitation, 5)3 -0.018  0.058 -0.228   0.183   0.388  -0.002
## poly(Precipitation, 5)4 -0.062  0.071 -0.107  -0.053   0.004   0.200
## poly(Precipitation, 5)5  0.010  0.015  0.165   0.024  -0.010  -0.043
##                         p(P,5)3 p(P,5)4
## Slope
## poly(Vegetation, 2)1
## poly(Vegetation, 2)2
## poly(Precipitation, 5)1
## poly(Precipitation, 5)2
## poly(Precipitation, 5)3
## poly(Precipitation, 5)4  0.012
## poly(Precipitation, 5)5 -0.005  -0.242
##
## Standardized Within-Group Residuals:
##         Min          Q1         Med          Q3         Max
## -5.35518367 -0.54625242  0.01446509  0.55111692  4.19933332
##
## Number of Observations: 1631
## Number of Groups: 81
```

```
lme6a = lme(log(Erosion) ~  Slope + poly(Vegetation,2) + poly(Precipitation, 6),
            method="ML", random = ~1|Citation, data = glob.all.complete)
summary(lme6a)
```

```
## Linear mixed-effects model fit by maximum likelihood
##  Data: glob.all.complete
##        AIC     BIC    logLik
##   3498.077 3562.84 -1737.038
##
## Random effects:
##  Formula: ~1 | Citation
##         (Intercept) Residual
## StdDev:    1.284052  0.63581
```

```
##
## Fixed effects: log(Erosion) ~ Slope + poly(Vegetation, 2) + poly(Precipitation,      6)
##                               Value Std.Error   DF   t-value p-value
## (Intercept)                3.015692 0.1555320 1541 19.389528  0.0000
## Slope                      0.063468 0.0033309 1541 19.054408  0.0000
## poly(Vegetation, 2)1      -2.685224 1.4344993 1541 -1.871889  0.0614
## poly(Vegetation, 2)2      -3.097306 0.9981025 1541 -3.103195  0.0019
## poly(Precipitation, 6)1    8.513181 2.1718333 1541  3.919813  0.0001
## poly(Precipitation, 6)2   -7.868523 2.2870974 1541 -3.440397  0.0006
## poly(Precipitation, 6)3    4.861471 1.7724358 1541  2.742819  0.0062
## poly(Precipitation, 6)4   -4.525387 1.3639585 1541 -3.317833  0.0009
## poly(Precipitation, 6)5    0.711235 1.2258205 1541  0.580211  0.5619
## poly(Precipitation, 6)6    1.895765 1.1041206 1541  1.716991  0.0862
##  Correlation:
##                           (Intr) Slope  p(V,2)1 p(V,2)2 p(P,6)1 p(P,6)2
## Slope                     -0.322
## poly(Vegetation, 2)1       0.078 -0.193
## poly(Vegetation, 2)2      -0.034  0.106 -0.252
## poly(Precipitation, 6)1    0.026 -0.099 -0.254   0.106
## poly(Precipitation, 6)2   -0.134 -0.009  0.230  -0.183  -0.013
## poly(Precipitation, 6)3   -0.027  0.062 -0.218   0.186   0.400   0.028
## poly(Precipitation, 6)4   -0.063  0.073 -0.106  -0.051   0.009   0.206
## poly(Precipitation, 6)5   -0.013  0.027  0.159   0.037   0.040   0.027
## poly(Precipitation, 6)6    0.046 -0.028 -0.026  -0.035  -0.105  -0.143
##                           p(P,6)3 p(P,6)4 p(P,6)5
## Slope
## poly(Vegetation, 2)1
## poly(Vegetation, 2)2
## poly(Precipitation, 6)1
## poly(Precipitation, 6)2
## poly(Precipitation, 6)3
## poly(Precipitation, 6)4    0.022
## poly(Precipitation, 6)5    0.089  -0.192
## poly(Precipitation, 6)6   -0.203  -0.051  -0.458
##
## Standardized Within-Group Residuals:
##        Min         Q1        Med         Q3        Max
## -5.3410517 -0.5354982  0.0176847  0.5519878  4.1879335
##
## Number of Observations: 1631
## Number of Groups: 81
```

```
lme7a = lme(log(Erosion) ~  Slope + poly(Vegetation,2) + poly(Precipitation, 7),
            method="ML", random = ~1|Citation, data = glob.all.complete)
summary(lme7a)
```

```
## Linear mixed-effects model fit by maximum likelihood
##  Data: glob.all.complete
##        AIC      BIC    logLik
##   3500.016 3570.176 -1737.008
##
## Random effects:
##  Formula: ~1 | Citation
##         (Intercept)  Residual
## StdDev:    1.283772 0.6358045
```

```
##
## Fixed effects: log(Erosion) ~ Slope + poly(Vegetation, 2) + poly(Precipitation,      7)
##                               Value Std.Error   DF   t-value p-value
## (Intercept)                3.013979 0.1557045 1540 19.357052  0.0000
## Slope                      0.063526 0.0033401 1540 19.019409  0.0000
## poly(Vegetation, 2)1      -2.668471 1.4365698 1540 -1.857530  0.0634
## poly(Vegetation, 2)2      -3.085548 0.9995285 1540 -3.087004  0.0021
## poly(Precipitation, 7)1    8.588042 2.1933515 1540  3.915489  0.0001
## poly(Precipitation, 7)2   -7.753682 2.3347587 1540 -3.320978  0.0009
## poly(Precipitation, 7)3    4.961704 1.8184570 1540  2.728524  0.0064
## poly(Precipitation, 7)4   -4.378545 1.4887024 1540 -2.941182  0.0033
## poly(Precipitation, 7)5    0.686918 1.2302150 1540  0.558372  0.5767
## poly(Precipitation, 7)6    1.980520 1.1570287 1540  1.711729  0.0871
## poly(Precipitation, 7)7   -0.291437 1.1827957 1540 -0.246397  0.8054
##  Correlation:
##                           (Intr) Slope  p(V,2)1 p(V,2)2 p(P,7)1 p(P,7)2
## Slope                     -0.324
## poly(Vegetation, 2)1       0.075 -0.189
## poly(Vegetation, 2)2      -0.036  0.108 -0.249
## poly(Precipitation, 7)1    0.020 -0.089 -0.245   0.112
## poly(Precipitation, 7)2   -0.141  0.005  0.235  -0.169   0.015
## poly(Precipitation, 7)3   -0.036  0.076 -0.201   0.192   0.417   0.071
## poly(Precipitation, 7)4   -0.076  0.094 -0.078  -0.028   0.063   0.265
## poly(Precipitation, 7)5   -0.009  0.021  0.154   0.033   0.028   0.010
## poly(Precipitation, 7)6    0.031 -0.006 -0.011  -0.019  -0.059  -0.074
## poly(Precipitation, 7)7    0.044 -0.070 -0.048  -0.048  -0.138  -0.200
##                           p(P,7)3 p(P,7)4 p(P,7)5 p(P,7)6
## Slope
## poly(Vegetation, 2)1
## poly(Vegetation, 2)2
## poly(Precipitation, 7)1
## poly(Precipitation, 7)2
## poly(Precipitation, 7)3
## poly(Precipitation, 7)4    0.109
## poly(Precipitation, 7)5    0.068  -0.208
## poly(Precipitation, 7)6   -0.122   0.075  -0.460
## poly(Precipitation, 7)7   -0.222  -0.400   0.081  -0.298
##
## Standardized Within-Group Residuals:
##         Min          Q1         Med          Q3         Max
## -5.34047578 -0.53809735  0.01588461  0.55610404  4.19804884
##
## Number of Observations: 1631
## Number of Groups: 81
```

```
lme8a = lme(log(Erosion) ~  Slope + poly(Vegetation,2) + poly(Precipitation, 8),
            method="ML", random = ~1|Citation, data = glob.all.complete)
summary(lme8a)
```

```
## Linear mixed-effects model fit by maximum likelihood
##  Data: glob.all.complete
##        AIC      BIC   logLik
##   3500.78 3576.337 -1736.39
##
## Random effects:
```

```
##  Formula: ~1 | Citation
##         (Intercept)  Residual
## StdDev:    1.271987 0.6358476
##
## Fixed effects: log(Erosion) ~ Slope + poly(Vegetation, 2) + poly(Precipitation,      8)
##                              Value Std.Error   DF   t-value p-value
## (Intercept)              3.012768 0.1545321 1539 19.496068  0.0000
## Slope                    0.063250 0.0033517 1539 18.871124  0.0000
## poly(Vegetation, 2)1    -2.610614 1.4380678 1539 -1.815362  0.0697
## poly(Vegetation, 2)2    -3.207482 1.0060211 1539 -3.188285  0.0015
## poly(Precipitation, 8)1  8.966202 2.2136023 1539  4.050502  0.0001
## poly(Precipitation, 8)2 -7.336575 2.3605734 1539 -3.107963  0.0019
## poly(Precipitation, 8)3  5.625871 1.9041336 1539  2.954557  0.0032
## poly(Precipitation, 8)4 -4.414495 1.4879011 1539 -2.966928  0.0031
## poly(Precipitation, 8)5  1.062673 1.2729317 1539  0.834823  0.4039
## poly(Precipitation, 8)6  1.561259 1.2138393 1539  1.286216  0.1986
## poly(Precipitation, 8)7  0.117409 1.2380576 1539  0.094833  0.9245
## poly(Precipitation, 8)8 -1.203535 1.0809846 1539 -1.113369  0.2657
##  Correlation:
##                         (Intr) Slope  p(V,2)1 p(V,2)2 p(P,8)1 p(P,8)2
## Slope                   -0.325
## poly(Vegetation, 2)1     0.076 -0.191
## poly(Vegetation, 2)2    -0.035  0.117 -0.251
## poly(Precipitation, 8)1  0.020 -0.099 -0.237   0.093
## poly(Precipitation, 8)2 -0.140 -0.008  0.238  -0.184   0.037
## poly(Precipitation, 8)3 -0.036  0.048 -0.180   0.148   0.436   0.114
## poly(Precipitation, 8)4 -0.076  0.096 -0.079  -0.025   0.058   0.256
## poly(Precipitation, 8)5 -0.010 -0.001  0.160   0.003   0.064   0.051
## poly(Precipitation, 8)6  0.031  0.019 -0.023   0.015  -0.100  -0.118
## poly(Precipitation, 8)7  0.041 -0.091 -0.033  -0.078  -0.085  -0.139
## poly(Precipitation, 8)8  0.005  0.081 -0.041   0.111  -0.148  -0.161
##                         p(P,8)3 p(P,8)4 p(P,8)5 p(P,8)6 p(P,8)7
## Slope
## poly(Vegetation, 2)1
## poly(Vegetation, 2)2
## poly(Precipitation, 8)1
## poly(Precipitation, 8)2
## poly(Precipitation, 8)3
## poly(Precipitation, 8)4  0.096
## poly(Precipitation, 8)5  0.140  -0.207
## poly(Precipitation, 8)6 -0.202   0.079  -0.501
## poly(Precipitation, 8)7 -0.112  -0.388   0.151  -0.362
## poly(Precipitation, 8)8 -0.301   0.024  -0.258   0.303  -0.297
##
## Standardized Within-Group Residuals:
##         Min          Q1         Med          Q3         Max
## -5.31825900 -0.54641218  0.01656766  0.56082429  4.18388449
##
## Number of Observations: 1631
## Number of Groups: 81
```

```
anova(lme2a, lme3a,lme4a,lme5a,lme6a,lme7a, lme8a)
```

```
##       Model df      AIC      BIC    logLik   Test   L.Ratio p-value
## lme2a     1  8 3514.235 3557.410 -1749.117
```

```
## lme3a     2  9 3506.107 3554.679 -1744.053 1 vs 2 10.127946  0.0015
## lme4a     3 10 3499.409 3553.379 -1739.705 2 vs 3  8.697321  0.0032
## lme5a     4 11 3499.023 3558.389 -1738.512 3 vs 4  2.386294  0.1224
## lme6a     5 12 3498.077 3562.840 -1737.038 4 vs 5  2.946309  0.0861
## lme7a     6 13 3500.016 3570.176 -1737.008 5 vs 6  0.061116  0.8047
## lme8a     7 14 3500.780 3576.337 -1736.390 6 vs 7  1.235923  0.2663
```

```
AIC(lme2a, lme3a,lme4a,lme5a,lme6a,lme7a, lme8a)
```

```
##       df      AIC
## lme2a  8 3514.235
## lme3a  9 3506.107
## lme4a 10 3499.409
## lme5a 11 3499.023
## lme6a 12 3498.077
## lme7a 13 3500.016
## lme8a 14 3500.780
```

Clearly stop at 3

refit order 3 polynomial with an REML fit

```
lme3.final = lme(log(Erosion) ~  Slope + poly(Vegetation,2) + poly(Precipitation, 3),
           method="ML", random = ~1|Citation, data = glob.all.complete)
summary(lme3.final)
```

```
## Linear mixed-effects model fit by maximum likelihood
##  Data: glob.all.complete
##        AIC      BIC    logLik
##   3506.107 3554.679 -1744.053
##
## Random effects:
##  Formula: ~1 | Citation
##         (Intercept) Residual
## StdDev:    1.277552 0.638853
##
## Fixed effects: log(Erosion) ~ Slope + poly(Vegetation, 2) + poly(Precipitation,      3)
##                              Value Std.Error   DF   t-value p-value
## (Intercept)              2.973089 0.1543598 1544 19.260776  0.0000
## Slope                    0.064336 0.0033311 1544 19.313476  0.0000
## poly(Vegetation, 2)1    -3.288882 1.4159441 1544 -2.322748  0.0203
## poly(Vegetation, 2)2    -3.214717 0.9997377 1544 -3.215560  0.0013
## poly(Precipitation, 3)1  8.955289 2.1634181 1544  4.139417  0.0000
## poly(Precipitation, 3)2 -5.866888 2.2214915 1544 -2.640968  0.0084
## poly(Precipitation, 3)3  5.569072 1.7394381 1544  3.201650  0.0014
##  Correlation:
##                         (Intr) Slope  p(V,2)1 p(V,2)2 p(P,3)1 p(P,3)2
## Slope                   -0.321
## poly(Vegetation, 2)1     0.075 -0.194
## poly(Vegetation, 2)2    -0.036  0.109 -0.265
## poly(Precipitation, 3)1  0.032 -0.103 -0.262   0.104
## poly(Precipitation, 3)2 -0.120 -0.028  0.259  -0.183  -0.031
## poly(Precipitation, 3)3 -0.017  0.058 -0.230   0.184   0.388  -0.005
```

```
##
## Standardized Within-Group Residuals:
##           Min            Q1           Med            Q3           Max
## -5.206163840 -0.552850519  0.008293124  0.549472635  4.170585799
##
## Number of Observations: 1631
## Number of Groups: 81
```

Check r-squared values

```
library(MuMIn)
r.squaredLR(lme3a)
```

```
## [1] 0.8124054
## attr(,"adj.r.squared")
## [1] 0.8307667
```

```
r.squaredLR(lme3.final)
```

```
## [1] 0.8124054
## attr(,"adj.r.squared")
## [1] 0.8307667
```

```
r.squaredGLMM(lme3.final)
```

```
##       R2m       R2c
## 0.1939938 0.8387677
```

Good overall model! but note that the fixed factors account for less of the variance than the random effect

How much of the variance does the precipitation polynomial account for?

Run model without it and compare

```
lmeNoPrecip = lme(log(Erosion) ~  Slope + poly(Vegetation,2),
                  method="ML", random = ~1|Citation, data = glob.all.complete)
r.squaredLR(lmeNoPrecip)
```

```
## [1] 0.8093964
## attr(,"adj.r.squared")
## [1] 0.8276897
```

```
r.squaredGLMM(lmeNoPrecip)
```

```
##       R2m       R2c
## 0.1389556 0.8426419
```

Not much overall, its taken up by the random effect – but improves the fixed effects by

about 40% (from about 0.13 to 0.19)

generate predictions for precipitation range and median values of slope and tree cover,

using a single citation with an erosion level close to average

Find the range of annual precipitation values

```
range(glob.all$Precipitation)
```

```
## [1]    3 3265
```

find the overal mean and citation means for log.erosion

```
glob.all$Erosion_log= log(glob.all$Erosion)
mean(glob.all$Erosion_log)  ## about 3.90
```

```
## [1] 3.835456
```

```
tapply(glob.all$Erosion_log, glob.all$Citation, mean) # Several have means very  close to the overall m
```

```
##        Abbuhl et al. (2010)        Acosta et al. (2015)
##                   3.9573536                   2.6411474
##         Belmont et al. 2007     Bierman and Caffee 2001
##                   5.2402029                   1.5937278
##         Bierman et al  2005         Bierman et al  2007
##                   4.4173538                   1.9655060
##        Bierman et al (2005)          Bierman et al 1998
##                   2.5122677                   1.0788654
##          Bierman et al 2001          Bierman et al 2009
##                   4.2329245                   2.8720743
##           Binnie et al 2006           Binnie et al 2008
##                   5.3051857                   5.6945818
##            Brown et al 1995            Brown et al 1998
##                   3.3196257                   3.8427232
##         Buechi et al.(2014)    Carretier, et al. (2013)
##                   4.6680739                   2.9118491
##         Chappell et al 2006           Clapp et al 2000
##                   4.1283158                   3.2496205
##            Clapp et al 2001           Clapp et al 2002
##                   4.2998318                   3.2112690
##               Codilean-2008               Codilean-2012
##                   2.1957997                   2.0718090
##              Cox et al 2009    Croke, J., et al. (2015)
##                   2.4313498                   2.5954528
##        Cyr and Granger 2008             Cyr et al 2010
##                   6.0113343                   7.1779379
##                Delunel-2010          Delunel et al 2010
```

```
##                 6.5135880                 6.5299152
##             Densmore-2009         DiBiase et al 2009
##                 6.8095365                 5.5764461
##          Dirks et al. 2016               Duxbury 2008
##                 0.9611333                 2.2133581
##     Duxbury et. al. (2014)         Ferrier et al 2005
##                 2.1443398                 5.2597126
##        Finnegan et al 2008    Glotzbach et al.,(2014)
##                 6.9985906                 4.2827084
##          Godard et al 2010         Granger et al 1996
##                 6.4963007                 3.7885362
##        Guralnik et al 2010         Harkins et al 2010
##                 3.2630126                 4.1682283
##        Heimsath et al 1999        Heimsath et al 2001
##                 4.1722217                 3.5457116
##        Heimsath et al 2006        Heimsath et al 2009
##                 3.6682352                 2.6500852
##        Heimsath et al 2010           Henck et al 2011
##                 1.0148766                 4.2031732
##       Hewawasam et al 2003        Hippe et al. (2012)
##                 2.9475616                 1.9897589
##           Insel et al 2010        Kirchner et al 2001
##                 5.1471373                 4.1599293
##          Kober et al 2009       Larsen et al. (2014)
##                 3.0301949                 5.6336211
##          Matmon et al 2003                Meyer-2010
##                 3.1452479                 3.8959038
##            Meyer-2010 (a)       Miller et al. (2013)
##                 3.9321666                 2.5803732
##           Morel et al 2003         Nichols et al 2002
##                 3.4637000                 3.7245979
##     Nichols et al 2005 (a)     Nichols et al 2005 (b)
##                 3.4175567                 5.0201630
##         Nichols et al 2007     Nichols et al., (2014)
##                 2.8088001                 3.1617442
##               Norton-2010               Norton-2011
##                 6.0643034                 4.0174907
##          Norton et al 2007          Ouimet et al 2009
##                 5.8367961                 4.9674828
##               Palumbo-2011         Palumbo et al 2009
##                 4.9673191                 5.0456836
##            Perg et al 2003         Placzek et al 2010
##                 4.9920080                -0.3906133
##         Placzek et al 2014        Pumin et al. (2015)
##                -0.4229516                 1.5556485
##        Quigley et al 2007a        Quigley et al 2007b
##                 3.3297014                 2.4895713
##       Reinhardt et al 2007                Reuter 2005
##                 5.6493420                 2.7043103
##           Riebe et al 2000           Riebe et al 2003
##                 3.5980253                 4.0551525
##          Safran et al 2005        Schaller et al 2001
##                 5.5087866                 3.5633208
##               Scharf-2012           Stock et al 2009
```

```
##                   1.4881506                   4.7364289
##               Sullivan 2007          Tomkins et al 2007
##                   2.6863033                   3.1069095
##         Vanacker et al 2007 von Blanckenburg et al 2004
##                   2.2380392                   2.3520408
##               Wittmann-2011         Wittmann et al 2007
##                   2.5872572                   6.3180681
##         Wittmann et al 2009
##                   5.4021486
## Granger et al 1996, Brown et al 1998, Meyer-2010
```

Specify a regularly-spaced vector of precipitation levels covering the observed range

Put it into a new dataframe

The new dataframe will be used to predict erosion levels with constant values for Citation, slope & tree cover

```
Precipitation=seq(0, 3265, 5)  # has 654 values
newdata=data.frame(Precipitation)
```

use selected citation, making sure it has the right level number

```
newdata$Citation = "Granger et al 1996"
newdata$Citation = factor(newdata$Citation, levels=levels(glob.all.complete$Citation))
```

use median basin slope

```
newdata$Slope = median(glob.all.complete$Slope)
```

use median tree cover

```
newdata$Vegetation = median(glob.all.complete$Vegetation)
```

generate and plot predicted values

```
newdata$pred.erosion = predict(lme3.final, newdata=newdata)
with(newdata, plot(pred.erosion ~ Precipitation, type="l", ylim=c(-3,9)))
with(glob.all.complete, points(Precipitation, Erosion))
```

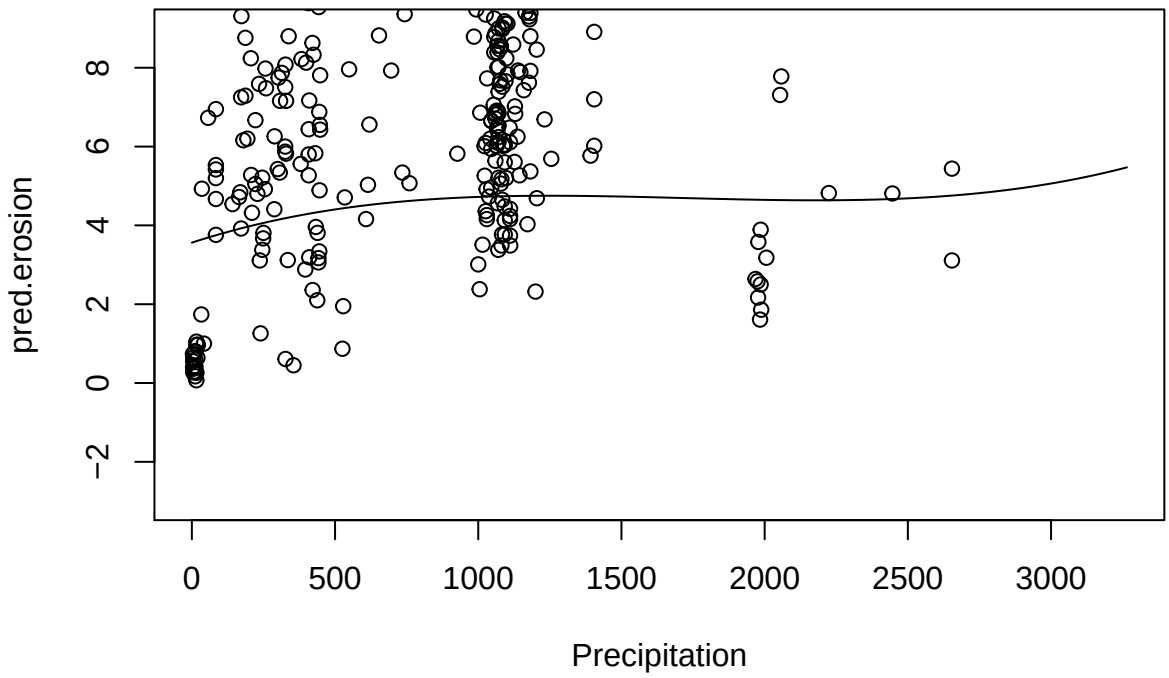

find inflexion points in the predicted sequence (to the nearest 5mm precipitation) (NB could do this more precisely by differentiating the

predictive equation)

NB because all the terms in the fitted model are additive, with no interaction terms, the inflection points will be the same regardless of the values of

the other covariates.

```
for (i in 2:653 )
{
  if (newdata$pred.erosion[i-1] <= newdata$pred.erosion[i]  && newdata$pred.erosion[i+1] <= newdata$pred
    cat("Maximum at ",newdata$Precipitation[i],"\n" )
  if (newdata$pred.erosion[i-1] >= newdata$pred.erosion[i]  && newdata$pred.erosion[i+1] >= newdata$pred
    cat("Minimum at ",newdata$Precipitation[i],"\n" )
}
```

```
## Maximum at  1250
## Minimum at  2180
```

finding inflection point of Precipitation

```
model.prec = lm(log(Erosion) ~  poly(Precipitation, 3),
             data = glob.all.complete)
model.veg = lm(log(Erosion)~  poly(Vegetation, 2),
             data = glob.all.complete)
```

trying New model (Only precip and erosion)

```
newdata$pred.erosion = predict(model.prec, newdata=newdata)
with(newdata, plot(pred.erosion ~ Precipitation, type="l", ylim=c(-3,9)))
with(glob.all.complete, points(Precipitation, Erosion))
```

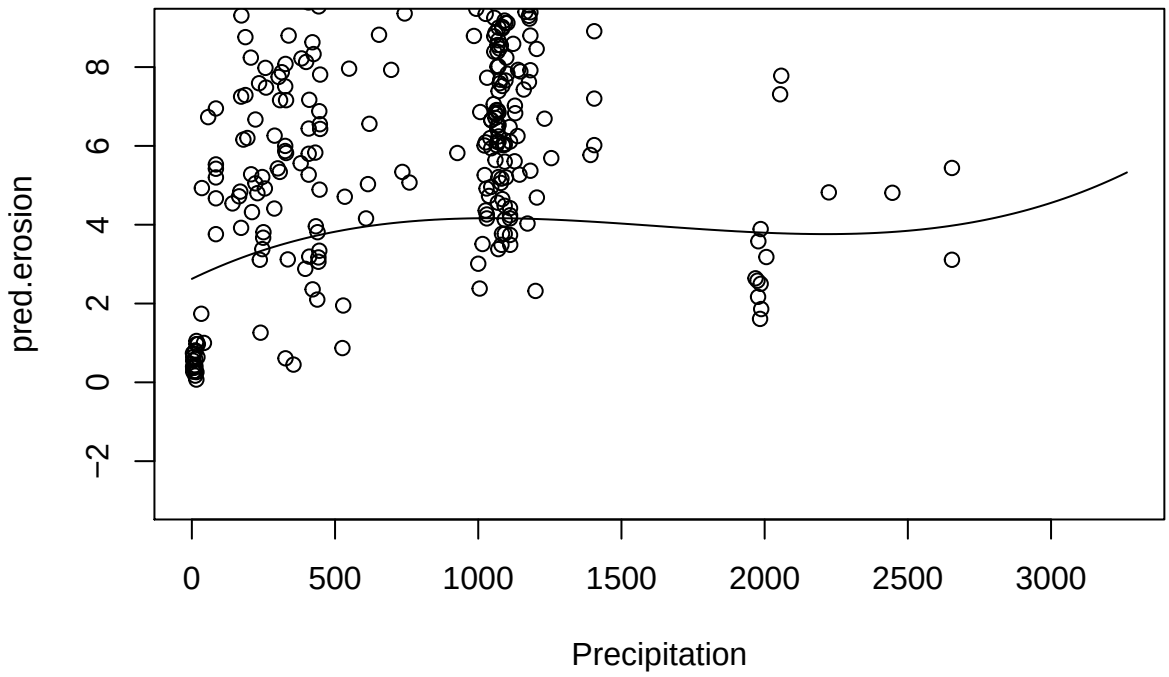

#Inflection point

```
for (i in 2:653 )
{
  if (newdata$pred.erosion[i-1] <= newdata$pred.erosion[i]  && newdata$pred.erosion[i+1] <= newdata$pred
    cat("Maximum at ",newdata$Precipitation[i],"\n" )
  if (newdata$pred.erosion[i-1] >= newdata$pred.erosion[i]  && newdata$pred.erosion[i+1] >= newdata$pred
    cat("Minimum at ",newdata$Precipitation[i],"\n" )
}
```

```
## Maximum at  1045
## Minimum at  2215
```

now for vegetation

```
range(glob.all.complete$Vegetation)
```

```
## [1]   0 100
```

```
Vegetation=seq(0, 100, 5)  # has 654 values
newdata=data.frame(Vegetation)
```

```
newdata$pred.erosion = predict(model.veg, newdata=newdata)
with(newdata, plot(pred.erosion ~ Vegetation, type="l", ylim=c(-3,9)))
with(glob.all.complete, points(Vegetation, Erosion))
```

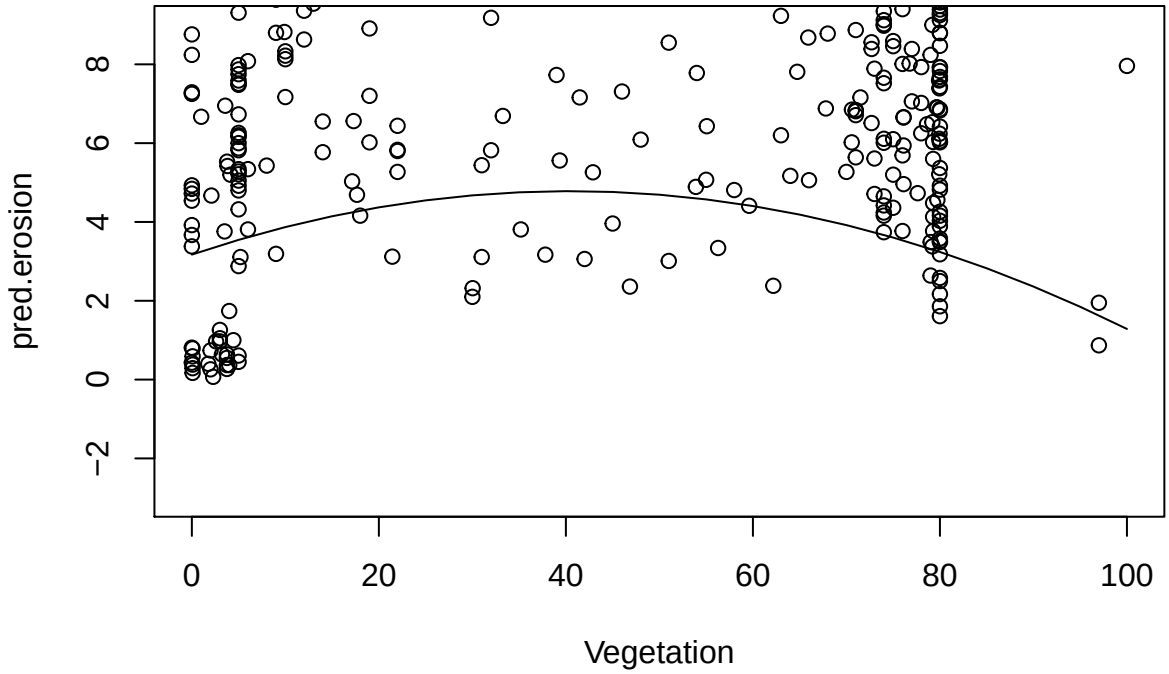


```
for (i in 2:20 )
{
  if (newdata$pred.erosion[i-1] <= newdata$pred.erosion[i]  && newdata$pred.erosion[i+1] <= newdata$pred
    cat("Maximum at ",newdata$Vegetation[i],"\n" )
  if (newdata$pred.erosion[i-1] >= newdata$pred.erosion[i]  && newdata$pred.erosion[i+1] >= newdata$pred
    cat("Minimum at ",newdata$Vegetation[i],"\n" )
}
```

```
## Maximum at  40
```

Now for areas less than 11 degree in slope

```
slopedata<-read.csv(file.choose())
```

erosion rate vs slope at areas <11 degree

```r
regression.A1<-lm(log(Erosion) ~ Slope, data=slopedata)
summary(regression.A1)
```

```
##
## Call:
## lm(formula = log(Erosion) ~ Slope, data = slopedata)
##
## Residuals:
##     Min      1Q  Median      3Q     Max
## -5.1259 -0.6805 -0.0088  0.7860  4.7266
##
## Coefficients:
##             Estimate Std. Error t value Pr(>|t|)
## (Intercept)  2.10900    0.12153  17.354  < 2e-16 ***
## Slope        0.15025    0.01856   8.098 2.48e-15 ***
## ---
## Signif. codes:  0 '***' 0.001 '**' 0.01 '*' 0.05 '.' 0.1 ' ' 1
##
## Residual standard error: 1.242 on 702 degrees of freedom
## Multiple R-squared:  0.08542,    Adjusted R-squared:  0.08412
## F-statistic: 65.57 on 1 and 702 DF,  p-value: 2.48e-15
```

erosion rate vs precipitation at areas <11 degree

```r
regression.A2<-lm(log(Erosion) ~ poly(Precipitation, 3), data=slopedata)
summary (regression.A2)
```

```
##
## Call:
## lm(formula = log(Erosion) ~ poly(Precipitation, 3), data = slopedata)
##
## Residuals:
##     Min      1Q  Median      3Q     Max
## -4.8787 -0.7841  0.0186  0.8131  4.2645
##
## Coefficients:
##                          Estimate Std. Error t value Pr(>|t|)
## (Intercept)               3.01717    0.04691  64.321  < 2e-16 ***
## poly(Precipitation, 3)1  3.35257    1.24462   2.694  0.00724 **
## poly(Precipitation, 3)2  0.25944    1.24462   0.208  0.83494
## poly(Precipitation, 3)3  9.38049    1.24462   7.537 1.49e-13 ***
## ---
## Signif. codes:  0 '***' 0.001 '**' 0.01 '*' 0.05 '.' 0.1 ' ' 1
##
## Residual standard error: 1.245 on 700 degrees of freedom
## Multiple R-squared:  0.08389,    Adjusted R-squared:  0.07997
## F-statistic: 21.37 on 3 and 700 DF,  p-value: 2.982e-13
```

```r
slopedata$Erosion_log<-log(slopedata$Erosion)
regression.A1<-lm(Erosion_log ~ Slope, data=slopedata)
regression.A2<-lm(Erosion_log ~ poly(Precipitation, 3), data=slopedata)
```

```r
summary(regression.A1)
```

```
##
## Call:
```

```
## lm(formula = Erosion_log ~ Slope, data = slopedata)
##
## Residuals:
##     Min      1Q  Median      3Q     Max
## -5.1259 -0.6805 -0.0088  0.7860  4.7266
##
## Coefficients:
##             Estimate Std. Error t value Pr(>|t|)
## (Intercept)  2.10900    0.12153  17.354  < 2e-16 ***
## Slope        0.15025    0.01856   8.098 2.48e-15 ***
## ---
## Signif. codes:  0 '***' 0.001 '**' 0.01 '*' 0.05 '.' 0.1 ' ' 1
##
## Residual standard error: 1.242 on 702 degrees of freedom
## Multiple R-squared:  0.08542,    Adjusted R-squared:  0.08412
## F-statistic: 65.57 on 1 and 702 DF,  p-value: 2.48e-15
```

```
summary(regression.A2)
```

```
##
## Call:
## lm(formula = Erosion_log ~ poly(Precipitation, 3), data = slopedata)
##
## Residuals:
##     Min      1Q  Median      3Q     Max
## -4.8787 -0.7841  0.0186  0.8131  4.2645
##
## Coefficients:
##                          Estimate Std. Error t value Pr(>|t|)
## (Intercept)               3.01717    0.04691  64.321  < 2e-16 ***
## poly(Precipitation, 3)1  3.35257    1.24462   2.694  0.00724 **
## poly(Precipitation, 3)2  0.25944    1.24462   0.208  0.83494
## poly(Precipitation, 3)3  9.38049    1.24462   7.537 1.49e-13 ***
## ---
## Signif. codes:  0 '***' 0.001 '**' 0.01 '*' 0.05 '.' 0.1 ' ' 1
##
## Residual standard error: 1.245 on 700 degrees of freedom
## Multiple R-squared:  0.08389,    Adjusted R-squared:  0.07997
## F-statistic: 21.37 on 3 and 700 DF,  p-value: 2.982e-13
```

Supplementary data for Chapter 2

Study number	Citation	Sample ID	Location	CRONUS SAMPLE ID	Latitude (decimal degrees)	Longitude (decimal degrees)	Mean Basin Elevation (m)
1	Abbuhl et al. (2010)	Piu2	Piura River, Peru	1	-5.162	-80.615	629
1	Abbuhl et al. (2010)	2_16	Piura River, Peru	2	-4.938	-80.344	718
1	Abbuhl et al. (2010)	Piu7	Piura River, Peru	3	-5.115	-80.173	876
1	Abbuhl et al. (2010)	Piu4	Piura River, Peru	4	-5.211	-80.016	1109
1	Abbuhl et al. (2010)	Piu6	Yapatera River Peru	5	-5.104	-80.158	1394
1	Abbuhl et al. (2010)	Piu8	Yapatera River Peru	6	-5.086	-80.132	1438
1	Abbuhl et al. (2010)	Piu9	Yapatera River Peru	7	-5.018	-80.054	1671
1	Abbuhl et al. (2010)	Piu3	Las Gallegas River, Peru	8	-5.138	-79.911	1750
1	Abbuhl et al. (2010)	2_12	Las Gallegas River, Peru	9	-5.114	-79.895	1824
1	Abbuhl et al. (2010)	Piu10	Yapatera River Peru	10	-4.945	-79.996	2080
1	Abbuhl et al. (2010)	2_10	Las Gallegas River, Peru	11	-5.061	-79.875	2005
1	Abbuhl et al. (2010)	2_9	Tributary to Las Gallegas River, Peru	12	-5.06	-79.876	2122
1	Abbuhl et al. (2010)	Piu1	Sechura Desert, Peru	13	-5.999	-80.568	15
1	Abbuhl et al. (2010)	2_8	Las Gallegas River, Peru	14	-5.047	-79.849	2189
1	Abbuhl et al. (2010)	2_6	Las Gallegas River, Peru	15	-5.029	-79.833	2507
1	Abbuhl et al. (2010)	2_2	Tributary to Yapatera River, Peru	16	-5.016	-80.048	1033
1	Abbuhl et al. (2010)	Piu13	Tributary to Yapatera River, Peru	17	-4.93	-79.952	2336
1	Abbuhl et al. (2010)	2_11	Tributary to Las Gallegas River, Peru	18	-5.104	-79.876	1480
1	Abbuhl et al. (2010)	Piu12	Tributary to Yapatera River, Peru	19	-4.926	-79.947	2143
1	Abbuhl et al. (2010)	2_5	Tributary to Las Gallegas River, Peru	20	-5.036	-79.806	2699
1	Abbuhl et al. (2010)	2_13	Tributary to Las Gallegas River, Peru	21	-5.116	-79.894	1114
1	Abbuhl et al. (2010)	2_4	Tributary to Yapatera River, Peru	22	-4.979	-80.014	1329
1	Abbuhl et al. (2010)	Piu11	Yapatera River Peru	23	-4.918	-79.894	3076
1	Abbuhl et al. (2010)	2_3	Tributary to Yapatera River, Peru	24	-4.989	-80.022	1178
1	Abbuhl et al. (2010)	2_1	Tributary to Yapatera River, Peru	25	-5.043	-80.074	463
1	Abbuhl et al. (2010)	2_7	Tributary to Las Gallegas River, Peru	26	-5.035	-79.825	2128
3	Belmont et al. 2007	Lower_EFMC	Clearwater River, WA, USA	27	47.654	-124.24	239
3	Belmont et al. 2007	Lower_WC	Clearwater River, WA, USA	28	47.729	-124.037	563
3	Belmont et al. 2007	Upper_WC	Clearwater River, WA, USA	29	47.739	-124.044	636
4	Bierman and Caffee 2001	NAM-57	Ugab River, Nambia	30	-21.166	13.667	1114
4	Bierman and Caffee 2001	NAM-52	Omaruru River, Nambia	31	-22.086	14.269	1147
4	Bierman and Caffee 2001	NAM-16	Kuiseb Canyon, Nambia	32	-23.303	15.773	1393
4	Bierman and Caffee 2001	NAM-46	Kahn River, Nambia	33	-21.915	15.571	1320
4	Bierman and Caffee 2001	NAM-08	Weissenfels, Nambia	34	-23.318	16.449	1828
4	Bierman and Caffee 2001	NAM-09	Escarpment, Nambia	35	-23.248	16.3	1669
4	Bierman and Caffee 2001	NAM-43	Phillips Cave, Nambia	36	-21.796	15.638	1109
6	Bierman et al 2007	S6s	Namibian Desert & Escarpment	37	-22.682	14.531	1227
5	Bierman et al 2005	RP-1	Rio Puerco, NM, USA	38	34.41	-106.853	2049
5	Bierman et al 2005	RP-2	Rio Puerco, NM, USA	39	34.545	-106.884	2066
5	Bierman et al 2005	RP-4	Rio Puerco, NM, USA	40	34.584	-106.885	2075
5	Bierman et al 2005	RP-5	Rio Puerco, NM, USA	41	34.869	-107.022	2097
6	Bierman et al 2007	S184s	Namibian Desert & Escarpment	42	-22.389	15.835	1442
6	Bierman et al 2007	S216s	Namibian Desert & Escarpment	43	-22.352	16.144	1498
6	Bierman et al 2007	S259s	Namibian Desert & Escarpment	44	-22.263	16.43	1535
6	Bierman et al 2007	O128o	Namibian Desert & Escarpment	45	-21.455	15.075	1280
6	Bierman et al 2007	O149o	Namibian Desert & Escarpment	46	-21.342	15.202	1305
5	Bierman et al 2005	RP-6	Rio Puerco, NM, USA	47	34.887	-107.033	2145

5	Bierman et al 2005	RP-7	Rio Puerco, NM, USA	48	34.892	-107.028	2052
5	Bierman et al 2005	RP-19	Rio Puerco, NM, USA	49	35.034	-106.942	2075
6	Bierman et al 2007	O171o	Namibian Desert & Escarpment	50	-21.348	15.406	1340
6	Bierman et al 2007	Sku	Namibian Desert & Escarpment	51	-22.008	15.588	1289
5	Bierman et al 2005	RP-21	Rio Puerco, NM, USA	52	35.348	-107.043	2128
5	Bierman et al 2005	RP-8A	Rio Puerco, NM, USA	53	35.039	-107.339	2216
5	Bierman et al 2005	RP-10	Rio Puerco, NM, USA	54	35.061	-107.344	2213
5	Bierman et al 2005	RP-22	Rio Puerco, NM, USA	55	35.571	-107.168	2140
6	Bierman et al 2007	O195o	Namibian Desert & Escarpment	56	-21.41	15.639	1421
6	Bierman et al 2007	S333s	Namibian Desert & Escarpment	57	-22.085	16.881	1564
5	Bierman et al 2005	RP-27	Rio Puerco, NM, USA	58	35.593	-107.192	2117
6	Bierman et al 2007	S337s	Namibian Desert & Escarpment	59	-22.038	16.922	1594
5	Bierman et al 2005	RP-29	Rio Puerco, NM, USA	60	35.627	-107.24	2154
9	Bierman et al 2009	QLD5	Queensland Escarpment, Australia	61	-16.852	145.648	593
9	Bierman et al 2009	QLD10	Queensland Escarpment, Australia	62	-16.801	145.617	598
5	Bierman et al 2005	RP-34	Rio Puerco, NM, USA	63	35.655	-107.392	2197
5	Bierman et al 2005	RP-28	Rio Puerco, NM, USA	64	35.642	-107.241	2057
5	Bierman et al (2005)	RP-38	Rio Puerco, NM, USA	65	34.962	-107.221	1990
5	Bierman et al 2005	RP-23	Rio Puerco, NM, USA	66	35.599	-107.18	2212
6	Bierman et al 2007	O269o	Namibian Desert & Escarpment	67	-21.304	16.217	103
6	Bierman et al 2007	S397s	Namibian Desert & Escarpment	68	-21.848	17.295	1681
5	Bierman et al 2005	RP-30	Rio Puerco, NM, USA	69	35.81	-107.255	2089
5	Bierman et al 2005	RP-14B	Rio Puerco, NM, USA	70	35.35	-108.01	2227
5	Bierman et al 2005	RP-14A	Rio Puerco, NM, USA	71	35.355	-108.011	2228
6	Bierman et al 2007	S160t	Namibian Desert & Escarpment	72	-22.519	15.858	1277
6	Bierman et al 2007	S337o	Namibian Desert & Escarpment	73	-22.038	16.921	1477
5	Bierman et al 2005	RP-33	Rio Puerco, NM, USA	74	35.657	-107.392	2061
5	Bierman et al 2005	RP-24	Rio Puerco, NM, USA	75	35.925	-106.986	2313
5	Bierman et al 2005	RP-37	Rio Puerco, NM, USA	76	35.58	-107.521	2139
8	Bierman et al 2001	tc-3	Trephina, Australia	77	-23.567	134.433	725
5	Bierman et al 2005	RP-32	Rio Puerco, NM, USA	78	35.82	-107.271	2087
5	Bierman et al (2005)	RP-3	Rio Puerco, NM, USA	79	34.575	-106.89	1800
5	Bierman et al 2005	RP-35	Rio Puerco, NM, USA	80	35.588	-107.486	2347
5	Bierman et al 2005	RP-41	Rio Puerco, NM, USA	81	35.336	-107.796	2291
6	Bierman et al 2007	S279sn	Namibian Desert & Escarpment	82	-22.154	16.577	1380
8	Bierman et al 2001	tc-2	Trephina, Australia	83	-23.524	134.392	737
8	Bierman et al 2001	tc-1	Trephina, Australia	84	-23.568	134.437	737
6	Bierman et al 2007	O291n	Namibian Desert & Escarpment	85	-21.166	16.348	1584
8	Bierman et al 2001	LUI35	Llano Uplift, TX, USA	86	30.554	-98.701	513
5	Bierman et al 2005	RP-26	Rio Puerco, NM, USA	87	35.956	-106.994	2386
5	Bierman et al 2005	RP-42	Rio Puerco, NM, USA	88	35.434	-108.042	2265
5	Bierman et al 2005	RP-9	Rio Puerco, NM, USA	89	35.093	-107.323	2334
6	Bierman et al 2007	S330o	Namibian Desert & Escarpment	90	-22.238	17.023	1789
5	Bierman et al 2005	RP-20	Rio Puerco, NM, USA	91	35.336	-107.035	2079
5	Bierman et al 2005	RP-31	Rio Puerco, NM, USA	92	35.824	-107.258	2093
9	Bierman et al 2009	QLD9	Queensland Escarpment, Australia	93	-16.824	145.512	535
9	Bierman et al 2009	QLD9a	Queensland Escarpment, Australia	94	-16.824	145.512	535
9	Bierman et al 2009	QLD9b	Queensland Escarpment, Australia	95	-16.824	145.512	535
9	Bierman et al 2009	QLD9c	Queensland Escarpment, Australia	96	-16.824	145.512	535
6	Bierman et al 2007	S393o	Namibian Desert & Escarpment	97	-21.84	17.262	1616

5	Bierman et al 2005	RP-39	Rio Puerco, NM, USA	98	35.34	-107.793	2199
6	Bierman et al 2007	O269ot	Namibian Desert & Escarpment	99	-21.306	16.216	1524
5	Bierman et al 2005	RP-36	Rio Puerco, NM, USA	100	35.577	-107.521	2141
5	Bierman et al 2005	RP-40	Rio Puerco, NM, USA	101	35.338	-107.795	2408
5	Bierman et al (2005)	RP-18	Rio Puerco, NM, USA	102	35.342	-108.214	2462
8	Bierman et al 2001	dc-23	Coast Range, OR, USA	103	44.428	-124.009	333
6	Bierman et al 2007	O149l	Namibian Desert & Escarpment	104	-21.289	15.237	1061
5	Bierman et al 2005	RP-25	Rio Puerco, NM, USA	105	35.95	-107.007	2173
8	Bierman et al 2001	dc-01	Coast Range, OR, USA	106	44.465	-123.967	356
8	Bierman et al 2001	dc-02	Coast Range, OR, USA	107	44.465	-123.967	356
6	Bierman et al 2007	O299s	Namibian Desert & Escarpment	108	-21.173	16.402	1555
9	Bierman et al 2009	QLD8	Queensland Escarpment, Australia	109	-16.899	145.551	592
9	Bierman et al 2009	QLD7	Queensland Escarpment, Australia	110	-16.907	145.561	520
8	Bierman et al 2001	dc-40	Coast Range, OR, USA	111	44.507	-123.859	372
7	Bierman et al 1998	wp-9	Wilpena Pound, Australia	112	-31.545	138.591	695
9	Bierman et al 2009	QLD3	Queensland Escarpment, Australia	113	-16.963	145.677	582
8	Bierman et al 2001	dc-38	Coast Range, OR, USA	114	44.508	-123.854	406
8	Bierman et al 2001	LUI34	Llano Uplift, TX, USA	115	30.497	-98.82	534
8	Bierman et al 2001	dc-31	Coast Range, OR, USA	116	44.509	-123.859	284
8	Bierman et al 2001	dc-30	Coast Range, OR, USA	117	44.524	-123.867	286
8	Bierman et al 2001	dc-37	Coast Range, OR, USA	118	44.514	-123.821	353
9	Bierman et al 2009	QLD6	Queensland Escarpment, Australia	119	-16.873	145.671	450
7	Bierman et al 1998	wp-8	Wilpena Pound, Australia	120	-31.557	138.576	701
9	Bierman et al 2009	QLD2	Queensland Escarpment, Australia	121	-16.822	145.637	405
9	Bierman et al 2009	QLD1	Queensland Escarpment, Australia	122	-16.822	145.637	406
8	Bierman et al 2001	dc-35	Coast Range, OR, USA	123	44.519	-123.818	337
8	Bierman et al 2001	dc-36	Coast Range, OR, USA	124	44.516	-123.818	383
9	Bierman et al 2009	QLD11	Queensland Escarpment, Australia	125	-16.792	145.644	412
8	Bierman et al 2001	dc-29	Coast Range, OR, USA	126	44.537	-123.852	281
9	Bierman et al 2009	QLD13	Queensland Escarpment, Australia	127	-16.833	145.682	318
8	Bierman et al 2001	dc-03	Coast Range, OR, USA	128	44.496	-123.922	334
8	Bierman et al 2001	dc-03a	Coast Range, OR, USA	129	44.496	-123.922	334
8	Bierman et al 2001	dc-03b	Coast Range, OR, USA	130	44.496	-123.922	334
8	Bierman et al 2001	dc-03c	Coast Range, OR, USA	131	44.496	-123.922	334
6	Bierman et al 2007	S259lc	Namibian Desert & Escarpment	132	-22.257	16.437	1088
9	Bierman et al 2009	QLD12	Queensland Escarpment, Australia	133	-16.827	145.654	460
6	Bierman et al 2007	Nlc4	Namibian Desert & Escarpment	134	-23.972	16.277	1584
9	Bierman et al 2009	QLD14	Queensland Escarpment, Australia	135	-16.816	145.682	300
9	Bierman et al 2009	QLD4	Queensland Escarpment, Australia	136	-16.948	145.689	307
6	Bierman et al 2007	Nlc6	Namibian Desert & Escarpment	137	-23.949	16.202	1416
6	Bierman et al 2007	Nlc7	Namibian Desert & Escarpment	138	-23.928	16.163	1607
6	Bierman et al 2007	Ulc1	Namibian Desert & Escarpment	139	-23.728	16.097	1558
6	Bierman et al 2007	Ulc3	Namibian Desert & Escarpment	140	-23.587	16.046	1194
6	Bierman et al 2007	Gaub	Namibian Desert & Escarpment	141	-23.477	16.053	1035
6	Bierman et al 2007	Ulc2	Namibian Desert & Escarpment	142	-23.684	16.183	1802
6	Bierman et al 2007	K2	Namibian Desert & Escarpment	143	-23.804	16.606	1550
7	Bierman et al 1998	wp-3	Wilpena Pound, Australia	144	-31.374	138.553	690
6	Bierman et al 2007	Nlc5	Namibian Desert & Escarpment	145	-23.944	16.302	1527
6	Bierman et al 2007	Nlc3	Namibian Desert & Escarpment	146	-23.952	16.228	1372
6	Bierman et al 2007	K1	Namibian Desert & Escarpment	147	-23.82	16.576	1570

6	Bierman et al 2007	Nsl	Namibian Desert & Escarpment	148	-23.937	16.177	1235
6	Bierman et al 2007	Nsf	Namibian Desert & Escarpment	149	-23.937	16.212	1249
6	Bierman et al 2007	Nnf	Namibian Desert & Escarpment	150	-23.957	16.158	1235
6	Bierman et al 2007	G1	Namibian Desert & Escarpment	151	-23.673	16.698	1599
6	Bierman et al 2007	N0	Namibian Desert & Escarpment	152	-23.972	16.089	1085
8	Bierman et al 2001	LUI33	Llano Uplift, TX, USA	153	30.499	-98.82	485
10	Binnie et al 2006	MHC-15	San Bernardino Mts, CA, USA	154	34.129	-116.989	2018
10	Binnie et al 2006	MHC-14	San Bernardino Mts, CA, USA	155	34.133	-116.988	1743
10	Binnie et al 2008	CLG	San Bernardino Mts, CA, USA	156	34.279	-117.044	1975
10	Binnie et al 2006	MHC-13	San Bernardino Mts, CA, USA	157	34.128	-116.985	2318
10	Binnie et al 2008	CRG	San Bernardino Mts, CA, USA	158	34.278	-117.064	1917
10	Binnie et al 2006	MHC-8	San Bernardino Mts, CA, USA	159	34.129	-116.976	2388
10	Binnie et al 2008	ARC	San Bernardino Mts, CA, USA	160	34.376	-117.092	1744
10	Binnie et al 2006	MHC-10	San Bernardino Mts, CA, USA	161	34.139	-116.99	1749
10	Binnie et al 2006	MHC-2	San Bernardino Mts, CA, USA	162	34.129	-116.961	2547
10	Binnie et al 2006	MHC-2a	San Bernardino Mts, CA, USA	163	34.129	-116.961	2547
10	Binnie et al 2006	MHC-2b	San Bernardino Mts, CA, USA	164	34.129	-116.961	2547
10	Binnie et al 2006	MHC-2c	San Bernardino Mts, CA, USA	165	34.129	-116.961	2547
10	Binnie et al 2008	EFKC	San Bernardino Mts, CA, USA	166	34.166	-117.049	1770
10	Binnie et al 2006	MHC-11	San Bernardino Mts, CA, USA	167	34.139	-116.99	1775
10	Binnie et al 2006	MHC-11a	San Bernardino Mts, CA, USA	168	34.139	-116.99	1775
10	Binnie et al 2006	MHC-11N	San Bernardino Mts, CA, USA	169	34.139	-116.99	1775
10	Binnie et al 2008	MC	San Bernardino Mts, CA, USA	170	34.18	-116.944	2076
10	Binnie et al 2008	BCT	San Bernardino Mts, CA, USA	171	34.208	-117.013	1964
10	Binnie et al 2008	EDC	San Bernardino Mts, CA, USA	172	34.184	-116.981	2076
10	Binnie et al 2008	OGC	San Bernardino Mts, CA, USA	173	34.094	-116.94	2396
10	Binnie et al 2008	WDC	San Bernardino Mts, CA, USA	174	34.184	-116.981	1922
10	Binnie et al 2008	CP	San Bernardino Mts, CA, USA	175	34.279	-117.035	2172
10	Binnie et al 2008	SGC	San Bernardino Mts, CA, USA	176	34.046	-116.934	2143
10	Binnie et al 2006	MHC-12	San Bernardino Mts, CA, USA	177	34.131	-116.991	1711
10	Binnie et al 2008	LLC	San Bernardino Mts, CA, USA	178	34.397	-117.076	1547
10	Binnie et al 2008	TBE	San Bernardino Mts, CA, USA	179	34.195	-116.928	2116
10	Binnie et al 2008	TBW	San Bernardino Mts, CA, USA	180	34.193	-116.932	2138
10	Binnie et al 2008	FC	San Bernardino Mts, CA, USA	181	34.05	-116.946	1894
10	Binnie et al 2008	UC	San Bernardino Mts, CA, USA	182	34.085	-116.969	1925
10	Binnie et al 2008	GCR	San Bernardino Mts, CA, USA	183	34.394	-117.055	1637
10	Binnie et al 2008	GC	San Bernardino Mts, CA, USA	184	34.41	-117.063	1647
10	Binnie et al 2006	MHCW	San Bernardino Mts, CA, USA	185	34.136	-116.961	2215
10	Binnie et al 2008	OC	San Bernardino Mts, CA, USA	186	34.089	-116.941	2115
10	Binnie et al 2008	RSC	San Bernardino Mts, CA, USA	187	34.089	-116.957	1934
10	Binnie et al 2008	TC	San Bernardino Mts, CA, USA	188	34.095	-116.984	1365
11	Brown et al 1998	CAY	Cayaguás, Puerto Rico	189	18.158	-65.959	280
11	Brown et al 1995	ICA	Rio Icacos, Puerto Rico	190	18.275	-65.785	220
11	Brown et al 1998	GUA	Quebrada Guaba, Puerto Rico	191	18.282	-65.787	700
14	Chappell et al 2006	2	Yangtse River, Penzhue, China	192	29.78	116.245	1858
14	Chappell et al 2006	8	Yangtse River, Dongting, China	193	29.779	112.47	2707
14	Chappell et al 2006	11	Yangtse River, Qongching, China	194	29.361	106.423	3429
14	Chappell et al 2006	16	Jinsha River, Yibin, China	195	28.629	104.134	3991
14	Chappell et al 2006	17	Jinsha River, Below Yalong, China	196	26.509	101.87	4231
14	Chappell et al 2006	19	Jinsha River, Panzhihua, China	197	26.596	101.552	4410

14	Chappell et al 2006	19a	Jinsha River, Panzhihua, China	198	26.596	101.552	4410
14	Chappell et al 2006	19b	Jinsha River, Panzhihua, China	199	26.596	101.552	4410
14	Chappell et al 2006	10	Jialing Jiang River, Qongqing, China	200	29.876	106.403	1324
14	Chappell et al 2006	10a	Jialing Jiang River, Qongqing, China	201	29.876	106.403	1324
14	Chappell et al 2006	10b	Jialing Jiang River, Qongqing, China	202	29.876	106.403	1324
14	Chappell et al 2006	4	Han Shui River, Xian Tao, China	203	30.522	112.888	769
14	Chappell et al 2006	18	Yalong River, China	204	26.821	101.788	3955
14	Chappell et al 2006	12	Min Jiang River, Yibin, China	205	28.829	104.395	2867
14	Chappell et al 2006	6	Xiang Jian River, Changsha, China	206	28.357	112.881	335
14	Chappell et al 2006	7	Yuan Jian River, Chande, China	207	29.047	111.552	608
14	Chappell et al 2006	3	Gan Jian River, Nanchang, China	208	28.262	115.846	303
14	Chappell et al 2006	13	Min Jiang River, Leshan, China	209	29.623	103.755	607
14	Chappell et al 2006	14	Qingyi Jiang River, China	210	29.952	103.403	2030
14	Chappell et al 2006	15	Min Jiang River, Dujiangan, China	211	30.377	103.846	717
15	Clapp et al 2000	NY20	Nahal Yael, Israel	212	29.58	34.93	244
15	Clapp et al 2000	NY20A	Nahal Yael, Israel	213	29.58	34.93	244
15	Clapp et al 2000	NY20A	Nahal Yael, Israel	214	29.58	34.93	244
15	Clapp et al 2000	NY20B	Nahal Yael, Israel	215	29.58	34.93	244
15	Clapp et al 2000	NY4	Nahal Yael, Israel	216	29.58	34.93	247
15	Clapp et al 2000	NY19	Nahal Yael, Israel	217	29.58	34.93	257
15	Clapp et al 2000	NY19A	Nahal Yael, Israel	218	29.58	34.93	257
15	Clapp et al 2000	NY19B	Nahal Yael, Israel	219	29.58	34.93	257
15	Clapp et al 2000	NY19C	Nahal Yael, Israel	220	29.58	34.93	257
15	Clapp et al 2000	NY18	Nahal Yael, Israel	221	29.58	34.93	272
15	Clapp et al 2000	NY18A	Nahal Yael, Israel	222	29.58	34.93	272
15	Clapp et al 2000	NY18B	Nahal Yael, Israel	223	29.58	34.93	272
15	Clapp et al 2000	NY18C	Nahal Yael, Israel	224	29.58	34.93	272
15	Clapp et al 2000	NY18C	Nahal Yael, Israel	225	29.58	34.93	272
17	Clapp et al 2002	2	Yuma Wash, AZ, USA	226	33.04	-114.522	281
17	Clapp et al 2002	5A	Yuma Wash, AZ, USA	227	33.089	-114.524	319
17	Clapp et al 2002	17A	Yuma Wash, AZ, USA	228	33.117	-114.505	336
17	Clapp et al 2002	19	Yuma Wash, AZ, USA	229	33.155	-114.516	375
17	Clapp et al 2002	4	Yuma Wash, AZ, USA	230	33.089	-114.531	348
17	Clapp et al 2002	4A	Yuma Wash, AZ, USA	231	33.089	-114.531	348
17	Clapp et al 2002	4B	Yuma Wash, AZ, USA	232	33.089	-114.531	348
17	Clapp et al 2002	21A	Yuma Wash, AZ, USA	233	33.177	-114.517	567
17	Clapp et al 2002	18A	Yuma Wash, AZ, USA	234	33.146	-114.499	307
17	Clapp et al 2002	3A	Yuma Wash, AZ, USA	235	33.098	-114.534	250
17	Clapp et al 2002	28	Yuma Wash, AZ, USA	236	33.207	-114.519	439
17	Clapp et al 2002	27	Yuma Wash, AZ, USA	237	33.169	-114.514	378
16	Clapp et al 2001	ECAC11	Arroyo Chavez, NM, USA	238	35.704	-107.107	1949
17	Clapp et al 2002	16A	Yuma Wash, AZ, USA	239	33.107	-114.524	254
17	Clapp et al 2002	15	Yuma Wash, AZ, USA	240	33.082	-114.535	227
17	Clapp et al 2002	22A	Yuma Wash, AZ, USA	241	33.17	-114.52	305
17	Clapp et al 2002	20A	Yuma Wash, AZ, USA	242	33.163	-114.522	303
17	Clapp et al 2002	14	Yuma Wash, AZ, USA	243	33.086	-114.558	246
16	Clapp et al 2001	ECAC10	Arroyo Chavez, NM, USA	244	35.699	-107.101	1978
17	Clapp et al 2002	13	Yuma Wash, AZ, USA	245	33.077	-114.57	123
17	Clapp et al 2002	11	Yuma Wash, AZ, USA	246	33.076	-114.572	264
16	Clapp et al 2001	ECAC9	Arroyo Chavez, NM, USA	247	35.693	-107.1	1992

17	Clapp et al 2002	12	Yuma Wash, AZ, USA	248	33.076	-114.572	255
16	Clapp et al 2001	ECAC8	Arroyo Chavez, NM, USA	249	35.669	-107.09	2004
19	Cox et al 2009	2005-3C	Amparafaravola, Madagascar	250	-17.55	48.208	867
19	Cox et al 2009	2004-9A	Ikopa watershed, Madagascar	251	-18.95	47.526	1453
19	Cox et al 2009	2004-6A	Onibe watershed, Madagascar	252	-19.005	47.125	1636
19	Cox et al 2009	2004-2A	Miarinarivo, Madagascar	253	-18.945	46.823	1328
19	Cox et al 2009	2005-7	Amparafaravola, Madagascar	254	-17.628	48.204	884
19	Cox et al 2009	2005-6	Amparafaravola, Madagascar	255	-17.565	48.264	855
19	Cox et al 2009	2005-3B	Amparafaravola, Madagascar	256	-17.55	48.208	880
20	Croke, J., et al. (2015)	1	Weany Left Arm, QLD, Australia	258	-19.89343	146.52303	290
20	Croke, J., et al. (2015)	2	Weany Right Arm, QLD, Australia	259	-19.88861	146.52331	291
20	Croke, J., et al. (2015)	3	Weany gauge, QLD, Australia	260	-19.9135	146.4945	282
20	Croke, J., et al. (2015)	4	Weany 2, QLD, Australia	261	-19.91866	146.49595	282
20	Croke, J., et al. (2015)	5	Stockyard Creek, QLD, Australia	262	-19.72106	146.42742	321
20	Croke, J., et al. (2015)	6	Weany 3, QLD, Australia	263	-19.92413	146.48448	280
20	Croke, J., et al. (2015)	7	Upper Fanning East, QLD, Australia	264	-19.64975	146.49481	460
20	Croke, J., et al. (2015)	8	Station Creek gauge, QLD, Australia	265	-19.90147	146.49101	300
20	Croke, J., et al. (2015)	9	Upper Fanning West, QLD, Australia	266	-19.63558	146.45411	476
20	Croke, J., et al. (2015)	10	Fanning River Station, QLD, Australia	267	-19.73394	146.42786	419
20	Croke, J., et al. (2015)	11	Fanning River, QLD, Australia	268	-19.90278	146.48525	382
20	Croke, J., et al. (2015)	12	Middle Fanning, QLD, Australia	269	-19.92411	146.48042	367
20	Croke, J., et al. (2015)	13	Lower Fanning River, QLD, Australia	270	-19.97968	146.44826	353
20	Croke, J., et al. (2015)	14	Upper Macrossan, QLD, Australia	271	-19.98681	146.42861	516
20	Croke, J., et al. (2015)	15	Macrossan Bridge, QLD, Australia	272	-19.99714	146.43553	511
20	Croke, J., et al. (2015)	16	pper Burdekin Falls dam, QLD, Austra	273	-20.26572	146.8625	493
20	Croke, J., et al. (2015)	18	en River (at Strathbowen), QLD, Aust	274	-20.53064	147.55733	350
20	Croke, J., et al. (2015)	19	Upper Suttor River, QLD, Australia	275	-21.53786	147.04741	279
20	Croke, J., et al. (2015)	20	Cape River, QLD, Australia	276	-20.99835	146.42478	345
20	Croke, J., et al. (2015)	21	elyando River Crossing, QLD, Australi	277	-21.53483	146.85979	330
20	Croke, J., et al. (2015)	22	er Suttor River (at St. Ann), QLD, Aust	278	-21.23696	146.92582	313
20	Croke, J., et al. (2015)	17	Lower Burdekin, QLD, Australia	279	-19.8924	147.23031	362
21	Cyr and Granger 2008	8	Montone at Davadola, Italy	280	44	12	585
21	Cyr and Granger 2008	6	Lamone at San Eufemia, Italy	281	44	12	616
21	Cyr and Granger 2008	4	Senio at Casoloa Valsenio, Italy (B)	282	44	12	592
21	Cyr and Granger 2008	3	Senio at Casoloa Valsenio, Italy	283	44	12	592
21	Cyr and Granger 2008	5	Lamone at Biforco, Italy	284	44	12	753
21	Cyr and Granger 2008	7	Montone at San Benetto, Italy	285	44	12	788
21	Cyr and Granger 2008	2	Senio at Palazzuolo, Italy	286	44	12	712
21	Cyr and Granger 2008	1	Visano at Palazzuolo, Italy	287	44	12	724
22	Cyr et al 2010	2	Fiumedinisi at Nizza di Scilia	288	38.003	15.405	667
22	Cyr et al 2010	5	Torno	289	38.005	16.084	433
22	Cyr et al 2010	1	Pagliara at Roccalumera	290	37.967	15.381	594
22	Cyr et al 2010	3	San Elia at Pentedatillo	291	37.943	15.758	564
22	Cyr et al 2010	4	San Pasquale at Palizzi	292	37.948	15.962	545
22	Cyr et al 2010	4a	San Pasquale at Palizzi	293	37.948	15.962	545
22	Cyr et al 2010	4b	San Pasquale at Palizzi	294	37.948	15.962	545
23	Delunel et al 2010	Rd01	Romanche, France	295	45.053	5.844	2079
23	Delunel et al 2010	Mb130	Drac, France	296	44.799	5.959	1765
23	Delunel et al 2010	Rd02	Veneon, France	297	45.015	6.062	2368
23	Delunel et al 2010	Rd09	Bonne, France	298	44.891	5.887	1801

23	Delunel et al 2010	Rd03	Upper Romanche, France	299	45.038	6.192	2402
23	Delunel et al 2010	Mb146	Severaisse, France	300	44.787	6.069	2024
23	Delunel et al 2010	Rd10	Upper Bonne, France	301	44.881	5.985	1996
23	Delunel et al 2010	Rd07	Gyr, France	302	44.87	6.485	2530
23	Delunel et al 2010	Rd08	Roizonne, France	303	44.949	5.868	1738
23	Delunel et al 2010	Rd05	Saint Pierre, France	304	44.893	6.445	2767
23	Delunel et al 2010	Rd06	Celse Niere, France	305	44.881	6.442	2687
23	Delunel et al 2010	Rd04	Tabuc, France	306	44.987	6.481	2491
25	DiBiase et al 2009	SGB1	San Gabriel Mts, CA, USA	307	34.304	-118.156	1402
25	DiBiase et al 2009	SGB12	San Gabriel Mts, CA, USA	308	34.24	-117.761	1801
25	DiBiase et al 2009	SG159	San Gabriel Mts, CA, USA	309	34.294	-117.741	1954
25	DiBiase et al 2009	SGB3	San Gabriel Mts, CA, USA	310	34.31	-118.121	1439
25	DiBiase et al 2009	SGB2	San Gabriel Mts, CA, USA	311	34.304	-118.108	1449
25	DiBiase et al 2009	SGB11	San Gabriel Mts, CA, USA	312	34.295	-117.739	1952
25	DiBiase et al 2009	SG158	San Gabriel Mts, CA, USA	313	34.304	-117.732	1950
25	DiBiase et al 2009	SG137	San Gabriel Mts, CA, USA	314	34.271	-117.889	1526
25	DiBiase et al 2009	SG141	San Gabriel Mts, CA, USA	315	34.252	-117.973	1522
25	DiBiase et al 2009	SGB13	San Gabriel Mts, CA, USA	316	34.295	-117.742	1960
25	DiBiase et al 2009	SG162	San Gabriel Mts, CA, USA	317	34.163	-117.635	1570
25	DiBiase et al 2009	SG157	San Gabriel Mts, CA, USA	318	34.304	-117.73	2019
25	DiBiase et al 2009	SG0743	San Gabriel Mts, CA, USA	319	34.303	-117.981	1726
25	DiBiase et al 2009	SG138	San Gabriel Mts, CA, USA	320	34.27	-117.891	1383
25	DiBiase et al 2009	SGB9	San Gabriel Mts, CA, USA	321	34.301	-118.255	1140
25	DiBiase et al 2009	SG161	San Gabriel Mts, CA, USA	322	34.301	-117.761	1955
25	DiBiase et al 2009	SGB6	San Gabriel Mts, CA, USA	323	34.327	-118.25	1260
25	DiBiase et al 2009	SGB5	San Gabriel Mts, CA, USA	324	34.328	-118.12	1353
25	DiBiase et al 2009	SG0703	San Gabriel Mts, CA, USA	325	34.307	-118.102	1348
25	DiBiase et al 2009	SG0728	San Gabriel Mts, CA, USA	326	34.36	-117.9	2088
25	DiBiase et al 2009	SG207	San Gabriel Mts, CA, USA	327	34.239	-117.806	1006
25	DiBiase et al 2009	SG140	San Gabriel Mts, CA, USA	328	34.241	-117.95	1073
25	DiBiase et al 2009	SGB10	San Gabriel Mts, CA, USA	329	34.28	-118.196	1108
25	DiBiase et al 2009	SG128	San Gabriel Mts, CA, USA	330	34.336	-118.01	1739
25	DiBiase et al 2009	SG0730	San Gabriel Mts, CA, USA	331	33.493	-118.152	1177
25	DiBiase et al 2009	SGB4	San Gabriel Mts, CA, USA	332	34.276	-118.026	1519
25	DiBiase et al 2009	SG206	San Gabriel Mts, CA, USA	333	34.23	-117.791	862
25	DiBiase et al 2009	SG0729	San Gabriel Mts, CA, USA	334	34.358	-117.904	2127
25	DiBiase et al 2009	SG116	San Gabriel Mts, CA, USA	335	34.278	-118.021	1530
25	DiBiase et al 2009	SG151	San Gabriel Mts, CA, USA	336	34.319	-117.799	2282
25	DiBiase et al 2009	SG163	San Gabriel Mts, CA, USA	337	34.163	-117.365	553
25	DiBiase et al 2009	SG123	San Gabriel Mts, CA, USA	338	34.35	-118.049	1732
25	DiBiase et al 2009	SGB7	San Gabriel Mts, CA, USA	339	34.296	-118.148	1318
25	DiBiase et al 2009	SG152	San Gabriel Mts, CA, USA	340	34.321	-117.801	2317
25	DiBiase et al 2009	SG127	San Gabriel Mts, CA, USA	341	34.217	-118.085	1347
25	DiBiase et al 2009	SG126	San Gabriel Mts, CA, USA	342	34.217	-118.083	1359
25	DiBiase et al 2009	SG131	San Gabriel Mts, CA, USA	343	34.364	-117.992	1739
25	DiBiase et al 2009	SG0740	San Gabriel Mts, CA, USA	344	34.32	-117.966	1912
25	DiBiase et al 2009	SG125	San Gabriel Mts, CA, USA	345	34.21	-118.08	1333
25	DiBiase et al 2009	SG124	San Gabriel Mts, CA, USA	346	34.337	-118.048	1543
25	DiBiase et al 2009	SG132	San Gabriel Mts, CA, USA	347	34.364	-117.99	1730
25	DiBiase et al 2009	SG150	San Gabriel Mts, CA, USA	348	34.281	-118.027	1511

25	DiBiase et al 2009	SG130	San Gabriel Mts, CA, USA	349	34.379	-117.99	1720
25	DiBiase et al 2009	SG129	San Gabriel Mts, CA, USA	350	34.339	-118.011	1761
25	DiBiase et al 2009	SG0702	San Gabriel Mts, CA, USA	351	34.38	-118.028	2072
25	DiBiase et al 2009	SG118	San Gabriel Mts, CA, USA	352	34.276	-118.026	1472
25	DiBiase et al 2009	SG0701	San Gabriel Mts, CA, USA	353	34.363	-117.992	1680
25	DiBiase et al 2009	SG136	San Gabriel Mts, CA, USA	354	34.327	-117.788	2259
25	DiBiase et al 2009	SG205	San Gabriel Mts, CA, USA	355	34.36	-117.991	1693
25	DiBiase et al 2009	SG204	San Gabriel Mts, CA, USA	356	34.359	-117.991	1704
27	Duxbury 2008	SH-56	Stanley, VA, USA	357	38.532	-78.603	529
27	Duxbury 2008	SH-01	Old Rag Mountain, VA, USA	358	38.571	-78.287	703
27	Duxbury 2008	SH-01A	Old Rag Mountain, VA, USA	359	38.571	-78.287	703
27	Duxbury 2008	SH-01B	Old Rag Mountain, VA, USA	360	38.571	-78.287	703
27	Duxbury 2008	SH-01C	Old Rag Mountain, VA, USA	361	38.571	-78.287	703
27	Duxbury 2008	SH-01D	Old Rag Mountain, VA, USA	362	38.571	-78.287	703
27	Duxbury 2008	SH-25	Browns Cove, VA, USA	363	38.148	-78.749	709
27	Duxbury 2008	SH-11	Washington, VA, USA	364	38.653	-78.245	558
27	Duxbury 2008	SH-52	Chester Gap, VA, USA	365	38.811	-78.234	572
27	Duxbury 2008	SH-23	Big Meadows, VA, USA	366	38.869	-78.178	494
27	Duxbury 2008	SH-48	Washington, VA, USA	367	38.838	-78.106	397
27	Duxbury 2008	SH-38	Grottoes, VA, USA	368	38.257	-78.769	643
27	Duxbury 2008	SH-12	Old Rag Mountain, VA, USA	369	38.615	-78.257	693
27	Duxbury 2008	SH-10	Thornton Gap, VA, USA	370	38.657	-78.282	651
27	Duxbury 2008	SH-16	Old Rag Mountain, VA, USA	371	38.542	-78.352	875
27	Duxbury 2008	SH-04	Crimora, VA, USA	372	38.199	-78.794	651
27	Duxbury 2008	SH-04A	Crimora, VA, USA	373	38.199	-78.794	651
27	Duxbury 2008	SH-04B	Crimora, VA, USA	374	38.199	-78.794	651
27	Duxbury 2008	SH-04C	Crimora, VA, USA	375	38.199	-78.794	651
27	Duxbury 2008	SH-04D	Crimora, VA, USA	376	38.199	-78.794	651
27	Duxbury 2008	SH-47	Washington, VA, USA	377	38.647	-78.209	301
27	Duxbury 2008	SH-19	Fletcher, VA, USA	378	38.471	-78.498	828
27	Duxbury 2008	SH-49	Front Royal, VA, USA	379	38.927	-78.176	277
27	Duxbury 2008	SH-03	McGaheysville, VA, USA	380	38.362	-78.654	498
27	Duxbury 2008	SH-03A	McGaheysville, VA, USA	381	38.362	-78.654	498
27	Duxbury 2008	SH-03B	McGaheysville, VA, USA	382	38.362	-78.654	498
27	Duxbury 2008	SH-03C	McGaheysville, VA, USA	383	38.362	-78.654	498
27	Duxbury 2008	SH-03D	McGaheysville, VA, USA	384	38.362	-78.654	498
27	Duxbury 2008	SH-17	Bentonville, VA, USA	385	38.78	-78.366	480
27	Duxbury 2008	SH-31	Crimora, VA, USA	386	38.16	-78.803	726
27	Duxbury 2008	SH-07	Big Meadows, VA, USA	387	38.582	-78.414	847
27	Duxbury 2008	SH-15	Old Rag Mountain, VA, USA	388	38.521	-78.29	430
27	Duxbury 2008	SH-28	Waynesboro East, VA, USA	389	38.099	-78.804	632
27	Duxbury 2008	SH-21	Thornton Gap, VA, USA	390	38.645	-78.369	699
27	Duxbury 2008	SH-08	Luray, VA, USA	391	38.634	-78.392	717
27	Duxbury 2008	SH-51	Chester Gap, VA, USA	392	38.796	-78.239	557
27	Duxbury 2008	SH-45	Old Rag Mountain, VA, USA	393	38.523	-78.265	259
27	Duxbury 2008	SH-24	Big Meadows, VA, USA	394	38.166	-78.745	726
27	Duxbury 2008	SH-27	Waynesboro East, VA, USA	395	38.1	-78.804	658
27	Duxbury 2008	SH-40	Browns Cove, VA, USA	396	38.239	-78.691	808
27	Duxbury 2008	SH-39	Crimora, VA, USA	397	38.222	-78.781	751
27	Duxbury 2008	SH-18*	Thornton Gap, VA, USA	398	38.664	-78.356	617

27	Duxbury 2008	SH-02	Thornton Gap, VA, USA	399	38.664	-78.356	618
27	Duxbury 2008	SH-02A	Thornton Gap, VA, USA	400	38.664	-78.356	618
27	Duxbury 2008	SH-02B	Thornton Gap, VA, USA	401	38.664	-78.356	618
27	Duxbury 2008	SH-02C	Thornton Gap, VA, USA	402	38.664	-78.356	618
27	Duxbury 2008	SH-02D	Thornton Gap, VA, USA	403	38.664	-78.356	618
27	Duxbury 2008	SH-22	Big Meadows, VA, USA	404	38.61	-78.418	517
27	Duxbury 2008	SH-26	Swift Run, VA, USA	405	38.293	-78.621	795
27	Duxbury 2008	SH-43	Swift Run, VA, USA	406	38.363	-78.574	639
27	Duxbury 2008	SH-13	Old Rag Mountain, VA, USA	407	38.543	-78.273	518
27	Duxbury 2008	SH-54	McGaheysville, VA, USA	408	38.29	-78.724	679
27	Duxbury 2008	SH-20	McGaheysville, VA, USA	409	38.357	-78.662	572
27	Duxbury 2008	SH-37	McGaheysville, VA, USA	410	38.252	-78.747	610
27	Duxbury 2008	SH-46	Washington, VA, USA	411	38.642	-78.246	442
27	Duxbury 2008	SH-05	Bentonville, VA, USA	412	38+D377	-75.888	899
27	Duxbury 2008	SH-06	Luray, VA, USA	413	38.676	-78.383	448
27	Duxbury 2008	SH-44	Stannardsville, VA, USA	414	38.341	-78.457	268
27	Duxbury 2008	SH-33	McGaheysville, VA, USA	415	38.311	-78.726	468
27	Duxbury 2008	SH-32	McGaheysville, VA, USA	416	38.31	-78.727	474
27	Duxbury 2008	SH-14	Old Rag Mountain, VA, USA	417	38.527	-78.279	281
27	Duxbury 2008	SH-30	Crimora, VA, USA	418	38.178	-78.789	767
27	Duxbury 2008	SH-42	Crimora, VA, USA	419	38.16	-78.785	791
27	Duxbury 2008	SH-34	Crimora, VA, USA	420	38.173	-78.809	628
27	Duxbury 2008	SH-50	Chester Gap, VA, USA	421	38.819	-78.208	520
27	Duxbury 2008	SH-36	Crimora, VA, USA	422	38.178	-78.806	648
27	Duxbury 2008	SH-41**	Crimora, VA, USA	423	38.178	-78.806	646
27	Duxbury 2008	SH-09	Thornton Gap, VA, USA	424	38.697	-78.322	778
27	Duxbury 2008	SH-35	Crimora, VA, USA	425	38.176	-78.807	541
27	Duxbury 2008	SH-29	Waynesboro East, VA, USA	426	38.109	-78.828	479
29	Ferrier et al 2005	ORK	ood Creek at Orick, Coast Range, CA	427	41.289	-124.06	575
29	Ferrier et al 2005	COY	Coyote Creek, Coast Range, CA, USA	428	41.117	-123.913	607
29	Ferrier et al 2005	PAN	Panther Creek, Coast Range, CA, USA	429	41.088	-123.908	504
29	Ferrier et al 2005	LLM	e Lost Man Creek, Coast Range, CA,	430	41.322	-124.02	457
29	Ferrier et al 2005	NFC	Fork, Caspar Creek, Coast Range, CA	431	39.361	-123.736	224
29	Ferrier et al 2005	SFC	Fork, Caspar Creek, Coast Range, CA	432	39.343	-123.754	187
29	Ferrier et al 2005	E	Eagle Creek, Coast Range, CA, USA	433	39.364	-123.718	257
29	Ferrier et al 2005	C	Carlson Creek, Coast Range, CA, USA	434	39.366	-123.73	235
29	Ferrier et al 2005	I	Iverson Creek, Coast Range, CA, USA	435	39.373	-123.718	262
29	Ferrier et al 2005	H	enningson Creek, Coast Range, CA, U	436	39.373	-123.721	246
30	Finnegan et al 2008	MEDOC	amche Barwa-Gyala Peri Massif, Tibe	437	29.326	95.312	4800
30	Finnegan et al 2008	NB-8-04	amche Barwa-Gyala Peri Massif, Tibe	438	29.604	94.937	4866
30	Finnegan et al 2008	NB-7-04	amche Barwa-Gyala Peri Massif, Tibe	439	29.71	94.328	4673
30	Finnegan et al 2008	NB-4-04	amche Barwa-Gyala Peri Massif, Tibe	440	30.097	95.065	4753
30	Finnegan et al 2008	NB-3-04	amche Barwa-Gyala Peri Massif, Tibe	441	30.096	95.066	4525
30	Finnegan et al 2008	NB-6-04	amche Barwa-Gyala Peri Massif, Tibe	442	29.948	94.801	4347
30	Finnegan et al 2008	NB-5-04	amche Barwa-Gyala Peri Massif, Tibe	443	29.945	94.804	4162
30	Finnegan et al 2008	NB-23-02	amche Barwa-Gyala Peri Massif, Tibe	444	30.102	95.111	4008
30	Finnegan et al 2008	NB-13-02	amche Barwa-Gyala Peri Massif, Tibe	445	29.909	95.514	3082
30	Finnegan et al 2008	NB-5-02	amche Barwa-Gyala Peri Massif, Tibe	446	30.066	95.18	3918
30	Finnegan et al 2008	NB-7-02	amche Barwa-Gyala Peri Massif, Tibe	447	30.045	95.263	3867
30	Finnegan et al 2008	NB-14-02	amche Barwa-Gyala Peri Massif, Tibe	448	29.947	95.411	4126

30	Finnegan et al 2008	P-6-02	amche Barwa-Gyala Peri Massif, Tibe	449	29.95	95.383	4295
31	Glotzbach et al.,(2014)	MR1 +	Black Forest in southwestern German	450	47.9037	8.014	1148
31	Glotzbach et al.,(2014)	MR2 +	Black Forest in southwestern German	451	47.9041	8.0133	1182
31	Glotzbach et al.,(2014)	MR3 +	Black Forest in southwestern German	452	47.9079	8.0046	1114
31	Glotzbach et al.,(2014)	MR4 +	Black Forest in southwestern German	453	47.9122	7.9996	1010
31	Glotzbach et al.,(2014)	MR5 +	Black Forest in southwestern German	454	47.9114	7.997	1099
31	Glotzbach et al.,(2014)	MR6 +	Black Forest in southwestern German	455	47.9186	7.9899	1027
31	Glotzbach et al.,(2014)	MR8 +	Black Forest in southwestern German	456	47.8827	7.9829	1248
31	Glotzbach et al.,(2014)	MR9 +	Black Forest in southwestern German	457	47.8838	7.9817	1241
31	Glotzbach et al.,(2014)	MR10 +	Black Forest in southwestern German	458	47.887	7.971	1180
31	Glotzbach et al.,(2014)	MR13 +	Black Forest in southwestern German	459	47.8982	7.9233	1090
31	Glotzbach et al.,(2014)	MR15 +	Black Forest in southwestern German	460	47.9089	7.9315	1011
31	Glotzbach et al.,(2014)	MR16 +	Black Forest in southwestern German	461	47.9244	7.9384	960
31	Glotzbach et al.,(2014)	MR18 +	Black Forest in southwestern German	462	47.9257	7.9396	1038
31	Glotzbach et al.,(2014)	MR20 +	Black Forest in southwestern German	463	47.9285	8.0991	1032
31	Glotzbach et al.,(2014)	MR21 +	Black Forest in southwestern German	464	47.9434	8.0045	955
32	Godard et al 2010	LM254	ongmen Shan, Eastern Tibetan Platea	465	31.059	103.488	3491
32	Godard et al 2010	SC086	ongmen Shan, Eastern Tibetan Platea	466	31.059	103.488	3491
32	Godard et al 2010	LM263	ongmen Shan, Eastern Tibetan Platea	467	31.284	103.467	3526
32	Godard et al 2010	LM261	ongmen Shan, Eastern Tibetan Platea	468	31.494	103.62	3523
32	Godard et al 2010	SC049	ongmen Shan, Eastern Tibetan Platea	469	31.704	103.853	3560
32	Godard et al 2010	LM259	ongmen Shan, Eastern Tibetan Platea	470	31.488	103.58	3622
32	Godard et al 2010	LM253	ongmen Shan, Eastern Tibetan Platea	471	31.057	103.485	3545
32	Godard et al 2010	SC082	ongmen Shan, Eastern Tibetan Platea	472	31.057	103.485	3545
32	Godard et al 2010	SC004	ongmen Shan, Eastern Tibetan Platea	473	30.761	103.469	1850
32	Godard et al 2010	SC016	ongmen Shan, Eastern Tibetan Platea	474	31.237	103.792	2637
32	Godard et al 2010	SC071	ongmen Shan, Eastern Tibetan Platea	475	31.516	104.113	2333
32	Godard et al 2010	SC031	ongmen Shan, Eastern Tibetan Platea	476	31.46	104.001	3042
32	Godard et al 2010	SC033	ongmen Shan, Eastern Tibetan Platea	477	31.318	103.996	1419
32	Godard et al 2010	SC059	ongmen Shan, Eastern Tibetan Platea	478	31.066	103.493	1520
33	Granger et al 1996	B-5	ond mountains batholiths, california	479	40.095	-120.065	1365
33	Granger et al 1996	B-5(a)	ond mountains batholiths, california	480	40.095	-120.065	1365
33	Granger et al 1996	B-5(b)	ond mountains batholiths, california	481	40.095	-120.065	1365
33	Granger et al 1996	B-5(c)	ond mountains batholiths, california	482	40.095	-120.065	1365
33	Granger et al 1996	B-5(d)	ond mountains batholiths, california	483	40.095	-120.065	1365
33	Granger et al 1996	A-4	ond mountains batholiths, california	484	40.094	-120.06	1383
33	Granger et al 1996	A-4(a)	ond mountains batholiths, california	485	40.094	-120.06	1383
33	Granger et al 1996	A-4(b)	ond mountains batholiths, california	486	40.094	-120.06	1383
33	Granger et al 1996	A-4(d)	ond mountains batholiths, california	487	40.094	-120.06	1383
33	Granger et al 1996	A-3	ond mountains batholiths, california	488	40.094	-120.06	1387
33	Granger et al 1996	B-3	ond mountains batholiths, california	489	40.095	-120.065	1487
33	Granger et al 1996	A-2	ond mountains batholiths, california	490	40.094	-120.06	1508
33	Granger et al 1996	B-2	ond mountains batholiths, california	491	40.095	-120.065	1533
33	Granger et al 1996	B-2(a)	ond mountains batholiths, california	492	40.095	-120.065	1533
33	Granger et al 1996	B-2(b)	ond mountains batholiths, california	493	40.095	-120.065	1533
33	Granger et al 1996	B-2(c)	ond mountains batholiths, california	494	40.095	-120.065	1533
33	Granger et al 1996	B-4	ond mountains batholiths, california	495	40.095	-120.065	1320
33	Granger et al 1996	A-1	ond mountains batholiths, california	496	40.094	-120.06	1554
33	Granger et al 1996	B-1	ond mountains batholiths, california	497	40.095	-120.065	1562
34	Guralnik et al 2010	N1-SD	Neqarot Gorge, Negev Desert, Israel	498	30.662	35.107	512

34	Guralnik et al 2010	N4-NR-SD	Neqarot Gorge, Negev Desert, Israel	499	30.591	34.943	604
34	Guralnik et al 2010	N4-R-SD	Neqarot Gorge, Negev Desert, Israel	500	30.6	34.937	594
34	Guralnik et al 2010	N4-N-SC	Neqarot Gorge, Negev Desert, Israel	501	30.487	34.938	555
35	Harkins et al 2010	KH-KCB-05-3	yemaqen Shan, Eastern Tibetan Plate	502	34.526	100.394	4167
35	Harkins et al 2010	NH-KCB-05-2	yemaqen Shan, Eastern Tibetan Plate	503	34.752	99.693	4295
35	Harkins et al 2010	NH-KCB-05-6	yemaqen Shan, Eastern Tibetan Plate	504	33.693	101.388	3929
35	Harkins et al 2010	NH-KE-04-2	yemaqen Shan, Eastern Tibetan Plate	505	34.1	100.761	3865
35	Harkins et al 2010	NH-KCB-05-1	yemaqen Shan, Eastern Tibetan Plate	506	34.777	100.813	3760
35	Harkins et al 2010	NH-KE-04-3	yemaqen Shan, Eastern Tibetan Plate	507	34.898	100.885	3951
35	Harkins et al 2010	NH-KE-04-4	yemaqen Shan, Eastern Tibetan Plate	508	34.798	100.811	3704
35	Harkins et al 2010	NH-KE-04-4A	yemaqen Shan, Eastern Tibetan Plate	509	34.798	100.811	3704
35	Harkins et al 2010	NH-KE-04-4B	yemaqen Shan, Eastern Tibetan Plate	510	34.798	100.811	3704
39	Heimsath et al 2009	TC-22/23	Tin Can Creek, NW Australia	511	-12.453	133.27	216
39	Heimsath et al 2009	TC-22	Tin Can Creek, NW Australia	512	-12.453	133.27	216
39	Heimsath et al 2009	TC-23	Tin Can Creek, NW Australia	513	-12.453	133.27	216
40	Heimsath et al 2010	MD-110	Mt. Sonder, Central Australia	514	-23.591	132.536	821
37	Heimsath et al 2001	FH-19	Bredbo River, Australia	515	-36	149.5	1121
38	Heimsath et al 2006	NR-58	Nunnock River Basin, SE Australia	516	-36.667	150	919
38	Heimsath et al 2006	NR-60	Nunnock River Basin, SE Australia	517	-36.667	150	919
38	Heimsath et al 2006	NR-61	Nunnock River Basin, SE Australia	518	-36.667	150	919
38	Heimsath et al 2006	NR-62	Nunnock River Basin, SE Australia	519	-36.667	150	919
38	Heimsath et al 2006	NR-65	Nunnock River Basin, SE Australia	520	-36.667	150	974
39	Heimsath et al 2009	TC-21	Tin Can Creek, NW Australia	521	-12.455	133.288	119
39	Heimsath et al 2009	TC-20	Tin Can Creek, NW Australia	522	-12.459	133.289	121
40	Heimsath et al 2010	MD-119	Tyler Pass, Central Australia	523	-23.699	132.355	792
40	Heimsath et al 2010	MD-119	Tyler Pass, Central Australia	524	-23.699	132.355	792
40	Heimsath et al 2010	MD-119	Tyler Pass, Central Australia	525	-23.699	132.355	792
38	Heimsath et al 2006	NR-32	Nunnock River Basin, SE Australia	526	-36.667	150	1005
38	Heimsath et al 2006	NR-33	Nunnock River Basin, SE Australia	527	-36.667	150	1005
38	Heimsath et al 2006	NR-38	Nunnock River Basin, SE Australia	528	-36.667	150	1018
37	Heimsath et al 2001	OR-16	Coast Range, OR, USA	529	43.469	-124.113	296
39	Heimsath et al 2009	TC-17	Tin Can Creek, NW Australia	530	-12.469	133.297	133
40	Heimsath et al 2010	MD-111	Tyler Pass, Central Australia	531	-23.661	132.364	812
40	Heimsath et al 2010	MD-108	Mt. Sonder, Central Australia	532	-23.592	132.57	1039
40	Heimsath et al 2010	MD-109	Mt. Sonder, Central Australia	533	-23.59	132.561	945
39	Heimsath et al 2009	TC-8	Tin Can Creek, NW Australia	534	-12.466	133.3	118
39	Heimsath et al 2009	TC-6	Tin Can Creek, NW Australia	535	-12.463	133.305	134
39	Heimsath et al 2009	TC-7	Tin Can Creek, NW Australia	536	-12.467	133.301	128
39	Heimsath et al 2009	TC-18	Tin Can Creek, NW Australia	537	-12.477	133.296	142
36	Heimsath et al 1999	creek2	nnessee Valley, Marin County, CA, U	538	37.85	-122.55	238
36	Heimsath et al 1999	creek1	nnessee Valley, Marin County, CA, U	539	37.85	-122.55	220
36	Heimsath et al 1999	creek1a	nnessee Valley, Marin County, CA, U	540	37.85	-122.55	220
36	Heimsath et al 1999	creek1b	nnessee Valley, Marin County, CA, U	541	37.85	-122.55	220
37	Heimsath et al 2001	FH-20	Bredbo River, Australia	542	-36	149.5	937
41	Henck et al 2011	05-3R-1b-YANG	Yangtze River, China	543	26.87	99.97	4556
41	Henck et al 2011	05-3R-3-YANG	Yangtze River, China	544	28.22	99.32	4608
41	Henck et al 2011	06-3R-41-YANG	Yangtze River, China	545	29.76	99	4675
41	Henck et al 2011	06-3R-17-YANG	Yangtze River, China	546	31.63	98.59	4743
41	Henck et al 2011	06-3R-17-YANGa	Yangtze River, China	547	31.63	98.59	4743
41	Henck et al 2011	06-3R-17-YANG	Yangtze River, China	548	31.63	98.59	4743

41	Henck et al 2011	05-3R-13b-SAL	Salween River, China	549	25.85	98.86	4538
41	Henck et al 2011	06-3R-26-MEK	branch of Mekong River at Chambo,	550	25.85	98.86	4538
41	Henck et al 2011	06-3R-26-MEK	branch of Mekong River at Chambo,	551	25.85	98.86	4538
41	Henck et al 2011	06-3R-26-MEK	branch of Mekong River at Chambo,	552	25.85	98.86	4538
41	Henck et al 2011	06-3R-27-MEK	branch of Mekong River at Chambo,	553	25.85	98.86	4538
41	Henck et al 2011	06-3R-27-MEK	branch of Mekong River at Chambo,	554	25.85	98.86	4538
41	Henck et al 2011	06-3R-27-MEK	branch of Mekong River at Chambo,	555	25.85	98.86	4538
41	Henck et al 2011	05-3R-12-SAL	Salween River, China	556	27.23	98.89	4574
41	Henck et al 2011	05-3R-11b-SAL	Salween River, China	557	27.23	98.89	4608
41	Henck et al 2011	05-3R-11b-SAL	Salween River, China	558	27.23	98.89	4608
41	Henck et al 2011	05-3R-11b-SAL	Salween River, China	559	27.23	98.89	4608
41	Henck et al 2011	05-3R-10-SAL	Salween River, China	560	27.58	98.79	4624
41	Henck et al 2011	05-3R-9-SAL	Salween River, China	561	28.02	98.63	4649
41	Henck et al 2011	05-3R-14a-MEK	Mekong River, China	562	25.43	99.29	4262
41	Henck et al 2011	06-3R-48-SAL	Salween River, China	563	30.1	97.21	4749
41	Henck et al 2011	05-3R-8-MEK	Mekong River, China	564	27.35	99.09	4443
41	Henck et al 2011	05-3R-7-MEK	Mekong River, China	565	27.57	99.04	4455
41	Henck et al 2011	05-3R-6-MEK	Mekong River, China	566	28.1	98.92	4477
41	Henck et al 2011	06-3R-38-MEK	Mekong River, China	567	29.62	98.35	4513
41	Henck et al 2011	06-3R-28-MEK	Mekong River, China	568	30.85	97.34	4541
41	Henck et al 2011	06-3R-29-MEK	Tributary to Mekong River, China	569	30.77	97.34	4621
41	Henck et al 2011	06-3R-32-SAL	butary to Salween River tributary, Ch	570	30.2	97.32	4739
41	Henck et al 2011	06-3R-49-SAL	Tributary to Salween River, China	571	30.11	97.19	4516
41	Henck et al 2011	06-3R-42-YANG	Tributary to Yangtze River, China	572	29.76	99.01	4211
41	Henck et al 2011	06-3R-36-SAL	butary to Salween River tributary, Ch	573	29.67	97.85	4590
41	Henck et al 2011	06-3R-30-SAL	butary to Salween River tributary, Ch	574	30.6	97.07	4754
41	Henck et al 2011	06-3R-20-YANG	Tributary to Yangtze River, China	575	31.59	98.37	4702
41	Henck et al 2011	06-3R-19a-YANG	Tributary to Yangtze River, China	576	31.65	98.37	4710
41	Henck et al 2011	06-3R-21-YANG	Tributary to Yangtze River, China	577	31.4	98.16	4526
41	Henck et al 2011	06-3R-34-SAL	butary to Salween River tributary, Ch	578	29.74	97.76	4612
41	Henck et al 2011	06-3R-16-YANG	Tributary to Yangtze River, China	579	31.64	98.59	4897
41	Henck et al 2011	06-3R-15-YANG	Tributary to Yangtze River, China	580	31.76	98.56	4910
41	Henck et al 2011	06-3R-19b-YANG	Tributary to Yangtze River, China	581	31.65	98.37	4684
41	Henck et al 2011	06-3R-53-SAL	Tributary to Salween River, China	582	29.78	96.71	4833
41	Henck et al 2011	05-3R-4-MEK	Tributary to Mekong River, China	583	28.56	98.81	4122
41	Henck et al 2011	06-3R-24-YANG	Tributary to Yangtze River, China	584	31.4	97.88	4574
41	Henck et al 2011	06-3R-22-YANG	Tributary to Yangtze River, China	585	31.3	98	1316
41	Henck et al 2011	06-3R-52-SAL	Tributary to Salween River, China	586	29.78	96.71	4889
41	Henck et al 2011	06-3R-43-MEK	Tributary to Mekong River, China	587	29.55	98.21	4885
41	Henck et al 2011	06-3R-50-SAL	Tributary to Salween River, China	588	30.04	97.15	3924
41	Henck et al 2011	06-3R-33-SAL	butary to Salween River tributary, Ch	589	29.85	97.69	4740
41	Henck et al 2011	06-3R-39-MEK	Tributary to Mekong River, China	590	29.66	98.37	4044
41	Henck et al 2011	06-3R-18-YANG	Tributary to Yangtze River, China	591	31.62	98.6	5057
41	Henck et al 2011	06-3R-35-SAL	butary to Salween River tributary, Ch	592	29.68	97.83	4667
41	Henck et al 2011	06-3R-46-SAL	Tributary to Salween River, China	593	30.1	97.3	4283
41	Henck et al 2011	05-3R-11a-SAL	butary to Salween River tributary, Ch	594	27.23	98.89	2061
42	Hewawasam et al 2003	M-MIN	Minipe, Sri Lanka	595	7.211	80.981	1033
42	Hewawasam et al 2003	M-VIC	Victoria, Sri Lanka	596	7.239	80.787	1016
42	Hewawasam et al 2003	M-HAG	Haragama, Sri Lanka	597	7.269	80.703	1068
42	Hewawasam et al 2003	M-PER	Peradeniya, Sri Lanka	598	7.261	80.595	1223

42	Hewawasam et al 2003	UO-1	Uma oya, Sri Lank	599	7.198	80.943	1219
42	Hewawasam et al 2003	BO-1	Belihul oya, Sri Lanka	600	7.144	80.836	1354
42	Hewawasam et al 2003	HUG-1	Huluganga, Sri Lanka	601	7.312	80.748	1005
42	Hewawasam et al 2003	MO-1	Maha oya, Sri Lanka	602	7.193	80.765	1103
42	Hewawasam et al 2003	UO-2	Uma oya, Sri Lank	603	6.908	80.908	1618
42	Hewawasam et al 2003	BO-2	Belihul oya, Sri Lanka	604	7.093	80.798	1533
42	Hewawasam et al 2003	HUG-2	Huluganga, Sri Lanka	605	7.374	80.747	1148
42	Hewawasam et al 2003	NO-1	Nilambe oya, Sri Lanka	606	7.188	80.631	935
42	Hewawasam et al 2003	AO-1	Atabage oya, Sri Lanka	607	7.133	80.593	1116
42	Hewawasam et al 2003	UO-3	Uma oya, Sri Lank	608	6.93	80.852	1867
42	Hewawasam et al 2003	AO-2	Atabage oya, Sri Lanka	609	7.148	80.638	1255
42	Hewawasam et al 2003	MO-2	Maha oya, Sri Lanka	610	7.13	80.765	1507
42	Hewawasam et al 2003	NO-2	Nilambe oya, Sri Lanka	611	7.153	80.663	1113
42	Hewawasam et al 2003	MO-3	Maha oya, Sri Lanka	612	7.133	80.713	1520
43	Hippe et al. (2012)	18-Feb	Altiplano basin, Bolivia	613	-16.6437	-68.324	4022
43	Hippe et al. (2012)	18-Apr	Altiplano basin, Bolivia	614	-16.5741	-68.3656	4355
43	Hippe et al. (2012)	18-May	Altiplano basin, Bolivia	615	-16.573	-68.3661	4022
43	Hippe et al. (2012)	18-Jun	Altiplano basin, Bolivia	616	-16.6659	-68.2869	4009
43	Hippe et al. (2012)	18-Jul	Altiplano basin, Bolivia	617	-16.6832	-68.2745	3915
43	Hippe et al. (2012)	19-Jan	Altiplano basin, Bolivia	618	-16.9152	-68.1612	4017
43	Hippe et al. (2012)	22-Mar	Altiplano basin, Bolivia	619	-16.7777	-68.1906	4085
43	Hippe et al. (2012)	22-Jun	Altiplano basin, Bolivia	620	-17.0328	-68.0941	4101
43	Hippe et al. (2012)	24-Jan	Altiplano basin, Bolivia	621	-17.106	-67.9911	4172
43	Hippe et al. (2012)	24-Feb	Altiplano basin, Bolivia	622	-17.1233	-67.9637	4094
43	Hippe et al. (2012)	24-Mar	Altiplano basin, Bolivia	623	-17.2678	-67.8591	4363
43	Hippe et al. (2012)	24-Apr	Altiplano basin, Bolivia	624	-17.2941	-67.8099	4324
43	Hippe et al. (2012)	24-May	Altiplano basin, Bolivia	625	-17.384	-67.6443	4214
43	Hippe et al. (2012)	24-Jun	Altiplano basin, Bolivia	626	-17.3847	-67.6353	4089
43	Hippe et al. (2012)	24-Aug	Altiplano basin, Bolivia	627	-17.4515	-67.6328	4015
43	Hippe et al. (2012)	25-Feb	Altiplano basin, Bolivia	628	-17.2831	-67.309	4334
43	Hippe et al. (2012)	25-Mar	Altiplano basin, Bolivia	629	-17.3304	-67.3922	4177
43	Hippe et al. (2012)	25-Apr	Altiplano basin, Bolivia	630	-17.3662	-67.5615	4057
43	Hippe et al. (2012)	122	Altiplano basin, Bolivia	631	-17.2297	-68.0686	4171
43	Hippe et al. (2012)	123	Altiplano basin, Bolivia	632	-17.4781	-68.3923	4076
44	Insel et al 2010	S10	Rio Parapeti, Bolivia	633	-20.01	-63.54	1454
44	Insel et al 2010	S04	Rio Azero, Bolivia	634	-19.61	-64.08	2278
44	Insel et al 2010	S04a	Rio Azero, Bolivia	635	-19.61	-64.08	2278
44	Insel et al 2010	S04b	Rio Azero, Bolivia	636	-19.61	-64.08	2278
44	Insel et al 2010	S15	Rio Nanachuazu, Bolivia	637	-19.17	-63.66	1085
44	Insel et al 2010	S06	Rio Cachu Mayu, Bolivia	638	-19.1	-65.3	3533
44	Insel et al 2010	S12	Rio Banado, Bolivia	639	-20.1	-63.89	1346
44	Insel et al 2010	N04	Rio Quiquibey, Bolivia	640	-15.39	-67.12	1110
44	Insel et al 2010	N04a	Rio Quiquibey, Bolivia	641	-15.39	-67.12	1110
44	Insel et al 2010	N04b	Rio Quiquibey, Bolivia	642	-15.39	-67.12	1110
44	Insel et al 2010	N05	Rio Inicua, Bolivia	643	-15.51	-67.17	1044
44	Insel et al 2010	S09	Rio Charagua, Bolivia	644	-19.79	-63.23	1142
44	Insel et al 2010	S09a	Rio Charagua, Bolivia	645	-19.79	-63.23	1142
44	Insel et al 2010	S09b	Rio Charagua, Bolivia	646	-19.79	-63.23	1142
44	Insel et al 2010	S08	Rio Saipuru, Bolivia	647	-19.52	-63.25	1101

44	Insel et al 2010	S13	Rio Zapaltar, Bolivia	648	-19.8	-63.94	1367
44	Insel et al 2010	S16	Rio Saladille, Bolivia	649	-19.2	-63.65	845
44	Insel et al 2010	N02	Rio Yucumo, Bolivia	650	-15.16	-67.04	626
44	Insel et al 2010	N06	Rio Pequende, Bolivia	651	-15.68	-67.43	1395
44	Insel et al 2010	N06a	Rio Pequende, Bolivia	652	-15.68	-67.43	1395
44	Insel et al 2010	N06b	Rio Pequende, Bolivia	653	-15.68	-67.43	1395
44	Insel et al 2010	S11	Rio Iviyeca, Bolivia	654	-19.93	-63.68	1329
44	Insel et al 2010	S05	Rio Canas, Bolivia	655	-19.53	-64.15	2039
44	Insel et al 2010	S05a	Rio Canas, Bolivia	656	-19.53	-64.15	2039
44	Insel et al 2010	S05b	Rio Canas, Bolivia	657	-19.53	-64.15	2039
44	Insel et al 2010	S03	Rio Bateon, Bolivia	658	-19.79	-64.03	1533
44	Insel et al 2010	S01	Rio El Chaleno, Bolivia	659	-19.79	-63.26	1109
45	Kirchner et al 2001	SalmonRiv	Salmon River, ID, USA	660	45.75	-116.323	2063
45	Kirchner et al 2001	SelwayRiv	Selway River, ID, USA	661	46.086	-115.514	1689
45	Kirchner et al 2001	LochsaRiv	Lochsa River, ID, USA	662	46.151	-115.587	1593
45	Kirchner et al 2001	SForkClrwtrRiv	South Fork, Clearwater, ID	663	45.887	-116.031	1577
45	Kirchner et al 2001	JohnsCreek	Johns Creek, ID, USA	664	45.823	-115.889	1775
45	Kirchner et al 2001	UpRedRiv	Red River, ID, USA	665	45.71	-115.343	1638
45	Kirchner et al 2001	SForkRedRiv	Red River, ID, USA	666	45.709	-115.344	1775
45	Kirchner et al 2001	TrapperCr	Trapper Creek, ID, USA	667	45.671	-115.327	1773
45	Kirchner et al 2001	HC-Wfork	Horse Creek, ID, USA	668	45.991	-115.337	1573
45	Kirchner et al 2001	HC-Efork	Horse Creek, ID, USA	669	45.989	-115.334	1602
45	Kirchner et al 2001	Tailholt_Main	Tailholt, ID, USA	670	45.043	-115.678	1719
45	Kirchner et al 2001	CircleEndMain	Circle End, ID, USA	671	45.047	-115.668	1667
45	Kirchner et al 2001	CircleEndB	Circle End, ID, USA	672	45.055	-115.672	1724
45	Kirchner et al 2001	TailholtA	Tailholt, ID, USA	673	45.053	-115.683	1825
45	Kirchner et al 2001	SC-6	Silver Creek, ID, USA	674	44.337	-115.806	1598
45	Kirchner et al 2001	TailholtB	Tailholt, ID, USA	675	45.053	-115.683	1783
45	Kirchner et al 2001	HC-8	Horse Creek, ID, USA	676	45.995	-115.358	1538
45	Kirchner et al 2001	TailholtC	Tailholt, ID, USA	677	45.053	-115.684	1721
45	Kirchner et al 2001	HC-4	Horse Creek, ID, USA	678	45.995	-115.346	1563
45	Kirchner et al 2001	SC-3	Silver Creek, ID, USA	679	44.368	-115.771	1678
45	Kirchner et al 2001	SC-2	Silver Creek, ID, USA	680	44.372	-115.767	1748
45	Kirchner et al 2001	SC-5	Silver Creek, ID, USA	681	44.346	-115.789	1578
45	Kirchner et al 2001	SC-8	Silver Creek, ID, USA	682	44.356	-115.785	1564
45	Kirchner et al 2001	HC-6	Horse Creek, ID, USA	683	45.994	-115.351	1540
45	Kirchner et al 2001	HC-12	Horse Creek, ID, USA	684	45.992	-115.386	1598
45	Kirchner et al 2001	CircleEndA	Circle End, ID, USA	685	45.055	-115.671	1663
45	Kirchner et al 2001	HC-10	Horse Creek, ID, USA	686	45.992	-115.373	1536
45	Kirchner et al 2001	HC-14	Horse Creek, ID, USA	687	45.99	-115.393	1617
45	Kirchner et al 2001	HC-2	Horse Creek, ID, USA	688	45.994	-115.342	1537
45	Kirchner et al 2001	HC-16	Horse Creek, ID, USA	689	45.991	-115.41	1672
45	Kirchner et al 2001	SC-7	Silver Creek, ID, USA	690	44.35	-115.776	1640
45	Kirchner et al 2001	HC-9	Horse Creek, ID, USA	691	45.994	-115.366	1496
46	Kober et al 2009	LL3	Rio Lluta, Chile	692	-18.399	-70.291	3463
46	Kober et al 2009	LL3	Rio Lluta, Chile	693	-18.399	-70.291	3463
46	Kober et al 2009	LL3a	Rio Lluta, Chile	694	-18.399	-70.291	3463
46	Kober et al 2009	LL2	Rio Lluta, Chile	695	-18.401	-70.017	3753
46	Kober et al 2009	LL1	Rio Lluta, Chile	696	-18.336	-69.862	4060
46	Kober et al 2009	LL1a	Rio Lluta, Chile	697	-18.336	-69.862	4060

46	Kober et al 2009	LL1b	Rio Lluta, Chile	698	-18.336	-69.862	4060
46	Kober et al 2009	LL1c	Rio Lluta, Chile	699	-18.336	-69.862	4060
46	Kober et al 2009	LL5	Rio Lluta, Chile	700	-17.999	-69.631	4342
46	Kober et al 2009	LL4	Rio Lluta, Chile	701	-17.983	-69.629	4319
48	Matmon et al 2003	GSCO-1	aluftee, Great Smoky Mts Nat'l Park,	702	35.505	-83.301	1230
48	Matmon et al 2003	GSCO-1a	aluftee, Great Smoky Mts Nat'l Park,	703	35.505	-83.301	1230
48	Matmon et al 2003	GSCO-1b	aluftee, Great Smoky Mts Nat'l Park,	704	35.505	-83.301	1230
48	Matmon et al 2003	GSRF-12	n Fork, Great Smoky Mts, Nat'l Park,	705	35.517	-83.295	1284
48	Matmon et al 2003	GSAC-1	m's Creek, Great Smoky Mts, Nat'l Pa	706	35.611	-83.936	759
48	Matmon et al 2003	GSLR-1	e River, Great Smoky Mts, Nat'l Park,	707	35.661	-83.707	1054
48	Matmon et al 2003	GSCA-1	hee River, Great Smoky Mts, Nat'l Pa	708	35.668	-83.071	1222
48	Matmon et al 2003	GSCO-2	aluftee, Great Smoky Mts Nat'l Park,	709	35.516	-83.306	1166
48	Matmon et al 2003	GSMP-1	e Prong, Great Smoky Mts, Nat'l Par	710	35.659	-83.709	919
48	Matmon et al 2003	GSLP-1	Pigeon, Great Smoky Mts, Nat'l Park	711	35.738	-83.415	1164
48	Matmon et al 2003	GSHC-1	Creek, Great Smoky Mts, Nat'l Park	712	35.476	-83.724	1100
48	Matmon et al 2003	GSDC-1	o Creek, Great Smoky Mts Nat'l Park,	713	35.464	-83.434	1121
48	Matmon et al 2003	GSLR-7	e River, Great Smoky Mts, Nat'l Park,	714	35.664	-83.598	1215
48	Matmon et al 2003	GSBC-1	Creek, Great Smoky Mts, Nat'l Park,	715	35.749	-83.115	1317
48	Matmon et al 2003	GSFC-1	y Creek, Great Smoky Mts, Nat'l Par	716	35.47	-83.566	1166
48	Matmon et al 2003	GSBC-2	Creek, Great Smoky Mts, Nat'l Park,	717	35.736	-83.13	1360
48	Matmon et al 2003	GSWP-1	Prong, Great Smoky Mts, Nat'l Park	718	35.688	-83.536	1225
48	Matmon et al 2003	GSEC-1	e Creek, Great Smoky Mts, Nat'l Park,	719	35.487	-83.774	1039
48	Matmon et al 2003	GSRF-11	n Fork, Great Smoky Mts, Nat'l Park,	720	35.58	-83.264	1466
48	Matmon et al 2003	GSRF-10	ht Fork, Great Smoky Mts, Nat'l Park	721	35.584	-83.238	1342
48	Matmon et al 2003	GSCO-4	aluftee, Great Smoky Mts Nat'l Park,	722	35.558	-83.312	1220
48	Matmon et al 2003	GSNC-1	n Creek, Great Smoky Mts, Nat'l Park	723	35.458	-83.528	1163
48	Matmon et al 2003	GSTM-1	Mile Creek, Great Smoky Mts, Nat'l P	724	35.467	-83.878	961
48	Matmon et al 2003	GSRF-1	n Fork, Great Smoky Mts, Nat'l Park,	725	35.61	-83.255	1520
48	Matmon et al 2003	GSLR-5	e River, Great Smoky Mts, Nat'l Park,	726	35.619	-83.54	1303
48	Matmon et al 2003	GSRF-6	ht Fork, Great Smoky Mts, Nat'l Park	727	35.622	-83.212	1440
48	Matmon et al 2003	GSPB-1	ranch Creek, Great Smoky Mts, Nat'l	728	35.499	-83.934	797
48	Matmon et al 2003	GSLR-3	e River, Great Smoky Mts, Nat'l Park,	729	35.598	-83.515	1471
48	Matmon et al 2003	GSCO-3	aluftee, Great Smoky Mts Nat'l Park,	730	35.521	-83.308	1028
48	Matmon et al 2003	GSLR-6	e River, Great Smoky Mts, Nat'l Park,	731	35.653	-83.582	1110
48	Matmon et al 2003	GSCO-5	aluftee, Great Smoky Mts Nat'l Park,	732	35.567	-83.336	1175
48	Matmon et al 2003	GSLR-2	e River, Great Smoky Mts, Nat'l Park,	733	35.599	-83.514	1433
48	Matmon et al 2003	GSRF-7	e Creek, Great Smoky Mts, Nat'l Park	734	35.618	-83.208	1293
48	Matmon et al 2003	GSCS-1	y Creek, Great Smoky Mts Nat'l Park,	735	35.754	-83.205	1173
48	Matmon et al 2003	GSLR-4	e River, Great Smoky Mts, Nat'l Park,	736	35.616	-83.529	1270
48	Matmon et al 2003	GSRF-8	ht Fork, Great Smoky Mts, Nat'l Park	737	35.613	-83.213	1367
48	Matmon et al 2003	GSRF-9	ht Fork, Great Smoky Mts, Nat'l Park	738	35.608	-83.224	1263
48	Matmon et al 2003	GSCO-7	aluftee, Great Smoky Mts Nat'l Park,	739	35.602	-83.413	1443
48	Matmon et al 2003	GSRF-2	e Creek, Great Smoky Mts, Nat'l Park	740	35.629	-83.193	1287
48	Matmon et al 2003	GSCO-6	aluftee, Great Smoky Mts Nat'l Park,	741	35.587	-83.36	1224
48	Matmon et al 2003	GSRF-3	e Creek, Great Smoky Mts, Nat'l Park	742	35.629	-83.194	1351
48	Matmon et al 2003	GSRF-5	e Creek, Great Smoky Mts, Nat'l Park	743	35.623	-83.199	1281
51	Morel et al 2003	Wut1	Wutach River, Germany	744	47.848	8.454	903
51	Morel et al 2003	Wut7	Wutach River, Germany	745	47.843	8.321	960
51	Morel et al 2003	Wut12	Wutach River, Germany	746	47.869	8.262	986
51	Morel et al 2003	Wut4	Wutach River, Germany	747	47.865	8.223	990

51	Morel et al 2003	Wut6	Wutach River, Germany	748	47.867	8.281	907
51	Morel et al 2003	Wut10	Wutach River, Germany	749	47.939	8.201	994
51	Morel et al 2003	Wut9	Wutach River, Germany	750	47.88	8.163	1030
51	Morel et al 2003	Don1	Danube River, Germany	751	47.983	8.242	1042
51	Morel et al 2003	Don3	Danube River, Germany	752	47.948	8.367	928
51	Morel et al 2003	Don2	Danube River, Germany	753	47.961	8.253	1066
51	Morel et al 2003	Don4	Danube River, Germany	754	47.967	8.367	920
51	Morel et al 2003	Wut8	Wutach River, Germany	755	47.859	8.276	829
51	Morel et al 2003	Wut5	Wutach River, Germany	756	47.905	8.218	1031
51	Morel et al 2003	Wut11	Wutach River, Germany	757	47.874	8.259	904
51	Morel et al 2003	Wut3	Wutach River, Germany	758	47.861	8.254	875
52	Nichols et al 2002	GMV-1	nite Mountain, Mojave Desert, CA, U	759	34.026	-115.138	555
52	Nichols et al 2002	IMV-2	on Mountain, Mojavee Desert, CA, US	760	34.116	-115.189	703
52	Nichols et al 2002	GMV-3	nite Mountain, Mojave Desert, CA, U	761	34.012	-115.134	653
52	Nichols et al 2002	IMV-3	on Mountain, Mojavee Desert, CA, US	762	34.109	-115.195	695
52	Nichols et al 2002	GMV-2	nite Mountain, Mojave Desert, CA, U	763	34.007	-115.133	776
52	Nichols et al 2002	IMV-1	on Mountain, Mojavee Desert, CA, US	764	34.117	-115.193	700
53	Nichols et al 2005 (a)	CMV-456b	vi Mountain Piedmont, Mojave Dese	765	34.602	-114.601	754
53	Nichols et al 2005 (a)	SRV-123b	vi Mountain Piedmont, Mojave Dese	766	34.592	-114.642	602
53	Nichols et al 2005 (a)	CMV-123a	vi Mountain Piedmont, Mojave Dese	767	34.613	-114.616	710
54	Nichols et al 2005 (b)	CLA	Rio Charges Basin, Panama	768	9.244	-79.531	452
54	Nichols et al 2005 (b)	CChC	Rio Charges Basin, Panama	769	9.267	-79.506	462
54	Nichols et al 2005 (b)	CHAG-19	Rio Charges Basin, Panama	770	9.269	-79.505	46
54	Nichols et al 2005 (b)	CPC	Rio Charges Basin, Panama	771	9.294	-79.416	487
54	Nichols et al 2005 (b)	CHAG-17	Rio Charges Basin, Panama	772	9.296	-79.411	454
54	Nichols et al 2005 (b)	PIED	Rio Charges Basin, Panama	773	9.293	-79.411	550
54	Nichols et al 2005 (b)	CCC	Rio Charges Basin, Panama	774	9.36	-79.325	511
54	Nichols et al 2005 (b)	Chico	Rio Charges Basin, Panama	775	9.271	-79.507	428
54	Nichols et al 2005 (b)	CHM-1	Rio Charges Basin, Panama	776	9.36	-79.321	534
54	Nichols et al 2005 (b)	CTOM	Rio Charges Basin, Panama	777	9.365	-79.323	486
54	Nichols et al 2005 (b)	CHAG-14	Rio Charges Basin, Panama	778	9.371	-79.261	548
54	Nichols et al 2005 (b)	CHAG-9	Rio Charges Basin, Panama	779	9.363	-79.272	622
54	Nichols et al 2005 (b)	CHAG-15	Rio Charges Basin, Panama	780	9.369	-79.263	550
54	Nichols et al 2005 (b)	CHAG-12	Rio Charges Basin, Panama	781	9.368	-79.272	535
54	Nichols et al 2005 (b)	CHAG-7	Rio Charges Basin, Panama	782	9.331	-79.352	452
54	Nichols et al 2005 (b)	CHAG-5	Rio Charges Basin, Panama	783	9.357	-79.326	434
54	Nichols et al 2005 (b)	CHT-2	Rio Charges Basin, Panama	784	9.357	-79.316	460
55	Nichols et al 2007	ERV-UB	Mojave Desert, CA, USA	785	35.41	-116.47	1103
56	Nichols et al., (2014)	QLD 1	Escarpment, Qld, Australia	786	-16.814895	145.63673	354
56	Nichols et al., (2014)	QLD 2	Escarpment, Qld, Australia	787	-16.814895	145.63673	354
56	Nichols et al., (2014)	QLD 3	Escarpment, Qld, Australia	788	-16.956362	145.677463	582
56	Nichols et al., (2014)	QLD 4	Escarpment, Qld, Australia	789	-16.9451699	145.6904252	351
56	Nichols et al., (2014)	QLD 5	Below gorge, Qld, Australia	790	-16.845445	145.648637	576
56	Nichols et al., (2014)	QLD 6	Escarpment, Qld, Australia	791	-16.867244	145.670755	451
56	Nichols et al., (2014)	QLD 7	Upland, Qld, Australia	792	-16.902909	145.561149	520
56	Nichols et al., (2014)	QLD 8	Upland, Qld, Australia	793	-16.894795	145.550538	600
56	Nichols et al., (2014)	QLD 9	Upland, Qld, Australia	794	-16.817066	145.51219	532
56	Nichols et al., (2014)	QLD 9xb	Upland, Qld, Australia	795	-16.816982	145.513026	532
56	Nichols et al., (2014)	QLD 10	Upland, Qld, Australia	796	-16.79409	145.612551	581

56	Nichols et al., (2014)	QLD 11	Escarpment, Qld, Australia	797	-16.785567	145.644501	382
56	Nichols et al., (2014)	QLD 12	Escarpment, Qld, Australia	798	-16.820043	145.654447	462
56	Nichols et al., (2014)	QLD 13	Escarpment, Qld, Australia	799	-16.826267	145.680866	324
56	Nichols et al., (2014)	QLD 14	Escarpment, Qld, Australia	800	-16.810561	145.681453	297
57	Norton et al 2007	Fon1	Fontanne River, Switzerland	802	47.03	8.061	936
57	Norton et al 2007	Trub6	Trub River, Switzerland	803	46.948	7.888	1072
57	Norton et al 2007	Mins	Minstigerbach River, Switzerland	804	46.491	8.261	2483
57	Norton et al 2007	Fon7	Fontanne River, Switzerland	805	46.982	8.002	1044
57	Norton et al 2007	Trub3	Trub River, Switzerland	806	46.968	7.893	1104
57	Norton et al 2007	Rec	Reckingerbach River, Switzerland	807	46.468	8.239	2446
57	Norton et al 2007	Ges	Geschinerbach River, Switzerland	808	46.499	8.281	2184
57	Norton et al 2007	Trub4	Trub River, Switzerland	809	46.979	7.934	1155
57	Norton et al 2007	Fon2	Fontanne River, Switzerland	810	47.037	8.033	902
57	Norton et al 2007	Fon4	Fontanne River, Switzerland	811	46.972	7.982	1053
57	Norton et al 2007	Ritz	Ritzibach River, Switzerland	812	46.452	8.226	2137
57	Norton et al 2007	Mil	Milibach River, Switzerland	813	46.522	8.323	2330
57	Norton et al 2007	Wil	Wilerbach River, Switzerland	814	46.442	8.197	2372
57	Norton et al 2007	Ober	Oberbach River, Switzerland	815	46.512	8.306	2275
57	Norton et al 2007	Nider3	Niderbach River, Switzerland	816	46.501	8.292	2422
57	Norton et al 2007	Fon3	Fontanne River, Switzerland	817	47.029	7.982	1002
57	Norton et al 2007	Spi	Spissbach River, Swtizerland	818	46.446	8.211	2231
57	Norton et al 2007	Chr	Chrimpebach River, Switzerland	819	46.436	8.204	2031
57	Norton et al 2007	Fon5	Fontanne River, Switzerland	820	46.97	7.967	1084
57	Norton et al 2007	Fon6	Fontanne River, Switzerland	821	46.986	7.972	1091
57	Norton et al 2007	Fon6s	Fontanne River, Switzerland	822	46.986	7.972	1091
57	Norton et al 2007	Fon6m	Fontanne River, Switzerland	823	46.986	7.972	1091
57	Norton et al 2007	Fon6l	Fontanne River, Switzerland	824	46.986	7.972	1091
57	Norton et al 2007	Bet	Bettulbach River, Switzerland	825	46.432	8.189	2119
57	Norton et al 2007	Trub5	Trub River, Switzerland	826	46.999	7.918	1175
57	Norton et al 2007	Trub1	Trub River, Switzerland	827	46.995	7.892	1181
57	Norton et al 2007	Hil	Hilperschbach River, Switzerland	828	46.448	8.208	2231
57	Norton et al 2007	Trub2	Trub River, Switzerland	829	46.99	7.883	1185
57	Norton et al 2007	Löü	Löümibach River, Switzerland	830	46.419	8.172	1906
57	Norton et al 2007	Nider2	Niderbach River, Switzerland	831	46.524	8.272	2650
57	Norton et al 2007	Nider1	Niderbach River, Switzerland	832	46.525	8.269	2700
57	Norton et al 2007	Wil2	Wilerbach River, Switzerland	833	46.459	8.173	2641
57	Norton et al 2007	Hil2	Hilperschbach River, Switzerland	834	46.463	8.183	2586
60	Ouimet et al 2009	wbo510	Dadu, Tibetan Plateau	835	31.72	100.93	3933
60	Ouimet et al 2009	wbo604	Min, Tibetan Plateau	836	32.02	103.28	3275
60	Ouimet et al 2009	wbo538	Yalong, Tibetan Plateau	837	30.04	101.22	4045
60	Ouimet et al 2009	wbo616	Dadu, Tibetan Plateau	838	32.43	101.05	3775
60	Ouimet et al 2009	wbo448	Dadu, Tibetan Plateau	839	29.91	102.19	3316
60	Ouimet et al 2009	wbo439	Yalong (Li Qui),Tibetan Plateau	840	29.41	101.23	4489
60	Ouimet et al 2009	wbo508	Dadu, Tibetan Plateau	841	32.2	101.02	4063
60	Ouimet et al 2009	wbo536	Yalong, Tibetan Plateau	842	30.04	100.98	3803
60	Ouimet et al 2009	wbo551	Dadu, Tibetan Plateau	843	29.34	102.25	2455
60	Ouimet et al 2009	wbo621	Yalong (Li Qui),Tibetan Plateau	844	30.32	101.38	4258
60	Ouimet et al 2009	wbo642	Yalong, Tibetan Plateau	845	28.93	101.54	4028
60	Ouimet et al 2009	wbo544	Yalong (Li Qui),Tibetan Plateau	846	29.98	101.58	3955
60	Ouimet et al 2009	wbo653	Dadu, Tibetan Plateau	847	31.03	101.87	3780

60	Ouimet et al 2009	wbo619	Yalong, Tibetan Plateau	848	31.03	101.07	3973
60	Ouimet et al 2009	wbo624	Yalong, Tibetan Plateau	849	29.77	101.1	3825
60	Ouimet et al 2009	wbo624s	Yalong, Tibetan Plateau	850	29.77	101.1	3825
60	Ouimet et al 2009	wbo624q	Yalong, Tibetan Plateau	851	29.77	101.1	3825
60	Ouimet et al 2009	wbo523	Dadu, Tibetan Plateau	852	30.73	102	3521
60	Ouimet et al 2009	wbo645	Yalong (Li Qui),Tibetan Plateau	853	29.93	101.39	4149
60	Ouimet et al 2009	wbo610	Dadu, Tibetan Plateau	854	32.53	100.67	4141
60	Ouimet et al 2009	wbo610s	Dadu, Tibetan Plateau	855	32.53	100.67	4141
60	Ouimet et al 2009	wbo610q	Dadu, Tibetan Plateau	856	32.53	100.67	4141
60	Ouimet et al 2009	wbo618	Yalong, Tibetan Plateau	857	31.45	100.72	3967
60	Ouimet et al 2009	wbo609	Dadu, Tibetan Plateau	858	32.42	100.81	4193
60	Ouimet et al 2009	wbo506	Dadu, Tibetan Plateau	859	31.89	100.75	4234
60	Ouimet et al 2009	wbo450	Dadu, Tibetan Plateau	860	30.23	102.18	3005
60	Ouimet et al 2009	wbo612	Dadu, Tibetan Plateau	861	32.22	100.39	4239
60	Ouimet et al 2009	wbo316	Yalong (Li Qui),Tibetan Plateau	862	29.43	101.23	4378
60	Ouimet et al 2009	wbo613	Dadu, Tibetan Plateau	863	32.61	101.19	4155
60	Ouimet et al 2009	wbo302	Yalong (Li Qui),Tibetan Plateau	864	30.27	101.53	4073
60	Ouimet et al 2009	wbo524	Dadu, Tibetan Plateau	865	30.38	102.13	3043
60	Ouimet et al 2009	wbo641	Yalong, Tibetan Plateau	866	28.61	101.68	3493
60	Ouimet et al 2009	wbo651	Dadu, Tibetan Plateau	867	31.29	102.05	3525
60	Ouimet et al 2009	wbo617	Dadu, Tibetan Plateau	868	32.34	101.22	3939
60	Ouimet et al 2009	wbo550	Dadu (Gonga), Tibetan Plateau	869	29.54	102.14	2612
60	Ouimet et al 2009	wbo643	Yalong (Li Qui),Tibetan Plateau	870	29.51	101.43	4327
60	Ouimet et al 2009	wbo521	Dadu, Tibetan Plateau	871	30.54	101.62	4197
60	Ouimet et al 2009	wbo502	Min, Tibetan Plateau	872	31.76	102.74	4145
60	Ouimet et al 2009	wbo514	Dadu, Tibetan Plateau	873	31.75	102	3672
60	Ouimet et al 2009	wbo444	Dadu, Tibetan Plateau	874	29.37	102.24	1948
60	Ouimet et al 2009	wbo518	Dadu, Tibetan Plateau	875	30.95	101.72	3634
60	Ouimet et al 2009	wbo305	Yalong (Li Qui),Tibetan Plateau	876	29.89	101.54	4295
60	Ouimet et al 2009	wbo644	Yalong (Li Qui),Tibetan Plateau	877	29.72	101.52	4218
60	Ouimet et al 2009	wbo512	Dadu, Tibetan Plateau	878	31.79	101.1	3663
60	Ouimet et al 2009	wbo607	Dadu, Tibetan Plateau	879	32.27	102.49	4003
60	Ouimet et al 2009	wbo545	Yalong (Li Qui),Tibetan Plateau	880	30.33	101.52	3918
60	Ouimet et al 2009	wbo424	Min, Tibetan Plateau	881	31.3	103.53	3004
60	Ouimet et al 2009	wbo614	Dadu, Tibetan Plateau	882	32.58	101.08	3951
60	Ouimet et al 2009	wbo505	Dadu, Tibetan Plateau	883	32.21	101.61	3577
60	Ouimet et al 2009	wbo513	Dadu, Tibetan Plateau	884	31.77	101.37	4210
60	Ouimet et al 2009	wbo530	Dadu, Tibetan Plateau	885	30.08	102.07	3798
60	Ouimet et al 2009	wbo515	Dadu, Tibetan Plateau	886	31.42	102.05	3233
60	Ouimet et al 2009	wbo647	Dadu, Tibetan Plateau	887	29.68	102.2	2388
60	Ouimet et al 2009	wbo637	Anning, Tibetan Plateau	888	28.77	102.25	2899
60	Ouimet et al 2009	wbo501	Min, Tibetan Plateau	889	31.56	103.49	2832
60	Ouimet et al 2009	wbo623	Yalong (Li Qui),Tibetan Plateau	890	30.14	101.51	3795
60	Ouimet et al 2009	wbo522	Dadu, Tibetan Plateau	891	30.68	101.75	4026
60	Ouimet et al 2009	wbo511	Dadu, Tibetan Plateau	892	31.77	100.99	4165
60	Ouimet et al 2009	wbo605	Min, Tibetan Plateau	893	32.13	102.89	3572
60	Ouimet et al 2009	wbo622	Yalong (Li Qui),Tibetan Plateau	894	30.31	101.42	4205
60	Ouimet et al 2009	wbo519	Dadu, Tibetan Plateau	895	31.02	102.28	3365
60	Ouimet et al 2009	wbo638	Yalong, Tibetan Plateau	896	28.38	101.88	2877
60	Ouimet et al 2009	wbo625	Yalong, Tibetan Plateau	897	30.05	101.31	4267

60	Ouimet et al 2009	wbo445	Dadu, Tibetan Plateau	898	29.5	102.18	1952
60	Ouimet et al 2009	wbo626	Yalong (Li Qui),Tibetan Plateau	899	30.06	101.36	4353
60	Ouimet et al 2009	wbo529	Dadu, Tibetan Plateau	900	30.1	102.06	3148
61	Palumbo et al 2009	L8	ngshou Shan Range, NE Tibetan Plate	901	39.053	100.703	2668
61	Palumbo et al 2009	Y9	Yumu Shan Range, NE Tibetan Plateau	902	39.117	99.925	2588
61	Palumbo et al 2009	L9	ngshou Shan Range, NE Tibetan Plate	903	38.957	100.805	2974
61	Palumbo et al 2009	Y5	Yumu Shan Range, NE Tibetan Plateau	904	39.193	99.757	2460
61	Palumbo et al 2009	Y3	Yumu Shan Range, NE Tibetan Plateau	905	39.221	99.621	2356
61	Palumbo et al 2009	Y4	Yumu Shan Range, NE Tibetan Plateau	906	39.198	99.743	2374
61	Palumbo et al 2009	Y8	Yumu Shan Range, NE Tibetan Plateau	907	39.119	99.877	2779
61	Palumbo et al 2009	L10*	ngshou Shan Range, NE Tibetan Plate	908	38.945	100.84	2859
61	Palumbo et al 2009	L10a	ngshou Shan Range, NE Tibetan Plate	909	38.945	100.84	2859
61	Palumbo et al 2009	L10b	ngshou Shan Range, NE Tibetan Plate	910	38.945	100.84	2859
61	Palumbo et al 2009	L2	ngshou Shan Range, NE Tibetan Plate	911	39.185	100.381	1758
61	Palumbo et al 2009	Y1	Yumu Shan Range, NE Tibetan Plateau	912	39.203	99.611	2140
61	Palumbo et al 2009	Y10*	Yumu Shan Range, NE Tibetan Plateau	913	39.046	100.021	2011
61	Palumbo et al 2009	Y10a	Yumu Shan Range, NE Tibetan Plateau	914	39.046	100.021	2011
61	Palumbo et al 2009	Y10b	Yumu Shan Range, NE Tibetan Plateau	915	39.046	100.021	2011
61	Palumbo et al 2009	Y6	Yumu Shan Range, NE Tibetan Plateau	916	39.157	99.863	2465
61	Palumbo et al 2009	L6	ngshou Shan Range, NE Tibetan Plate	917	39.053	100.634	2173
61	Palumbo et al 2009	L1	ngshou Shan Range, NE Tibetan Plate	918	39.193	100.368	2639
61	Palumbo et al 2009	Y11	Yumu Shan Range, NE Tibetan Plateau	919	39.027	100.036	1852
61	Palumbo et al 2009	Y7	Yumu Shan Range, NE Tibetan Plateau	920	39.147	99.888	2385
61	Palumbo et al 2009	Y2*	Yumu Shan Range, NE Tibetan Plateau	921	39.21	99.614	1997
61	Palumbo et al 2009	Y2a	Yumu Shan Range, NE Tibetan Plateau	922	39.21	99.614	1997
61	Palumbo et al 2009	Y2b	Yumu Shan Range, NE Tibetan Plateau	923	39.21	99.614	1997
61	Palumbo et al 2009	Y13	Yumu Shan Range, NE Tibetan Plateau	924	38.976	100.113	1703
61	Palumbo et al 2009	L5	ngshou Shan Range, NE Tibetan Plate	925	39.098	100.538	1579
61	Palumbo et al 2009	L3	ngshou Shan Range, NE Tibetan Plate	926	39.161	100.403	1711
61	Palumbo et al 2009	Y12	Yumu Shan Range, NE Tibetan Plateau	927	39.018	100.057	1904
61	Palumbo et al 2009	L7*	ngshou Shan Range, NE Tibetan Plate	928	39.046	100.649	2204
61	Palumbo et al 2009	L7a	ngshou Shan Range, NE Tibetan Plate	929	39.046	100.649	2204
61	Palumbo et al 2009	L7b	ngshou Shan Range, NE Tibetan Plate	930	39.046	100.649	2204
61	Palumbo et al 2009	L4	ngshou Shan Range, NE Tibetan Plate	931	39.119	100.487	1786
63	Perg et al 2003	SLR	San Lorenzo River, CA, USA	932	36.972	-122.024	361
63	Perg et al 2003	PC	Pescadero Creek, CA, USA	933	37.264	-122.406	313
63	Perg et al 2003	SGC	San Gregori Creek, CA, USA	934	37.326	-122.387	326
63	Perg et al 2003	WC	Waddell Creek, CA, USA	935	37.113	-122.27	368
63	Perg et al 2003	SC	Scott Creek, CA, USA	936	37.066	-122.23	434
64	Placzek et al 2010	ADBA-13SD	Atacama Desert, Chile	937	-23.583	-69.275	2695
64	Placzek et al 2010	ADBA-2SD	Atacama Desert, Chile	938	-23.534	-69.08	2775
64	Placzek et al 2010	ADBA-5SD	Atacama Desert, Chile	939	-23.4	-69.463	2040
64	Placzek et al 2010	ADBA-12SDsm	Atacama Desert, Chile	940	-23.398	-69.462	2043
64	Placzek et al 2010	ASOI-SD	Atacama Desert, Chile	941	-24.093	-70.269	1799
64	Placzek et al 2010	ADSA-1SD	Atacama Desert, Chile	942	-23.786	-68.107	3369
64	Placzek et al 2010	ADSO-6SD	Atacama Desert, Chile	943	-24.115	-70.57	3610
64	Placzek et al 2010	ADSO-3SD	Atacama Desert, Chile	944	-24.089	-70.06	1238
66	Quigley et al 2007a	YG07	Northern Flinders Range, Australia	945	-30.187	139.428	530
67	Quigley et al 2007b	DCF01	ot Creek, Central Flinders Range, Aust	946	-32.231	137.932	512
67	Quigley et al 2007b	NWF01	tana Fan, Central Flinders Range, Aus	947	-32.117	137.955	586

67	Quigley et al 2007b	SWC01	tana Fan, Central Flinders Range, Aus	948	-32.151	137.948	564
67	Quigley et al 2007b	SWC01	tana Fan, Central Flinders Range, Aus	949	-32.151	137.948	564
67	Quigley et al 2007b	SWC01R	tana Fan, Central Flinders Range, Aus	950	-32.151	137.948	564
67	Quigley et al 2007b	SWF04	tana Fan, Central Flinders Range, Aus	951	-32.151	137.946	469
68	Reinhardt et al 2007	MRS 21b	Rio Torrente, Sierra Nevada, Spain	952	37	-3.48	2028
68	Reinhardt et al 2007	MRS 21a	Rio Torrente, Sierra Nevada, Spain	953	37	-3.48	2119
68	Reinhardt et al 2007	MRS 14	Rio Torrente, Sierra Nevada, Spain	954	37	-3.48	2292
68	Reinhardt et al 2007	MRS 17	Rio Torrente, Sierra Nevada, Spain	955	37	-3.48	2021
68	Reinhardt et al 2007	MRS 18	Rio Torrente, Sierra Nevada, Spain	956	37	-3.48	2126
68	Reinhardt et al 2007	MRS 12B	Rio Torrente, Sierra Nevada, Spain	957	37	-3.48	2350
68	Reinhardt et al 2007	MRS 3	Rio Torrente, Sierra Nevada, Spain	958	37	-3.48	2439
69	Reuter 2005	JSQ4	squehanna River at Harrisburg, PA, U	959	40.255	-76.886	429
69	Reuter 2005	JSQ7	Juniata River at Newport , PA, USA	960	40.478	-77.129	385
69	Reuter 2005	JSQ12	wn Branch Juniata River at Saxton, P	961	40.216	-78.266	462
69	Reuter 2005	JSQ2	Conewago Creek near Manchester, P	962	40.082	-76.72	192
69	Reuter 2005	JS42	onestoga River at Conestoga, PA, US	963	39.946	-76.368	148
69	Reuter 2005	JS39	vatara Creek at Harper Tavern, PA, U	964	40.043	-76.578	236
69	Reuter 2005	JSQ11	ranch Susquehanna River at Bower, P	965	40.897	-78.677	527
69	Reuter 2005	JSQ101	nch of Sinnemahoning Creek at Stirlin	966	41.413	-78.197	545
69	Reuter 2005	JSQ10	gle Creek Spring Creek at Milesbur, P	967	40.943	-77.787	407
69	Reuter 2005	JSQ1	Cordorus Creek near York, PA, USA	968	39.946	-76.756	215
69	Reuter 2005	JSQ3	w Breeches Creek near Camp Hill, PA	969	40.225	-76.898	248
69	Reuter 2005	JSQ5	erman Creek at Shermans Dale, PA,U	970	40.323	-77.169	312
69	Reuter 2005	JSQ13	Dunning Creek at Belden, PA, USA	971	40.072	-78.493	489
69	Reuter 2005	JS45	equea Creek at Martic Forge, PA, US	972	39.906	-76.329	157
69	Reuter 2005	JSQ9	Spring Creek near Axeman, PA, USA	973	40.89	-77.794	392
69	Reuter 2005	JS43	k at Eshelman Mill Road near Lyndon	974	40.01	-76.278	134
69	Reuter 2005	JSQ165	Conestoga Creek near Millersville, PA	975	40.021	-76.359	119
69	Reuter 2005	JSQ6	Bixler Run near Loysville, PA, USA	976	40.371	-77.043	285
69	Reuter 2005	JSQ153	ributary to Conowingo Creek, PA, US	977	39.829	-76.188	192
69	Reuter 2005	JSQ120	Yost Run-low, PA, USA	978	41.209	-77.921	608
69	Reuter 2005	JS44	Conestoga Creek near Churchtown, P	979	40.145	-75.989	194
69	Reuter 2005	JSQ125	Gottshall Run-low, PA, USA	980	41.098	-77.246	528
69	Reuter 2005	JSQ137	Minehart Run, PA, USA	981	40.53	-77.61	445
69	Reuter 2005	JSQ159	other tributary to East Branch, PA, U	982	39.806	-76.62	281
69	Reuter 2005	JSQ158	Alum Rock Run, PA,USA	983	39.776	-76.493	214
69	Reuter 2005	JSQ116	Little Birch Island Run, PA, USA	984	41.204	-78.039	549
69	Reuter 2005	JSQ114	Pebble Run, PA, USA	985	41.245	-78.278	633
69	Reuter 2005	JSQ130	Mud Creek, PA, USA	986	41.074	-76.618	202
69	Reuter 2005	JSQ134	Independence Run, PA, USA	987	40.686	-76.898	209
69	Reuter 2005	JSQ103	Crooked Run, PA, USA	988	41.592	-78.187	565
69	Reuter 2005	JSQ127	Jamison Run, PA, USA	989	41.069	-77.308	555
69	Reuter 2005	JSQ154	Kellys Run, PA, USA	990	39.837	-76.339	215
69	Reuter 2005	JSQ108	Bell Draft, PA, USA	991	41.396	-78.357	628
69	Reuter 2005	JSQ119	Laurely Fork, PA, USA	992	41.274	-77.768	569
69	Reuter 2005	JSQ131	ributary to Spruce Run Creek, PA, US	993	41.075	-76.522	281
69	Reuter 2005	JSQ148	ibutary from Kettle Mountain, PA, US	994	40.982	-77.49	533
69	Reuter 2005	JSQ115	Sanders Draft, PA, USA	995	41.276	-78.233	626
69	Reuter 2005	JSQ111	Wykoff Branch-low, PA, USA	996	41.451	-77.952	583
69	Reuter 2005	JSQ141	Laurel Run PA, USA	997	40.332	-78.111	516

69	Reuter 2005	JSQ156	Tributary to Beaver Creek, PA, USA	998	39.901	-76.52	241
69	Reuter 2005	JSQ155	Tributary to Tucquan Creek, PA, USA	999	39.865	-76.34	199
69	Reuter 2005	JSQ118	Drake Hollow, PA, USA	1000	41.286	-77.789	582
69	Reuter 2005	JSQ135	Boyers Run, PA, USA	1001	40.625	-76.956	219
69	Reuter 2005	JSQ150	Anderson Run, PA, USA	1002	39.812	-76.33	165
69	Reuter 2005	JSQ157	Tributary to Bald Eagle Creek, PA, USA	1003	39.75	-76.435	192
69	Reuter 2005	JSQ113	Lebo Branch, PA, USA	1004	41.358	-77.969	540
69	Reuter 2005	JSQ160	Tributary to East Branch, PA, USA	1005	39.816	-76.65	259
69	Reuter 2005	JSQ132	Tributary to Plum Creek, PA, USA	1006	40.852	-76.716	213
69	Reuter 2005	JSQ138	Tributary to Minehart Run, PA, USA	1007	40.531	-77.609	424
69	Reuter 2005	JSQ104	Heth Run, PA,USA	1008	41.704	-78.038	636
69	Reuter 2005	JSQ151	Mill Creek-low, PA, USA	1009	39.817	-76.339	177
69	Reuter 2005	JSQ112	Left Fork Bearfield Run, PA, USA	1010	41.386	-77.949	506
69	Reuter 2005	JSQ107	Another Middle Branch, PA, USA	1011	41.427	-78.359	573
69	Reuter 2005	JSQ161	Green Branch, PA, USA	1012	39.936	-76.473	198
69	Reuter 2005	JSQ117	butary to Little Birch Island Run, PA, U	1013	41.205	-78.034	504
69	Reuter 2005	JSQ146	Pine Swamp Run, PA, USA	1014	40.832	-77.476	558
69	Reuter 2005	JSQ136	Tributary to Lick Run, PA, USA	1015	40.369	-77.656	331
69	Reuter 2005	JSQ145	Swift Run, PA, USA	1016	40.816	-77.418	523
69	Reuter 2005	JSQ147	Bear Run, PA, USA	1017	40.985	-77.485	503
69	Reuter 2005	JSQ102	Russell Hollow Run, PA, USA	1018	41.459	-78.153	573
69	Reuter 2005	JSQ106	East Branch, PA, USA	1019	41.448	-78.359	604
69	Reuter 2005	JSQ128	Tributary to White Deer Hole, PA, USA	1020	41.075	-77.119	516
69	Reuter 2005	JSQ105	Big Run, PA, USA	1021	41.459	-78.43	611
69	Reuter 2005	JSQ109	uth Branch Little Portage Creek, PA, U	1022	41.598	-78.104	637
69	Reuter 2005	JSQ139	Wharton Run, PA, USA	1023	40.407	-77.766	509
69	Reuter 2005	JSQ144	Another Laurel Run, PA, USA	1024	40.738	-77.79	637
69	Reuter 2005	JSQ129	Buffalo Creek, PA, USA	1025	40.94	-77.223	624
69	Reuter 2005	JSQ140	Shores Branch, PA, USA	1026	40.326	-78.048	473
69	Reuter 2005	JSQ123	Middle Branch, PA, USA	1027	41.203	-77.798	649
69	Reuter 2005	JSQ149	Greens Run, PA, USA	1028	41.015	-77.707	371
69	Reuter 2005	JSQ152	Mill Creek-high, PA, USA	1029	39.815	-76.346	180
69	Reuter 2005	JSQ143	Croyle Run, PA, USA	1030	40.696	-77.803	583
69	Reuter 2005	JSQ133	Wolf Run, PA,USA	1031	40.522	-76.746	491
69	Reuter 2005	JSQ100	Dry Run, PA, USA	1032	41.376	-78.154	532
69	Reuter 2005	JSQ142	y to Frankstown Branch Juniata River,	1033	40.443	-78.303	356
69	Reuter 2005	JSQ124	Sulphur Run, PA, USA	1034	41.206	-77.34	292
69	Reuter 2005	JSQ126	Gottshall Run-high, PA, USA	1035	41.085	-77.275	551
69	Reuter 2005	JSQ110	Wykoff Branch-high, PA, USA	1036	41.453	-77.976	614
69	Reuter 2005	JSQ121	Kyler Fork of Yost Run, PA, USA	1037	41.164	-77.905	674
70	Riebe et al 2000	AP-11	Antelope Lake, CA, USA	1038	39.892	-120.144	1812
70	Riebe et al 2000	AP-7	Antelope Lake, CA, USA	1039	39.883	-120.128	2088
70	Riebe et al 2000	AL-8	Antelope Lake, CA, USA	1040	40.149	-120.647	1764
70	Riebe et al 2000	AP-3	Antelope Lake, CA, USA	1041	39.899	-120.135	1983
70	Riebe et al 2000	SP-19	Sunday Peak, CA, USA	1042	35.788	-118.58	2207
70	Riebe et al 2000	SP-1	Sunday Peak, CA, USA	1043	35.794	-118.59	2124
70	Riebe et al 2000	NP-17	Nichols Peak, CA, USA	1044	35.523	-118.209	1118
70	Riebe et al 2000	AL-10	Antelope Lake, CA, USA	1045	40.155	-120.638	1726
70	Riebe et al 2000	FR-6	Fall River, CA, USA	1046	39.639	-121.332	761
70	Riebe et al 2000	SP-3	Sunday Peak, CA, USA	1047	35.798	-118.583	2267

70	Riebe et al 2000	AL-6	Antelope Lake, CA, USA	1048	40.184	-120.638	1752
70	Riebe et al 2000	AP-1	Antelope Lake, CA, USA	1049	39.903	-120.129	1988
70	Riebe et al 2000	SP-7	Sunday Peak, CA, USA	1050	35.779	-118.584	2296
70	Riebe et al 2000	FR-10	Fall River, CA, USA	1051	39.647	-121.343	959
70	Riebe et al 2000	NP-1	Nichols Peak, CA, USA	1052	35.592	-118.226	1035
70	Riebe et al 2000	AL-7	Antelope Lake, CA, USA	1053	40.162	-120.653	1797
70	Riebe et al 2000	NP-7	Nichols Peak, CA, USA	1054	35.6	-118.212	1228
70	Riebe et al 2000	GD-2	Grizzly Dome, CA, USA	1055	39.881	-121.347	1273
70	Riebe et al 2000	GD-3	Grizzly Dome, CA, USA	1056	39.88	-121.348	1324
70	Riebe et al 2000	GD-5	Grizzly Dome, CA, USA	1057	39.886	-121.331	1509
70	Riebe et al 2000	AP-2	Antelope Lake, CA, USA	1058	39.902	-120.135	1937
70	Riebe et al 2000	AP-9	Antelope Lake, CA, USA	1059	39.883	-120.13	1845
70	Riebe et al 2000	NP-4	Nichols Peak, CA, USA	1060	35.585	-118.218	1262
70	Riebe et al 2000	NP-6	Nichols Peak, CA, USA	1061	35.587	-118.218	1174
70	Riebe et al 2000	NP-18	Nichols Peak, CA, USA	1062	35.522	-118.201	1172
70	Riebe et al 2000	FR-7	Fall River, CA, USA	1063	39.639	-121.331	784
70	Riebe et al 2000	FR-8	Fall River, CA, USA	1064	39.659	-121.323	1058
70	Riebe et al 2000	FR-9	Fall River, CA, USA	1065	39.655	-121.327	1039
70	Riebe et al 2000	GD-4	Grizzly Dome, CA, USA	1066	39.886	-121.331	1503
70	Riebe et al 2000	GD-6	Grizzly Dome, CA, USA	1067	39.888	-121.327	1499
70	Riebe et al 2000	GD-9	Grizzly Dome, CA, USA	1068	39.887	-121.316	1513
70	Riebe et al 2000	AL-2	Antelope Lake, CA, USA	1069	40.172	-120.646	1796
70	Riebe et al 2000	AL-3	Antelope Lake, CA, USA	1070	40.18	-120.637	1724
70	Riebe et al 2000	AL-4	Antelope Lake, CA, USA	1071	40.178	-120.638	1727
70	Riebe et al 2000	AL-5	Antelope Lake, CA, USA	1072	40.179	-120.629	1693
70	Riebe et al 2000	AL-9	Antelope Lake, CA, USA	1073	40.155	-120.645	1794
70	Riebe et al 2000	AL-11	Antelope Lake, CA, USA	1074	40.163	-120.634	2087
70	Riebe et al 2000	AP-4	Antelope Lake, CA, USA	1075	39.892	-120.141	1837
70	Riebe et al 2000	AP-5	Antelope Lake, CA, USA	1076	39.89	-120.134	1859
70	Riebe et al 2000	AP-6	Antelope Lake, CA, USA	1077	39.887	-120.134	1842
70	Riebe et al 2000	AP-13	Antelope Lake, CA, USA	1078	39.88	-120.128	1832
70	Riebe et al 2000	AP-14	Antelope Lake, CA, USA	1079	39.879	-120.128	1834
70	Riebe et al 2000	SP-4	Sunday Peak, CA, USA	1080	35.815	-118.575	2278
70	Riebe et al 2000	SP-8	Sunday Peak, CA, USA	1081	35.783	-118.592	2408
70	Riebe et al 2000	SP-9	Sunday Peak, CA, USA	1082	35.783	-118.602	2233
70	Riebe et al 2000	NP-10	Nichols Peak, CA, USA	1083	35.582	-118.181	1398
70	Riebe et al 2000	NP-14	Nichols Peak, CA, USA	1084	35.578	-118.198	1360
71	Riebe et al 2003	RI-8	na, Luquillo Experimental Forest, Pue	1085	18.269	-65.796	704
71	Riebe et al 2003	RI-6	os, Luquillo Experimental Forest, Pue	1086	18.276	-65.786	692
71	Riebe et al 2003	RI-4	os, Luquillo Experimental Forest, Pue	1087	18.289	-65.791	713
71	Riebe et al 2003	RI-2	os, Luquillo Experimental Forest, Pue	1088	18.269	-65.783	678
71	Riebe et al 2003	RI-1	os, Luquillo Experimental Forest, Pue	1089	18.282	-65.789	729
71	Riebe et al 2003	RI-7	os, Luquillo Experimental Forest, Pue	1090	18.282	-65.789	722
72	Safran et al 2005	bol50	per Beni River basin, Andes Mts, Boli	1091	-13.98	-67.506	2146
72	Safran et al 2005	bol18	per Beni River basin, Andes Mts, Boli	1092	-15.495	-67.881	2285
72	Safran et al 2005	bol42	per Beni River basin, Andes Mts, Boli	1093	-16.262	-67.25	3200
72	Safran et al 2005	bol15	per Beni River basin, Andes Mts, Boli	1094	-15.308	-68.213	3016
72	Safran et al 2005	bol38	per Beni River basin, Andes Mts, Boli	1095	-16.55	-67.396	3635
72	Safran et al 2005	bol38a	per Beni River basin, Andes Mts, Boli	1096	-16.55	-67.396	3635
72	Safran et al 2005	bol38b	per Beni River basin, Andes Mts, Boli	1097	-16.55	-67.396	3635

72	Safran et al 2005	bol21	per Beni River basin, Andes Mts, Boli	1098	-15.508	-67.842	1905
72	Safran et al 2005	bol13	per Beni River basin, Andes Mts, Boli	1099	-15.299	-68.275	3188
72	Safran et al 2005	bol7	per Beni River basin, Andes Mts, Boli	1100	-15.45	-68.598	3341
72	Safran et al 2005	bol20	per Beni River basin, Andes Mts, Boli	1101	-15.509	-67.868	2652
72	Safran et al 2005	bol19	per Beni River basin, Andes Mts, Boli	1102	-15.502	-67.886	2979
72	Safran et al 2005	bol43	per Beni River basin, Andes Mts, Boli	1103	-16.32	-67.433	2159
72	Safran et al 2005	bol22	per Beni River basin, Andes Mts, Boli	1104	-15.763	-67.675	2441
72	Safran et al 2005	bol37	per Beni River basin, Andes Mts, Boli	1105	-16.554	-67.336	3264
72	Safran et al 2005	bol32	per Beni River basin, Andes Mts, Boli	1106	-16.061	-67.659	3992
72	Safran et al 2005	bol44	per Beni River basin, Andes Mts, Boli	1107	-16.405	-67.646	3721
72	Safran et al 2005	bol14	per Beni River basin, Andes Mts, Boli	1108	-15.311	-68.237	2209
72	Safran et al 2005	bol30	per Beni River basin, Andes Mts, Boli	1109	-16.058	-68.016	3931
72	Safran et al 2005	bol41	per Beni River basin, Andes Mts, Boli	1110	-16.323	-67.433	3011
72	Safran et al 2005	bol45	per Beni River basin, Andes Mts, Boli	1111	-16.402	-67.642	3340
72	Safran et al 2005	bol17	per Beni River basin, Andes Mts, Boli	1112	-15.402	-68.154	1535
72	Safran et al 2005	bol8	per Beni River basin, Andes Mts, Boli	1113	-15.45	-68.598	3461
72	Safran et al 2005	bol34	per Beni River basin, Andes Mts, Boli	1114	-16.801	-67.213	3335
72	Safran et al 2005	bol24	per Beni River basin, Andes Mts, Boli	1115	-16.001	-68.589	1813
72	Safran et al 2005	bol40	per Beni River basin, Andes Mts, Boli	1116	-16.404	-67.478	2515
72	Safran et al 2005	bol27	per Beni River basin, Andes Mts, Boli	1117	-16.157	-68.12	4517
72	Safran et al 2005	bol25	per Beni River basin, Andes Mts, Boli	1118	-16.044	-67.626	1902
72	Safran et al 2005	bol 1	per Beni River basin, Andes Mts, Boli	1119	-15.793	-68.639	4359
72	Safran et al 2005	bol28	per Beni River basin, Andes Mts, Boli	1120	-16.107	-68.074	4100
72	Safran et al 2005	bol16	per Beni River basin, Andes Mts, Boli	1121	-15.377	-68.167	1671
72	Safran et al 2005	bol31	per Beni River basin, Andes Mts, Boli	1122	-16.88	-67.97	3964
72	Safran et al 2005	bol39	per Beni River basin, Andes Mts, Boli	1123	-16.429	-67.468	2103
72	Safran et al 2005	bol 48	per Beni River basin, Andes Mts, Boli	1124	-16.314	-67.909	4291
72	Safran et al 2005	bol49	per Beni River basin, Andes Mts, Boli	1125	-16.313	-67.892	4294
72	Safran et al 2005	bol33	per Beni River basin, Andes Mts, Boli	1126	-17.06	-67.197	2651
72	Safran et al 2005	bol2	per Beni River basin, Andes Mts, Boli	1127	-15.783	-68.636	4062
72	Safran et al 2005	bol26	per Beni River basin, Andes Mts, Boli	1128	-16.281	-67.652	2230
72	Safran et al 2005	bol29	per Beni River basin, Andes Mts, Boli	1129	-16.083	-68.039	3418
72	Safran et al 2005	bol5	per Beni River basin, Andes Mts, Boli	1130	-15.713	-68.672	3660
72	Safran et al 2005	bol6	per Beni River basin, Andes Mts, Boli	1131	-15.67	-68.679	4213
72	Safran et al 2005	bol9	per Beni River basin, Andes Mts, Boli	1132	-15.41	-68.544	2516
72	Safran et al 2005	bol23	per Beni River basin, Andes Mts, Boli	1133	-15.981	-68.577	1533
72	Safran et al 2005	bol46	per Beni River basin, Andes Mts, Boli	1134	-16.357	-67.809	3753
72	Safran et al 2005	bol36	per Beni River basin, Andes Mts, Boli	1135	-16.754	-67.231	2787
72	Safran et al 2005	bol36a	per Beni River basin, Andes Mts, Boli	1136	-16.754	-67.231	2787
72	Safran et al 2005	bol 36b	per Beni River basin, Andes Mts, Boli	1137	-16.754	-67.231	2787
72	Safran et al 2005	bol3	per Beni River basin, Andes Mts, Boli	1138	-15.764	-68.646	3830
72	Safran et al 2005	bol11	per Beni River basin, Andes Mts, Boli	1139	-15.343	-68.481	1849
72	Safran et al 2005	bol35	per Beni River basin, Andes Mts, Boli	1140	-16.779	-67.222	2731
72	Safran et al 2005	bol35a	per Beni River basin, Andes Mts, Boli	1141	-16.779	-67.222	2731
72	Safran et al 2005	bol35b	per Beni River basin, Andes Mts, Boli	1142	-16.779	-67.222	2731
72	Safran et al 2005	bol10	per Beni River basin, Andes Mts, Boli	1143	-15.348	-68.49	1767
72	Safran et al 2005	bol4	per Beni River basin, Andes Mts, Boli	1144	-15.763	-68.646	3830
73	Schaller et al 2001	loi-2	Loire River, France	1145	47.419	0.926	473
73	Schaller et al 2001	loi-2	Loire River, France	1146	47.419	0.926	473
73	Schaller et al 2001	loi-2	Loire River, France	1147	47.419	0.926	473

73	Schaller et al 2001	loi-7	Loire River, France	1148	47.87	1.894	521
73	Schaller et al 2001	loi-10	Loire River, France	1149	47.001	3.059	570
73	Schaller et al 2001	meu-15C	Meuse River, Belgium & France	1150	51.5	6.164	267
73	Schaller et al 2001	meu-15C	Meuse River, Belgium & France	1151	51.5	6.164	267
73	Schaller et al 2001	meu-15C	Meuse River, Belgium & France	1152	51.5	6.164	267
73	Schaller et al 2001	meu-14	Meuse River, Belgium & France	1153	51.284	6.048	270
73	Schaller et al 2001	meu-13	Meuse River, Belgium & France	1154	51.033	5.763	287
73	Schaller et al 2001	meu-13A	Meuse River, Belgium & France	1155	51.033	5.763	287
73	Schaller et al 2001	meu-13	Meuse River, Belgium & France	1156	51.033	5.763	287
73	Schaller et al 2001	meu-13D	Meuse River, Belgium & France	1157	51.033	5.763	287
73	Schaller et al 2001	loi-11	Loire River, France	1158	46.961	3.133	504
73	Schaller et al 2001	meu-10	Meuse River, Belgium & France	1159	50.472	5.006	283
73	Schaller et al 2001	loi-12	Loire River, France	1160	46.95	3.066	657
73	Schaller et al 2001	loi-12	Loire River, France	1161	46.95	3.066	657
73	Schaller et al 2001	loi-12	Loire River, France	1162	46.95	3.066	657
73	Schaller et al 2001	loi-14	Loire River, France	1163	46.651	3.235	691
73	Schaller et al 2001	loi-14A	Loire River, France	1164	46.651	3.235	691
73	Schaller et al 2001	loi-14	Loire River, France	1165	46.651	3.235	691
73	Schaller et al 2001	neck-6	Neckar River, Germany	1166	49.45	8.936	448
73	Schaller et al 2001	neck-6a	Neckar River, Germany	1167	49.45	8.936	448
73	Schaller et al 2001	neck-6b	Neckar River, Germany	1168	49.45	8.936	448
73	Schaller et al 2001	neck-6D	Neckar River, Germany	1169	49.45	8.936	448
73	Schaller et al 2001	loi-15	Loire River, France	1170	46.436	3.328	709
73	Schaller et al 2001	loi-41	Loire River, France	1171	46.487	3.899	597
73	Schaller et al 2001	neck-7	Neckar River, Germany	1172	49.31	9.145	451
73	Schaller et al 2001	neck-7a	Neckar River, Germany	1173	49.31	9.145	451
73	Schaller et al 2001	neck-7b	Neckar River, Germany	1174	49.31	9.145	451
73	Schaller et al 2001	meu-9	Meuse River, Belgium & France	1175	50.322	4.878	300
73	Schaller et al 2001	meu-7	Meuse River, Belgium & France	1176	49.896	4.705	302
73	Schaller et al 2001	loi-17	Loire River, France	1177	46.075	3.455	786
73	Schaller et al 2001	loi-40	Loire River, France	1178	45.998	4.045	792
73	Schaller et al 2001	loi-19	Loire River, France	1179	45.923	3.36	869
73	Schaller et al 2001	neck-8	Neckar River, Germany	1180	49.004	9.158	497
73	Schaller et al 2001	loi-39	Loire River, France	1181	45.945	4.212	850
73	Schaller et al 2001	loi-23	Loire River, France	1182	45.462	3.285	956
73	Schaller et al 2001	meu-4	Meuse River, Belgium & France	1183	49.535	5.1	317
73	Schaller et al 2001	neck-3	Neckar River, Germany	1184	48.704	9.419	560
73	Schaller et al 2001	neck-4	Neckar River, Germany	1185	48.704	9.419	560
73	Schaller et al 2001	reg-5	Regen River, Germany	1186	49.121	12.121	589
73	Schaller et al 2001	loi-55	Loire River, France	1187	46.364	3.314	616
73	Schaller et al 2001	reg-7	Regen River, Germany	1188	49.181	12.4	618
73	Schaller et al 2001	loi-25	Loire River, France	1189	45.117	3.492	1097
73	Schaller et al 2001	loi-25A	Loire River, France	1190	45.117	3.492	1097
73	Schaller et al 2001	loi-25	Loire River, France	1191	45.117	3.492	1097
73	Schaller et al 2001	loi-50	Loire River, France	1192	46.837	3.501	291
73	Schaller et al 2001	loi-18	Loire River, France	1193	45.944	3.449	738
73	Schaller et al 2001	loi-45	Loire River, France	1194	47.492	1.285	117
73	Schaller et al 2001	reg-12	Regen River, Germany	1195	49.187	12.736	706
73	Schaller et al 2001	reg-12A	Regen River, Germany	1196	49.187	12.736	706
73	Schaller et al 2001	reg-12	Regen River, Germany	1197	49.187	12.736	706

73	Schaller et al 2001	reg-12D	Regen River, Germany	1198	49.187	12.736	706
73	Schaller et al 2001	reg-14	Regen River, Germany	1199	49.146	12.838	730
73	Schaller et al 2001	meu-1	Meuse River, Belgium & France	1200	48.401	5.68	372
73	Schaller et al 2001	neck-2	Neckar River, Germany	1201	48.396	8.648	669
73	Schaller et al 2001	loi-21	Loire River, France	1202	45.666	3.648	867
73	Schaller et al 2001	loi-52	Loire River, France	1203	46.517	3.683	459
73	Schaller et al 2001	loi-49	Loire River, France	1204	47.036	3.207	286
73	Schaller et al 2001	neck-1	Neckar River, Germany	1205	48.179	8.617	705
73	Schaller et al 2001	loi-37	Loire River, France	1206	44.867	3.926	1187
73	Schaller et al 2001	reg-11	Regen River, Germany	1207	49.243	12.738	525
73	Schaller et al 2001	loi-51	Loire River, France	1208	46.771	3.45	247
73	Schaller et al 2001	neck-10	Neckar River, Germany	1209	48.854	8.617	704
73	Schaller et al 2001	reg-20	Regen River, Germany	1210	49.011	13.216	871
73	Schaller et al 2001	loi-36	Loire River, France	1211	44.732	3.862	1172
73	Schaller et al 2001	reg-13	Regen River, Germany	1212	49.171	12.845	698
73	Schaller et al 2001	loi-48	Loire River, France	1213	47.138	3.206	286
73	Schaller et al 2001	reg-18	Regen River, Germany	1214	49.048	13.233	904
73	Schaller et al 2001	reg-18A	Regen River, Germany	1215	49.048	13.233	904
73	Schaller et al 2001	reg-18	Regen River, Germany	1216	49.048	13.233	904
73	Schaller et al 2001	reg-18D	Regen River, Germany	1217	49.048	13.233	904
73	Schaller et al 2001	loi-56	Loire River, France	1218	46.006	3.459	347
73	Schaller et al 2001	loi-29	Loire River, France	1219	45.146	3.43	1006
73	Schaller et al 2001	reg-19	Regen River, Germany	1220	49.015	13.255	870
73	Schaller et al 2001	reg-19	Regen River, Germany	1221	49.015	13.255	870
73	Schaller et al 2001	reg-19	Regen River, Germany	1222	49.015	13.255	870
73	Schaller et al 2001	loi-33	Loire River, France	1223	44.933	3.383	1268
73	Schaller et al 2001	loi-34	Loire River, France	1224	45	3.4	1340
73	Schaller et al 2001	loi-32	Loire River, France	1225	45.067	3.3	1143
75	Stock et al 2009	HoC	olbrook Creek, Wasatch MTS, UT, US	1226	40.88	-111.84	2228
75	Stock et al 2009	CC	enterville Creek, Wasatch Mts, UT, US	1227	40.91	-111.86	2118
75	Stock et al 2009	HC	Holmes Creek, Wasatch Mts, UT, USA	1228	41.06	-111.84	2295
75	Stock et al 2009	FC	Ford Canyon, Wasatch, Mts, UT, USA	1229	40.94	-111.87	2232
75	Stock et al 2009	SC	hepards Creek, Wasatch Mts, UT, US	1230	41.01	-111.84	2149
75	Stock et al 2009	HCN	mes Creek North, Wasatch Mts, UT,	1231	41.07	-111.84	2272
75	Stock et al 2009	StC	Steed Creek, Wasatch Mts, UT, USA	1232	40.97	-111.84	2279
75	Stock et al 2009	RC	cky Mouth Creek, Wasatch Mts, UT, U	1233	40.54	-111.8	2540
75	Stock et al 2009	RC	cky Mouth Creek, Wasatch Mts, UT, U	1234	40.54	-111.8	2540
75	Stock et al 2009	RC	cky Mouth Creek, Wasatch Mts, UT, U	1235	40.54	-111.8	2540
75	Stock et al 2009	KC	ys Creek North, Wasatch Mts, UT, US	1236	41.12	-111.84	2153
75	Stock et al 2009	BC	Bear Creek, Wasatch Mts, UT, USA	1237	40.52	-111.82	2327
75	Stock et al 2009	SG	Stairs Gulch, Wasatch Mts, UT, USA	1238	40.62	-111.74	2387
75	Stock et al 2009	LF	Lisa Falls, Wasatch Mts, UT, USA	1239	40.57	-111.73	2788
75	Stock et al 2009	CG	Coalpit Gulch, Wasatch Mts, UT, USA	1240	40.57	-111.74	2727
75	Stock et al 2009	TG	Tanner Gulch, Wasatch Mts, UT, USA	1241	40.58	-111.7	2884
76	Sullivan 2007	CS-32	Blue Ridge Escarpment NC & VA, USA	1242	36.616	-80.451	829
76	Sullivan 2007	CS-03	Blue Ridge Escarpment NC & VA, USA	1243	36.466	-80.834	549
76	Sullivan 2007	CS-03A	Blue Ridge Escarpment NC & VA, USA	1244	36.466	-80.834	549
76	Sullivan 2007	CS-03B	Blue Ridge Escarpment NC & VA, USA	1245	36.466	-80.834	549
76	Sullivan 2007	CS-03C	Blue Ridge Escarpment NC & VA, USA	1246	36.466	-80.834	549
76	Sullivan 2007	CS-03D	Blue Ridge Escarpment NC & VA, USA	1247	36.466	-80.834	549

76	Sullivan 2007	CS-21	Blue Ridge Escarpment NC & VA, USA	1248	35.584	-82.164	593
76	Sullivan 2007	CS-20	Blue Ridge Escarpment NC & VA, USA	1249	35.621	-82.179	678
76	Sullivan 2007	CS-29	Blue Ridge Escarpment NC & VA, USA	1250	36.725	-80.226	566
76	Sullivan 2007	CS-15	Blue Ridge Escarpment NC & VA, USA	1251	35.34	-82.182	457
76	Sullivan 2007	CS-16	Blue Ridge Escarpment NC & VA, USA	1252	35.542	-82.381	884
76	Sullivan 2007	CS-22	Blue Ridge Escarpment NC & VA, USA	1253	35.569	-82.217	718
76	Sullivan 2007	CS-27	Blue Ridge Escarpment NC & VA, USA	1254	36.76	-80.372	950
76	Sullivan 2007	CS-19	Blue Ridge Escarpment NC & VA, USA	1255	35.636	-82.219	701
76	Sullivan 2007	CS-28	Blue Ridge Escarpment NC & VA, USA	1256	36.785	-80.298	622
76	Sullivan 2007	CS-31	Blue Ridge Escarpment NC & VA, USA	1257	36.664	-80.34	690
76	Sullivan 2007	CS-25	Blue Ridge Escarpment NC & VA, USA	1258	36.717	-80.433	902
76	Sullivan 2007	CS-24	Blue Ridge Escarpment NC & VA, USA	1259	35.548	-82.405	1057
76	Sullivan 2007	CS-26	Blue Ridge Escarpment NC & VA, USA	1260	36.774	-80.463	924
76	Sullivan 2007	CS-30	Blue Ridge Escarpment NC & VA, USA	1261	36.659	-80.18	427
76	Sullivan 2007	CS-09	Blue Ridge Escarpment NC & VA, USA	1262	35.33	-82.391	685
76	Sullivan 2007	CS-05	Blue Ridge Escarpment NC & VA, USA	1263	36.474	-80.859	478
76	Sullivan 2007	CS-23	Blue Ridge Escarpment NC & VA, USA	1264	35.525	-82.168	679
76	Sullivan 2007	CS-08	Blue Ridge Escarpment NC & VA, USA	1265	36.552	-80.791	858
76	Sullivan 2007	CS-18	Blue Ridge Escarpment NC & VA, USA	1266	35.621	-82.33	812
76	Sullivan 2007	CS-13	Blue Ridge Escarpment NC & VA, USA	1267	35.311	-82.221	390
76	Sullivan 2007	CS-02	Blue Ridge Escarpment NC & VA, USA	1268	36.446	-80.848	477
76	Sullivan 2007	CS-02A	Blue Ridge Escarpment NC & VA, USA	1269	36.446	-80.848	477
76	Sullivan 2007	CS-02B	Blue Ridge Escarpment NC & VA, USA	1270	36.446	-80.848	477
76	Sullivan 2007	CS-02C	Blue Ridge Escarpment NC & VA, USA	1271	36.446	-80.848	477
76	Sullivan 2007	CS-02D	Blue Ridge Escarpment NC & VA, USA	1272	36.446	-80.848	477
76	Sullivan 2007	CS-01	Blue Ridge Escarpment NC & VA, USA	1273	36.618	-80.778	867
76	Sullivan 2007	CS-01A	Blue Ridge Escarpment NC & VA, USA	1274	36.618	-80.778	867
76	Sullivan 2007	CS-01B	Blue Ridge Escarpment NC & VA, USA	1275	36.618	-80.778	867
76	Sullivan 2007	CS-01C	Blue Ridge Escarpment NC & VA, USA	1276	36.618	-80.778	867
76	Sullivan 2007	CS-01D	Blue Ridge Escarpment NC & VA, USA	1277	36.618	-80.778	867
76	Sullivan 2007	CS-07	Blue Ridge Escarpment NC & VA, USA	1278	36.556	-80.799	720
76	Sullivan 2007	CS-07A	Blue Ridge Escarpment NC & VA, USA	1279	36.556	-80.799	720
76	Sullivan 2007	CS-07B	Blue Ridge Escarpment NC & VA, USA	1280	36.556	-80.799	720
76	Sullivan 2007	CS-07C	Blue Ridge Escarpment NC & VA, USA	1281	36.556	-80.799	720
76	Sullivan 2007	CS-07D	Blue Ridge Escarpment NC & VA, USA	1282	36.556	-80.799	720
76	Sullivan 2007	CS-04	Blue Ridge Escarpment NC & VA, USA	1283	36.472	-80.858	502
76	Sullivan 2007	CS-04A	Blue Ridge Escarpment NC & VA, USA	1284	36.472	-80.858	502
76	Sullivan 2007	CS-04B	Blue Ridge Escarpment NC & VA, USA	1285	36.472	-80.858	502
76	Sullivan 2007	CS-04C	Blue Ridge Escarpment NC & VA, USA	1286	36.472	-80.858	502
76	Sullivan 2007	CS-04D	Blue Ridge Escarpment NC & VA, USA	1287	36.472	-80.858	502
76	Sullivan 2007	CS-14	Blue Ridge Escarpment NC & VA, USA	1288	35.292	-82.234	566
76	Sullivan 2007	CS-10	Blue Ridge Escarpment NC & VA, USA	1289	35.357	-82.401	714
76	Sullivan 2007	CS-06	Blue Ridge Escarpment NC & VA, USA	1290	36.539	-80.86	601
76	Sullivan 2007	CS-06A	Blue Ridge Escarpment NC & VA, USA	1291	36.539	-80.86	601
76	Sullivan 2007	CS-06B	Blue Ridge Escarpment NC & VA, USA	1292	36.539	-80.86	601
76	Sullivan 2007	CS-06C	Blue Ridge Escarpment NC & VA, USA	1293	36.539	-80.86	601
76	Sullivan 2007	CS-06D	Blue Ridge Escarpment NC & VA, USA	1294	36.539	-80.86	601
77	Tomkins et al 2007	BM-21	Blue Mts Plateau, Australia	1295	-33.415	150.16	1125
77	Tomkins et al 2007	BM-23	Blue Mts Plateau, Australia	1296	-33.417	150.16	1101
78	Vanacker et al 2007	BO-R2F	igh Plateau and Escarpment, Sri Lank	1297	6.757	80.762	2069

78	Vanacker et al 2007	ESP-5	carpment Zone, Sri Lankan Escarpme	1298	6.72	80.78	1447
78	Vanacker et al 2007	BO-U4	High Plateau, Sri Lankan Escarpment	1299	6.783	80.782	2143
78	Vanacker et al 2007	HP-2	High Plateau, Sri Lankan Escarpment	1300	6.803	80.808	2146
78	Vanacker et al 2007	ESP-3	carpment Zone, Sri Lankan Escarpme	1301	6.732	80.815	1223
78	Vanacker et al 2007	BO-F2F	carpment Zone, Sri Lankan Escarpme	1302	6.766	80.754	1361
78	Vanacker et al 2007	BO-U2	High Plateau, Sri Lankan Escarpment	1303	6.791	80.789	2096
78	Vanacker et al 2007	HP-4	High Plateau, Sri Lankan Escarpment	1304	6.797	80.778	2206
78	Vanacker et al 2007	KO-F4	carpment Zone, Sri Lankan Escarpme	1305	6.771	80.8	1677
78	Vanacker et al 2007	BO-U3	High Plateau, Sri Lankan Escarpment	1306	6.789	80.797	2194
78	Vanacker et al 2007	HP-3	High Plateau, Sri Lankan Escarpment	1307	6.812	80.799	2118
78	Vanacker et al 2007	HP-1	High Plateau, Sri Lankan Escarpment	1308	6.8	80.785	2161
78	Vanacker et al 2007	BO-U1	High Plateau, Sri Lankan Escarpment	1309	6.8	80.803	2132
78	Vanacker et al 2007	KO-G1	carpment Zone, Sri Lankan Escarpme	1310	6.759	80.789	1755
78	Vanacker et al 2007	BO-F1	carpment Zone, Sri Lankan Escarpme	1311	6.725	80.76	1033
78	Vanacker et al 2007	KO-R1F	carpment Zone, Sri Lankan Escarpme	1312	6.775	80.814	1721
78	Vanacker et al 2007	KO-T1	carpment Zone, Sri Lankan Escarpme	1313	6.771	80.797	1524
78	Vanacker et al 2007	KO-G3	carpment Zone, Sri Lankan Escarpme	1314	6.746	80.782	1441
78	Vanacker et al 2007	BO-U5	High Plateau, Sri Lankan Escarpment	1315	6.784	80.783	2076
79	von Blanckenburg et al 2004	HG(F)-3	Hakgala Forest, Sri Lanka	1322	6.926	80.817	1875
79	von Blanckenburg et al 2004	HG(F)-4	Hakgala Forest, Sri Lanka	1323	6.931	80.808	1875
79	von Blanckenburg et al 2004	KN(F)-10	Knuckles Forest, Sri Lanka	1324	7.364	80.832	1427
79	von Blanckenburg et al 2004	KN(F)-1	Knuckles Forest, Sri Lanka	1325	7.365	80.831	1453
79	von Blanckenburg et al 2004	GH(F)-1	Galaha Forest, Sri Lanka	1326	7.119	80.693	1568
79	von Blanckenburg et al 2004	GH(F)-2	Galaha Forest, Sri Lanka	1327	7.117	80.693	1584
79	von Blanckenburg et al 2004	KN(F)-3	Knuckles Forest, Sri Lanka	1328	7.366	80.83	1556
79	von Blanckenburg et al 2004	KN(F)-2	Knuckles Forest, Sri Lanka	1329	7.366	80.83	1448
79	von Blanckenburg et al 2004	KN(F)-5	Knuckles Forest, Sri Lanka	1330	7.366	80.83	1449
79	von Blanckenburg et al 2004	KN(F)-6	Knuckles Forest, Sri Lanka	1331	7.366	80.829	1567
79	von Blanckenburg et al 2004	KN(F)-7	Knuckles Forest, Sri Lanka	1332	7.364	80.83	1339
79	von Blanckenburg et al 2004	KN(F)-11	Knuckles Forest, Sri Lanka	1333	7.363	80.829	1324
81	Wittmann et al 2009	MAD20a	Madeira at Porto Velho, Boliva	1334	-8.77	-63.909	689
81	Wittmann et al 2009	MAD20a-1	Madeira at Porto Velho, Boliva	1335	-8.77	-63.909	689
81	Wittmann et al 2009	MAD20q-2	Madeira at Porto Velho, Boliva	1336	-8.77	-63.909	689
81	Wittmann et al 2009	MAD19a	Madeira at Ribeirao, Boliva	1337	-10.229	-65.281	728
81	Wittmann et al 2009	MAR18a	Mamoré at Guayaramerin, Boliva	1338	-10.808	-65.346	584
81	Wittmann et al 2009	MAR18a-1	Mamoré at Guayaramerin, Boliva	1339	-10.808	-65.346	584
81	Wittmann et al 2009	MAR18a-2	Mamoré at Guayaramerin, Boliva	1340	-10.808	-65.346	584
81	Wittmann et al 2009	BE17a	at Cachuela Esperanza, Beni Basin, B	1341	-10.55	-66.6	1017
81	Wittmann et al 2009	Mar_16	Mamoré at Puerto Ganadero, Boliva	1342	-14.864	-64.99	1085
81	Wittmann et al 2009	MAR16a	Mamoré at Puerto Ganadero, Boliva	1343	-14.864	-64.99	1085
81	Wittmann et al 2009	MAR16b	Mamoré at Puerto Ganadero, Boliva	1344	-14.864	-64.99	1085
81	Wittmann et al 2009	MD15a	e de Dios at Miraflores, Beni Basin, B	1345	-11.112	-66.416	858
81	Wittmann et al 2009	BE12a	Beni River at Riberalta, Bolivia	1346	-11.212	-66.249	1467
81	Wittmann et al 2009	BE10a	Beni River, Bolivia	1347	-11.559	-66.677	1551
81	Wittmann et al 2009	BE8a	Beni River, Bolivia	1348	-12.078	-66.882	1716
81	Wittmann et al 2009	BE7	Beni River, Bolivia	1349	-12.512	-66.95	1737
81	Wittmann et al 2009	BE7a	Beni River, Bolivia	1350	-12.512	-66.95	1737
81	Wittmann et al 2009	BE7b	Beni River, Bolivia	1351	-12.512	-66.95	1737
81	Wittmann et al 2009	BE4a	Beni River, Bolivia	1352	-13.119	-67.185	2086
81	Wittmann et al 2009	BE4a-1	Beni River, Bolivia	1353	-13.119	-67.185	2086

81	Wittmann et al 2009	BE4a-2	Beni River, Bolivia	1354	-13.119	-67.185	2086
81	Wittmann et al 2009	BE3a	Beni River, Bolivia	1355	-13.571	-67.353	2112
81	Wittmann et al 2009	BE3a-1	Beni River, Bolivia	1356	-13.571	-67.353	2112
81	Wittmann et al 2009	BE3a-2	Beni River, Bolivia	1357	-13.571	-67.353	2112
81	Wittmann et al 2009	BE2	Beni River, Bolivia	1358	-14.284	-67.474	2179
81	Wittmann et al 2009	BE2a	Beni River, Bolivia	1359	-14.284	-67.474	2179
81	Wittmann et al 2009	BE2b	Beni River, Bolivia	1360	-14.284	-67.474	2179
81	Wittmann et al 2009	BE1	Beni River at Rurrenabaque, Bolivia	1361	-14.527	-67.497	2192
81	Wittmann et al 2009	BE1a	Beni River at Rurrenabaque, Bolivia	1362	-14.527	-67.497	2192
81	Wittmann et al 2009	BE1b	Beni River at Rurrenabaque, Bolivia	1363	-14.527	-67.497	2192
81	Wittmann et al 2009	GR17b	de at Puerto Pailas, Mamore Basin, B	1364	-17.655	-62.777	2297
81	Wittmann et al 2009	GR19c	rande at Abapo, Mamore Basin, Boliv	1365	-17.866	-63.41	2518
81	Wittmann et al 2009	OR16b	Orthón at Caracoles, Beni Basin, Boliv	1366	-10.82	-66.11	281
81	Wittmann et al 2009	GR25a	le near Puente Arce, Mamore Basin,	1367	-18.609	-65.162	3311
81	Wittmann et al 2009	ICH21a	at Puerto Villarroel, Mamore Basin, B	1368	-16.841	-64.787	901
81	Wittmann et al 2009	CHA23a	paré at Villa Tunari, Mamore Basin, B	1369	-16.974	-65.414	2418
81	Wittmann et al 2009	MAN15b	niqui at San Borja, Mamore Basin, Bo	1370	-14.864	-66.738	490
81	Wittmann et al 2009	PIR18	rai at Angostura, Mamore Basin, Boli	1371	-18.082	-63.457	1392
81	Wittmann et al 2009	PIR18b	rai at Angostura, Mamore Basin, Boli	1372	-18.082	-63.457	1392
81	Wittmann et al 2009	PIR18c	rai at Angostura, Mamore Basin, Boli	1373	-18.082	-63.457	1392
80	Wittmann et al 2007	Emme	Emme, Mittelland	1374	47.047	7.633	978
80	Wittmann et al 2007	Reuss	Reuss, Reuss-Valley	1375	46.827	8.641	2103
80	Wittmann et al 2007	Reussa	Reuss, Reuss-Valley	1376	46.827	8.641	2103
80	Wittmann et al 2007	Reussb	Reuss, Reuss-Valley	1377	46.827	8.641	2103
80	Wittmann et al 2007	Sesia	Sesia, Valle delle Sesia	1378	45.812	8.256	1599
80	Wittmann et al 2007	Mag11-apr	Maggia, Val di Maggia Moghegno	1379	46.242	8.711	1727
80	Wittmann et al 2007	Mag11-feb	Maggia, Val di Maggia Riveo	1380	46.3	8.617	1820
80	Wittmann et al 2007	Klem	Kleine Emme, Emmental	1381	47.043	8.206	1075
80	Wittmann et al 2007	Klema	Kleine Emme, Emmental	1382	47.043	8.206	1075
80	Wittmann et al 2007	Klemb	Kleine Emme, Emmental	1383	47.043	8.206	1075
80	Wittmann et al 2007	Toce	Toce, Valle Antigorio	1384	46.146	8.309	1893
80	Wittmann et al 2007	Tocea	Toce, Valle Antigorio	1385	46.146	8.309	1893
80	Wittmann et al 2007	Toceb	Toce, Valle Antigorio	1386	46.146	8.309	1893
80	Wittmann et al 2007	Mela3	Melezza, Centovalli at Verscio	1387	46.181	8.711	1341
80	Wittmann et al 2007	Mela3a	Melezza, Centovalli at Verscio	1388	46.181	8.711	1341
80	Wittmann et al 2007	Mela3b	Melezza, Centovalli at Verscio	1389	46.181	8.711	1341
80	Wittmann et al 2007	Anza	Anza, Valle Anzasca	1390	46.023	8.262	1782
80	Wittmann et al 2007	Mela2	Melezza, Centovalli at Intragna	1391	46.177	8.704	1227
80	Wittmann et al 2007	Verz	Verzasca, Valle Verzasca	1392	46.253	8.843	1655
80	Wittmann et al 2007	Verza	Verzasca, Valle Verzasca	1393	46.253	8.843	1655
80	Wittmann et al 2007	Verzb	Verzasca, Valle Verzasca	1394	46.253	8.843	1655
80	Wittmann et al 2007	Sense	Sense, Mittelland	1395	46.825	7.32	1292
80	Wittmann et al 2007	Chie	Chietalbach, Chietal	1396	46.503	8.307	2363
80	Wittmann et al 2007	Mag8	Bavona, Val Bavona	1397	46.34	8.608	1936
80	Wittmann et al 2007	Mag16	Maggia, Val Lavizzara and Val di Pecci	1398	46.395	8.656	1978
80	Wittmann et al 2007	Mela1	Melezza, Centovalli at Dissimo	1399	46.14	8.583	1336
80	Wittmann et al 2007	Lonza	Lonza, northern Valais	1400	46.402	7.783	2550
80	Wittmann et al 2007	Tic	Ticino, Val Bedretto	1401	46.52	8.561	2181
80	Wittmann et al 2007	Tica	Ticino, Val Bedretto	1402	46.52	8.561	2181
80	Wittmann et al 2007	Ticb	Ticino, Val Bedretto	1403	46.52	8.561	2181

80	Wittmann et al 2007	Mag4	Rovana, Valle di Campo	1404	46.288	8.532	1879
80	Wittmann et al 2007	Mag17	Maggia, Val di Peccia	1405	46.409	8.642	1976
80	Wittmann et al 2007	Mag10	Maggia, Val di Prato	1406	46.389	8.667	1988
80	Wittmann et al 2007	Furka	Furkareuss, Furkatal	1407	46.588	8.494	2488
80	Wittmann et al 2007	Taf	Tafersbach, Mittelland	1408	46.882	7.302	705
80	Wittmann et al 2007	Mag2	Maggia, Val del Salto	1409	46.253	8.713	1474
80	Wittmann et al 2007	Wasen	Liechtguetbach, Mittelland	1410	47.043	7.795	1012
80	Wittmann et al 2007	Wasen1-jan	Liechtguetbach, Mittelland	1411	47.043	7.795	1012
80	Wittmann et al 2007	Wasen1-feb	Liechtguetbach, Mittelland	1412	47.043	7.795	1012
80	Wittmann et al 2007	Buetsch1	Butschelbach, Mitteland	1413	46.847	7.407	883
80	Wittmann et al 2007	Mag13	Maggia, Lago Bianco and Lago Nero	1414	46.448	8.526	2505
80	Wittmann et al 2007	Mag18	Maggia, side valley of Val Lavizzara	1415	46.447	8.666	2104
80	Wittmann et al 2007	Mag1	Maggia, Val di Gei	1416	46.223	8.741	1387
80	Wittmann et al 2007	Gren	Milibach, southern Valais	1417	46.375	8.101	1924
80	Wittmann et al 2007	Buetsch2	Butschelbach, Mitteland	1418	46.84	7.438	923
18	Codilean-2008	N2C	Gaub River catchment, Namibia	1419	-23.484712	16.231486	1565
18	Codilean-2008	N2G	Gaub River catchment, Namibia	1420	-23.469645	16.313166	1619
18	Codilean-2008	N3E	Gaub River catchment, Namibia	1421	-23.342974	16.419892	1835
18	Codilean-2008	N3F	Gaub River catchment, Namibia	1422	-23.325474	16.344922	1867
24	Densmore-2009	04A10	Sweetwater range, Montana, USA	1423	45.108579	-112.406058	2399
24	Densmore-2009	05WS1	Wassuk Range, Montana, USA	1424	38.376422	-118.586352	2188
24	Densmore-2009	05WS4	Wassuk Range, Montana, USA	1425	38.344388	-118.599138	2306
24	Densmore-2009	05WS5	Wassuk Range, Montana, USA	1426	38.226099	-118.650396	2537
24	Densmore-2009	05WS7	Wassuk Range, Montana, USA	1427	38.516671	-118.700458	2130
24	Densmore-2009	05WS9	Wassuk Range, Montana, USA	1428	38.388598	-118.638663	2510
24	Densmore-2009	05WS11	Wassuk Range, Montana, USA	1429	38.402022	-118.600408	2289
24	Densmore-2009	05WS12	Wassuk Range, Montana, USA	1430	38.421474	-118.620121	2060
24	Densmore-2009	05WS13	Wassuk Range, Montana, USA	1431	38.333078	-118.648968	2531
24	Densmore-2009	05WS14	Wassuk Range, Montana, USA	1432	38.325045	-118.626639	2503
49	Meyer-2010	06D1	cher catchment, Black Forest, Germa	1433	48.551791	8.158167	642
49	Meyer-2010	06D4	cher catchment, Black Forest, Germa	1434	48.584761	8.126739	645
49	Meyer-2010	06D8	cher catchment, Black Forest, Germa	1435	48.578201	8.196057	858
49	Meyer-2010	06D9	cher catchment, Black Forest, Germa	1436	48.597116	8.17339	844
49	Meyer-2010	07D3	cher catchment, Black Forest, Germa	1437	48.568775	8.162143	635
49	Meyer-2010	07D5	cher catchment, Black Forest, Germa	1438	48.569325	8.140844	499
49	Meyer-2010	08D23	cher catchment, Black Forest, Germa	1439	48.568768	8.161078	763
49	Meyer-2010	08D25	cher catchment, Black Forest, Germa	1440	48.589276	8.163934	608
49	Meyer-2010	06D10	tach catchment, Black Forest, Germa	1441	48.132081	8.253707	876
49	Meyer-2010	06D11	tach catchment, Black Forest, Germa	1442	48.106374	8.212937	1014
49	Meyer-2010	06D12	tach catchment, Black Forest, Germa	1443	48.117648	8.208545	990
49	Meyer-2010	06D13	tach catchment, Black Forest, Germa	1444	48.186311	8.227562	824
49	Meyer-2010	06D14	tach catchment, Black Forest, Germa	1445	48.214709	8.248278	737
49	Meyer-2010	06D15	tach catchment, Black Forest, Germa	1446	48.239915	8.214064	723
49	Meyer-2010	07D9	tach catchment, Black Forest, Germa	1447	48.131914	8.228379	931
49	Meyer-2010	07D14	tach catchment, Black Forest, Germa	1448	48.209645	8.230383	676
49	Meyer-2010	08D4	tach catchment, Black Forest, Germa	1449	48.234256	8.213093	598
49	Meyer-2010	08D10	tach catchment, Black Forest, Germa	1450	48.207246	8.297008	840
49	Meyer-2010	08D22	tach catchment, Black Forest, Germa	1451	48.150359	8.239716	922
49	Meyer-2010 (a)	05D2	Aabach subcatchments, Germany	1452	51.474517	8.750964	449
49	Meyer-2010 (a)	05D3	Aabach subcatchments, Germany	1453	51.49134	8.745479	439

49	Meyer-2010 (a)	05D1	Mo¨hne subcatchments, Germany	1454	51.487683	8.460753	443
49	Meyer-2010 (a)	06D16	Mo¨hne subcatchments, Germany	1455	51.468904	8.343457	390
49	Meyer-2010 (a)	06D17	Mo¨hne subcatchments, Germany	1456	51.47872	8.190185	292
49	Meyer-2010 (a)	06D19	Mo¨hne subcatchments, Germany	1457	51.477896	8.38754	436
49	Meyer-2010 (a)	07D16	Mo¨hne subcatchments, Germany	1458	51.457261	8.435243	452
49	Meyer-2010 (a)	07D17	Mo¨hne subcatchments, Germany	1459	51.483578	8.446782	399
49	Meyer-2010 (a)	07D18	Mo¨hne subcatchments, Germany	1460	51.431221	8.348306	481
49	Meyer-2010 (a)	07D21	Mo¨hne subcatchments, Germany	1461	51.491598	8.308613	409
49	Meyer-2010 (a)	07D23	Mo¨hne subcatchments, Germany	1462	51.485462	8.418717	346
49	Meyer-2010 (a)	07D24	Mo¨hne subcatchments, Germany	1463	51.487829	8.356128	324
49	Meyer-2010 (a)	06D18	Heve subcatchment, Germany	1464	51.456907	8.152845	388
23	Delunel-2010	Rd01	manche catchment, French western A	1465	45.054517	5.846541	1801
23	Delunel-2010	Rd02	eneon catchment, French western Al	1466	45.013714	6.062101	2404
23	Delunel-2010	Rd03	Romanche catchment, French weste	1467	45.038462	6.207552	2413
23	Delunel-2010	Rd04	abuc catchment, French western Alp	1468	44.985941	6.482774	2534
23	Delunel-2010	Rd05	t Pierre catchment, French western	1469	44.891281	6.445973	2776
23	Delunel-2010	Rd06	se Niere catchment, French western	1470	44.881765	6.443325	2744
23	Delunel-2010	Rd07	Gyr catchment, French western Alps	1471	44.871068	6.485743	2574
23	Delunel-2010	Rd08	izonne catchment, French western A	1472	44.941459	5.861961	1747
23	Delunel-2010	Rd09	onne catchment, French western Alp	1473	44.890781	5.897468	1611
23	Delunel-2010	Rd10	er Bonne catchment, French western	1474	44.880868	5.989066	2010
23	Delunel-2010	Mb130	Drac catchment, French western Alps	1475	44.793878	5.973164	1694
23	Delunel-2010	Mb146	eraisse catchment, French western A	1476	44.783874	6.063577	2044
82	Wittmann-2011	Cb-1a	ian shield- upper Madeira River tribu	1477	-15.240897	-59.444380	436
82	Wittmann-2011	Cb-5b	lian shield- upper Tapajós River tribu	1478	-9.935722	-56.928892	326
59	Norton-2011	Ahrn	Eastern Alps	1479	47.0504	12.130092	2362
59	Norton-2011	Antholzer	Eastern Alps	1480	46.815501	12.0817	2014
59	Norton-2011	Arno	Eastern Alps	1481	46.004134	10.678137	1886
59	Norton-2011	Avisio	Eastern Alps	1482	46.280755	11.450457	1874
59	Norton-2011	Bergler	Eastern Alps	1483	46.8196	11.536071	1923
59	Norton-2011	Bitto	Eastern Alps	1484	46.129038	9.569365	1547
59	Norton-2011	Castello	Eastern Alps	1485	46.159883	9.980053	1764
59	Norton-2011	Fersina	Eastern Alps	1486	46.068272	11.255438	1457
59	Norton-2011	Flagger	Eastern Alps	1487	46.800532	11.582781	2029
59	Norton-2011	Fusino	Eastern Alps	1488	46.333174	10.249209	2312
59	Norton-2011	Hoeller	Eastern Alps	1489	47.273618	12.419984	1969
59	Norton-2011	Krimmler	Eastern Alps	1490	47.213734	12.171716	2313
59	Norton-2011	Lagorai	Eastern Alps	1491	46.283248	11.505395	1928
59	Norton-2011	Masino	Eastern Alps	1492	46.165778	9.634395	2008
59	Norton-2011	Melach	Eastern Alps	1493	47.252811	11.264602	2083
59	Norton-2011	Muehl	Eastern Alps	1494	47.277822	12.376702	1667
59	Norton-2011	Nero	Eastern Alps	1495	46.137498	11.114619	1666
59	Norton-2011	Novate	Eastern Alps	1496	46.219925	9.459539	1834
59	Norton-2011	Oglio	Eastern Alps	1497	46.159059	10.34916	1940
59	Norton-2011	Pfitsch	Eastern Alps	1498	46.902141	11.473587	2096
59	Norton-2011	Pitze	Eastern Alps	1499	47.148834	10.740581	2381
59	Norton-2011	Plima	Eastern Alps	1500	46.598113	10.82564	2439
59	Norton-2011	Schnalz	Eastern Alps	1501	46.64895	10.97801	2372
59	Norton-2011	Silla	Eastern Alps	1502	46.086612	11.19962	988
59	Norton-2011	Talfer	Eastern Alps	1503	46.514723	11.354447	1693

59	Norton-2011	Tauern	Eastern Alps	1504	47.086253	12.527477	2377
59	Norton-2011	Watten	Eastern Alps	1505	47.278617	11.596998	1934
59	Norton-2011	Widschoenau	Eastern Alps	1506	47.460168	11.990226	1313
59	Norton-2011	Zemm	Eastern Alps	1507	47.151232	11.831783	2249
59	Norton-2011	Ziel	Eastern Alps	1508	46.670583	11.061324	2349
59	Norton-2011	diAdame	Eastern Alps	1509	46.078298	10.35134	2049
59	Norton-2011	valMoena	Eastern Alps	1510	46.274329	11.452084	1844
59	Norton-2011	diVenina	Eastern Alps	1511	46.162458	9.91247	1867
58	Norton-2010	Mil	Upper Rhone Valley, Swiss Alps	1512	46.522058	8.324613	2758
58	Norton-2010	Ober	Upper Rhone Valley, Swiss Alps	1513	46.511348	8.307186	2478
58	Norton-2010	Nider1	Upper Rhone Valley, Swiss Alps	1514	46.502099	8.293027	2313
58	Norton-2010	Ges	Upper Rhone Valley, Swiss Alps	1515	46.498635	8.28307	2337
58	Norton-2010	Mins	Upper Rhone Valley, Swiss Alps	1516	46.490468	8.262189	2487
58	Norton-2010	Rec	Upper Rhone Valley, Swiss Alps	1517	46.465828	8.235452	2485
58	Norton-2010	Hil	Upper Rhone Valley, Swiss Alps	1518	46.447794	8.20629	2147
58	Norton-2010	Wil	Upper Rhone Valley, Swiss Alps	1519	46.441928	8.197988	2383
58	Norton-2010	Wil2	Upper Rhone Valley, Swiss Alps	1520	46.457049	8.170429	2672
58	Norton-2010	Ritz	Upper Rhone Valley, Swiss Alps	1521	46.453712	8.228852	2196
58	Norton-2010	Spi	Upper Rhone Valley, Swiss Alps	1522	46.447851	8.216287	2180
58	Norton-2010	Chr	Upper Rhone Valley, Swiss Alps	1523	46.437143	8.203014	2038
58	Norton-2010	Bet	Upper Rhone Valley, Swiss Alps	1524	46.432071	8.189667	2072
58	Norton-2010	Lou	Upper Rhone Valley, Swiss Alps	1525	46.419511	8.173021	1874
62	Palumbo-2011	07C44-(Q1)	Qilian Shan, Tibet	1526	39.716	97.227	3493
62	Palumbo-2011	07C41-(Q2)	Qilian Shan, Tibet	1527	39.68	97.512	3872
62	Palumbo-2011	07C42-(Q3)	Qilian Shan, Tibet	1528	39.643	97.66	3678
62	Palumbo-2011	07C43-(Q4)	Qilian Shan, Tibet	1529	39.403	97.695	4317
62	Palumbo-2011	07C45-(Q5)	Qilian Shan, Tibet	1530	39.4	97.629	4227
62	Palumbo-2011	07C46-(Q6)	Qilian Shan, Tibet	1531	39.339	98.815	3787
62	Palumbo-2011	07C19-(Q7)	Qilian Shan, Tibet	1532	39.25	99.053	3286
62	Palumbo-2011	07C13-(Q8)	Qilian Shan, Tibet	1533	39.162	99.169	3766
62	Palumbo-2011	07C12-(Q9)	Qilian Shan, Tibet	1534	39.075	99.246	3594
62	Palumbo-2011	07C20-(Q10)	Qilian Shan, Tibet	1535	39.027	99.287	3823
62	Palumbo-2011	07C23-(Q11)	Qilian Shan, Tibet	1536	38.856	99.529	3632
62	Palumbo-2011	06C16-(Q12)	Qilian Shan, Tibet	1537	38.795	99.555	3784
62	Palumbo-2011	06C32-(Q13)	Qilian Shan, Tibet	1538	38.671	100.036	3730
62	Palumbo-2011	06C34-(L12)	Qilian Shan, Tibet	1539	39.036	100.954	2687
62	Palumbo-2011	06C12-(H3)	Qilian Shan, Tibet	1540	39.649268	100.073342	1906
19	Codilean-2012	N2A	Gaub River catchment, Namibia	1541	-23.478488	16.089481	1357
19	Codilean-2012	N2B	Gaub River catchment, Namibia	1542	-23.480911	16.09039	1335
19	Codilean-2012	N2D	Gaub River catchment, Namibia	1543	-23.482986	16.245457	1359
19	Codilean-2012	N2F	Gaub River catchment, Namibia	1544	-23.477074	16.278043	1632
19	Codilean-2012	N3A	Gaub River catchment, Namibia	1545	-23.365757	16.459222	1764
19	Codilean-2012	N3B	Gaub River catchment, Namibia	1546	-23.387140	16.434851	1751
19	Codilean-2012	N3C	Gaub River catchment, Namibia	1547	-23.357052	16.433583	1817
74	Scharf-2012	S3.1	Cape Mountains, Southern Africa	1548	-33.995580	20.664803	848
74	Scharf-2012	S4.1	Cape Mountains, Southern Africa	1549	-33.993210	20.70578	636
74	Scharf-2012	S6.1	Cape Mountains, Southern Africa	1550	-33.434303	21.407692	1252
74	Scharf-2012	S07	Cape Mountains, Southern Africa	1551	-34.021483	21.351937	463
74	Scharf-2012	S08	Cape Mountains, Southern Africa	1552	-33.983784	20.846127	737
74	Scharf-2012	S09	Cape Mountains, Southern Africa	1553	-33.981517	20.376457	906

74	Scharf-2012	S10	Cape Mountains, Southern Africa	1554	-33.984923	20.423264	1014
74	Scharf-2012	S11	Cape Mountains, Southern Africa	1555	-33.463145	21.214118	1337
74	Scharf-2012	S12	Cape Mountains, Southern Africa	1556	-33.398385	22.356838	1435
74	Scharf-2012	S13	Cape Mountains, Southern Africa	1557	-33.360599	22.180246	1367
28	Duxbury et. al. (2014)	SH-01 (0.25-0.85 mm)	ANDOAH NATIONAL PARK, VIRGINIA	1558	38.57121	-78.28735	717
28	Duxbury et. al. (2014)	SH-01 (0.85-2 mm)	ANDOAH NATIONAL PARK, VIRGINIA	1559	38.57121	-78.28735	717
28	Duxbury et. al. (2014)	SH-01 (2-10 mm)	ANDOAH NATIONAL PARK, VIRGINIA	1560	38.57121	-78.28735	717
28	Duxbury et. al. (2014)	SH-01 (>10 mm)	ANDOAH NATIONAL PARK, VIRGINIA	1561	38.57121	-78.28735	717
28	Duxbury et. al. (2014)	SH-07	ANDOAH NATIONAL PARK, VIRGINIA	1562	38.58155	-78.41427	831
28	Duxbury et. al. (2014)	SH-08	ANDOAH NATIONAL PARK, VIRGINIA	1563	38.6341	-78.39168	732
28	Duxbury et. al. (2014)	SH-10	ANDOAH NATIONAL PARK, VIRGINIA	1564	38.65694	-78.28215	659
28	Duxbury et. al. (2014)	SH-11	ANDOAH NATIONAL PARK, VIRGINIA	1565	38.65282	-78.24489	569
28	Duxbury et. al. (2014)	SH-12	ANDOAH NATIONAL PARK, VIRGINIA	1566	38.61456	-78.25663	702
28	Duxbury et. al. (2014)	SH-13	ANDOAH NATIONAL PARK, VIRGINIA	1567	38.54308	-78.27286	321
28	Duxbury et. al. (2014)	SH-14	ANDOAH NATIONAL PARK, VIRGINIA	1568	38.52742	-78.27909	470
28	Duxbury et. al. (2014)	SH-15	ANDOAH NATIONAL PARK, VIRGINIA	1569	38.52129	-78.29047	440
28	Duxbury et. al. (2014)	SH-21	ANDOAH NATIONAL PARK, VIRGINIA	1570	38.64484	-78.36921	707
28	Duxbury et. al. (2014)	SH-22	ANDOAH NATIONAL PARK, VIRGINIA	1571	38.61039	-78.41763	507
28	Duxbury et. al. (2014)	SH-45	ANDOAH NATIONAL PARK, VIRGINIA	1572	38.52343	-78.26451	258
28	Duxbury et. al. (2014)	SH-46	ANDOAH NATIONAL PARK, VIRGINIA	1573	38.64164	-78.24595	442
28	Duxbury et. al. (2014)	SH-47	ANDOAH NATIONAL PARK, VIRGINIA	1574	38.64702	-78.20854	304
28	Duxbury et. al. (2014)	SH-50	ANDOAH NATIONAL PARK, VIRGINIA	1575	38.81878	-78.20828	508
28	Duxbury et. al. (2014)	SH-51	ANDOAH NATIONAL PARK, VIRGINIA	1576	38.796	-78.23921	562
28	Duxbury et. al. (2014)	SH-52	ANDOAH NATIONAL PARK, VIRGINIA	1577	38.81109	-78.23393	583
28	Duxbury et. al. (2014)	SH-02 (0.25-0.85 mm)	ANDOAH NATIONAL PARK, VIRGINIA	1578	38.6635	-78.3555	607
28	Duxbury et. al. (2014)	SH-02 (0.85-2 mm)	ANDOAH NATIONAL PARK, VIRGINIA	1579	38.6635	-78.3555	607
28	Duxbury et. al. (2014)	SH-02 (2-10 mm)	ANDOAH NATIONAL PARK, VIRGINIA	1580	38.6635	-78.3555	607
28	Duxbury et. al. (2014)	SH-02 (>10 mm)	ANDOAH NATIONAL PARK, VIRGINIA	1581	38.6635	-78.3555	607
28	Duxbury et. al. (2014)	SH-05	ANDOAH NATIONAL PARK, VIRGINIA	1582	38.75965	-78.29867	819
28	Duxbury et. al. (2014)	SH-09	ANDOAH NATIONAL PARK, VIRGINIA	1583	38.6973	-78.32236	804
28	Duxbury et. al. (2014)	SH-16	ANDOAH NATIONAL PARK, VIRGINIA	1584	38.54164	-78.35171	890
28	Duxbury et. al. (2014)	SH-18*	ANDOAH NATIONAL PARK, VIRGINIA	1585	38.66361	-78.35552	605
28	Duxbury et. al. (2014)	SH-19	ANDOAH NATIONAL PARK, VIRGINIA	1586	38.47084	-78.49769	836
28	Duxbury et. al. (2014)	SH-25	ANDOAH NATIONAL PARK, VIRGINIA	1587	38.14798	-78.7487	714
28	Duxbury et. al. (2014)	SH-26	ANDOAH NATIONAL PARK, VIRGINIA	1588	38.2931	-78.62078	797
28	Duxbury et. al. (2014)	SH-40	ANDOAH NATIONAL PARK, VIRGINIA	1589	38.23854	-78.69121	815
28	Duxbury et. al. (2014)	SH-03 (0.25-0.85 mm)	ANDOAH NATIONAL PARK, VIRGINIA	1590	38.3617	-78.654	502
28	Duxbury et. al. (2014)	SH-03 (0.85-2 mm)	ANDOAH NATIONAL PARK, VIRGINIA	1591	38.3617	-78.654	502
28	Duxbury et. al. (2014)	SH-03 (2-10 mm)	ANDOAH NATIONAL PARK, VIRGINIA	1592	38.3617	-78.654	502
28	Duxbury et. al. (2014)	SH-03 (>10 mm)	ANDOAH NATIONAL PARK, VIRGINIA	1593	38.3617	-78.654	502
28	Duxbury et. al. (2014)	SH-20	ANDOAH NATIONAL PARK, VIRGINIA	1594	38.3568	-78.6621	569
28	Duxbury et. al. (2014)	SH-29	ANDOAH NATIONAL PARK, VIRGINIA	1595	38.1092	-78.8283	584
28	Duxbury et. al. (2014)	SH-30	ANDOAH NATIONAL PARK, VIRGINIA	1596	38.1782	-78.7893	778
28	Duxbury et. al. (2014)	SH-32	ANDOAH NATIONAL PARK, VIRGINIA	1597	38.3101	-78.7269	472
28	Duxbury et. al. (2014)	SH-34	ANDOAH NATIONAL PARK, VIRGINIA	1598	38.1728	-78.8094	616
28	Duxbury et. al. (2014)	SH-35	ANDOAH NATIONAL PARK, VIRGINIA	1599	38.1759	-78.8071	555
28	Duxbury et. al. (2014)	SH-36	ANDOAH NATIONAL PARK, VIRGINIA	1600	38.1775	-78.8057	645
28	Duxbury et. al. (2014)	SH-41**	ANDOAH NATIONAL PARK, VIRGINIA	1601	38.1776	-78.8059	639
28	Duxbury et. al. (2014)	SH-04 (0.25-0.85 mm)	ANDOAH NATIONAL PARK, VIRGINIA	1602	38.19886	-78.79376	656
28	Duxbury et. al. (2014)	SH-04 (0.85-2 mm)	ANDOAH NATIONAL PARK, VIRGINIA	1603	38.3617	-78.654	656

28	Duxbury et. al. (2014)	SH-04 (2-10 mm)	ANDOAH NATIONAL PARK, VIRGINIA	1604	38.3617	-78.654	656
28	Duxbury et. al. (2014)	SH-04 (>10 mm)	ANDOAH NATIONAL PARK, VIRGINIA	1605	38.3617	-78.654	656
28	Duxbury et. al. (2014)	SH-06	ANDOAH NATIONAL PARK, VIRGINIA	1606	38.6762	-78.38344	452
28	Duxbury et. al. (2014)	SH-27	ANDOAH NATIONAL PARK, VIRGINIA	1607	38.09966	-78.80402	636
28	Duxbury et. al. (2014)	SH-28	ANDOAH NATIONAL PARK, VIRGINIA	1608	38.09913	-78.8043	636
28	Duxbury et. al. (2014)	SH-37	ANDOAH NATIONAL PARK, VIRGINIA	1609	38.25227	-78.74652	620
28	Duxbury et. al. (2014)	SH-39	ANDOAH NATIONAL PARK, VIRGINIA	1610	38.22154	-78.78121	756
28	Duxbury et. al. (2014)	SH-42	ANDOAH NATIONAL PARK, VIRGINIA	1611	38.15973	-78.78496	788
28	Duxbury et. al. (2014)	SH-54	ANDOAH NATIONAL PARK, VIRGINIA	1612	38.28971	-78.72392	679
28	Duxbury et. al. (2014)	SH-17	ANDOAH NATIONAL PARK, VIRGINIA	1613	38.77959	-78.3656	489
28	Duxbury et. al. (2014)	SH-23	ANDOAH NATIONAL PARK, VIRGINIA	1614	38.869	-78.178	497
28	Duxbury et. al. (2014)	SH-24	ANDOAH NATIONAL PARK, VIRGINIA	1615	38.166	-78.745	730
28	Duxbury et. al. (2014)	SH-31	ANDOAH NATIONAL PARK, VIRGINIA	1616	38.16031	-78.80311	728
28	Duxbury et. al. (2014)	SH-33	ANDOAH NATIONAL PARK, VIRGINIA	1617	38.31137	-78.72635	467
28	Duxbury et. al. (2014)	SH-38	ANDOAH NATIONAL PARK, VIRGINIA	1618	38.25673	-78.76888	647
28	Duxbury et. al. (2014)	SH-43	ANDOAH NATIONAL PARK, VIRGINIA	1619	38.36257	-78.5739	640
28	Duxbury et. al. (2014)	SH-44	ANDOAH NATIONAL PARK, VIRGINIA	1620	38.34114	-78.45703	269
28	Duxbury et. al. (2014)	SH-48	ANDOAH NATIONAL PARK, VIRGINIA	1621	38.838	-78.106	403
28	Duxbury et. al. (2014)	SH-49	ANDOAH NATIONAL PARK, VIRGINIA	1622	38.92655	-78.17554	277
28	Duxbury et. al. (2014)	SH-56	ANDOAH NATIONAL PARK, VIRGINIA	1623	38.53189	-78.60295	634
13	Carretier, et al. (2013)	SAN1	San Andres	1624	-27.2	-69.92	1250
13	Carretier, et al. (2013)	HUA12	Huasco	1625	-28.6	-70.73	600
13	Carretier, et al. (2013)	HUA10	Huasco	1626	-28.7	-70.55	600
13	Carretier, et al. (2013)	HUA7	Huasco	1627	-28.8	-70.46	600
13	Carretier, et al. (2013)	HUA1	Huasco	1628	-28.99	-70.28	600
13	Carretier, et al. (2013)	ELK1	Elqui	1629	-29.85	-70.49	1195
13	Carretier, et al. (2013)	ELK2	Elqui	1630	-29.85	-70.49	1195
13	Carretier, et al. (2013)	HUR1	Hurtado	1631	-30.31	-70.73	485
13	Carretier, et al. (2013)	ILL1	Illapel	1632	-31.6	-71.11	1079
13	Carretier, et al. (2013)	CHO0823S	Choapa	1633	-31.61	-71.4	500
13	Carretier, et al. (2013)	CHO0820	Choapa	1634	-31.66	-71.22	500
13	Carretier, et al. (2013)	CHO0822S	Choapa	1635	-31.66	-71.3	500
13	Carretier, et al. (2013)	CHO1	Choapa	1636	-31.69	-71.27	500
13	Carretier, et al. (2013)	ACO1	Aconcagua	1637	-32.83	-70.54	1420
13	Carretier, et al. (2013)	MAI1	Maipo	1638	-33.58	-70.44	850
13	Carretier, et al. (2013)	CAC1	Cachapoal	1639	-34.21	-70.53	700
13	Carretier, et al. (2013)	TIN1	Tingirririca	1640	-34.68	-70.87	518
13	Carretier, et al. (2013)	TEN1	Teno	1641	-34.99	-70.86	900
13	Carretier, et al. (2013)	LON1	Lontue	1642	-35.18	-71.12	900
13	Carretier, et al. (2013)	MAU1	Maule	1643	-35.73	-71.02	900
2	Acosta et al. (2015)	S-01	Southern kenya rift	1644	–1.876	36.779	1707
2	Acosta et al. (2015)	S-02	Southern kenya rift	1645	–1.446	36.971	1567
2	Acosta et al. (2015)	S-03	Southern kenya rift	1646	–1.809	36.045	2246
2	Acosta et al. (2015)	C-01	Central Kenya rift	1647	0.658	35.883	1400
2	Acosta et al. (2015)	C-02	Central Kenya rift	1648	0.633	34.999	1830
2	Acosta et al. (2015)	C-03	Central Kenya rift	1649	0.612	34.962	2010
2	Acosta et al. (2015)	C-04	Central Kenya rift	1650	0.655	34.839	2244
2	Acosta et al. (2015)	C-05	Central Kenya rift	1651	0.631	35.569	1511
2	Acosta et al. (2015)	C-06	Central Kenya rift	1652	0.608	35.579	1540
2	Acosta et al. (2015)	C-07	Central Kenya rift	1653	0.582	35.57	1540

2	Acosta et al. (2015)	C-08	Central Kenya rift	1654	0.513	35.586	1657
2	Acosta et al. (2015)	C-09	Central Kenya rift	1655	0.395	35.64	1621
2	Acosta et al. (2015)	C-10	Central Kenya rift	1656	0.442	35.628	1803
2	Acosta et al. (2015)	N-01	Northern Kenya rift	1657	1.812	36.715	1306
2	Acosta et al. (2015)	N-02	Northern Kenya rift	1658	1.908	36.837	1415
2	Acosta et al. (2015)	N-03	Northern Kenya rift	1659	1.792	36.799	1405
2	Acosta et al. (2015)	N-04	Northern Kenya rift	1660	1.773	36.794	1347
2	Acosta et al. (2015)	N-05	Northern Kenya rift	1661	2.005	36.89	1555
2	Acosta et al. (2015)	N-06	Northern Kenya rift	1662	2.125	36.588	1318
2	Acosta et al. (2015)	N-07	Northern Kenya rift	1663	2.148	36.594	1258
50	Miller et al. (2013)	100	Dry Run	1664	41.376	-78.154	443
50	Miller et al. (2013)	102	Russell Hollow Run	1665	41.459	-78.153	514
50	Miller et al. (2013)	103	Crooked Run	1666	41.592	-78.187	448
50	Miller et al. (2013)	104	Heth Run	1667	41.704	-78.038	444
50	Miller et al. (2013)	105	Big Run	1668	41.459	-78.43	500
50	Miller et al. (2013)	106	East Branch	1669	41.448	-78.359	504
50	Miller et al. (2013)	107	another Middle Branch	1670	41.427	-78.359	524
50	Miller et al. (2013)	108	Bell Draft	1671	41.396	-78.357	570
50	Miller et al. (2013)	109	South Branch Little Portage Creek	1672	41.598	-78.104	587
50	Miller et al. (2013)	110	Wykoff Branch, high elevation sample	1673	41.453	-77.976	378
50	Miller et al. (2013)	111	Wykoff Branch, low elevation sample §	1674	41.451	-77.952	586
50	Miller et al. (2013)	112	Left Fork Bearfield Run	1675	41.386	-77.949	566
50	Miller et al. (2013)	113	Lebo Branch	1676	41.358	-77.969	464
50	Miller et al. (2013)	114	Pebble Run	1677	41.245	-78.278	391
50	Miller et al. (2013)	115	Sanders Draft	1678	41.276	-78.233	411
50	Miller et al. (2013)	116	Little Birch Island Run	1679	41.204	-78.039	343
50	Miller et al. (2013)	117	tributary to Little Birch Island Run	1680	41.205	-78.034	314
50	Miller et al. (2013)	118	Drake Hollow	1681	41.286	-77.789	312
50	Miller et al. (2013)	119	Laurely Fork	1682	41.274	-77.768	419
50	Miller et al. (2013)	120	Yost Run, low elevation sample §§	1683	41.209	-77.921	378
50	Miller et al. (2013)	121	t Run (Kyler Fork), high elevation sam	1684	41.164	-77.905	412
50	Miller et al. (2013)	123	Middle Branch	1685	41.203	-77.798	498
50	Miller et al. (2013)	124	Sulphur Run	1686	41.206	-77.34	510
50	Miller et al. (2013)	125	Gottshall Run, low elevation sample §	1687	41.098	-77.246	412
50	Miller et al. (2013)	126	Gottshall Run, high elevation sample	1688	41.085	-77.275	310
50	Miller et al. (2013)	127	Jamison Run	1689	41.069	-77.308	281
50	Miller et al. (2013)	128	tributary to White Deer Hole Run	1690	41.075	-77.119	310
50	Miller et al. (2013)	129	Buffalo Creek	1691	40.94	-77.223	341
50	Miller et al. (2013)	130	Mud Creek	1692	41.074	-76.618	500
50	Miller et al. (2013)	131	tributary to Spruce Run Creek	1693	41.075	-76.522	381
50	Miller et al. (2013)	132	tributary to Plum Creek	1694	40.852	-76.716	264
50	Miller et al. (2013)	133	Wolf Run	1695	40.522	-76.746	563
50	Miller et al. (2013)	134	Independence Run	1696	40.686	-76.898	357
50	Miller et al. (2013)	135	Boyers Run	1697	40.625	-76.956	391
50	Miller et al. (2013)	136	tributary to Lick Run	1698	40.369	-77.656	343
50	Miller et al. (2013)	137	Minehart Run	1699	40.53	-77.61	646
50	Miller et al. (2013)	138	tributary to Minehart Run	1700	40.531	-77.609	633
50	Miller et al. (2013)	139	Wharton Run	1701	40.407	-77.766	573
50	Miller et al. (2013)	140	Shores Branch	1702	40.326	-78.048	570
50	Miller et al. (2013)	141	Laurel Run	1703	40.332	-78.111	562

50	Miller et al. (2013)	142	utary to Frankstown Branch Juniata R	1704	40.443	-78.303	382
50	Miller et al. (2013)	143	Croyle Run	1705	40.696	-77.803	344
50	Miller et al. (2013)	144	another Laurel Run	1706	40.738	-77.79	309
50	Miller et al. (2013)	145	Swift Run	1707	40.816	-77.418	509
50	Miller et al. (2013)	146	Pine Swamp Run	1708	40.832	-77.476	469
50	Miller et al. (2013)	147	Bear Run	1709	40.985	-77.485	368
50	Miller et al. (2013)	148	tributary to Kettle Mountain	1710	40.982	-77.49	478
50	Miller et al. (2013)	149	Greens Run	1711	41.015	-77.707	311
50	Miller et al. (2013)	150	Anderson Run	1712	39.812	-76.33	387
50	Miller et al. (2013)	152	Mill Creek	1713	39.815	-76.346	110
50	Miller et al. (2013)	153	tributary to Conowingo Creek	1714	39.829	-76.188	123
50	Miller et al. (2013)	154	Kellys Run	1715	39.837	-76.339	93
50	Miller et al. (2013)	155	tributary to Tucquan Creek	1716	39.865	-76.34	104
50	Miller et al. (2013)	156	tributary to Beaver Creek	1717	39.901	-76.52	547
50	Miller et al. (2013)	157	tributary to Bald Eagle Creek	1718	39.75	-76.435	340
50	Miller et al. (2013)	158	Alum Rock Run	1719	39.776	-76.493	417
50	Miller et al. (2013)	159	tributary to East Branch	1720	39.806	-76.62	249
50	Miller et al. (2013)	160	tributary to East Branch	1721	39.816	-76.65	400
50	Miller et al. (2013)	161	Green Branch	1722	39.936	-76.473	471
12	Buechi et al.(2014)	BR1a	region, Swiss northerns alpine, Switz	1728	47.342	8.945	935
12	Buechi et al.(2014)	BR3	region, Swiss northerns alpine, Switz	1729	47.335	8.967	1021
12	Buechi et al.(2014)	DI1	region, Swiss northerns alpine, Switz	1730	47.346	9.077	889
12	Buechi et al.(2014)	DI2	region, Swiss northerns alpine, Switz	1731	47.329	9.027	973
12	Buechi et al.(2014)	FEa	region, Swiss northerns alpine, Switz	1732	47.3	9.08	963
12	Buechi et al.(2014)	FIa	region, Swiss northerns alpine, Switz	1733	47.345	8.932	883
12	Buechi et al.(2014)	GO1a	region, Swiss northerns alpine, Switz	1734	47.393	9.072	811
12	Buechi et al.(2014)	GO2	region, Swiss northerns alpine, Switz	1735	47.375	9.039	832
12	Buechi et al.(2014)	GO3a	region, Swiss northerns alpine, Switz	1736	47.348	9	947
12	Buechi et al.(2014)	HOE	region, Swiss northerns alpine, Switz	1737	47.243	9.035	755
12	Buechi et al.(2014)	HT	region, Swiss northerns alpine, Switz	1738	47.309	8.969	1049
12	Buechi et al.(2014)	JO	region, Swiss northerns alpine, Switz	1739	47.184	8.544	864
12	Buechi et al.(2014)	ST1a	region, Swiss northerns alpine, Switz	1740	47.414	8.862	760
12	Buechi et al.(2014)	ST2a	region, Swiss northerns alpine, Switz	1741	47.387	8.942	885
12	Buechi et al.(2014)	TOa	region, Swiss northerns alpine, Switz	1743	47.34	8.943	999
12	Buechi et al.(2014)	VT	region, Swiss northerns alpine, Switz	1744	47.311	8.96	1049
47	Larsen et al. (2014)	Karangarua-Pit-1	southern Alps, New Zealand	1745	-43.6485	169.8466	1030
47	Larsen et al. (2014)	Karangarua-Pit-2	southern Alps, New Zealand	1746	-43.6493	169.8499	1082
47	Larsen et al. (2014)	Karangarua-Pit-3	southern Alps, New Zealand	1747	-43.6486	169.8521	1112
47	Larsen et al. (2014)	Karangarua-Pit-4	southern Alps, New Zealand	1748	-43.648	169.8458	959
47	Larsen et al. (2014)	Karangarua-Pit-5	southern Alps, New Zealand	1749	-43.6479	169.8458	961
47	Larsen et al. (2014)	Fox-Pit-1	southern Alps, New Zealand	1752	-43.4943	169.9984	932
47	Larsen et al. (2014)	Fox-Pit-2	southern Alps, New Zealand	1753	-43.4944	169.9986	942
47	Larsen et al. (2014)	Alex-Knob-Pit-2	southern Alps, New Zealand	1755	-43.4168	170.1574	846
47	Larsen et al. (2014)	Alex-Knob-Pit-3	southern Alps, New Zealand	1756	-43.4199	170.1534	947
47	Larsen et al. (2014)	Alex_Knob_Pit_4_0- 10_cm	southern Alps, New Zealand	1757	-43.4169	170.1577	836
47	Larsen et al. (2014)	Alex_Knob_Pit_4_10 -20_cm	southern Alps, New Zealand	1758	-43.4169	170.1577	836
47	Larsen et al. (2014)	Alex_Knob_Pit_4_20 -30_cm	southern Alps, New Zealand	1759	-43.4169	170.1577	836
47	Larsen et al. (2014)	Gunn-Pit-1	southern Alps, New Zealand	1761	-43.404	170.4046	866

47	Larsen et al. (2014)	Gunn_Pit_2	southern Alps, New Zealand	1762	-43.4047	170.405	832
47	Larsen et al. (2014)	Gunn-Pit-3	southern Alps, New Zealand	1763	-43.4044	170.4048	856
47	Larsen et al. (2014)	Gunn_Pit_4	southern Alps, New Zealand	1764	-43.4027	170.4027	953
47	Larsen et al. (2014)	Gunn-Pit-5	southern Alps, New Zealand	1765	-43.4034	170.4037	910
47	Larsen et al. (2014)	Gunn-Pit-6	southern Alps, New Zealand	1766	-43.4046	170.4048	838
47	Larsen et al. (2014)	Gunn-Pit-7	southern Alps, New Zealand	1767	-43.405	170.4102	555
47	Larsen et al. (2014)	Rapid-Creek-Pit-1	southern Alps, New Zealand	1770	-43.0294	171.0175	966
47	Larsen et al. (2014)	Rapid-Creek-Pit-2	southern Alps, New Zealand	1771	-43.0282	171.0173	897
47	Larsen et al. (2014)	Rapid-Creek-Pit-3	southern Alps, New Zealand	1772	-43.0267	171.017	856
47	Larsen et al. (2014)	Rapid-Creek-Pit-4	southern Alps, New Zealand	1773	-43.0289	171.0175	946
47	Larsen et al. (2014)	Rapid-Creek-Pit-5	southern Alps, New Zealand	1774	-43.0273	171.0173	832
65	Pumin et al. (2015)	BRC-21	Upper Paraguay river basin, Brazil	1777	-15.906966	-56.435038	204
65	Pumin et al. (2015)	BRC-22	Upper Paraguay river basin, Brazil	1778	-15.682199	-56.300522	237
65	Pumin et al. (2015)	BRC-23	Upper Paraguay river basin, Brazil	1779	-15.746988	-56.536631	235
65	Pumin et al. (2015)	BRC-24	Upper Paraguay river basin, Brazil	1780	-16.015374	-56.852482	188
65	Pumin et al. (2015)	BRC-25	Upper Paraguay river basin, Brazil	1781	-16.169074	-56.743175	190
65	Pumin et al. (2015)	BRC-26	Upper Paraguay river basin, Brazil	1782	-16.236074	-56.403351	139
65	Pumin et al. (2015)	BRC-28	Upper Paraguay river basin, Brazil	1783	-15.933417	-56.128678	146
65	Pumin et al. (2015)	BRC-29	Upper Paraguay river basin, Brazil	1784	-15.845387	-56.846956	331
65	Pumin et al. (2015)	BRC-30	Upper Paraguay river basin, Brazil	1785	-15.807032	-56.718341	452
65	Pumin et al. (2015)	BRC-31	Upper Paraguay river basin, Brazil	1786	-15.736972	-56.543542	285
26	Dirks et al. 2016	CHK110	pruit river sub-catchment, Malapa, S	1787	-25.893	27.8	1398
26	Dirks et al. 2016	CHK111	pruit river sub-catchment, Malapa, S	1788	-25.896	27.808	1423
26	Dirks et al. 2016	CHK112	pruit river sub-catchment, Malapa, S	1789	-25.875	27.789	1337
26	Dirks et al. 2016	CHK113	ort river sub-catchment, Malapa, Sou	1790	-25.875	27.78	1292
26	Dirks et al. 2016	CHK118	ort river sub-catchment, Malapa, Sou	1791	-25.838	27.85	1248
26	Dirks et al. 2016	CHK207	dile river catchment, Malapa, South	1792	-25.933	27.905	1282
64	Placzek et al 2014	ADSO-6SD	Atacama dessert, Chile	1793	-24.1153	-68.59555	2913
64	Placzek et al 2014	ADBA-2SD	Atacama dessert, Chile	1794	-23.5335	-69.0796333	2472
64	Placzek et al 2014	ASOI-SD	Atacama dessert, Chile	1795	-24.09328	-70.16883333	1040
64	Placzek et al 2014	ADBA-5SD	Atacama dessert, Chile	1796	-23.40005	-69.46306667	1517
64	Placzek et al 2014	ADSA-1SD	Atacama dessert, Chile	1797	-23.78565	-68.1071	2364
64	Placzek et al 2014	ADSO-3SD	Atacama dessert, Chile	1798	-24.08873333	-70.0597	1057
64	Placzek et al 2014	ADBA-12SDsm	Atacama dessert, Chile	1799	-23.39783333	-69.4624	1527
64	Placzek et al 2014	ADBA-13SD	Atacama dessert, Chile	1800	-23.58311667	-69.27523	1862
64	Placzek et al 2014	ADCA-1SD	Atacama dessert, Chile	1801	-22.6654	-68.4706	3204
64	Placzek et al 2014	ADS0-8BA	Atacama dessert, Chile	1802	-24.1529	-68.547	3128
64	Placzek et al 2014	ADBA-4SD	Atacama dessert, Chile	1803	-23.4037	-69.4623	1565
64	Placzek et al 2014	ADSO-13SD	Atacama dessert, Chile	1804	-24.1955	-68.81	3028
64	Placzek et al 2014	ADBA-6SD	Atacama dessert, Chile	1805	-23.34218333	-69.9295	1009
64	Placzek et al 2014	ADPC-5SD	Atacama dessert, Chile	1806	-24.0728	-70.2038	979
64	Placzek et al 2014	ADSA-3SD	Atacama dessert, Chile	1807	-22.9147	-68.1193	2490
64	Placzek et al 2014	ADPC-1SD	Atacama dessert, Chile	1808	-24.06927	-70.1975	1047
64	Placzek et al 2014	ADSA-2SD	Atacama dessert, Chile	1809	-23.259	-68.0644	2357
64	Placzek et al 2014	ADCT-56	Atacama dessert, Chile	1810	-24.20825	-70.06821667	1979
64	Placzek et al 2014	ADBA-12SDLA	Atacama dessert, Chile	1811	-23.39783333	-69.4624	1527

Mean Basin Slope (°)	Rock Type (general)	Mean Annual Precipitation (mm yr-1)	Mean Annual Temperature (°C)	Vegetation (tree cover %)	Original 10Be Concentration (at g-1)	Original 10Be Concentraion Error (at g-1)
10.8	Mixed	338	22	8	191000	14000
12.4	Mixed	378	22	8	282000	40000
14.9	Mixed	429	21	9	82000	11000
19.3	Mixed	510	21	10	152000	15000
18.6	Mixed	626	19	9	79200	3900
19.2	Mixed	639	19	9	59100	5300
20.8	Mixed	716	18	9	62400	5200
21.4	Mixed	743	18	13	54200	3700
21.1	Mixed	763	18	13	70000	12000
20.1	Mixed	815	17	9	73200	5600
21	Mixed	789	17	10	36800	4300
19.3	Mixed	801	17	15	81800	6200
0.8	Mixed	35	23	0	373000	23000
22.3	Mixed	792	16	12	60000	10000
26.1	Mixed	800	15	13	349000	42000
23.7	Mixed	546	21	8	47700	4900
22.8	Mixed	844	15	5	75000	15000
22.2	Mixed	730	20	7	198000	13000
20.8	Mixed	845	17	5	58400	3900
21.5	Mixed	843	14	26	255000	18000
29.9	Mixed	646	21	13	219000	12000
23.9	Mixed	686	20	10	73400	7100
7.2	Mixed	735	12	5	2233000	54000
29.7	Mixed	686	20	5	34600	4800
17.8	Mixed	262	23	5	62100	4900
20.3	Mixed	751	17	21	58000	12000
18.1	Sedimentary	3265	8	76	27450	745
24.4	Sedimentary	3060	7	79	22310	1162
25.8	Sedimentary	3028	7	80	29770	880
3	Mixed	300	20	8	810000	30000
2.7	Mixed	240	20	3	2950000	80000
8.1	Metamorphic	57	18	5	830000	20000
2.4	Mixed	307	20	6	950000	30000
2.4	Igneous	250	16	6	1840000	50000
12	Igneous	233	16	5	570000	20000
7.5	Mixed	194	21	5	720000	20000
4.3	Mixed	257	19	5	631132	11311
4.3	Mixed	300	9	8	290000	9000
4.3	Mixed	302	9	8	382000	11000
4.4	Mixed	303	9	9	209000	7000
4.4	Mixed	307	9	9	158000	5000
4.8	Mixed	338	19	9	653404	11911
4.9	Mixed	360	19	10	577052	9433
4.3	Mixed	383	19	10	734629	24671
2.9	Mixed	303	19	5	652011	11842
3	Mixed	314	19	5	651451	12471
4.7	Mixed	315	9	72	204000	7000

4.2	Mixed	300	9	8	127000	5000
4.3	Mixed	304	9	8	111000	4000
3.1	Mixed	327	19	6	649777	11808
2.7	Igneous	289	20	5	982071	17565
4.4	Mixed	311	8	9	121000	6000
5	Mixed	358	8	11	269000	8000
5	Mixed	325	8	11	317000	16000
4.2	Mixed	311	8	9	124000	5000
3.4	Mixed	357	19	7	655208	14016
2.7	Mixed	421	19	12	862026	25309
3.6	Mixed	289	8	6	126000	5000
2.9	Mixed	429	19	12	665431	17811
4	Mixed	295	8	7	202000	7000
5.7	Sedimentary	1930	21	45	230713	8435
5.6	Sedimentary	1923	21	44	256434	5845
4.2	Mixed	308	8	7	213000	8000
2.9	Mixed	278	8	5	94000	4000
3.8	Mixed	282	10	6	640000	18000
5.8	Mixed	382	7	16	99000	5000
3.1	Mixed	410	18	9	836078	13491
3.2	Metamorphic	443	18	13	836416	14777
2.4	Mixed	279	8	5	74000	3000
4.4	Mixed	317	8	5	268000	8000
4.4	Mixed	317	8	5	304000	9000
5.9	Mixed	207	19	2	536872	8938
1.5	Igneous	399	19	10	863452	159814
3.1	Mixed	259	9	5	219000	8000
5.4	Mixed	412	6	17	72000	4000
3.1	Mixed	280	8	5	245000	9000
4.1	Sedimentary	316	20	5	339000	31000
2.3	Mixed	272	8	5	87000	4000
3.4	Mixed	260	11	5	708000	21000
5.5	Mixed	363	7	12	344000	11000
5	Mixed	335	8	11	555000	23000
1.5	Igneous	346	19	7	627592	12697
3.8	Sedimentary	318	20	5	251000	20000
3.7	Sedimentary	318	20	5	271000	20000
3.7	Mixed	425	18	10	887690	16003
3	Igneous	748	18	23	222000	18000
6.3	Mixed	452	6	23	49000	3000
5.1	Mixed	325	8	5	159000	6000
5.5	Mixed	376	8	14	117000	7000
7.9	Metamorphic	407	18	9	889801	15393
6.6	Mixed	313	9	8	118000	4000
2.4	Mixed	291	8	5	58000	3000
7.9	Sedimentary	2086	22	50	249084	3761
7.9	Sedimentary	2086	22	50	251487	3368
7.9	Sedimentary	2086	22	50	246089	4259
7.9	Sedimentary	2086	22	50	249677	3656
1.7	Mixed	447	18	14	1133940	20075

4.2	Mixed	301	8	5	388000	14000
3.8	Igneous	394	18	10	653968	13554
4.3	Mixed	288	8	5	375000	13000
6.1	Mixed	379	7	19	558000	21000
4.8	Mixed	431	6	22	2400000	60000
20	Sedimentary	2366	9	80	37000	13000
1.5	Mixed	222	20	1	646570	14470
3.5	Mixed	335	7	5	104000	5000
20.4	Sedimentary	2383	9	80	38000	13000
20.4	Sedimentary	2383	9	80	42000	14000
3.4	Igneous	410	18	10	826250	18397
8.8	Sedimentary	2050	21	44	196561	3232
8.2	Sedimentary	2161	22	67	181189	2985
19.4	Sedimentary	2376	9	80	20000	13000
7.5	Metamorphic	438	15	30	1709392	63051
14.2	Sedimentary	2233	21	80	101792	2649
20	Sedimentary	2385	9	80	44000	10000
4.1	Igneous	746	18	19	146000	14000
17.9	Sedimentary	2352	10	80	83000	11000
17.9	Sedimentary	2351	10	80	31000	16000
18.1	Sedimentary	2362	9	80	40000	15000
17	Sedimentary	2224	22	80	499372	8204
8.2	Metamorphic	433	16	45	991108	41871
6.7	Sedimentary	2160	22	71	172467	5143
6.7	Sedimentary	2160	22	71	183822	3102
17.4	Sedimentary	2336	9	80	42000	6000
19.2	Sedimentary	2398	9	80	39000	9000
5.3	Sedimentary	2162	22	60	189202	3114
14.9	Sedimentary	2320	10	80	49000	18000
19.3	Sedimentary	2213	22	80	60577	2102
20.8	Sedimentary	2457	9	80	37667	14000
20.8	Sedimentary	2457	9	80	41000	14000
20.8	Sedimentary	2457	9	80	34000	15000
20.8	Sedimentary	2457	9	80	38000	13000
3.7	Igneous	259	21	5	601257	10075
12.2	Sedimentary	2204	22	80	130897	2162
10.3	Metamorphic	210	16	5	1427360	26280
23	Sedimentary	2227	23	80	65629	1932
20.5	Sedimentary	2315	22	80	74661	1489
17.9	Metamorphic	187	16	0	665840	11932
24.2	Igneous	206	15	0	796701	14184
21.2	Igneous	187	17	0	862677	15383
12.6	Mixed	172	18	0	683461	14468
11.8	Igneous	165	19	0	909168	19131
6.7	Igneous	222	14	5	654804	11944
1.6	Metamorphic	249	17	0	1606237	28183
12.7	Metamorphic	442	15	42	1228665	40477
8.1	Metamorphic	207	16	5	1144898	20021
13.3	Metamorphic	180	17	5	898302	25724
1.8	Igneous	246	17	0	1753056	30694

10.2	Igneous	173	18	5	559684	18665
3.8	Metamorphic	172	17	0	1249150	41195
12.3	Igneous	169	17	0	1024171	24902
1.3	Igneous	255	17	5	1268894	22416
0.9	Igneous	142	18	0	983395	26428
10.5	Igneous	739	18	17	121000	13000
23.6	Igneous	740	8	49	52000	6000
21.8	Igneous	748	10	48	43000	5000
8.6	Igneous	688	9	12	180600	10000
25.7	Igneous	734	7	50	29000	5000
12.4	Igneous	708	9	16	127700	5800
25.3	Igneous	739	7	50	52000	7000
8	Igneous	700	10	8	215100	9400
20.3	Igneous	753	10	46	56000	4000
23.4	Igneous	747	6	46	131000	13000
23.4	Igneous	747	6	46	152000	17000
23.4	Igneous	747	6	46	120000	11000
23.4	Igneous	747	6	46	121000	11000
27.7	Igneous	697	10	19	7700	1300
21.3	Igneous	746	10	48	52500	8500
21.3	Igneous	747	10	48	46000	11000
21.3	Igneous	748	10	48	59000	6000
21.8	Igneous	703	9	32	26800	2000
27.7	Igneous	714	8	38	74400	5200
24.8	Igneous	697	9	31	20800	1900
33	Igneous	707	9	20	62100	3200
29.2	Igneous	723	10	19	10300	1300
19.4	Igneous	692	7	48	97300	5500
30.9	Metamorphic	716	9	29	10800	1200
18.4	Igneous	770	10	41	47000	7000
16.9	Igneous	682	11	5	110600	7200
23.9	Igneous	661	8	55	50300	2700
23.6	Igneous	684	8	54	62000	3000
32.1	Metamorphic	714	12	38	10100	1100
27.9	Igneous	752	10	57	5600	1100
17.5	Igneous	685	10	5	100900	6100
15.6	Igneous	648	11	5	84200	6500
30.1	Igneous	704	8	61	17000	2000
31	Metamorphic	713	7	63	4700	8600
34.8	Metamorphic	713	8	53	11000	1200
25.8	Metamorphic	674	12	35	42000	3900
9.7	Igneous	2198	23	24	60600	9057
12.8	Igneous	3001	20	72	117571	12100
13.3	Igneous	3001	20	73	114386	11814
4.3	Mixed	1001	10	24	120000	9000
5.5	Mixed	818	7	25	160000	12000
5.9	Mixed	706	4	24	440000	19000
5.8	Mixed	584	1	21	580000	30000
5.6	Mixed	537	0	21	450000	40000
4.9	Mixed	447	-2	16	1095000	41500

4.9	Metamorphic	845.59	1.69	48.19	1140000	47000
4.9	Metamorphic	845.59	1.69	48.19	1050000	36000
5.3	Mixed	883	12	37	170000	12500
5.3	Mixed	883	12	37	200000	16000
5.3	Mixed	883	12	37	140000	9000
4.1	Mixed	891	13	34	100000	6000
7.1	Mixed	728	2	33	130000	16000
7.7	Mixed	965	6	35	70000	6000
2.5	Mixed	1504	17	18	100000	7000
3	Mixed	1335	15	20	120000	9000
2.5	Mixed	1569	18	22	140000	15000
1.3	Mixed	1253	16	8	50000	4000
9.7	Mixed	1141	11	34	40000	3000
1.9	Mixed	1281	15	10	60000	8000
8.4	Mixed	30	23	0	123000	5000
8.4	Mixed	31	23	0	125000	5000
8.4	Mixed	32	23	0	125000	5000
8.4	Mixed	33	23	0	123000	5000
8.3	Mixed	30	23	0	132000	10000
6.9	Metamorphic	30	23	0	123333	7000
6.9	Metamorphic	31	23	0	120000	8000
6.9	Metamorphic	32	23	0	131000	6000
6.9	Metamorphic	33	23	0	119000	7000
5.8	Metamorphic	30	22	0	137000	7500
5.8	Metamorphic	31	22	0	120000	7000
5.8	Metamorphic	32	22	0	127000	7000
5.8	Metamorphic	33	22	0	142000	9000
5.8	Metamorphic	34	22	0	159000	7000
6.2	Igneous	105	22	5	114276	10447
6.1	Igneous	110	21	5	135793	7495
6	Igneous	112	21	5	154444	6361
7.4	Igneous	116	21	5	184715	9131
6.4	Igneous	97	22	5	124484	10699
6.4	Igneous	98	22	5	114601	10596
6.4	Igneous	99	22	5	134367	10803
7.8	Igneous	120	21	5	218972	8081
3.9	Igneous	110	22	5	156371	6095
7	Igneous	99	22	5	116113	7081
9.2	Igneous	125	21	5	216229	9673
8	Igneous	117	21	5	165897	8879
4.2	Sedimentary	279	10	5	119333	13000
8.4	Igneous	103	22	5	83805	5252
6.1	Igneous	96	22	4	125762	7641
5.4	Igneous	107	21	5	153171	14132
6.8	Igneous	105	22	5	191961	11049
6.9	Igneous	97	22	5	123954	6274
4.7	Sedimentary	283	10	5	198000	9000
6.3	Igneous	97	22	5	157606	9770
6.6	Igneous	98	22	5	160561	7699
5.3	Sedimentary	289	9	5	135000	6000

6.2	Igneous	96	22	5	136070	8437
5.3	Sedimentary	289	9	5	174000	9000
7.3	Metamorphic	1135	20	5	340000	11000
8.5	Metamorphic	1392	16	14	1000000	23000
8.4	Metamorphic	1436	16	5	590000	18000
8.7	Metamorphic	1528	18	6	370000	14000
8.6	Metamorphic	1150	21	5	210000	6000
8.3	Metamorphic	1121	20	7	430000	12000
6.2	Metamorphic	1134	20	5	410000	13000
1.45	Mixed	678.00	23.00	6.52	266000	18000
1.35	Mixed	678.00	23.00	6.50	209000	10000
1.41	Mixed	676.02	23.00	7.87	202000	25000
1.43	Mixed	677.24	23.00	8.89	245000	11000
2.68	Mixed	653.59	22.00	9.90	387000	31000
1.45	Mixed	675.41	23.00	8.90	190000	10000
8.5	Mixed	773.68	22.00	34.67	203000	12000
1.78	Mixed	694.93	22.34	7.94	180000	16000
6.17	Mixed	754.52	22.00	31.14	269000	22000
5.73	Mixed	728.11	22.00	25.70	240000	15000
4.62	Mixed	705.57	22.08	20.75	219000	11000
4.13	Mixed	703.36	22.13	18.57	256000	15000
3.73	Mixed	696.83	22.26	17.43	247000	11000
2.91	Mixed	671.27	22.57	20.05	289000	15000
2.94	Mixed	677.66	22.50	19.35	282000	22000
2.9	Mixed	683.45	22.61	16.77	276000	14000
6.73	Mixed	730.65	22.03	16.38	149000	78000
0.9	Mixed	608.18	21.75	18.00	731000	27000
1.41	Mixed	644.33	22.86	12.41	352000	15000
1.25	Mixed	620.00	23.00	17.30	514000	19000
1.21	Mixed	614.95	22.11	17.14	634000	25000
2.4	Mixed	666.14	22.46	15.82	263000	12000
16.8	Sedimentary	860	10	51	9576	1482
18.1	Sedimentary	901	10	63	18354	912
17.7	Sedimentary	905	10	58	11628	2052
17.7	Sedimentary	905	10	58	18354	1482
19.2	Sedimentary	942	9	76	20178	1026
19	Sedimentary	919	9	76	17784	2736
18.1	Sedimentary	951	10	67	16986	2736
18.8	Sedimentary	963	9	62	19152	2052
22.6	Mixed	729	14	49	4200	1100
16.3	Mixed	824	15	46	7900	500
21.7	Mixed	715	14	50	5900	400
16.3	Mixed	796	14	26	2800	300
19.2	Mixed	813	15	34	4100	750
19.2	Mixed	814	15	34	5400	600
19.2	Mixed	815	15	34	2800	900
28.4	Mixed	1458	2	26	38700	6700
24.7	Mixed	1232	4	35	22400	4200
32.7	Mixed	1554	0	18	25000	4400
30.8	Mixed	1311	3	40	50700	9800

26	Mixed	1584	0	12	17100	3000
31.8	Mixed	1356	2	29	24700	4500
31.4	Mixed	1388	2	30	41100	8200
29.8	Mixed	1629	-1	13	14500	2500
31	Mixed	1300	3	48	38700	6800
30.4	Mixed	1747	-2	6	22300	4300
30.7	Mixed	1694	-1	19	19800	3400
27.6	Mixed	1627	0	25	16000	3300
22.2	Mixed	621	12	23	73201	14600
32.5	Mixed	741	10	38	11070	630
32.2	Metamorphic	768	9	37	17150	1670
20.4	Mixed	657	12	26	96740	13990
20.2	Mixed	659	12	25	69030	17250
31.9	Metamorphic	764	9	37	14820	670
30.9	Metamorphic	758	9	41	11680	1390
31.8	Mixed	694	11	42	15050	1400
27.9	Mixed	691	11	28	30450	2380
32.9	Metamorphic	776	9	37	28220	1840
32.1	Mixed	762	12	34	33690	4630
33.1	Metamorphic	782	8	27	11680	1570
25.4	Igneous	741	10	16	42700	2890
32.6	Mixed	648	13	40	18650	2750
29.8	Mixed	508	14	33	15330	560
33.4	Metamorphic	805	9	37	12030	1690
29.5	Mixed	516	13	36	29390	12460
23.1	Mixed	537	13	17	56530	10860
25.8	Mixed	654	12	46	12540	830
22.4	Igneous	796	8	37	110910	6080
30.5	Mixed	579	15	38	23040	2330
27.5	Mixed	564	14	31	32490	1990
28.3	Mixed	518	13	45	22560	760
13.5	Igneous	794	10	19	250690	20680
25.8	Mixed	492	13	20	11550	2640
19.7	Igneous	737	11	43	244330	243440
27.7	Mixed	610	15	51	18560	5210
21.5	Igneous	800	7	34	155050	7650
19.9	Igneous	749	11	50	27150	2540
28.9	Metamorphic	791	7	29	34820	10270
1.7	Metamorphic	458	17	6	43130	2830
26.2	Igneous	679	11	32	93680	3950
31.9	Igneous	627	12	50	29160	4740
29.1	Metamorphic	798	7	35	199290	9520
35.8	Mixed	593	13	50	10260	870
33.9	Mixed	587	13	53	12940	900
12.3	Igneous	796	10	16	102880	12700
23.2	Igneous	784	10	5	78640	4280
31.1	Mixed	617	13	49	16140	1320
24.5	Igneous	632	12	11	52550	3060
14.5	Igneous	804	10	18	94480	4540
22.4	Igneous	661	12	19	23820	2570

18.9	Igneous	746	10	11	138470	9040
15	Igneous	805	10	10	213830	57300
18.5	Igneous	790	8	36	167580	8310
23.2	Igneous	726	11	26	2570	2250
8.8	Igneous	769	10	5	81270	3490
23.3	Metamorphic	789	7	44	103090	4450
9.2	Igneous	770	10	5	89340	5770
9	Igneous	768	10	5	16000	2180
8.7	Mixed	1026	10	48	813862	15338
16.8	Igneous	1144	9	80	187000	6750
16.8	Igneous	1145	9	80	213000	6000
16.8	Igneous	1146	9	80	209000	8000
16.8	Igneous	1147	9	80	187000	9000
16.8	Igneous	1148	9	80	139000	4000
17.3	Metamorphic	1147	10	73	729171	32513
16.2	Igneous	1094	10	80	359862	8625
14.6	Igneous	1069	10	79	487595	10520
12.5	Mixed	1053	10	73	332805	7324
10.6	Mixed	1045	10	77	380207	8347
19.2	Mixed	1098	10	79	671159	12349
15.1	Igneous	1145	9	80	428488	10094
16.7	Igneous	1115	9	80	362424	7784
13.7	Metamorphic	1197	8	80	332717	6933
21.3	Sedimentary	1111	10	74	1167500	152500
21.3	Sedimentary	1111	10	74	1230000	160000
21.3	Sedimentary	1111	10	74	1350000	170000
21.3	Sedimentary	1111	10	74	1210000	160000
21.3	Sedimentary	1111	10	74	1350000	170000
21.3	Sedimentary	1111	10	74	1210000	160000
21.3	Sedimentary	1111	10	74	880000	120000
11	Igneous	1045	11	63	394263	8380
15.9	Metamorphic	1173	9	78	534730	10366
8	Mixed	1000	11	51	1242250	20355
15.4	Metamorphic	1060	11	71	717500	92500
15.4	Metamorphic	1060	11	71	570000	70000
15.4	Metamorphic	1060	11	71	730000	100000
15.4	Metamorphic	1060	11	71	850000	110000
15.4	Metamorphic	1060	11	71	720000	90000
15	Mixed	1026	10	75	1056020	19891
18.4	Mixed	1128	10	78	818823	12646
21	Igneous	1154	9	79	503169	10110
16.4	Igneous	1085	11	80	422521	8403
16.6	Sedimentary	1127	10	73	934511	14468
19.2	Igneous	1101	10	79	457692	9139
18	Igneous	1134	9	78	325720	6571
15.1	Igneous	1070	10	80	522320	10285
11.3	Igneous	1056	12	68	488209	10544
19.7	Mixed	1160	10	79	522736	12825
16.6	Sedimentary	1144	10	70	1005568	14824
15.1	Metamorphic	1159	9	80	824001	14358
24.4	Sedimentary	1122	10	75	695758	35597
11.9	Metamorphic	1084	10	74	1099416	20422

11.9	Metamorphic	1084	10	74	612250	17750
11.9	Metamorphic	1084	10	74	721000	20000
11.9	Metamorphic	1084	10	74	615000	19000
11.9	Metamorphic	1084	10	74	557000	15000
11.9	Metamorphic	1084	10	74	556000	17000
14.3	Igneous	1031	11	39	655439	12312
13.9	Metamorphic	1158	9	80	625662	12462
13.9	Mixed	1117	10	80	423655	9205
10.8	Igneous	1112	10	80	454679	8782
22.4	Sedimentary	1104	10	79	418702	9658
16.8	Metamorphic	1067	10	75	835514	15639
19.6	Sedimentary	1077	10	80	698748	12237
17	Igneous	1073	10	80	275669	6898
8.2	Metamorphic	1172	8	80	1513025	21462
18	Sedimentary	1022	11	74	779880	14890
5.7	Mixed	1074	12	80	506253	12459
10.6	Mixed	1030	11	80	1058720	16091
10.8	Metamorphic	1030	11	80	1085886	16797
15.7	Igneous	1053	11	80	336424	14098
15.3	Metamorphic	1137	10	78	933658	15392
19.5	Sedimentary	1162	10	79	445668	8579
17.9	Metamorphic	1097	10	75	391194	7865
15	Igneous	1054	10	77	713664	12625
19.9	Metamorphic	1095	11	74	614022	16232
19.8	Metamorphic	1095	11	74	717160	13866
14.4	Metamorphic	1129	9	80	877415	18758
16.6	Metamorphic	1097	10	75	937424	33479
14	Metamorphic	1081	11	80	1262680	19046
15.6	Mixed	1554	10	78	10600	800
16.2	Mixed	1534	10	74	25100	2500
16	Mixed	1542	10	80	19000	1200
13.2	Mixed	1678	10	80	29400	2300
14.1	Sedimentary	1184	11	80	31600	2000
13.5	Sedimentary	1170	11	80	44900	3600
16.9	Sedimentary	1184	11	80	48700	3100
14.6	Sedimentary	1226	11	80	33900	2200
14.3	Sedimentary	1181	11	80	43900	4800
12.4	Sedimentary	1189	11	80	33400	2100
8.4	Metamorphic	355	-1	10	157453	4885
7.5	Metamorphic	316	-1	9	390239	19954
11.3	Metamorphic	391	0	20	195657	4999
14.2	Metamorphic	475	-1	15	19641	776
9.7	Metamorphic	598	1	17	22349	960
14.3	Metamorphic	504	2	28	23554	949
10.4	Metamorphic	526	3	41	127553	4669
19	Metamorphic	561	2	12	11761	855
18.3	Metamorphic	591	3	17	15818	564
13	Metamorphic	594	3	16	15810	990
21.6	Metamorphic	599	3	18	7226	353
13.6	Metamorphic	836	9	55	12374	449

22.9	Metamorphic	571	2	23	10630	531
17.6	Mixed	1303.00	6.00	80.00	133000	13000
21.2	Mixed	1297.28	6.05	79.75	76000	5600
19.5	Mixed	1282.53	6.17	79.83	86500	8000
23.8	Mixed	1266.51	6.30	79.86	69600	5800
17.1	Mixed	1182.00	7.00	79.93	152000	11000
17.7	Mixed	1248.47	6.45	79.89	126000	12000
19.8	Mixed	1184.12	6.98	71.97	112000	8200
16.4	Mixed	1183.45	6.99	74.44	143000	11000
19.9	Mixed	1182.81	6.99	76.82	751000	7100
12.2	Mixed	1182.00	7.00	79.29	118000	8400
20.2	Mixed	1182.21	7.00	78.60	74600	10000
19.8	Mixed	1182.19	7.00	78.75	90900	7100
18.5	Mixed	1182.18	7.00	78.81	90400	7500
8.6	Mixed	1303.00	6.00	66.82	165000	12000
14.1	Mixed	1302.27	6.01	75.63	75400	5400
27.7	Sedimentary	888	3	48	34920	680
27.7	Sedimentary	888	3	48	34920	680
27.5	Sedimentary	884	3	48	35310	6480
26.1	Sedimentary	858	3	47	35240	5890
26	Sedimentary	852	3	48	35580	5570
31.4	Sedimentary	952	3	52	36220	7520
31.3	Sedimentary	1052	3	25	44900	8750
31.3	Sedimentary	1052	3	25	48880	8750
30.6	Sedimentary	1077	11	16	19420	5990
22.2	Sedimentary	1044	7	11	26950	6900
27	Sedimentary	977	8	18	22940	7650
23.4	Sedimentary	1051	4	18	29380	7970
22.4	Sedimentary	994	12	6	14270	2910
29.7	Sedimentary	1040	13	26	15560	2340
8.7	Igneous	316	9	5	217500	15000
8.7	Igneous	316	9	5	290000	10000
8.7	Igneous	316	9	5	190000	20000
8.7	Igneous	316	9	5	210000	20000
8.7	Igneous	316	9	5	180000	10000
11.1	Igneous	314	9	5	136667	10000
11.1	Igneous	315	9	5	140000	10000
11.1	Igneous	316	9	5	120000	10000
11.1	Igneous	317	9	5	150000	10000
11.3	Igneous	314	9	5	190000	10000
11.6	Igneous	314	9	5	240000	20000
14.4	Igneous	314	8	5	430000	20000
8.5	Igneous	315	8	5	323333	26667
8.5	Igneous	316	8	5	300000	10000
8.5	Igneous	317	8	5	300000	20000
8.5	Igneous	318	8	5	370000	50000
10	Igneous	317	10	5	310000	30000
16.5	Igneous	314	8	5	340000	20000
6.5	Igneous	314	8	5	480000	20000
6.4	Sedimentary	119	19	0	113000	6000

5.7	Sedimentary	136	18	0	157000	14000
5.8	Sedimentary	139	18	0	166000	8000
8.6	Sedimentary	120	18	0	308000	18000
19.7	Metamorphic	527	-3	11	545990	80426
23.4	Metamorphic	458	-4	15	448257	16764
23.2	Metamorphic	662	0	13	567528	21790
15.7	Metamorphic	508	-2	5	634156	14849
26.7	Metamorphic	522	-1	59	430129	13786
14.8	Metamorphic	532	-3	20	707902	11392
23.9	Metamorphic	515	-1	5	433156	9584
23.9	Metamorphic	515	-1	5	426520	8827
23.9	Metamorphic	515	-1	5	439792	10340
4	Sedimentary	1405	26	19	314500	43500
4	Sedimentary	1405	26	19	260000	40000
4	Sedimentary	1405	26	19	369000	47000
5	Sedimentary	327	20	5	4001000	286000
5.7	Mixed	828	10	45	256957	7600
9	Igneous	801	10	80	153000	11000
9	Igneous	801	10	80	82000	4000
9	Igneous	801	10	80	64000	7000
9	Igneous	801	10	80	175000	11000
7.7	Igneous	799	10	80	92000	7000
4.1	Sedimentary	1407	27	28	88000	6000
4.2	Sedimentary	1407	27	28	70000	6000
2.9	Metamorphic	326	20	5	611000	94500
2.9	Metamorphic	326	20	5	498000	41000
2.9	Metamorphic	326	20	5	624000	148000
6.7	Igneous	801	9	80	258000	12000
6.7	Igneous	801	9	80	251000	12000
6.9	Igneous	804	9	80	307000	23000
21.1	Sedimentary	1748	10	80	55540	4972
6.5	Sedimentary	1408	27	29	148000	10000
2.8	Metamorphic	329	20	5	636000	102000
23.1	Sedimentary	355	19	5	5605000	254000
20.2	Sedimentary	396	18	5	1299000	111000
6.4	Sedimentary	1398	27	24	117000	7000
7.7	Sedimentary	1401	27	22	154000	10000
7.9	Sedimentary	1398	27	24	159000	7000
9.4	Sedimentary	1407	27	30	179000	10000
15.6	Sedimentary	920	13	30	41000	5000
14.4	Sedimentary	920	13	30	63000	5500
14.4	Sedimentary	920	13	30	63000	5000
14.4	Sedimentary	920	13	30	63000	6000
7.3	Mixed	828	10	5	250037	8186
5.5	Mixed	423	-3	14	2661264	52493
5.2	Mixed	405	-3	13	2814015	45255
4.5	Mixed	378	-4	11	3262761	97513
3.6	Mixed	343	-5	6	4139052	76948
3.6	Mixed	344	-5	6	4215088	94795
3.6	Mixed	345	-5	6	4063015	59101

8.4	Mixed	544	-1	12	294362	12158
7.2	Mixed	527	-1	12	307301	10325
7.2	Mixed	527	-1	12	296760	10966
7.2	Mixed	527	-1	12	317841	9684
6.7	Mixed	497	-1	12	404244	12955
6.7	Mixed	497	-1	12	375523	13219
6.7	Mixed	497	-1	12	432965	12691
8.2	Mixed	531	-1	12	402267	15524
8.1	Mixed	517	-1	11	562165	16183
8.1	Mixed	518	-1	11	532386	18243
8.1	Mixed	519	-1	11	591943	14123
8	Mixed	512	-1	11	427659	11859
7.004453	Mixed	504	-1	11	518500	12296
8.5	Mixed	593	1	19	261412	14464
7.2	Mixed	476	-2	9	784949	20449
8.2	Mixed	533	0	16	352419	10543
8.1	Mixed	529	0	16	295439	12621
8	Mixed	522	-1	15	308766	17071
7.5	Mixed	512	-1	14	352113	10049
6.9	Mixed	506	-1	13	399126	18332
8.3	Mixed	536	-1	14	678376	26294
6.3	Mixed	533	-1	5	2120444	58616
6.3	Mixed	567	-1	7	231103	10285
8.2	Mixed	524	2	31	984334	38432
7	Mixed	552	0	7	1772162	37815
6	Mixed	533	-1	5	2078252	62058
7.2	Mixed	535	1	17	948113	30610
7	Mixed	535	1	16	651735	29344
6.6	Mixed	525	1	17	949300	36916
6.7	Mixed	548	0	6	1092820	26768
6.5	Mixed	567	0	26	384297	13299
6.2	Mixed	566	0	26	360619	11421
7.7	Mixed	534	1	13	924199	20444
3.3	Mixed	563	-3	2	111701	7259
14.2	Mixed	653	2	31	70117	5195
6.6	Mixed	519	0	13	881427	39199
6.4	Mixed	518	1	15	782810	33147
3.7	Mixed	561	-3	1	277111	14909
8.1	Mixed	567	-2	12	2768030	67592
5.5	Mixed	573	0	16	105850	5784
6.3	Mixed	551	-1	6	1553608	50391
10.4	Mixed	529	3	34	344713	14531
5.6	Mixed	567	0	29	360839	26401
6.8	Mixed	553	0	5	1237683	50806
14.4	Mixed	552	2	7	367464	15764
19	Mixed	1473	15	60	161438	7129
13.6	Metamorphic	2428	21	43	205000	12000
12.5	Metamorphic	2563	21	42	103000	10000
11.9	Metamorphic	2572	21	42	216000	15000
12.9	Metamorphic	2677	20	41	392000	20000

14.1	Metamorphic	2039	20	45	257000	26000
17.9	Metamorphic	2371	19	46	145000	16000
16	Metamorphic	2570	21	48	264000	16000
14.2	Metamorphic	2554	21	39	241000	21000
11.9	Metamorphic	2030	17	54	400000	78000
19.6	Metamorphic	2321	18	57	230000	17000
16.4	Metamorphic	2575	20	48	207000	30000
13.6	Metamorphic	2675	21	22	266000	16000
13.8	Metamorphic	2663	20	45	313000	19000
12.8	Metamorphic	2052	16	70	258000	34000
7.1	Metamorphic	2618	19	50	349000	53000
14.9	Metamorphic	2446	18	58	1020000	26000
14.3	Metamorphic	2614	21	28	257000	13000
6.9	Metamorphic	2553	19	72	245000	13000
2.1		515.6697209			1830000	75000
7.7		515.6697209			7845000	236000
3.8		515.6697209			3663000	110000
3.4		515.6697209			5183000	156000
2.8		515.6697209			4765000	143000
4.6		515.6697209			2645000	80000
6.4		515.6697209			1592000	48000
6.6		515.6697209			4268000	154000
10.3		515.6697209			4600000	138000
9		515.6697209			4843000	145000
15.8		515.6697209			1365000	90000
17.2		515.6697209			955000	32000
11.4		515.6697209			3117000	94000
10		515.6697209			4109000	123000
7.8		515.6697209			2577000	77000
8.6		515.6697209			1938000	62000
4.5		515.6697209			5687000	216000
8		515.6697209			2681000	81000
6.4		515.6697209			2206000	66000
4.8		515.6697209			437000	16000
14.6	Sedimentary	820	20	75	30200	1700
18.3	Sedimentary	755	17	45	104250	2450
18.3	Sedimentary	755	17	45	136900	3800
18.3	Sedimentary	757	17	45	71600	1100
12.5	Sedimentary	919	21	69	12900	900
10.8	Sedimentary	583	12	6	734700	28800
14	Sedimentary	862	20	75	26200	1500
15.2	Sedimentary	1829	22	79	35550	1500
15.2	Sedimentary	1829	22	79	36400	1800
15.2	Sedimentary	1829	22	79	34700	1200
14.2	Sedimentary	1812	22	76	51100	3500
15.8	Sedimentary	797	21	77	15800	2050
15.8	Sedimentary	797	21	77	15600	1300
15.8	Sedimentary	797	21	77	16000	2800
13.9	Sedimentary	797	21	73	16300	1300

16.2	Sedimentary	929	20	74	10400	900
15.6	Sedimentary	975	22	75	2700	500
17.1	Sedimentary	1831	23	79	5200	600
20	Sedimentary	1552	20	79	41200	1800
20	Sedimentary	1553	20	79	54700	2100
20	Sedimentary	1554	20	79	27700	1500
21	Sedimentary	865	20	80	11400	1100
25.3	Sedimentary	832	18	60	267900	17900
25.3	Sedimentary	832	18	60	288600	8400
25.3	Sedimentary	832	18	60	247200	27400
21.5	Sedimentary	927	20	74	9600	500
27.5	Sedimentary	778	21	72	20900	2200
17.9	Igneous	509	1	46	147000	8000
20.8	Igneous	571	3	68	132000	7000
18.3	Igneous	594	3	74	105000	4000
13.8	Igneous	733	3	77	275000	9000
16.6	Igneous	753	2	79	260000	9000
11.3	Igneous	682	2	76	303000	10000
11.5	Igneous	719	2	73	465000	13000
10.3	Igneous	700	2	73	467000	12000
15.2	Igneous	725	2	80	272000	7000
16.2	Igneous	719	3	80	312000	9000
22.3	Igneous	661	3	63	122000	6000
23.1	Igneous	664	3	63	130000	7000
22.5	Igneous	675	2	66	126000	5000
22.3	Igneous	672	2	59	118000	7000
15.2	Igneous	582	3	48	172000	11000
22	Igneous	687	1	65	115000	5000
13.5	Igneous	720	3	80	264000	13000
21.2	Igneous	664	3	54	141000	5000
16.2	Igneous	717	2	80	271000	11000
16	Igneous	601	3	46	161000	6000
16.5	Igneous	569	4	54	92000	4000
12.2	Igneous	568	4	52	187000	7000
13.2	Igneous	558	4	52	206000	9000
12.8	Igneous	717	3	80	294000	11000
17	Igneous	731	2	80	248000	8000
23.8	Igneous	661	3	50	123000	5000
14.9	Igneous	729	2	80	258000	9000
15.7	Igneous	728	3	80	309000	15000
17.3	Igneous	712	2	80	246000	9000
13.4	Igneous	738	2	80	436000	15000
22.2	Igneous	566	4	72	288000	11000
13.1	Igneous	708	3	80	286000	9000
11.8	Mixed	196	7	3	867000	49500
11.8	Mixed	196	7	3	866000	54000
11.8	Mixed	196	7	3	868000	45000
12	Mixed	217	6	4	975000	40000
11.5	Mixed	249	5	4	1120000	114000
11.5	Mixed	249	5	4	1069000	56000

11.5	Mixed	249	5	4	1033000	180000
11.5	Mixed	249	5	4	1258000	106000
8.4	Mixed	292	4	5	2373000	149000
8.7	Mixed	291	4	5	2435000	306000
19.2	Metamorphic	1663	9	80	295000	0
19.2	Metamorphic	1663	9	80	279500	9000
19.2	Metamorphic	1663	9	80	264000	10000
18.9	Metamorphic	1681	9	80	310000	9000
12.5	Metamorphic	1525	11	79	362000	11000
16.8	Metamorphic	1605	10	80	264000	7000
17	Metamorphic	1600	9	80	379000	11000
19.8	Metamorphic	1644	9	80	234000	7000
16.4	Metamorphic	1563	11	79	267000	7000
20.1	Metamorphic	1593	9	80	225000	7000
17.7	Metamorphic	1682	10	80	318000	10000
18.7	Metamorphic	1663	10	80	316000	8000
17.8	Metamorphic	1681	9	80	240000	8000
20.8	Metamorphic	1620	9	80	234000	6000
18.6	Metamorphic	1722	9	80	359000	11000
21.1	Metamorphic	1653	9	80	247000	8000
20.7	Metamorphic	1677	9	80	242000	6000
17.6	Metamorphic	1674	10	80	341000	11000
17.8	Metamorphic	1783	8	80	452000	11000
20.7	Metamorphic	1696	9	80	325000	9000
21.1	Metamorphic	1655	9	80	200000	6000
19.1	Metamorphic	1697	10	80	363000	12000
16.3	Metamorphic	1658	10	80	309000	9000
17.1	Metamorphic	1807	8	80	434000	11000
17.5	Metamorphic	1733	9	79	301000	9000
20.6	Metamorphic	1749	8	80	341000	9000
16.8	Metamorphic	1559	11	80	295000	12000
20.5	Metamorphic	1800	8	80	178000	6000
18.3	Metamorphic	1598	10	80	312000	8000
16.3	Metamorphic	1641	10	80	282000	10000
19.3	Metamorphic	1657	9	80	317000	8000
19.4	Metamorphic	1783	8	80	256000	8000
17.9	Metamorphic	1652	9	80	376000	11000
22.3	Metamorphic	1513	10	80	191000	5000
18.7	Metamorphic	1661	9	79	224000	7000
21.7	Metamorphic	1649	9	80	297000	9000
20.2	Metamorphic	1691	9	80	274000	8000
19.5	Metamorphic	1801	8	80	278000	7000
17.3	Metamorphic	1652	9	80	335000	9000
17.3	Metamorphic	1633	10	80	361000	12000
17.6	Metamorphic	1727	8	80	461000	12000
17.1	Metamorphic	1644	9	80	322000	9000
6.4	Mixed	1229	6	61	117000	13000
9.9	Mixed	1279	6	71	172000	16000
11.3	Igneous	1299	6	70	166000	16000
11.2	Igneous	1314	6	73	77000	10000

5.1	Mixed	1221	6	72	200000	16000
11.6	Igneous	1300	6	69	199000	21000
10.5	Igneous	1354	6	11	119000	14000
10	Igneous	1344	6	79	261000	23000
3.3	Sedimentary	1210	6	80	686000	41000
8.7	Igneous	1347	6	80	269000	26000
3.4	Sedimentary	1225	6	80	658000	37000
4	Mixed	1170	7	79	454000	26000
14.7	Igneous	1360	5	71	219000	23000
8.2	Igneous	1245	6	80	228000	17000
3	Igneous	1204	6	75	439000	32000
9.1	Igneous	117	21	0	168000	9000
23.4	Igneous	135	20	0	162000	5000
15.2	Igneous	136	21	0	148000	5000
22.6	Igneous	127	21	0	143000	4000
22.5	Igneous	144	20	5	131000	5000
22.6	Igneous	131	20	0	140000	4000
12.5	Igneous	179	19	5	128000	4000
12.7	Igneous	154	20	5	462000	18000
10.9	Igneous	172	19	5	132000	4000
13.3	Igneous	3044	24	79	25600	1600
13.4	Igneous	3067	24	79	22200	1500
13.2	Igneous	3074	24	79	27900	2300
12.6	Igneous	3104	24	79	27600	1700
11.9	Igneous	3085	24	79	32100	2100
14	Igneous	3141	23	80	27200	1500
10.2	Igneous	3134	23	79	30000	1700
14.6	Igneous	3015	24	79	24100	2200
10.5	Igneous	3139	23	79	37100	1800
9.8	Igneous	3136	23	80	30400	1800
8.1	Igneous	3186	23	77	52200	2800
11.6	Igneous	3209	23	80	25500	1500
9	Igneous	3136	23	80	29500	1700
10.6	Igneous	3222	23	80	37800	2200
15.9	Igneous	2913	24	80	45500	4500
11.6	Igneous	2969	24	80	28600	1500
11.2	Igneous	3078	24	80	21000	1500
13.1	Sedimentary	139	16	5	459000	15000
6.4		2157.026297			184000	3000
6.4		2157.026297			172000	5000
17		2052.697711			102000	3000
22		2052.697711			231000	1000
8.6		2157.026297			231000	8000
20		2052.697711			499000	8000
11		2157.026297			181000	3000
12		2157.026297			197000	3000
11		2157.026297			251000	3000
11		2157.026297			248000	4000
8.5		2157.026297			256000	6000

6.8		2157.026297			189000	3000
16		2157.026297			131000	2000
22		2052.697711			61000	2000
24		2052.697711			66000	2000
17.3	Sedimentary	1265	6	79	13800	3200
17.3	Sedimentary	1310	6	79	15900	5100
29.1	Metamorphic	1955	-1	6	7400	1900
19	Sedimentary	1315	6	80	20300	2300
18.7	Sedimentary	1320	5	80	30100	3300
29.1	Metamorphic	1906	0	19	15800	3900
27.5	Metamorphic	1809	0	17	46700	4700
19.4	Sedimentary	1379	5	80	25400	2900
15.9	Sedimentary	1247	6	79	16400	2000
16.2	Sedimentary	1314	6	79	29300	3300
28.2	Metamorphic	1884	-1	38	64500	9100
24.4	Metamorphic	1856	-1	11	41400	4400
23.4	Metamorphic	1885	-1	19	233000	15000
26.3	Metamorphic	1818	0	16	54400	6900
25.7	Metamorphic	1884	-1	5	86300	9600
16.2	Sedimentary	1294	6	80	20800	2200
23.5	Metamorphic	1850	-1	36	30400	4800
27.9	Metamorphic	1843	-1	39	20100	4200
18.2	Sedimentary	1345	6	78	25900	8500
18.4	Sedimentary	1330	6	80	25667	2833
18.4	Sedimentary	1330	6	80	28500	3100
18.4	Sedimentary	1330	6	80	23200	2600
18.4	Sedimentary	1330	6	80	25300	2800
25	Metamorphic	1839	-1	32	11800	2500
19.5	Sedimentary	1396	5	80	32500	2700
21.6	Sedimentary	1322	6	80	29400	3100
28.2	Metamorphic	1843	-1	16	57800	5800
22.5	Sedimentary	1381	5	80	23200	2600
27.5	Metamorphic	1731	1	47	17200	4100
20.5	Metamorphic	2035	-3	5	145900	9900
19.8	Metamorphic	2089	-3	5	134000	13000
20.6	Metamorphic	2105	-3	5	233000	17000
23.5	Metamorphic	2041	-3	5	140000	13000
13.1	Igneous	705	2	18	1024500	33400
31.5	Igneous	867	4	66	98800	4200
25.8	Igneous	827	2	60	412200	11200
18.9	Metamorphic	696	2	51	228100	9100
33	Igneous	976	4	46	65800	2400
26.3	Igneous	900	0	32	124200	5400
18.6	Igneous	723	0	49	968400	16100
28.5	Igneous	749	4	74	346000	14100
31.7	Igneous	986	10	70	96500	8600
7.4	Metamorphic	857	1	15	914200	29600
26.8	Metamorphic	952	2	73	100200	3600
21.7	Igneous	900	2	31	808600	20300
31.2	Igneous	811	3	69	99100	4800

24.3	Metamorphic	741	2	22	174900	6200
28	Metamorphic	804	4	63	275550	8850
28	Metamorphic	804	4	63	318500	11000
28	Metamorphic	804	4	63	232600	6700
33.8	Igneous	834	4	71	27900	1800
15	Metamorphic	872	1	33	1418700	24500
22.9	Metamorphic	683	-1	28	407750	13600
22.9	Metamorphic	683	-1	28	455900	15000
22.9	Metamorphic	683	-1	28	359600	12200
25.3	Metamorphic	697	2	55	358300	12400
23.9	Metamorphic	696	-1	48	272000	6100
25.6	Igneous	715	0	30	274300	6500
34.9	Igneous	909	6	73	84400	3700
16.7	Metamorphic	677	-1	32	769800	30000
27.1	Igneous	892	0	37	196000	8500
26.4	Metamorphic	725	-1	11	389800	12400
6.1	Igneous	879	1	8	1087600	19400
34.2	Igneous	845	6	75	45800	1800
30.9	Igneous	990	5	72	94600	4300
29.2	Igneous	801	4	74	267600	7500
20.1	Metamorphic	725	1	27	548000	14600
37.1	Igneous	959	9	78	14300	1700
28	Metamorphic	931	0	53	204800	7200
23.1	Igneous	874	0	35	142200	8100
26	Igneous	938	0	37	202300	5800
29.5	Igneous	789	3	75	211500	5300
30.2	Igneous	946	13	57	42400	4900
33.3	Igneous	771	4	78	127300	5000
4.3	Igneous	921	0	20	1805000	48900
23.8	Metamorphic	924	1	52	756300	22100
29.7	Igneous	696	4	61	370200	8300
21.1	Metamorphic	837	1	30	203000	6000
15.6	Igneous	836	3	9	1581800	46300
34.8	Igneous	1014	6	32	66500	3400
24	Metamorphic	708	0	47	314800	10000
28.1	Igneous	740	3	66	189300	10000
27.9	Igneous	772	0	52	267900	8800
35.5	Igneous	985	2	52	74300	3600
27.8	Igneous	761	6	77	170900	4500
35.3	Igneous	960	9	55	31200	1600
22.7	Igneous	1110	7	51	11500	1100
32.1	Igneous	949	7	73	89600	3600
21.4	Metamorphic	836	3	19	763700	15500
34.9	Igneous	871	1	66	78300	5200
25.3	Igneous	735	0	42	472800	9500
29.5	Metamorphic	837	3	68	112300	3600
10	Metamorphic	861	1	5	633600	13200
31.7	Igneous	842	5	75	178000	6600
32	Igneous	1018	10	38	52600	2200
22.1	Metamorphic	867	1	33	366000	12900

32.1	Igneous	911	13	28	19500	1700
9.9	Metamorphic	885	0	17	900600	19700
19.5	Igneous	865	6	75	57700	3700
16.2	Mixed	251	1	6	178000	20000
21.9	Sedimentary	216	1	5	39000	16000
22.7	Mixed	285	0	5	125000	15000
16.7	Sedimentary	195	2	5	98000	17000
18.3	Sedimentary	185	3	5	159000	21000
17.6	Sedimentary	188	2	5	98000	16000
22	Mixed	235	0	5	87000	14000
20.9	Metamorphic	276	0	5	191000	25000
20.9	Metamorphic	276	0	5	174000	24000
20.9	Metamorphic	276	0	5	208000	26000
8.4	Sedimentary	142	6	4	371000	43000
14.2	Sedimentary	165	4	5	188000	27000
16.6	Sedimentary	162	5	5	52500	13500
16.6	Sedimentary	162	5	5	70000	15000
16.6	Sedimentary	162	5	5	35000	12000
23.2	Metamorphic	200	2	5	89000	16000
19.1	Mixed	185	4	1	76000	18000
6.5	Sedimentary	132	6	3	267000	29000
9.3	Sedimentary	153	5	4	91000	15000
23	Metamorphic	195	2	5	112000	16000
10.2	Sedimentary	151	5	5	118000	16500
10.2	Sedimentary	151	5	5	102000	15000
10.2	Sedimentary	151	5	5	134000	18000
8.1	Sedimentary	138	6	5	25000	14000
11.5	Sedimentary	127	7	0	22300	8200
14	Metamorphic	136	6	5	96000	13000
17.7	Sedimentary	155	5	5	40800	8800
26.8	Metamorphic	210	3	5	89000	16000
26.8	Metamorphic	210	3	5	108000	17000
26.8	Metamorphic	210	3	5	70000	15000
13.6	Sedimentary	147	6	5	29000	13000
15.7	Sedimentary	868	13	77	26700	1600
16.2	Sedimentary	811	13	67	22700	1600
14.4	Sedimentary	800	12	48	23700	1800
16.8	Sedimentary	889	12	80	19400	1300
16.1	Sedimentary	923	12	79	59300	5300
4.4	Igneous	16	11	2	20260000	460000
4.5	Igneous	16	11	3	8840000	300000
3.7	Igneous	12	14	0	6920000	210000
3.6	Igneous	12	14	0	10400000	190000
8	Igneous	4	14	2	6470000	260000
5.9	Igneous	33	9	4	8040000	580000
8.2	Igneous	21	8	3	15380000	540000
9	Igneous	5	16	4	6770000	610000
15.1	Mixed	275	17	13	137000	14000
11.9	Sedimentary	387	16	18	163757	12750
13.8	Sedimentary	407	15	23	92868	10832

15	Sedimentary	408	15	22	626009	46485
15	Sedimentary	408	15	22	682778	52396
15	Sedimentary	408	15	22	569241	40574
14.8	Sedimentary	408	15	22	317983	32945
20.3	Metamorphic	817	8	5	10500	2700
21	Metamorphic	853	8	5	14200	3500
21.3	Metamorphic	904	7	5	11000	1000
18.1	Metamorphic	824	8	5	17000	1000
14.1	Metamorphic	838	8	5	397000	45000
12.7	Metamorphic	917	8	5	650000	25000
20.3	Metamorphic	962	6	5	211000	11000
7.3	Sedimentary	999	8	72	128899	5648
8	Sedimentary	1009	9	70	219838	10315
7.7	Sedimentary	997	9	77	468240	14504
3.2	Mixed	1033	11	39	246188	8239
3.2	Mixed	1086	10	32	184442	5960
5.3	Sedimentary	1107	9	61	263900	8634
6.4	Sedimentary	1118	8	73	242597	8345
11.8	Sedimentary	1083	7	80	221594	10099
7.5	Sedimentary	1002	9	63	258375	8288
4.7	Mixed	1062	10	24	260956	8193
4.9	Sedimentary	1047	10	49	192281	6291
8.1	Sedimentary	1042	10	70	346742	10808
7.5	Sedimentary	1026	9	67	490938	15285
3.5	Mixed	1093	10	23	173767	5851
4.8	Sedimentary	1002	9	44	314446	9782
2.2	Mixed	1082	11	12	298671	9377
2.1	Mixed	1044	11	12	334063	10388
6.8	Sedimentary	1026	10	74	481188	26325
3.2	Metamorphic	1102	10	21	300399	10178
9.4	Sedimentary	1054	7	80	245627	10634
3.6	Sedimentary	1130	10	65	355968	11825
4.9	Sedimentary	1049	8	80	200677	7824
12.6	Sedimentary	1046	9	79	383304	10751
4.1	Metamorphic	1111	10	33	433082	13904
3.6	Metamorphic	1101	11	48	380355	10594
4.2	Sedimentary	1054	7	78	375191	11560
2.6	Sedimentary	1096	7	80	457999	15264
2.7	Sedimentary	989	9	31	307621	11301
5.2	Sedimentary	1058	10	53	227316	10329
15.4	Sedimentary	1063	7	80	149983	8907
3.6	Sedimentary	1056	8	80	526496	14588
5.5	Metamorphic	1088	10	37	412688	12205
7.5	Sedimentary	1109	6	80	347370	11558
16.7	Sedimentary	1041	7	80	148010	7089
7.3	Sedimentary	1016	8	74	247895	13324
14	Sedimentary	1066	7	80	228363	8038
5.1	Sedimentary	1087	7	80	348755	12150
6.5	Sedimentary	1053	7	79	351631	12576
5.4	Sedimentary	1009	9	76	468412	15564

4.7	Metamorphic	1084	10	45	367538	11857
5	Metamorphic	1083	10	63	395062	12225
12.8	Sedimentary	1051	7	80	236567	10930
7.3	Sedimentary	1060	10	75	190707	5620
4.5	Metamorphic	1079	11	51	372548	11576
3.3	Metamorphic	1101	11	70	283104	7558
10.2	Sedimentary	1052	7	80	254724	8995
4.1	Metamorphic	1092	10	32	376441	11952
4.2	Sedimentary	1042	9	63	525364	18147
12.7	Sedimentary	1048	9	78	289935	8549
7.9	Sedimentary	1036	6	80	166509	8260
3.5	Metamorphic	1079	11	66	604858	20465
12.7	Sedimentary	1045	7	80	122066	7231
11.4	Sedimentary	1097	7	80	140802	7170
4.8	Metamorphic	1067	10	76	406983	13547
3.6	Sedimentary	1048	7	79	369524	12310
5.2	Sedimentary	1076	8	80	335221	9413
5.4	Sedimentary	1015	9	80	956312	24512
12.4	Sedimentary	1080	8	80	271829	11085
13.6	Sedimentary	1056	8	80	159739	6625
17.7	Sedimentary	1071	7	80	92307	5806
10.2	Sedimentary	1104	7	80	226187	9902
8.1	Sedimentary	1052	8	80	334049	10145
4.1	Sedimentary	1122	6	80	272911	8831
15.9	Sedimentary	1069	6	80	131392	8528
15.3	Sedimentary	1051	8	76	199937	7269
11.2	Sedimentary	1067	7	80	712165	19272
3.1	Sedimentary	1091	7	80	747159	19521
3.3	Sedimentary	1007	9	80	586240	19651
4.8	Sedimentary	1056	7	80	516210	14232
10.8	Metamorphic	1013	9	80	199993	11171
3.3	Metamorphic	1081	11	64	594961	25704
8.5	Sedimentary	1029	8	80	869883	23392
3.6	Sedimentary	1139	8	80	521875	14003
18.4	Sedimentary	1063	7	80	187297	14016
6.6	Sedimentary	985	9	80	426230	12610
8.4	Sedimentary	993	9	80	381397	20540
3.2	Sedimentary	1056	7	79	281435	8154
2.9	Sedimentary	1056	7	77	552113	17486
1.6	Sedimentary	1064	7	80	782941	31106
12.2	Igneous	446	6	46	591500	41100
15.1	Igneous	431	6	42	235100	12900
11.9	Igneous	647	6	58	417000	26400
10.4	Igneous	450	6	54	303000	19200
20.1	Igneous	696	7	78	1587000	89200
22.9	Igneous	711	7	80	318900	24200
5.8	Igneous	265	14	5	205400	20600
9.4	Igneous	664	6	72	400800	27400
20.3	Igneous	1457	12	67	256200	16900
14.1	Igneous	711	7	80	506300	27500

7.5	Igneous	623	6	52	497500	32300
7.7	Igneous	482	5	51	435100	13700
29.7	Igneous	747	5	79	277000	21800
5.1	Igneous	1275	11	55	275100	18500
19.4	Igneous	248	15	5	164700	19400
7.6	Igneous	670	6	56	822400	47200
14.7	Igneous	309	13	5	206700	25000
42.8	Igneous	1049	8	80	96300	7700
40.5	Igneous	1049	8	80	90500	7500
6.7	Igneous	1111	8	80	180700	11200
9.5	Igneous	495	5	32	396100	12700
8.1	Igneous	431	6	24	256000	12400
29.4	Igneous	280	14	5	304000	24200
22.4	Igneous	280	14	5	229000	19200
6.5	Igneous	264	14	5	261200	20800
11.9	Igneous	1457	12	77	341200	21500
3.2	Igneous	1182	11	80	552300	31400
3	Igneous	1206	11	80	475800	30500
6.8	Igneous	1111	8	80	171900	10500
12.2	Igneous	1111	8	80	151500	11600
3.9	Igneous	1110	8	80	171700	12300
7	Igneous	652	6	59	346700	24200
19.6	Igneous	635	6	80	328400	19800
10.1	Igneous	635	6	80	532800	34900
5.9	Igneous	613	6	58	418900	30700
24.1	Igneous	661	6	57	312200	21500
18.1	Igneous	648	6	80	622100	35400
6.6	Igneous	450	6	37	409000	19300
5.6	Igneous	440	6	26	253800	12200
5.4	Igneous	440	6	26	311800	28700
4.3	Igneous	431	6	22	323900	20900
5.4	Igneous	431	6	22	282600	21600
4.2	Igneous	688	7	80	167500	12100
9.3	Igneous	747	5	80	606300	37300
12.9	Igneous	708	7	79	395600	22700
27.2	Igneous	360	12	5	134300	33100
19.8	Igneous	322	13	5	139300	21800
14.3	Igneous	2947	20	75	66000	4000
12.8	Igneous	2969	20	72	108000	6000
14.4	Igneous	2979	21	74	41000	3000
11.8	Igneous	3004	21	76	96000	7000
14.2	Igneous	2941	20	74	129000	8000
16.2	Igneous	2986	20	73	122000	9000
20.5	Mixed	1307	17	51	21466	1185
22	Mixed	1140	16	44	89004	3417
24.6	Metamorphic	799	12	28	46946	2967
25.4	Mixed	939	13	31	75514	3243
22	Sedimentary	618	10	12	53872	2396
22	Sedimentary	618	10	12	52845	2606
22	Sedimentary	618	10	12	54899	2185

23.6	Metamorphic	1245	18	59	55880	3700
24.6	Mixed	865	12	20	89171	3327
24.1	Mixed	828	11	15	89110	2968
26.7	Metamorphic	1011	14	41	33070	2307
26.2	Metamorphic	949	12	37	32534	1779
25.9	Metamorphic	1131	17	48	41700	2452
28.1	Metamorphic	1037	15	49	36474	2973
27.5	Mixed	850	11	46	52434	2700
18.9	Metamorphic	496	7	7	134207	4332
28.8	Metamorphic	703	9	32	46659	2761
27.6	Metamorphic	1089	17	61	58620	7796
27.6	Metamorphic	717	7	22	66577	3329
27.9	Metamorphic	892	13	45	18899	1492
28.4	Metamorphic	785	11	41	30501	2414
25.5	Metamorphic	1241	20	72	38226	2572
26.5	Mixed	816	10	30	90797	3028
27.2	Sedimentary	757	11	69	57124	5019
23.9	Metamorphic	1311	19	72	32297	2617
27.6	Metamorphic	982	15	58	48428	3182
26.1	Sedimentary	657	4	14	57964	2628
29.1	Metamorphic	1249	18	67	53260	3417
22.7	Sedimentary	680	5	6	35337	2109
25.8	Metamorphic	694	6	27	48125	2387
26.4	Metamorphic	1208	19	65	103468	7887
15.1	Metamorphic	472	7	6	119512	5683
24.2	Metamorphic	1161	18	37	81173	3772
26.9	Metamorphic	630	6	16	51780	2261
24.1	Metamorphic	622	6	21	85676	3371
22.4	Sedimentary	941	15	65	69926	4736
24.6	Sedimentary	685	7	5	78304	6234
24.4	Metamorphic	1072	17	53	44659	2604
27.1	Metamorphic	763	11	30	45685	3290
27	Sedimentary	733	10	22	30668	2365
24.8	Sedimentary	689	6	13	131582	8091
30	Metamorphic	1077	16	50	38057	3054
16.9	Metamorphic	1384	20	74	153546	5040
28.1	Metamorphic	656	8	36	64187	5493
30.5	Sedimentary	916	15	76	76581	3911
30.5	Sedimentary	916	15	76	77350	4571
30.5	Sedimentary	916	15	76	75812	3251
25.2	Sedimentary	704	9	9	38628	3736
27.6	Metamorphic	1199	19	64	24294	3018
32.9	Sedimentary	903	15	78	97954	4111
32.9	Sedimentary	903	15	78	93362	3428
32.9	Sedimentary	903	15	78	102546	4794
25.9	Metamorphic	1207	20	69	93577	5342
16.6	Sedimentary	704	9	5	36143	3468
4.8	Mixed	746	9	32	139750	9000
4.8	Mixed	746	9	32	140000	18000
4.8	Mixed	746	9	32	139500	0

5.3	Mixed	759	9	30	176000	18000
5.7	Mixed	766	9	36	176000	21000
4	Sedimentary	915	9	31	91250	4500
4	Sedimentary	915	9	31	97000	9000
4	Sedimentary	915	9	31	85500	0
4	Sedimentary	917	9	31	142000	11000
4.3	Sedimentary	927	8	32	395333	22000
4.3	Sedimentary	927	8	32	235000	35000
4.3	Sedimentary	927	8	32	165000	20000
4.3	Sedimentary	927	8	32	786000	11000
5.4	Mixed	777	9	32	201000	42000
4.3	Sedimentary	912	9	33	196000	30000
6.2	Mixed	753	9	42	154250	9500
6.2	Mixed	753	9	42	157000	19000
6.2	Mixed	753	9	42	151500	0
6.5	Mixed	753	8	44	153000	19000
6.5	Mixed	753	8	44	144000	17000
6.5	Mixed	753	8	44	162000	21000
5.9	Sedimentary	780	8	38	77000	2667
5.9	Sedimentary	780	8	38	75000	7000
5.9	Sedimentary	780	8	38	67000	0
5.9	Sedimentary	780	8	38	89000	1000
6.7	Mixed	753	8	46	133000	15000
6.1	Mixed	786	9	34	215000	21000
5.7	Sedimentary	781	8	37	55000	3500
5.7	Sedimentary	781	8	37	56000	7000
5.7	Sedimentary	781	8	37	54000	0
5.7	Sedimentary	781	8	37	56000	7000
5.7	Sedimentary	781	8	37	54000	0
4.5	Sedimentary	916	9	38	154000	14000
4.4	Sedimentary	893	9	36	252000	25000
7.6	Mixed	746	8	50	155000	11000
7.1	Mixed	786	8	44	137000	16000
8.2	Mixed	755	8	50	117000	13000
6.2	Sedimentary	816	8	38	49000	5000
7.2	Mixed	790	8	47	109000	12000
8.7	Mixed	770	8	57	155000	13000
4.1	Sedimentary	807	9	32	304000	27000
6	Sedimentary	882	8	37	63000	9000
6	Sedimentary	882	8	37	70000	7000
7.5	Mixed	825	6	52	231000	33000
5	Mixed	788	9	42	189000	16000
8	Mixed	851	6	54	244000	19000
8.5	Mixed	803	7	64	171500	18500
8.5	Mixed	803	7	64	178000	20000
8.5	Mixed	803	7	64	165000	17000
4	Mixed	765	10	28	242000	15000
8.2	Mixed	747	8	63	162000	14000
1.5	Mixed	664	11	28	194000	16000
9.2	Mixed	927	6	66	248000	19000
9.2	Mixed	927	6	66	245000	24000
9.2	Mixed	927	6	66	245000	17000

9.2	Mixed	927	6	66	254000	16000
9.1	Mixed	953	6	67	293000	21000
3.8	Sedimentary	841	9	30	212000	15000
5.4	Sedimentary	986	7	34	71000	9000
8.7	Mixed	763	8	69	215000	26000
5.9	Mixed	770	9	35	215000	15000
3.9	Mixed	764	10	51	381000	23000
4.8	Sedimentary	1015	7	36	133000	12000
8.7	Mixed	872	6	70	120000	15000
6.8	Mixed	758	7	47	268000	21000
1.7	Mixed	743	10	12	385000	28000
10.6	Sedimentary	989	7	80	144000	18000
10	Mixed	1028	5	76	249000	18000
10.2	Mixed	857	6	77	245000	26000
10.6	Mixed	887	6	67	237000	17000
3	Mixed	760	10	55	700000	39000
10.8	Mixed	1031	5	79	255667	32000
10.8	Mixed	1031	5	79	269000	52000
10.8	Mixed	1031	5	79	262000	21000
10.8	Mixed	1031	5	79	236000	23000
2.3	Mixed	695	10	15	243000	21000
10.3	Mixed	772	7	71	165000	19000
9.3	Mixed	1047	5	75	291000	22500
9.3	Mixed	1047	5	75	291000	23000
9.3	Mixed	1047	5	75	291000	22000
7.7	Mixed	867	5	78	254000	25000
8.3	Mixed	897	6	80	337000	26000
9.2	Mixed	828	6	75	236000	22000
22.6	Igneous	734	4	46	173000	3900
22.8	Igneous	699	5	34	223500	7200
25.6	Igneous	713	4	22	196100	7400
23.3	Igneous	733	4	16	157300	4400
26.6	Igneous	685	5	11	128400	3900
27.1	Igneous	691	5	10	273300	7100
25.9	Igneous	747	4	44	227000	6200
30	Igneous	872	2	26	119200	3100
30	Igneous	872	2	26	120200	3100
30	Igneous	872	2	26	118200	3100
23.4	Igneous	701	4	10	239800	6200
27.4	Igneous	803	4	15	182200	7900
36.3	Metamorphic	903	2	44	109300	9100
35	Igneous	822	4	53	50700	7100
33.6	Igneous	899	2	58	29300	2200
35.3	Igneous	930	2	51	49100	3400
9.1	Metamorphic	1217	10	75	269000	8000
9.5	Metamorphic	1165	11	76	375250	11500
9.5	Metamorphic	1165	11	76	373000	12000
9.5	Metamorphic	1165	11	76	368000	12000
9.5	Metamorphic	1165	11	76	324000	10000
9.5	Metamorphic	1165	11	76	436000	12000

10.7	Metamorphic	1310	13	79	251000	7000
12.7	Metamorphic	1323	12	78	211000	8000
11.2	Metamorphic	1255	12	76	704000	20000
9.7	Metamorphic	1375	13	73	321000	9000
13.7	Metamorphic	1363	11	78	422000	12000
14.7	Metamorphic	1332	12	80	197000	7000
5.7	Metamorphic	1209	10	62	680000	24000
16.2	Metamorphic	1316	12	80	188000	6000
14.2	Metamorphic	1203	11	80	331000	11000
16.3	Metamorphic	1236	11	79	181000	6000
5.5	Metamorphic	1204	10	75	761000	32000
16.4	Metamorphic	1491	10	80	226000	7000
10.6	Metamorphic	1186	10	79	643000	19000
4.8	Metamorphic	1252	12	76	483000	26000
3.3	Metamorphic	1395	12	40	416000	12000
8.4	Metamorphic	1164	12	78	480000	15000
13.7	Metamorphic	1369	12	80	221000	13000
4.8	Metamorphic	1179	10	63	681000	21000
11.1	Metamorphic	1317	11	77	513000	14000
7.7	Metamorphic	1399	14	75	339000	14000
6.2	Metamorphic	1177	12	80	524250	15000
6.2	Metamorphic	1177	12	80	511000	16000
6.2	Metamorphic	1177	12	80	500000	13000
6.2	Metamorphic	1177	12	80	460000	12000
6.2	Metamorphic	1177	12	80	626000	19000
4.8	Metamorphic	1182	10	80	787250	22000
4.8	Metamorphic	1182	10	80	644000	17000
4.8	Metamorphic	1182	10	80	716000	20000
4.8	Metamorphic	1182	10	80	675000	19000
4.8	Metamorphic	1182	10	80	1114000	32000
17.9	Metamorphic	1184	11	80	342750	11250
17.9	Metamorphic	1184	11	80	481000	16000
17.9	Metamorphic	1184	11	80	355000	12000
17.9	Metamorphic	1184	11	80	287000	10000
17.9	Metamorphic	1184	11	80	248000	7000
13.4	Metamorphic	1170	12	80	321250	10000
13.4	Metamorphic	1170	12	80	330000	11000
13.4	Metamorphic	1170	12	80	344000	11000
13.4	Metamorphic	1170	12	80	301000	9000
13.4	Metamorphic	1170	12	80	310000	9000
18	Metamorphic	1422	14	80	121000	4000
7.5	Metamorphic	1372	12	62	378000	11000
16.6	Metamorphic	1148	12	80	237500	7000
16.6	Metamorphic	1148	12	80	239000	6000
16.6	Metamorphic	1148	12	80	220000	7000
16.6	Metamorphic	1148	12	80	225000	7000
16.6	Metamorphic	1148	12	80	266000	8000
7.4	Sedimentary	1095	11	80	340000	10000
6.6	Sedimentary	1049	11	80	250000	10000
11.1	Metamorphic	2002	15	80	732000	48000

26.4	Metamorphic	2134	18	58	201000	17000
7	Metamorphic	1978	15	80	2301000	180000
4.8	Metamorphic	1968	14	79	3003000	60000
25.7	Metamorphic	2100	20	67	177000	17000
27.3	Metamorphic	2265	20	64	179000	17000
8.1	Metamorphic	2006	16	80	2119000	74000
12.6	Metamorphic	1988	14	80	3600000	76000
27.4	Metamorphic	2071	17	55	145000	14000
11.6	Metamorphic	1986	14	80	2774000	83000
5.1	Metamorphic	1975	15	80	2584000	65000
7.6	Metamorphic	1984	15	80	3956000	88000
4.9	Metamorphic	1977	15	80	3027000	112000
28	Metamorphic	2008	15	80	322000	27000
24.2	Metamorphic	2375	21	35	133000	18000
23.5	Metamorphic	2009	16	80	125000	22000
37.8	Metamorphic	2048	20	48	106000	11000
37.8	Metamorphic	2110	17	57	177000	21000
11.5	Metamorphic	1986	15	80	1748000	60000
8.7	Metamorphic	2058	16	54	820000	22000
8	Metamorphic	2054	16	46	869000	22000
18.6	Metamorphic	2334	19	59	275000	21000
19.3	Metamorphic	2320	19	80	371000	22000
17.2	Metamorphic	2654	18	31	948000	53000
16.5	Metamorphic	2654	18	31	1584000	30000
30.3	Metamorphic	2234	17	80	363000	15000
30.1	Metamorphic	2368	19	59	363000	18000
28	Metamorphic	2368	19	69	434000	18000
23.6	Metamorphic	2301	18	69	276000	20000
17.2	Metamorphic	2368	19	59	479000	29000
13.2	Metamorphic	2368	19	59	319000	19000
5.8	Mixed	1674	23	61	35250	3750
5.8	Mixed	1674	23	61	38700	4100
5.8	Mixed	1674	23	61	31800	3400
6	Mixed	1662	23	60	39700	5200
4.1	Mixed	1516	23	59	50000	15700
4.1	Mixed	1516	23	59	46700	10600
4.1	Mixed	1516	23	59	53300	20800
9.7	Mixed	1915	22	63	36600	6500
7.3	Mixed	1477	21	52	11400	3950
7.3	Mixed	1477	21	52	13200	4200
7.3	Mixed	1477	21	52	9600	3700
8.5	Mixed	2353	22	67	20900	9600
13.8	Mixed	1453	20	55	40400	9800
14.6	Mixed	1448	19	54	41400	3800
16.2	Mixed	1431	19	54	35300	4500
16.4	Mixed	1428	18	54	25200	3550
16.4	Mixed	1428	18	54	24200	4400
16.4	Mixed	1428	18	54	26200	2700
19.6	Mixed	1322	17	52	66950	7900
19.6	Mixed	1322	17	52	64800	7900

19.6	Mixed	1322	17	52	69100	7900
19.9	Mixed	1317	17	51	31450	3950
19.9	Mixed	1317	17	51	31300	4300
19.9	Mixed	1317	17	51	31600	3600
20.5	Mixed	1300	16	51	22450	4150
20.5	Mixed	1300	16	51	28700	4200
20.5	Mixed	1300	16	51	16200	4100
14.8	Mixed	1296	16	50	38050	5950
14.8	Mixed	1296	16	50	39200	5000
14.8	Mixed	1296	16	50	36900	6900
12.8	Mixed	692	16	34	27700	4900
14	Mixed	665	16	32	24700	3200
2.3	Mixed	1885	25	78	110600	11300
10.9	Mixed	578	12	11	142400	8200
12	Mixed	2000	22	63	16500	3400
21.5	Mixed	1704	16	33	58800	7300
9.1	Mixed	1976	24	76	11600	2800
18	Mixed	799	20	76	15350	4750
18	Mixed	799	20	76	17500	4000
18	Mixed	799	20	76	13200	5500
14.2	Sedimentary	1229	6	64	35400	4200
29.4	Mixed	1838	0	19	12250	4250
29.4	Mixed	1838	0	19	14500	4300
29.4	Mixed	1838	0	19	10000	4200
29.5	Metamorphic	1366	4	50	29000	5600
29.9	Metamorphic	1570	3	40	19300	3100
29.5	Metamorphic	1605	2	37	21000	3600
16.1	Sedimentary	1349	6	64	21550	4700
16.1	Sedimentary	1349	6	64	24300	4800
16.1	Sedimentary	1349	6	64	18800	4600
27.2	Metamorphic	1644	2	34	15700	3000
27.2	Metamorphic	1644	2	34	19500	3300
27.2	Metamorphic	1644	2	34	11900	2700
27.8	Metamorphic	1395	5	63	20150	4300
27.8	Metamorphic	1395	5	63	18400	4400
27.8	Metamorphic	1395	5	63	21900	4200
30.8	Metamorphic	1492	3	40	18800	5800
26.5	Metamorphic	1358	6	66	10700	4000
31.7	Metamorphic	1495	3	39	24550	4800
31.7	Metamorphic	1495	3	39	24400	4500
31.7	Metamorphic	1495	3	39	24700	5100
17.7	Sedimentary	1349	4	62	39900	7500
24.5	Mixed	1925	-1	11	25600	6200
29.2	Metamorphic	1670	1	28	21000	4100
28.9	Metamorphic	1676	1	28	16800	4300
25	Metamorphic	1375	5	60	9600	1900
28.9	Mixed	2029	-2	6	14200	3500
26.1	Metamorphic	1813	0	18	24650	5100
26.1	Metamorphic	1813	0	18	19500	4500
26.1	Metamorphic	1813	0	18	29800	5700

26.6	Metamorphic	1600	2	44	15300	3800
29.7	Metamorphic	1681	1	26	50600	7300
31.9	Metamorphic	1637	1	24	23800	4100
24.3	Mixed	2015	-2	6	16800	2900
6.9	Sedimentary	988	7	14	43200	5000
35.4	Metamorphic	1427	5	41	35500	5900
17.7	Sedimentary	1265	6	75	32550	6700
17.7	Sedimentary	1265	6	75	31300	7500
17.7	Sedimentary	1265	6	75	33800	5900
10.3	Sedimentary	1096	6	22	70000	11400
23.6	Metamorphic	1953	-2	6	32400	5400
28.7	Metamorphic	1723	0	16	32700	4500
30.2	Metamorphic	1399	5	29	30500	6200
32.5	Metamorphic	1643	1	40	13000	4200
9.2	Sedimentary	1125	6	30	80600	8900
11.7	Mixed	231.08	16.14	5.03	425000	16000
11.3	Mixed	234.54	16.11	5.09	493000	16000
2.5	Mixed	221.88	16.90	5.00	1294000	42000
5	Mixed	234.74	16.37	5.00	904000	29000
10.5	Igneous	287.8976973	8.1	14.98	782000	38000
19.4	Igneous	175.00	9.00	14.55	6670	990
18.5	Igneous	175.86	8.93	6.41	4700	1200
15	Igneous	244.11	5.49	5.40	23400	1100
21.8	Igneous	235.19	6.99	5.23	16400	2000
19.2	Igneous	204.30	7.74	19.87	15500	2800
19.1	Igneous	189.11	8.39	15.47	7510	510
20	Igneous	175.00	9.00	5.24	9480	510
14	Igneous	258.49	5.43	15.98	34800	4100
14.4	Igneous	252.19	5.57	15.33	5900	950
16.3	Mixed	995.79	7.52	79.95	99300	7900
16.4	Mixed	948.05	7.84	79.09	128000	8200
17.8	Mixed	1073.00	7.00	79.73	130600	7300
16.1	Mixed	1068.29	7.03	80.00	320000	18000
18.3	Mixed	1053.51	7.13	79.54	68300	4600
15.1	Mixed	970.37	7.69	79.45	82400	5400
16.9	Mixed	1027.48	7.31	79.72	121000	10000
14.2	Mixed	1064.20	7.06	80.00	141000	12000
11.3	Mixed	1231.00	6.00	74.79	104100	6300
6.5	Mixed	1231.00	6.00	74.91	190000	11000
6.3	Mixed	1230.57	6.01	72.45	222000	15000
12.7	Mixed	1024.72	7.76	78.15	124800	7800
15.5	Mixed	997.00	8.00	78.79	136200	8800
14.9	Mixed	1116.08	6.98	74.62	92400	6400
9.3	Mixed	1231.00	6.00	72.09	118600	6400
18.2	Mixed	1173.04	6.50	73.34	87800	5000
17.1	Mixed	996.76	8.00	78.52	90500	9900
7	Mixed	997.00	8.00	80.00	145400	9900
9.7	Mixed	1230.95	6.00	74.17	107000	6700
4.7	Mixed	994.00	7.00	71.74	140900	8500
4.3	Mixed	994.00	7.00	79.01	138000	24000

5.2	Mixed	1033.78	7.00	43.01	102000	19000
5	Mixed	1003.49	7.00	53.85	114800	6600
4.4	Mixed	1003.93	7.08	47.53	74500	5300
5.6	Mixed	1017.23	7.00	61.88	217000	13000
5.5	Mixed	1018.06	7.00	68.80	133000	11000
5.2	Mixed	1020.94	7.00	76.82	116000	6200
6.1	Mixed	1008.90	7.00	62.84	127800	6100
5.1	Mixed	1009.47	7.07	47.89	117300	7000
2.9	Mixed	937.14	7.56	7.40	73500	4600
2.7	Mixed	925.66	7.65	7.52	110200	6700
5.3	Mixed	982.35	7.12	72.33	122000	7600
26.4	Mixed	1444.27	1.94	25.44	38700	6700
33.5	Mixed	1187.71	4.73	47.02	25000	4400
26.5	Mixed	1305.16	3.25	38.21	17100	3000
27.5	Mixed	1397.54	2.12	27.93	16000	3300
32.6	Mixed	1296	4.3	62	22300	4300
34	Mixed	1544	1.3	35	19800	3400
31.7	Mixed	1590	0.366666667	46	14500	2500
29.5	Mixed	1590	0.366666667	16	38700	6800
29.4	Mixed	1590	0.366666667	18	50700	9300
33.3	Mixed	1590	0.366666667	30	41100	8200
21.5	Mixed	1121.29	5.00	40.98	22400	4200
32.1	Mixed	1130	5.533333333	72	24700	4500
3.2		1361.582022			231800	11200
2.6		1361.582022			267600	9500
26.5	Mixed	1336.24	-1.64	5.89	153000	27000
26.5	Mixed	1125.46	0.37	37.43	491000	52000
27	Mixed	938.24	1.86	61.43	304000	24000
23.2	Mixed	905.53	2.89	48.72	404000	63000
28	Mixed	909.27	3.36	62.41	584000	61000
28.4	Mixed	1122.37	6.01	58.03	261000	32000
29.9	Mixed	1056.45	1.77	31.83	121000	21000
22	Mixed	807.25	7.34	64.67	351000	55000
28.1	Mixed	898.52	3.70	53.20	111000	22000
27.3	Mixed	1095.26	0.61	21.45	510000	35000
28.1	Mixed	1188.12	1.13	40.08	227000	26000
27.5	Mixed	1291.25	-0.91	17.15	332000	34000
25.4	Mixed	855.01	3.26	47.04	693000	70000
30.1	Mixed	1255.78	2.14	31.80	475000	76000
26.1	Mixed	1176.52	1.45	48.11	290000	22000
21.8	Mixed	1135.86	2.00	63.72	153000	22000
22.4	Mixed	870.17	4.11	55.25	397000	47000
34.1	Mixed	1233.25	4.35	25.26	169000	22000
25.9	Mixed	932.85	2.41	37.29	221000	25000
27	Mixed	1077.95	0.97	28.76	293000	40000
27.7	Mixed	1281.48	-0.81	23.97	260000	35000
25.5	Mixed	1039.83	0.54	26.10	153000	37000
28.2	Mixed	1252.26	-1.47	23.36	299000	36000
15.3	Mixed	802.00	8.00	63.29	366000	56000
22	Mixed	869.94	3.98	55.42	411000	50000

25.7	Mixed	1328.19	-1.57	10.67	149000	21000
23.9	Mixed	1068.83	3.46	50.16	293000	33000
21	Mixed	1020.41	5.05	70.96	153000	29000
29.6	Mixed	1169.07	0.03	22.13	215000	27000
28.3	Mixed	1113.16	0.47	24.73	238000	33000
27.5	Mixed	924.96	2.67	37.39	280000	30000
25.9	Mixed	801.42	4.81	53.20	827000	63000
30.9	Mixed	1031.00	4.00	38.78	160000	39000
9.5	Metamorphic	1941.00	-1.00	30.71	41400	4400
13.6	Metamorphic	1941.00	-1.00	26.56	54400	6900
25.6	Metamorphic	1938.86	-0.98	15.23	134000	13000
27.5	Metamorphic	1928.33	-0.90	26.99	46700	4700
27.7	Metamorphic	1902.20	-0.69	12.54	7400	1900
29.3	Metamorphic	1830.44	-0.12	21.29	15800	3900
26.8	Metamorphic	1816.00	0.00	51.02	57800	5800
22.7	Metamorphic	1810.00	0.00	42.88	233000	15000
18.4	Metamorphic	1804.63	0.00	35.38	233000	17000
27.7	Metamorphic	1816.00	0.00	32.32	64500	9100
23.4	Metamorphic	1901.54	-0.97	15.71	30400	4800
27.7	Metamorphic	1816.00	0.00	41.40	20100	4200
25.1	Metamorphic	1894.43	-0.89	17.91	11800	2500
27.9	Metamorphic	1816.00	0.00	15.71	17200	4100
14.9	Mixed	184.40	-3.21	4.82	449000	19000
17.4	Mixed	225.55	-5.25	4.05	1104000	35000
17.8	Mixed	233.17	-4.99	4.70	393000	19000
26.5	Mixed	257.00	-6.00	5.00	337000	18000
22.6	Mixed	255.92	-6.92	4.30	1064000	44000
26.3	Mixed	294.59	-4.99	6.79	47600	3900
28.6	Mixed	185.43	1.97	9.07	78300	5100
26.5	Mixed	303.62	-4.92	6.88	92400	6100
27.6	Mixed	247.61	-1.09	12.31	71200	5600
28.8	Mixed	295.55	-3.91	8.19	36300	5100
27.3	Mixed	286.79	-2.93	14.84	353000	18000
22.9	Mixed	321.78	-5.00	12.27	220000	12000
16.2	Mixed	340.31	-4.29	8.39	113000	6200
11.2	Mixed	215.23	3.00	4.41	1272000	50000
8	Mixed	119.00	6.00	1.38	137000	21000
10.6	Mixed	203.77	17.70	3.16	405000	14000
10.8	Mixed	224.67	16.39	4.48	393000	14000
11.9	Mixed	231.96	16.14	5.04	402000	22000
12.6	Mixed	233.12	16.10	5.08	501000	16000
1.6	Mixed	237.32	16.25	5.20	1916000	53000
1.8	Mixed	229.00	16.00	5.00	1286000	38000
2.3	Mixed	245.83	16.08	5.00	1243000	40000
23.5	Mixed	446.00	15.00	53.90	857000	27000
12.1	Mixed	439.03	15.00	35.18	921000	29000
20.3	Mixed	335.00	13.00	21.44	1682000	53000
14.6	Mixed	421.73	15.38	46.85	1471000	46000
19.8	Mixed	445.00	15.00	56.28	1334000	42000
22.9	Mixed	448.00	15.00	55.07	843000	26000

31.2	Mixed	448.00	15.00	64.74	759000	24000
28	Mixed	329.00	13.00	41.48	998000	31000
23.1	Mixed	442.00	14.00	37.80	2185000	69000
24.3	Mixed	380.07	14.00	39.34	1272000	40000
16.8	Mixed	1074.99	10.69	80.00	348000	10000
16.8	Mixed	1074.99	10.69	80.00	342000	13000
16.8	Mixed	1074.99	10.69	80.00	306000	14000
16.8	Mixed	1074.99	10.69	80.00	229000	7000
21	Mixed	1086.00	10.00	79.17	503000	10000
18	Mixed	1086.00	10.00	78.05	326000	7000
16.7	Mixed	1068.78	10.80	76.71	362000	8000
16.2	Mixed	1070.00	11.00	79.20	360000	9000
15.1	Mixed	1070.00	11.00	65.86	428000	10000
10.8	Mixed	1070.00	11.00	73.02	455000	9000
15.7	Mixed	1086.00	10.00	80.00	336000	14000
16.4	Mixed	1016.76	10.63	78.21	423000	8000
19.2	Mixed	986.70	10.98	73.09	458000	9000
14.3	Mixed	1074.89	11.00	79.91	655000	12000
11.3	Mixed	1070.00	11.00	65.92	488000	11000
17	Mixed	1070.00	11.00	51.86	276000	7000
11	Mixed	1070.00	11.00	54.92	394000	8000
15	Mixed	1064.00	10.00	79.64	714000	13000
15.1	Mixed	1064.00	10.00	79.64	522000	10000
14.6	Mixed	1064.00	10.00	79.46	488000	11000
11.9	Mixed	1045.49	10.45	76.11	1023000	29000
11.9	Mixed	1045.49	10.45	76.11	873000	27000
11.9	Mixed	1045.49	10.45	76.11	790000	21000
11.9	Mixed	1045.49	10.45	76.11	789000	25000
8.2	Mixed	1082.839942	11	76	1513000	21000
14.4	Mixed	1068.25	10.71	79.73	877000	19000
13.7	Mixed	1086.00	10.00	80.00	333000	7000
11.9	Mixed	1068.25	10.71	79.73	1099000	20000
15.9	Mixed	1086.00	10.00	78.94	535000	10000
17.3	Mixed	1102.00	11.00	80.00	729000	33000
13.9	Mixed	1070.00	11.00	79.20	626000	12000
15.1	Mixed	1071.00	11.00	79.95	824000	14000
15.4	Mixed	1067.32	11.00	72.69	744000	20000
15.4	Mixed	1067.32	11.00	72.69	584000	16000
15.4	Mixed	1067.32	11.00	72.69	506000	17000
15.4	Mixed	1067.32	11.00	72.69	595000	16000
16.8	Mixed	1086.00	10.00	70.57	836000	16000
14	Mixed	1092.47	11.00	79.27	1263000	19000
15.3	Mixed	1071.00	11.00	79.96	934000	15000
10.8		885.28324			1086000	17000
17.9	Mixed	1071.00	11.00	79.93	391000	8000
16.6	Mixed	1071.00	11.00	79.93	937000	33000
19.9	Mixed	1071.00	11.00	79.19	614000	16000
19.8	Mixed	1092.47	11.00	79.27	717000	14000
21.3	Mixed	1070.90	11.00	76.76	404000	13000
21.3	Mixed	1070.90	11.00	76.76	369000	12000

21.3	Mixed	1070.90	11.00	76.76	409000	13000
21.3	Mixed	1070.90	11.00	76.76	558000	17000
18	Mixed	1037.62	10.58	77.62	780000	15000
16.6	Mixed	1092.47	11.00	79.27	1006000	15000
16.6	Mixed	1092.47	11.00	79.27	935000	14000
19.6	Mixed	1071.00	11.00	79.93	699000	12000
24.4	Mixed	1071.00	11.00	70.59	696000	36000
19.5	Mixed	1071.00	11.00	79.96	446000	9000
22.4	Mixed	1071.00	11.00	78.87	419000	10000
15	Mixed	1111.55	10.10	79.01	1056000	20000
12.5	Mixed	1084.20	11.00	79.92	333000	7000
19.7	Mixed	1102.00	11.00	80.00	523000	13000
18.4	Mixed	1092.47	11.00	79.27	819000	13000
10.6	Mixed	1070.00	11.00	79.20	1059000	16000
19.2	Mixed	1071.00	11.00	79.19	671000	12000
13.9	Mixed	1056.00	11.00	75.12	424000	9000
5.7	Mixed	1109.47	10.21	78.62	506000	12000
10.6	Mixed	1020.15	11.00	71.90	380000	8000
8	Mixed	1004.95	11.00	62.18	1242000	20000
8.7	Mixed	1022.52	10.98	42.89	814000	15000
13.49573328	Mixed	83.96829003		2.09	1027511	153842
23.26770481	Mixed	83.96829003		3.82	598649	24962
23.74949449	Mixed	83.96829003		3.77	588998	16567
24.22774532	Mixed	83.96829003		3.5	833051	53481
24.22774532	Mixed	83.96829003		3.57	479983	13641
26.10485401	Mixed	83.96829003		2.66	177039	23322
26.10485401	Mixed	83.96829003		2.66	186943	16714
24.22774532	Mixed	83.96829003		4.13	593076	38635
20.80679101	Mixed	369.7749591		10.76	468966	13507
18.26288994	Mixed	369.7749591		12.76	218067	9450
18.77803322	Mixed	369.7749591		11.01	234948	10795
18.26288994	Mixed	369.7749591		12.84	198207	5803
18.77803322	Mixed	369.7749591		13.44	195648	6708
28.36904629	Mixed	369.7749591		7.28	101191	2915
27.47443163	Mixed	294.099972		6.88	87032	5010
27.92358972	Mixed	294.099972		7.67	91404	10713
26.56505118	Mixed	294.099972		16.17	99370	5275
25.17352452	Mixed	294.099972		20.72	73331	48099
19.29004622	Mixed	294.099972		32.48	64381	29145
22.29362916	Mixed	294.099972		16.57	129351	14825
1.99	Metamorphic	528.52	20.40	97.00	2243000	34000
1.93	Metamorphic	525.85	20.00	97.00	3890000	51000
7.23	Metamorphic	549.09	20.08	100.00	874000	14000
9.91	Metamorphic	773.89	22.00	33.00	48000	2800
2.23	Metamorphic	1231.52	18.12	33.26	806000	16000
3.33	Metamorphic	1199.94	16.49	30.03	2320000	27000
2.97	Metamorphic	1204.70	17.33	17.66	1422000	15000
8.6	Metamorphic	1037.20	18.17	69.86	78000	2200
9.96	Metamorphic	950.00	21.00	29.95	78000	2100
10.67	Metamorphic	950.00	21.00	40.38	73000	2100

17.7	Metamorphic	1129.21	18.07	58.01	432000	10000
17.89	Metamorphic	1195.00	17.00	59.93	202000	4700
14.4	Metamorphic	1195.00	17.00	64.20	199000	2800
1.64	Mixed	445		67.8	714000	15000
1.86	Mixed	288		59.6	1122000	25000
1.7	Mixed	534		73	1053000	11000
1.2	Mixed	308		71.5	705000	9400
5.12	Mixed	341		76	169000	3300
3.86	Mixed	307		56.9	237000	4600
7.32	Mixed	611		55.1	65000	1800
21.7	Sedimentary	1074.139518			187000	14000
21.8	Sedimentary	1074.139518			92300	5800
19.4	Sedimentary	1074.139518			150000	9000
10	Sedimentary	835.7627191			167000	8000
4.4	Sedimentary	1074.139518			273000	9000
13.6	Sedimentary	1074.139518			226000	10000
14	Sedimentary	1074.139518			141000	7000
8.8	Sedimentary	1074.139518			347000	12000
20.6	Sedimentary	1074.139518			131000	9000
0.7	Sedimentary	973.4216739			552000	17000
8	Sedimentary	973.4216739			352000	13000
16.4	Sedimentary	973.4216739			122000	7000
12.2	Sedimentary	973.4216739			255000	9000
2.6	Sedimentary	1074.139518			458000	15000
6.6	Sedimentary	1074.139518			349000	12000
5.8	Sedimentary	973.4216739			375000	12000
4.9	Sedimentary	973.4216739			370000	12000
15.9	Sedimentary	973.4216739			237000	11000
20	Sedimentary	973.4216739			148000	7000
12.4	Sedimentary	973.4216739			246000	11000
2	Sedimentary	973.4216739			783000	31000
5.8	Sedimentary	973.4216739			516000	14000
13.1	Sedimentary	1032.193934			381000	21000
7.5	Sedimentary	1032.193934			201000	8000
3.6	Sedimentary	1032.193934			281000	8000
3.8	Sedimentary	1032.193934			526000	15000
9.7	Sedimentary	1030.181554			334000	10000
3.7	Metamorphic	1030.181554			747000	20000
4.6	Sedimentary	1030.181554			308000	11000
10.5	Sedimentary	1030.181554			248000	13000
4.8	Sedimentary	1030.181554			525000	18000
4.4	Sedimentary	1030.181554			522000	14000
8.6	Sedimentary	1030.181554			227000	10000
11.5	Sedimentary	1030.181554			191000	6000
5.8	Sedimentary	973.4216739			956000	25000
14.7	Sedimentary	973.4216739			383000	11000
14.8	Sedimentary	973.4216739			290000	9000
19.1	Sedimentary	973.4216739			200000	7000
3.9	Sedimentary	1021.909045			586000	20000
6.4	Sedimentary	1021.909045			468000	16000

12.4	Sedimentary	1171.621856			426000	13000
9.2	Metamorphic	973.4216739			870000	23000
12.1	Metamorphic	973.4216739			712000	19000
14.3	Sedimentary	973.4216739			272000	11000
6.1	Sedimentary	973.4216739			335000	9000
20	Sedimentary	973.4216739			160000	7000
17.2	Sedimentary	973.4216739			228000	8000
15.5	Sedimentary	973.4216739			200000	11000
7.8	Metamorphic	1041.214224			373000	12000
5.7	Metamorphic	1041.214224			595000	26000
4.4	Metamorphic	1041.214224			300000	10000
8.4	Metamorphic	1041.214224			413000	12000
7.9	Metamorphic	1041.214224			395000	12000
6.7	Metamorphic	1041.214224			368000	12000
5.4	Metamorphic	1041.214224			283000	8000
5.9	Metamorphic	1041.214224			380000	11000
5.7	Metamorphic	1041.214224			433000	14000
5.4	Metamorphic	1041.214224			376000	12000
6.9	Metamorphic	1041.214224			407000	14000
32	Mixed	2450.723183			163000	10400
33.2	Mixed	2450.723183			19400	3750
24.9	Mixed	2450.723183			267000	10900
29.1	Mixed	2450.723183			285000	9580
28	Mixed	2450.723183			24900	5660
19.8	Mixed	2450.723183			36200	5240
20.9	Mixed	2450.723183			410000	25900
21.7	Mixed	2450.723183			23800	4610
30.6	Mixed	2450.723183			24200	2810
13	Mixed	2450.723183			201000	9330
32.7	Mixed	2450.723183			22000	3250
16.3	Mixed	1142.510507			308000	12300
23.5	Mixed	2450.723183			25300	6760
28	Mixed	2450.723183			30100	2530
32.4	Mixed	2450.723183			7150	6730
30.1	Mixed	2450.723183			29800	3360
24		2787.444293			28100	1300
28		2787.444293			57000	2300
37		2787.444293			73800	1600
29		2787.444293			20840	590
44		2787.444293			24800	1000
25		2787.444293			35200	900
27		2787.444293			70600	1300
36		2787.444293			48700	1100
35		2787.444293			43000	1500
29		2787.444293			49800	1300
29		2787.444293			55700	2300
29		2787.444293			57500	1100
25		2787.444293			14440	680

32		2787.444293			20080	830
40		2787.444293			19530	770
26		2787.444293			43600	1900
25		2787.444293			30400	1500
31		2787.444293			20300	800
31		2787.444293			23900	900
35		2787.444293			24900	1100
44		2787.444293			11100	560
0		2787.444293			8020	330
50		2787.444293			3160	500
28		2787.444293			6830	340
2.6	Mixed	1361.581991			2179000	22000
2.8	Mixed	1361.581991			2655000	24000
3.1	Metamorphic	1361.581991			120000	2000
7.4	Sedimentary	1361.581991			281000	5000
2.2	Metamorphic	1361.581991			522000	9000
1.6	Metamorphic	1361.581991			1290000	15000
1.5	Metamorphic	1361.581991			1430000	20000
6.4	Sedimentary	1361.581991			258000	5000
8.5	Metamorphic	1361.581991			142000	3000
3.7	Sedimentary	1361.581991			266000	6000
2.92		678.2528859			2000000	52600
3.45		678.2528859			2260000	60700
2.92		678.2528859			2110000	58800
2.92		678.2528859			2110000	68600
3.18		678.2528859			2180000	63200
3.45		678.2528859			1690000	49400
30.91	Igneous	19.59	8.64	3.22	15381745.42	539944.9586
2.38	Igneous	16.20	11.17	2.59	8840389.017	300252.0981
11.30	Igneous	4.38	14.35	1.76	6473567.45	255793.3143
2.38	Igneous	11.98	13.44	0.08	6922665.965	214371.3035
30.91	Igneous	42.17	6.06	4.44	8044806.384	582606.6322
5.76	Igneous	5.00	16.00	3.75	6771286.373	609028.8429
2.38	Igneous	11.98	13.44	0.08	10395268.18	185475.9973
2.38	Igneous	15.74	11.45	2.28	20264589.01	460795.0031
0.00	Igneous	3			6973985.448	231641.2978
30.91	Igneous	3			6491339.198	248591.319
2.38	Igneous	11.98	13.44	0.08	5157501.08	271803.8885
30.91	Igneous	25			24252380.67	949032.6626
27.63	Igneous	11.98	13.44	0.08	8085039.68	365595.4141
3.70	Igneous	5.00	16.00	3.75	6612062.456	170924.6032
30.91	Igneous	50			1125639.983	49547.94776
3.70	Igneous	5.00	16.00	3.75	4269465.755	103275.7989
30.91	Igneous	55			1237650.535	43962.27098
5.79	Igneous	5.00	16.00	3.75	8835959.01	447552.4995
2.38	Igneous	11.98	13.44	0.08	7928725.228	250532.4693

AMS Standard	Published Erosion Rate (m My-1)	Published Erosion Rate Error (m My-1)	CRONUS Erosion Rate (m My-1)	CRONUS Erosion Rate Error (m My-1)	timescale
NIST_30300	24.35	2.47	15.94	1.71	27170.68283
NIST_30300	16.63	2.81	11.1	1.91	39851.55297
NIST_30300	68.42	10.47	45.6	7.13	9533.342867
NIST_30300	39.34	4.79	27.71	3.5	16191.05444
NIST_30300	89.53	7.33	64.94	5.74	6997.196748
NIST_30300	122.11	13.64	89.96	10.49	5054.525696
NIST_30300	126.29	13.51	97.63	10.95	4739.982344
NIST_30300	149.27	14.2	117.97	11.92	3940.896406
NIST_30300	118.49	22.53	94.94	18.31	4929.234675
NIST_30300	128.23	13.19	105.01	11.35	4528.101112
NIST_30300	246.47	33.57	201.82	28.31	2337.643363
NIST_30300	117.04	12.01	96.08	10.36	4964.33436
NIST_30300	7.04	0.72	4.93	0.53	85634.76772
NIST_30300	162.25	30.06	136.52	25.68	3500.665126
NIST_30300	29.84	4.31	27.11	4	18166.54177
NIST_30300	113.13	13.76	87.79	11.09	4992.776077
NIST_30300	136.37	30.09	118.14	26.33	4081.216202
NIST_30300	32.31	3.09	26.54	2.69	17460.00567
NIST_30300	161.52	15.39	136.72	13.83	3485.83878
NIST_30300	47.01	4.8	41.53	4.43	11904.23047
NIST_30300	21.69	1.9	18.92	1.79	23914.14821
NIST_30300	82.41	9.68	67.46	8.27	6695.204978
NIST_30300	6.95	0.72	5.34	0.48	96044.18032
NIST_30300	160.25	24.85	132.92	21.13	3333.854248
NIST_30300	65.23	6.61	47.21	5.01	8783.053099
NIST_30300	160.2	36.47	136.53	31.39	3487.685202
KNSTD	229.89	15.64	149.98	11.27	2940.030723
KNSTD	370.14	30.97	238.18	21.26	1920.945874
KNSTD	263.74	18.83	188.12	14.82	2453.494773
KNSTD	6.79	0.6	5.43	0.51	88052.39117
KNSTD	1.51	0.16	1.26	0.72	392445.4256
KNSTD	8.25	0.67	6.73	0.59	72355.62791
KNSTD	6.51	0.56	5.34	0.49	90888.43445
KNSTD	4.48	0.4	3.81	0.36	131980.5329
KNSTD	14.62	1.22	12.05	1.07	40505.30366
KNSTD	7.68	0.63	6.2	0.55	76960.07696
KNSTD	10.13	0.79	7.98	0.67	60039.77635
KNSTD	48.46	3.95	39.13	3.36	12807.27453
KNSTD	36.85	3	29.94	2.56	16796.84219
KNSTD	68.85	5.65	55.74	4.81	8977.315446
KNSTD	92.72	7.5	75.52	6.44	6621.886161
KNSTD	11	0.86	8.8	0.74	54971.48354
KNSTD	13.02	1	10.41	0.86	46477.8504
KNSTD	10.21	0.86	8.22	0.74	59259.25926
KNSTD	9.77	0.76	7.75	0.65	61792.76252
KNSTD	9.92	0.78	7.87	0.66	60966.31611
KNSTD	73.1	6.03	60.09	5.21	8353.433783

KNSTD	113.33	9.5	91.64	8.08	5440.122947
KNSTD	131.72	10.83	106.9	9.27	4666.450843
KNSTD	10.16	0.79	8.08	0.68	59497.24825
KNSTD	6.25	0.51	6.26	0.51	96200.0962
KNSTD	124.33	11.12	122.55	10.95	4905.973943
KNSTD	57.39	4.67	56.71	4.61	10606.63312
KNSTD	48.36	4.43	47.86	4.39	12568.24162
KNSTD	122.14	10.34	120.94	10.23	4971.414367
KNSTD	10.58	0.83	10.56	0.83	56980.05698
KNSTD	8.63	0.72	8.63	0.72	69716.7756
KNSTD	118.18	9.95	117.46	9.89	5118.705991
KNSTD	11.66	0.94	11.65	0.94	51619.56381
KNSTD	74.61	6.17	74.3	6.14	8094.421426
07KNSTD	17.19	1.34	17.01	1.33	35294.37716
07KNSTD	15.33	1.11	15.16	1.1	39611.80432
KNSTD	72.43	6.1	72.2	6.08	8329.949291
KNSTD	153.75	13.08	152.81	12.99	3934.094089
KNSTD	20.25	1.67	20.16	1.67	29853.53111
KNSTD	161.62	14.57	158.5	14.27	3793.563745
KNSTD	8.63	0.68	3.19	0.27	188723.7556
KNSTD	9.61	0.77	9.54	0.76	63041.76517
KNSTD	199.67	16.77	199.02	16.72	3020.503556
KNSTD	57.95	4.72	57.71	4.7	10421.95907
KNSTD	50.94	4.16	50.76	4.14	11851.85185
KNSTD	12.34	0.94	12.24	0.93	49137.03089
KNSTD	8.11	1.8	8.13	1.8	73981.59708
KNSTD	64.89	5.41	64.76	5.4	9285.374375
KNSTD	236.81	22.09	233.52	21.76	2574.922189
KNSTD	60.48	5.07	60.35	5.06	9966.239364
KNSTD	14.55	1.77	14.61	1.77	41123.70525
KNSTD	169.29	14.72	168.82	14.67	3561.253561
KNSTD	16.05	1.34	15.96	1.33	37696.72981
KNSTD	48.45	4.03	48.22	4.01	12478.26053
KNSTD	28.57	2.53	28.34	2.51	21232.26774
KNSTD	10.87	0.85	10.89	0.85	55227.64143
KNSTD	20.31	2.21	20.47	2.23	29336.26696
KNSTD	18.7	1.95	18.83	1.97	31894.11155
KNSTD	8.32	0.67	8.33	0.67	72267.38934
KNSTD	22.47	2.47	22.87	2.51	26255.76396
KNSTD	364.92	35.37	358.85	34.74	1675.599708
KNSTD	101.04	8.5	100.67	8.46	5973.715651
KNSTD	144.61	13.92	141.83	13.64	4239.769569
KNSTD	9.7	0.78	9.64	0.77	62443.89806
KNSTD	123.27	10.03	122.15	9.93	4921.865387
KNSTD	256.02	23.01	255.17	22.93	2355.76463
07KNSTD	15.2	1.06	15.07	1.05	39824.77101
07KNSTD	14.84	1.03	14.91	1.04	40257.64895
07KNSTD	15.2	1.07	15.28	1.08	39296.59102
07KNSTD	14.96	1.04	15.03	1.05	39932.1154
KNSTD	6.54	0.54	6.55	0.54	91874.82056

KNSTD	38.91	3.3	38.81	3.29	15500.72175
KNSTD	11.26	0.89	11.24	0.88	53531.39951
KNSTD	39.12	3.28	39.03	3.28	15416.04039
KNSTD	30.54	2.66	25.67	2.32	19912.3855
KNSTD	6.77	0.6	5.83	0.53	89111.66806
KNSTD	155.16	63.65	115.6	47.49	3845.756328
KNSTD	8.46	0.67	6.67	0.57	71054.2677
KNSTD	148.94	13.2	124.06	11.5	4044.448489
KNSTD	153.14	60.78	114.54	45.54	3893.000871
KNSTD	138.15	53.18	103.4	39.87	4315.413578
KNSTD	8.86	0.72	7.17	0.62	68035.88893
07KNSTD	20.51	1.41	14.86	1.14	29541.00661
07KNSTD	21.41	1.46	15.45	1.18	28151.66711
KNSTD	297.81	91.94	222.73	252.49	1998.625945
KNSTD	2.6	0.26	2.1	0.22	233304.1703
07KNSTD	41.75	2.86	29.76	2.27	14474.6603
KNSTD	135.88	34.08	102.5	25.88	4380.489301
KNSTD	35.78	4.3	27.22	3.38	16492.97502
KNSTD	64.51	9.84	48.48	7.54	9200.319711
KNSTD	179.52	60.09	133.66	95.33	3303.559999
KNSTD	144.46	64.44	108.49	48.44	4110.658939
07KNSTD	6.49	0.5	4.82	0.41	93616.52332
KNSTD	4.94	0.47	3.96	0.39	121932.6322
07KNSTD	21.07	1.53	15.08	1.21	28490.02849
07KNSTD	19.62	1.34	14.08	1.08	30577.53316
KNSTD	135.95	21.84	101.95	16.68	4367.897049
KNSTD	151.28	38.5	113.92	29.18	3927.315214
07KNSTD	19.06	1.3	13.7	1.05	31487.38537
KNSTD	111.51	48.62	83.35	36.35	5314.731772
07KNSTD	62.75	4.41	43.52	3.36	9531.809435
KNSTD	154.38	70.35	113.67	50.15	3912.535274
KNSTD	140.62	55.74	104.23	41.38	4269.706698
KNSTD	170.47	94.96	126.19	70.32	3521.677023
KNSTD	152.06	60.36	112.65	44.79	3948.248335
KNSTD	9.48	0.73	7.48	0.62	63446.74439
07KNSTD	29.5	1.95	21.03	1.56	20364.00662
KNSTD	5.24	0.44	4.32	0.39	115066.5228
07KNSTD	57.24	3.89	39.56	2.97	10480.94433
07KNSTD	50.02	3.23	34.7	2.5	11988.52099
KNSTD	10.88	0.85	8.76	0.74	55330.77429
KNSTD	10.1	0.8	8.24	0.7	59557.04448
KNSTD	8.96	0.72	7.29	0.62	67340.06734
KNSTD	9.12	0.72	7.25	0.62	66211.46286
KNSTD	5.92	0.49	4.72	0.42	101820.0331
KNSTD	14.05	1.1	11.49	0.96	42879.34823
KNSTD	4.45	0.38	3.67	0.33	135604.7123
KNSTD	3.81	0.35	3.06	0.3	158447.2173
KNSTD	6.43	0.53	5.28	0.46	93616.52332
KNSTD	7.58	0.64	6.16	0.55	79223.60864
KNSTD	4.09	0.36	3.38	0.31	147411.0927

KNSTD	11.73	0.97	9.31	0.82	51395.71488
KNSTD	4.83	0.43	3.92	0.37	124756.3353
KNSTD	5.99	0.5	4.84	0.43	100609.9478
KNSTD	5.97	0.5	4.92	0.43	100781.0532
KNSTD	5.66	0.48	4.54	0.41	106390.0525
KNSTD	42.15	5.48	32.07	4.28	13881.29755
NIST_30000	279.99	38.66	215.64	30.37	2300.258492
NIST_30000	282.09	38.9	219.63	30.98	2225.198425
NIST_30000	75.23	6.98	59.86	5.8	8324.098786
NIST_30000	594.63	114.62	465.99	90.66	1077.754606
NIST_30000	103.61	8.94	81.99	7.45	6046.86319
NIST_30000	341.86	53.46	270.55	42.89	1863.381525
NIST_30000	54.73	4.69	43.25	3.91	11422.37071
NIST_30000	216.01	21.88	168.97	17.84	2896.063887
NIST_30000	146.11	18.43	117.5	15.11	4327.0726
NIST_30000	125.7	17.21	101.15	14.08	5030.07039
NIST_30000	159.65	19.14	128.36	15.72	3959.85695
NIST_30000	158.31	18.89	127.29	15.52	3993.21154
NIST_30000	1642.09	308.22	1255.96	238.62	388.6923563
NIST_30000	234.38	42.54	183.33	33.7	2672.224894
NIST_30000	267.87	70.79	209.44	55.68	2338.104528
NIST_30000	208.28	26.13	162.98	21.01	3007.320947
NIST_30000	553.34	57.86	435.42	47.16	1140.895617
NIST_30000	184.76	18.71	145.58	15.32	3403.161963
NIST_30000	714.6	83.89	561.54	67.79	884.3741588
NIST_30000	289.02	26.31	227.26	21.52	2219.780464
NIST_30000	1321.4	194.17	1032.25	154.61	477.0316704
NIST_30000	158.73	14.82	126.65	12.33	3953.780308
NIST_30000	1426.48	191.26	1124.94	154.08	442.4908474
NIST_30000	252.07	42.47	196.76	33.66	2480.089531
NIST_30000	96.28	9.33	74.89	7.6	6489.898068
NIST_30000	299.01	27.19	237.23	22.57	2100.647262
NIST_30000	245.23	21.6	194.86	18	2561.454906
NIST_30000	1322.12	173.66	1031.69	138.83	476.4295417
NIST_30000	2420.85	524.12	1899.71	415.02	259.1078431
NIST_30000	111.56	10.48	87.15	8.59	5600.534851
NIST_30000	136.07	14.38	105.4	11.58	4628.544814
NIST_30000	937.45	131.33	747.71	106.77	668.2973121
NIST_30000	3214.67	613.91	2545.24	521.14	195.2580604
NIST_30000	1237.39	162.88	971.8	131.02	506.9486822
NIST_30000	230.67	26.85	176.35	21.26	2707.014721
NIST_Certified	70.06	17.12	58.68	9.93	10208.3134
NIST_Certified	61.72	10.68	27.65	3.52	21682.86105
NIST_Certified	50.77	7.69	37.09	4.67	16168.96569
NIST_30000	157.53	16.88	93.68	9.79	6415.422676
NIST_30000	46.03	4.45	113.23	12.14	5312.349553
NIST_30000	52.14	5.69	58.69	5.31	10256.01579
NIST_30000	67.82	6.55	57.19	5.49	10527.49321
NIST_30000	95.08	11.53	77.83	9.4	7735.18591
NIST_30000	41.78	3.8	34.31	3.1	17553.09812

NIST_30000	40.11	3.71	32.93	3.03	18289.89483
NIST_30000	43.6	3.9	35.8	3.18	16820.68103
NIST_30000	44.86	4.55	47.77	4.91	12576.24348
NIST_30000	163.21	17.76	32.05	3.61	14904.24026
NIST_30000	61.65	6.41	46.26	4.65	10273.79668
NIST_30000	157.53	16.88	46	4.41	9896.335882
NIST_30000	276.7	41.08	208.56	31.17	2499.230706
NIST_30000	75.27	7.29	232.31	27.34	2187.092056
NIST_30000	30.92	4.05	33.24	3.39	13081.51419
NIST_30000	67.14	6.08	33.39	3.56	13437.47375
NIST_30000	30.92	4.05	22.77	3.06	19183.96221
NIST_30000	75.11	6.86	83.91	9.08	5294.787282
NIST_30000	365.67	42.51	254.97	27.56	1925.314639
NIST_30000	103.45	15.72	75.4	11.71	5973.113523
KNSTD	36.94	2.84	26.78	2.24	16248.76865
KNSTD	36.28	2.78	26.32	2.2	16534.39153
KNSTD	36.28	2.78	26.32	2.2	16534.39153
KNSTD	36.92	2.84	26.78	2.24	16248.76865
KNSTD	34.28	3.52	24.9	2.68	17506.42814
KNSTD	37.17	3.28	26.94	2.52	16173.37862
KNSTD	38.2	3.62	27.73	2.78	15701.97649
KNSTD	34.75	2.79	25.27	2.2	17261.65431
KNSTD	38.55	3.43	27.98	2.65	15557.69474
KNSTD	33.79	2.95	24.35	2.26	17962.79456
KNSTD	38.49	3.41	28.01	2.64	15565.86794
KNSTD	36.21	3.13	26.38	2.44	16548.2433
KNSTD	32.08	2.99	23.44	2.31	18676.0981
KNSTD	28.37	2.28	20.79	1.81	21126.29564
KNSTD	43.01	5.1	31.06	3.72	14153.15483
KNSTD	36.16	3.15	26.62	2.48	16641.18485
KNSTD	31.83	2.51	23.53	2.01	18914.54174
KNSTD	27.09	2.3	20.03	1.82	22404.25681
KNSTD	38	4.26	29.78	3.44	14893.00308
KNSTD	41.24	4.8	32.48	3.91	13629.08447
KNSTD	34.75	3.71	27.48	3.06	16164.55517
KNSTD	22.66	1.78	19.19	1.64	23875.60808
KNSTD	30.78	2.39	22.76	1.92	19512.43308
KNSTD	40.99	3.71	29.9	2.88	14664.50365
KNSTD	23.55	1.95	17.76	1.58	25520.78349
KNSTD	30.27	2.63	22.5	2.09	19899.01251
KNSTD	113.54	16.41	93.22	12.67	5330.028716
KNSTD	58.23	5.27	42.21	4.06	10323.91276
KNSTD	37.16	3.45	27.03	2.61	16208.76894
KNSTD	31.5	3.7	23.24	2.83	19103.5652
KNSTD	24.57	2.23	18.26	1.76	24456.97865
KNSTD	38.11	3.22	27.83	2.5	15773.02615
KNSTD	68.53	5.98	56.83	5.21	8784.355064
KNSTD	29.9	2.84	19.71	1.94	22128.17747
KNSTD	29.18	2.42	21.44	1.92	20647.82553
KNSTD	102.04	8.79	84.54	7.66	5893.511612

KNSTD	34.55	3.19	25.38	2.48	17347.55833
KNSTD	79.39	7.2	65.83	6.24	7583.729109
07KNSTD	12.95	1.02	9.84	0.84	46405.05815
07KNSTD	5.79	0.49	5.77	0.48	104329.6818
07KNSTD	11.81	0.97	11.67	0.96	51574.63817
07KNSTD	15.97	1.31	15.96	1.31	37672.76495
07KNSTD	22.27	1.64	22.26	1.64	26972.80804
07KNSTD	9.87	0.78	9.88	0.78	60841.1286
07KNSTD	10.59	0.85	10.59	0.85	56761.74259
NIST_30000	15.33	± 1.41	13.35	1.35	44995.64105
NIST_30000	19.89	± 1.67	17.55	1.48	34174.89
NIST_30000	20.52	± 3.02	18.15	2.74	33068.78307
NIST_30000	16.68	± 1.37	14.59	1.22	41152.26337
NIST_30000	10.35	± 0.81	8.82	1.02	68114.0911
NIST_30000	21.88	± 1.88	19.42	1.69	30896.38126
NIST_30000	22.62	± 3.07	19.99	1.83	30019.88818
NIST_30000	23.42	± 2.75	20.87	2.42	28752.6731
NIST_30000	16.95	± 1.91	14.73	1.66	40756.02425
NIST_30000	18.51	± 2.24	16.19	1.55	37083.39128
NIST_30000	19.98	± 1.70	17.57	1.51	34155.19266
NIST_30000	16.76	± 1.52	14.61	1.36	41095.18673
NIST_30000	17.28	± 1.43	15.09	1.26	39798.02502
NIST_30000	16.14	± 1.43	13.96	1.24	43035.04667
NIST_30000	16.51	± 1.76	14.3	1.56	41968.31392
NIST_30000	16.61	± 1.43	14.56	1.28	41238.17624
NIST_30000	29.56	± 2.49	26.7	20.49	22463.70707
NIST_30000	4.93	± 0.44	4.16	0.38	144888.1644
NIST_30000	11.8	± 0.99	10.2	0.87	58905.82431
NIST_30000	7.69	± 0.65	6.56	0.57	91590.81802
NIST_30000	5.96	± 0.53	5.03	0.46	119715.6753
NIST_30000	16.22	± 1.35	14.12	1.19	42510.22902
07KNSTD	659.56	112.81	651.06	111.5	921.0615695
07KNSTD	347.18	28.31	344.12	28.05	1742.970654
07KNSTD	543.03	105.25	537.67	104.06	1115.363434
07KNSTD	340.68	35.31	338.97	35.2	1769.355645
07KNSTD	342.75	28.54	340.81	28.33	1760.472335
07KNSTD	398.25	68.24	395.87	67.79	1515.698372
07KNSTD	397.13	70.85	395.31	70.47	1517.60037
07KNSTD	353.67	44.77	352.78	44.76	1700.604352
07KNSTD	1554.14	448.43	1477.41	426.24	405.8214066
07KNSTD	720.27	63.94	684.16	60.66	875.9036178
07KNSTD	1059.23	98.26	1006.43	93.25	595.6422811
07KNSTD	2189.54	274.05	2089.79	261.44	286.8211593
07KNSTD	1495.22	298.35	1410.16	281.27	425.0443574
07KNSTD	1079.22	139.03	1069.39	137.7	560.5037527
07KNSTD	2086.31	759.7	2067.39	752.78	289.913843
NIST_27900	446.13	86.6	415.37	80.55	1447.713563
NIST_27900	623.86	129.79	588.41	122.31	1021.500022
NIST_27900	807.35	159.31	768.81	151.6	782.3520927
NIST_27900	280.86	60.27	265	56.83	2268.470668

NIST_27900	1190.44	234.17	1148.79	225.86	523.5795695
NIST_27900	658.99	133.79	627.51	127.31	958.1589933
NIST_27900	388.06	85.87	370.25	81.89	1623.941774
NIST_27900	1527.4	296.13	1459.2	282.72	412.2440609
NIST_27900	347.47	68.11	334.46	65.53	1797.151066
NIST_27900	1128.09	242.69	1090.82	234.59	551.5824383
NIST_27900	1211.92	234.43	1172.33	226.67	513.1960341
NIST_27900	1319.85	302.08	1294.42	296.2	464.7128975
07KNSTD	121.88	26.9	120.4	26.57	4988.993034
07KNSTD	1063.98	97.13	1020.8	92.82	588.5258788
07KNSTD	737.79	90	719	87.6	835.7557191
07KNSTD	93.62	15.44	92.55	15.27	6491.319888
07KNSTD	132.95	36.89	131.44	36.47	4570.005341
07KNSTD	853.69	72.66	831.52	70.58	722.6562676
07KNSTD	1077.39	151.48	1054.73	148.17	569.7129217
07KNSTD	657.28	76.75	640.66	74.7	937.3647046
07KNSTD	321.59	33.83	314.29	33.01	1910.972566
07KNSTD	448.71	43.8	437.46	42.62	1373.713646
07KNSTD	304.06	47.76	291.25	45.69	2062.339363
07KNSTD	1129.5	175.02	1097.16	169.86	547.7281776
07KNSTD	255.87	25.2	251.79	24.77	2386.214837
07KNSTD	487.31	80.81	475.45	78.8	1262.823579
07KNSTD	510.45	38.74	504.13	38.19	1190.446961
07KNSTD	1044.44	167.58	1026.91	164.68	585.1494911
07KNSTD	281.97	147.58	280.13	146.62	2143.114508
07KNSTD	153.43	32.58	152.27	32.34	3944.043877
07KNSTD	699.42	66.45	695.23	66.02	863.5229036
07KNSTD	118.85	10.97	118.45	10.93	5076.174341
07KNSTD	314.18	38.29	309.12	37.65	1941.144499
07KNSTD	228.92	20.78	226.74	20.56	2647.038873
07KNSTD	337.33	25.13	335.03	24.94	1791.338208
07KNSTD	41.73	4.69	41.67	4.68	14428.84326
07KNSTD	688.86	172.63	676.63	169.53	886.9287763
07KNSTD	37.41	9.71	37.31	5229.14	16116.19779
07KNSTD	355.4	111.13	354.46	110.84	1692.251392
07KNSTD	86.48	7.75	86.19	7.72	6976.60222
07KNSTD	355.33	41.69	354.67	41.61	1693.411992
07KNSTD	428.09	142.1	426.05	141.43	1411.069132
07KNSTD	125.81	11.58	125.69	11.57	4770.892783
07KNSTD	114.85	9.59	114	9.51	5271.707078
07KNSTD	293.38	53.07	291.88	52.79	2057.041768
07KNSTD	74.85	6.72	74.53	6.69	8070.170129
07KNSTD	854.9	93.25	848.85	92.54	707.2270203
07KNSTD	682.51	66.55	676.95	65.96	886.8491359
07KNSTD	104.11	15.14	104.06	15.14	5775.193379
07KNSTD	152.28	13.85	151.36	13.76	3971.267877
07KNSTD	538	57.44	533.93	56.98	1124.378781
07KNSTD	184.46	16.86	183.45	16.76	3274.534965
07KNSTD	112.95	9.79	112.9	9.78	5323.325481
07KNSTD	401.25	51.94	400.27	51.81	1500.386349

07KNSTD	76.01	7.46	75.96	7.45	7912.840067
07KNSTD	49.85	15.07	49.79	15.05	12076.47427
07KNSTD	77.14	6.92	77.14	6.92	7795.219582
07KNSTD	3658.42	1006.73	3654.38	13706.87	164.2996225
07KNSTD	127.76	10.66	127.76	10.66	4703.489107
07KNSTD	140.85	12.15	140.76	12.14	4271.86125
07KNSTD	116.91	11.32	116.91	11.32	5140.017283
07KNSTD	668.69	104.15	668.68	104.15	898.3439591
KNSTD	6.59	0.54	6.09	0.5	98765.4321
KNSTD	36.12	2.83	34.67	2.71	17322.20382
KNSTD	30.49	2.3	30.19	2.27	19899.01251
KNSTD	31.11	2.49	30.81	2.46	19499.59173
KNSTD	35.01	2.98	34.67	2.95	17322.20382
KNSTD	47.88	3.54	47.42	3.5	12662.23488
KNSTD	7.92	0.73	7.89	0.72	76266.74293
KNSTD	15.63	1.19	15.51	1.19	38756.87329
KNSTD	11.33	0.88	11.25	0.88	53434.85957
KNSTD	16.2	1.22	16.18	1.22	37129.86169
KNSTD	13.07	0.99	13	0.99	46224.07119
KNSTD	8.27	0.66	8.24	0.66	72979.38332
KNSTD	14.24	1.11	14.13	1.1	42540.74606
KNSTD	16.58	1.26	16.46	1.25	36512.17453
KNSTD	21.31	1.61	21.1	1.59	28490.02849
KNSTD	4.58	0.79	4.42	0.76	136228.1822
KNSTD	4.18	0.72	4.16	0.72	144888.1644
KNSTD	3.75	0.64	3.74	0.64	161469.3713
KNSTD	4.26	0.74	4.24	0.74	142108.5354
KNSTD	6.13	1.07	6.11	1.06	98601.09694
KNSTD	11.61	0.88	11.57	0.88	51936.24826
KNSTD	12.27	0.96	12.21	0.95	49259.56713
KNSTD	3.02	0.27	3.01	0.27	200200.2002
KNSTD	7.03	1.15	6.84	1.13	87921.74964
KNSTD	8.89	1.39	8.87	1.39	67802.35613
KNSTD	6.73	1.17	6.71	1.17	89650.92172
KNSTD	5.66	0.95	5.64	0.95	106773.4401
KNSTD	6.83	1.1	6.81	1.1	88314.84241
KNSTD	4.37	0.37	4.36	0.37	138133.4715
KNSTD	7.03	0.57	7.02	0.57	85758.69647
KNSTD	13.1	1.02	13.25	1.03	45374.62424
KNSTD	11.87	0.91	11.8	0.9	50953.79128
KNSTD	5.63	0.46	5.61	0.46	107353.7305
KNSTD	13.27	1.02	13.21	1.02	45514.02401
KNSTD	19.54	1.46	19.36	1.45	31042.04257
KNSTD	10.35	0.81	10.3	0.8	58383.50666
KNSTD	8.78	0.69	8.78	0.69	68428.70584
KNSTD	11.58	0.92	11.55	0.92	52073.16279
KNSTD	5.15	0.43	5.27	0.44	114400.1144
KNSTD	7.47	0.61	7.43	0.6	80955.27221
KNSTD	8.62	0.82	8.59	0.82	70046.40574
KNSTD	4.6	0.39	4.65	0.4	129387.029

KNSTD	9.06	0.75	9.02	0.75	66658.33437
KNSTD	7.45	0.62	7.52	0.63	80080.08008
KNSTD	8.9	0.74	8.98	0.75	66959.61498
KNSTD	9.94	0.8	10.02	0.81	59979.00735
KNSTD	9.96	0.82	10.04	0.83	59857.83764
KNSTD	7.67	0.61	7.73	0.62	77870.2487
KNSTD	10.01	0.79	10	0.79	60161.68453
KNSTD	13.69	1.05	13.69	1.05	43895.7476
KNSTD	9.99	0.77	11.62	0.89	51709.65031
KNSTD	14.25	1.1	14.26	1.1	42147.41057
KNSTD	6.08	0.5	6.1	0.5	98601.09694
KNSTD	7.74	0.62	7.68	0.61	78385.26357
KNSTD	19.06	1.43	19.08	1.43	31470.66344
KNSTD	3.82	0.33	4.03	0.35	149267.6556
KNSTD	6.03	0.49	6.01	0.49	100100.1001
KNSTD	8.48	0.68	8.47	0.68	71054.2677
KNSTD	4.25	0.36	4.26	0.36	141430.213
KNSTD	4.13	0.35	4.16	0.35	144888.1644
KNSTD	15.66	1.32	13.59	1.15	44223.32781
KNSTD	6.31	0.52	6.25	0.51	96200.0962
KNSTD	14.36	1.1	14.41	1.1	41731.87272
KNSTD	14.65	1.11	14.77	1.12	40700.0407
KNSTD	6.99	0.56	7.06	0.57	85265.12124
KNSTD	9.1	0.74	9.12	0.74	65916.86236
KNSTD	7.62	0.61	7.66	0.62	78593.18204
KNSTD	6.98	0.58	6.83	0.57	88052.39117
KNSTD	5.26	0.48	5.2	0.47	115740.7407
KNSTD	3.82	0.33	3.49	0.3	172767.5197
KNSTD	644.5	63.89	630.46	62.39	951.0240449
KNSTD	270.2	32.37	268.51	32.16	2233.585589
KNSTD	335.84	30.12	334.23	29.96	1793.832579
KNSTD	208.76	21.17	208.53	21.15	2875.26731
KNSTD	165.24	14.7	165.23	14.7	3626.637654
KNSTD	112.29	11.54	112.22	11.54	5340.596545
KNSTD	107.43	9.68	107.84	9.72	5558.508513
KNSTD	153.74	13.88	154.75	13.98	3872.394907
KNSTD	120.11	15.43	120.49	15.48	4974.753128
KNSTD	158.63	14.1	158.23	14.06	3787.26013
07KNSTD	290.94	25.32	285.33	24.81	2110.071901
07KNSTD	119	11.49	118.65	11.46	5074.435628
07KNSTD	223.69	19.04	218.19	18.55	2759.324793
07KNSTD	2377.23	214.58	2279.75	205.38	264.0681045
07KNSTD	1887.4	172.56	1810.26	165.2	332.5267481
07KNSTD	1613.11	144.78	1579.14	141.58	381.1644718
07KNSTD	270.53	23.81	266.77	23.46	2256.292235
07KNSTD	2695.4	290.42	2710.47	292.1	222.0329391
07KNSTD	1314.12	110.74	1269.31	106.65	473.8390499
07KNSTD	1820.59	183.25	1929.8	194.77	311.8383181
07KNSTD	4151.28	385.18	4119.53	382.07	146.0756992
07KNSTD	2814.94	246.51	2713.71	237.15	221.7794949

07KNSTD	3557.75	336.1	3417.19	322.22	176.136712
S2007N	33.3	± 4.3	67.14	8.26	8951.549737
S2007N	91.5	± 10	121.95	12.54	4926.775795
S2007N	88	± 11	102.02	12	5888.82632
S2007N	108	± 12	118.72	13	5059.27254
S2007N	35.2	± 3.9	56.54	5.82	10629.46354
S2007N	48.6	± 5.9	65.28	7.87	9203.177397
S2007N	52.8	± 5.9	85.79	8.87	7005.468644
S2007N	28.5	± 3.3	66.43	7.08	9047.215154
S2007N	92.3	± 12	11.16	0.89	53921.07303
S2007N	35.9	± 4.0	72.95	7.4	8236.172239
S2007N	86.2	± 14	110.66	17.08	5427.666171
S2007N	83.6	± 8.9	87.27	9.22	6882.608509
S2007N	63.7	± 7.5	92.6	10.16	6487.766505
S2007N	37.4	± 3.9	49.55	5.12	12128.37889
S2007N	85.4	± 9.0	105.4	10.58	5698.005698
NIST_27900	802.25	64.97	742.81	59.77	810.0174863
NIST_27900	802.25	64.97	742.81	59.77	810.0174863
NIST_27900	804.45	165.46	751.78	154.51	800.3789794
NIST_27900	803.76	152.06	756.57	143.01	795.3088706
NIST_27900	807.52	144.43	768.21	137.3	783.2931406
NIST_27900	820.78	189.61	773.24	178.54	778.2218506
NIST_27900	641.21	139.46	593.24	128.94	1014.296509
NIST_27900	588.89	118.46	544.82	109.51	1104.429314
NIST_27900	588.64	205.24	552.8	192.7	1086.647949
NIST_27900	684.61	194.75	619.36	176.07	970.8266589
NIST_27900	677.9	259.52	620.88	237.63	968.1461756
NIST_27900	758.36	229.78	709.18	214.81	848.1845141
NIST_27900	609.07	136.2	599.42	134.01	1001.457747
NIST_27900	583.41	98.32	578.53	97.47	1037.797224
KNSTD	48.65	5.26	46.73	4.73	12865.66636
KNSTD	34.82	2.84	34.65	2.83	17352.63814
KNSTD	53.99	7.02	53.74	6.99	11183.10233
KNSTD	48.68	5.93	48.46	5.9	12405.12021
KNSTD	57.09	5.23	56.83	5.21	10576.34468
KNSTD	77.37	8.07	76.33	7.88	7872.892156
KNSTD	74.8	7.63	74.47	7.6	8070.170129
KNSTD	87.62	9.71	87.23	9.66	6889.009447
KNSTD	69.68	6.88	69.37	6.85	8663.634395
KNSTD	54.86	4.94	54.51	4.91	11027.03001
KNSTD	45.77	5.15	45.68	5.14	13162.87411
KNSTD	25.42	2.27	25.25	2.26	23827.60726
KNSTD	35	3.88	34.56	3.9	17403.60037
KNSTD	37.44	3.06	37.35	3.05	16098.68494
KNSTD	37.44	3.78	37.35	3.77	16098.68494
KNSTD	30.11	4.81	30.03	4.8	20026.78583
KNSTD	31.52	3.92	31.37	3.9	19165.34905
KNSTD	33.31	3.2	33.25	3.19	18088.90698
KNSTD	23.35	2.04	23.33	2.04	25787.31909
NIST_27900	43.05	3.68	42.97	3.67	13963.06769

NIST_27900	31.97	3.68	31.89	3.67	18824.41527
NIST_27900	29.95	2.52	29.86	2.51	20108.33365
NIST_27900	14.87	1.41	11.39	1.14	40477.63611
KNSTD	76.89	13.22	68.46	11.82	7726.109421
KNSTD	100.2	8.99	89.26	8.13	5934.233853
KNSTD	64.69	5.8	57.32	5.24	9190.331771
KNSTD	57.81	4.88	50.03	4.31	10529.36376
KNSTD	80.69	6.99	71.42	6.33	7358.656309
KNSTD	53.73	4.46	47.83	4.05	11037.29917
KNSTD	77.85	6.49	68.91	5.89	7619.8096
KNSTD	79.07	6.56	69.99	5.96	7502.121694
KNSTD	76.66	6.42	67.87	5.83	7738.216148
NIST_30200	10.09	1.75	7.2	1.25	59497.24825
NIST_30200	12.43	2.34	8.91	1.68	47674.38396
NIST_30200	8.25	1.36	6.02	0.99	71829.40516
NIST_30200	0.75	0.12	0.61	0.42	800800.8008
KNSTD	31.41	2.44	25.08	2.1	19146.77197
KNSTD	48.37	4.89	37.68	3.99	12486.14818
KNSTD	92.44	7.71	71.51	6.4	6529.22645
KNSTD	119.44	15.56	92.08	12.35	5058.408814
KNSTD	42.07	3.99	32.8	3.28	14376.33655
KNSTD	84.56	8.71	66.04	7.12	7107.983598
NIST_30200	40.42	3.82	27.31	2.71	14825.93427
NIST_30200	51.88	5.62	34.93	3.92	11538.01777
NIST_30200	7.7	1.47	6	1.15	78178.44229
NIST_30200	9.55	1.12	7.51	0.9	61986.67287
NIST_30200	7.4	2.14	5.87	1.68	80080.08008
NIST_30000	28.46	2.45	22.62	2.07	21126.29564
NIST_30000	29.3	2.54	23.27	2.14	20519.13409
KNSTD	24.63	2.62	19.64	2.17	24416.67048
KNSTD	99.49	11.1	73.39	8.52	6043.779629
NIST_30200	22.83	2.21	15.69	1.6	26244.13608
NIST_30200	7.45	1.47	5.82	1.15	80734.68564
NIST_30200	0.57	0.08	0.45	0.34	1077441.077
NIST_30200	3.61	0.47	2.88	0.38	168350.1684
NIST_30200	29.47	2.63	20.07	1.9	20322.10537
NIST_30200	21.85	2.08	15.03	1.51	27434.84225
NIST_30200	21.03	1.68	14.46	1.25	28531.17923
NIST_30200	18.51	1.65	12.81	1.21	32399.8137
KNSTD	125.3	17.55	91.36	13.11	4760.162203
KNSTD	79.2	8.69	57.86	6.61	7536.469447
KNSTD	79.2	8.15	57.86	6.24	7536.469447
KNSTD	79.2	9.23	57.86	6.99	7536.469447
KNSTD	28.66	2.25	22.63	1.91	20961.88867
KNSTD	18.1	1.56	13.39	1.17	39638.30051
KNSTD	17.44	1.5	13.39	1.16	39691.39937
KNSTD	15.71	1.41	12.28	1.12	43349.86047
KNSTD	12.64	1.1	10.5	0.93	50866.31696
KNSTD	12.4	1.1	10.3	0.92	51845.37118
KNSTD	12.88	1.11	10.7	0.93	49923.55456

KNSTD	162.04	14.79	121.4	11.21	4335.937606
KNSTD	159.53	14.06	116.26	10.36	4528.101112
KNSTD	165.23	14.79	137.71	12.21	4371.441374
KNSTD	154.21	13.42	128.52	11.07	4684.156135
KNSTD	117.24	10.27	100.86	8.76	5968.90202
KNSTD	126.27	11.21	108.64	9.57	5541.355831
KNSTD	109.41	9.49	94.12	8.09	6396.724877
KNSTD	119.52	10.79	105.92	9.51	5684.341416
KNSTD	31.41	2.62	76.72	6.62	7847.869058
KNSTD	33.22	2.83	81.05	7.15	7427.833951
KNSTD	29.79	2.44	72.82	6.17	8268.349276
KNSTD	114.21	9.85	102.58	8.8	5869.577977
KNSTD	94.8	8.07	86.24	7.31	6981.533843
KNSTD	164.12	16.1	136.94	13.33	4395.43534
KNSTD	64.8	5.59	61.95	5.34	9719.412704
KNSTD	129.46	11.21	114.31	9.83	5266.553436
KNSTD	155.27	14.26	137.9	12.59	4365.64456
KNSTD	149.85	14.75	134.72	13.2	4468.687072
KNSTD	133.2	11.49	123.7	10.63	4866.890544
KNSTD	119.39	11.18	113.85	10.64	5288.172342
KNSTD	70.68	6.41	69.01	6.25	8726.146261
KNSTD	22.98	2.02	22.53	1.98	26729.48095
KNSTD	202.72	18.77	191.24	17.67	3148.069446
KNSTD	38.78	3.52	38.09	3.45	15810.90162
KNSTD	25.33	2.17	24.97	2.14	24118.54264
KNSTD	23.64	2.1	23.42	2.08	25720.16461
KNSTD	53.13	4.71	52.29	4.63	11515.59644
KNSTD	77.84	7.3	76.77	7.19	7843.713999
KNSTD	48.51	4.42	47.91	4.36	12568.24162
KNSTD	41.89	3.6	41.31	3.55	14577.92356
KNSTD	144.34	12.85	142.02	12.64	4239.769569
KNSTD	154.71	13.6	152.77	13.42	3941.420636
KNSTD	54.22	4.62	53.32	4.55	11296.08449
KNSTD	458.49	47.79	454.03	47.31	1326.007144
KNSTD	529.23	57.72	511.95	55.77	1175.615674
KNSTD	52.92	4.95	52.77	4.94	11411.37286
KNSTD	56.08	5.17	9.72	0.87	61921.901
KNSTD	189.01	18.5	187.01	18.3	3219.562059
KNSTD	18.2	1.6	18.05	1.58	33366.70003
KNSTD	321.66	31.02	317.13	30.57	1897.753771
KNSTD	30.95	2.76	30.69	2.74	19622.27128
KNSTD	103.18	9.36	101.61	9.21	5924.148681
KNSTD	163.29	18.02	162.09	17.89	3715.08114
KNSTD	37.64	3.47	37.29	3.44	16151.33804
KNSTD	109.78	10.05	107.67	9.85	5591.023612
KNSTD	76.24	6.5	74.93	6.37	8022.100888
S555	27.39	2.48	26.3	2.38	22827.14147
S555	56.54	6.73	54.35	6.47	11037.29917
S555	26.51	2.62	25.36	2.51	23675.29335
S555	15.09	1.35	14.52	1.3	41382.16429

S555	23.57	2.99	22.92	2.91	26197.72735
S555	46.98	6.22	45.5	6.02	13192.17704
S555	23.08	2.16	14.79	1.47	30546.00993
S555	23.49	2.68	17.37	2.06	26128.42119
S555	18.31	4.1	14.15	3.18	33536.64927
S555	36.96	3.82	23.97	2.59	19473.95966
S555	28.21	4.74	21	3.58	21595.93996
S555	18.85	1.76	14	1.39	32101.44055
S555	17.71	1.67	13.27	1.33	34493.16604
S555	33.2	5.13	26.07	4.1	18289.89483
S555	17.02	3.04	12.95	2.34	35762.98084
S555	6.05	0.51	4.81	0.43	100439.4225
S555	21.74	1.88	16.33	1.51	27860.4886
S555	28.8	2.54	22.26	2.1	20976.72894
S2007N	12.9	± 1.2	10.72	1.02	48692.89997
S2007N	3.2	±0.3	2.65	0.26	198856.5747
S2007N	6.2	±0.6	5.16	0.48	101471.3343
S2007N	4.2	±0.4	3.53	0.34	148892.6112
S2007N	4.4	±0.4	3.69	0.35	142450.1425
S2007N	8.8	±0.8	7.29	0.67	71742.44462
S2007N	15.3	± 1.4	12.77	1.15	40868.45466
S2007N	5.5	±0.5	4.58	0.44	114843.5257
S2007N	5.2	±0.5	4.37	0.41	120201.3372
S2007N	4.8	±0.4	3.98	0.38	131980.5329
S2007N	20.5	± 2.2	17.06	1.84	30688.37869
S2007N	29	± 2.7	24.15	2.17	21619.57653
S2007N	8.1	±0.7	6.76	0.62	77666.13271
S2007N	5.7	±0.5	4.74	0.45	110764.9706
S2007N	9.1	±0.8	7.5	0.69	69798.89194
S2007N	14.1	± 1.3	11.75	1.07	44622.93619
S2007N	4.2	±0.4	3.48	0.35	151171.5797
S2007N	8.8	±0.8	7.34	0.67	71396.6979
S2007N	11.4	± 1.1	9.52	0.86	55022.52485
S2007N	57.2	± 5.4	47.88	4.3	10821.63244
07KNSTD	248.34	21.54	183.52	16.96	2514.608303
07KNSTD	107.68	8.12	84.79	6.87	5761.716992
07KNSTD	81.54	6.3	64.3	5.32	7611.979353
07KNSTD	157.76	11.48	124.01	9.75	3930.962472
07KNSTD	467.82	43.9	343.86	34.15	1295.369298
07KNSTD	26.61	2.36	22.54	2.06	22871.1923
07KNSTD	262.16	22.66	198.29	18.34	2306.076945
07KNSTD	163.44	12.38	120.46	9.96	3696.541654
07KNSTD	159.53	12.79	117.6	10.2	3787.26013
07KNSTD	167.55	12.01	123.47	9.75	3605.893833
07KNSTD	108.98	10.23	79.8	7.94	5562.682743
07KNSTD	392.02	57.44	292.14	43.86	1535.333297
07KNSTD	397.1	41.67	295.92	32.54	1515.698372
07KNSTD	387.06	74.22	288.46	56.1	1555.034619
07KNSTD	370.89	37.78	275.51	29.49	1621.453451

07KNSTD	670.11	72.51	507.63	57.39	899.4893711
07KNSTD	1987.16	399.66	1435.32	292.24	302.6488966
07KNSTD	906.93	118.88	633.25	85.2	665.9391282
07KNSTD	163.02	12.74	161.66	12.62	3711.125956
07KNSTD	121.93	9.22	120.91	9.14	4962.671406
07KNSTD	244.29	20.56	242.28	20.38	2475.73777
07KNSTD	601.06	70.05	597.35	69.6	1003.985824
07KNSTD	34.92	3.49	34.6	3.45	17372.98718
07KNSTD	32.31	2.54	32.02	2.52	18776.69812
07KNSTD	37.97	5.14	37.63	5.1	15977.15267
07KNSTD	789.53	65.82	787.54	65.63	761.7850528
07KNSTD	289.67	35.9	289.04	35.82	2074.322993
KNSTD	121.49	11.39	119.36	11.19	5039.052658
KNSTD	108.43	9.93	105.1	9.61	5721.110181
KNSTD	129.09	10.71	124.68	10.31	4821.353776
KNSTD	46.66	3.83	45.89	3.76	13107.55569
KNSTD	56.48	4.71	55.43	4.62	10851.35676
KNSTD	43.31	3.58	43.09	3.56	13956.49064
KNSTD	30.53	2.51	30.37	2.5	19812.52399
KNSTD	30.26	2.46	30.17	2.46	19939.18548
KNSTD	46.46	3.69	46.33	3.67	12981.2178
KNSTD	41.12	3.33	41.01	3.32	14664.50365
KNSTD	115.56	10.3	113.96	10.15	5275.46152
KNSTD	104.34	9.57	103.29	9.46	5820.573545
KNSTD	111.7	9.4	110.67	9.31	5432.64203
KNSTD	128.09	12.25	126.26	12.06	4762.457547
KNSTD	73.48	7.22	73.43	7.21	8188.373533
KNSTD	127.48	10.99	126.14	10.87	4766.671433
KNSTD	46.73	4.2	46.66	4.2	12888.05117
KNSTD	99.03	8.16	98.51	8.11	6103.538908
KNSTD	46.39	3.97	46.19	3.95	13018.2907
KNSTD	83.19	6.91	82.81	6.88	7261.274263
KNSTD	153.64	13.16	153.03	13.11	3928.617029
KNSTD	66.67	5.53	66.53	5.52	9037.556697
KNSTD	59.86	5.16	59.69	5.15	10072.96605
KNSTD	41.93	3.53	41.81	3.52	14383.31535
KNSTD	52.04	4.25	51.82	4.23	11605.80871
KNSTD	109.66	9.25	109.01	9.19	5515.054375
KNSTD	47.81	3.95	47.71	3.94	12602.99006
KNSTD	41.88	3.78	41.85	3.77	14372.84969
KNSTD	50.36	4.19	50.15	4.17	11990.94684
KNSTD	30.46	2.57	30.43	2.57	19766.26393
KNSTD	44.44	3.76	44.47	3.76	13526.42302
KNSTD	41.75	3.39	41.75	3.39	14404.29248
S555	26.31	2.59	23.46	2.31	25653.35899
S555	26.34	2.68	23.49	2.39	25620.08615
S555	26.28	2.51	23.44	2.23	25686.71836
S555	25.33	2.29	23.83	2.15	25259.7013
S555	24.27	3.21	23.76	3.14	25346.13313
S555	25.46	2.46	24.92	2.41	24157.87169

S555	26.37	5.26	25.81	5.16	23321.23544
S555	21.53	2.55	21.08	2.5	28572.44902
S555	12.39	1.31	12.3	1.3	48974.59443
S555	11.91	1.86	11.85	1.85	50822.69233
KNSTD	31.91	2.46	28.74	2.27	20917.49356
KNSTD	30.95	2.23	30.41	2.19	19759.67298
KNSTD	32.86	2.69	25.94	2.27	18611.5764
KNSTD	28.77	2.27	22.83	1.92	21278.01051
KNSTD	17.12	1.35	13.28	1.13	35548.44587
KNSTD	29.48	2.25	22.98	1.9	20800.0208
KNSTD	22.19	1.76	17.78	1.51	27321.00473
KNSTD	35.71	2.77	28.1	2.35	17082.51924
KNSTD	26.57	2.02	20.6	1.7	23004.37083
KNSTD	37.66	2.94	29.37	2.47	16342.87349
KNSTD	24.69	1.96	19.49	1.66	24670.79903
KNSTD	25.33	1.95	19.9	1.65	24177.58436
KNSTD	35.88	2.85	28.43	2.42	16945.74185
KNSTD	39.39	3.02	31.4	2.59	15436.11859
KNSTD	22.82	1.82	18	1.54	26874.94751
KNSTD	38.17	3.03	30.59	2.6	15891.46132
KNSTD	36.36	2.77	28.4	2.33	16979.73045
KNSTD	22.07	1.76	17.34	1.49	27665.38714
KNSTD	21.61	1.71	17.57	1.48	28071.65289
KNSTD	28.31	2.22	22.68	1.91	21501.90829
KNSTD	43.53	3.36	34.35	2.86	13989.43797
KNSTD	22.52	1.82	17.75	1.53	27245.63644
KNSTD	23.27	1.81	18.16	1.53	26232.51849
KNSTD	23.32	1.85	19.05	1.61	25934.03031
KNSTD	29.69	2.34	23.91	2.02	20329.07693
KNSTD	28.64	2.25	23.13	1.94	21201.88167
KNSTD	21.85	1.81	16.92	1.5	27834.31623
KNSTD	57.2	4.55	46.08	3.92	10570.68485
KNSTD	23.87	1.83	18.89	1.57	25335.29682
KNSTD	28.08	2.26	22.33	1.93	21509.71298
KNSTD	25.81	1.99	20.67	1.71	23367.2158
KNSTD	38.42	3.05	30.93	2.62	15785.63113
KNSTD	23.4	1.86	18.84	1.6	25877.40579
KNSTD	44.09	3.33	35	2.86	13685.74117
KNSTD	39.76	3.11	31.69	2.67	15233.74274
KNSTD	31.49	2.5	25.35	2.15	19233.77451
KNSTD	31.92	2.5	25.61	2.15	18908.50646
KNSTD	35.29	2.73	28.61	2.37	17092.3736
KNSTD	26.34	2.06	21.16	1.77	22986.52415
KNSTD	23.39	1.89	18.7	1.62	25956.74957
KNSTD	19.52	1.55	15.89	1.35	30896.38126
KNSTD	27.28	2.14	21.95	1.85	22136.4435
S555	71.29	9.53	56.4	7.73	8461.981902
S555	49.73	5.93	39.7	4.88	12128.37889
S555	52.61	6.41	42.03	5.28	11471.01418
S555	116.15	17.46	92.36	14.16	5181.817004

S555	40.87	4.45	32.64	3.69	14733.77903
S555	43.75	5.71	35.15	4.7	13762.02026
S555	76.36	10.68	61.13	8.74	7882.317007
S555	34.12	3.98	34.07	3.97	17647.18858
S555	11.21	1.12	11.19	1.12	53774.28245
S555	33.62	4.16	33.57	4.16	17908.5099
S555	11.66	1.14	11.64	1.14	51709.65031
S555	16.19	1.55	16.16	1.55	37223.1528
S555	40.7	5.31	40.55	5.29	14822.22593
S555	35.44	3.73	35.49	3.73	16936.0558
S555	17.35	1.86	17.35	1.86	34654.53758
KNSTD	2.93	-16	33.56	2.93	17886.88779
KNSTD	2.87	-2	38.27	2.86	15689.5047
KNSTD	3.08	2	40.79	3.08	14715.48529
KNSTD	3.18	12	43.46	3.17	13813.34715
KNSTD	3.89	25	50	3.89	12007.95527
KNSTD	3.27	15	44.58	3.26	13464.95325
KNSTD	50.95	3.79	50.92	3.78	11790.54104
KNSTD	11.6	0.98	11.6	0.98	51845.37118
KNSTD	48.01	3.54	48.01	3.54	12504.59153
KNSTD	177.69	15.35	176.6	15.25	3389.148371
KNSTD	206.85	18.64	205.51	18.51	2912.289132
KNSTD	163.72	16.79	134.29	13.78	4453.239593
KNSTD	167.13	14.35	166.12	14.26	3603.481864
KNSTD	140.51	12.5	139.84	12.44	4280.501247
KNSTD	175.07	14.23	173.78	14.12	3445.105474
KNSTD	154.78	12.75	154.15	12.7	3883.561128
KNSTD	186.75	20.53	185.86	20.43	3220.086902
KNSTD	125.6	9.69	125.03	9.65	4789.401055
KNSTD	150.65	12.69	150.25	12.65	3984.35146
KNSTD	88.27	7.18	88.08	7.16	6800.465832
KNSTD	192.82	16.19	192.26	16.14	3114.31886
KNSTD	160.45	13.34	159.82	13.28	3746.318072
KNSTD	122.94	10.32	122.68	10.29	4880.920786
KNSTD	97.66	11.52	97.05	11.45	6169.626159
KNSTD	156.59	12.41	156.16	12.37	3832.821891
KNSTD	217.58	20.25	217.41	20.23	2752.787628
KNSTD	16.6	1.36	16.59	1.36	36244.19527
KNSTD	19.6	1.3	21.28	1.43	28178.43997
KNSTD	21.1	1.5	22.94	1.65	26139.94674
KNSTD	41.8	2.9	46.05	3.21	13018.2907
KNSTD	50	3.2	16.47	1.1	36422.40889
KNSTD	17.2	1.3	18.81	1.44	31911.28662
KNSTD	6.5	0.5	7.24	0.55	82996.16143
KNSTD	21.4	1.5	23.85	1.61	25152.48695
KNSTD	20.5	1.4	22.76	1.54	26372.61204
KNSTD	15.2	1.1	16.7	1.14	35936.48227
KNSTD	15.2	1.1	16.93	1.17	35463.35084
KNSTD	15.3	1.1	16.82	1.21	35676.85687

KNSTD	19.1	1.3	20.99	1.42	28586.23216
KNSTD	29.5	2	32.88	2.15	18233.61823
KNSTD	62.8	4.4	69.65	4.81	8599.515202
KNSTD	57.2	3.9	63.18	4.3	9479.964687
S555	635.48	161.78	497.89	127.69	948.9376643
S555	600.73	219.09	476.66	174.42	1002.542071
S555	3236.7	924.35	2686.61	769.62	191.61259
S555	461.37	61.71	365.47	50.19	1305.356285
S555	322.51	42.23	256.89	34.56	1867.786405
S555	1491.82	408.85	1227.82	337.62	418.8259106
S555	425.92	54.16	349.71	45.27	1457.792356
S555	395.54	53.43	316.34	43.82	1521.848513
S555	520.88	73.45	408.32	59.01	1154.093896
S555	320.19	42.72	254.27	34.83	1879.396761
S555	296.95	48.43	244.92	40.39	2078.761682
S555	515.96	68.18	434.54	58.34	1179.499995
S555	93.65	9.51	78.54	8.17	6563.214006
S555	380.49	57.11	318.72	48.44	1605.506889
S555	260.22	35.61	220.69	30.62	2332.398916
S555	437.82	55.58	346.01	45.24	1374.223349
S555	663.32	118.79	554.27	100.17	920.918432
S555	893.78	206.64	734.26	170.78	689.1813602
S555	369.89	138.82	294.5	110.84	1625.991474
S555	375.3	49.33	298.76	40.35	1603.638656
S555	337.67	43.93	268.88	35.96	1782.394179
S555	415.55	55.23	330.73	45.13	1448.244275
S555	380.79	50.15	303.13	41.01	1580.499794
S555	1593.88	373.56	1327.38	312.89	382.5596781
S555	312.17	34.02	250.54	28.36	1925.815192
S555	347.02	44.26	278.34	36.5	1733.69004
S555	346.3	43.99	291.03	37.64	1755.413806
S555	441.74	58.86	354.21	48.43	1361.906124
S555	957.58	252.42	788.47	208.87	638.0333261
S555	174.69	18.18	150.68	16.02	3443.704048
S555	196.01	24.65	169.36	21.6	3067.408213
S555	108.43	11.7	93.43	10.27	5559.551483
S555	174.89	21.38	150.67	18.71	3437.312022
KNSTD	34.09	3	29.8	2.67	17684.0523
KNSTD	274.54	24.42	227.76	20.85	2269.600125
KNSTD	87.46	7.43	75.43	6.55	6960.213679
KNSTD	147.62	13.17	127.88	11.68	4093.05562
KNSTD	420.06	36.15	329.66	29.21	1563.115171
KNSTD	355.68	32.6	307.03	28.63	1717.311249
KNSTD	39.19	3.27	34.2	2.91	15436.11859
KNSTD	92.95	8.33	79.46	7.29	6576.32441
KNSTD	178.89	20.94	137.19	16.44	3652.567755
KNSTD	43.18	3.8	37.86	3.39	13949.91979
KNSTD	354.38	30.92	302.89	27.07	1726.618084
KNSTD	42.28	3.59	36.58	3.18	14365.88103
KNSTD	340.88	31.7	286.21	27.2	1823.474037

KNSTD	207	18.1	177.26	15.85	2956.60626
KNSTD	120.82	10.34	100.57	8.86	5193.624826
KNSTD	101.83	8.85	86.92	7.75	6011.28619
KNSTD	139.81	11.82	137.48	11.61	4377.900359
KNSTD	1078.52	109.64	1027.55	104.22	585.5484448
KNSTD	26.04	2.19	25.9	2.18	23257.16611
KNSTD	99.83	8.75	97.95	8.58	6146.588451
KNSTD	87.94	7.69	87.52	7.65	6879.412498
KNSTD	111.72	9.8	111.18	9.75	5415.266313
KNSTD	100.27	8.78	99.52	8.71	6049.332305
KNSTD	151.37	12.68	150.6	12.62	3997.521537
KNSTD	151.46	12.75	149.92	12.61	4015.671157
KNSTD	277.61	24.6	257.1	22.66	2339.581478
KNSTD	53.7	4.86	53.43	4.84	11268.16111
NIST_Certified	186.83	17.12	182.82	16.74	3292.912828
KNSTD	104.78	9.12	103.7	9.02	5805.746964
NIST_Certified	28.64	2.4	28.62	2.4	21043.77104
KNSTD	507.65	43.74	486.22	41.76	1237.067809
KNSTD	295.07	26.68	283.36	25.56	2123.378933
KNSTD	110.57	9.29	107.82	9.05	5581.544623
KNSTD	66	5.62	65.73	5.59	9160.497644
KNSTD	1289.59	182.82	1223.82	173.19	491.2399634
KNSTD	200.5	17.61	197.86	17.37	3042.524991
KNSTD	278.65	27.45	276.27	27.21	2178.889556
KNSTD	199.31	17.03	197.05	16.83	3054.915933
KNSTD	151.82	12.64	148.9	12.39	4041.965709
KNSTD	291.35	39.98	286.3	39.26	2098.56432
KNSTD	242.91	21.42	238.01	20.96	2528.449002
NIST_Certified	18.79	1.65	18.78	1.65	32084.06024
KNSTD	50.99	4.41	50.61	4.38	11897.06068
KNSTD	84.85	7.03	83.85	6.95	7178.589856
KNSTD	186.3	15.93	185.57	15.86	3243.883253
KNSTD	20.94	1.83	20.92	1.83	28780.60187
KNSTD	344.64	31.81	336.95	31.06	1785.186301
KNSTD	117.25	10.14	116.4	10.06	5171.867626
KNSTD	163.7	15.61	160.24	15.26	3755.815646
KNSTD	153.75	13.4	151.9	13.23	3963.034793
KNSTD	464.82	43.23	434.25	40.24	1385.824917
KNSTD	149.78	12.33	146.35	12.03	4111.514553
KNSTD	517.03	46.35	497.83	44.49	1207.40137
KNSTD	1773.83	217.18	1747.01	213.76	344.208382
KNSTD	237.64	20.52	229.1	19.73	2625.460071
KNSTD	41.31	3.44	41.18	3.43	14617.47885
KNSTD	475.71	49.47	465.93	48.41	1291.783129
KNSTD	84.45	7.05	83.67	6.98	7196.024197
KNSTD	274.47	23.38	271.56	23.11	2216.044997
KNSTD	58.21	4.87	61.05	5.11	9863.392021
KNSTD	151.44	13.13	149.17	12.92	4033.986335
KNSTD	381.89	32.98	372.31	32.08	1615.265878
KNSTD	108.79	9.59	108.48	9.56	5549.659043

KNSTD	640.53	72.24	628.05	70.75	956.5041686
KNSTD	45.51	3.85	45.49	3.85	13239.33406
KNSTD	406.5	40.75	404.13	40.5	1488.477325
S555	124.81	17.24	105.06	14.71	4897.459443
S555	543.5	271.6	460.19	230.21	1111.680848
S555	209.83	30.43	179.11	26.26	2893.659811
S555	202.44	39.47	169.15	33.23	3016.659502
S555	115.51	17.92	97.46	15.31	5225.684238
S555	192.18	35.49	160.43	29.88	3171.148887
S555	268.06	48.98	230.59	42.47	2234.596299
S555	129.07	20.14	109.34	17.11	4730.900468
S555	140.66	22.69	120.1	19.55	4306.006341
S555	117.47	17.58	100.35	15.18	5156.566243
S555	33.55	4.76	27.92	4.02	17941.04125
S555	85.35	14.17	71.74	12.04	7049.638265
S556	326.23	112	238.28	68.38	2099.382126
S557	216.77	51.42	178.41	42.58	2806.234752
S558	435.68	172.58	358.05	142.14	1395.87919
S555	220.24	44.33	186.78	37.87	2731.470812
S555	217.43	57.1	182.3	48.1	2766.409563
S555	43.69	5.86	68.79	9.44	7487.902358
S555	149.5	27.72	123.5	23.15	4027.680232
S555	168.48	27.8	141.07	23.53	3608.968286
S555	128.25	20.93	104.78	17.16	4786.306377
S556	145.88	24.55	121.38	20.68	4128.989636
S557	110.61	17.31	92.15	14.63	5446.122531
S555	503.55	165.33	410.7	337.08	1196.890777
S555	524.73	226.58	426.01	184.34	1145.704218
S555	130.25	20.4	107.02	17.03	4618.084419
S555	346.71	82.58	286.41	68.67	1736.484184
S555	199.77	42.82	158.57	32.13	3185.981681
S555	156.73	28.01	130.5	23.56	3874.167054
S555	242.8	57.63	201.9	48.2	2500.496192
S555	454.98	257.84	374.95	212.7	1317.838843
KNSTD	210.93	18.28	153.15	14.14	2866.08915
KNSTD	242.33	22.83	175.24	17.41	2490.512703
KNSTD	233.85	23.06	169.4	17.54	2581.203034
KNSTD	292.61	26.8	213.25	20.67	2057.613169
KNSTD	96.93	10.81	71.36	8.28	6243.731879
07KNSTD	0.34	0.06	0.26	0.26	1851851.852
07KNSTD	1.25	0.14	1.05	0.62	493827.1605
07KNSTD	2.26	0.23	0.81	0.51	630417.6517
07KNSTD	0.54	0.07	0.43	0.33	1161946.26
07KNSTD	0.91	0.11	0.74	0.47	689061.1542
07KNSTD	2.07	0.26	1.74	0.23	300808.4226
07KNSTD	1.14	0.13	0.97	0.58	538720.5387
07KNSTD	0.47	0.1	0.37	0.31	1316872.428
NIST_30000	37.57	4.72	27.93	3.62	16037.68857
NIST_30000	31.34	3.31	23.57	2.6	19146.77197
NIST_30000	59.81	8.2	44.78	6.31	10028.64432

NIST_30000	7.46	0.84	5.8	0.67	81512.0485
NIST_30000	6.69	0.78	5.27	0.63	89923.00343
NIST_30000	8.23	0.9	6.44	0.73	73159.57933
NIST_30000	14.1	2.08	14.78	1.96	40672.10656
NIST_30000	1408.1	401.32	1371.01	390.66	438.3762216
NIST_30000	1094.56	298.49	1068.14	291.22	562.7446181
NIST_30000	1550.07	182.99	1524.3	179.81	394.4122629
NIST_30000	859	80.62	842.39	78.94	713.4770008
NIST_30000	37.22	5.2	36.85	5.15	16324.86481
NIST_30000	25.61	2.25	25.41	2.23	23684.7559
NIST_30000	85.45	7.94	84.85	7.88	7090.124343
KNSTD		44.59	43.8	3.52	13704.73156
KNSTD	24.1	2.04	24.02	2.03	25003.90686
KNSTD	11.09	0.9	11.06	0.9	54366.2929
KNSTD	18.34	1.43	18.33	1.42	32776.13897
KNSTD	24.47	1.84	24.34	1.83	24660.53236
KNSTD	17.66	1.37	17.54	1.37	34234.11858
KNSTD	23.96	1.88	24.01	1.88	25014.46149
KNSTD	27.04	2.27	26.99	2.27	22252.81985
KNSTD	20.66	1.6	20.58	1.6	29191.75333
KNSTD	17.45	1.34	17.46	1.35	34393.0698
KNSTD	25.17	1.91	25.09	1.9	23933.46497
KNSTD	13.83	1.09	13.78	1.09	43605.04728
KNSTD	10.76	0.88	10.69	0.87	56276.59949
KNSTD	26.13	1.97	26.14	1.97	22959.80599
KNSTD	16.44	1.29	16.41	1.29	36625.00572
KNSTD	14.12	1.1	14.13	1.1	42510.22902
KNSTD	12.31	0.97	12.31	0.97	48813.22838
KNSTD	9.37	0.9	9.35	0.9	64342.30104
KNSTD	14.67	1.17	14.66	1.16	40981.50709
KNSTD	25.21	2.1	25.22	2.1	23827.60726
KNSTD	12.19	0.98	12.19	0.98	49300.54847
KNSTD	29.5	2.35	29.55	2.36	20322.10537
KNSTD	13.7	1.08	13.68	1.07	43928.28707
KNSTD	10.44	0.85	10.43	0.85	57645.19383
KNSTD	11.44	0.9	11.44	0.9	52534.80431
KNSTD	15.3	1.22	15.27	1.22	39348.77773
KNSTD	13.09	1.08	13.09	1.08	45937.41028
KNSTD	14.56	1.18	14.57	1.18	41238.17624
KNSTD	20.43	1.71	20.39	1.71	29452.91216
KNSTD	41.67	3.81	41.56	3.8	14446.43083
KNSTD	10.57	0.85	10.56	0.85	56980.05698
KNSTD	10.45	0.84	10.45	0.84	57533.26142
KNSTD	17.68	1.42	17.65	1.42	34037.48378
KNSTD	42.2	3.54	42.11	3.53	14258.72456
KNSTD	19.64	1.76	19.65	1.77	30561.76341
KNSTD	25.84	2.03	25.78	2.03	23302.89393
KNSTD	17.53	1.42	17.53	1.42	34293.55281
KNSTD	16.85	1.37	16.87	1.37	35633.95025
KNSTD	11.54	0.95	11.54	0.95	52118.96153

KNSTD	12.14	0.97	12.16	0.98	49423.90263
KNSTD	10.85	0.87	10.84	0.87	55434.29304
KNSTD	25.8	2.19	25.8	2.19	23284.58124
KNSTD	24.83	1.84	18.59	1.51	24128.36289
KNSTD	11.25	0.9	8.55	0.74	53338.6672
KNSTD	15.65	1.18	11.78	0.97	38405.22311
KNSTD	23.11	1.83	17.95	1.54	25968.12413
KNSTD	12.01	0.96	9.18	0.79	50092.35778
KNSTD	8.03	0.68	6.2	0.56	75011.72058
KNSTD	18.29	1.41	14.09	1.18	32848.81334
KNSTD	39	3.33	30.36	2.78	15344.18935
KNSTD	6.54	0.56	5.06	0.47	92017.48332
KNSTD	49.52	4.48	37.73	3.62	12128.37889
KNSTD	44.52	3.81	34.28	3.14	13468.01347
KNSTD	10.47	0.86	8.01	0.7	57310.69561
KNSTD	15	1.21	11.73	1.02	40040.04004
KNSTD	17.32	1.34	13.53	1.14	34735.79089
KNSTD	4.42	0.39	3.51	0.32	136542.072
KNSTD	21.15	1.74	16.42	1.45	28380.87129
KNSTD	36.95	2.96	28.3	2.45	16235.4135
KNSTD	69.6	6.43	53.07	5.19	8640.895197
KNSTD	27.57	2.3	21.43	1.91	21810.54813
KNSTD	16.91	1.33	13.17	1.12	35569.78347
KNSTD	22.65	1.78	17.69	1.5	26537.95757
KNSTD	50.39	4.8	38.78	3.89	11959.48724
KNSTD	29.05	2.28	22.3	1.89	20691.08214
KNSTD	8.02	0.67	6.42	0.57	75202.10566
KNSTD	7.54	0.63	6.05	0.54	79864.23081
KNSTD	8.7	0.74	6.86	0.62	69228.10661
KNSTD	11.62	0.94	9.25	0.8	51754.81158
KNSTD	26.5	2.39	20.12	1.92	22669.95381
KNSTD	6.69	0.61	5.17	0.5	90059.66453
KNSTD	6.12	0.52	4.92	0.44	98437.30774
KNSTD	10.08	0.81	7.93	0.69	59737.15651
KNSTD	32.14	3.34	24.64	2.68	18770.75048
KNSTD	11.34	0.91	8.79	0.76	53052.1569
KNSTD	12.33	1.15	9.48	0.93	48773.05289
KNSTD	20.91	1.61	16.25	1.36	28780.60187
KNSTD	10.53	0.87	8.39	0.74	57089.84514
KNSTD	7.47	0.67	6.02	0.57	80624.84253
KNSTD	26.39	2.79	18.53	2.01	27283.26854
KNSTD	68	6.39	57.23	5.58	8845.985857
KNSTD	30.92	3.09	25.86	2.68	19442.01419
KNSTD	49.12	4.89	41.28	4.25	12238.59134
KNSTD	10.29	1.04	7.93	0.82	64977.25796
KNSTD	52.18	5.67	39.38	4.39	12821.12922
KNSTD	40.04	5.03	31.33	4.05	15253.34859
KNSTD	32.94	3.41	26.24	2.8	19128.23088
KNSTD	28.05	2.77	20.62	2.13	22915.41348
KNSTD	33.03	3.15	26.92	2.65	18926.62385

KNSTD	25.65	2.61	21.4	2.25	23534.25705
KNSTD	34.9	2.91	28.63	2.5	17705.18651
KNSTD	64.93	7.19	50.66	5.74	10015.08522
KNSTD	28.11	2.81	27.83	2.79	21595.93996
KNSTD	48.77	6.85	47.15	6.62	12741.18668
KNSTD	15.77	1.56	15.56	1.54	38680.97863
KNSTD	42.68	6.16	41.98	6.06	14313.83074
KNSTD	101.98	10.95	101.98	10.95	5891.168035
KNSTD	112.22	12.32	112.22	12.32	5353.623567
KNSTD	62.38	6.01	62.14	5.98	9673.401773
KNSTD	36.59	3.04	36.25	3.01	16599.23229
KNSTD	53.91	4.84	53.57	4.81	11227.59743
KNSTD	29.23	3.21	28.63	3.15	20999.02879
KNSTD	37.12	4.16	36.45	4.09	16488.38599
KNSTD	31.84	3.48	31.68	3.46	18975.10703
KNSTD	19.61	1.92	19.61	1.92	30656.62662
KNSTD	14.17	1.37	14.17	1.37	42449.32612
KNSTD	16.41	1.65	16.41	1.65	36647.6557
KNSTD	65.16	6.23	65.16	6.23	9224.666759
KNSTD	74	7.87	74	7.87	8123.270632
KNSTD	65.66	6.76	65.65	6.76	9156.251431
KNSTD	38.25	3.98	38.25	3.98	15726.97963
KNSTD	38.62	3.76	38.62	3.76	15574.04974
KNSTD	23.41	2.4	23.41	2.4	25697.85744
KNSTD	29.41	3.15	29.41	3.15	20455.38808
KNSTD	42.55	4.39	42.55	4.39	14136.27368
KNSTD	18.54	1.8	25.17	2.46	23914.14821
KNSTD	32.89	2.97	32.89	2.97	18289.89483
KNSTD	54.53	4.88	54.53	4.88	11029.08231
KNSTD	43.66	5.27	43.66	5.27	13778.01889
KNSTD	41.71	4.18	41.71	4.18	14421.82021
KNSTD	48.05	5.21	48.05	5.21	12515.15507
KNSTD	99.26	10.42	99.26	10.42	6059.228963
KNSTD	28.74	2.89	28.74	2.89	20939.66758
KNSTD	40.15	3.87	40.15	3.87	14983.37782
KNSTD	72.9	20.06	72.9	20.06	8241.899758
KNSTD	68.59	12.16	68.59	12.16	8759.683556
KNSTD	77.66	6.8	77.57	6.79	7727.116868
KNSTD	45.78	3.91	45.75	3.91	13107.55569
KNSTD	128.05	12.32	128.05	12.32	4679.347699
KNSTD	51.51	5.06	51.48	5.05	11646.86699
KNSTD	38.61	3.51	38.61	3.51	15537.29923
KNSTD	40.76	4.07	40.83	4.08	14689.95024
KNSTD	636.18	57.27	507.31	44.64	1183.670087
KNSTD	153.41	12.52	129.91	10.43	4624.932433
KNSTD	428.56	42.11	391.07	38.19	1537.44446
KNSTD	245.12	21.09	220.13	18.77	2731.093154
KNSTD	438.87	38.85	415.98	36.6	1445.876766
KNSTD	40.65		424.1	38.4	1418.19455
KNSTD	37.05		408.17	34.98	1473.561091

KNSTD	198.49	19.11	171.24	16.3	3506.465045
KNSTD	219.5	18.4	201.93	16.81	2977.702591
KNSTD	231.63	19.11	216.75	17.78	2774.43978
KNSTD	525.51	53.4	348.04	36.35	1413.391353
KNSTD	607.73	56.3	419.97	40.15	1186.965634
KNSTD	277.49	25.34	210.62	20.25	2281.308102
KNSTD	411.88	45.05	281.84	31.69	1729.086696
KNSTD	401	36.64	302.29	28.58	1667.677696
KNSTD	199.14	16.73	166.15	14.46	3097.875438
KNSTD	535.68	51.93	423.44	42.22	1205.902592
KNSTD	207.92	31.83	152.64	23.79	3157.630908
KNSTD	402.56	37.06	326.05	30.92	1574.452927
KNSTD	1010.4	109.89	739.01	82.45	675.2807163
KNSTD	695.51	76.23	539.48	60.61	935.8991007
KNSTD	216.1	20.4	158.93	15.84	2898.755528
KNSTD	237.35	19.66	189.62	16.39	2674.757809
KNSTD	352.85	41	287.82	34.25	1755.985992
KNSTD	288.74	30.51	221.78	24.49	2117.460847
KNSTD	287.09	27.98	220.91	22.45	2216.044997
KNSTD	569.89	51.68	485.8	45.24	1069.256406
KNSTD	183.71	17.24	141.77	14.04	3340.996745
KNSTD	899.11	88.53	740.84	74.64	698.6637183
KNSTD	584.38	53.77	487.45	46.2	1056.766875
KNSTD	85.72	8.84	62.61	6.75	7484.119634
KNSTD	217.05	19.71	184.9	17.34	2782.25547
KNSTD	133.34	11.19	104.02	9.3	4619.164335
KNSTD	580.86	51.89	493.98	45.47	1047.112881
KNSTD	353.16	30.88	298.63	26.92	1733.081603
KNSTD	203.71	20.23	164.78	17.05	2993.647853
KNSTD	350.05	39.02	292.6	33.29	1759.374718
KNSTD	260.01	23.68	204.43	19.64	2359.98643
KNSTD	456.1	47.64	372.96	40.1	1357.320581
KNSTD	752.07	81.63	620.99	69.14	820.1065523
KNSTD	219.93	21.88	185.73	18.94	2782.516752
KNSTD	357.2	38.5	278.99	31.15	1751.833129
KNSTD	49.83	3.77	38.29	3.16	12185.74116
KNSTD	377.92	43.59	312.05	36.76	1638.263277
KNSTD	199.06	17.77	161.67	15.12	3068.996802
KNSTD	18.53		160.05	15.73	3100.14435
KNSTD	17.01		163.32	14.58	3037.845863
KNSTD	639.56	79.34	534.08	67.5	957.9886071
KNSTD	389.99	55.79	301.03	44.13	1561.714567
KNSTD	150.77	12.67	122.43	10.88	4047.763611
KNSTD	12.88		128.5	11.11	3855.514591
KNSTD	12.45		116.89	10.67	4240.072929
KNSTD	94.72	8.44	73.25	6.94	6429.343524
KNSTD	402.18	48.55	570.86	71.79	896.2109322
S555	44.37	4.84	33.41	3.35	13800.47957
S555	44.28	6.67	33.35	5.12	13826.23874
S555	44.45	3.01	33.48	5.15	13774.81619

S555	35.86	4.56	27.48	3.59	16940.89744
S555	37.06	5.29	28.3	4.12	16497.56661
S555	60.7	5.4	45.36	4.03	9921.188558
S555	56.67	6.59	56.7	6.59	10582.01058
S555	64.72	4.2	64.76	7.54	9263.601572
S555	37.91	3.98	37.91	3.98	15832.02224
S555	20.26	3.03	12.62	1.2	47636.0605
S555	22.3	3.9	22.32	3.91	26911.56188
S555	32.66	4.73	32.69	4.73	18369.26821
S555	5.81	0.47	5.82	0.47	103419.3006
S555	30.61	7.26	30.12	7.15	19945.89676
S555	26.97	4.8	27.04	4.81	22211.11666
S555	45.25	4.78	44.49	4.17	13498.69231
S555	44.4	6.38	43.68	6.28	13752.43891
S555	46.09	3.17	45.34	6.7	13245.2524
S555	46.81	6.83	45.81	6.71	13110.45559
S555	49.69	6.98	48.82	6.86	12302.10904
S555	43.92	6.67	43.14	6.56	13920.42736
S555	82.64	6.86	81.28	6.06	7382.491499
S555	83.73	9.73	83.53	9.7	7182.940516
S555	94.13	6.16	93.91	11.8	6389.138465
S555	70.06	4.7	69.9	4.69	8585.809803
S555	54.61	7.39	53.59	7.26	11206.36522
S555	30.38	3.76	29.86	3.7	20121.98956
S555	115.68	12.02	115.22	10.57	5206.858735
S555	113.51	16.37	113.1	16.31	5304.740781
S555	117.85	7.66	117.42	17.44	5109.43777
S555	35.35	4.12	35.47	4.14	16926.38082
S555	20.76	2.63	20.85	2.65	28808.58496
S555	48.91	4.93	47.99	4.83	12517.79875
S555	55.49	7.72	54.79	7.63	10963.78525
S555	69	9.22	67.96	9.08	8838.069986
S555	134.13	16.49	133.49	16.41	4494.445147
S555	72.87	9.65	72.25	9.57	8312.422396
S555	54.25	6.03	53.56	5.95	11216.97128
S555	17.02	2.02	17.14	2.04	35064.65045
S555	107.7	17.43	107.22	17.35	5596.832193
S555	96.6	11.79	96.17	11.73	6240.44432
S555	28.59	4.77	28.23	4.72	21278.01051
S555	34.93	3.92	34.65	3.88	17337.40762
S555	27.56	2.97	27.24	2.94	22054.06001
S555	53.3	7.02	52.88	6.98	11363.23284
S555	51.2	6.97	50.88	6.93	11811.6921
S555	55.39	7.07	55.04	7.03	10917.32853
S555	21.07	2.02	20.98	2.01	28627.66148
S555	44.87	5.07	44.24	5	13579.11532
S555	23.44	2.6	23.43	2.6	25620.08615
S555	28.9	3.12	28.6	3.06	21013.92172
S555	29.27	3.65	28.97	3.61	20741.77783
S555	29.27	2.97	28.97	2.94	20741.77783

S555	28.17	2.73	27.88	2.7	21556.66033
S555	24.58	2.56	24.38	2.53	24660.53236
S555	26.09	2.65	26.14	2.65	22977.61119
S555	101.88	14.94	79.05	11.85	5894.097798
S555	36.25	5.25	28.57	4.22	16754.10214
S555	27.25	2.75	20.85	2.2	22252.81985
S555	12.74	1.25	9.84	1.01	47293.90204
S555	54.35	6.28	42.58	5.1	11055.83195
S555	81.25	11.93	65.38	9.79	7415.750126
S555	23.08	2.51	18.02	2.03	26139.94674
S555	12.1	1.3	9.36	1.05	49547.87563
S555	50.53	7.43	39.59	5.94	11918.59599
S555	32.45	3.37	25.75	2.78	18729.22227
S555	38.4	5.06	31.09	4.19	15710.30203
S555	30.19	3.11	23.62	2.54	20149.35711
S555	6.42	0.65	5.07	0.53	93913.24764
S555	32.39	4.84	25.74	3.91	18788.60471
S555	30.6	6.71	24.42	5.38	19819.15025
S555	31.46	3.46	25.09	2.86	19277.57295
S555	35.11	4.35	27.96	3.56	17271.71648
S555	21.65	2.49	16.59	1.98	27769.09993
S555	52.07	7.21	41.41	5.86	11614.90773
S555	27.49	2.98	21.89	2.46	22086.93972
S555	27.49	3.02	21.89	2.49	22086.93972
S555	27.49	2.94	21.89	2.43	22086.93972
S555	39.52	4.95	32.25	4.14	15237.65988
S555	31	3.38	25.46	2.86	19448.3949
S555	39.23	4.73	31.73	3.93	15360.0983
NIST_Certified	87.98	7	74.71	6.24	6809.843629
NIST_Certified	63.43	5.26	53.72	4.66	9448.223734
NIST_Certified	81.11	6.94	68.95	6.14	7402.780669
NIST_Certified	97.55	7.92	82.56	7.02	6160.64656
NIST_Certified	114.22	9.31	96.22	8.23	5265.149645
NIST_Certified	57.3	4.67	48.55	4.13	10527.49321
NIST_Certified	68.9	5.62	58.74	5.01	8690.315187
07KNSTD	159.24	12.96	136.97	11.61	3745.370956
07KNSTD	161.91	13.17	135.83	11.5	3777.121503
NIST_Certified	156.57	12.75	132.47	11.24	3873.1542
NIST_Certified	61.35	4.96	51.38	4.35	9899.642375
07KNSTD	92.16	8.13	78.19	7.16	6526.350139
07KNSTD	161.42	18.34	136.2	15.83	3747.265667
07KNSTD	438.05	71.27	375.42	61.67	1374.637761
07KNSTD	731.55	78.99	627.21	69.29	820.8676879
07KNSTD	481.37	50.32	410.28	43.83	1261.237826
KNSTD	24.9	1.92	19.48	1.63	24236.91585
KNSTD	14.49	1.15	11.05	0.95	42267.65996
KNSTD	14.41	1.15	11.12	0.96	41998.05759
KNSTD	14.62	1.17	11.28	0.97	41382.16429
KNSTD	16.81	1.32	12.92	1.1	35980.12098
KNSTD	12.13	0.96	9.4	0.8	49881.53136

KNSTD	22.51	1.7	17.26	1.42	26777.79451
KNSTD	28.75	2.28	22.08	1.9	20984.15696
KNSTD	7.2	0.6	5.69	0.51	83936.62785
KNSTD	15.63	1.2	15.57	1.2	38580.24691
KNSTD	15.59	1.24	15.57	1.23	38630.54711
KNSTD	31.67	2.47	31.59	2.46	19011.63274
KNSTD	9.93	0.85	9.92	0.85	60654.30835
KNSTD	32.96	2.5	32.88	2.5	18267.34256
KNSTD	17.31	1.38	17.26	1.37	34817.42612
KNSTD	34.52	2.64	34.51	2.64	17398.49068
KNSTD	8.46	0.76	8.46	0.76	71139.56694
KNSTD	34.18	2.65	34.02	2.63	17662.96848
KNSTD	10.35	0.86	10.35	0.86	58097.313
KNSTD	9.85	0.94	9.85	0.94	61029.10325
KNSTD	13.72	1.09	13.73	1.09	43798.41778
KNSTD	10.27	0.84	10.28	0.84	58498.77518
KNSTD	27.3	2.52	27.22	2.52	22070.48762
KNSTD	9.23	0.77	9.23	0.77	65191.70436
KNSTD	12.01	0.96	11.99	0.96	50177.1882
KNSTD	13.99	1.17	13.98	1.17	42972.63181
KNSTD	9.44	0.77	9.3	0.76	64622.96539
KNSTD	9.57	0.79	9.57	0.79	62841.20812
KNSTD	9.8	0.78	9.81	0.78	61281.55042
KNSTD	10.76	0.85	10.77	0.85	55852.27074
KNSTD	7.61	0.64	7.62	0.64	79012.34568
KNSTD	8.36	0.7	7.92	0.66	75973.40931
KNSTD	9.89	0.81	9.89	0.81	60841.1286
KNSTD	8.8	0.73	8.8	0.73	68349.78
KNSTD	9.39	0.78	9.39	0.78	64064.06406
KNSTD	5.37	0.47	5.37	0.47	112233.4456
KNSTD	19.2	1.52	17.72	1.41	33920.58343
KNSTD	12.4	1.02	12.25	1.01	49096.32084
KNSTD	17.26	1.39	17.06	1.37	35231.42643
KNSTD	21.72	1.73	21.47	1.71	27992.09223
KNSTD	25.41	1.93	25.12	1.91	23914.14821
KNSTD	16.37	1.28	16.32	1.28	36829.86902
KNSTD	15.84	1.26	15.84	1.26	37938.06611
KNSTD	15.14	1.2	15.14	1.2	39718.00218
KNSTD	17.52	1.36	17.52	1.36	34293.55281
KNSTD	16.97	1.31	16.97	1.31	35420.95592
KNSTD	48.74	3.62	47.9	3.56	12528.38462
KNSTD	15.57	1.22	15.56	1.22	38630.54711
KNSTD	24.4	1.85	24.28	1.84	24742.90574
KNSTD	24.09	1.79	24.12	1.79	24909.31453
KNSTD	26.33	2.01	26.37	2.02	22783.26
KNSTD	25.7	1.96	25.74	1.96	23339.60585
KNSTD	21.46	1.65	21.48	1.65	27965.67214
NIST_Certified	23.52	1.86	19.12	1.52	31437.27282
NIST_Certified	32.11	2.65	26.13	2.16	23004.37083
S555	12.2	1.26	12.14	1.25	49547.87563

S555	34.71	3.85	33.89	3.76	17721.07035
S555	3.58	0.44	3.58	0.44	168350.1684
S555	2.64	0.25	2.64	0.24	228800.2288
S555	34.6	4.16	25.92	3.23	17532.32522
S555	36.9	4.4	27.94	3.46	16433.51616
S555	3.83	0.36	3.18	0.31	157604.4129
S555	2.22	0.21	1.86	0.19	271831.4645
S555	54.93	6.6	42.15	5.24	11091.00866
S555	2.99	0.28	2.5	0.25	201562.1063
S555	3.09	0.29	2.58	0.25	195575.1131
S555	1.92	0.19	1.61	0.16	315208.8258
S555	2.59	0.26	2.17	0.22	233304.1703
S555	24.67	2.78	19.34	2.26	24609.32693
S555	41.7	6.51	31.01	4.94	14358.91913
S555	65.51	12.87	50.4	10.02	9283.919671
S555	69.39	8.71	53.08	6.88	8682.675349
S555	38.4	5.41	29.71	4.29	15541.37405
S555	4.7	0.43	3.89	0.37	128545.0309
S555	9.59	0.79	7.78	0.68	62774.63905
S555	9	0.74	7.31	0.64	66884.0398
S555	24.07	2.54	18.62	2.06	24993.36114
S555	17.71	1.67	13.81	1.38	33998.42757
S555	6.78	0.67	5.44	0.56	88977.86676
S555	3.81	0.33	3.11	0.29	158024.6914
S555	19.24	1.6	15.09	1.35	31271.37692
S555	18.07	1.59	14.09	1.32	33310.43241
S555	14.87	1.25	11.66	1.05	40394.85975
S555	25.94	2.66	20.26	2.18	23175.30671
S555	12.5	1.22	9.77	1	48100.0481
S555	19.29	1.81	14.91	1.48	31139.91553
S555	186.22	23.33	99.18	12.72	4265.097111
S555	169.26	21.16	90.09	11.54	4698.640918
S555	206.87	25.99	110.25	14.17	3833.813758
S555	169.28	25.14	90.47	13.69	4705.730109
S555	117.52	42.12	65.67	23.72	6406.406406
S555	126.1	31.54	70.48	17.81	5964.096141
S555	109.99	51.81	61.45	29.14	6851.573507
S555	221.94	43.41	117.33	23.2	3734.748803
S555	725.26	289.92	412.44	165.34	1072.041885
S555	625.81	225.68	355.79	128.74	1243.114312
S555	862.02	394.75	490.34	225.04	901.4460321
S555	353.67	207.91	189.62	111.83	2270.295734
S555	258.08	69.07	139.87	37.66	3263.534489
S555	261.17	30.2	143.73	16.99	3198.189825
S555	320.15	47.14	186.84	27.93	2489.884843
S555	453.24	72.4	266.65	43.14	1746.103461
S555	472.09	94.74	277.75	56.2	1676.07363
S555	435.82	54.56	330.43	40.79	1816.153093
S555	192.49	26.88	153.41	21.27	3915.120194
S555	198.96	28.49	158.58	22.55	3787.26013

S555	186.43	25.43	148.55	20.11	4043.06879
S555	416.03	60.8	335.27	48.63	1791.067499
S555	418.04	65.69	336.89	52.6	1782.447791
S555	414.04	56.14	333.67	44.84	1799.661664
S555	597.34	122.06	489.93	99.78	1225.732413
S555	466.69	77.36	382.58	63.09	1569.74012
S555	828.82	231.89	680.15	189.98	882.8852691
S555	362.74	63.77	290.35	50.81	2068.530413
S555	352.03	52.2	281.75	41.49	2131.704711
S555	374.12	77.41	299.48	61.77	2005.389484
S555	498.55	97.88	436.97	85.6	1374.701539
S555	602.11	90.52	548.55	82.22	1095.344989
S555	33.57	4.21	34.17	4.28	17532.32522
S555	141.69	13.52	138.06	13.16	4356.337518
S555	393.45	88.43	355.26	79.79	1686.616174
S555	247.53	36.06	214.32	31.09	2803.446838
S555	419.93	110.94	411.23	108.65	1455.393552
S555	508.41	177.47	496.12	173.18	1208.97787
S555	445.44	111.49	434.65	108.77	1379.983682
S555	591.9	301.52	577.62	294.25	1038.360947
S555	253.61	35.2	251.39	34.88	2388.426878
S555	1504.45	604.31	1507.86	605.72	398.7944444
S555	1270.67	424.26	1273.56	425.27	472.1665213
S555	1843.42	950.56	1847.6	952.75	325.4608424
S555	464.52	99.21	454.53	97.07	1322.161072
S555	747.76	134.91	746.9	134.8	804.7265615
S555	722.75	138.36	728.86	139.59	824.752046
S555	450.62	107.98	442.14	105.93	1358.036008
S555	399.25	86.75	391.72	85.1	1532.870981
S555	517.02	139.45	507.31	136.81	1183.551884
S555	1042.64	220.87	1019.86	216.01	589.4625465
S555	839.02	158.97	820.67	155.47	732.5453892
S555	1376.31	344.79	1346.28	337.24	446.5353462
S555	556.92	130.72	557.33	130.84	1077.833017
S555	610.17	160.82	610.62	160.96	983.7357735
S555	512.17	108.32	512.55	108.43	1171.988594
S555	817.77	285.49	791.97	276.48	758.9848388
S555	1145.98	505.02	977.66	430.69	614.2638202
S555	545.69	117.88	560.2	121.09	1072.857052
S555	549.06	112.22	563.66	115.28	1066.255092
S555	542.36	123.52	556.78	126.88	1079.442953
S555	273.98	56.95	273.38	56.83	2197.473181
S555	840.94	225.89	842.45	226.31	713.992786
S555	775.72	167.74	785.06	169.83	765.8213913
S555	985.63	279.89	1009.08	286.63	595.8279383
S555	1178.4	256.6	1168.94	254.53	513.8412783
S555	1677.54	459.02	1700.39	465.37	353.792959
S555	772.07	176.92	662.34	152.7	769.0714088
S555	976.5	249.34	837.56	214.92	608.0616818
S555	638.3	135.73	547.68	117.28	930.2428341

S555	1038.21	285.5	868.4	239.95	578.3817529
S555	323.41	53.48	280.13	46.94	1804.209446
S555	688.89	132.66	601.58	117.03	839.6398155
S555	1379.5	267.57	1188.56	232.21	433.3401043
S555	369.64	51.4	132.53	18.45	3505.220588
S555	334.75	62.12	281.46	52.9	1747.390654
S555	278.35	63.01	222.11	50.73	2145.597569
S555	289.6	76.51	231.05	61.44	2062.267592
S555	267.94	51.78	213.82	41.85	2229.048684
S555	117.72	21.45	92.77	17.14	5103.717101
S555	709.32	133.43	620.88	117.7	830.1941617
S555	539	85.8	473.46	76.42	1072.701686
S555	377.51	84.58	308.05	69.61	1587.145707
S555	1262.97	465.37	1055.77	390.04	476.7783609
S555	104.65	13.84	82.82	11.25	5742.176285
07KNSTD	18.02	2.05	13.86	1.23	34940.60098
07KNSTD	15.75	1.75	12.28	1.07	39664.83217
07KNSTD	6.29	0.7	5.05	0.47	99095.75127
07KNSTD	9.59	1.08	7.59	0.68	65552.27794
S555	30.02	3.57	22.45	2.17	23103.02505
S555	270.99	48.71	2089.39	357.32	240.6125394
S555	420.28	118.73	3188.71	906.83	158.4315436
S555	89.28	10.42	734.54	68.12	694.2112329
S555	107.25	17.51	821.48	120.54	610.8635205
S555	145.21	30.93	1095.39	222.51	465.0703128
S555	259.7	32.69	1976.73	206.46	255.4454586
S555	177.09	21.17	1357.69	129.16	368.216305
S555	64.76	10.41	492.93	70.9	1034.807028
S555	379.07	74.66	2863.36	525.5	177.7944905
S555	72.4	9.73	55.03	6.08	8480.145859
S555	56.12	7.08	42.5	4.25	11022.92769
S555	63.98	7.98	49.22	4.69	9687.63434
S555	24.94	2.98	19.29	1.89	25056.76924
S555	107	13.78	80.32	8.1	5783.083757
S555	79.76	9.96	59.53	5.93	7714.040518
S555	63.33	8.14	49.42	5.61	9567.203626
S555	48.99	6.69	37.34	4.32	12523.08945
S555	81.53	9.99	62.53	6.11	7611.001703
S555	48.56	5.96	37.54	3.67	12899.2728
S555	40.69	5.25	31.4	3.28	15432.09877
S555	64.85	8.04	49.93	4.96	9513.446662
S555	56.02	6.92	42.65	4.3	11072.35786
S555	87.05	10.93	62.86	6.48	7467.144564
S555	74.19	8.77	57.09	5.37	8382.976271
S555	84.2	10.14	63.82	6.04	7319.572537
S555	77.2	11.76	58.22	7.85	7969.238738
S555	56.29	7.01	43.23	4.47	11024.97847
S555	82.03	10.06	79.21	7.47	7582.758702
S555	44.2	5.33	43.7	4.02	13739.6845
S555	44.85	9.12	44.35	8.72	13538.78439

S555	61.67	13.52	61.12	12.73	9820.891491
S555	53.35	6.41	51.93	4.63	11558.27175
S555	82.32	10.08	76.11	7.43	7881.268687
S555	27.77	3.44	27.34	2.56	21972.28745
S555	46.97	6.35	46.55	5.08	12899.2728
S555	52.23	6.04	51.71	4.47	11608.08213
S555	50.24	5.74	49.59	4.14	12108.55318
S555	52.03	6.51	51.49	4.68	11658.32368
S555	80.56	9.57	80.25	7.33	7475.622462
S555	52.08	6.44	51.65	4.71	11619.4626
S555	49.18	5.93	48.64	4.51	12343.10753
NIST_27900	498.32	859.79	348.68	67.44	1724.00603
NIST_27900	927.57	1647.35	785.73	154.98	765.5245997
NIST_27900	1353.92	2453.9	1156.47	227.4	520.1100553
NIST_27900	1529.42	3300.67	1328.08	303.98	452.9520157
NIST_27900	1305.81	2616.11	1096.51	235.82	548.7222488
NIST_27900	1499.1	2608.01	1212.12	234.47	496.3710622
NIST_27900	1823.74	3247.37	1497.91	290.33	401.6079378
NIST_27900	376.08	689.24	336.35	65.9	1787.124439
NIST_27900	308.14	582.08	234.66	47.84	2561.23349
NIST_27900	426.17	911.22	373.52	82.62	1609.78103
NIST_27900	686.13	1339.51	562.51	116.85	1068.427435
NIST_27900	740.14	1379.79	635.34	128.92	946.3916453
S555N	17.08	2	15.26	1.3	39348.77773
S555N	13.21	1.49	11.58	0.92	51845.37118
S555	1616.5	333.99	140.89	27.99	4270.322062
S555	399.77	61.41	34.21	4.59	17589.56939
S555	589.45	77.95	50.73	5.63	11856.59449
S555	439.1	81.59	37.75	6.79	15938.47748
S555	374.82	55.03	26.9	3.59	22370.4263
S555	543.66	88.51	47.33	6.95	12705.67308
S555	1391.64	285.88	120.03	23.39	5009.659249
S555	377.24	73.95	32.73	5.91	18374.96411
S555	1836.09	392.51	157.07	34.65	3829.106957
S555	461.36	56.97	39.64	4.18	15183.00263
S555	1144.5	361.7	73.69	10.3	8163.556862
S555	723.08	106.5	62.47	8.15	9632.519385
S555	262.11	38.87	22.41	2.94	26850.59323
S555	424.82	83.97	34.87	6.43	17256.62762
S555	723.26	94.68	61.8	6.74	9735.380197
S555	993.67	185.58	90.15	14.94	6670.335351
S555	396.12	63.35	33.31	4.81	18061.34083
S555	1044.67	177.59	89.57	13.72	6714.169415
S555	882.25	135.57	72.98	10.1	8243.046218
S555	714.43	125.07	61.34	9.84	9809.511548
S555	990.27	170.25	83.44	13.24	7211.787667
S555	1745.45	468.49	146.53	39.47	4106.101667
S555	850.3	135.84	61.23	9.03	8429.482114
S555	255.49	48.17	18.2	3.28	26777.79451
S555	383.29	60.16	27.64	4.13	18278.61174

S555	1686.35	299.85	125.15	20.71	4115.226337
S555	638.38	99.26	46.92	6.6	10845.39884
S555	784.31	178.69	58.12	12.41	8458.358444
S555	1085.7	181.23	79.5	12.06	6460.183065
S555	1057.9	179.84	75.98	12.44	6781.011473
S555	735.84	109.43	52.13	7.09	9786.830596
S555	207.53	26.72	14.96	1.71	34214.35292
S555	1100.65	295.32	81.15	22.13	6221.444542
S555	580.35	88.4	570.11	76.86	911.2463173
S555	427.38	72.1	363.56	55.34	1417.380451
S555	176.65	24.51	132.08	16.79	3887.382528
S555	514.71	74.79	386.71	50.15	1325.858804
S555	3668.85	1011.17	2693.44	771.59	191.1527346
S555	1711.96	463	1258.76	346.17	409.0654006
S555	342.33	49.89	275.25	35.56	1850.00185
S555	105.59	13.15	79.1	8.23	6518.453334
S555	127.38	16.28	95.28	10.48	5456.151299
S555	337.98	61.66	254.74	42.02	2003.220176
S555	710.68	138.2	535.93	96.82	950.5358943
S555	984.54	236.41	737.74	171.59	686.1490101
S555	1709.63	417.19	1286.41	303.17	393.9481682
S555	998	260.38	771.45	204.35	651.0933281
S555	98.09	11.6	67.28	6.26	7819.90753
S555	49.93	5.57	33.16	2.97	16003.04058
S555	130.69	15.64	84.83	8.14	6218.180405
S555	209.37	25.13	136.04	13.47	3909.695801
S555	62.51	7.02	40.89	3.83	13021.15123
S555	1119.14	149.98	740.76	86.32	711.3871293
S555	498.51	62.38	343.18	35.92	1520.911102
S555	563.56	69.68	375.37	39.69	1403.61589
S555	660.57	88.62	444.05	50.64	1182.512706
S555	1482.13	265.64	981.47	162.25	537.0069982
S555	134.62	16.35	90.35	8.79	5828.015269
S555	235.97	28.42	157.15	15.57	3355.563944
S555	422.97	49.6	297.33	29.44	1770.307082
S555	19.79	2.21	14.4	1.34	36177.81396
S555	113.8	20.5	85.91	15.17	5824.578264
07KNSTD	16.59	1.92	12.7	1.11	37696.72981
07KNSTD	16.95	1.92	12.91	1.13	36990.79854
07KNSTD	16.7	1.99	12.8	1.26	37363.97179
07KNSTD	15.76	1.78	12.18	1.06	40013.00423
07KNSTD	3.85	0.44	3.11	0.3	161469.3713
07KNSTD	6	0.7	4.8	0.44	103963.6127
07KNSTD	6.51	0.74	5.21	0.48	95888.76903
07KNSTD	6.13	0.68	4.89	0.45	99595.39371
07KNSTD	4.72	0.54	3.81	0.36	126893.4888
07KNSTD	3.86	0.44	3.12	0.3	161030.5958
07KNSTD	2.32	0.29	2.36	0.23	255427.8416
07KNSTD	3.35	0.39	3.34	0.31	180668.4734
07KNSTD	6.49	0.72	6.43	0.56	93616.52332

07KNSTD	7.95	0.9	7.81	0.67	77060.15508
07KNSTD	7.44	0.85	7.16	0.62	84175.08418
07KNSTD	3.3	0.39	3.17	0.3	189933.5233
07KNSTD	5.77	0.67	5.56	0.5	108335.0261
KNSTD	18	± 1.4	18	1.41	33385.49817
KNSTD	18	± 1.4	18.35	1.51	32758.0206
KNSTD	18	± 1.4	20.68	1.78	29048.6565
KNSTD	18	± 1.4	28.22	2.16	21293.30193
NIST_30600	13.1	± 1.0	12.97	1.01	46368.74746
NIST_30600	19.5	± 1.5	19.34	1.46	31074.59846
NIST_30600	16.6	± 1.3	16.4	1.25	36647.6557
NIST_30600	15.6	± 1.2	15.46	1.19	38858.53066
NIST_30600	14.2	± 1.1	14.09	1.09	42663.25361
NIST_30600	10	± 0.8	9.88	0.76	60841.1286
NIST_30600	15.7	± 1.3	15.49	1.3	38807.6354
NIST_30600	11.9	± 0.9	11.75	0.89	51173.79901
NIST_30600	13.3	± 1.0	13.14	1.01	45760.04576
NIST_30600	7.7	± 0.6	7.59	0.61	79329.66434
NIST_30600	8.8	± 0.7	8.68	0.68	69228.10661
NIST_30600	19.1	± 1.4	18.86	1.42	31859.81681
NIST_30600	11.6	± 0.9	11.48	0.87	52349.16896
NIST_30600	7	± 0.6	6.91	0.56	87018.00185
NIST_30600	10.4	± 0.8	10.24	0.8	58730.68311
NIST_30600	11.3	± 0.9	11.21	0.88	53628.28892
NIST_30600	5	± 0.4	4.96	0.44	121432.9083
NIST_30600	5	± 0.4	5.94	0.52	101297.8791
NIST_30600	5	± 0.4	6.65	0.56	90472.15154
NIST_30600	5	± 0.4	6.66	0.58	90334.23668
NIST_30600	3.8	± 0.3	3.77	0.33	160160.1602
NIST_30600	7	± 0.6	6.9	0.57	87274.31408
NIST_30600	21.3	± 1.6	21.08	1.59	28517.44911
NIST_30600	4.6	± 0.4	4.56	0.39	132275.1323
NIST_30600	12.3	± 1.0	12.14	0.94	49547.87563
NIST_30600	7.9	± 0.7	7.83	0.72	76860.25844
NIST_30600	10	± 0.8	9.9	0.78	60778.72745
NIST_30600	7.5	± 0.6	7.39	0.6	81400.0814
NIST_30600	6.6	± 0.6	6.51	0.55	92448.14237
NIST_30600	6.6	± 0.6	8.56	0.7	70212.39249
NIST_30600	6.6	± 0.6	10.05	0.84	59797.43618
NIST_30600	6.6	± 0.6	8.39	0.69	71742.44462
NIST_30600	6.1	± 0.5	6.02	0.5	100100.1001
NIST_30600	3.8	± 0.3	3.77	0.33	159728.4616
NIST_30600	6.3	± 0.5	6.24	0.51	96513.45156
NIST_30600	4.1	± 0.4	4.11	0.35	146681.3348
NIST_30600	14.7	± 1.1	14.5	1.1	41469.04077
NIST_30600	5.3	± 0.5	5.21	0.47	115740.7407
NIST_30600	9.1	± 0.7	9	0.73	66808.63502
NIST_30600	7.6	± 0.6	6.03	0.52	79864.23081
NIST_30600	14.6	± 1.2	11.34	0.98	41731.87272
NIST_30600	--		12.49	1.08	37792.89494

NIST_30600	--		11.19	0.97	42297.82959
NIST_30600	--		8.02	0.71	59557.04448
NIST_30600	6	± 0.5	4.73	0.42	100952.7415
NIST_30600	5.2	± 0.4	4.13	0.36	117811.6486
NIST_30600	5.6	± 0.5	4.48	0.39	108335.0261
NIST_30600	7.7	± 0.6	6.11	0.52	78593.18204
NIST_30600	8.6	± 0.8	6.85	0.69	70546.73721
NIST_30600	14.4	± 1.1	11.31	0.94	42297.82959
NIST_30600	14.3	± 1.1	11.13	0.93	42632.56062
NIST_30600	4.4	± 0.4	3.49	0.32	138780.4666
NIST_30600	16.2	± 1.2	12.43	1.02	37482.13742
NIST_30600	11.6	± 0.9	9.12	0.78	52534.80431
NIST_30600	7	± 0.6	5.6	0.48	86636.34395
NIST_30600	4.3	± 0.4	3.38	0.3	143138.3074
NIST_30600	8.3	± 0.7	6.53	0.56	73522.65417
NIST_30600	13.7	± 1.1	10.67	0.89	44388.95825
NIST_30600	8.5	± 0.7	6.48	0.56	71742.44462
NIST_30600	13.1	± 1.0	9.99	0.83	46477.8504
NIST_30600	3	± 0.3	2.38	0.22	202250.0316
NIST_30600	6.6	± 0.5	5.26	0.46	91874.82056
NIST_27900	0.02	0	4.67	0.88	105256.2331
NIST_27900	0.04	0.01	5.42	0.52	86763.19072
NIST_27900	0.04	0.01	5.53	0.49	85142.61388
NIST_27900	0.03	0.01	3.76	0.42	126893.4888
NIST_27900	0.05	0.01	6.95	0.61	67187.36877
NIST_27900	0.14	0.03	30.57	4.8	15468.35272
NIST_27900	0.13	0.02	28.89	3.47	16379.0103
NIST_27900	0.05	0.01	5.2	0.57	90334.23668
NIST_27900	0.03	0	10.65	0.92	45236.07577
NIST_27900	0.05	0.01	15.97	1.42	28476.33794
NIST_27900	0.04	0.01	14.76	1.34	30896.38126
NIST_27900	0.06	0.01	17.69	1.45	25653.35899
NIST_27900	0.06	0.01	17.94	1.51	25281.25395
NIST_27900	0.2	0.03	67.47	5.52	7117.374401
NIST_27900	0.27	0.04	54.75	5.18	8428.283211
NIST_27900	0.21	0.04	47.52	6.74	9612.207504
NIST_27900	0.17	0.03	38.7	3.54	11644.57836
NIST_27900	0.18	0.12	69.26	80.85	6701.261931
NIST_27900	0.13	0.06	79.42	46.07	5839.501307
NIST_27900	0.1	0.02	39.17	5.5	11957.0741
07KNSTD	0.003	0.0003	1.95	0.19	254331.5848
07KNSTD	0.0014	0.0001	0.87	0.53	569800.5698
07KNSTD	0.0111	0.0009	7.96	0.67	62116.62396
07KNSTD	0.1315	0.0112	97.71	9.09	4618.084419
07KNSTD	0.0101	0.0008	6.69	0.57	72800.0728
07KNSTD	0.0029	0.0003	2.32	0.22	215488.2155
07KNSTD	0.0062	0.0005	4.69	0.41	106390.0525
07KNSTD	0.0877	0.0062	83.28	5.92	7205.649229
07KNSTD	0.0885	0.0062	84.53	5.98	7099.467984
07KNSTD	0.095	0.0067	90.51	6.46	6630.035719

07KNSTD	0.0174	0.0013	14.75	1.13	40756.02425
07KNSTD	0.0358	0.0026	32.58	2.37	18432.11797
07KNSTD	0.0407	0.0028	36.53	2.58	16442.63575
07KNSTD	0.0086	0.0007	6.88	0.55	87403.03726
07KNSTD	0.0052	0.0004	4.41	0.38	136542.072
07KNSTD	0.0058	0.0005	4.71	0.38	127713.9208
07KNSTD	0.0086	0.0007	7.16	0.56	84055.68689
07KNSTD	0.0422	0.0029	38.21	2.7	15714.46811
07KNSTD	0.0245	0.0017	23.39	1.67	25686.71836
07KNSTD	0.0962	0.0066	88.8	6.17	6754.731478
07KNSTD	32.1	± 3.3	27.01	2.82	22236.1198
07KNSTD	69.6	± 6.4	60.1	5.55	9986.393539
07KNSTD	41.7	± 3.8	34.41	3.17	17444.58618
07KNSTD	39	± 3.3	30.63	2.59	19602.7983
07KNSTD	22.7	± 1.8	18.72	1.48	32101.44055
07KNSTD	27.6	± 2.3	23.03	1.93	26082.42045
07KNSTD	44.5	± 3.8	38.69	3.29	15521.02128
07KNSTD	17.9	± 1.4	15.17	1.24	39611.80432
07KNSTD	50.4	± 4.8	43.77	4.29	13717.42112
07KNSTD	10.5	± 0.9	7.8	0.66	77060.15508
07KNSTD	16.9	± 1.4	15.13	1.25	39718.00218
07KNSTD	49.5	± 4.9	46.39	4.16	12941.52856
07KNSTD	23.1	± 1.8	19.61	1.56	30640.77521
07KNSTD	13.1	± 1.1	9.7	0.81	61986.67287
07KNSTD	17.5	± 1.2	13.34	1.09	45029.83226
07KNSTD	15.3	± 1.2	11.68	0.95	51485.02108
07KNSTD	15	± 1.2	11.58	0.94	51890.76993
07KNSTD	25.8	± 2.2	18.95	1.62	31689.44345
07KNSTD	42.2	± 3.5	34.09	2.84	17610.47823
07KNSTD	25.2	± 2.1	19.1	1.62	31453.95927
07KNSTD	7.47	± 0.67	5.37	0.49	112233.4456
07KNSTD	11.6	± 0.9	9.24	0.75	65048.58316
07KNSTD	12.3	± 1.2	13.06	1.23	46044.49049
07KNSTD	29.5	± 2.4	24.36	1.96	24650.27423
07KNSTD	20.9	± 1.6	15.66	1.21	38380.34926
07KNSTD	10.6	± 0.9	7.57	0.63	79436.00437
07KNSTD	16.9	± 1.3	12.93	1.02	46477.8504
07KNSTD	7.54	± 0.63	5.32	0.46	113090.1894
07KNSTD	14.6	± 1.2	16.35	1.33	36761.32708
07KNSTD	19.6	± 1.8	18.95	1.7	31689.44345
07KNSTD	8.03	± 0.68	7.47	0.64	80515.29791
07KNSTD	10.1	± 0.8	9.52	0.77	63176.18258
07KNSTD	20.4	± 1.7	20.42	1.71	29423.66398
07KNSTD	24.8	± 1.8	25.23	1.92	23798.8993
07KNSTD	4.42	± 0.39	3.96	0.35	151946.8186
07KNSTD	13.7	± 1.1	14.26	1.13	42177.40873
07KNSTD	18.3	± 1.4	19.1	1.5	31470.66344
07KNSTD	29.1	± 2.3	21.1	1.79	22045.85538
07KNSTD	8.7	± 0.74	6.68	0.61	71742.44462
07KNSTD	11.5	± 1.0	8.47	0.75	56169.91399

07KNSTD	11.3	± 0.9	8.06	0.7	58097.313
07KNSTD	6.12	± 0.52	3.55	0.33	135295.1125
07KNSTD	8.02	± 0.67	4.31	0.39	110352.4381
07KNSTD	21.2	± 1.7	14.58	1.3	31997.4402
07KNSTD	17.3	± 1.3	11.3	0.95	41411.08264
07KNSTD	37	± 3.0	22.83	2.01	19912.3855
07KNSTD	25.8	± 2.0	17.18	1.47	26972.80804
07KNSTD	26.5	± 2.4	17.22	1.65	26419.643
07KNSTD	11.3	± 0.9	9.28	0.81	50262.30641
07KNSTD	6.7	± 0.6	4.32	0.42	107744.1077
07KNSTD	14.7	± 1.2	9.34	0.81	48374.90552
07KNSTD	10.5	± 0.8	6.4	0.56	71482.82178
07KNSTD	10.9	± 0.9	6.79	0.6	67187.36877
07KNSTD	12.1	± 1.0	10.76	0.94	43798.41778
07KNSTD	15.7	± 1.2	11.99	1	38355.50761
07KNSTD	11.4	± 0.9	9.32	0.8	50177.1882
07KNSTD	10.4	± 0.9	7	0.62	66285.5249
07KNSTD	12	± 1.0	9.3	0.81	50177.1882
07KNSTD	10.5	± 0.9	9.08	0.8	51800.0518
07KNSTD	50	5	37.17	3.76	12930.23331
07KNSTD	466	99	343.99	73.88	1384.982805
07KNSTD	29	2	21.52	1.92	22438.1898
07KNSTD	29	2	21.49	1.86	22618.03789
07KNSTD	351	88	256.25	64.53	1851.562545
07KNSTD	228	37	165.6	27.53	2850.373221
07KNSTD	17	2	12.91	1.34	37577.20942
07KNSTD	336	72	243.54	52.38	1926.253389
07KNSTD	357	49	260.76	36.43	1817.099818
07KNSTD	36	3	25.96	2.36	18329.4956
07KNSTD	421	70	309.33	52.29	1544.094514
07KNSTD	25	2	18.16	1.62	26621.41027
07KNSTD	303	90	217.09	64.73	2147.308014
07KNSTD	275	30	199.93	22.59	2359.610546
07KNSTD	1253	335	922.05	7618.08	514.9486371
07KNSTD	309	41	227.88	31.25	2097.969952
07KNSTD	290	20	234.54	20.71	2029.357188
07KNSTD	150	10	119.16	10.26	4023.578168
07KNSTD	110	10	93.72	7.45	5136.007909
07KNSTD	370	30	301.2	24	1569.781702
07KNSTD	300	20	253.15	21.49	1869.082456
07KNSTD	220	20	220.7	15.94	2720.186333
07KNSTD	110	10	109.23	7.76	5498.168423
07KNSTD	150	10	149.88	10.64	4005.357165
07KNSTD	180	10	181.67	13.88	3304.84966
07KNSTD	140	10	145.55	10.51	4124.391652
07KNSTD	130	10	129.8	10.29	4625.293417
07KNSTD	120	10	125.64	8.82	4778.201843
07KNSTD	510	40	520.43	42.41	1153.128221

07KNSTD	360	30	365.21	28.56	1643.214909
07KNSTD	380	30	381.36	29.5	1573.70032
07KNSTD	180	10	179.79	14.54	3339.302336
07KNSTD	250	20	252.25	21.08	2379.69879
07KNSTD	360	30	362.59	28.01	1655.101644
07KNSTD	250	20	256.83	19.17	2335.340266
07KNSTD	280	20	318.52	25.71	1884.656657
07KNSTD	670	50	688.6	57.52	871.5237776
07KNSTD	960	70	930.42	72.4	644.9215251
07KNSTD	2380	420	2504.41	439.48	239.6288628
07KNSTD	1070	90	1077.03	88.93	557.0945292
NIST_27900	0.76	± 0.09	0.77	0.49	790123.4568
NIST_27900	0.57	± 0.07	0.58	0.4	1058201.058
NIST_27900	28.32	± 1.91	28.48	1.87	21051.24663
NIST_27900	10.51	± 0.77	10.58	0.76	56761.74259
NIST_27900	5.04	± 0.40	5.08	0.41	118281.9546
NIST_27900	1.53	± 0.15	1.54	0.15	392445.4256
NIST_27900	1.33	± 0.14	1.34	0.14	448933.7823
NIST_27900	12.64	± 0.91	12.72	0.91	47218.53327
NIST_27900	26.92	± 1.87	26.64	1.81	22506.36508
NIST_27900	11.85	± 0.87	11.93	0.87	50347.7139
NIST SRM-4325	3.72	0.33	2.83	0.27	251098.5562
NIST SRM-4325	3.3	0.3	2.5	0.24	283537.1256
NIST SRM-4325	3.33	0.31	2.54	0.24	280849.5699
NIST SRM-4325	3.23	0.3	2.46	0.24	290486.565
NIST SRM-4325	3	0.28	2.28	0.22	313541.0543
NIST SRM-4325	4.15	0.37	3.17	0.3	225320.3774
07KNSTD	1.01	0.14	0.64	0.43	1097393.69
07KNSTD	1.43	0.18	0.97	0.58	713966.979
07KNSTD	0.55	0.09	0.4	0.32	1911589.008
07KNSTD	0.82	0.11	0.59	0.41	1234567.901
07KNSTD	1.44	0.21	1	0.6	697167.756
07KNSTD	0.52	0.11	0.37	0.31	2043422.733
07KNSTD	0.37	0.07	0.29	0.27	2693602.694
07KNSTD	0.13	0.04	0.07	0.17	19753086.42
07KNSTD	2.76	0.31	1.82	0.19	323821.0888
07KNSTD	2.99	0.344	1.96	0.21	300808.4226
07KNSTD	1.1	0.16	0.79	0.5	750117.2058
07KNSTD	0.488	0.08	0.27	0.26	2194787.38
07KNSTD	0.29	0.06	0.17	0.21	3485838.78
07KNSTD	0.42	0.07	0.27	0.26	2116402.116
07KNSTD	12.38	1.27	8.67	0.83	68035.88893
07KNSTD	0.91	0.12	0.64	0.43	925925.9259
07KNSTD	10.37	1.03	7.26	0.67	81177.06748
07KNSTD	0.955	0.14	0.55	0.39	1058201.058
07KNSTD	0.6	0.09	0.38	0.31	1519468.186

Appendix 2

Figure 1: Location of NQBR8

Figure 2: Sample BR-1

Figure 3: Sample location of CN3

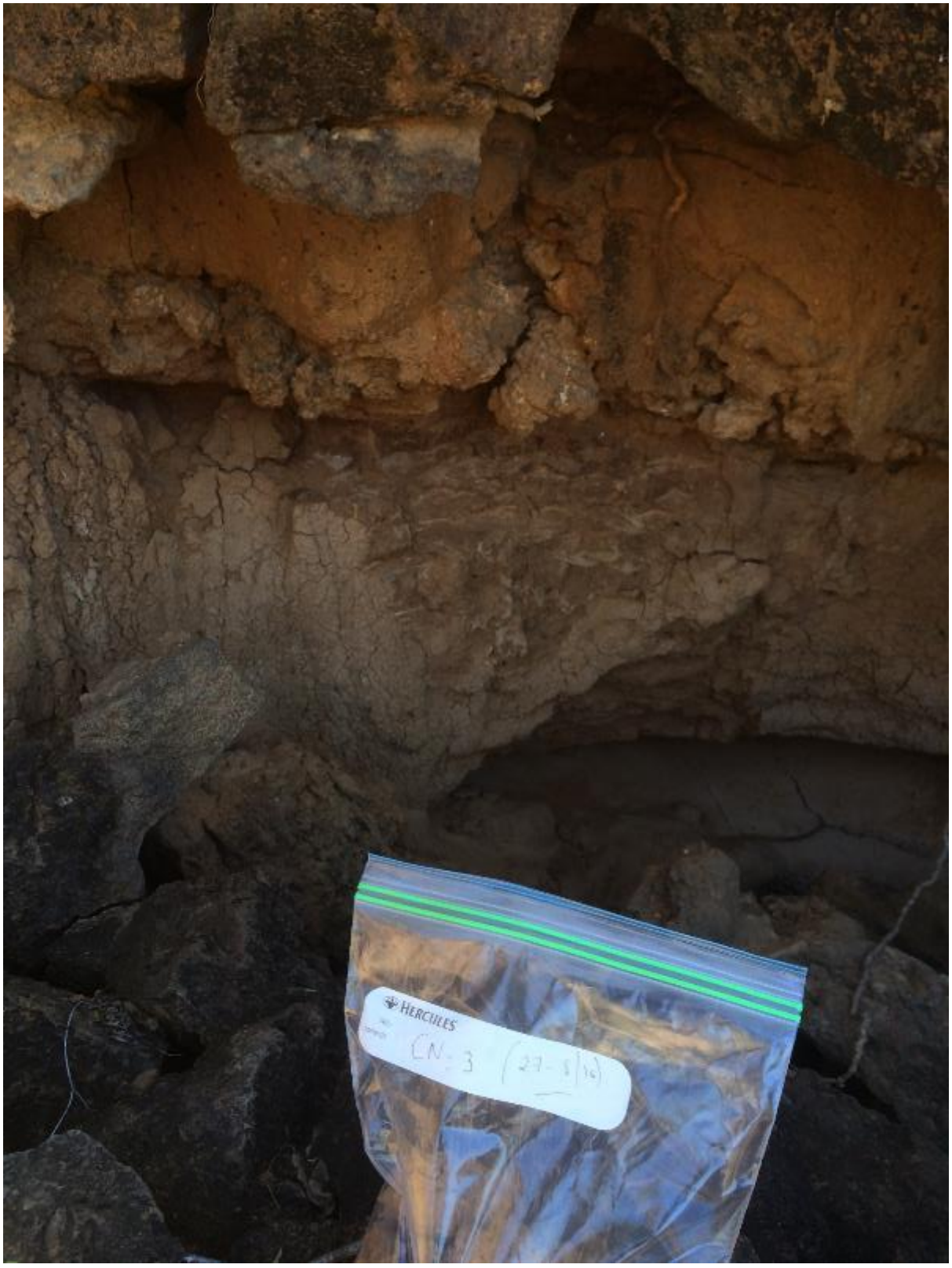

Figure 4: Sample location of CN3

Figure 5: The Great Dividing Range board near sample PGBR6, PGBR7, and PGBR8

Figure 6: Location of bedrock sample in southern study area

Figure 7: Location of sample PGBR6, PGBR7, and PGBR8

Figure 8: Location of sample NQ1

Figure 9: Location of sample NQ2

Figure 10: Location of sample NQ3

Figure 11: Location of sample NQ5

Figure 12: Location of sample NQ7

Figure 13: Location of sample NQ10

Figure 14: Location of sample NQ13

Figure 15: Location of sample NQBR1

Figure 16: Location of sample NQBR2

Figure 17: Location of sample NQBR3

Figure 18: Sampling area of NQBR3

Figure 19: Location of sample NQBR4

Figure 20: Sample NQBR5

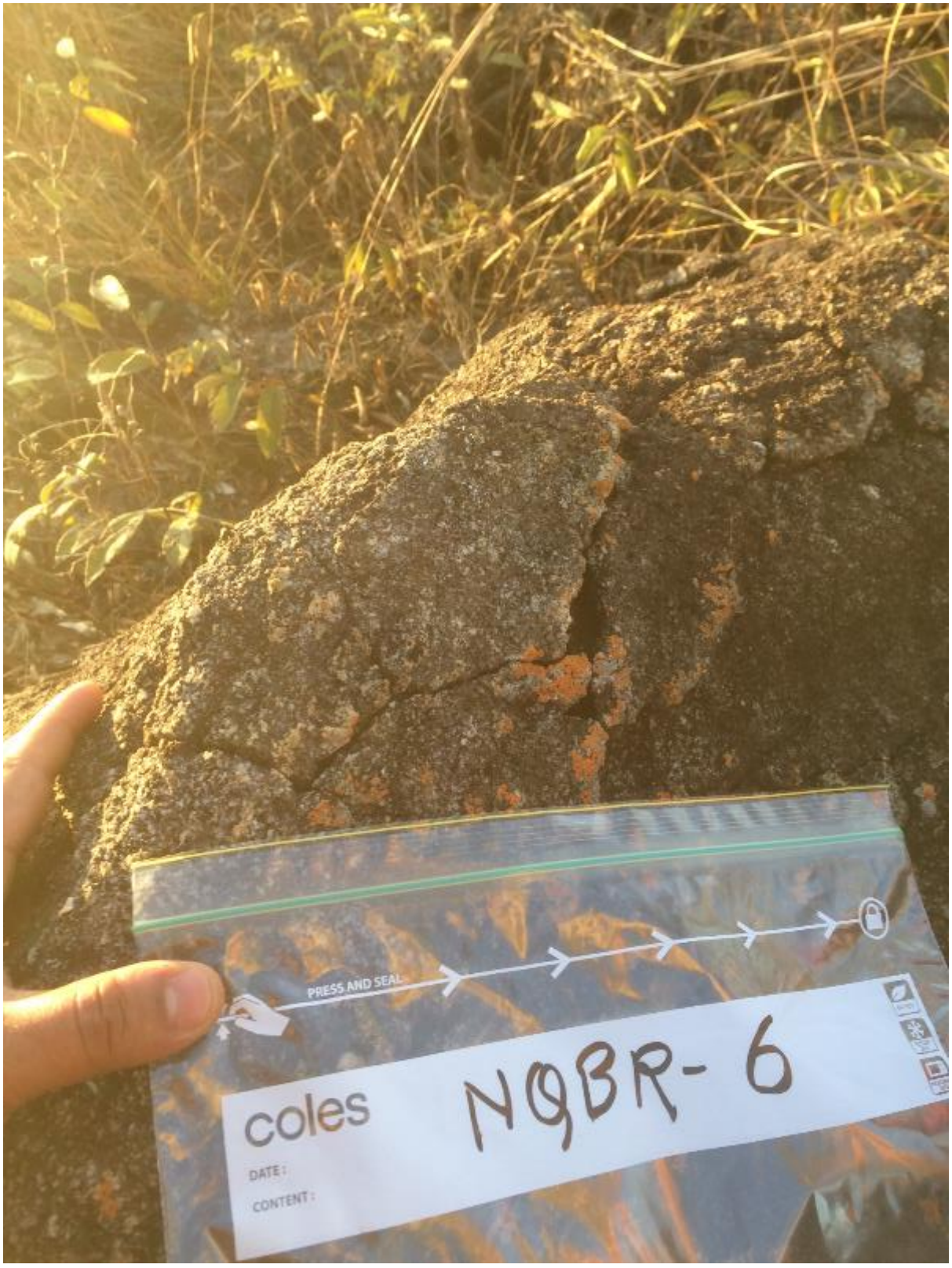

Figure 21: Sample NQBR6

Figure 22: Location of sample NQBR8

Figure 23: Sample PG1

Figure 24: location of sample PG2

Figure 25: Location of sample PG3

Figure 26: Location of sample PG4

Figure 27: Location of sample PG5

Figure 28: Location of sample PG6

Figure 29: Sample PGBR1

Figure 30: Sample PGBR2

Figure 31: Location of sample PGBR3

Appendix 3

Data for Chapter-3

CRONUS SAMPLE ID	Location	Type	Sample Point	Latitude (decimal degrees)	Longitude (decimal degrees)	Mean Basin Elevation (m)	Mean Basin Slope (°)
BR1	Toomba basalt(burdekin river),QLD, Australia	sediments	South	-20.331433	144.440417	253	2.3
CN2	Toomba basalt, Qld, Australia	Buried sediments	South	-19.8601	146.137767	257	3.1
CN3	Toomba basalt, Qld, Australia	Buried sediments	South	-19.8592	146.132617	260	3.1
PG1	flinders creek, Qld, Australia	sediments	South	-20.755967	144.4822	379	10
PG2	Creek near buried samples, Qld, Australia	sediments	South	-20.24795	144.465983	505	12
PG3	Porcupine creek, Qld, Australia	sediments	South	-20.61015	144.404183	361	8.2
PG4	Torrens creek, Qld, Australia	sediments	South	-20.767167	145.028983	457	11
PG5	Warrigal Creek, Qld, Australia	sediments	South	-20.6456	145.292167	435	11
PG6	Campaspi river, Qld, Australia	sediments	South	-20.442217	145.53335	354	12
PGBR2	Porcupine gorge, Qld, Australia	Bedrock	South	-20.3495	144.462867	592	n/a
PGBR3	Porcupine gorge, Qld, Australia	Bedrock	South	-20.349167	144.46285	584	n/a
PGBR6	white Mountains, Qld, Australia	Bedrock	South	-20.715617	145.225333	526	n/a
PGBR7	white Mountains, Qld, Australia	Bedrock	South	-20.715283	145.22475	539	n/a
PGBR8	white Mountains, Qld, Australia	Bedrock	South	-20.71585	145.22335	558	n/a
NQ1	Henrietta Creek, QLD,Australia	sediments	North	-17.59745	145.75739	401	9.4
NQ2	Kelly St. George Cxreek, QLD, Australia	sediments	North	-16.43639	144.78011	404	9.4
NQ3	Boulder creek, QLD, Australia	sediments	North	-16.56328	144.69536	280	11
NQ4	Mitchell river, QLD, Australia	sediments	North	-16.56049	144.88808	304	9.7
NQ5	McLeod river QLD, Australia	sediments	North	-16.49823	145.00208	345	11
NQ6	Granite gorge, QLD, Australia	sediments	North	-17.038116	145.34903	480	9.4
NQ7	Mary Creek, QLD, Austgralia	sediments	North	-16.57277	145.18692	353	9.1
NQ8	Rifle Creek, QLD, Australia	sediments	North	-16.66477	145.3269	379	8.5
NQ9	Creek 1(from top), Mt. Lewis National Park	sediments	North	-16.51646	145.27654	1172	26
NQ10	creek 2 (from top), Mt. lewis, Qld	sediments	North	-16.56949	145.2942	975	24
NQ11	Babinda boulders, QLD, Australia	sediments	North	-17.3416	145.86955	64	4.7
NQ13	Mulgrave river, QLD, Australia	sediments	North	-17.17688	145.72331	37	3
NQBR1	Mt carbine, QLD, Australia	Bedrock	North	-16.435	144.78174	420	n/a
NQBR2	Mt carbine, QLD, Australia	Bedrock	North	-16.45232	144.80215	454	n/a
NQBR3	Mt carbine, QLD, Australia	Bedrock	North	-16.46419	144.81448	504	n/a
NQBR4	Mt carbine, QLD, Australia	Bedrock	North	-16.46419	144.86877	543	n/a
NQBR5	Granite Gorge, QLD, Australia	Bedrock	North	-17.03805	145.3501	470	n/a
NQBR7	Mt carbine, QLD, Australia	Bedrock	North	-16.65986	145.31317	426	n/a
NQBR8	The track Crest, Gordonvale, Qld, Australia	Bedrock	North	-17.23764	145.78204	150	n/a
NQBR9	Hitchinbrook Lookout, Qld, Australia	Bedrock	North	-18.53297	146.18896	141	n/a
NQBR10	Paluma Range, Qld, Australia	Bedrock	North	-18.99236	146.29106	99	n/a
Croke-Hillslope	weany hillslope	sediments	South	-19.88504	146.53522	284	0
Croke-1	Weany Left Arm	sediments	South	-19.89343	146.52303	290	1.45
Croke-2	Weany Right Arm	sediments	South	-19.88861	146.52331	291	1.35
Croke-3	Weany gauge	sediments	South	-19.9135	146.4945	282	1.41
Croke-4	Weany 2	sediments	South	-19.91866	146.49595	282	1.43
Croke-5	Stockyard Creek	sediments	South	-19.72106	146.42742	321	2.68
Croke-6	Weany 3	sediments	South	-19.92413	146.48448	280	1.45
Croke-7	Upper Fanning East	sediments	South	-19.64975	146.49481	460	8.5
Croke-8	Station Creek gauge	sediments	South	-19.90147	146.49101	300	1.78
Croke-9	Upper Fanning West	sediments	South	-19.63558	146.45411	476	6.17
Croke-10	Fanning River Station	sediments	South	-19.73394	146.42786	419	5.73
Croke-11	Fanning River	sediments	South	-19.90278	146.48525	382	4.62

Croke-12	Middle Fanning	sediments	South	-19.92411	146.48042	367	4.13
Croke-13	Lower Fanning River	sediments	South	-19.97968	146.44826	353	3.73
Croke-14	Upper Macrossan	sediments	South	-19.98681	146.42861	516	2.91
Croke-15	Macrossan Bridge	sediments	South	-19.99714	146.43553	511	2.94
Croke-16	Upper Burdekin Falls dam	sediments	South	-20.26572	146.8625	493	2.9
Croke-17	Lower Burdekin	sediments	South	-19.8924	147.23031	362	6.73
Croke-18	Bowen River (at Strathbowen)	sediments	South	-20.53064	147.55733	350	2.4
Croke-19	Upper Suttor River	sediments	South	-21.53786	147.04741	279	1.41
Croke-20	Cape River	sediments	South	-20.99835	146.42478	345	1.25
Croke-21	Belyando River Crossing	sediments	South	-21.53483	146.85979	330	1.21
Croke-22	Lower Suttor River (at St. Ann)	sediments	South	-21.23696	146.92582	313	2.4
QLD1	Escarpment, Qld, Australia	sediments	North	-16.814895	145.63673	354	6.4
QLD2	Escarpment, Qld, Australia	sediments	North	-16.814895	145.63673	354	6.4
QLD3	Escarpment, Qld, Australia	sediments	North	-16.956362	145.677463	582	17
QLD4	Escarpment, Qld, Australia	sediments	North	-16.9451699	145.6904252	351	22
QLD5	Below gorge, Qld, Australia	sediments	North	-16.845445	145.648637	576	8.6
QLD6	Escarpment, Qld, Australia	sediments	North	-16.867244	145.670755	451	20
QLD7	Upland, Qld, Australia	sediments	North	-16.902909	145.561149	520	11
QLD8	Upland, Qld, Australia	sediments	North	-16.894795	145.550538	600	12
QLD9	Upland, Qld, Australia	sediments	North	-16.817066	145.51219	532	11
QLD9xb	Upland, Qld, Australia	sediments	North	-16.816982	145.513026	532	11
QLD10	Upland, Qld, Australia	sediments	North	-16.79409	145.612551	581	8.5
QLD11	Escarpment, Qld, Australia	sediments	North	-16.785567	145.644501	382	6.8
QLD12	Escarpment, Qld, Australia	sediments	North	-16.820043	145.654447	462	16
QLD13	Escarpment, Qld, Australia	sediments	North	-16.826267	145.680866	324	22
QLD14	Escarpment, Qld, Australia	sediments	North	-16.810561	145.681453	297	24
QLD15	Beach, Qld, Australia	sediments	North	-16.8001	145.725962	0	0

Original 10Be Concentration (at g-1)	Original 10Be Concentraion Error (at g-1)	AMS Standard	Erosion rate(m/My)	Erosion Rate (m/My)	Precipitation(mean) mm	Precipitation (Max) mm	Lithology
176712.6887	4337.284035	07KNSTD	15.72	1.34	598.5	1082.4	NA
1220519.276	28457.89417	07KNSTD	1.82	0.97	643.4	1286.8	NA
254644.6019	5968.437213	07KNSTD	10.72	0.94	643.4	1286.8	NA
200905.8418	4943.910036	07KNSTD	15.06	1.29	463.4	1107.1	NA
455353.1819	10634.36261	07KNSTD	6.93	0.64	598.5	1082.4	NA
197904.643	4856.013999	07KNSTD	15.09	1.29	463.4	1107.1	NA
217153.4656	5081.398494	07KNSTD	14.65	1.26	547.2	1442	NA
416055.5424	10182.52603	07KNSTD	7.27	0.67	666.7	1574.8	NA
283046.717	7500.801791	07KNSTD	10.31	0.92	681.6	1540.7	NA
57472.68293	1321.736008	07KNSTD	58.54	4.66	598.5	1082.4	sedimentary
42063.22136	1031.247571	07KNSTD	79.22	6.25	598.5	1082.4	Sedimentary
269203.876	7286.279358	07KNSTD	12.1	1.07	547.2	1442	sedimentary
87166.16165	2152.104586	07KNSTD	37.6	3.07	547.2	1442	sedimentary
138809.4162	3417.699834	07KNSTD	24.21	2.03	547.2	1442	sedimentary
78739.56646	1895.151179	07KNSTD	38.08	3.06	3089	4552.4	NA
176411.9502	4689.801282	07KNSTD	16.83	1.44	615.8	969.2	NA
231011.4377	6144.366335	07KNSTD	11.73	1.03	615.8	969.2	NA
244788.926	6920.491261	07KNSTD	11.22	0.99	615.8	969.2	NA
285417.2762	7579.965481	07KNSTD	9.82	0.87	615.8	969.2	NA
1181354.187	31146.13111	07KNSTD	2.23	1.15	914	1266.6	NA
169781.2426	4218.626233	07KNSTD	16.94	1.43	879.4	1784.2	NA
147092.2777	3652.553091	07KNSTD	19.96	1.67	1101.8	3594.8	NA
460448.4854	12164.73051	07KNSTD	10.52	0.96	2227	4146.6	NA
189922.5718	5043.934883	07KNSTD	22.57	1.96	1611.5	3014.3	NA
45449.10863	1282.561808	07KNSTD	53.56	4.16	4267.3	7040.2	NA
70845.90508	1942.493681	07KNSTD	33.76	2.68	1648.5	3486.9	NA
167639.7799	4458.752137	07KNSTD	17.82	1.52	933.5	1879	sedimentary
409817.7649	9620.411647	07KNSTD	7.07	0.64	933.5	1879	Granitic
775558.8687	20424.60686	07KNSTD	3.57	0.35	933.5	1879	Granitic
176805.7267	4722.473634	07KNSTD	17.75	1.52	933.5	1879	Granitic
193561.7141	5151.689321	07KNSTD	15.75	1.36	983	1623	Granitic
131396.3916	3525.494459	07KNSTD	22.94	1.92	836	1394.6	Granitic
43026.45405	1450.492735	07KNSTD	56.49	4.5	1611.5	3014.3	Granitic
359226.844	9523.541862	07KNSTD	6.68	0.61	8053.6	12461	Granitic
365933.6333	8602.962087	07KNSTD	6.28	0.57	2210.9	3937.8	Granitic
231000	16000	NIST_30000	13.02	1.44	1952.1	3289.2	NA
266000	18000	NIST_30000	11.28	1.25	650	1531	NA
209000	10000	NIST_30000	14.51	1.39	650	1531	NA
202000	25000	NIST_30000	14.94	2.33	650	1531	NA
245000	11000	NIST_30000	12.23	1.17	618.3	1340.7	NA
387000	31000	NIST_30000	7.73	0.95	618.3	1340.7	NA
190000	10000	NIST_30000	15.9	1.56	627.9	1293.3	NA
203000	12000	NIST_30000	16.73	1.72	618.3	1340.7	NA
180000	16000	NIST_30000	17.04	2.11	627.9	1293.3	NA
269000	22000	NIST_30000	12.66	1.53	618.3	1340.7	NA
240000	15000	NIST_30000	13.71	1.45	627.9	1293.3	NA
219000	11000	NIST_30000	14.72	1.44	627.9	1293.3	NA

256000	15000	NIST_30000	12.39	1.29	618.3	1340.7	NA
247000	11000	NIST_30000	12.75	1.22	618.3	1340.7	NA
289000	15000	NIST_30000	12.12	1.22	618.3	1340.7	NA
282000	22000	NIST_30000	12.39	1.46	618.3	1340.7	NA
276000	14000	NIST_30000	12.54	1.25	618.3	1340.7	NA
263000	12000	NIST_30000	12	1.16	668.7	1342.2	NA
149000	78000	NIST_30000	21.47	16.25	839.7	1732.5	NA
731000	27000	NIST_30000	3.76	0.39	724.9	1731.5	NA
352000	15000	NIST_30000	8.81	0.86	586.3	1146.6	NA
514000	19000	NIST_30000	5.81	0.57	551.6	1187.1	NA
634000	25000	NIST_30000	4.53	0.46	586.3	1146.6	NA
184000	3000	07KNSTD	15.64	1.3	599.3	1076.4	NA
172000	5000	07KNSTD	16.76	1.45	2129.4	4921.9	NA
102000	3000	07KNSTD	32.76	2.75	2328.9	3400	NA
231000	1000	07KNSTD	12.35	1.02	2328.9	3400	NA
231000	8000	07KNSTD	14.36	1.3	2129.4	4921.9	NA
499000	8000	07KNSTD	5.83	0.53	2129.4	4921.9	NA
181000	3000	07KNSTD	17.75	1.48	1127.7	2325.7	NA
197000	3000	07KNSTD	17.16	1.43	1127.7	2325.7	NA
251000	3000	07KNSTD	12.8	1.08	1127.7	2325.7	NA
248000	4000	07KNSTD	12.96	1.1	1127.7	2325.7	NA
256000	6000	07KNSTD	12.96	1.13	2129.4	4921.9	NA
189000	3000	07KNSTD	15.5	1.29	2129.4	4921.9	NA
131000	2000	07KNSTD	23.68	1.91	2129.4	4921.9	NA
61000	2000	07KNSTD	46.47	3.81	2129.4	4921.9	NA
66000	2000	07KNSTD	42.31	3.43	2129.4	4921.9	NA
275000	8000	07KNSTD	7.97	0.72	2064.5	2851.8	NA

Calculation 10Be/9Be ratio and Blank correction

Sample Id	ABAZ conc.	ABAZ added	9Be added	Quartz	Be10/Be9	10/9 err	10/9 err%	Blk fraction	Be10/Be9	10/9 Err	10/9 err%	10Be
	(ppm)	(g)	(g)	(g)					blk-corrected	blk-corrected	blk-corrected	(atoms/g)
BR1	1027	0.30918	0.000318	78.4	6.541E-13	1.462E-14	2.2%	0.2%	6.530E-13	1.464E-14	2.2%	1.767E+05
CN2	1027	0.30972	0.000318	33.3	1.913E-12	4.027E-14	2.1%	0.1%	1.912E-12	4.028E-14	2.1%	1.221E+06
CN3	1027	0.30592	0.000314	44.8	5.445E-13	1.150E-14	2.1%	0.2%	5.434E-13	1.152E-14	2.1%	2.546E+05
PG1	1027	0.30525	0.000313	63.6	6.111E-13	1.370E-14	2.2%	0.2%	6.100E-13	1.371E-14	2.2%	2.009E+05
PG2	1027	0.30470	0.000313	42.2	9.201E-13	1.938E-14	2.1%	0.1%	9.190E-13	1.939E-14	2.1%	4.554E+05
PG3	1027	0.30570	0.000314	77.8	7.349E-13	1.643E-14	2.2%	0.2%	7.337E-13	1.644E-14	2.2%	1.979E+05
PG4	1027	0.30991	0.000318	77.0	7.871E-13	1.661E-14	2.1%	0.1%	7.860E-13	1.663E-14	2.1%	2.172E+05
PG5	1027	0.30690	0.000315	75.4	1.491E-12	3.327E-14	2.2%	0.1%	1.489E-12	3.327E-14	2.2%	4.161E+05
PG6	1027	0.30630	0.000315	24.5	3.310E-13	8.069E-15	2.4%	0.3%	3.299E-13	8.096E-15	2.5%	2.830E+05
PGBR2	1027	0.30629	0.000315	69.3	1.906E-13	3.867E-15	2.0%	0.6%	1.895E-13	3.924E-15	2.1%	5.747E+04
PGBR3	1027	0.30505	0.000313	80.1	1.621E-13	3.540E-15	2.2%	0.7%	1.609E-13	3.603E-15	2.2%	4.206E+04
PGBR6	1027	0.30574	0.000314	78.5	1.008E-12	2.532E-14	2.5%	0.1%	1.007E-12	2.533E-14	2.5%	2.692E+05
PGBR7	1027	0.30740	0.000316	78.7	3.263E-13	7.310E-15	2.2%	0.3%	3.252E-13	7.341E-15	2.3%	8.717E+04
PGBR8	1027	0.30605	0.000314	68.1	4.512E-13	1.010E-14	2.2%	0.2%	4.501E-13	1.013E-14	2.2%	1.388E+05
Blank-1	1027	0.30680	0.000315	0	2.304E-15	3.214E-16	13.9%					
Blank-2	1027	0.30638	0.000315	0	7.423E-16	1.803E-16	24.3%					
				Error-weighted mean blk:	**1.116E-15**	**6.665E-16**	**59.7%**					
NQ 1	1027	0.30592	0.000314	75.22	2.8436E-13	6.02837E-15	**2.1%**	0.79%	2.821E-13	6.17634E-15	2.19%	78739.56646
NQ 2	1027	0.30603	0.000314	73.31	6.1804E-13	1.51086E-14	**2.4%**	0.36%	6.158E-13	1.51682E-14	2.46%	176411.9502
NQ 3	1027	0.30163	0.00031	49.94	5.5958E-13	1.36703E-14	**2.4%**	0.40%	5.573E-13	1.37362E-14	2.46%	231011.4377
NQ 4	1027	0.30587	0.000314	55.98	6.5507E-13	1.72107E-14	**2.6%**	0.34%	6.528E-13	1.72631E-14	2.64%	244788.926
NQ 5	1027	0.30772	0.000316	48.25	6.5437E-13	1.59878E-14	**2.4%**	0.34%	6.521E-13	1.60442E-14	2.46%	285417.2762
NQ 6	1027	0.30608	0.000314	53.7	3.0224E-12	7.36635E-14	**2.4%**	0.07%	3.020E-12	7.36758E-14	2.44%	1181354.187
NQ 7	1027	0.30194	0.00031	56.26	4.6322E-13	1.0399E-14	**2.2%**	0.48%	4.610E-13	1.04855E-14	2.27%	169781.2426
NQ 8	1027	0.30251	0.000311	68.75	4.8936E-13	1.09899E-14	**2.2%**	0.46%	4.871E-13	1.10717E-14	2.27%	147092.2777
NQ 9	1027	0.30762	0.000316	64.69	1.4132E-12	3.44768E-14	**2.4%**	0.16%	1.411E-12	3.4503E-14	2.45%	460448.4854
NQ 10	1027	0.29283	0.000301	64.47	6.1154E-13	1.49303E-14	**2.4%**	0.37%	6.093E-13	1.49907E-14	2.46%	189922.5718
NQ 11	1027	0.30674	0.000315	57	1.2531E-13	2.95645E-15	**2.4%**	1.79%	1.231E-13	3.24754E-15	2.64%	45449.10863
NQ 13	1027	0.30222	0.00031	61.02	2.1068E-13	5.14889E-15	**2.4%**	1.06%	2.084E-13	5.32137E-15	2.55%	70845.90508
NQBR 1	1027	0.305	0.000313	70.54	5.6721E-13	1.3859E-14	**2.4%**	0.40%	5.650E-13	1.3924E-14	2.46%	167639.7799
NQBR 2	1027	0.30247	0.000311	52.826	1.0452E-12	2.21099E-14	**2.1%**	0.21%	1.043E-12	2.21507E-14	2.12%	409817.7649
NQBR 3	1027	0.3055	0.000314	57.843	2.142E-12	5.21133E-14	**2.4%**	0.10%	2.140E-12	5.21306E-14	2.44%	775558.8687
NQBR 4	1027	0.30251	0.000311	50.07	4.2867E-13	1.04756E-14	**2.4%**	0.52%	4.264E-13	1.05615E-14	2.48%	176805.7267
NQBR 5	1027	0.3024	0.000311	57.237	5.361E-13	1.30989E-14	**2.4%**	0.42%	5.339E-13	1.31677E-14	2.47%	193561.7141
NQBR 7	1027	0.30251	0.000311	53.38	3.401E-13	8.30385E-15	**2.4%**	0.66%	3.379E-13	8.41189E-15	2.49%	131396.3916
NQBR 8	1027	0.30165	0.00031	46.334	9.8547E-14	2.79405E-15	**2.8%**	2.28%	9.630E-14	3.10043E-15	3.22%	43026.45405
NQBR 9	1027	0.30226	0.00031	48.1	8.3524E-13	2.04083E-14	**2.4%**	0.27%	8.330E-13	2.04525E-14	2.46%	359226.844
NQBR 10	1027	0.30648	0.000315	49.264	8.5936E-13	1.81871E-14	**2.1%**	0.26%	8.571E-13	1.82367E-14	2.13%	365933.6333
Blank-3	1027	0.30431	0.000313	0	1.7777E-15	2.85946E-16	**16.1%**					
Blank-4	1027	0.30216	0.00031	0	1.4717E-15	3.2984E-16	**22.4%**					
Blank 5	1027	0.30302	0.000311	0	8.2574E-15	6.8568E-16	**8.3%**					
				Error-weighted mean blk:	**2.244E-15**	**1.344E-15**	**59.9%**					

10Be err	10Be err%
4.34E+03	2.5%
2.85E+04	2.3%
5.97E+03	2.3%
4.94E+03	2.5%
1.06E+04	2.3%
4.86E+03	2.5%
5.08E+03	2.3%
1.02E+04	2.4%
7.50E+03	2.7%
1.32E+03	2.3%
1.03E+03	2.5%
7.29E+03	2.7%
2.15E+03	2.5%
3.42E+03	2.5%
1.90E+03	2.4%
4.69E+03	2.7%
6.14E+03	2.7%
6.92E+03	2.8%
7.58E+03	2.7%
3.11E+04	2.6%
4.22E+03	2.5%
3.65E+03	2.5%
1.22E+04	2.6%
5.04E+03	2.7%
1.28E+03	2.8%
1.94E+03	2.7%
4.46E+03	2.7%
9.62E+03	2.3%
2.04E+04	2.6%
4.72E+03	2.7%
5.15E+03	2.7%
3.53E+03	2.7%
1.45E+03	3.4%
9.52E+03	2.7%
8.60E+03	2.4%

CRONUS INPUT FILE

CRONUS SAMPLE ID	Latitude (decimal degrees)	Longitude (decimal degrees)	Mean Basin Elevation (m)a	Elevation/Pressure Flag	Thickness(cm)	Density(g/cm^2)	Shielding Correction	Original 10Be Concentration (at g-1)
BR1	-20.331433	144.440417	253	std	1	2.7	1	176712.6887
CN2	-19.8601	146.137767	257	std	1	2.7	1	1220519.276
CN3	-19.8592	146.132617	260	std	1	2.7	1	254644.6019
PG1	-20.755967	144.4822	379	std	1	2.7	1	200905.8418
PG2	-20.24795	144.465983	505	std	1	2.7	1	455353.1819
PG3	-20.61015	144.404183	361	std	1	2.7	1	197904.643
PG4	-20.767167	145.028983	457	std	1	2.7	1	217153.4656
PG5	-20.6456	145.292167	435	std	1	2.7	1	416055.5424
PG6	-20.442217	145.53335	354	std	1	2.7	1	283046.717
PGBR2	-20.3495	144.462867	592	std	4	2.7	0.998148	57472.68293
PGBR3	-20.349167	144.46285	584	std	3.5	2.7	0.996547	42063.22136
PGBR6	-20.715617	145.225333	526	std	3	2.7	0.99895	269203.876
PGBR7	-20.715283	145.22475	539	std	5	2.7	1	87166.16165
PGBR8	-20.71585	145.22335	558	std	3.5	2.7	1	138809.4162
NQ1	-17.59745	145.75739	401	std	1	2.7	1	78739.56646
NQ2	-16.43639	144.78011	404	std	1	2.7	1	176411.9502
NQ3	-16.56328	144.69536	280	std	1	2.7	1	231011.4377
NQ4	-16.56049	144.88808	304	std	1	2.7	1	244788.926
NQ5	-16.49823	145.00208	345	std	1	2.7	1	285417.2762
NQ6	-17.038116	145.34903	480	std	1	2.7	1	1181354.187
NQ7	-16.57277	145.18692	353	std	1	2.7	1	169781.2426
NQ8	-16.66477	145.3269	379	std	1	2.7	1	147092.2777
NQ9	-16.51646	145.27654	1172	std	1	2.7	1	460448.4854
NQ10	-16.56949	145.2942	975	std	1	2.7	1	189922.5718
NQ11	-17.3416	145.86955	64	std	1	2.7	1	45449.10863
NQ13	-17.17688	145.72331	37	std	1	2.7	1	70845.90508
NQBR1	-16.435	144.78174	420	std	1.75	2.7	1	167639.7799
NQBR2	-16.45232	144.80215	454	std	3.5	2.7	0.999867	409817.7649
NQBR3	-16.46419	144.81448	504	std	4.5	2.7	0.994047	775558.8687
NQBR4	-16.46419	144.86877	543	std	6	2.7	1	176805.7267
NQBR5	-17.03805	145.3501	470	std	3.75	2.7	1	193561.7141
NQBR7	-16.65986	145.31317	426	std	1.5	2.7	0.998248	131396.3916
NQBR8	-17.23764	145.78204	150	std	6.5	2.7	0.977417	43026.45405
NQBR9	-18.53297	146.18896	141	std	1.5	2.7	1	359226.844
NQBR10	-18.99236	146.29106	99	std	2	2.7	0.990771	365933.6333

Original 10Be Concentraion Error (at g-1)	AMS Standard	Al 26 concentration	eroor- Al concentration	AL Standard
4337.284035	07KNSTD	0	0	KNSTD
28457.89417	07KNSTD	0	0	KNSTD
5968.437213	07KNSTD	0	0	KNSTD
4943.910036	07KNSTD	0	0	KNSTD
10634.36261	07KNSTD	0	0	KNSTD
4856.013999	07KNSTD	0	0	KNSTD
5081.398494	07KNSTD	0	0	KNSTD
10182.52603	07KNSTD	0	0	KNSTD
7500.801791	07KNSTD	0	0	KNSTD
1321.736008	07KNSTD	0	0	KNSTD
1031.247571	07KNSTD	0	0	KNSTD
7286.279358	07KNSTD	0	0	KNSTD
2152.104586	07KNSTD	0	0	KNSTD
3417.699834	07KNSTD	0	0	KNSTD
1895.151179	07KNSTD	0	0	KNSTD
4689.801282	07KNSTD	0	0	KNSTD
6144.366335	07KNSTD	0	0	KNSTD
6920.491261	07KNSTD	0	0	KNSTD
7579.965481	07KNSTD	0	0	KNSTD
31146.13111	07KNSTD	0	0	KNSTD
4218.626233	07KNSTD	0	0	KNSTD
3652.553091	07KNSTD	0	0	KNSTD
12164.73051	07KNSTD	0	0	KNSTD
5043.934883	07KNSTD	0	0	KNSTD
1282.561808	07KNSTD	0	0	KNSTD
1942.493681	07KNSTD	0	0	KNSTD
4458.752137	07KNSTD	0	0	KNSTD
9620.411647	07KNSTD	0	0	KNSTD
20424.60686	07KNSTD	0	0	KNSTD
4722.473634	07KNSTD	0	0	KNSTD
5151.689321	07KNSTD	0	0	KNSTD
3525.494459	07KNSTD	0	0	KNSTD
1450.492735	07KNSTD	0	0	KNSTD
9523.541862	07KNSTD	0	0	KNSTD
8602.962087	07KNSTD	0	0	KNSTD

sample Id	Start weight(g)	weight after heavy liquid, frantz and etching (g)	Weight of quartz before dissolving(without bottle)	Wt of bottle(empty)	Wt of bottle (with final dissolved quartz)	wt of ONLY dissolved quartz liquid(g)	Wt of bottles after taking out liquid	wt of **REMOVED** liquid for 27Al and 9Be
NQBR-1	189	92.54	70.54	79.83	612.63	532.8	595.32	17.31
NQ-1	188	117.69	75.22	79.84	617.35	537.51	599.93	17.42
NQ-2	380	197.38	73.31	79.32	609.5	530.18	591.93	17.57
NQ-4	181	96.42	55.98	80.11	506.38	426.27	492.154	14.226
NQ-5*	109	57.2	48.25	81.53	470.16	388.63	457.51	12.65
NQ-6	485	173.25	53.7	79.31	481.46	402.15	468.24	13.22
NQ-9	128	148.06	64.69	79.45	611.95	532.5	594.93	17.02
NQ-11**	243	89.51	57	80.238	491.57	411.332	478.31	13.26
Blank-3	-	-	-	79.46	464.77	385.31	453.89	10.88
2ND batch								
NQBR-2	244	77.27	52.826	80.623	534.304	453.681	523.369	10.935
NQBR-3	149	86.96	57.843	81.87	571.241	489.371	559.877	11.364
NQBR-4	260	55.46	50.07	78.457	524.227	445.77	513.144	11.083
NQBR-5	235	63.1	57.237	78.92	579.856	500.936	568.396	11.46
NQBR-8	286	51.2	46.334	80.644	514.483	433.839	503.592	10.891
NQBR-10	254	54.49	49.264	79.316	522.843	443.527	511.86	10.983
NQ-3	389	83.98	49.94	81.22	531.167	449.947	520.215	10.952
NQ-7	175	62.13	56.26	77.316	531.441	454.125	520.464	10.977
NQ-10	149	71.02	64.47	76.777	612.838	536.061	601.754	11.084
NQ-13**	298	75.9	61.02	78.561	580.127	501.566	569.019	11.108
Blank -4	-	-	-	76.685	474.994	398.309	464.796	10.198
3RD batch								
NQBR-7	285	80.27	53.38	80.24	574.01	493.77	564.973	9.037
NQBR-9	281	81.09	48.1	80.3	513.14	432.84	504.834	8.306
NQ-8	211	92.88	68.75	76.9	646.1	569.2	637.81	8.29
Blank 5	-	-	-	76.425	447.193	370.768	442.396	4.797
*(0.5-0.7)								
**(grinded)								

% of liquid removed	Qartz in removed samples
3.248873874	2.291756
3.240869937	2.437782
3.313968841	2.429471
3.337321416	1.868233
3.255024059	1.570549
3.287330598	1.765297
3.196244131	2.06765
3.223673334	1.837494
2.823700397	#VALUE!
	0
	0
	0
	0
2.410283878	1.273257
2.322164575	1.34321
2.48625973	1.24487
2.287717393	1.309421
2.510378274	1.163159
2.476286675	1.219918
2.434064456	1.215572
2.417175888	1.359903
2.067675134	1.33303
2.214663673	1.351388
2.560323769	#VALUE!
	0
	0
	0
1.830204346	0.976963
1.918953886	0.923017
1.456430077	1.001296
1.293800975	#VALUE!

sample Id	Start weight(g)	weight after heavy liquid, frantz and etching (g)	Weight of quartz before dissolving(without bottle)	Wt of bottle(empty)	Wt of bottle (with final dissolved quartz)	wt of ONLY dissolved quartz liquid(g)	Wt of bottles after taking out liquid	wt of **REMOVED** liquid for 27Al and 9Be
PG-1	429.92	75	63.6	80.56	615.9	535.34	600.36	15.54
PG-2	161.49	58	42	76.767	421.2	344.433	401.67	19.53
PG-3	246.13	89	2	78.443	706.3	627.857	679.63	26.67
PG-4	860	91	77.78	77.085	709.6	632.515	696.74	12.86
PG-5	492.5	123	76.98	77.717	701.2	623.483	691.36	9.84
PG-6	118.1	34	24.5	78.096	278.9	200.804	266.05	12.85
PGBR-2(2)	257	177	69.3	77.907	635.3	557.393	623.53	11.77
PGBR-3	167.69	117	80.1	78.007	792.5	714.493	777.39	15.11
PGBR-6	253.5	94	78.5	77.827	699.8	621.973	691.45	8.35
PGBR-7	212.7	95	78.7	79.396	690	610.604	679.79	10.21
PGBR-8	199.3	83	68.1	77.001	688	610.999	675.82	12.18
BR-1	176.56	61	78.4	78.091	671.8	593.709	658.86	12.94
CN-2	230	109	33.3	77.562	723.4	645.838	708.39	15.01
CN-3	253	50	44.8	78.334	438.2	359.866	432.2	6
PGBR 2	257	177	na	0	0	0	0	0
Blank 1	-			78.244	457.33	379.086	446.871	10.459
Blank 2	-			77.982	461.73	383.748	450.593	11.137

% of liquid removed
2.902828109
5.670188397
4.247782536
2.033153364
1.578230682
6.399274915
2.111616041
2.114786289
1.342502006
1.672114824
1.993456618
2.179518923
2.324112239
1.667287268
0
2.759004553
2.902164962

The online erosion rate calculator formerly known as the CRONUS-Earth ^{10}Be - ^{26}Al erosion rate calculator -- results

Version information --

Component	Version
Wrapper script:	2.3
Main calculator:	2.1
Objective function:	2.0
Constants:	2.3
Muons:	1.1

Comments:

Production rate calibration information: Using default calibration data set

^{10}Be results:

Results not dependent on spallogenic production rate model:

Erosion rates -- constant production rate model:

Scaling scheme for spallation: Lal(1991) / Stone(2000)

Sample name	Shielding factor	Production rate (muons) (atoms/g/yr)	Internal uncertainty (m/Myr)	Erosion rate (g/cm2/yr)	Erosion rate (m/Myr)	External uncertainty (m/Myr)	Production rate (spallation) (atoms/g/yr)
BR1	1.0000	0.082	0.36	0.00371	13.72	1.08	3.36
CN2	1.0000	0.082	0.04	0.00040	1.47	0.15	3.33
CN3	1.0000	0.083	0.23	0.00247	9.15	0.74	3.34
PG1	1.0000	0.086	0.34	0.00354	13.10	1.04	3.72
PG2	1.0000	0.089	0.15	0.00156	5.76	0.49	4.03
PG3	1.0000	0.085	0.34	0.00354	13.12	1.04	3.66
PG4	1.0000	0.088	0.32	0.00343	12.69	1.01	3.94
PG5	1.0000	0.087	0.16	0.00165	6.10	0.52	3.86
PG6	1.0000	0.085	0.25	0.00237	8.79	0.73	3.62
PGBR2	0.9981	0.092	1.29	0.01484	54.95	4.03	4.30
PGBR3	0.9965	0.091	1.89	0.02045	75.72	5.53	4.27
PGBR6	0.9990	0.090	0.30	0.00280	10.36	0.85	4.13
PGBR7	1.0000	0.090	0.88	0.00929	34.40	2.59	4.17
PGBR8	1.0000	0.091	0.55	0.00581	21.52	1.67	4.23
NQ1	1.0000	0.087	0.87	0.00943	34.94	2.59	3.62
NQ2	1.0000	0.087	0.41	0.00396	14.66	1.16	3.60
NQ3	1.0000	0.083	0.29	0.00272	10.06	0.82	3.29
NQ4	1.0000	0.084	0.29	0.00259	9.59	0.79	3.34
NQ5	1.0000	0.085	0.24	0.00225	8.32	0.69	3.44
NQ6	1.0000	0.089	0.06	0.00049	1.80	0.18	3.82
NQ7	1.0000	0.085	0.39	0.00399	14.78	1.16	3.47
NQ8	1.0000	0.086	0.46	0.00475	17.57	1.36	3.54
NQ9	1.0000	0.111	0.25	0.00239	8.86	0.75	6.31
NQ10	1.0000	0.104	0.55	0.00537	19.90	1.59	5.47
NQ11	1.0000	0.078	1.48	0.01372	50.82	3.67	2.83
NQ13	1.0000	0.077	0.89	0.00842	31.18	2.30	2.77
NQBR1	1.0000	0.087	0.44	0.00420	15.57	1.23	3.64
NQBR2	0.9999	0.088	0.15	0.00159	5.89	0.50	3.73
NQBR3	0.9940	0.089	0.09	0.00079	2.91	0.27	3.85
NQBR4	1.0000	0.090	0.44	0.00418	15.47	1.23	3.98
NQBR5	1.0000	0.088	0.39	0.00368	13.64	1.09	3.79
NQBR7	0.9982	0.087	0.57	0.00550	20.35	1.58	3.65
NQBR8	0.9774	0.079	1.86	0.01448	53.65	3.99	2.94
NQBR9	1.0000	0.079	0.17	0.00152	5.64	0.48	3.03
NQBR10	0.9908	0.078	0.14	0.00144	5.32	0.45	2.92

Erosion rates -- time-varying production models:

Scaling scheme for spallation:	Desilets and others (2003,2006)			Dunai (2001)			Lifton and others (2005)			Time-dependent Lal (1991)/Stone (2000)		
Sample name	Erosion rate	Erosion rate	External uncertainty	Erosion rate	Erosion rate	External uncertainty	Erosion rate	Erosion rate	External uncertainty	Erosion rate	Erosion rate	External uncertainty

	(g/cm2/yr)	(m/Myr)	(m/Myr)	(g/cm2/yr)	(m/Myr)	(m/Myr)	(g/cm2/yr)	(m/Myr)	(m/Myr)	(g/cm2/yr)	(m/Myr)	(m/Myr)
BR1	0.00372	13.78	8.11	0.00387	14.32	1.49	0.00375	13.91	1.40	0.00424	15.72	1.34
CN2	0.00041	1.52	0.80	0.00043	1.59	0.84	0.00042	1.54	0.82	0.00049	1.82	0.97
CN3	0.00252	9.35	4.33	0.00262	9.71	4.51	0.00255	9.43	0.98	0.00289	10.72	0.94
PG1	0.00358	13.24	6.10	0.00371	13.76	8.05	0.00362	13.39	1.37	0.00407	15.06	1.29
PG2	0.00163	6.05	2.83	0.00169	6.28	2.95	0.00165	6.13	2.89	0.00187	6.93	0.64
PG3	0.00358	13.27	6.11	0.00372	13.78	6.35	0.00362	13.41	1.37	0.00407	15.09	1.29
PG4	0.00349	12.92	7.60	0.00362	13.40	6.18	0.00353	13.07	1.34	0.00395	14.65	1.26
PG5	0.00171	6.33	2.96	0.00178	6.58	3.08	0.00173	6.41	3.02	0.00196	7.27	0.67
PG6	0.00243	9.00	4.17	0.00253	9.36	4.35	0.00246	9.11	4.25	0.00278	10.31	0.92
PGBR2	0.01438	53.24	5.24	0.01490	55.19	5.33	0.01444	53.48	5.00	0.01581	58.54	4.66
PGBR3	0.01955	72.42	7.04	0.02031	75.23	7.19	0.01960	72.58	6.70	0.02139	79.22	6.25
PGBR6	0.00288	10.67	4.93	0.00299	11.07	5.12	0.00292	10.81	5.02	0.00327	12.10	1.07
PGBR7	0.00914	33.83	3.42	0.00947	35.06	3.47	0.00920	34.09	3.27	0.01015	37.60	3.07
PGBR8	0.00584	21.63	9.90	0.00605	22.40	2.29	0.00590	21.85	2.17	0.00654	24.21	2.03
NQ1	0.00932	34.51	3.42	0.00962	35.61	3.47	0.00933	34.55	3.26	0.01028	38.08	3.06
NQ2	0.00408	15.12	6.95	0.00419	15.52	1.62	0.00408	15.11	1.53	0.00455	16.83	1.44
NQ3	0.00281	10.40	4.81	0.00289	10.69	4.96	0.00281	10.39	1.08	0.00317	11.73	1.03
NQ4	0.00269	9.95	4.61	0.00276	10.23	4.75	0.00268	9.94	1.04	0.00303	11.22	0.99
NQ5	0.00235	8.70	4.04	0.00241	8.94	5.78	0.00235	8.70	4.06	0.00265	9.82	0.87
NQ6	0.00052	1.93	0.99	0.00054	1.99	1.02	0.00052	1.93	1.00	0.00060	2.23	1.15
NQ7	0.00410	15.17	6.98	0.00421	15.59	1.61	0.00409	15.16	1.52	0.00457	16.94	1.43
NQ8	0.00484	17.94	1.87	0.00498	18.44	1.88	0.00484	17.93	1.78	0.00539	19.96	1.67
NQ9	0.00263	9.75	4.49	0.00266	9.84	4.54	0.00263	9.75	4.51	0.00284	10.52	0.96
NQ10	0.00565	20.92	9.53	0.00574	21.25	11.28	0.00564	20.89	2.16	0.00610	22.57	1.96
NQ11	0.01302	48.24	4.54	0.01351	50.05	4.64	0.01302	48.22	4.32	0.01446	53.56	4.16
NQ13	0.00814	30.15	2.92	0.00843	31.22	2.97	0.00814	30.14	2.78	0.00912	33.76	2.68
NQBR1	0.00433	16.04	9.09	0.00444	16.45	1.71	0.00433	16.02	1.61	0.00481	17.82	1.52
NQBR2	0.00169	6.27	2.94	0.00173	6.43	3.01	0.00169	6.27	2.95	0.00191	7.07	0.64
NQBR3	0.00085	3.13	1.52	0.00087	3.21	1.57	0.00084	3.13	1.53	0.00096	3.57	0.35
NQBR4	0.00434	16.07	9.06	0.00444	16.45	1.72	0.00434	16.06	1.63	0.00479	17.75	1.52
NQBR5	0.00382	14.14	6.50	0.00392	14.51	6.69	0.00382	14.15	1.45	0.00425	15.75	1.36
NQBR7	0.00559	20.71	2.15	0.00574	21.28	2.17	0.00559	20.71	2.05	0.00619	22.94	1.92
NQBR8	0.01382	51.19	4.89	0.01432	53.05	4.99	0.01381	51.17	4.66	0.01525	56.49	4.50
NQBR9	0.00156	5.77	2.72	0.00162	5.99	2.82	0.00157	5.80	2.75	0.00180	6.68	0.61
NQBR10	0.00146	5.40	2.55	0.00152	5.62	2.66	0.00147	5.43	2.58	0.00170	6.28	0.57

^{26}Al results:

Results not dependent on spallogenic production rate model:

Erosion rates -- constant production rate model:

Scaling scheme for spallation: Lal(1991) / Stone(2000)

Sample name	Shielding factor	Production rate (muons) (atoms/g/yr)	Internal uncertainty (m/Myr)	Erosion rate (g/cm2/yr)	Erosion rate (m/Myr)	External uncertainty (m/Myr)	Production rate (spallation) (atoms/g/yr)
BR1	--	--	--	--	--	--	
CN2	--	--	--	--	--	--	
CN3	--	--	--	--	--	--	
PG1	--	--	--	--	--	--	
PG2	--	--	--	--	--	--	
PG3	--	--	--	--	--	--	
PG4	--	--	--	--	--	--	
PG5	--	--	--	--	--	--	
PG6	--	--	--	--	--	--	
PGBR2	--	--	--	--	--	--	
PGBR3	--	--	--	--	--	--	
PGBR6	--	--	--	--	--	--	
PGBR7	--	--	--	--	--	--	
PGBR8	--	--	--	--	--	--	
NQ1	--	--	--	--	--	--	
NQ2	--	--	--	--	--	--	
NQ3	--	--	--	--	--	--	
NQ4	--	--	--	--	--	--	
NQ5	--	--	--	--	--	--	
NQ6	--	--	--	--	--	--	
NQ7	--	--	--	--	--	--	
NQ8	--	--	--	--	--	--	
NQ9	--	--	--	--	--	--	
NQ10	--	--	--	--	--	--	
NQ11	--	--	--	--	--	--	

NQ13	--	--	--	--	--	--
NQBR1	--	--	--	--	--	--
NQBR2	--	--	--	--	--	--
NQBR3	--	--	--	--	--	--
NQBR4	--	--	--	--	--	--
NQBR5	--	--	--	--	--	--
NQBR7	--	--	--	--	--	--
NQBR8	--	--	--	--	--	--
NQBR9	--	--	--	--	--	--
NQBR10	--	--	--	--	--	--

Erosion rates -- time-varying production models:

Scaling scheme for spallation:	Desilets and others (2003,2006)			Dunai (2001)			Lifton and others (2005)			Time-dependent Lal (1991)/Stone (2000)		
Sample name	Erosion rate (g/cm2/yr)	Erosion rate (m/Myr)	External uncertainty (m/Myr)	Erosion rate (g/cm2/yr)	Erosion rate (m/Myr)	External uncertainty (m/Myr)	Erosion rate (g/cm2/yr)	Erosion rate (m/Myr)	External uncertainty (m/Myr)	Erosion rate (g/cm2/yr)	Erosion rate (m/Myr)	External uncertainty (m/Myr)
BR1	--	--	--	--	--	--	--	--	--	--	--	--
CN2	--	--	--	--	--	--	--	--	--	--	--	--
CN3	--	--	--	--	--	--	--	--	--	--	--	--
PG1	--	--	--	--	--	--	--	--	--	--	--	--
PG2	--	--	--	--	--	--	--	--	--	--	--	--
PG3	--	--	--	--	--	--	--	--	--	--	--	--
PG4	--	--	--	--	--	--	--	--	--	--	--	--
PG5	--	--	--	--	--	--	--	--	--	--	--	--
PG6	--	--	--	--	--	--	--	--	--	--	--	--
PGBR2	--	--	--	--	--	--	--	--	--	--	--	--
PGBR3	--	--	--	--	--	--	--	--	--	--	--	--
PGBR6	--	--	--	--	--	--	--	--	--	--	--	--
PGBR7	--	--	--	--	--	--	--	--	--	--	--	--
PGBR8	--	--	--	--	--	--	--	--	--	--	--	--
NQ1	--	--	--	--	--	--	--	--	--	--	--	--
NQ2	--	--	--	--	--	--	--	--	--	--	--	--
NQ3	--	--	--	--	--	--	--	--	--	--	--	--
NQ4	--	--	--	--	--	--	--	--	--	--	--	--
NQ5	--	--	--	--	--	--	--	--	--	--	--	--
NQ6	--	--	--	--	--	--	--	--	--	--	--	--
NQ7	--	--	--	--	--	--	--	--	--	--	--	--
NQ8	--	--	--	--	--	--	--	--	--	--	--	--
NQ9	--	--	--	--	--	--	--	--	--	--	--	--
NQ10	--	--	--	--	--	--	--	--	--	--	--	--
NQ11	--	--	--	--	--	--	--	--	--	--	--	--
NQ13	--	--	--	--	--	--	--	--	--	--	--	--
NQBR1	--	--	--	--	--	--	--	--	--	--	--	--
NQBR2	--	--	--	--	--	--	--	--	--	--	--	--
NQBR3	--	--	--	--	--	--	--	--	--	--	--	--
NQBR4	--	--	--	--	--	--	--	--	--	--	--	--
NQBR5	--	--	--	--	--	--	--	--	--	--	--	--
NQBR7	--	--	--	--	--	--	--	--	--	--	--	--
NQBR8	--	--	--	--	--	--	--	--	--	--	--	--
NQBR9	--	--	--	--	--	--	--	--	--	--	--	--
NQBR10	--	--	--	--	--	--	--	--	--	--	--	--

Plotting discontinued in this version. Use version 3 instead.

$^{26}Al/^{10}Be$ ratios (relative to 07KNSTD!):

Sample	$^{26}Al/^{10}Be$ ratio
BR1	--
CN2	--
CN3	--
PG1	--
PG2	--
PG3	--
PG4	--
PG5	--
PG6	--
PGBR2	--
PGBR3	--
PGBR6	--

PGBR7	--
PGBR8	--
NQ1	--
NQ2	--
NQ3	--
NQ4	--
NQ5	--
NQ6	--
NQ7	--
NQ8	--
NQ9	--
NQ10	--
NQ11	--
NQ13	--
NQBR1	--
NQBR2	--
NQBR3	--
NQBR4	--
NQBR5	--
NQBR7	--
NQBR8	--
NQBR9	--
NQBR10	--

Solver diagnostics:

Sample name:	Nuclide	fzero output status	Objective function value (atoms)	Solution time (s)	P_mu(z) calculation time (s)
BR1	Be-10	1 1 1 1 1	-0.488 0.618 4.93e-05 0.586 -0.56	0.01 0.01 0.01 0.01 0.01	4.93
	Al-26	--	--	--	--
CN2	Be-10	1 1 1 1 1	23.8 32.7 29.1 32.4 -26.9	0.01 0.01 0.01 0.01 0.01	4.87
	Al-26	--	--	--	--
CN3	Be-10	1 1 1 1 1	-0.986 1.17 -1.26 0.878 -1.12	0.01 0.01 0.01 0.01 0.01	4.88
	Al-26	--	--	--	--
PG1	Be-10	1 1 1 1 1	-0.559 0.744 0.268 0.72 -0.669	0.01 0.01 0.01 0.01 0.01	5.03
	Al-26	--	--	--	--
PG2	Be-10	1 1 1 1 1	-2.86 3.36 -3.43 2.43 -3	0.01 0.01 0.01 0.01 0.01	5.19
	Al-26	--	--	--	--
PG3	Be-10	1 1 1 1 1	-0.544 0.729 0.126 0.7 -0.656	0.01 0.01 0.01 0.01 0.01	5.01
	Al-26	--	--	--	--
PG4	Be-10	1 1 1 1 1	-0.589 0.827 0.359 0.799 -0.745	0.01 0.01 0.01 0.01 0.01	5.13
	Al-26	--	--	--	--
PG5	Be-10	1 1 1 1 1	-2.62 3.05 -3 2.7 -2.65	0.01 0.01 0.01 0.01 0.01	5.09
	Al-26	--	--	--	--
PG6	Be-10	1 1 1 1 1	-1.14 1.46 -1.46 1.25 -1.32	0.01 0.01 0.01 0.01 0.01	4.99
	Al-26	--	--	--	--
PGBR2	Be-10	1 1 1 1 1	-0.0515 0.0563 0.054 0.0564 -0.0521	0.01 0.01 0.01 0.01 0.01	5.13
	Al-26	--	--	--	--
PGBR3	Be-10	1 1 1 1 1	-0.0278 -0.0143 0.0289 0.00452 0.028	0.01 0.01 0.01 0.01 0.01	5.09
	Al-26	--	--	--	--
PGBR6	Be-10	1 1 1 1 1	-0.839 1.21 0.000105 1.11 -1.1	0.01 0.01 0.01 0.01 0.01	5.07
	Al-26	--	--	--	--
PGBR7	Be-10	1 1 1 1 1	-0.117 0.133 0.0553 0.132 3.4e-06	0.01 0.01 0.01 0.01 0.01	5.08
	Al-26	--	--	--	--
PGBR8	Be-10	1 1 1 1 1	-0.251 0.215 0.305 -0.325 -0.292	0.01 0.01 0.01 0.01 0.01	5.01
	Al-26	--	--	--	--
NQ1	Be-10	1 1 1 1 1	-0.105 0.105 -0.114 0.102 -0.109	0.01 0.01 0.01 0.01 0.01	5.02
	Al-26	--	--	--	--
NQ2	Be-10	1 1 1 1 1	-0.413 0.465 -0.566 0.476 -0.529	0.01 0.01 0.01 0.01 0.01	5.03
	Al-26	--	--	--	--
NQ3	Be-10	1 1 1 1 1	-0.81 0.247 -1.04 0.311 -0.938	0.01 0.01 0.01 0.01 0.01	4.93
	Al-26	--	--	--	--
NQ4	Be-10	1 1 1 1 1	-0.885 0.201 -1.15 0.27 -1.03	0.01 0.01 0.01 0.01 0.01	4.84
	Al-26	--	--	--	--
NQ5	Be-10	1 1 1 1 1	-1.17 0.000117 -1.52 0.028 -1.35	0.01 0.01 0.01 0.01 0.01	4.86
	Al-26	--	--	--	--
NQ6	Be-10	1 1 1 1 1	9.16 25.6 0.0102 25.4 -21.4	0.00 0.01 0.01 0.01 0.01	4.96
	Al-26	--	--	--	--
NQ7	Be-10	1 1 1 1 1	-0.409 0.442 -0.541 0.448 -0.505	0.01 0.01 0.01 0.01 0.01	4.79
	Al-26	--	--	--	--
NQ8	Be-10	1 1 1 1 1	-0.313 0.379 1.72e-05 0.38 -0.376	0.01 0.01 0.01 0.01 0.01	4.81
	Al-26	--	--	--	--

NQ9	Be-10	1 1 1 1 1	-1.42 1.43 0.000145 1.49 -2.21	0.01 0.01 0.01 0.01 0.01	5.64
	Al-26	--	--	--	--
NQ10	Be-10	1 1 1 1 1	-0.317 -0.47 0.454 -0.471 -0.441	0.01 0.01 0.01 0.01 0.01	5.55
	Al-26	--	--	--	--
NQ11	Be-10	1 1 1 1 1	-0.0439 0.0466 -0.0463 0.0467 -0.0442	0.01 0.01 0.01 0.01 0.01	3.93
	Al-26	--	--	--	--
NQ13	Be-10	1 1 1 1 1	-0.108 -0.119 0.0819 -0.119 -0.1	0.01 0.01 0.01 0.01 0.01	3.73
	Al-26	--	--	--	--
NQBR1	Be-10	1 1 1 1 1	-0.376 0.439 -0.478 0.447 -0.477	0.01 0.01 0.01 0.01 0.01	4.83
	Al-26	--	--	--	--
NQBR2	Be-10	1 1 1 1 1	-2.54 0.000494 -2.96 0.000433 -2.52	0.01 0.01 0.01 0.01 0.01	4.80
	Al-26	--	--	--	--
NQBR3	Be-10	1 1 1 1 1	-11.5 7.72 -10.7 7.84 -8.38	0.01 0.01 0.01 0.01 0.01	4.84
	Al-26	--	--	--	--
NQBR4	Be-10	1 1 1 1 1	-0.379 0.452 -0.461 0.459 -0.507	0.01 0.01 0.01 0.01 0.01	4.84
	Al-26	--	--	--	--
NQBR5	Be-10	1 1 1 1 1	-0.457 0.532 -0.663 0.511 -0.619	0.01 0.01 0.01 0.01 0.01	4.80
	Al-26	--	--	--	--
NQBR7	Be-10	1 1 1 1 1	-0.253 0.311 0.172 0.311 -0.163	0.01 0.01 0.01 0.01 0.01	4.82
	Al-26	--	--	--	--
NQBR8	Be-10	1 1 1 1 1	-0.0394 0.0398 -0.0414 0.0399 -0.0398	0.01 0.01 0.01 0.01 0.01	4.12
	Al-26	--	--	--	--
NQBR9	Be-10	1 1 1 1 1	-2.66 2.65 -2.77 2.4 -2.21	0.01 0.01 0.01 0.01 0.01	4.26
	Al-26	--	--	--	--
NQBR10	Be-10	1 1 1 1 1	-2.94 2.98 -2.99 2.77 -2.35	0.01 0.01 0.01 0.01 0.01	4.03
	Al-26	--	--	--	--

The online erosion rate calculator formerly known as the CRONUS-Earth ^{10}Be - ^{26}Al erosion rate calculator -- results

Version information --

Component	Version
Wrapper script:	2.3
Main calculator:	2.1
Objective function:	2.0
Constants:	2.3
Muons:	1.1

Comments:

Production rate calibration information: Using default calibration data set

^{10}Be results:

Results not dependent on spallogenic production rate model:

Erosion rates -- constant production rate model:

Scaling scheme for spallation: Lal(1991) / Stone(2000)

Sample name	Shielding factor	Production rate (muons) (atoms/g/yr)	Internal uncertainty (m/Myr)	Erosion rate (g/cm2/yr)	Erosion rate (m/Myr)	External uncertainty (m/Myr)	Production rate (spallation) (atoms/g/yr)
Croke-Hillslope	1.0000	0.083	0.84	0.00302	11.20	1.19	3.40
Croke-1	1.0000	0.083	0.71	0.00260	9.63	1.02	3.41
Croke-2	1.0000	0.083	0.64	0.00339	12.55	1.14	3.42
Croke-3	1.0000	0.083	1.74	0.00350	12.95	1.99	3.39
Croke-4	1.0000	0.083	0.51	0.00283	10.49	0.94	3.40
Croke-5	1.0000	0.084	0.58	0.00175	6.48	0.77	3.49
Croke-6	1.0000	0.083	0.78	0.00373	13.83	1.29	3.39
Croke-7	1.0000	0.088	0.91	0.00391	14.49	1.41	3.86
Croke-8	1.0000	0.084	1.41	0.00401	14.86	1.79	3.44
Croke-9	1.0000	0.089	0.95	0.00291	10.80	1.26	3.90
Croke-10	1.0000	0.087	0.79	0.00318	11.76	1.19	3.75
Croke-11	1.0000	0.086	0.68	0.00343	12.69	1.17	3.65
Croke-12	1.0000	0.085	0.67	0.00286	10.59	1.05	3.61
Croke-13	1.0000	0.085	0.52	0.00295	10.92	0.98	3.58
Croke-14	1.0000	0.090	0.57	0.00278	10.30	0.98	4.03
Croke-15	1.0000	0.090	0.88	0.00285	10.54	1.20	4.02
Croke-16	1.0000	0.089	0.58	0.00289	10.71	1.01	3.99
Croke-17	1.0000	0.085	0.50	0.00277	10.25	0.93	3.60
Croke-18	1.0000	0.085	14.43	0.00514	19.03	14.49	3.61
Croke-19	1.0000	0.083	0.14	0.00085	3.16	0.31	3.51
Croke-20	1.0000	0.085	0.35	0.00203	7.51	0.69	3.64
Croke-21	1.0000	0.084	0.20	0.00133	4.92	0.45	3.64
Croke-22	1.0000	0.084	0.17	0.00102	3.80	0.37	3.57
QLD1	1.0000	0.085	0.24	0.00367	13.58	1.04	3.48
QLD2	1.0000	0.085	0.45	0.00395	14.62	1.17	3.48
QLD3	1.0000	0.092	0.90	0.00802	29.70	2.31	4.12
QLD4	1.0000	0.085	0.05	0.00286	10.59	0.81	3.47
QLD5	1.0000	0.092	0.45	0.00333	12.34	1.04	4.10
QLD6	1.0000	0.088	0.09	0.00130	4.82	0.41	3.74
QLD7	1.0000	0.090	0.27	0.00418	15.47	1.18	3.93
QLD8	1.0000	0.092	0.24	0.00402	14.90	1.14	4.17
QLD9	1.0000	0.090	0.14	0.00295	10.94	0.85	3.96
QLD9xb	1.0000	0.090	0.19	0.00299	11.08	0.87	3.96
QLD10	1.0000	0.092	0.28	0.00299	11.08	0.89	4.11
QLD11	1.0000	0.086	0.23	0.00363	13.44	1.03	3.55
QLD12	1.0000	0.088	0.34	0.00568	21.04	1.56	3.77
QLD13	1.0000	0.085	1.46	0.01171	43.36	3.31	3.40
QLD14	1.0000	0.084	1.23	0.01060	39.25	2.96	3.34
QLD15	1.0000	0.076	0.22	0.00185	6.84	0.58	2.69

Erosion rates -- time-varying production models:

Scaling scheme for spallation:	Desilets and others (2003,2006)			Dunai (2001)			Lifton and others (2005)			Time-dependent Lal (1991)/Stone (2000)		
Sample name	Erosion rate (g/cm2/yr)	Erosion rate (m/Myr)	External uncertainty (m/Myr)	Erosion rate (g/cm2/yr)	Erosion rate (m/Myr)	External uncertainty (m/Myr)	Erosion rate (g/cm2/yr)	Erosion rate (m/Myr)	External uncertainty (m/Myr)	Erosion rate (g/cm2/yr)	Erosion rate (m/Myr)	External uncertainty (m/Myr)
Croke-Hillslope	0.00308	11.40	5.33	0.00320	11.84	5.54	0.00311	11.50	1.43	0.00351	13.02	1.44
Croke-1	0.00266	9.85	6.27	0.00276	10.23	4.80	0.00269	9.94	1.24	0.00304	11.28	1.25
Croke-2	0.00344	12.74	5.90	0.00357	13.23	6.14	0.00347	12.85	1.42	0.00392	14.51	1.39
Croke-3	0.00354	13.12	6.29	0.00368	13.62	2.28	0.00357	13.23	2.19	0.00404	14.94	2.33
Croke-4	0.00289	10.69	4.96	0.00300	11.11	5.16	0.00291	10.79	1.20	0.00330	12.23	1.17
Croke-5	0.00181	6.72	3.19	0.00188	6.98	3.32	0.00183	6.78	4.80	0.00209	7.73	0.95
Croke-6	0.00377	13.97	6.47	0.00392	14.51	1.67	0.00381	14.09	1.58	0.00429	15.90	1.56
Croke-7	0.00401	14.85	6.87	0.00415	15.36	8.81	0.00404	14.97	1.74	0.00452	16.73	1.72
Croke-8	0.00405	15.00	7.04	0.00420	15.57	2.14	0.00409	15.13	2.05	0.00460	17.04	2.11
Croke-9	0.00302	11.19	5.24	0.00313	11.58	5.44	0.00305	11.29	1.51	0.00342	12.66	1.53
Croke-10	0.00327	12.10	5.62	0.00338	12.53	7.50	0.00330	12.21	1.47	0.00370	13.71	1.45
Croke-11	0.00350	12.97	6.01	0.00363	13.45	6.24	0.00354	13.09	1.47	0.00397	14.72	1.44
Croke-12	0.00294	10.88	6.71	0.00305	11.29	5.26	0.00297	10.99	1.30	0.00335	12.39	1.29
Croke-13	0.00302	11.19	5.18	0.00313	11.61	5.39	0.00305	11.30	1.25	0.00344	12.75	1.22
Croke-14	0.00289	10.71	4.97	0.00299	11.09	5.15	0.00292	10.83	5.05	0.00327	12.12	1.22
Croke-15	0.00296	10.95	5.12	0.00306	11.34	6.91	0.00299	11.07	5.21	0.00335	12.39	1.46
Croke-16	0.00299	11.07	5.13	0.00310	11.47	5.33	0.00302	11.19	5.22	0.00339	12.54	1.25
Croke-17	0.00284	10.53	4.89	0.00295	10.93	6.73	0.00287	10.63	1.19	0.00324	12.00	1.16
Croke-18	0.00513	18.99	14.52	0.00532	19.72	15.04	0.00517	19.16	14.64	0.00580	21.47	16.25
Croke-19	0.00086	3.19	1.55	0.00090	3.34	1.63	0.00087	3.24	1.59	0.00102	3.76	0.39
Croke-20	0.00207	7.65	3.57	0.00215	7.97	3.73	0.00209	7.75	3.64	0.00238	8.81	0.86
Croke-21	0.00135	4.99	2.37	0.00141	5.22	3.99	0.00137	5.07	3.93	0.00157	5.81	0.57
Croke-22	0.00104	3.87	3.32	0.00109	4.04	1.95	0.00106	3.93	1.90	0.00122	4.53	0.46
QLD1	0.00377	13.97	8.15	0.00388	14.37	1.47	0.00377	13.98	1.38	0.00422	15.64	1.30
QLD2	0.00405	14.99	6.90	0.00416	15.42	1.61	0.00405	14.99	1.52	0.00453	16.76	1.45
QLD3	0.00808	29.94	3.10	0.00830	30.74	3.12	0.00808	29.94	2.95	0.00885	32.76	2.75
QLD4	0.00296	10.98	5.06	0.00305	11.29	5.22	0.00297	10.98	1.10	0.00333	12.35	1.02
QLD5	0.00350	12.95	5.96	0.00358	13.26	6.12	0.00350	12.96	1.38	0.00388	14.36	1.30
QLD6	0.00139	5.14	3.89	0.00142	5.28	2.49	0.00139	5.14	3.90	0.00158	5.83	0.53
QLD7	0.00432	16.02	9.03	0.00443	16.43	1.68	0.00433	16.03	1.59	0.00479	17.75	1.48
QLD8	0.00419	15.54	7.12	0.00430	15.91	8.95	0.00420	15.55	1.55	0.00463	17.16	1.43
QLD9	0.00310	11.50	5.29	0.00318	11.78	5.43	0.00311	11.50	1.17	0.00346	12.80	1.08
QLD9xb	0.00314	11.64	5.36	0.00322	11.93	5.50	0.00315	11.65	1.19	0.00350	12.96	1.10
QLD10	0.00315	11.67	6.96	0.00323	11.95	5.51	0.00315	11.68	1.21	0.00350	12.96	1.13
QLD11	0.00374	13.86	6.37	0.00385	14.25	1.46	0.00374	13.87	1.38	0.00418	15.50	1.29
QLD12	0.00578	21.42	2.18	0.00594	22.00	2.19	0.00578	21.42	2.06	0.00639	23.68	1.91
QLD13	0.01142	42.28	4.21	0.01179	43.66	4.27	0.01141	42.25	4.01	0.01255	46.47	3.81
QLD14	0.01036	38.38	3.80	0.01070	39.63	3.86	0.01036	38.36	3.62	0.01142	42.31	3.43
QLD15	0.00187	6.92	3.25	0.00193	7.16	3.36	0.00187	6.91	3.26	0.00215	7.97	0.72

^{26}Al results:

Results not dependent on spallogenic production rate model:

Erosion rates -- constant production rate model:

Scaling scheme for spallation: Lal(1991) / Stone(2000)

Sample name	Shielding factor	Production rate (muons) (atoms/g/yr)	Internal uncertainty (m/Myr)	Erosion rate (g/cm2/yr)	Erosion rate (m/Myr)	External uncertainty (m/Myr)	Production rate (spallation) (atoms/g/yr)
Croke-Hillslope	--	--	--	--	--	--	
Croke-1	--	--	--	--	--	--	
Croke-2	--	--	--	--	--	--	
Croke-3	--	--	--	--	--	--	
Croke-4	--	--	--	--	--	--	
Croke-5	--	--	--	--	--	--	
Croke-6	--	--	--	--	--	--	
Croke-7	--	--	--	--	--	--	
Croke-8	--	--	--	--	--	--	
Croke-9	--	--	--	--	--	--	
Croke-10	--	--	--	--	--	--	
Croke-11	--	--	--	--	--	--	
Croke-12	--	--	--	--	--	--	
Croke-13	--	--	--	--	--	--	
Croke-14	--	--	--	--	--	--	
Croke-15	--	--	--	--	--	--	
Croke-16	--	--	--	--	--	--	

Croke-17	--	--	--	--	--	--
Croke-18	--	--	--	--	--	--
Croke-19	--	--	--	--	--	--
Croke-20	--	--	--	--	--	--
Croke-21	--	--	--	--	--	--
Croke-22	--	--	--	--	--	--
QLD1	--	--	--	--	--	--
QLD2	--	--	--	--	--	--
QLD3	--	--	--	--	--	--
QLD4	--	--	--	--	--	--
QLD5	--	--	--	--	--	--
QLD6	--	--	--	--	--	--
QLD7	--	--	--	--	--	--
QLD8	--	--	--	--	--	--
QLD9	--	--	--	--	--	--
QLD9xb	--	--	--	--	--	--
QLD10	--	--	--	--	--	--
QLD11	--	--	--	--	--	--
QLD12	--	--	--	--	--	--
QLD13	--	--	--	--	--	--
QLD14	--	--	--	--	--	--
QLD15	--	--	--	--	--	--

Erosion rates -- time-varying production models:

Scaling scheme for spallation:	Desilets and others (2003,2006)			Dunai (2001)			Lifton and others (2005)			Time-dependent Lal (1991)/Stone (2000)		
Sample name	Erosion rate (g/cm2/yr)	Erosion rate (m/Myr)	External uncertainty (m/Myr)	Erosion rate (g/cm2/yr)	Erosion rate (m/Myr)	External uncertainty (m/Myr)	Erosion rate (g/cm2/yr)	Erosion rate (m/Myr)	External uncertainty (m/Myr)	Erosion rate (g/cm2/yr)	Erosion rate (m/Myr)	External uncertainty (m/Myr)
Croke-Hillslope	--	--	--	--	--	--	--	--	--	--	--	--
Croke-1	--	--	--	--	--	--	--	--	--	--	--	--
Croke-2	--	--	--	--	--	--	--	--	--	--	--	--
Croke-3	--	--	--	--	--	--	--	--	--	--	--	--
Croke-4	--	--	--	--	--	--	--	--	--	--	--	--
Croke-5	--	--	--	--	--	--	--	--	--	--	--	--
Croke-6	--	--	--	--	--	--	--	--	--	--	--	--
Croke-7	--	--	--	--	--	--	--	--	--	--	--	--
Croke-8	--	--	--	--	--	--	--	--	--	--	--	--
Croke-9	--	--	--	--	--	--	--	--	--	--	--	--
Croke-10	--	--	--	--	--	--	--	--	--	--	--	--
Croke-11	--	--	--	--	--	--	--	--	--	--	--	--
Croke-12	--	--	--	--	--	--	--	--	--	--	--	--
Croke-13	--	--	--	--	--	--	--	--	--	--	--	--
Croke-14	--	--	--	--	--	--	--	--	--	--	--	--
Croke-15	--	--	--	--	--	--	--	--	--	--	--	--
Croke-16	--	--	--	--	--	--	--	--	--	--	--	--
Croke-17	--	--	--	--	--	--	--	--	--	--	--	--
Croke-18	--	--	--	--	--	--	--	--	--	--	--	--
Croke-19	--	--	--	--	--	--	--	--	--	--	--	--
Croke-20	--	--	--	--	--	--	--	--	--	--	--	--
Croke-21	--	--	--	--	--	--	--	--	--	--	--	--
Croke-22	--	--	--	--	--	--	--	--	--	--	--	--
QLD1	--	--	--	--	--	--	--	--	--	--	--	--
QLD2	--	--	--	--	--	--	--	--	--	--	--	--
QLD3	--	--	--	--	--	--	--	--	--	--	--	--
QLD4	--	--	--	--	--	--	--	--	--	--	--	--
QLD5	--	--	--	--	--	--	--	--	--	--	--	--
QLD6	--	--	--	--	--	--	--	--	--	--	--	--
QLD7	--	--	--	--	--	--	--	--	--	--	--	--
QLD8	--	--	--	--	--	--	--	--	--	--	--	--
QLD9	--	--	--	--	--	--	--	--	--	--	--	--
QLD9xb	--	--	--	--	--	--	--	--	--	--	--	--
QLD10	--	--	--	--	--	--	--	--	--	--	--	--
QLD11	--	--	--	--	--	--	--	--	--	--	--	--
QLD12	--	--	--	--	--	--	--	--	--	--	--	--
QLD13	--	--	--	--	--	--	--	--	--	--	--	--
QLD14	--	--	--	--	--	--	--	--	--	--	--	--
QLD15	--	--	--	--	--	--	--	--	--	--	--	--

Plotting discontinued in this version. Use version 3 instead.

$^{26}Al/^{10}Be$ ratios (relative to 07KNSTD!):

Sample	$^{26}Al/^{10}Be$ ratio
Croke-Hillslope	--
Croke-1	--
Croke-2	--
Croke-3	--
Croke-4	--
Croke-5	--
Croke-6	--
Croke-7	--
Croke-8	--
Croke-9	--
Croke-10	--
Croke-11	--
Croke-12	--
Croke-13	--
Croke-14	--
Croke-15	--
Croke-16	--
Croke-17	--
Croke-18	--
Croke-19	--
Croke-20	--
Croke-21	--
Croke-22	--
QLD1	--
QLD2	--
QLD3	--
QLD4	--
QLD5	--
QLD6	--
QLD7	--
QLD8	--
QLD9	--
QLD9xb	--
QLD10	--
QLD11	--
QLD12	--
QLD13	--
QLD14	--
QLD15	--

Solver diagnostics:

Sample name:	Nuclide	fzero output status	Objective function value (atoms)	Solution time (s)	P_mu(z) calculation time (s)
Croke-Hillslope	Be-10	1 1 1 1 1	-0.655 0.848 -0.888 0.709 -0.806	0.01 0.01 0.01 0.01 0.01	5.00
	Al-26	--	--	--	--
Croke-1	Be-10	1 1 1 1 1	-0.876 1.09 -1.17 0.83 -1.05	0.01 0.01 0.01 0.01 0.01	4.92
	Al-26	--	--	--	--
Croke-2	Be-10	1 1 1 1 1	-0.529 0.707 -0.724 0.624 -0.663	0.01 0.01 0.01 0.01 0.01	4.92
	Al-26	--	--	--	--
Croke-3	Be-10	1 1 1 1 1	-0.503 0.668 -0.68 0.598 -0.623	0.01 0.01 0.01 0.01 0.01	4.92
	Al-26	--	--	--	--
Croke-4	Be-10	1 1 1 1 1	-0.743 0.946 -1 0.761 -0.902	0.01 0.01 0.01 0.01 0.01	4.92
	Al-26	--	--	--	--
Croke-5	Be-10	1 1 1 1 1	-2.04 2.28 -2.43 1.58 -2.07	0.01 0.01 0.01 0.01 0.01	4.95
	Al-26	--	--	--	--
Croke-6	Be-10	1 1 1 1 1	-0.449 0.598 -0.603 0.548 -0.554	0.01 0.01 0.01 0.01 0.01	4.92
	Al-26	--	--	--	--
Croke-7	Be-10	1 1 1 1 1	-0.385 0.618 2.77e-05 0.584 -0.572	0.01 0.01 0.01 0.01 0.01	5.10
	Al-26	--	--	--	--
Croke-8	Be-10	1 1 1 1 1	-0.395 0.536 -0.415 0.502 -0.493	0.01 0.01 0.01 0.01 0.01	4.92
	Al-26	--	--	--	--
Croke-9	Be-10	1 1 1 1 1	-0.632 1.01 -1.07 0.824 -0.979	0.01 0.01 0.01 0.01 0.01	5.08
	Al-26	--	--	--	--
Croke-10	Be-10	1 1 1 1 1	-0.555 0.851 -0.88 0.732 -0.809	0.01 0.01 0.01 0.01 0.01	5.05
	Al-26	--	--	--	--
Croke-11	Be-10	1 1 1 1 1	-0.493 0.738 -0.75 0.658 -0.691	0.01 0.01 0.01 0.01 0.01	5.00
	Al-26	--	--	--	--

Croke-12	Be-10	1 1 1 1 1	-0.693 0.981 -1.03 0.783 -0.94	0.01 0.01 0.01 0.01 0.01	4.98
	Al-26	--	--	--	--
Croke-13	Be-10	1 1 1 1 1	-0.659 0.928 -0.971 0.759 -0.884	0.01 0.01 0.01 0.01 0.01	4.98
	Al-26	--	--	--	--
Croke-14	Be-10	1 1 1 1 1	-0.664 1.14 -1.19 0.896 -1.1	0.01 0.01 0.01 0.01 0.01	5.19
	Al-26	--	--	--	--
Croke-15	Be-10	1 1 1 1 1	-0.634 1.1 -1.14 0.879 -1.05	0.01 0.01 0.01 0.01 0.01	5.16
	Al-26	--	--	--	--
Croke-16	Be-10	1 1 1 1 1	-0.692 1.1 -1.1 0.964 -1.02	0.01 0.01 0.01 0.01 0.01	5.16
	Al-26	--	--	--	--
Croke-17	Be-10	1 1 1 1 1	-0.744 1.03 -1.09 0.8 -0.992	0.01 0.01 0.01 0.01 0.01	4.99
	Al-26	--	--	--	--
Croke-18	Be-10	1 1 1 1 1	-0.288 -0.367 0.286 0.361 -0.171	0.01 0.01 0.01 0.01 0.01	4.98
	Al-26	--	--	--	--
Croke-19	Be-10	1 1 1 1 1	-9.5 8.75 8.48 9.33 -7.94	0.01 0.01 0.01 0.01 0.01	4.88
	Al-26	--	--	--	--
Croke-20	Be-10	1 1 1 1 1	-1.72 2.02 -1.75 1.9 -1.77	0.01 0.01 0.01 0.01 0.01	4.95
	Al-26	--	--	--	--
Croke-21	Be-10	1 1 1 1 1	-4.24 4.42 2.64 4.34 -3.79	0.01 0.01 0.01 0.01 0.01	4.95
	Al-26	--	--	--	--
Croke-22	Be-10	1 1 1 1 1	-6.83 6.88 4.6 6.78 -5.75	0.01 0.01 0.01 0.01 0.01	4.93
	Al-26	--	--	--	--
QLD1	Be-10	1 1 1 1 1	-0.469 0.493 -0.634 0.488 -0.588	0.01 0.01 0.01 0.01 0.01	5.00
	Al-26	--	--	--	--
QLD2	Be-10	1 1 1 1 1	-0.417 0.466 -0.554 0.463 -0.516	0.01 0.01 0.01 0.01 0.01	5.00
	Al-26	--	--	--	--
QLD3	Be-10	1 1 1 1 1	-0.152 0.133 -0.171 0.13 -0.164	0.01 0.01 0.01 0.01 0.01	5.18
	Al-26	--	--	--	--
QLD4	Be-10	1 1 1 1 1	-0.727 0.522 -0.998 0.478 -0.909	0.01 0.01 0.01 0.01 0.01	4.89
	Al-26	--	--	--	--
QLD5	Be-10	1 1 1 1 1	-0.533 0.714 -0.867 0.698 -0.811	0.01 0.01 0.01 0.01 0.01	4.99
	Al-26	--	--	--	--
QLD6	Be-10	1 1 1 1 1	-4.08 2.15 -4.36 1.78 -3.59	0.01 0.01 0.01 0.01 0.01	4.93
	Al-26	--	--	--	--
QLD7	Be-10	1 1 1 1 1	-0.38 0.524 0.0118 0.52 -0.52	0.01 0.01 0.01 0.01 0.01	5.02
	Al-26	--	--	--	--
QLD8	Be-10	1 1 1 1 1	-0.402 0.593 0.127 0.589 -0.586	0.01 0.01 0.01 0.01 0.01	5.07
	Al-26	--	--	--	--
QLD9	Be-10	1 1 1 1 1	-0.66 0.692 -1.05 0.66 -0.976	0.01 0.01 0.01 0.01 0.01	5.02
	Al-26	--	--	--	--
QLD9xb	Be-10	1 1 1 1 1	-0.645 0.692 -1.03 0.664 -0.954	0.01 0.01 0.01 0.01 0.01	5.01
	Al-26	--	--	--	--
QLD10	Be-10	1 1 1 1 1	-0.641 0.746 -1.06 0.719 -0.988	0.01 0.01 0.01 0.01 0.01	5.00
	Al-26	--	--	--	--
QLD11	Be-10	1 1 1 1 1	-0.476 0.512 -0.657 0.508 -0.611	0.01 0.01 0.01 0.01 0.01	4.83
	Al-26	--	--	--	--
QLD12	Be-10	1 1 1 1 1	-0.243 0.305 0.223 0.305 -0.236	0.01 0.01 0.01 0.01 0.01	4.95
	Al-26	--	--	--	--
QLD13	Be-10	1 1 1 1 1	-0.0683 0.0728 -0.0566 0.0731 1.85e-06	0.01 0.01 0.01 0.01 0.01	4.77
	Al-26	--	--	--	--
QLD14	Be-10	1 1 1 1 1	-0.0807 0.0769 -0.0854 0.0777 -0.0819	0.01 0.01 0.01 0.01 0.01	4.75
	Al-26	--	--	--	--
QLD15	Be-10	1 1 1 1 1	-1.72 1.18 -1.77 1.29 -1.44	0.01 0.01 0.01 0.01 0.01	3.74
	Al-26	--	--	--	--

CERTIFICATE OF ANALYSIS

Work Order	: **CA1803836**	Page	: 1 of 11
Client	: **Ashish Kumar Mishra**	Laboratory	: ALS Water Resources Group
Contact	: Mr Ashish Kumar Mishra	Contact	: Client Services
Address	: Room 152, Building 34 EGRU James Cook Uni QLD Townsville 4814	Address	: 16B Lithgow Street Fyshwick ACT Australia 2609
Telephone	: ----	Telephone	: +61 2 6202 5404
Project	: Al & Be Analysis	Date Samples Received	: 22-Jun-2018 13:00
Order number	: ----	Date Analysis Commenced	: 22-Jun-2018
C-O-C number	: ----	Issue Date	: 06-Jul-2018 15:32
Sampler	: Ashish Kumar Mishra		
Site	: Al & Be Analysis		
Quote number	: ----		
No. of samples received	: 44		
No. of samples analysed	: 44		

Accreditation No. 992
Accredited for compliance with
ISO/IEC 17025 - Testing

This report supersedes any previous report(s) with this reference. Results apply to the sample(s) as submitted. This document shall not be reproduced, except in full.

This Certificate of Analysis contains the following information:

- General Comments
- Analytical Results

Additional information pertinent to this report will be found in the following separate attachments: Quality Control Report, QA/QC Compliance Assessment to assist with Quality Review and Sample Receipt Notification.

Signatories

This document has been electronically signed by the authorized signatories below. Electronic signing is carried out in compliance with procedures specified in 21 CFR Part 11.

Signatories	*Position*	*Accreditation Category*
Titus Vimalasiri	Metals Teamleader	Inorganics, Fyshwick, ACT

General Comments

The analytical procedures used by the Environmental Division have been developed from established internationally recognized procedures such as those published by the USEPA, APHA, AS and NEPM. In house developed procedures are employed in the absence of documented standards or by client request.

Where moisture determination has been performed, results are reported on a dry weight basis.

Where a reported less than (<) result is higher than the LOR, this may be due to primary sample extract/digestate dilution and/or insufficient sample for analysis.

Where the LOR of a reported result differs from standard LOR, this may be due to high moisture content, insufficient sample (reduced weight employed) or matrix interference.

When sampling time information is not provided by the client, sampling dates are shown without a time component. In these instances, the time component has been assumed by the laboratory for processing purposes.

Where a result is required to meet compliance limits the associated uncertainty must be considered. Refer to the ALS Contact for details.

Key : CAS Number = CAS registry number from database maintained by Chemical Abstracts Services. The Chemical Abstracts Service is a division of the American Chemical Society.
LOR = Limit of reporting
^ = This result is computed from individual analyte detections at or above the level of reporting
ø = ALS is not NATA accredited for these tests.
~ = Indicates an estimated value.

- **For samples collected by ALS WRG, sampling was carried out in accordance with Procedure EN67**

Analytical Results

Sub-Matrix: **WATER** (Matrix: **WATER**)				Client sample ID	BR1	CN2	CN3	PG1	PG2
				Client sampling date / time	[21-Jun-2018]	[21-Jun-2018]	[21-Jun-2018]	[21-Jun-2018]	[21-Jun-2018]
Compound	*CAS Number*	*LOR*	*Unit*		**CA1803836-001**	**CA1803836-002**	**CA1803836-003**	**CA1803836-004**	**CA1803836-005**
					Result	Result	Result	Result	Result
EG005F: Dissolved Metals by ICP-OES									
Aluminium	7429-90-5	0.02	mg/L		**4.79**	**21.0**	**5.16**	**9.38**	**8.79**
Beryllium	7440-41-7	0.001	mg/L		**0.326**	**0.362**	**0.197**	**0.427**	**0.862**

Analytical Results

Sub-Matrix: **WATER** (Matrix: **WATER**)				Client sample ID	PG3	PG4	PG5	PG6	PGBR2
				Client sampling date / time	[21-Jun-2018]	[21-Jun-2018]	[21-Jun-2018]	[21-Jun-2018]	[21-Jun-2018]
Compound	CAS Number	LOR	Unit		CA1803836-006	CA1803836-007	CA1803836-008	CA1803836-009	CA1803836-010
					Result	Result	Result	Result	Result
EG005F: Dissolved Metals by ICP-OES									
Aluminium	7429-90-5	0.02	mg/L		**21.1**	**9.04**	**7.46**	**6.50**	**7.87**
Beryllium	7440-41-7	0.001	mg/L		**0.726**	**0.309**	**0.248**	**0.958**	**0.313**

Analytical Results

Sub-Matrix: **WATER** (Matrix: **WATER**)				Client sample ID	PGBR3	PGBR6	PGBR7	PGBR8	Blank-1
				Client sampling date / time	[21-Jun-2018]	[21-Jun-2018]	[21-Jun-2018]	[21-Jun-2018]	[21-Jun-2018]
Compound	*CAS Number*	*LOR*	*Unit*		**CA1803836-011**	**CA1803836-012**	**CA1803836-013**	**CA1803836-014**	**CA1803836-015**
					Result	Result	Result	Result	Result
EG005F: Dissolved Metals by ICP-OES									
Aluminium	7429-90-5	0.02	mg/L		**8.54**	**7.94**	**9.40**	**8.56**	**1.02**
Beryllium	7440-41-7	0.001	mg/L		**0.323**	**0.200**	**0.277**	**0.315**	**0.160**

Analytical Results

Sub-Matrix: WATER (Matrix: WATER)				Client sample ID	Blank-2	NQ 1	NQ 2	NQ 3	NQ 4
				Client sampling date / time	[21-Jun-2018]	[21-Jun-2018]	[21-Jun-2018]	[21-Jun-2018]	[21-Jun-2018]
Compound	CAS Number	LOR	Unit		CA1803836-016	CA1803836-017	CA1803836-018	CA1803836-019	CA1803836-020
					Result	Result	Result	Result	Result
EG005F: Dissolved Metals by ICP-OES									
Aluminium	7429-90-5	0.02	mg/L		**0.95**	**5.99**	**21.0**	**23.9**	**14.5**
Beryllium	7440-41-7	0.001	mg/L		**0.149**	**0.490**	**0.488**	**0.411**	**0.519**

Analytical Results

Sub-Matrix: **WATER** (Matrix: **WATER**)				Client sample ID	NQ 5	NQ 6	NQ 7	NQ 8	NQ 9
				Client sampling date / time	[21-Jun-2018]	[21-Jun-2018]	[21-Jun-2018]	[21-Jun-2018]	[21-Jun-2018]
Compound	CAS Number	LOR	Unit		CA1803836-021	CA1803836-022	CA1803836-023	CA1803836-024	CA1803836-025
					Result	Result	Result	Result	Result
EG005F: Dissolved Metals by ICP-OES									
Aluminium	7429-90-5	0.02	mg/L		**10.8**	**13.2**	**13.9**	**12.4**	**15.2**
Beryllium	7440-41-7	0.001	mg/L		**0.480**	**0.537**	**0.456**	**0.262**	**0.524**

Analytical Results

Sub-Matrix: **WATER**
(Matrix: **WATER**)

Compound	CAS Number	LOR	Unit	Client sample ID	NQ 10	NQ 11	NQ 13	NQBR 1	NQBR 2
				Client sampling date / time	[21-Jun-2018]	[21-Jun-2018]	[21-Jun-2018]	[21-Jun-2018]	[21-Jun-2018]
					CA1803836-026	**CA1803836-027**	**CA1803836-028**	**CA1803836-029**	**CA1803836-030**
					Result	Result	Result	Result	Result
EG005F: Dissolved Metals by ICP-OES									
Aluminium	7429-90-5	0.02	mg/L		**13.1**	**14.8**	**10.9**	**10.6**	**6.62**
Beryllium	7440-41-7	0.001	mg/L		**0.424**	**0.540**	**0.353**	**0.493**	**0.392**

Analytical Results

Sub-Matrix: **WATER**
(Matrix: **WATER**)

Compound	CAS Number	LOR	Unit	Client sample ID	NQBR 3	NQBR 4	NQBR 5	NQBR 7	NQBR 8
				Client sampling date / time	[21-Jun-2018]	[21-Jun-2018]	[21-Jun-2018]	[21-Jun-2018]	[21-Jun-2018]
					CA1803836-031	CA1803836-032	CA1803836-033	CA1803836-034	CA1803836-035
					Result	Result	Result	Result	Result
EG005F: Dissolved Metals by ICP-OES									
Aluminium	7429-90-5	0.02	mg/L		**16.3**	**5.12**	**8.49**	**35.8**	**8.93**
Beryllium	7440-41-7	0.001	mg/L		**0.359**	**0.387**	**0.373**	**0.272**	**0.418**

Analytical Results

Sub-Matrix: WATER (Matrix: WATER)				Client sample ID	NQBR 9	NQBR 10	Blank-3	Blank-4	Blank 5
				Client sampling date / time	[21-Jun-2018]	[21-Jun-2018]	[21-Jun-2018]	[21-Jun-2018]	[21-Jun-2018]
Compound	CAS Number	LOR	Unit		CA1803836-036	CA1803836-037	CA1803836-038	CA1803836-039	CA1803836-040
					Result	Result	Result	Result	Result
EG005F: Dissolved Metals by ICP-OES									
Aluminium	7429-90-5	0.02	mg/L		**9.96**	**6.79**	**4.25**	**3.90**	**1.95**
Beryllium	7440-41-7	0.001	mg/L		**0.318**	**0.418**	**0.446**	**0.407**	**0.206**

Analytical Results

Sub-Matrix: **WATER** (Matrix: **WATER**)				Client sample ID	**ABAZ-1**	**ABAZ-2**	**ABAZ-3**	**ABAZ-4**	**----**
				Client sampling date / time	[21-Jun-2018]	[21-Jun-2018]	[21-Jun-2018]	[21-Jun-2018]	----
Compound	*CAS Number*	*LOR*	*Unit*		**CA1803836-041**	**CA1803836-042**	**CA1803836-043**	**CA1803836-044**	**--------**
					Result	Result	Result	Result	----
EG005F: Dissolved Metals by ICP-OES									
Beryllium	7440-41-7	0.001	mg/L		**1.05**	**1.04**	**1.03**	**1.05**	**----**

Appendix 4

This administrative form
has been removed

This administrative form
has been removed

This administrative form
has been removed

This administrative form
has been removed

This administrative form
has been removed

This administrative form
has been removed

This administrative form
has been removed

Appendix 5

Beta Analytic
RADIOCARBON DATING
Consistent accuracy delivered on time

DR. M.A. TAMERS and MR. D.G. HOOD
4985 S.W. 74th Court
Miami, Florida, USA 33155
PH: 305-667-5167 FAX: 305-663-0964
beta@radiocarbon.com

REPORT OF RADIOCARBON DATING ANALYSES

Mr. Ashish Kumar Mishra

James Cook University

Report Date: June 30, 2017

Material Received: June 12, 2017

Sample Information and Data	Sample Code Number	Conventional Radiocarbon Age (BP) or Percent Modern Carbon (pMC) & Stable Isotopes Calendar Calibrated Results: 95.4 % Probability High Probability Density Range Method (HPD)	
Beta - 467008	**TB-5**	**17130 +/- 50 BP**	IRMS δ13C: -29.1 o/oo
Submitter Material: Charcoal		**(95.4%) 18866 - 18480 cal BC**	**(20815 - 20429 cal BP)**
Analyzed Material: Charred material			
Pretreatment: (charred material) none			
Analysis Service: AMS-Standard delivery			
Percent Modern Carbon: 11.85 +/- 0.07 pMC			
Fraction Modern Carbon: 0.1185 +/- 0.0007			
D14C: -881.46 +/- 0.74 o/oo			
Δ14C: -882.41 +/- 0.74 o/oo(1950:2017)			
Measured Radiocarbon Age: (without d13C correction): 17200 +/- 50 BP			
Calibration: BetaCal3.21: HPD method: SHCAL13			

Results are ISO/IEC-17025:2005 accredited. No sub-contracting or student labor was used in the analyses. All work was done at Beta in 4 in-house NEC accelerator mass spectrometers and 4 Thermo IRMSs. The "Conventional Radiocarbon Age" was calculated using the Libby half-life (5568 years), is corrected for total isotopic fraction and was used for calendar calibration where applicable. The Age is rounded to the nearest 10 years and is reported as radiocarbon years before present (BP), “present" = AD 1950. Results greater than the modern reference are reported as percent modern carbon (pMC). The modern reference standard was 95% the 14C signature of NIST SRM-4990C (oxalic acid). Quoted errors are 1 sigma counting statistics. Calculated sigmas less than 30 BP on the Conventional Radiocarbon Age are conservatively rounded up to 30. d13C values are on the material itself (not the AMS d13C). d13C and d15N values are relative to VPDB-1. References for calendar calibrations are cited at the bottom of calibration graph pages.

Beta Analytic
RADIOCARBON DATING
Consistent accuracy delivered on time

DR. M.A. TAMERS and MR. D.G. HOOD
4985 S.W. 74th Court
Miami, Florida, USA 33155
PH: 305-667-5167 FAX: 305-663-0964
beta@radiocarbon.com

REPORT OF RADIOCARBON DATING ANALYSES

Mr. Ashish Kumar Mishra

Rerport Date: July 31, 2017

James Cook University

Material Received: July 10, 2017

Sample Information and Data	Sample Code Number	Conventional Radiocarbon Age (BP) or Percent Modern Carbon (pMC) & Stable Isotopes Calendar Calibrated Results: 95.4 % Probability High Probability Density Range Method (HPD)	
Beta - 469122	**TB-6**	**16580 +/- 50 BP**	IRMS δ13C: -35.7 o/oo
Submitter Material: Charcoal		**(95.4%) 18199 - 17777 cal BC**	**(20148 - 19726 cal BP)**

Analyzed Material: Charred material
Pretreatment: (charred material) none

Analysis Service: AMS-Standard delivery
Percent Modern Carbon: 12.69 +/- 0.08 pMC
Fraction Modern Carbon: 0.1269 +/- 0.0008
D14C: -873.06 +/- 0.79 o/oo
Δ14C: -874.08 +/- 0.79 o/oo(1950:2017)
Measured Radiocarbon Age: (without d13C correction): 16760 +/- 50 BP
Calibration: BetaCal3.21: HPD method: SHCAL13

Results are ISO/IEC-17025:2005 accredited. No sub-contracting or student labor was used in the analyses. All work was done at Beta in 4 in-house NEC accelerator mass spectrometers and 4 Thermo IRMSs. The "Conventional Radiocarbon Age" was calculated using the Libby half-life (5568 years), is corrected for total isotopic fraction and was used for calendar calibration where applicable. The Age is rounded to the nearest 10 years and is reported as radiocarbon years before present (BP), “present" = AD 1950. Results greater than the modern reference are reported as percent modern carbon (pMC). The modern reference standard was 95% the 14C signature of NIST SRM-4990C (oxalic acid). Quoted errors are 1 sigma counting statistics. Calculated sigmas less than 30 BP on the Conventional Radiocarbon Age are conservatively rounded up to 30. d13C values are on the material itself (not the AMS d13C). d13C and d15N values are relative to VPDB-1. References for calendar calibrations are cited at the bottom of calibration graph pages.

BetaCal 3.21

Calibration of Radiocarbon Age to Calendar Years

(High Probability Density Range Method (HPD): SHCAL13)

(Variables: d13C = -35.7 o/oo)

Laboratory number **Beta-469122**

Conventional radiocarbon age **16580 ± 50 BP**

95.4% probability

(95.4%) 18199 - 17777 cal BC (20148 - 19726 cal BP)

68.2% probability

(68.2%) 18113 - 17909 cal BC (20062 - 19858 cal BP)

TB-6

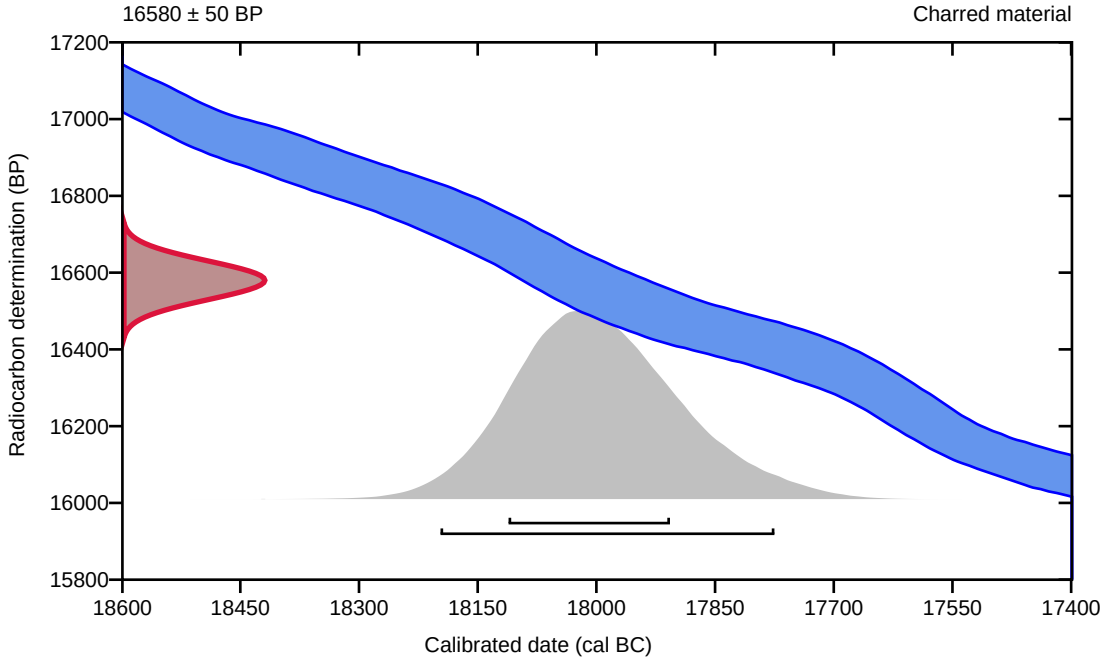

Database used

SHCAL13

References

References to Probability Method

Bronk Ramsey, C. (2009). Bayesian analysis of radiocarbon dates. Radiocarbon, 51(1), 337-360.

References to Database SHCAL13

Hogg, et.al.,2013, Radiocarbon 55(4).

Beta Analytic Radiocarbon Dating Laboratory
4985 S.W. 74th Court, Miami, Florida 33155 • Tel: (305)667-5167 • Fax: (305)663-0964 • Email: beta@radiocarbon.com

BetaCal 3.21

Calibration of Radiocarbon Age to Calendar Years

(High Probability Density Range Method (HPD): SHCAL13)

(Variables: d13C = -29.1 o/oo)

Laboratory number **Beta-467008**

Conventional radiocarbon age **17130 ± 50 BP**

95.4% probability

(95.4%) 18866 - 18480 cal BC (20815 - 20429 cal BP)

68.2% probability

(68.2%) 18746 - 18566 cal BC (20695 - 20515 cal BP)

TB-5

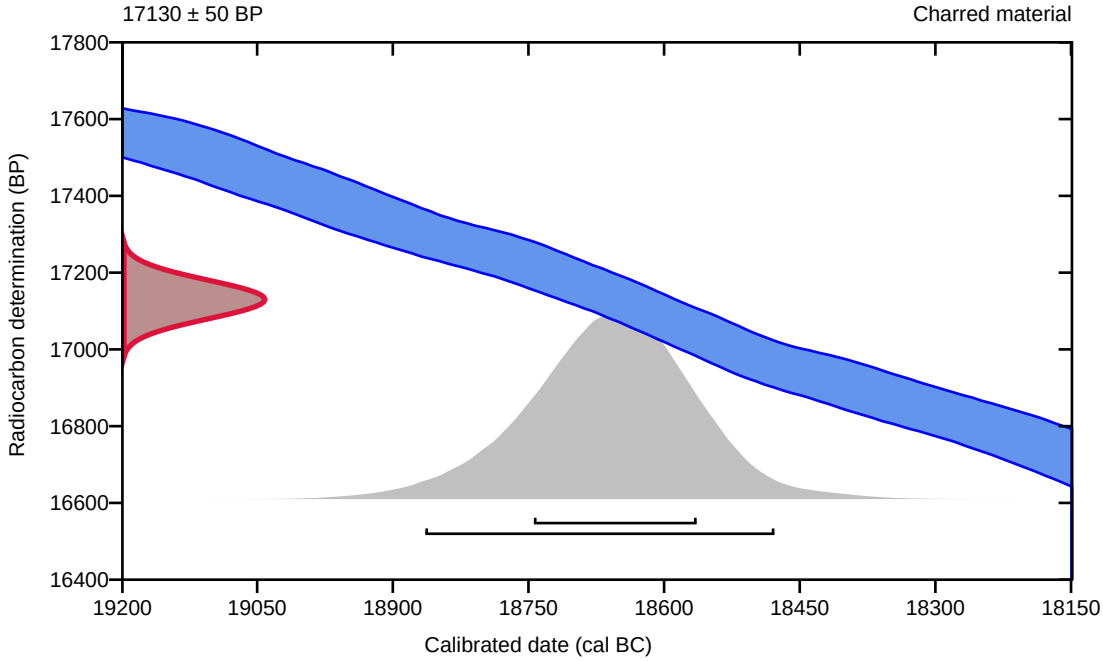

Database used

SHCAL13

References

References to Probability Method

Bronk Ramsey, C. (2009). Bayesian analysis of radiocarbon dates. Radiocarbon, 51(1), 337-360.

References to Database SHCAL13

Hogg, et.al.,2013, Radiocarbon 55(4).

Beta Analytic Radiocarbon Dating Laboratory

4985 S.W. 74th Court, Miami, Florida 33155 • Tel: (305)667-5167 • Fax: (305)663-0964 • Email: beta@radiocarbon.com